Design, Synthesis and Evaluation of Non-Canonical Hsp90 Modulators

By

Alison C. Donnelly

Submitted to the graduate degree program in Department of Medicinal Chemistry and the Graduate Faculty of the University of Kansas in partial fulfillment of the requirements for the degree of Doctor of Philosophy.

Committee Members:

_____

Chairperson: Brian S. J. Blagg, Ph.D.

_____

Thomas E. Prisinzano, Ph.D.

_____

Apurba Dutta, Ph.D.

_____

Paul R. Hanson, Ph.D.

_____

Jon A. Tunge, Ph.D.

Date Defended: March 24, 2011

The Dissertation Committee for Alison C. Donnelly

certifies that this is the approved version of the following dissertation:

Design, Synthesis and Evaluation of Non-Canonical Hsp90 Modulators

_____

Chairperson: Brian S. J. Blagg, Ph.D

Date approved: April 13, 2011

Design, Synthesis and Evaluation of Non-Canonical Hsp90 Modulators

Abstract

Novobiocin, a known DNA gyrase inhibitor, binds to a nucleotide-binding site located on the Hsp90 *C*-terminus and induces degradation of Hsp90-dependent client proteins at ~700 μM in breast cancer cells (SKBr3). Although many analogues of novobiocin have been synthesized in an attempt to improve upon this activity, it was only recently demonstrated that monomeric species can exhibit antiproliferative activity against various cancer cell lines. To further refine the essential elements of the coumarin core, a series of modified coumarin derivatives was synthesized and evaluated. Structure–activity relationships for novobiocin as an anti-cancer agent were elucidated through analogues that manifest low micromolar to nanomolar activity against several cancer cell lines. The compound that exhibited the best and most consistent activity has been further evaluated against a broader panel of cancers as well as taken into an *in vivo* model. Studies are ongoing to further refine the coumarin core, with the potential to replace it with a more suitable heterocyclic ring system.

In addition to the coumarin portion, a noviose sugar and benzamide side chain are appended to the natural product. Because limited information exists regarding the role of the sugar appendage, a series of non-sugar derivatives was synthesized and evaluated to establish structure–activity relationships for the noviose region of novobiocin. These studies have produced simplified novobiocin analogues that manifest low micromolar activity against a panel of cancer cell lines. Likewise, studies have been executed to elucidate details concerning the benzamide side chain and its potential to make hydrophobic interactions with the binding pocket. The most promising compound from each of these series has demonstrated impressive activity against several cancer cell lines and have been evaluated *in vivo*.

Efforts to understand the mechanism of action manifested by these diverse Hsp90 modulators are ongoing and have resulted in the existence of at least three distinct classes of Hsp90 *C*-terminal modulators. Moreover, collaborative studies with the NCI have revealed promising results with a compound that modulates Hsp90 through yet another disparate, but synergistic, mechanism. Through current studies, we hope to better solubilize the most potent compounds and advance novel Hsp90 modulators into clinical development.

Acknowledgments

There are several people I would like to thank for their support and guidance during my graduate school years. Through the good times as well as the bad, there have been people that I have turned to that have provided the support I needed to persevere.

Firstly, many thanks go to my mentor Professor Dr. Blagg. Dr. Blagg provided guidance, patience, understanding and encouragement, always challenging me to reach my full potential. I would not have achieved the many successes or received the accolades I have without his belief that I could achieve great things. Thank you to him for having confidence in me and helping me develop into the scientist I am today.

I am also very grateful to my family for their support. Thanks to mom and dad for supporting me in my decisions and helping me through the tough times, I would not have made it through graduate school without you both. Also, many thanks to Paul, Patrick and Becky, who are both my siblings and close friends. Likewise, I am appreciative of my extended family, especially Julie, AN and UM, AP and UBR, and Grandpa Donnelly, who have provided a network of support and guidance through my graduate years. Finally, I would like to thank Matt, who has been like family to me and has been my rock for the last several years.

I would also like to thank many current and former Blagg lab members. Former co-workers Donna, Gang, Joe, Jed, and Geraldine eased my transition into the lab and were instrumental in teaching me lab techniques and engaging in helpful discussions. Moreover, several of these individuals were great friends and remain so today. In addition, current co-workers, especially Matt, Gary and Teather, have been some of my closest friends during my time in the Blagg laboratory. I will stay in close contact with these individuals, as they were

great friends both in and out of the lab. Thanks also to Laura, Huiping and Bhaskar for helpful discussions and collaborative work during my graduate school years.

Outside of the Blagg lab, I would also like to thank my committee members, Dr. Prisinzano, Dr. Hanson, Dr. Dutta and Dr. Tunge. Each of these individuals offered support and mentorship during graduate school, helping me make difficult decisions and develop as a scientist. In addition, Drs. Aubé and Rafferty acted as invaluable mentors and friends during my time at KU. Moreover, Dr. Neckers, Mehdi and Fabi at the NIH were very helpful during my time at the NIH as well as when I returned to KU and remain good friends and invaluable resources. Several Medicinal Chemistry friends outside of the Blagg lab group, especially Juhienah, Tim, Kim, and Angelica, have been great friends to me. Finally, Sarah Neuenswander, Justin Douglas, and David VanderVelde were invaluable assets in solving spectroscopy puzzles and offered many helpful discussions throughout the years.

I would also like to mention and thank several of my friends in Lawrence. I offer sincere gratitude to Amy and the Brandt family, James and Shayna, Jack and Nancy, Dr. Mark, and Scott and Molly for being great friends during my time in Lawrence. Likewise, thanks to the Dog Days Running Club as well as my teammates from LASL teams, especially Emily, Nick, Anne, Pedro, Dave, Thomas and Dan.

Finally, I would like to thank the Medicinal Chemistry Department, Goetsch Family Scholarship, NIH Training Grant in Chemical Biology and the ACS Division of Organic Chemistry Graduate Fellowship for funding my research. I would not have accomplished all that I have without the generous support from the department and these agencies.

Table of Contents

List of Sections:

Chapter III

Examination of the Sugar Appendage on Novobiocin

Chapter IV

Studies on the Novobiocin Benzamide Side Chain

Chapter V

Modulation of Hsp90 with Small Molecules

List of Figures:

Chapter I

Novobiocin and Additional Inhibitors of the Hsp90 *C*-terminal Nucleotide-binding Pocket

Chapter II

Studies on the Novobiocin Coumarin Core

Chapter III

Examination of the Sugar Appendage on Novobiocin

Chapter IV

Studies on the Novobiocin Benzamide Side Chain

Chapter V

Modulation of Hsp90 with Small Molecules

List of Schemes:

Chapter II

Studies on the Novobiocin Coumarin Core

Chapter III

Examination of the Sugar Appendage on Novobiocin

Chapter IV

Studies on the Novobiocin Benzamide Side Chain

Chapter V

Modulation of Hsp90 with Small Molecules

List of Tables:

Chapter II

Studies on the Novobiocin Coumarin Core

Chapter III

Examination of the Sugar Appendage on Novobiocin

Chapter IV

Studies on the Novobiocin Benzamide Side Chain

Chapter V

Modulation of Hsp90 with Small Molecules

Chapter I

Novobiocin and Additional Inhibitors of the Hsp90 C-terminal Nucleotide-binding Pocket

I. Introduction

The goal of several research groups, internationally, has been to better understand the ubiquitously expressed 90 kDa heat shock proteins (Hsp90). Many studies have been published, revealing these proteins to be integrally involved in cell signaling, proliferation and survival. This family of proteins plays an essential role as molecular chaperones and is responsible for the conformational maturation of nascent polypeptides and the refolding of denatured proteins.[1] More than 150 Hsp90-dependent client proteins have been identified,[2,3] many of which are associated with cellular signaling networks such as steroid hormone receptors, transcription factors and protein kinases, which represent individually sought after targets for the development of cancer chemotherapeutics.[1,4-8] Hsp90 is an abundant molecular chaperone and is constitutively expressed in eukaryotic cells. Under homeostatic conditions, this protein accounts for nearly 1% of the total cellular protein in eukaryotic cells.[9] Cells exposed to heat shock and other stressed conditions, such as in the case of cancer, overexpress Hsp90.[10] Many proteins in tumor cells are dependent upon the Hsp90 protein folding machinery for their maturation, stability and activation.[2,3] Since Hsp90 inhibition uniquely targets client proteins associated with all six hallmarks of cancer, Hsp90 has emerged as a promising target for cancer chemotherapy.[11,12] Moreover, this molecular chaperone has exhibited exceptional neuroprotective properties due to its essential role in the refolding of aggregated proteins associated with several neurodegenerative diseases.[13,14]

Human Hsp90 exists as a homodimer, which contains three highly conserved domains. These regions consist of a 25 kDa *N*-terminal ATP-binding domain, a 35 kDa middle domain, and a 12 kDa *C*-terminal dimerization domain (Figure 1). Inhibitors that bind to the various Hsp90 domains block the ability of the chaperone to stabilize and/or fold client proteins, leading to an unproductive heteroprotein complex that is degraded by the ubiquitin-proteasome pathway.[15-20] Natural products geldanamycin (GDA) and radicicol (Figure 2), for example, are known to bind the *N*-terminal ATP-binding site.[21-24] These molecules inhibit the ability of the Hsp90 *N*-terminus to bind and hydrolyze ATP, which is essential for its chaperoning function.[25-27] While the solution structure of Hsp90 exists as a continuum of C-terminally dimerized conformations, the ATP-bound state is a highly constrained structure.[28] The formation of this structure involves coupled conformational switches to position the catalytic apparatus for ATP hydrolysis.[25] An unstructured, highly charged linker joins the *N*-terminus to the middle domain.[14]

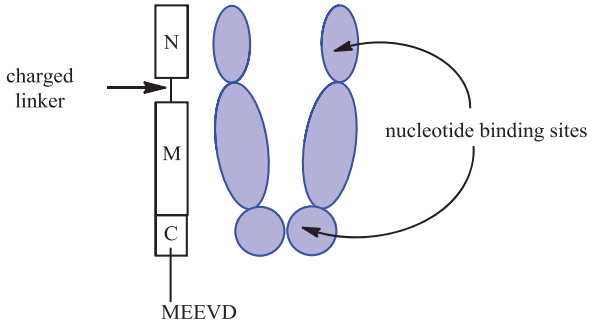

Figure 1. Structure of Hsp90 in open state.[14]

The middle domain exhibits high affinity for co-chaperones as well as client proteins.[29-35] Structural and functional analyses have demonstrated that the middle domain of Hsp90 contains a catalytic loop which may serve as an acceptor for the γ-phosphate of ATP, when it is bound to the *N*-terminus.[33] The structure of the *C*-terminus of Hsp90 is characterized by the MEEVD sequence, which is known to bind co-chaperones that contain multiple copies of the tetratricopeptide repeat (TPR), a 34 amino acid sequence. Chadli and co-workers recently

identified a second, novel site near the *N*-terminus that also binds TPR proteins. This second site is either within or near the ATP-binding pocket at the *N*-terminus of Hsp90 and thus is strongly regulated by nucleotide binding.[14,36]

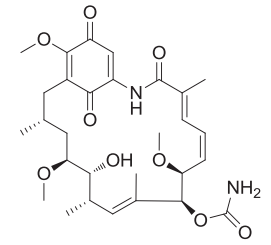

GDA

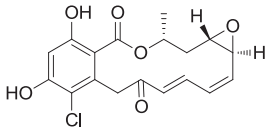

Radicicol

Figure 2. Structures of GDA and radicicol.[14]

Initial studies by Csermely and co-workers suggested a second ATP-binding site located in the Hsp90 *C*-terminus.[37] This *C*-terminal nucleotide binding pocket has been shown to not only bind ATP, but also novobiocin, cisplatin, epilgallocatechin-3-gallate (EGCG) and Taxol.[21] This review examines the different classes of Hsp90 *C*-terminal inhibitors, with specific emphasis on structure-activity relationships for novobiocin and their implications for neuroprotection and/or anti-cancer activity.[14]

II. The Hsp90 Family

Heat shock proteins consist of several subfamilies of molecular chaperones classified by their molecular weights. These subfamilies include Hsp90, Hsp70, Hsp60 and the small Hsps.[38] Each of these subfamilies plays critical cellular roles, such as the prevention of protein

aggregation and the direction of misfolded and transient proteins to proteasomal degradation.[39] Hsp90 proteins are highly conserved and four isoforms have been identified. The two major cytosolic isoforms include the major, inducible Hsp90α and the minor, constitutively expressed, Hsp90β.[40-43] Although there is a relatively high conservation within these two isoforms (85% sequence identity), it is suggested that they may display altering chaperone activity.[44] Due to slight perturbations in amino acid sequence, it has been proposed that the α and β forms may exhibit differential binding to client protein substrates.[14,40]

Millson and co-workers used yeast to show that activation of certain Hsp90 clients, such as heat shock transcription factor and v-src were more efficient with Hsp90α, rather than Hsp90β. In contrast, activation of other clients, such as glucocorticoid receptor and extracellular signal-regulated kinase-5 mitogen-activated protein kinase, demonstrated less dependence on the human Hsp90 isoform expressed. Differential expression patterns were observed when inhibitors, such as radicicol, were selectively introduced to each isoform. It was concluded that in yeast and mammalian systems, cellular susceptibility to Hsp90 inhibitors may be dependent on alternations to the Hsp90α/β ratio. Heat shock is known to induce such an alteration in this isoform ratio.[14,45]

Other Hsp90 isoforms include glucose-regulated protein 94 (Grp94) in the endoplasmic reticulum and Hsp75/TRAP1 in the mitochondrial matrix.[46,47] Hsp75 is unique in both its expression of a LxCxE motif,[42] which is absent in all other Hsp90 family members, as well as its dependence on stress kinases for transcriptional activation.[48] Moreover, Hsp75 is structurally unique because it lacks the highly charged hinge region located in the *N*-terminal domain of the other isoforms.[42,47] A recent report added Hsp90N to the Hsp90 family and revealed its role to be associated with cellular transformation. It has been proposed that the newly discovered Hsp90N

represents a recent Hsp90α gene rearrangement.[49] Although Hsp90N shares high sequence homology with the α and β isoforms, it lacks the 25 kDa *N*-terminus.[49] Structures of the five Hsp90 isoforms are summarized and compared in Figure 3.[14]

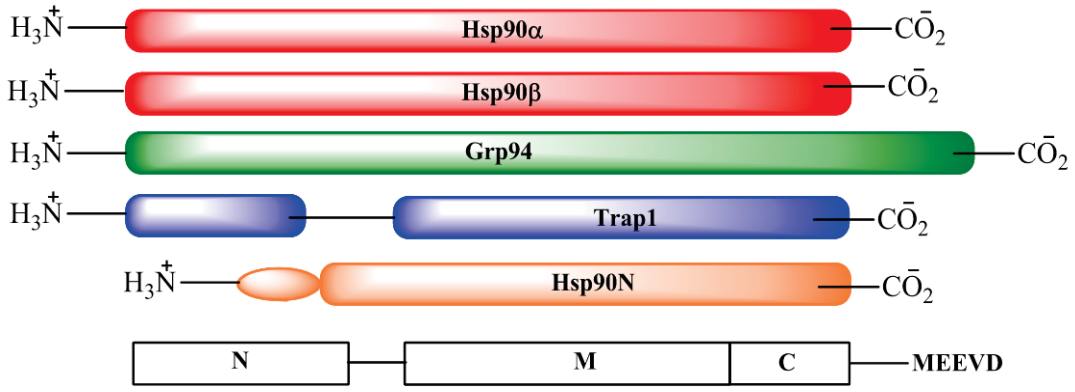

Figure 3. Summary of various Hsp90 isoforms.[14,40]

There is selective dimerization amongst the two cytosolic isoforms. The two dominant isoforms differ in their ability to dimerize, with the α form doing so readily and the β with much less efficiency.[40] Upon dimerization, Hsp90 exists mainly as a constitutive dimer (αα or ββ), but monomers (α or β), heterodimers (αβ) and higher oligomers of both isoforms may also exist.[40] Dimerization is dependent upon the last 190 amino acids in the *C*-terminus.[47,49] This *C*-terminal dimerization is essential for efficient ATP hydrolysis and dependent on both intra- and inter-domain interactions for its formation and stability.[50] 16 amino acids located in the 561-685 amino acid region of the *C*-terminal dimerization domain were suggested to be responsible for dimerization of Hsp90β.[51] Kobayakawa and co-workers defined which specific amino acid substitutions impeded dimerization and explained the results in terms of the differences between the two major isoforms.[14,52]

In addition to the structures of the isolated domains have been published previously, the full length crystal structure of the closed chaperone complex of yeast Hsp90 bound to nucleotide-

p23/Sba1 was published in 2006 by Ali and associates. The crystal structure was solved in complex with a non-hydrolyzable ATP analogue and the Hsp90 co-chaperone p23/Sba1. This crystal structure revealed several novel aspects of Hsp90 which were previously unknown. Firstly, the complex architecture of the 'closed' state of Hsp90 was elucidated. In addition, the experimentally described interactions between Hsp90 and partner proteins were confirmed. Moreover, a detailed conformational change in the *N*-terminal domain was demonstrated to result from ATP binding in the closed, ATP-bound state. Finally, the structural and stabilizing role of co-chaperone p23/Sba1 in the ATP-bound closed dimer state was clarified. This closed Hsp90 state was shown to provide a binding surface for protein substrates rather than enclosing them. Formation and disruption of this surface was found to be directly coupled to the Hsp90 ATPase cycle. The full-length crystal structure verified the widely accepted ATPase-coupled molecular clamp mechanism and structurally elucidated the ATP-dependent activation of Hsp90 client proteins. In contrast to the closed ATP-bound state, the relaxed, structurally unconstrained structure was described as a continuum between *C*-terminally dimerized conformations.[14,25]

In addition to the crystal structure of Hsp90 bound to p23/Sba1, the structures of other Hsp90 complexes have been published. The structure of the Hsp90-Cdc37-Cdk4 complex was published by Vaughan and co-workers in 2005. The 3D structure of this complex was determined by single-particle electron microscopy. This study helped elucidate the locations of Cdc37 and Cdk4 in the complex as well as the link between conformational changes in the kinase and the Hsp90 ATPase cycle.[53] Another important structure, solved by Meyer and co-workers, was that of Aha1 bound to Hsp90. Aha1 plays an important role in stimulating the ATPase activity of Hsp90. Through a crystal structure of the *N*-terminal domain of Aha1 in complex with the middle segment of Hsp90, it was confirmed that this activity is mediated

through an interaction between Aha1 and the central segment of Hsp90. This binding promotes a conformational switch in the middle-segment catalytic loop and enables the interaction of the *N*-terminus with ATP.[14,33]

More recently, Bron and co-workers reported the solution structures of two open conformational states of eukaryotic Hsp90. This group presented the first nucleotide-free structure of the full-length chaperone and confirmed that, in solution, apo-Hsp90 is in conformational equilibrium between two states. Switching between the two Hsp90 conformations was described to require movement of the *N*-terminal and middle domains around two flexible hinge regions. Due to the intrinsic flexibility and dynamic nature of the Hsp90 dimer observed, Bron and associates challenged the accepted ATPase cycle and proposed an alternative mechanism for chaperone activity.[14,54]

III. Hsp90 as a Molecular Chaperone

Eukaryotic Hsp90 is constitutively expressed under normal conditions,[55] and significantly overexpressed upon exposure to stress. Stress to the cell, including elevated temperature, non-physiological pH, nutrient deprivation and malignancy, results in the accumulation of misfolded proteins and increased translation of new proteins.[21] Heat shock proteins are overexpressed to refold both denatured and newly synthesized polypeptides into their native conformation.[14,55-57]

The induction of the molecular chaperones Hsp27, Hsp40 and Hsp70 depends on Hsp90.[4] Release of heat-shock transcription factor 1 (HSF1) is responsible for this Hsp upregulation. While Hsp90 is bound to HSF1 in resting cells, it dissociates upon cellular stress and is translocated to the cell nucleus. Once in the nucleus, HSF1 is phosphorylated and then undergoes

trimerization.[58,59] The activated HSF1 trimer binds to heat shock response elements (HSE), the consensus sequence for Hsp promoters,[60] and elicits transcription of Hsps.[14]

After the synthesis of single-stranded polypeptides by the ribosome, nascent polypeptides have the propensity to aggregate through interactions between amino acid side chains. This aggregation is prevented through the action of molecular chaperones. Because of their role in the transformation of linear polypeptides into tertiary and quaternary structures, chaperones are considered essential for the second half of the genetic code.[61] Linear polypeptides released from the ribosome are subsequently bound by the promiscuous molecular chaperone, Hsp70, in complex with ATP and Hsp40. The bound ATP is then hydrolyzed to stabilize and prevent aggregation of these proteins.[14,61]

Hsp70 interacting protein (HIP), subsequently, binds to and stabilizes the Hsp70-ADP-client complex. BAG (Bcl2-associated athanogene) homologues, on the contrary, cause the dissociation of this Hsp70-protein complex by stimulating exchange of ATP for ADP and polypeptide release.[21] Hsp90-Hsp70 organizing protein (HOP), which contains highly conserved tetratricopeptide repeats (TPRs), unites the Hsp70-protein complex with Hsp90, thus forming a multiprotein complex .[62] HOP has been shown to interact with the Hsp90 *C*-terminus through its TPR domain as well as at additional sites in the middle domain of Hsp90. Onuoha and co-workers utilized biophysical analysis of the structure and binding of HOP to Hsp90 using a variety of truncation mutants of both the client and chaperone. Their results confirmed that while the primary binding site of HOP is the C-terminal MEEVD peptide, binding also occurs at additional sites in the *C*-terminal and middle domains.[63] Immunophilins, co-chaperones, and partner proteins bind to the newly formed heteroprotein complex and facilitate the transfer of client proteins from Hsp70 to Hsp90. Simultaneously, Hsp70, HIP and HOP are released from

the complex.[64] The action of immunophilins, such as FKBP51, FKBP52 and CyP-40, or PP5 enable *cis/trans* peptidylprolylisomerase activity and form a heteroprotein complex that represents the activated Hsp90 protein folding machine.[64-66] Figure 4 summarizes essential co-chaperones and partner proteins involved in the protein folding mechanism of Hsp90 and highlights those participants containing a TPR domain.[14]

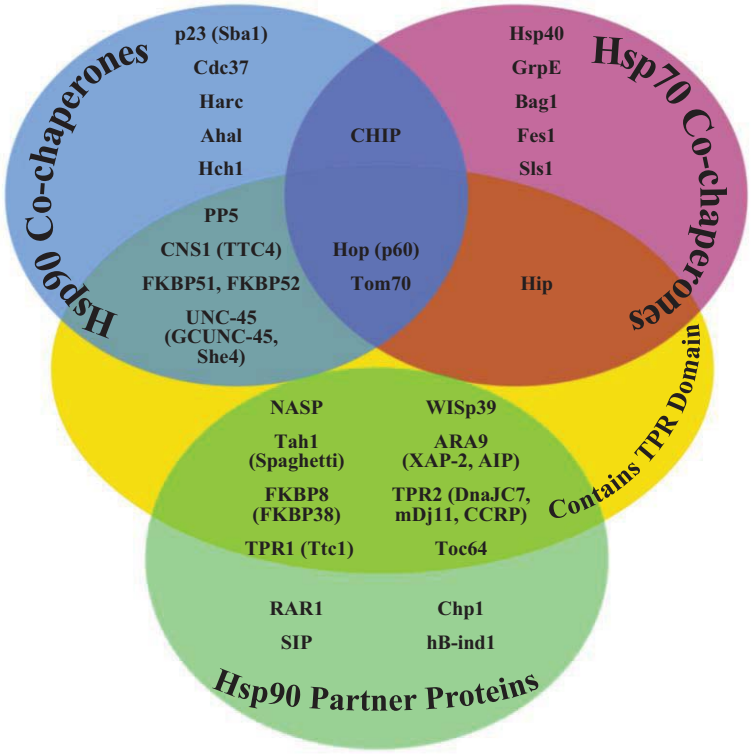

Figure 4. Co-chaperones and partner proteins involved in Hsp90 protein folding.[14,67,68]

At this point of the folding process, ATP binds to the open conformation and Hsp90 clamps around the client protein substrate resulting in a closed clamp.[69] It is at this stage of the folding process that an inhibitor, instead of ATP, can bind competitively to the multiprotein complex, and cause destabilization of the heteroprotein complex, which will transform it into a substrate for the ubiquitin-proteasome pathway. During the protein folding cycle, ATP hydrolysis occurs through the binding co-chaperone p23 to the ATP-bound Hsp90 multiprotein

complex. Co-chaperone p23 is also responsible for stabilizing this clamped, high-affinity client-bound Hsp90 conformation. The bound client protein is then folded into its three-dimensional structure by this complex. Release of the folded protein has not been fully characterized, but is thought to also be stimulated by p23.[2] Once the mature protein is released, Hsp90 can reenter the next catalytic protein folding cycle. The schematic diagram shown in Figure 5 represents a simplified Hsp90-mediated protein folding mechanism. This process has been shown to utilize more than 20 associated proteins for the maturation of various clients.[1,14,21,70-76]

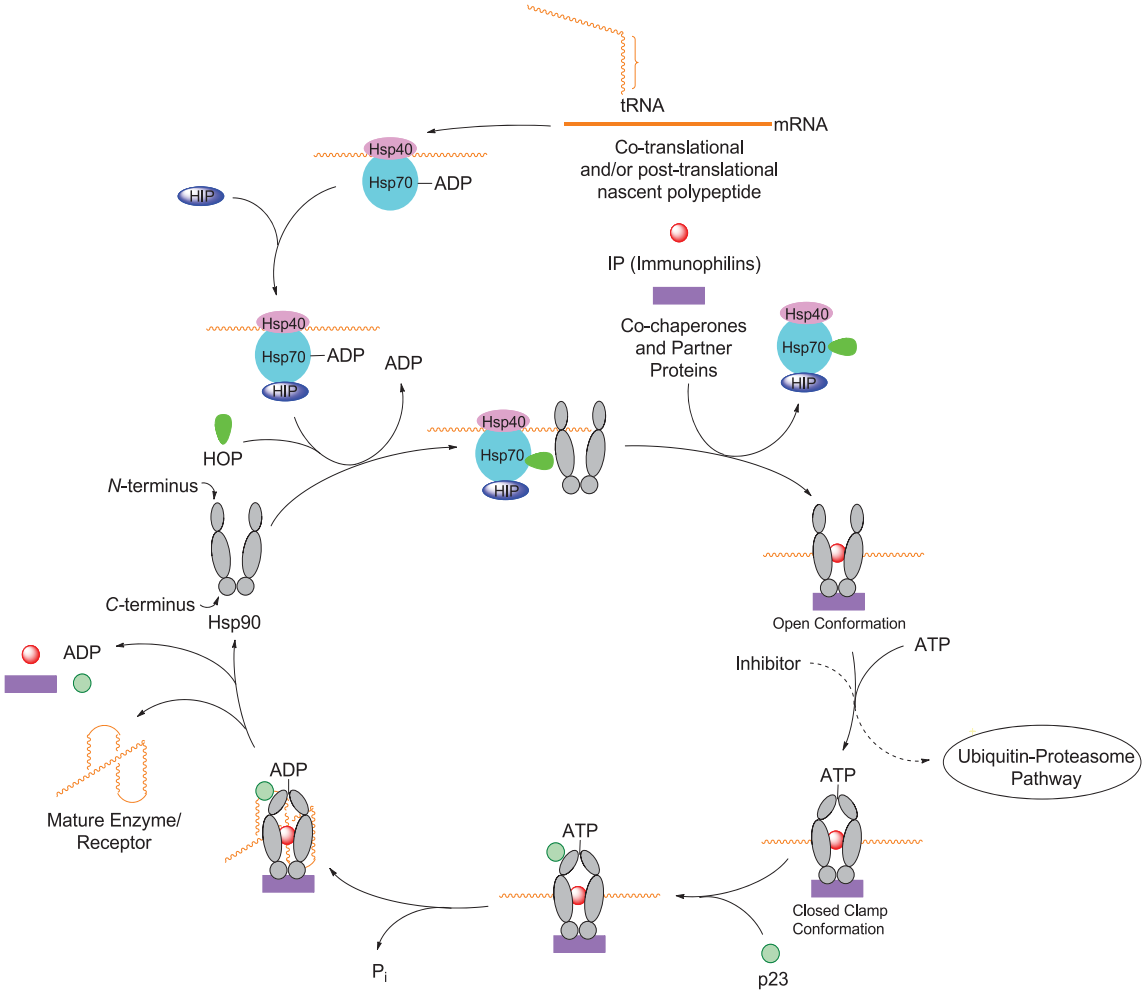

Figure 5. Proposed Hsp90-mediated protein folding mechanism.[14]

IV. Description of the *C*-terminal ATP Binding Pocket

The existence of a second ATP binding site on the Hsp90 carboxyl terminus, separate from the well-documented *N*-terminal ATP binding site, has only recently been reported.[9,77,78] Since no co-crystal structure of the Hsp90 *C*-terminus bound to inhibitors has been published, knowledge of the binding pocket is limited, but many hypotheses have been proposed to account for its function. The Hsp90 *C*-terminal domain is known to display chaperone activity independent of the *N*-terminus, as well as mediate dimerization and oligimerization of Hsp90 monomeric species. Structurally, the *C*-terminus of Hsp90 contains a conserved pentapeptide sequence (MEEVD) that is recognized by co-chaperones.[9,79] The co-chaperones that recognize this sequence all contain multiple copies of the tetratricopeptide repeat (TPR), a 34 amino acid sequence that elicits specific binding to Hsp90.[65,80-82] This sequence, though conserved, has been reported as dispensable for activity.[14,83]

Many groups have used novobiocin to study Hsp90 *C*-terminal binding, as it was the first and remains the most studied inhibitor of the Hsp90 carboxyl terminus.[84] Neckers and co-workers revealed via truncation studies that the novobiocin binding site resides in the Hsp90 *C*-terminus, in a region that is proximal to the carboxyl-terminal dimerization domain. Several amino-terminal point mutations known to disrupt binding of geldanamycin and radicicol were tested for their ability to perturb binding to immobilized novobiocin. These mutants bound novobiocin-Sepharose as well as or better than did wild type Hsp90. Moreover, the *N*-terminal Hsp90 fragment containing the ATP-binding site of GDA and radicicol failed to bind. Upon demonstration that the amino-terminus did not bind novobiocin, several *C*-terminal fragments were analyzed for novobiocin binding. These fragments revealed that novobiocin binds to a carboxyl-terminal Hsp90 fragment containing amino acids 538–728. Moreover, this group

demonstrated that novobiocin competes with ATP for binding and that association of the co-chaperones Hsc70 and p23 with Hsp90 is disrupted by novobiocin. Through immobilization of ATP, the same fragments that demonstrated binding to immobilized novobiocin were tested for ATP binding. The same fragments that bound novobiocin were also shown to bind ATP, demonstrating a competitive nature between the two small molecules. Finally, novobiocin preincubation with rabbit reticulocyte lysate, which contains Hsc70- and p23-Hsp90-multichaperone complexes, caused a marked decrease in the amounts of both p23 and Hsc70 when co-precipitated with Hsp90. This study confirmed the disruption of co-chaperone binding by novobiocin.[14,77]

Csermely and co-workers reported that the *C*-terminal site becomes available for binding only after occupancy of the *N*-terminal site. Moreover, through oxidative nucleotide affinity cleavage, this group characterized that while the *N*-terminal binding site is fairly specific for adenine nucleotides, the *C*-terminus binds both purines and pyrimidines (GTP and UTP preferentially).[37] Garnier and co-workers utilized isothermal titration calorimetry, scanning differential calorimetry and fluorescence spectroscopy to study the interaction of ATP with native Hsp90 and its recombinant *C*-terminal domain. Results clearly demonstrated that a second ATP-binding site is present in the carboxyl terminus and that the secondary structure of this site may resemble a Rossmann fold.[9,85] Garnier and co-workers concluded that the nucleotide-binding site overlaps with the dimerization domain, which explains the close relationship between ATP binding, dimerization, and magnesium-dependent oligomerization.[9,14]

Although the Hsp90 *C*-terminus does not exhibit ATPase activity, it is involved in the conformational rearrangement of Hsp90 upon ATP binding.[79,86] The ATPase activity of Hsp90, which leads to a conformational change of the entire homodimer, is dependent upon the Hsp90

C-terminal region to trap the nucleotide during the ATPase cycle.[9] Yun and co-workers suggested that the conformational switch upon novobiocin binding causes changes to Hsp90/cochaperone/client interactions and may be responsible for the observed biological activities.[86] Complex interactions between the *N*- and *C*-terminus is a critical regulatory component of chaperone function. Garnier and co-workers have alluded to the cross-talk observed as allosteric interactions between the two termini.[9,37,87-90] Garnier also observed that when a nucleotide is bound to the *N*-terminus, the molecule exhibits a strong negative impact on the binding of nucleotides to the *C*-terminus. Furthermore, affinity of the truncated *C*-terminus for ATP was higher than that of the entire protein. This result confirms that the presence of the amino-terminus negatively affects binding to the carboxyl-terminus and that interdomain cross-talk occurs. The development of improved analogues should further refine knowledge on the Hsp90 *C*-terminal nucleotide-binding pocket and provide insight into the unique mechanism exhibited by Hsp90 during the protein folding process.[14,79]

V. Inhibitors of the *C*-terminal ATP Binding Pocket

A. Novobiocin and analogues

The coumarin antibiotics novobiocin, chlorobiocin, and coumermycin A1 (Figure 6) have been isolated from several *streptomyces* strains and all exhibit potent activity against Gram-positive bacteria. These compounds bind to type II topoisomerases, including DNA gyrase, and inhibit the enzyme-catalyzed hydrolysis of ATP.[79,91-94] As a result, novobiocin analogues have garnered the attention of numerous researchers as attractive agents for the treatment of bacterial infections. In addition, novobiocin was reported to bind weakly to the newly discovered Hsp90

C-terminal nucleotide-binding site (~700 μM in SKBr3 cells) and induce degradation of Hsp90 client proteins. Structural modification of this compound has led to analogues with 1000-fold greater efficacy in anti-proliferative assays against various cancer cell lines.[14]

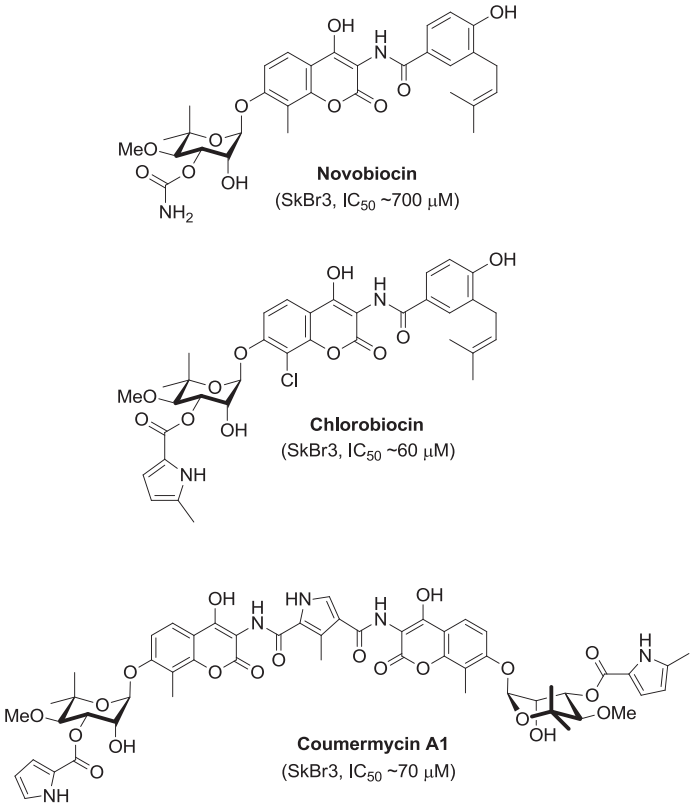

Figure 6. Structures of novobiocin, chlorobiocin and coumermycin A1.[14]

Co-crystal structures of GyrB bound to novobiocin and ADP revealed that both small molecules bind GyrB in a bent conformation,[95-97] exactly as Hsp90 binds ADP.[23] With the observations that novobiocin binds in this bent conformation and also exhibits cytotoxicity,[94,98-101] Neckers and co-workers hypothesized and subsequently proved that it also binds Hsp90. It is through binding to Hsp90 that novobiocin exerts its anti-tumor activity against breast cancer cells. Using SKBr3 breast cancer cells, Neckers and co-workers demonstrated that 16-hour exposure to novobiocin induces degradation of Hsp90-dependent clients ErbB2, mutant p53 and Raf-1 in a concentration-dependent manner. The same laboratory eluted truncated Hsp90 from

an immobilized novobiocin solid-support and led to the conclusion that, in contrast to all other Hsp90 inhibitors that bind to the well-established *N*-terminal ATP-binding site, only the Hsp90 *C*-terminus is capable of binding novobiocin.[84] Binding of novobiocin to the *C*-terminus was found to displace inhibitors bound to the Hsp90 *N*-terminus, a phenomenon that is not reciprocal with *N*-terminal inhibitors.[77,84] Allan and co-workers proposed that novobiocin may lead to substrate release by inducing a conformational change that results in separation of the homodimeric *C*-terminal domains.[14,79]

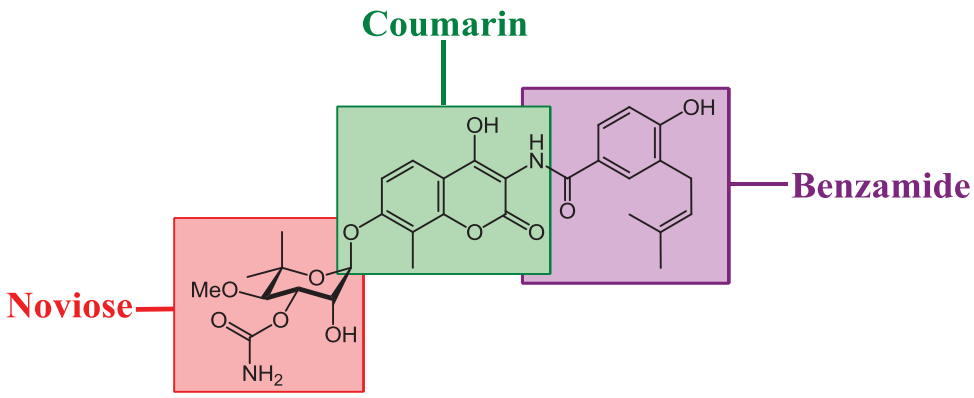

Figure 7. Structural analysis of novobiocin.[14]

Two research laboratories have synthesized analogues of novobiocin in an attempt to improve upon its poor Hsp90 inhibitory activity.[84] Novobiocin is composed of three distinct parts upon which modifications can be made: the benzamide side chain, the coumarin core and the noviose sugar (Figure 7). The role of each contributing part can be studied through the development of analogues to probe specific structure-activity relationships for this molecule. To this end, a library of novobiocin analogues published in 2005 reported that **A4** (Figure 8), with a shortened *N*-acyl side chain, an absent 4-hydroxy substituent and a missing carbamoyl group on the noviose appendage, induced degradation of Hsp90-dependent client proteins at ~70-fold lower concentration than novobiocin.[15] This study demonstrated that attachment of the noviose appendage to the 7-position and an amide linker at the 3-position of the coumarin ring are

essential for Hsp90 inhibition.[15] To confirm the observed SAR trends elucidated from this library, the natural product analogues **DHN1** and **DHN2** (Figure 8) were prepared and evaluated. These molecules were evaluated in several assays, which confirmed that while the 4-hydroxyl and 3'-carbamate are essential for DNA gyrase inhibition, they are detrimental to Hsp90 inhibitory activity.[18] Thus, the first selective inhibitors of the Hsp90 *C*-terminus were born.[14]

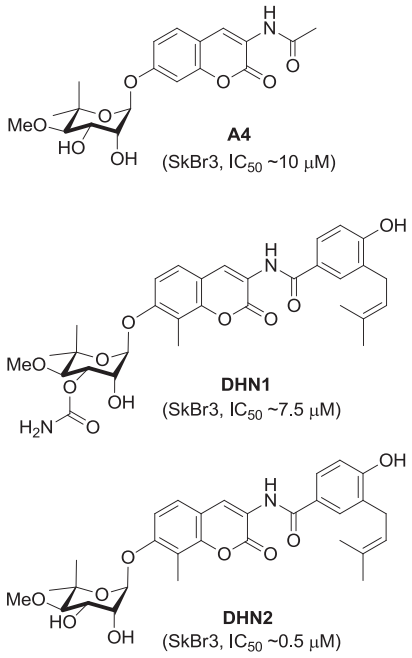

Figure 8. Structures of **A4**, **DHN1** and **DHN2**.[14]

Compound **A4** was found to exhibit unique properties unbenounced previously. **A4** induced Hsp90 levels at concentrations 1000–10000-fold lower than that required for client protein degradation and was thus evaluated for neuroprotective activity. **A4** was found to produce an EC_{50} at 6 nM and exhibited no toxicity at any concentration tested in a model for Alzheimer's disease.[15,102] In contrast to the monomeric species, dimers of **A4** (based on the structure of coumermycin A1, Figure 9) were found to manifest anti-proliferative activity. This study sought to fully investigate variants of **A4** through preparation of dimers that were linked through *meta*- and *para*-phthalic acids and others that contained methylene spacers in the tether.

The phthalic acid derivatives were proposed to represent steric mimics of the pyrrole linker found in the natural product, coumermycin A1. Unfortunately, the phthalic acid-linked derivatives manifested no activity against cell cultures.[14]

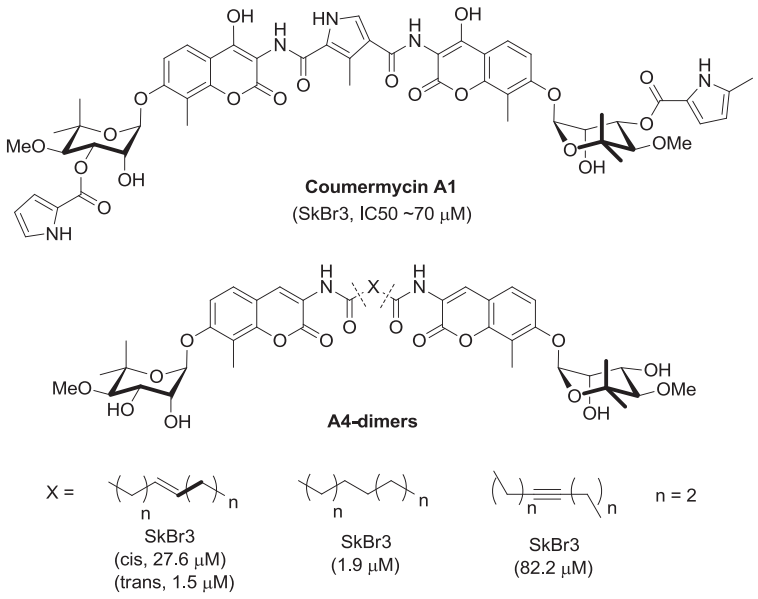

Figure 9. Structures of coumermycin A1 and **A4**-dimers.[14]

Through the synthesis and biological evaluation of methylene linked dimers, the optimal tether length and degree of unsaturation were determined. The saturated **A4**-dimer with a tether length of eight carbons was found to be the most potent compound in this series and exhibited anti-proliferative activity against two different breast cancer cell lines at low micromolar concentrations. The fact that the dimeric species exhibited anti-proliferative activity led to the hypothesis that conversion of a nontoxic molecule into a potent anti-proliferative agent was accomplished through modification of the amide side chain.[103] Consequently, a series of monomeric species based on **A4** were synthesized and evaluated against a series of cancer cell lines. Both biaryl and heterocyclic amide derivatives were prepared to explore potential hydrogen-bonding interactions with the putative novobiocin binding pocket that is responsible for binding the prenylated benzamide of the natural product. This study led to the first SAR for

the amide side chain and led to identification of the biaryl and the 2-indolyl side chains (Figure 10), both of which exhibited anti-proliferative activity.[14,102]

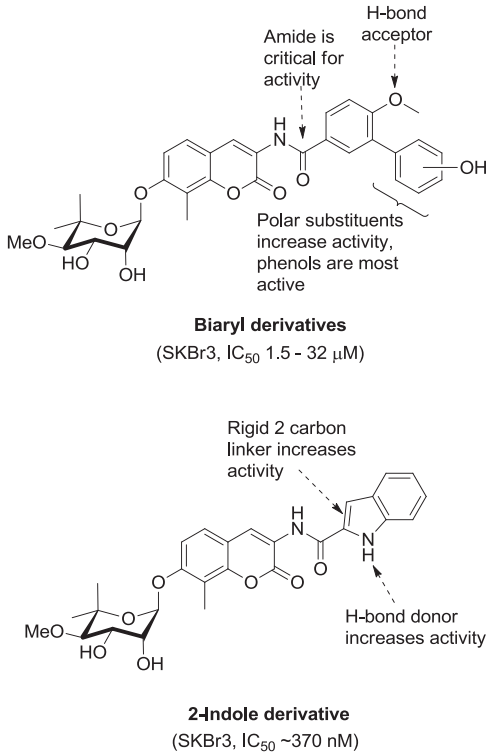

Figure 10. SAR elucidated for novobiocin.[14]

A paper published by Huang and co-workers in 2007 represented the first combinatorial library of coumarin analogues aimed at Hsp90 inhibition. The library was designed to probe hydrophobic and hydrogen bonding interactions produced by the binding pocket. The analogues incorporated previously determined SAR trends as well as strategically placed H-bond donors/acceptors.[14,104]

Renoir and co-workers were the first to publish studies on the role of noviose in Hsp90 inhibition. Their structure–activity relationship studies demonstrated that when analogues lack the noviose moiety, the inclusion of a tosyl substituent at C-4 or C-7 of the coumarin results in Hsp90 inhibition. These analogues were more potent than novobiocin and manifested mid-micromolar IC_{50} values.[105] A subsequent paper by the same group suggested that Hsp90

inhibition can be enhanced by removal of C7/C8 substituents in desnoviose analogues bearing a tosyl group at the 4-position. These studies produced inhibitors with simplified coumarins that also exhibited mid-micromolar IC_{50} values.[106] A summary of the novobiocin SAR determined thus far is summarized in Figure 11.[14]

To extend SAR for novobiocin, modified coumarin derivatives of **A4** were designed to complement and probe interactions typically manifested by the purine ring of ATP. These coumarin-modified ring systems possess hydrogen bonding capabilities that mimic those of the nucleotide bases, adenine and guanine. In addition, these derivatives contain strategically placed hydrogen bond acceptors and donors and alkyl groups of variable size to probe the size and nature of the binding pocket. The results from such studies are currently under review and should be available in the near future.[14]

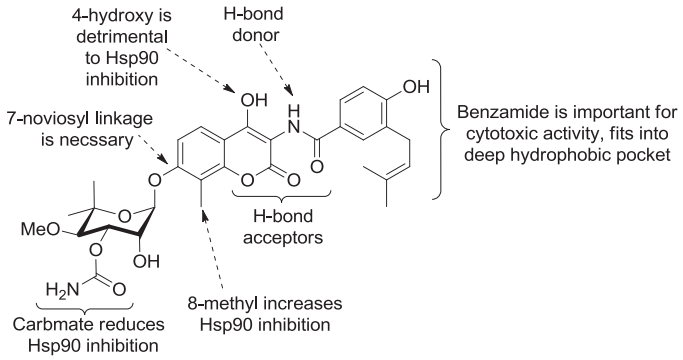

Figure 11. Summary of SAR between novobiocin and Hsp90.[14]

B. Cisplatin

Cisplatin (Figure 12) is a platinum-containing chemotherapeutic used to treat various types of cancers, including testicular, ovarian, bladder, and small cell lung cancer.[107] Most notably, cisplatin coordinates to DNA bases, resulting in cross-linked DNA, which prohibits rapidly dividing cells from duplicating DNA during mitosis.[108-110] In addition to its DNA-

mediated effects, Sreedhar and co-workers reported that cisplatin binds to the Hsp90 *C*-terminal domain and interferes with nucleotide binding.[111] Rosenhagen points to physiological effects as indicators of the interaction between cisplatin and Hsp90. The hyperactive Hsp90-androgen receptor (AR) in prostate cancer is treated with cisplatin through Hsp90 inhibition. Likewise, Hsp90 inhibitors can be used to treat cisplatin-resistance in cells transfected with the Hsp90-dependent protein kinase v-src.[14,112]

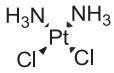

Figure 12. Structure of cisplatin.[14]

Itoh and co-workers reported that cisplatin decreases Hsp90 chaperone activity. They applied bovine brain cytosol to a cisplatin-affinity column, eluted with cisplatin and detected Hsp90 in the eluent. The results of this study indicated that cisplatin has a high affinity for Hsp90. Moreover, through the use of proteolyzed Hsp90 fragments and affinity purification, it was demonstrated that cisplatin binds near the *C*-terminus.[113] Upon treatment of neuroblastoma cells with cisplatin, Rosenhagen and co-workers observed degradation of the androgen and glucocorticoid steroid receptors but not other Hsp90 clients, such as raf-1, lck and c-src. The steroid-receptor-specific proteolysis induced by cisplatin suggests that the compound does not complex Hsp90 and other client proteins, but rather it specifically inhibits steroid receptor-Hsp90 complexes.[112] Csermely and co-workers determined that the cisplatin binding site is located proximal to the *C*-terminal nucleotide binding site. This study concluded that cisplatin can be used to inhibit the *in vitro* chaperone activity of Hsp90 as well as to efficiently and selectively block *C*-terminal nucleotide binding.[14,78]

Acquired resistance to cisplatin can limit its therapeutic potential and many resistance mechanisms have been reported.[114] These pathways include decreased intracellular drug

accumulation, enhanced cellular detoxification by glutathione and metallothionein, altered DNA repair and inhibition of apoptosis.[114,115] The observed *in vivo* unresponsiveness of certain tumors to cisplatin cannot be explained by these mechanisms, however, pointing to novel pathways mediating cisplatin resistance.[116,117] Genomic screening *in vivo* has helped to elucidate the mechanisms of both cisplatin toxicity and acquired cisplatin resistance.[14,118]

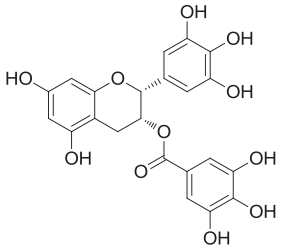

Figure 13. Structure of EGCG.[14]

C. Epigallocatechin-3-gallate

EGCG (Figure 13) is a one of the active polyphenolic components found in green tea. EGCG is known to inhibit the activity of many Hsp90 client proteins, including telomerase, multiple kinases, and the aryl hydrocarbon receptor (AhR). EGCG is also involved in growth factor signaling, which involves epidermal and vascular endothelial growth factors as well as transcription factors such as AP-1 and NF-κB. Recently Palermo and co-workers demonstrated via affinity chromatography that EGCG manifests its antagonistic activity against AhR through Hsp90 binding.[119] Affinity purification of Hsp90 fragments from immobilized EGCG revealed that EGCG binds to the Hsp90 *C*-terminus. This interaction was reported to occur specifically with amino acids 538–728, suggesting that binding takes place at the *C*-terminal ATP-binding site. Unlike previously identified *N*-terminal Hsp90 inhibitors, EGCG does not appear to prevent Hsp90 from forming heteroprotein complexes. Studies are currently underway to determine whether EGCG competes with novobiocin or cisplatin binding.[14,119]

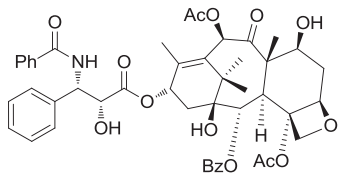

Figure 14. Structure of taxol.[14]

D. Taxol

Taxol (Figure 14), a well-known drug for the treatment of cancer, is responsible for the stabilization of microtubules and blockage of mitosis.[120] Previous studies have shown that Taxol induces transcription factors and kinase activation, mimicking the effect of bacterial lipopolysaccharide (LPS), an attribute unrelated to its tubulin-binding properties.[121] A significant amount of evidence suggests that the LPS-mimetic activity of Taxol is independent of β-tubulin binding. Thus, Rosen and co-workers prepared a biotinylated Taxol derivative and performed affinity chromatography experiments with lysates from both mouse brain and macrophage cell lines. These studies led to affinity purification of two chaperones, Hsp70 and Hsp90, by mass spectrometry from the mouse brain. In contrast to typical Hsp90-binding drugs, Taxol exhibits a stimulatory response, mediating the activation of macrophages and exerting the LPS-mimetic effects observed.[14,122]

Recently it was reported that the geldanamycin derivative **17-AAG** (Figure 15) behaves synergistically with Taxol-induced apoptosis. The mechanism by which these two interact is best explained as sensitization of tumor cells to Taxol-induced apoptosis by **17-AAG** through suppression of Akt kinase.[123] The use of Hsp90 inhibitors in combination with proapoptotic therapies represents an exciting new strategy for chemotherapy.[14]

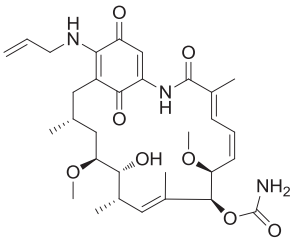

Figure 15. Structure of **17-AAG**.[14]

VI. Implications for Hsp90 Inhibitors

Key roles of Hsp90 involve the folding of client proteins and refolding of aggregated or misfolded proteins. These functions of Hsp90 make it an attractive target for the development of potential therapeutics. By taking advantage of these roles, Hsp90 can be transformed from a mechanism for protein folding to a means of therapy delivery. Moreover, the divergence of these functions makes Hsp90 amenable to the treatment of a broad range of disease states (Figure 16). Also included in Figure 16 is a summary of the structural modifications to novobiocin that have been shown to convert it between a cytotoxic and non-toxic agent.[14]

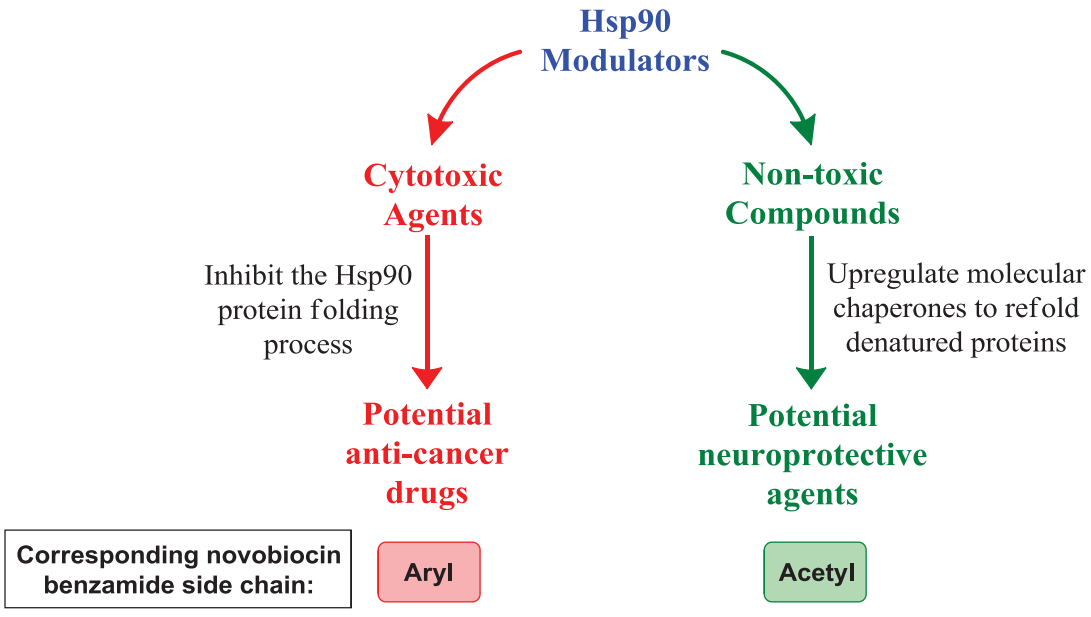

Figure 16. Bidirectional approach to Hsp90 modulation.[14]

A. Cancer

Many proteins responsible for malignant progression within tumor cells are Hsp90-dependent and more than 40 oncogenic substrates have been identified to date.[124] Therefore, targeting Hsp90 can simultaneously disrupt all six hallmarks of cancer (Figure 18) and offer a unified mechanism for chemotherapy.[11] Moreover, Hsp90 is overexpressed in malignant cells, and its expression correlates directly with the proliferation of these cells.[41,125-127] Hsp90 inhibitors represent a unique class of compounds that demonstrate high differential selectivity for malignant versus normal cells[10] at concentrations that are well tolerated by humans.[128,129] There are currently more than 20 Hsp90-targeted clinical trials in progress and many more inhibitors are in preclinical development.[14]

The mechanism by which Hsp90 inhibitors exert their anti-cancer effect is by competitively binding in the nucleotide binding site. Upon inhibitor binding, the heteroprotein complex becomes unable to fold or stabilize client proteins. This unproductive complex becomes ubiquitinylated and marked for degradation by the ubiquitin-proteasome pathway. Figure 17 demonstrates at which step this disruption of the protein folding process occurs.[14]

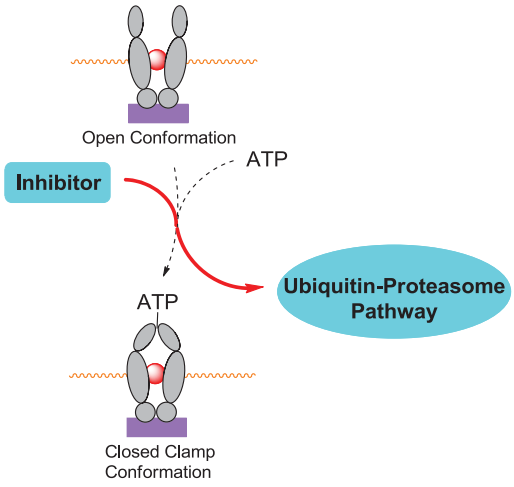

Figure 17. Hsp90 inhibition by anti-cancer agents.[14]

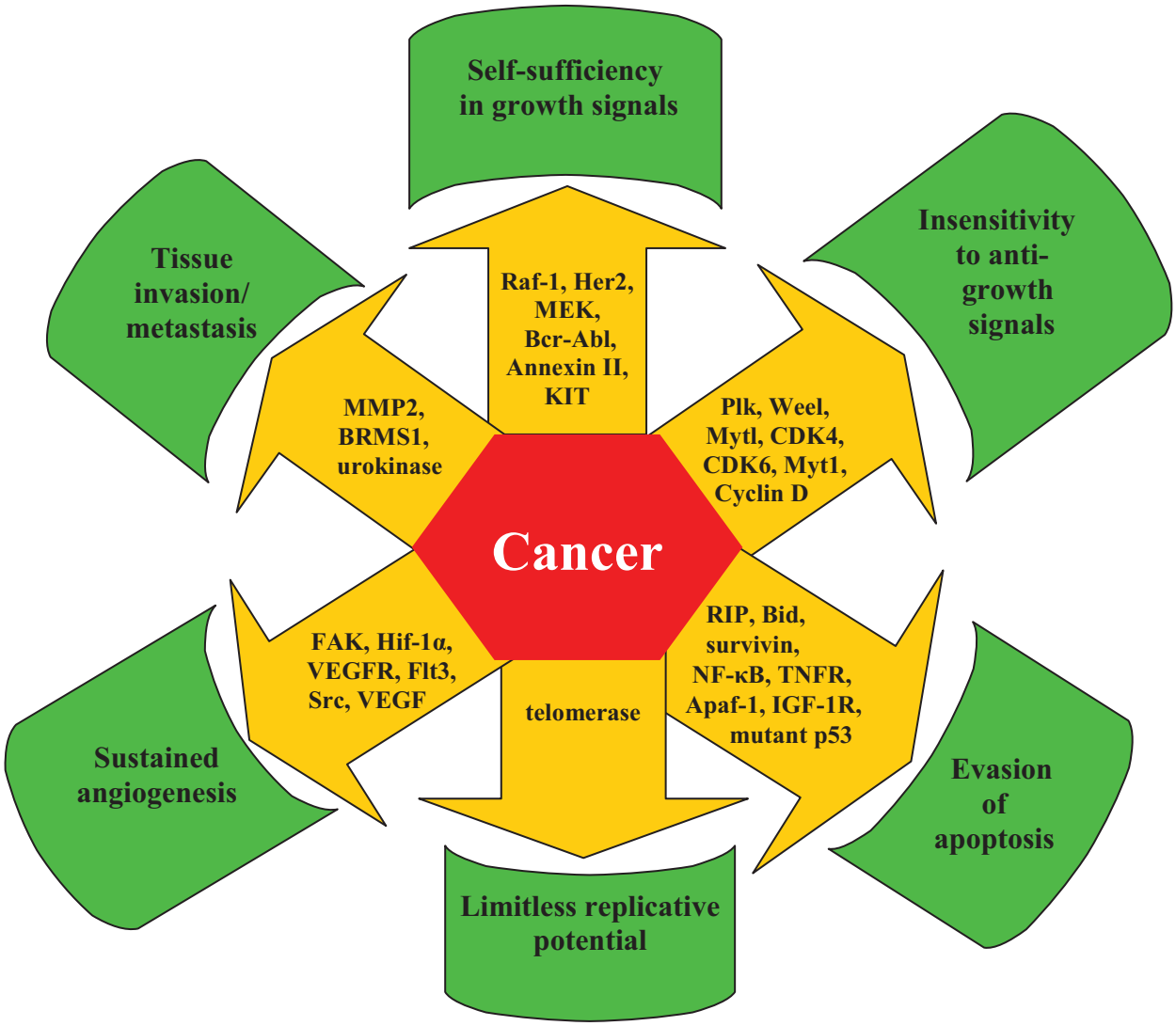

Figure 18. Hallmarks of cancer and corresponding Hsp90 client proteins.[14,16,130-133]

Figure 18 lists the six hallmarks of cancer as defined by Weinberg as well as associated client proteins for each.[11] A cell is defined as cancerous only if all six of these hallmarks are present. The manifestation of each is mediated through a number of proteins, many of which are Hsp90-dependent. The proteins associated with the first two hallmarks are those which facilitate and/or inhibit mitogenic signaling. Those listed with the third hallmark inhibit programmed cell death by preventing normal apoptotic pathways from killing the transformed cell. Telomerase enables DNA replication without harming valuable genetic material and thus provides

immortality.[134] Hallmark five is related to the recruitment of vasculature, a process which is directly regulated by several Hsp90 clients. Finally, several Hsp90-dependent clients enable metastasis, leading to the spread of cancer from the initial tumor site to other parts of the body.[14]

While many of these proteins are associated with only one hallmark of cancer, other Hsp90-dependent proteins fall into many. The Hsp90 client HDAC6 is involved with the control of gene expression through deacetylation of histones, many of which are Hsp90 clients as well. Deacetylation of histones causes DNA to become too tightly wound, inhibiting gene expression. Therefore, inhibition of this deacetylation may lead to the increased expression of genes responsible for tumor suppression. Moreover, HDAC6 inhibition can inhibit cancer cell proliferation, induce apoptosis and block tumor angiogenesis.[135] Similarly, the SMYD family of proteins also contains several Hsp90-dependent clients which are directly related to modification of histones. SMYD1, SMYD2 and SMYD3 are histone methyltransferases which act much like HDACs in their ability to alter gene expression.[136,137] Inhibition of these Hsp90-dependent proteins will lead to the same anti-cancer effects as associated with histone deacetylase inhibition.[14]

Akt is another Hsp90-dependent protein which is associated with several hallmarks of cancer. Akt (protein kinase B) is a serine/threonine kinase involved in signal transduction pathways that has implications in self-sufficiency of growth signals, evasion of apoptosis and sustained angiogenesis. Inhibition of apoptosis by Akt is accomplished through inhibition of a number of proapoptotic proteins, such as kinase ASK1,[138] glycogen synthase kinase 3, BAD, caspase 9 and Forkhead transcription factors.[139-142] Moreover, through interaction with phosphatidylinositol-3 kinase (PI3K), Akt signaling regulates many angiogenic growth factors involved with recruitment of vasculature.[143] The PI3K-Akt interaction is responsible for an

important cell survival signal pathway that is targeted by many anti-cancer drugs.[144] The ability of Hsp90 inhibitors to disrupt the many associations of Akt with oncogenic pathways has generated much interest in studying the interaction between Akt and Hsp90.[14]

The receptor tyrosine kinase c-Met is another example of an Hsp90-client that is involved with several of the hallmarks defined by Weinberg. This kinase plays important roles in cell growth, apoptosis, angiogenesis and apoptosis[145] and thus can be categorized as fitting into several hallmarks. Met is overexpressed and mutated in a variety of cancers, and its function and stability depend on Hsp90. Hsp90 inhibitors, such as geldanamycin, have been shown to block c-Met oncogenic signaling.[146-148] Clinical trials are under way to study the effects of such inhibitors in a variety of cancers that demonstrate an overactive c-Met pathway.[14,149]

Although the anti-cancer drug effects of many Hsp90 inhibitors have been previously ascribed to the specific inhibition of growth-related (tyrosine) protein kinases, a more complicated mechanism has been recently suggested. MAP kinases, which play an important role in cellular signaling, have been known to be activated by various stresses and growth stimuli.[150-157] The recently identified and cloned member of the MAP kinase superfamily, MOK, was found to be Hsp90-dependent for its intracellular stability and solubility. The Hsp90/Cdc37 complex that binds MOK specifically binds closely related protein kinases MAK and MRK, but not conventional MAP kinases, such as ERK, p38 and JNK.[158] With the knowledge that Hsp90 inhibition leads to degradation of certain other kinases, such as MOK, it was concluded that molecular chaperones play an essential role in the stability of signal transuding protein kinases. This role may be directly related to the anti-cancer effects observed upon introduction of Hsp90 inhibitors.[14]

The more than 40 client proteins associated with oncogenesis include proteins from the classes of transcription factors, kinases, and other proteins..[21,47,125-127] Many of these proteins are individually sought after anti-cancer targets for which therapies have been developed. While many of these proteins can be associated with a specific hallmark of cancer as defined by Weinberg, other examples exist that regulate factors upstream to cancer development. Oncogenic proteins like Mdm2 and SV40 large T-antigen are associated with tumor suppressor genes. These Hsp90-dependent proteins play essential roles in regulating p53, a tumor suppressor which is commonly mutated in many cancers. Ral-binding protein 1 is another example of an oncogenic Hsp90-dependent protein. This protein interacts with RalA and RalB, both or which are associated with Ras and many signaling pathways directly related to the malignant phenotype. Hsp90 inhibitors, therefore, offer the opportunity to treat cancer through disrupting many targets at different stages as it advances, further increasing their utility to treat a variety of cancers. The possibility to disrupt many targets is also what gives Hsp90 inhibition its seemingly divergent role in the treatment of neurodegenerative diseases.[14]

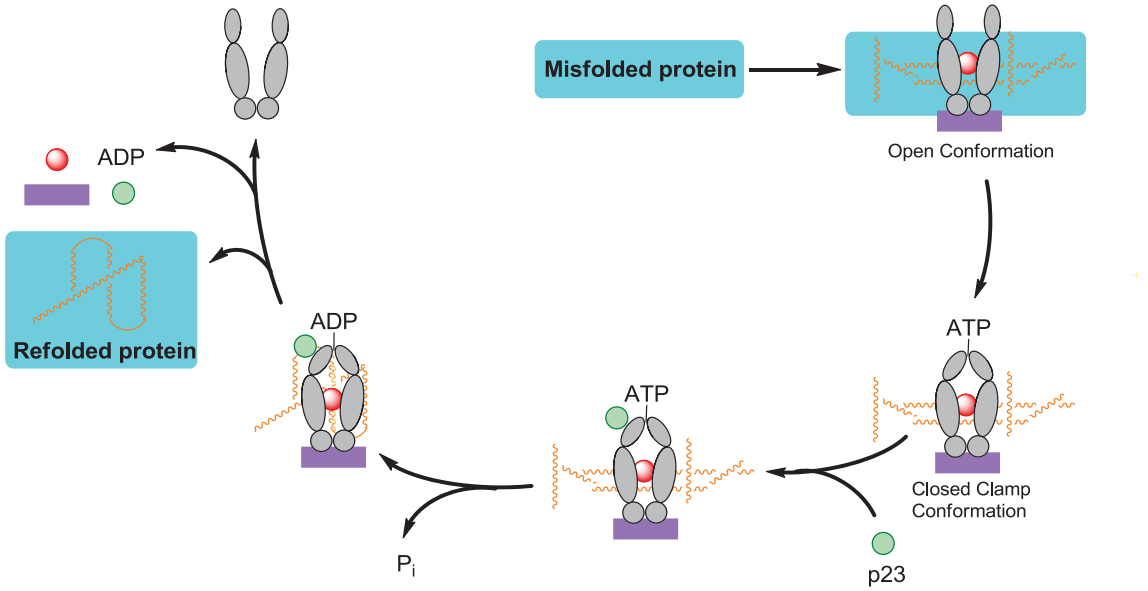

Figure 19. Hsp90 inhibition by neuroprotective agents.[14]

B. Neurodegenerative diseases

The accumulation of misfolded proteins that result in plaque formation causes neurodegenerative diseases including Alzheimer's, Parkinson's, Huntington's, and prion disease.[13] Hsp90 is a major molecular chaperone responsible for the rematuration, disaggregation, and resolubilization of these misfolded proteins and their aggregates. Hsp90 inhibitors can lead to Hsp induction, refolding of aggregated proteins and provide neuroprotective activities via this mechanism.[159] Figure 19 summarizes this role of Hsp90 as it fits into the generally accepted protein folding scheme.[14]

There are several Hsp90-dependent proteins with roles within the central nervous system related to disease states. Tau proteins are associated with microtubules and are abundant in neurons within the central nervous system. These proteins promote tubulin assembly into microtubules and the different Tau isoforms stabilize these microtubules, often after phosphorylation by a series of kinases. Hyperphosphorylation of the Tau protein results in the self-assembly of filament tangles, which are involved in the pathogenesis of Alzheimer's disease.[160] This aggregation of Tau protein into neurofibrillary tangles has also been associated with diseases such as progressive supranuclear palsy, corticobasal degeneration, and Pick's disease.[14,161]

Soluble protein levels correlate well with high levels of Hsp90. In contrast, high levels of granular Tau oligomers (Tau filaments and intermediates) have been observed when Hsp levels are low. Although it has been suggested that Hsp90 functions to regulate levels of soluble Tau levels, the chaperone system can become saturated.[162] Chiosis and co-workers studied Tau hyperphosphorylation as the direct result of the aberrant activation of several kinases, such as cyclin-dependent protein kinase 5 (cdk5) and glycogen synthase kinase-3β. The group

specifically studied the cdk5/p35 kinase complex, demonstrating in mice that cdk5 inhibitors reduce Tau hyperphosphorylation and apoptosis in neurons.[163,164] In addition to abnormal phosphorylation of Tau by kinases, the accumulation of aggregated Tau in several tauopathies has been linked to mutations in human Tau isoforms on chromosome 17.[164-166] Chiosis and co-workers demonstrated that the expression of the most common mutation, TauP301L, can be suppressed to inhibit neuronal loss and led to function improvement in mice. Both cdk5/p35 and TauP301L were cited as clients that require Hsp90 assistance for their stability and proper function.[14,167]

Another Hsp90-dependent client associated with neurological disease is alpha-synuclein. This protein is found predominantly at presynaptic terminals in neural tissue, but its primary function remains unknown. Although it is usually a soluble protein, alpha-synuclein can aggregate to form insoluble fibrils in diseases characterized by Lewy bodies, such as Parkinson's disease, dementia with Lewy bodies and multiple system atrophy.[168] An alpha-synuclein fragment, the non-Abeta component (NAC), is also found in the amyloid plaques associated with Alzheimer's disease.[14,169]

Hsp90 offers a new range of therapies for treating neurodegenerative diseases. Whether through the induction of Hsp90 to allow refolding of denatured or aggregated proteins or through directly inhibiting clients related to neurodegeneration, Hsp90 offers a unique target for therapy. Hsp90 modulators have already demonstrated efficacy in the treatment of neurodegenerative diseases and represent an exciting avenue for the development of clinical drugs to slow the progression of and cure these debilitating diseases.[14]

VII. Conclusion and Future Directions in the Field of *C*-terminal Inhibition

Mechanistic implications for targeting the Hsp90 protein folding machinery continue to evolve at a high rate. Newly identified client proteins and co-chaperones have led to additional biological targets that can be modulated by small molecules that bind Hsp90. Crystal and co-crystal structures of nearly the entire Hsp90 scaffold have provided significant advancements in the field. These structures allow for a more precise understanding of the protein and provide a scaffold upon which rationally-designed inhibitors can be developed. Biochemical and spectroscopic techniques, molecular modeling and inhibitor design have indirectly revealed much about the *C*-terminus, but much remains speculative without confirmation through co-crystal structures. The mechanism of action for *C*-terminal inhibitors will finally be clarified through further understanding of the *C*-terminal structure and its nucleotide binding site. Thus, although considerable advancements have been made, continued efforts that focus on the Hsp90 *C*-terminus are required to fully understand the Hsp90 protein folding machine and its potential role against various diseases.[14]

Chapter II

Studies on the Novobiocin Coumarin Core

I. Introduction

Research groups have attempted to develop analogues of novobiocin that improve its comparatively poor Hsp90 inhibitory activity.[84] A library of novobiocin analogues disclosed in 2005 demonstrated that **A4** (Figure 20) induced degradation of Hsp90-dependent client proteins at ~70-fold lower concentration than novobiocin.[15] Notably, this study highlighted that attachment of the noviose moiety to the 7-position and an amide linker at the 3-position of the coumarin ring are critical for anti-Hsp90 activity.[15] To confirm the observed SAR trends elucidated from this library, two natural product analogues were prepared and evaluated, **DHN1** and **DHN2** (Figure 20). Upon evaluation of these molecules in several assays, it was confirmed that the 4-hydroxyl and the 3'-carbamate are detrimental to Hsp90 inhibitory activity, but critical for DNA gyrase inhibition.[18]

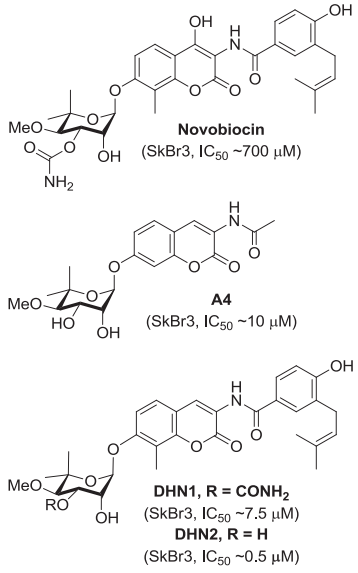

Figure 20. Structures of **A4**, **DHN1**, and **DHN2** versus novobiocin. [15,18]

While several publications have focused on the goal of enhancing the understanding of the benzamide side chain, these initial reports involving **A4**, **DHN1** and **DHN2** represent the only reports to examine specifically the coumarin core.[102,103] The goal of expanding our knowledge and the development of SAR for the novobiocin coumarin core, a rational approach toward coumarin analogues was proposed. It was anticipated that manipulation of the coumarin nucleus could result in enhanced potency and efficacy, leading to the development of novel novobiocin analogues with greater promise.

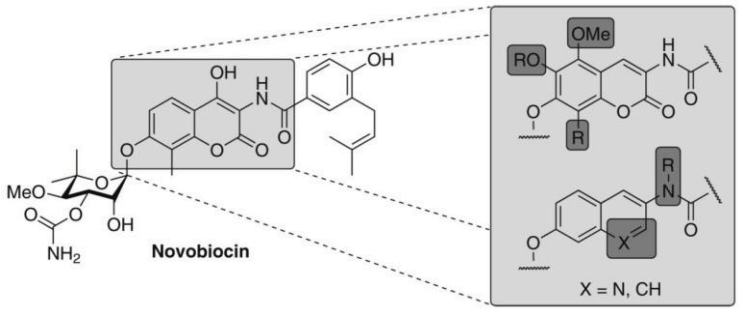

Figure 21. Summary of coumarin-replacement strategy.[170]

II. Initial efforts to explore the novobiocin coumarin core

Although the Hsp90 *C*-terminus does not exhibit ATPase activity, it does play a critical role in conformational rearrangement upon ATP binding.[79] To further explore SAR, derivatives of **A4** with variations to the coumarin scaffold were designed to probe the importance of interactions typically manifested by the purine ring (Figure 21). A purine ring was chosen as the model system since the *C*-terminal site is known to bind nucleotides, with a partiality for GTP and UTP.[37] The coumarin-derived motifs possess hydrogen bonding capabilities similar to the nucleotide bases adenine and guanine, and contain strategically placed hydrogen bond acceptors and donors and alkyl groups of variable size to probe the size and nature of the complementary

binding pocket. The design, synthesis and evaluation of such compounds are described in the next section.

A. Design of novobiocin analogues with modified coumarin cores

To elucidate structure-activity relationships for the coumarin ring system of novobiocin, we envisioned construction of novobiocin analogues with modified coumarin cores. As shown in Scheme 1, the derivatives were assembled in a modular fashion allowing sequential coupling of noviose and a series of benzoic acids with the modified coumarin cores.[170] We previously demonstrated that the trichloroacetimidate of noviose carbonate couples readily to coumarin phenols in good yield, to afford the corresponding α-anomer.[171] The benzoic acids selected were based upon previously obtained SAR for the amide side chain as described by Burlison and co-workers.[102]

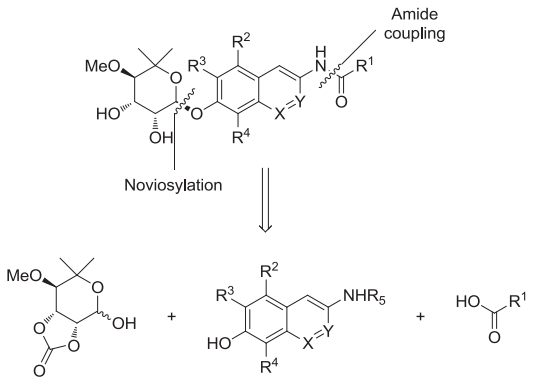

Scheme 1. Retrosynthesis of novobiocin analogues.[170]

The coumarin scaffolds were designed to complement interactions present on the purine nucleus, via probing the importance of hydrogen bond donor and acceptors in positions surrounding the aromatic ring system. Rationale for these analogues is based on the identification of additional interactions with the nucleotide-binding domain that typically binds the

corresponding purine substrate and may lead to enhanced inhibitory affinity for these compounds.[170] Minor perturbations were made on each analogue; however, the addition of one hydrogen bond can produce 1-2 kcal/mol of binding energy and thus increase binding by 10-fold.[172] Therefore, these complementary interactions can exhibit a substantial impact on binding and subsequent inhibition. While it has been demonstrated that the *N*-terminal site is fairly specific for adenine nucleotides, the *C*-terminal site has been shown to be more promiscuous, and binds both purines and pyrimidines. Unlike the *N*-terminus, which specifically binds adenine, GTP and UTP are specific *C*-terminal substrates.[37] Based on these previous studies, mimics of the guanosine nucleus were chosen to take advantage of this differential. Hydrogen-bond acceptors were placed at the 5-, 6- and 8-positions of the coumarin ring to mimic those at the 6-, 7- and 3-positions of guanine, respectively (Figure 22). Additionally, analogues bearing modification to the coumarin lactone were constructed to probe the importance of hydrogen bond donors/acceptors as well as to potentially improve upon the solubility of the novobiocin scaffold. The activity of such compounds is likely to provide insight into the interactions that are essential or those that can be further optimized.[170]

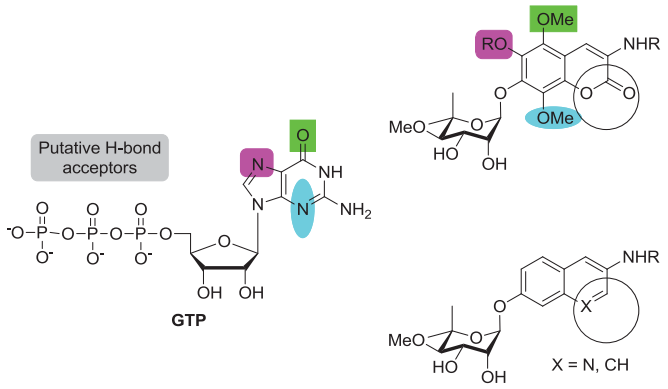

Figure 22. Complementarity of GTP and coumarin analogues.[170]

There is limited knowledge regarding the shape and dimension of the pocket since discovery of the *C*-terminal binding site is a recent achievement, and no Hsp90 co-crystal

structure bound to *C*-terminal inhibitors exists. Therefore, several analogues were designed to probe the pocket at positions that potentially project into unoccupied regions. Alkyl and aryl groups of variable size were attached at the 5-, 6- and 8-positions of the coumarin ring to maximize putative hydrophobic interactions and to optimize affinity. A methoxy group was attached at the 5-position of the coumarin ring, while methoxy, propoxy, and isopropoxy ethers were installed at the 6-position. Methyl, methoxy, benzyl and phenyl substituents were placed at the 8-position, offering a variety of possible interactions with residues within this region of the pocket. The culmination of structure–activity relationships elucidated by such compounds is likely to provide a platform upon which improved analogues can be sought.[170]

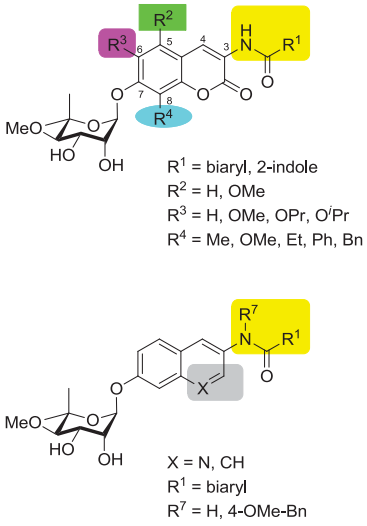

Figure 23. Proposed coumarin, quinoline and naphthalene analogues.

As seen in Figure 23, great diversity was incorporated into the various analogues designed as part of this study. While R^1 groups were selected based upon their demonstrated cytotoxic efficacy in the aforementioned benzamide study, rationale for substituents installed at the other positions varies.[102] A methoxy group was placed at the 5-position of the coumarin ring, corresponding to the 6-position carbonyl of the guanine ring, to probe if there is a potential hydrogen bonding network in this portion of the binding pocket. Choices for R^3 were focused on

investigating the space into which the 6-position of the coumarin and 7-position of guanine extend. Firstly, ethers were chosen because of their incorporation of an electronegative oxygen, which can accept hydrogen bonds like the nitrogen found at the corresponding position of the purine ring. Moreover, groups of increasing bulk were incorporated to explore the space and potentially capitalize on interactions with hydrophobic residues.

Next, R^4, which corresponds to the 8-position of the coumarin ring and 3-position of guanine, was outfitted with a number of substituents with variable goals. While a methyl group is consistent with the substituent found at this position in novobiocin, a methoxy group more closely mimics the hydrogen bonding capability of the nitrogen found at the corresponding position of the guanine ring. In contrast, bulky ethyl, phenyl and benzyl substituents were installed with the aim of capitalizing on additional interactions with hydrophobic residues to gain binding affinity. Within the naphthalene and quinoline systems, R^7 sought to explore the importance of hydrogen bonding to the amide nitrogen and whether another bulky substituent was well tolerated at this position. Position X was varied to probe the importance of the coumarin lactone in binding. While it is envisioned that the quinoline would exclude one potential hydrogen bond, the naphthalene core would offer a comparison that lacked the ability to hydrogen bond at this position.

1. Syntheses of 5-, 6-, and 8-alkyl(oxy) novobiocin analogues

To prepare the resorcinol precursors with substitutions at the 4-position, which result in coumarin ring systems with appendages at the 6-position, the phenols of benzaldehyde **1** were protected as the corresponding ethers (Scheme 2). The resulting benzaldehydes (**2a**–**b**)[173] were converted to their formate esters via Dakin oxidation, and then hydrolyzed to afford phenols **3a**–

b.[174,175] *O*-Alkylation with the requisite alkyl iodide proceeded in good yield and generated a series of protected 4-substituted resorcinolic ethers (**4a**–**c**). *Ortho*-lithiation of **4a**–**c**, followed by alkylation with methyl iodide provided the 2-methyl protected resorcinols, **5a**–**c**.[176] Deprotection[177] of the alkoxy ethers by exposure to acidic conditions gave resorcinols **6a**–**c**.[170]

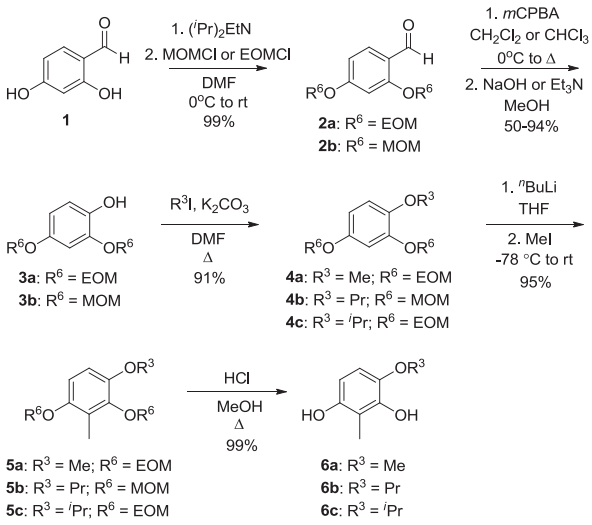

Scheme 2. Syntheses of 4-substituted resorcinols. OEOM = OCH_2OEt.[170]

To generate resorcinol precursors with substitutions at the 5-position, the phenols of 5-methoxy resorcinol **7** were once again protected as the corresponding alkoxy ethers, **8** (Scheme 3). *Ortho*-lithiation of **8**, followed by treatment with methyl iodide, led to installation of a methyl group at the 2-position of **9**.[176] Acidic deprotection[177] was employed to afford resorcinol **10**.[170]

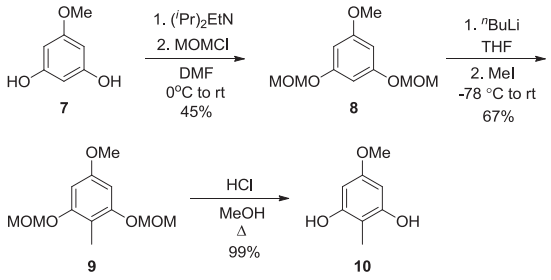

Scheme 3. Synthesis of 5-substituted resorcinol.[170]

To synthesize the resorcinol precursors with aryl substituents at the 2-position, the phenols of resorcinol **11** were protected as the corresponding alkoxy ethers, **12** (Scheme 4).

Subsequent *ortho*-lithiation of **12**, followed by the addition of benzyl bromide provided the benzyl derivative, **13**.[176] Removal of the ether protecting groups[177] gave diphenol **14**.[176] The anion of resorcinol **12** was also employed to construct the corresponding 2-iodide via reaction with iodine to yield **15**.[178] A Suzuki coupling in the presence of biaryl ligand S-Phos,[179] was used to generate biaryl **16**, which underwent deprotection[177] to provide **17**.[170]

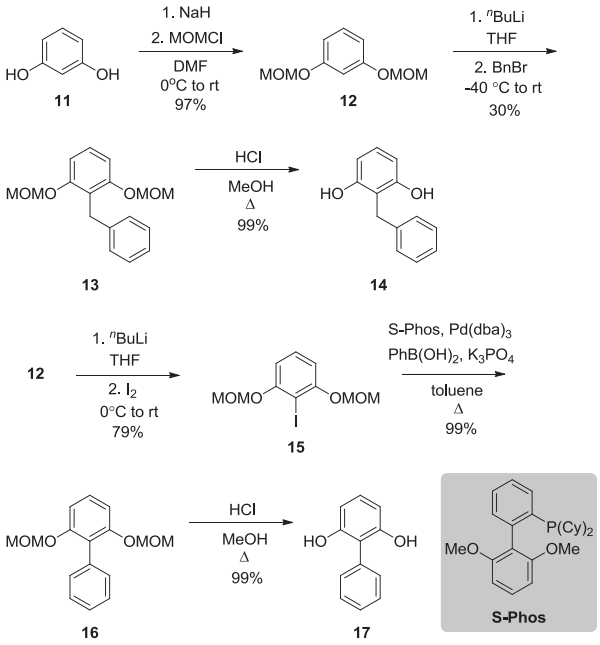

Scheme 4. Syntheses of 2-substituted resorcinols.[170]

To generate resorcinol precursors with alkyl substitutions at the 2-position, pyragallol (**18**) was *O*-alkylated with methyl iodide to generate 2-methoxy resorcinol amongst an inseparable mixture of regioisomers (Scheme 5). The mixture was subsequently subjected to coumarin formation and the corresponding products isolated.[170] Preparation of 2-ethyl resorcinol (**21**) from 2,6-dihydroxyacetophenone (**20**) was accomplished according to published procedures.[180]

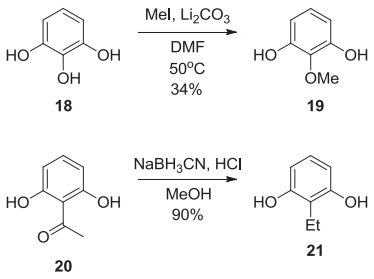

Scheme 5. Synthesis of 2-methoxy resorcinol and 2-ethyl resorcinol.[170,180]

Once resorcinols **6a**–**c, 10**, **14**, **17**, **19**, and **21** were obtained, the corresponding coumarins **23a**–**h** were synthesized through a modified Pechmann condensation with eneamine **22** as previously described.[181,182] The resulting coumarin phenols were noviosylated with the trichloroacetimidate of noviose cyclic carbonate (**24**) in the presence of catalytic boron trifluoride etherate to generate scaffolds **25a**–**h** in good yield.[171] The benzyl carbamate was removed via hydrogenolysis to produce the aminocoumarin, which was readily coupled with preselected benzoic acids in the presence of *N*-(3-dimethylamino-propyl)-*N*'-ethylcarbodiimide hydrochloride (EDCI) and pyridine. Benzoic acids were chosen based on previously determined SAR trends reported by Burlison and co-workers.[102] The cyclic carbonates were treated with triethylamine in methanol to give the solvolyzed products, **26a**–**p** in moderate to good yield over three steps (Scheme 6). The ethyl coumarin and corresponding derivatives were synthesized by a co-worker as part of this study.[170]

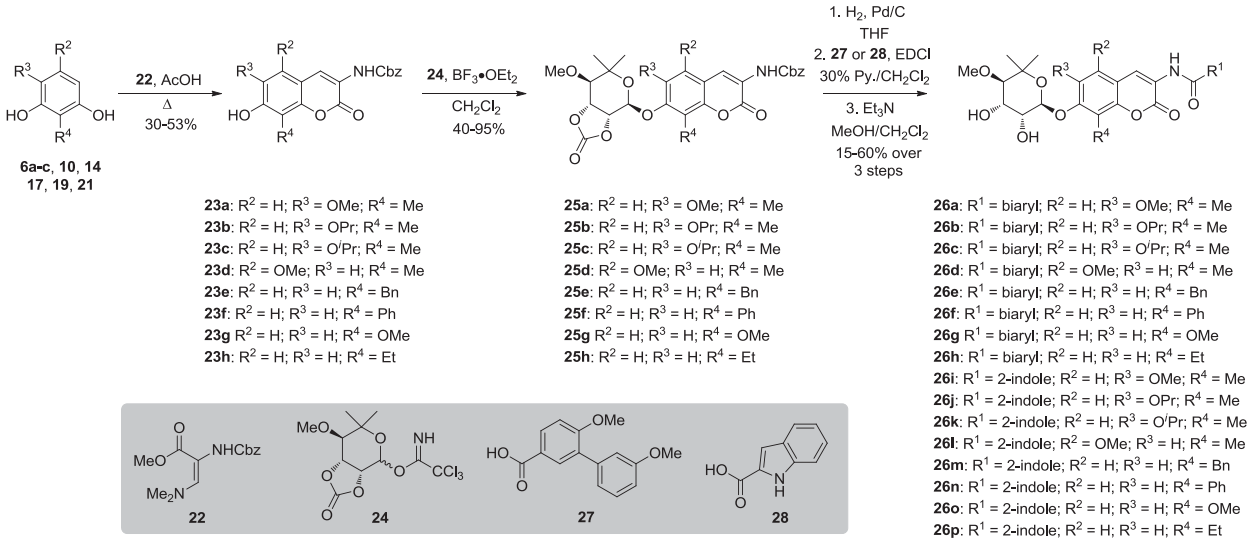

Scheme 6. Preparation of 5-, 6-, and 8-modified novobiocin analogues.[170]

2. Syntheses of quinoline- and naphthalene-containing novobiocin analogues

Novobiocin analogues containing a quinoline or naphthalene ring in lieu of the 8-methylcoumarin of novobiocin were synthesized to probe the importance of the coumarin lactone moiety in binding the Hsp90 *C*-terminus, as well as to potentially circumvent the limited solubility of coumarin-containing analogues. Preparation of the quinolone and naphthalene cores, followed by appendage of the biaryl side chain and noviose was accomplished by a co-worker as part of this study.[170]

3. Biological evaluation of novobiocin analogues with modified coumarins

Upon construction of the library of novobiocin analogues, the compounds were evaluated for anti-proliferative activity against SKBr3 (estrogen receptor negative, Her2 over-expressing breast cancer cells), MCF-7 (estrogen receptor positive breast cancer cells), LNCaP (androgen receptor sensitive prostate cancer cells) and PC-3 (androgen receptor insensitive prostate cancer

cells) cell lines. As shown in Table 1, the 6-substituted analogues containing the biaryl side chain (**26a**–**26c**) were 3- to 7-fold less active against the two breast cancer cells than analogues containing hydrogen at this position.[38] These analogues were more active against prostate cancer cells than breast cancer cells versus the corresponding 6-H derivative. For reasons that remain unclear, the putative binding pocket for biaryl-containing analogues does not appear to tolerate incorporation of steric bulk at the 6-position. Analogues containing the 2-indole side chain (**26i**–**26k**) were consistently more active than their corresponding biaryl derivatives, in-line with previously-observed trends.[38] Analogue **26j**, containing a 6-propoxy-coumarin, was consistently the most potent derivative in this library exhibiting 2-fold enhanced potency relative to its 6-H analogue against LNCaP cells.[170]

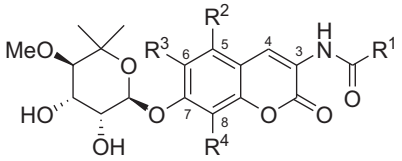

Table 1. Anti-proliferative activities of coumarin-derived novobiocin analogues.[170]

Compound	R^1	R^2	R^3	R^4	MCF-7 (IC_{50}, μM)	SKBr3 (IC_{50}, μM)	PC-3 (IC_{50}, μM)	LNCaP (IC_{50}, μM)
26a	biaryl	H	OMe	Me	> 100[a]	58.8 ± 1.3	35.4	6.6
26b	biaryl	H	OPr	Me	> 100	> 100	5.6 ± 5.7	3.0 ± 0.6
26c	biaryl	H	O^{i}Pr	Me	66.9 ± 3.1	58.6 ± 5.4	60.7 ± 9.1	14.4 ± 4.2
26d	biaryl	OMe	H	Me	82.8	55.7 ± 6.9	11.3 ± 2.0	2.0 ± 0.8
26e	biaryl	H	H	Bn	> 100	> 100	> 100	49.7 ± 25.0
26f	biaryl	H	H	Ph	> 100	17.3 ± 3.4	> 100	1.0 ± 0.1
26g	biaryl	H	H	OMe	9.0 ± 5.4	13.9 ± 1.2	2.3 ± 2.9	1.1 ± 0.1
26h	biaryl	H	H	Et	41.7 ± 14.0	28.6 ± 1.1	1.8 ± 0.6	1.6 ± 0.3
26i	2-indole	H	OMe	Me	24.4 ± 1.2	25.1 ± 7.7	20.2 ± 9.8	10.5 ± 0.3

26j	2-indole	H	OPr	Me	2.1 ± 0.1	2.1 ± 0.8	6.2 ± 1.8	1.8 ± 0.7
26k	2-indole	H	O^{i}Pr	Me	20.0 ± 1.0	20.7 ± 0.4	11.9	11.4
26l	2-indole	OMe	H	Me	6.1 ± 1.7	9.0 ± 0.8	11.8 ± 1.3	12.9 ± 4.4
26m	2-indole	H	H	Bn	13.2 ± 0.6	38.0 ± 3.0	73.3 ± 3.7	67.6 ± 6.3
26n	2-indole	H	H	Ph	22.9 ± 2.1	38.8 ± 8.3	28.0 ± 12.1	27.6 ± 10.8
26o	2-indole	H	H	OMe	> 100	9.7 ± 1.0	> 100	> 100
26p	2-indole	H	H	Et	4.3 ± 2.5	4.3 ± 3.4	> 100	> 100

[a] Values represent mean ± standard deviation for at least two separate experiments performed in triplicate.

By comparison, incorporation of a hydrogen-bond acceptor at the 5-position (**26d**, **26l**) resulted in equivalent or decreased activity versus corresponding 6-H analogues, especially against both breast cancer cell lines.[38] In general, 5-methoxy functionalized coumarins do not appear beneficial for anti-proliferative activity.[170]

It was previously demonstrated that 8-methyl analogues were ~10-fold more active than the corresponding 8-hydrogen derivatives.[38] To further elaborate upon this trend, a larger selection of 8-fuctionalized coumarins were evaluated. Incorporation of an 8-methoxy (**26g**) led to 2-fold improved activity over its 8-methyl counterpart, and 5-fold increased activity over the similarly-sized 8-ethyl derivative **26h**. Introduction of steric bulk (**26e**, **26f**) generally decreased anti-proliferative activity, especially against MCF-7 cells. It appears that while short alkoxy side chains take advantage of putative interactions, steric bulk appears detrimental to inhibitory activity at this location. A similar trend was observed against prostate cancer cells, with **26g** and **26h** exhibiting 10-fold increased activity versus their 8-methyl counterparts.[38] Surprisingly, 8-benzyl **26e** was more than twice as active as the 8-methyl derivative against LNCaP cells. In contrast, 8-position analogues containing the 2-indole side chain (**26m**–**26p**) did not exhibit

similar, consistent trends against prostate and breast cancer cells. Against breast cancer cells, compounds **26m**, **26n**, and **26p** exhibited significantly reduced activity versus the 8-methyl derivative. The 8-methoxy **26o** was inactive against MCF-7 cells, while both **26o** and **26p** were inactive against both PC-3 and LNCaP cells. The selectivity of **26o** and **26p** for breast cancer cells versus prostate cancer cells is intriguing and requires further investigation.[170]

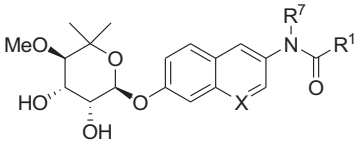

Table 2. Anti-proliferative activities of quinoline and naphthalene novobiocin analogues.[170]

Compound	R^1	R^7	X	MCF-7 (IC_{50}, μM)	SKBr3 (IC_{50}, μM)	PC-3 (IC_{50}, μM)	LNCaP (IC_{50}, μM)
29a	biaryl	4-OMe-Bn	N	> 100[a]	> 100	> 100	> 100
29b	biaryl	H	N	13.1 ± 4.1	16.5 ± 6.2	17.6 ± 4.6	14.2 ± 0.4
29c	biaryl	4-OMe-Bn	CH	> 100	> 100	> 100	> 100
29d	biaryl	H	CH	46.4 ± 5.3	38.9 ± 2.4	10.9 ± 0.7	19.6 ± 1.6

[a] Values represent mean ± standard deviation for at least two separate experiments performed in triplicate.

As shown in Table 2, compounds **29a** and **29c** containing the *p*-MeOBn-alkylated amides did not exhibit anti-proliferative activity against the cell lines tested. This is in contrast to analogues **29b** and **29d** lacking the *p*-MeOBn functionality, which manifested modest antiproliferative activity. This stark difference suggests one of two scenarios regarding the role of the *p*-MeOBn functionality; either the *p*-MeOBn group of tertiary amides **29a** and **29c** is unable to occupy the same pocket as the 4-aryloxy substituted novobiocin analogues[60,61] or more simply, the secondary amide is required for benzamide-containing novobiocin analogues to manifest anti-proliferative activity, an observation consistent with prior structure–activity

trends.[38] It is plausible that the steric congestion of amides **29a** and **29c** forces adoption of a more static conformation that disallows *cis*/*trans* isomerization of the amide, a feature that has been hypothesized to be essential for anti-proliferative activity of novobiocin analogues against bacteria. Further evidence was gathered upon realization that the lack of reactivity for tertiary amides **29a** and **29c** to all but the harshest conditions for *p*-MeOBn removal[58,62,63] suggest these compounds may adopt a highly-organized and stable conformation.[170]

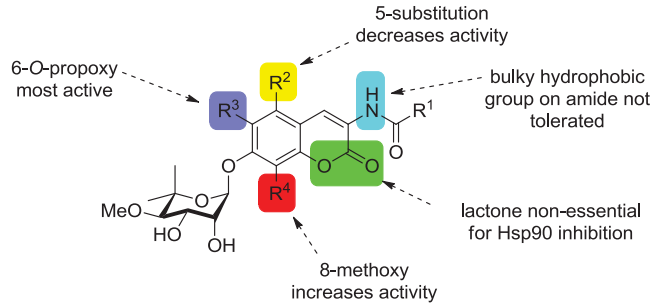

Figure 24. SAR observed for the novobiocin coumarin scaffold.[170]

Against breast cancer cells, analogue **29b** exhibited similar anti-proliferative activities as the corresponding 8-methylcoumarin analogue, while **29d** was between 2- and 5-fold less active.[38] In contrast, both **29b** and **29d** were significantly more active against PC-3 cells than the corresponding 8-methylcoumarin; **29b** and **29d** exhibited between 7- to 9-fold reduced activity against LNCaP cells. Given that both **29b** and **29d** lack the 8-methyl feature that yields an increased activity of ~10-fold, it is reasonable to hypothesize that the quinoline- and naphthalene-derived analogues that include an 8-methyl substituent could exhibit anti-proliferative activities between 1-5 μM against breast cancer cells and 1-2 μM against prostate cancer cells, approximately an order of magnitude less than the novobiocin analogue containing a coumarin. These results suggest that, while the lactone moiety may provide beneficial hydrogen-bonding interactions with the novobiocin binding pocket, these interactions may not be required to manifest anti-proliferative activity. More importantly, these results implicate that

continued optimization of the coumarin scaffold connecting the sugar and benzamide motifs is likely to produce compounds with enhanced anti-proliferative activity. A summary of the observed trends for anti-proliferative activities of coumarin-derived novobiocin analogues is depicted in Figure 24.[170]

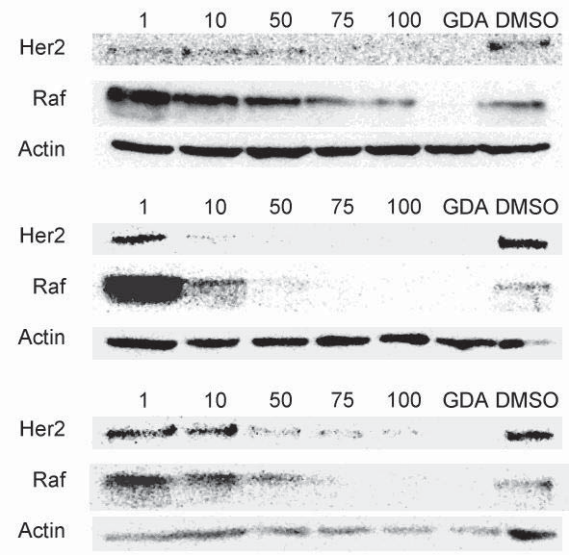

Figure 25. Western blot analyses of Hsp90 client protein degradation assays against MCF-7 cells following treatment with coumarin analogues. Concentrations (in μM) of **26g** (top), **26j** (middle), and **29d** (bottom) are indicated above each lane. GDA (geldanamycin, 500 nM) and DMSO were respectively.[170]

To provide additional support that the anti-proliferative activities exhibited by coumarin-derived novobiocin analogues results from Hsp90 inhibition, analogues **26g**, **26j**, and **29d** were evaluated for their abilities to induce degradation of Hsp90-dependent client proteins. As shown in Figure 25, the Hsp90 client proteins Her2 and Raf were degraded in MCF-7 cells in a concentration-dependent manner upon treatment with coumarin-derived novobiocin analogs. Moreover, Hsp90 client protein degradation correlates well with observed anti-proliferative

IC_{50}s; **26g** (IC_{50} = 9.0 μM) and **26j** (IC_{50} = 2.1 μM) induced client degradation at ~10 μM, while **29d**, with its more modest anti-proliferative activity (IC_{50} = 46.4 μM), induced client degradation at ~50 μM. Since actin, a non-Hsp90-dependent protein, is not affected by these analogues, anti-proliferative activities of these analogues correlate directly with Hsp90-client protein degradation.[170]

Compound **26g** and **26j** demonstrated the most potent anti-proliferative activity against the cancer cell lines tested and represent scaffolds that will be further probed to improve activity. Derivatives **26f** and **26o** appear to represent compounds that exhibit differential selectivity for one cancer cell lines versus another, for reasons that remain unclear. Since these compounds demonstrated low micromolar activity against one cell line and are inactive against others, they may provide a tool for further exploration and perhaps unraveling of the complicated processes affected. The activities of analogues **29b** and **29d**, the first documented novobiocin analogues lacking the coumarin functionality, implicate that, while the coumarin ring may participate in hydrogen bonding interactions with Hsp90 that abrogate activity, these interactions are not essential for anti-proliferation activity through inhibition of Hsp90. These analogues provide sufficient evidence to continue the search for optimal ring systems that bridge the benzamide and noviose functionalities.[170]

B. Neuroprotection studies using modified coumarins

As previously discussed, Hsp90 modulation has demonstrated efficacy in the treatment of neurodegenerative diseases. Notably, the *C*-terminal Hsp90 modulator **A4**, that contains a shortened *N*-acyl side chain, lacks of the 4-hydroxy substituent and the carbamoyl group on the noviose appendage, was found to induce Hsp90 at concentrations 1000–10000-fold lower than

that required for client protein degradation. This induction of the heat shock response was hypothesized to possess potential utility in the refolding of denatured proteins, such as the amyloid plaques associated with Alzheimer's disease (Figure 26). Due to this unique activity, **A4** was tested in a model for Alzheimer's disease, in which it was found to produce an EC_{50} at 6 nM and exhibit no toxicity at any concentration.[15] This study, in conjunction with studies involving the benzamide side chain, suggested that modification of the amide side chain results in conversion of a nontoxic molecule into an anti-proliferative agent and visa versa.[103] Consequently, the set of coumarin analogues described in Section I were outfitted with an acetamide side chain in an attempt to convert them into potential neuroprotective agents (Figure 16).[170]

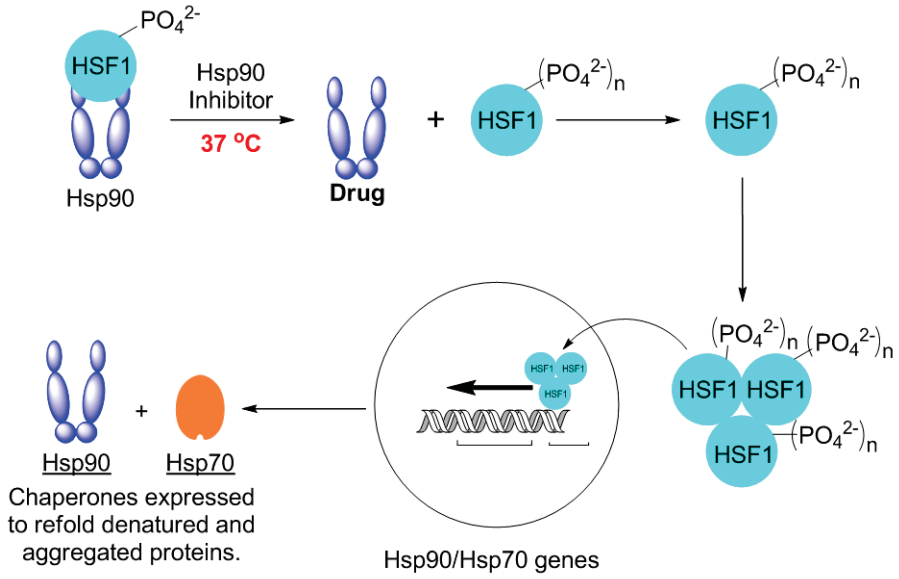

Figure 26. Induction of the heat shock response.

1. Syntheses of 5-, 6-, and 8-alkyl(oxy) acetamide-containing analogues

As previously shown, coumarins modified at the 5-, 6-, and 8-modified with protected noviose appended at the 7-position (**25a**–**g**) were obtained in good yield (Scheme 6).[170,171] The

benzyl carbamate was subsequently removed via hydrogenolysis to produce the corresponding aminocoumarin, which was readily coupled with acetic anhydride in the presence of pyridine (**Scheme 7**). The cyclic carbonates were exposed to triethylamine in methanol to give the solvolyzed products **30a**–**g** over three steps.

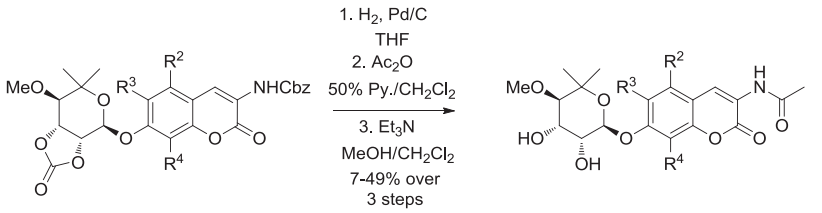

25a: R^2 = H; R^3 = OMe; R^4 = Me
25b: R^2 = H; R^3 = OPr; R^4 = Me
25c: R^2 = H; R^3 = O^{i}Pr; R^4 = Me
25d: R^2 = OMe; R^3 = H; R^4 = Me
25e: R^2 = H; R^3 = H; R^4 = Bn
25f: R^2 = H; R^3 = H; R^4 = Ph
25g: R^2 = H; R^3 = H; R^4 = OMe

30a: R^2 = H; R^3 = OMe; R^4 = Me (8%)
30b: R^2 = H; R^3 = OPr; R^4 = Me (7%)
30c: R^2 = H; R^3 = O^{i}Pr; R^4 = Me (19%)
30d: R^2 = OMe; R^3 = H; R^4 = Me (26%)
30e: R^2 = H; R^3 = H; R^4 = Bn (12%)
30f: R^2 = H; R^3 = H; R^4 = Ph (49%)
30g: R^2 = H; R^3 = H; R^4 = OMe (34%)

Scheme 7. Synthesis of 5-, 6-, and 8-modified acetamide-containing novobiocin analogues.

2. Biological evaluation of acetamide-containing novobiocin analogues

Upon preparation, analogues **30a**–**g** were submitted to a range of biological assays. An assay was developed in collaboration with Dr. Chaguturu in the KU high throughput screening (HTS) lab to evaluate these compounds for their potential neuroprotective activity. Based on an assay previously developed in collaboration between the Blagg and Michaelis labs at KU, the dose-dependent protection that these compounds offer against $A\beta_{25\text{-}35}$ toxicity in SH-SY5Y neuroblastoma cells was to be evaluated in a high throughput screen.[183] Unfortunately, the HTS laboratory was unable to perform this assay in an HTS format that was reproducible.

Recent studies have implicated that Hsp70 plays a key regulatory role in colonic tumorigenesis.[184] Therefore, induction of Hsp70, potentially through small molecules, is thought to exhibit the potential to reverse this oncogenic progression. Since analogues **30a**–**g** were designed to mimic **A4** in both structure and function, these compounds were perceived to be

inducers of Hsp70 levels. Due to their interest in the underlying mechanisms for growth control of normal intestinal tissue and explaining how disruption of this normal state leads to tumor formation, the Neufeld lab at KU demonstrated interest in compounds of this type. The Neufeld lab used Western blot analyses to examine the ability of these compounds, as well as a collection of structurally related analogues, to induce Hsp70 levels. Although this study is ongoing, several Hsp90 *C*-terminal modulators have been identified to induce Hsp70 at the same or greater levels than **A4**. These compounds represent promising tools in understanding the progression of colon cancer, with the potential to become therapeutic agents in the future.

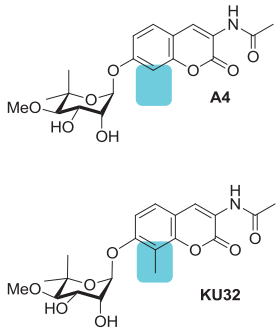

Figure 27. Structure of **KU32** versus **A4**.

Another recent publication, resulting from a collaborative effort between the Blagg and Dobrowsky laboratories, highlighted the role of Hsp70 in the inhibition of sensory neuron degeneration after axotomy. Since the onset of DPN (diabetic peripheral neuropathy) is associated with the gradual decline of sensory neuron function, it was proposed that increasing Hsp70 levels could improve several indices of neuronal function. KU-32 (**Figure 27**), which is a structurally related analogue of **A4**, was shown to protect against glucose-induced death of embryonic DRG (dorsal root ganglia) neurons cultured for 3 days *in vitro*.[185] The success of KU-32 in this assay, as well as in *in vivo* models, has generated interest in screening compounds of similar origins. As part of continued collaborative studies, the Dobrowsky lab assays novobiocin-

derived compounds, including analogues **30a**–**g**, for their potential to protect against glucose-induced death of embryonic DRG neurons.

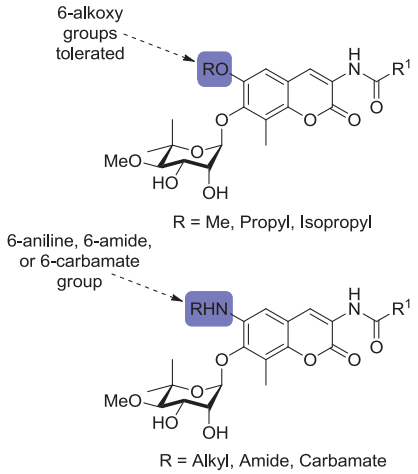

Figure 28. Complementarity of 6-alkoxy and 6-amino groups.[170]

III. Further exploration of the 6-, and 8-position of the coumarin core

A. Modifications to the 6-position

Initial studies of coumarin-derived novobiocin analogues revealed that the 6-position was tolerant of alkoxy substituents. Although alkoxy substituents offered insight about the steric environment and a potential hydrogen bonding network, it was envisioned that other analogues could be proposed to capitalize upon additional interactions within this area of the binding pocket. These analogues were designed to make similar interactions with polar residues in the area as well as probe the impact of an additional hydrogen bond donor. Moreover, through incorporation of functionalities containing variable bulk and electrostatics and the potential to pi-stack at the 6-position, further insights could be gained. As seen in Figure 28, the 6-alkoxy and 6-amino coumarins would complement each other, and the 6-amino group would provide a handle upon which to build more diversity.

1. Synthesis of 6-amino coumarins

Installation of a nitro group at the 6-position of the coumarin ring was proposed as a method to access 6-amide and 6-amino groups. As seen in Scheme 8, 8-methyl coumarin **31**[102] was treated with zirconyl nitrate in acetone, then heated at reflux overnight to yield 6-nitro coumarin **32** in good yield.[186] Nitration at the desired position was confirmed by HMBC NMR spectroscopy. Following acetylation, 6-nitro coumarin **33** was subjected to a variety of conditions in an attempt to cleave the benzyl carbamate. Since removal of the benzyl carbamate proved problematic, the nitro group of coumarin **33** was instead reduced to the corresponding aniline using tin (II) chloride dihydrate in methanol at reflux.[187] 6-Aniline coumarin **34** was treated with benzyl chloride in the presence of cesium chloride and potassium iodide to install a single benzyl group. Although compound **35** was not carried on further, it is envisioned that this methodology could be utilized to access amines, amides and carbamates at the 6-position of the coumarin ring.

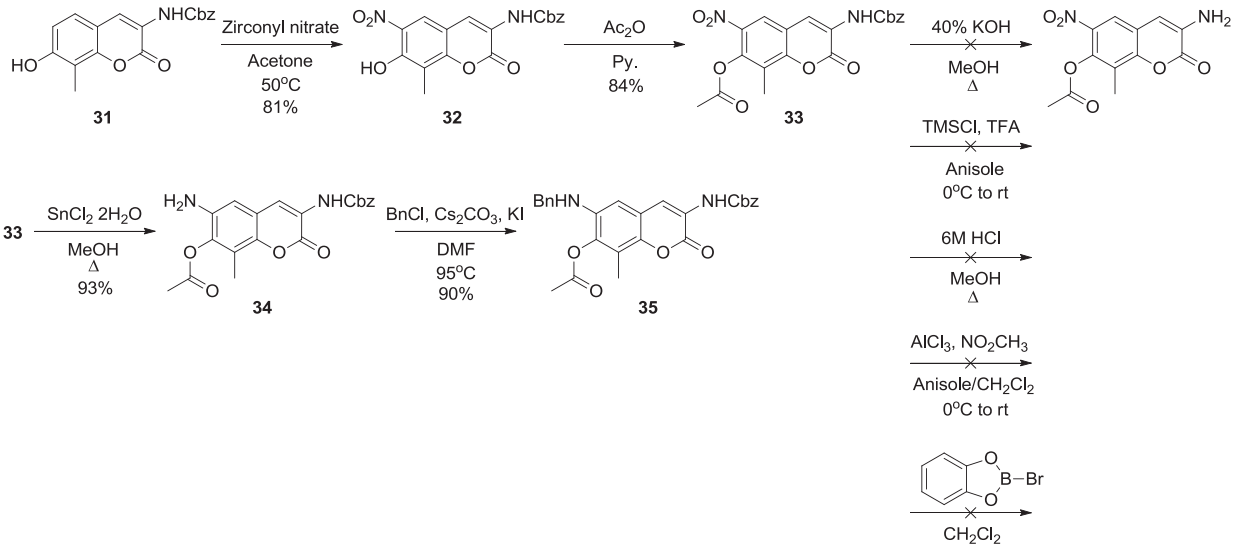

Scheme 8. Synthesis of 6-amino coumarins.

Due to the difficulties encountered with cleavage of the benzyl carbamate from 6-nitro coumarin **33**, it was proposed that a more amenable group should be installed at the 4-position of the coumarin. As seen in Scheme 9, the benzyl carbamate of 8-methyl coumarin **31**[102] was removed via hydrogenolysis to produce the corresponding aminocoumarin, which was sequentially treated with allyl carbonochloridate in the presence of pyridine to afford the Alloc-protected 8-methyl coumarin.[188] Nitration was carried out as previously described with zirconyl nitrate in acetone, leading to quantitative conversion to 6-nitro coumarin, **37**.[186] While acetylation of the 7-position yielded compound **38** in modest yield, attempts to noviosylate the 7-position of coumarin **37** proved unsuccessful due to loss of the nitro group.

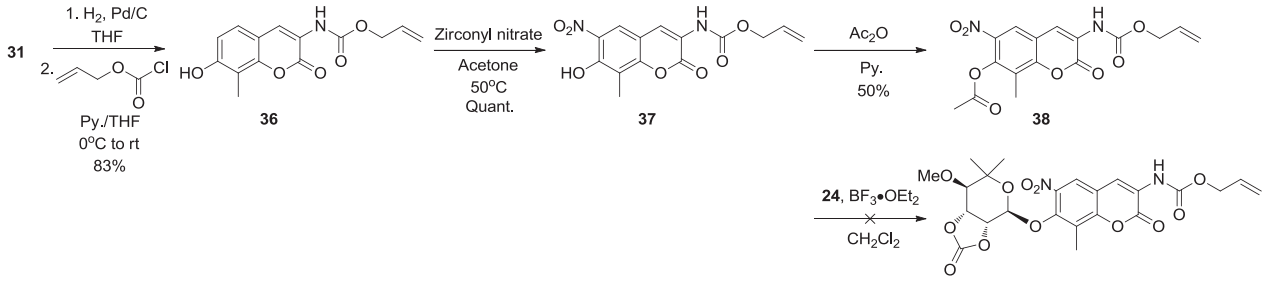

Scheme 9. Synthesis of 6-nitro 4-alloc coumarins.

B. Incorporation of GTP structural elements

As previously discussed, it has been demonstrated that unlike the *N*-terminal site, which is fairly specific for adenine nucleotides, the *C*-terminal site is more promiscuous, binding both purines and pyrimidines. Moreover, GTP and UTP are specific *C*-terminal substrates.[37] Based on these studies and the studies with GTP-complementarity as described in Section I, a coumarin-containing guanosine nucleus was designed (Figure 29).[170] It was envisioned that the key structural elements preserved by the purine-like coumarin would offer selectivity for binding to the Hsp90 *C*-terminus.

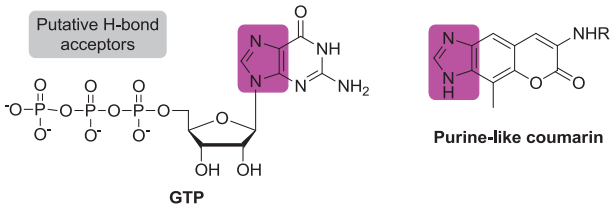

Figure 29. Complementarity of GTP and purine-like coumarin scaffold.

1. Synthesis of GTP mimic coumarin

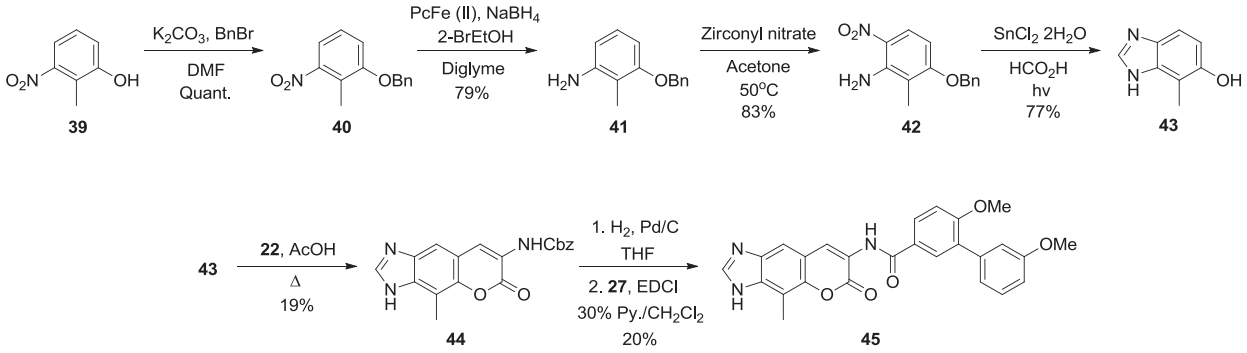

Scheme 10. Synthesis of purine-like coumarin.

As shown in Scheme 10, phenol **39** was quantitatively protected as the corresponding benzyl ether **40**. A benzyl group was selected to protect the phenol because of its stability to a variety of conditions and to assist in preventing its ortho nitration. Benzyl-protected nitroarene **40** was reduced using a bromoethanol-assisted phthalocyanatoiron/sodium borohydride protocol.[189] It was predicted that the mechanism that drives nitration ortho to a phenol with zirconyl nitrate would also have efficacy in nitrating the position ortho to aniline **41**. Thus, zirconyl nitrate was employed for this purpose, yielding the desired product, as confirmed by HSQC and HMBC experiments, in good yield.[186] Next, nitrated aniline **42** was treated with tin (II) chloride dihydrate in formic acid to execute a one-pot *in situ* reduction and cyclization under microwave conditions.[190] These microwave conditions also resulted in cleavage of the benzyl ether to yield phenol **43** in good yield. The corresponding coumarin **44** was synthesized through

a modified Pechmann condensation with eneamine **22** as previously described.[181,182] Finally, the benzyl carbamate was removed via hydrogenolysis to produce the corresponding aminocoumarin, which was coupled with biaryl acid **27** in the presence of EDCI and pyridine to afford compound **45**.

2. Biological evaluation of coumarin 45

Upon construction of analogue **45**, it was evaluated for anti-proliferative activity against SKBr3 and MCF-7 breast cancer cell lines. This compound proved to be inactive against both cell lines in these assays. It is hypothesized that attachment of a sugar to scaffold **45** may result in modest gains in anti-proliferative activity.

C. Modifications to the 8-position

The coumarin-derived novobiocin analogues study revealed that an 8-methoxy group was a favorable substitution versus the 8-hydrogen and 8-methyl group. Moreover, this group was much better tolerated than benzyl and phenyl substituents, which implied a smaller binding pocket with potential polar residues. This finding was also in agreement with the ~12-fold improvement in activity when compared to novobiocin, which has an 8-methyl group, and chlorobiocin, bearing an 8-chloro substituent. Several additional 8-position analogues of the coumarin ring were proposed to further probe this position. These analogues were designed with the potential to interact with surrounding polar residues as well as to probe for additional hydrogen bonds. As seen in Figure 30, the 8-amino, 8-acetyl, and 8-amide were designed to complement interactions made by the 8-methoxy group, while exploring other potential features

of this cavity into which the 8-substituent projects. Finally, while it has been shown that 8-acetyl coumarins demonstrate a wide range of biological activities, most are reported to exhibit modest anti-cancer activity. This finding further supports the design of structurally-related coumarins modified at the 8-position.

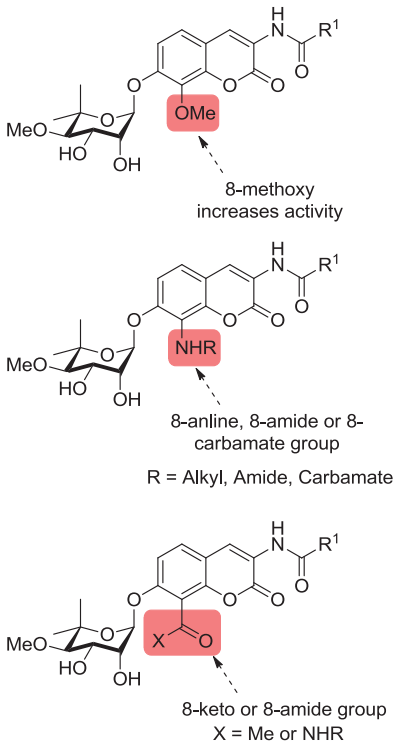

Figure 30. Complementarity of various 8-position substituents.

1. Synthetic steps toward 8-amino coumarins

As seen in Scheme 11, repeated attempts to employ a modified Pechmann condensation between eneamine **22** and resorcinol **46** proved to be problematic, as loss of the nitro group was observed.[181,182] As an alternative, 2-nitroresorcinol **46** was quantitatively reduced using hydrogen and palladium on carbon to afford aniline **47**. Molecular iodine was used to catalyze the protection of the aniline as the corresponding benzyl carbamate, **48**.[191] Although further steps to cyclize to the corresponding coumarin were not attempted, it is envisioned that a modified

Pechmann condensation using an alternatively functionalized eneamine, potentially bearing the desired amide functionality, would yield the desired coumarin. Subsequent cleavage of the benzyl carbamate would then yield a free aniline that could be used to gain access to the proposed functionalized anilines, amides and carbamates. Moreover, this aniline could be converted to a variety of 8-position halogens, which has proven problematic in prior studies, enlisting Sandmeyer chemistry to prepare analogues that bear resemblance to chlorobiocin.

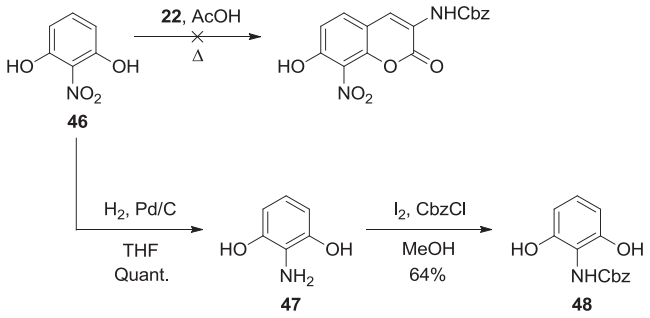

Scheme 11. Efforts toward 8-amino analogues.

2. Synthesis of 8-acetyl coumarins

As shown in Scheme 12, coumarin **50** was obtained in modest yield through employment of a modified Pechmann condensation between eneamine **22** and resorcinol **49**.[181,182] While acetylation of coumarin **50** proceeded in good yield, noviosylation was low yielding and the two anomers were collected as an inseparable mixture of **51**. The benzyl carbamate of acetylated coumarin **52** was removed via hydrogenolysis to produce the corresponding aminocoumarin, which was readily coupled with biaryl acid **27** in the presence of EDCI and pyridine to afford compound **53**. Following deacetylation, compound **54** was prepared for biological evaluation.

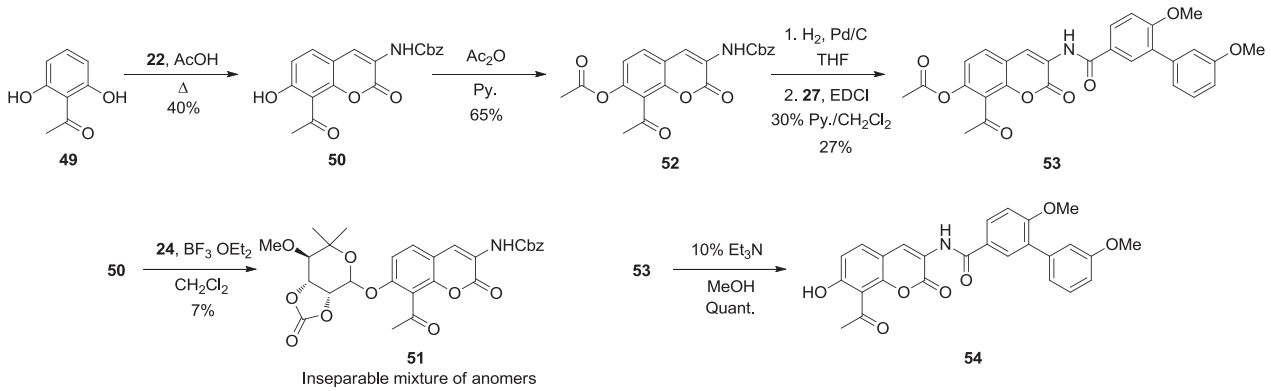

Scheme 12. Synthesis of 8-acetyl analogues.

3. Biological evaluation of 8-acetyl coumarin 54

Upon construction of analogue **54**, this compound was evaluated for anti-proliferative activity against SKBr3 and MCF-7 breast cell lines. Although this compound proved inactive in these assays, it is hypothesized it has the potential to be transformed into an active agent through appendage of a sugar moiety.

4. Synthesis toward 8-amido coumarins

As shown in Scheme 13, coumarin **56** was obtained through employment of a modified Pechmann condensation between eneamine **22** and resorcinol **55**.[181,182] Formation of coumarin **56** was confirmed by crude ^{1}HNMR and mass spectrometry studies, but was difficult to purify further. Thus, this coumarin was taken on crude into an acetylation reaction, yielding compound **57** in modest yield over both steps. It was envisioned that conversion of the 8-acid to the corresponding ester would enable functionalization of the 7-position without difficulty. Attempts to esterify the 8-position resulted in loss of the acetate protecting group, despite our efforts to keep the reaction under anhydrous conditions. The desired compounds could be easily accessed through coupling of compound **57** to a variety of amines to yield 8-amide coumarins. In addition,

functionalization of the 7-position of compound **58**, followed by hydrolysis to liberate the free 8-acid and subsequent coupling reactions would also provide a route to the desired analogues.

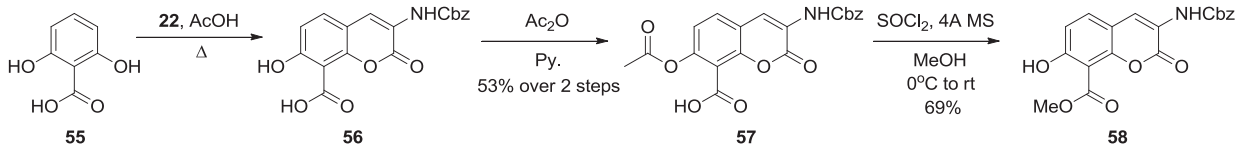

Scheme 13. Synthesis toward 8-amide analogues.

This study enabled the development of methodologies toward the preparation of molecules that probe the 6- and 8-positions of the coumarin ring. Moreover, these synthetic methods demonstrate the broad applicability of the modified Pechmann condensation towards coumarin-ring formation. Due to the creation of a binding model, these efforts were abandoned in favor of a more rational approach to the design of analogues that probe this region of the binding pocket.

IV. Coumarin-replacement study

A. Molecular modeling

These preliminary studies on the coumarin core generated several interesting compounds with a broad range of activities that add to a growing library of novobiocin analogues. Addition of these compounds to the library enabled a co-worker in the Blagg group to create a CoMFA model for the compilation of novobiocin-based congeners. Through overlaying the presumed conformations of the biologically active compounds, a correlation between the anti-proliferative activity of the novobiocin analogues and their 3D shape, electrostatic and hydrogen bonding characteristics was derived. This CoMFA study was pivotal toward the development of an

HTPG-based docking model with Dr. Verkhivker on campus.[192] Since its development, this model for novobiocin binding the Hsp90 *C*-terminus has been instrumental towards rational inhibitor design and has enabled a better understanding of observed trends in biological activity.

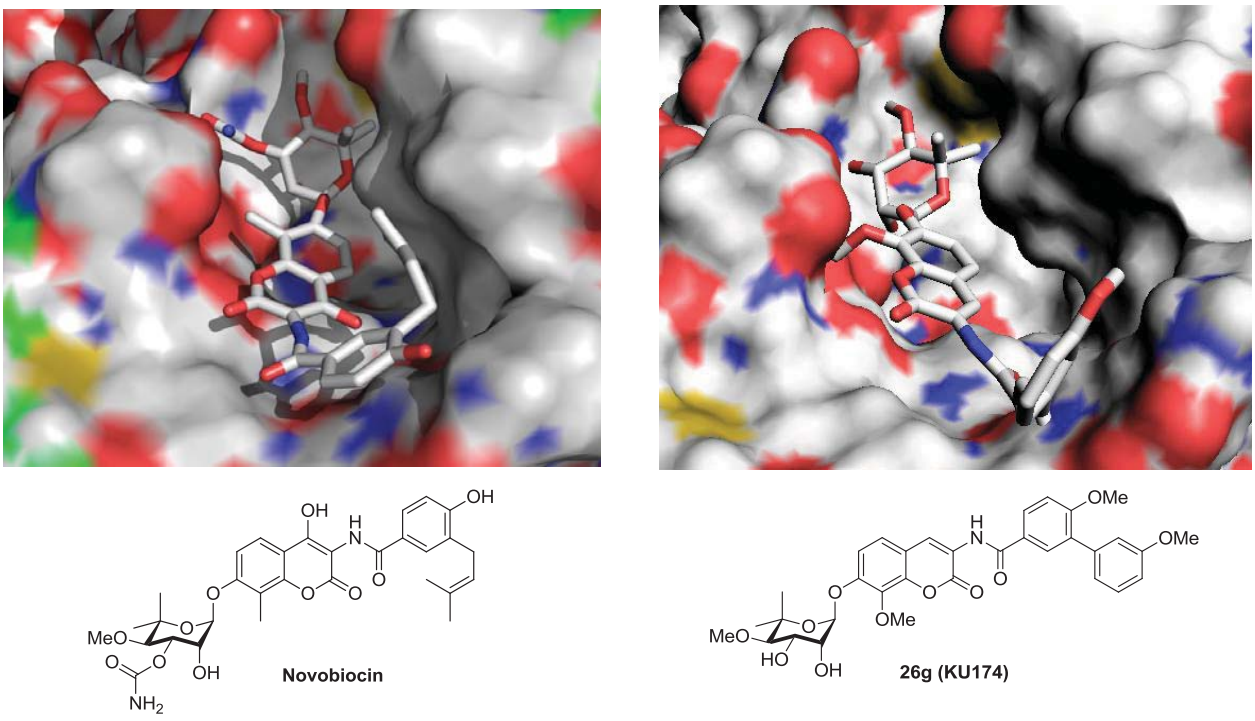

Figure 31. Novobiocin versus **26g** bound to Hsp90α model.

1. Docking of novobiocin versus 26g

Promising compounds that were synthesized prior to the creation of the model, such as those that are part of the coumarin study in Section I, have been docked and examined for key interactions. Due to the promising activity that **26g** (KU174) manifested, it was one of the compounds that has been docked and studied extensively as part of the modeling studies. The conformation exhibited by novobiocin versus that which **26g,** adopts is shown in Figure 31. It was observed that the two compounds assume similar orientations within the binding pocket and that structural features within the two congeners overlap. Key hydrogen bonds within the noviose

binding pocket are proposed to anchor these compounds deep within the cavity, while the benzamide side chain resides in a largely hydrophobic region. Interactions with the 8-position and lactone moiety of the coumarin core have also been proposed as important in binding.

2. Specific interactions made by the coumarin core of novobiocin

Confirmation that novobiocin and **26g** bind in similar orientations within the proposed binding site was an important finding. This discovery verified that analogues like **26g** manifest the same interactions as novobiocin within the pocket and that the slight perturbations to the coumarin core that lead to improvements in activity could be due its ability to make additional interactions. With the model verified, it was important to explore the area around the coumarin and to identify key residues that could offer additional interactions and further improve binding affinity.

As shown in Figure 32, the novobiocin coumarin core makes several important interactions with surrounding residues. Firstly, Glu-537, an acidic glutamic acid residue is located in the vicinity of the 8-methyl group of novobiocin. The two oxygens that make up the carboxylic acid of this residue are 3.6, 2.9, and 2.9 Å away from the three hydrogens attached to the 8-methyl group. It is hypothesized that since these interactions are within 4.0 Å, hydrogen bonds could be made between the coumarin and this part of the pocket. The existence of these H-bonds confirms the importance of the 8-position and explains the 10-fold increase in activity when a methyl group replaces the 8-hydrogen.[170] Moreover, the steric clash between this residue and bulkier aryl groups explains the inactivity of compounds bearing an 8-aryl substituent.

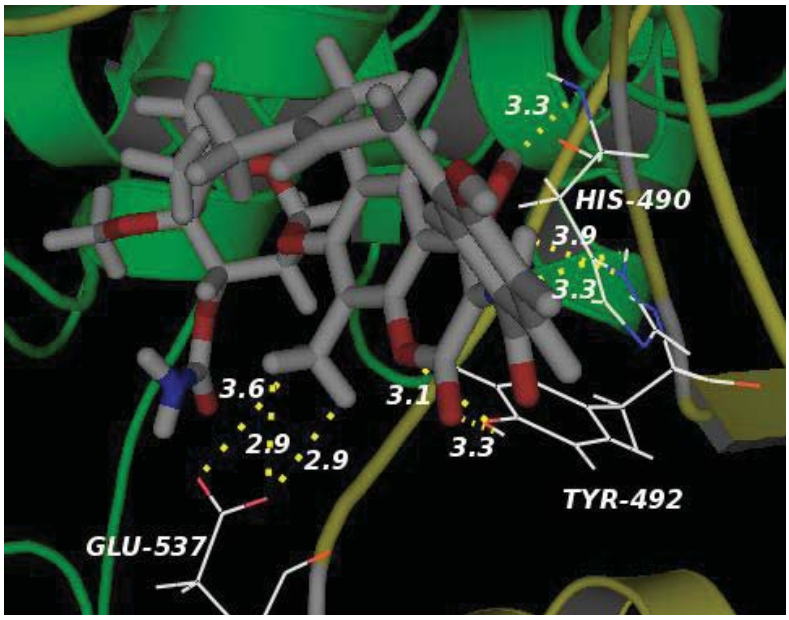

Figure 32. Novobiocin bound to model.

Next, Tyr-492, a tyrosine residue, is located in the proximity of the coumarin lactone. The free phenol of this tyrosine residue is 3.1 and 3.3 Å away from the two oxygens that comprise the coumarin lactone. It is proposed that the phenolic hydrogen on this tyrosine could hydrogen bond with the lactone, making it an essential portion of the structure. Although the lactone was deemed 'not essential' as part of the first coumarin study, there is a definitive 2-4-fold loss in activity when comparing the quinoline directly to the naphthalene in breast cancer cells. While the quinoline could potentially preserve this hydrogen bond to Tyr-492, the naphthalene does not contain a heteroatom capable of making such an interaction. This potential H-bond offers an explanation for the trends in activity and is believed to be essential in binding analogues of this type.

Finally, His-490, a histidine residue, resides proximal to the northern region of the coumarin lactone ring. This histidine could potentially make several interactions with this part of the coumarin. The nitrogen of the amide backbone, which connects His-490 to the neighboring residue, is 3.3 Å away from the hydrogen connected to the 4-hydroxyl group of novobiocin. A

hydrogen bond could exist between this backbone amide and the hydroxyl group on novobiocin. Moreover, the amide that connects the coumarin core to the prenylated side chain of novobiocin also has the potential to interact with this histidine residue. While the hydrogen attached to the amide is 3.9 Å from one of the nitrogens that makes up the imidazole core, the amide nitrogen is 3.3 Å from the protonated imidazole nitrogen. These potential interactions confirm what has been shown through synthesis of analogues lacking the amide linkage, that the amide bond is essential in attaching a side chain to the coumarin core.[15]

Upon identification of the important interactions made by novobiocin, it was a logical next step to examine the effect of structural changes on the ability of various analogues to preserve these essential contacts.

3. Specific interactions made by the coumarin core of 59

Compound **59** (Figure 33) was a promising compound developed as part of the benzamide side chain study by Burlison and co-workers.[102] This novobiocin analogue was designed with the knowledge that the 4-hydroxyl group on the coumarin and 3'-carbamate on the noviose sugar were detrimental to Hsp90 inhibition.[18] In addition to these structural deviations from novobiocin, the biaryl acid **27**, also found in **26g**, was appended in place of the prenylated side chain of novobiocin.[102]

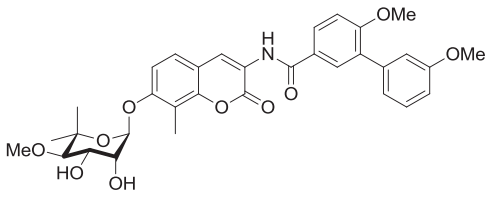

Figure 33. Structure of **59**.[102]

As seen in Figure 34, this simplified coumarin structure can still capitalize on the same hydrogen bonding network as novobiocin. Glu-537 interacts with the 8-methyl group of analogue **59** in an analogous fashion, making multiple hydrogen bond contacts between the glutamic acid oxygens and methyl group hydrogens. Although the compound is skewed slightly, possibly due to the sugar reorienting and extending deeper into the pocket due to excision of the bulky carbamate, two of the three contacts are preserved and are actually in closer proximity to this residue than in novobiocin.

Next, like with the glutamic acid residue, **59** is in closer contact with Tyr-492 as well. Both oxygens of the lactone ring are within 3.2 Å of the phenolic hydrogen of this tyrosine residue, preserving those hydrogen bonds found when novobiocin is docked. When **59** is docked, His-490 is just outside of hydrogen bonding distance for the same interaction made by the amide nitrogen of novobiocin to the imidazole ring. Finally, the 4-position of novobiocin versus that found in **59** differs greatly and was examined for potential different interactions. Like the amide nitrogen, the 4-hydrogen is just outside of the distance required for it to hydrogen bond to the imidazole ring of histidine 490. Despite the predicted distances, it is likely that the hydrogen bond is preserved between the amide side chain and His-490, while it is possible that an additional contact is made between the 4-hydrogen and the same residue. Preservation of many of the proposed coumarin interactions for compound **59** may contribute to the remarkable 70-fold improvement in activity observed for this compound versus novobiocin.[102]

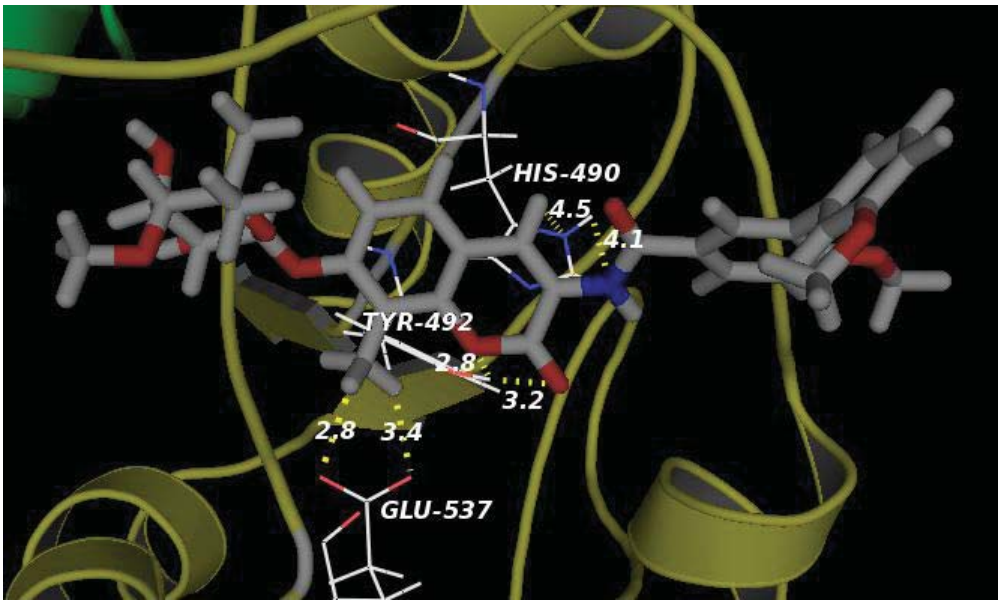

Figure 34. 59 bound to the model.

Overall, these slight structural perturbations to the coumarin core and sugar, combined with a major change to the side chain, did not augment many of the potential interactions. This finding supports that major changes can be made to the benzamide side chain, potentially to capitalize on additional interactions, without disruption of coumarin binding. Moreover, the slight modifications to the coumarin and sugar were well tolerated. One final analogue was docked to examine the combined effect of major changes to both the sugar and benzamide side chain, while maintaining the same coumarin core as **59**.

4. Specific interactions made by the coumarin core of 60

While the development of compound **60** (Figure 35) will discussed in more detail as part of Chapter 2, it was identified as a promising compound as part of a study of possible sugar surrogates by Zhao and co-workers.[193] This novobiocin analogue maintains the excised 4-hydroxyl group on the coumarin and biaryl side chain found in compound **59**.[18,102] In contrast,

compound **60** lacks the noviose sugar found in the natural product, bearing an *N*-methyl piperidine in its place.

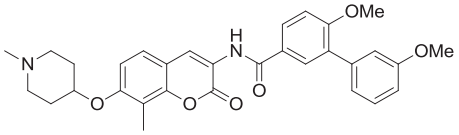

Figure 35. Structure of **60**.[194]

As seen in Figure 36, despite more modest structural changes, the energy-minimized conformation of compound **60** still adopts a similar binding orientation to novobiocin. Glu-537 interacts with the 8-methyl group of analogue **60** in an analogous fashion to novobiocin, making the same number of potential hydrogen bond contacts between the glutamic acid oxygens and methyl group hydrogens. Despite obvious changes in the sugar orientation, the three contacts are preserved and are all within the proper distance to hydrogen bond.

Likewise, **60** mimics the interactions that novobiocin makes with Tyr-492 almost exactly. Both oxygens of the lactone ring are within 3.4 Å of the phenolic hydrogen of this tyrosine residue, suggesting that these hydrogen bonds are made when **60** binds to the putative pocket. Like when **59** is docked, His-490 is the same distance, just outside of hydrogen bonding range, for the same interaction made by the amide nitrogen of novobiocin to the imidazole ring. Moreover, the 4-position hydrogen is just outside of the distance required for it to hydrogen bond to the imidazole ring of histidine 490, but slightly closer than when analogue **59** is bound. It is proposed that analogue **60** could augment its position slightly to take advantage of these additional hydrogen bonds with His-490. Since this compound manifests another 10-fold improvement in activity versus compound **59** and 700-fold versus novobiocin, it is believed that key coumarin interactions are preserved while additional contacts are made within the sugar binding region.

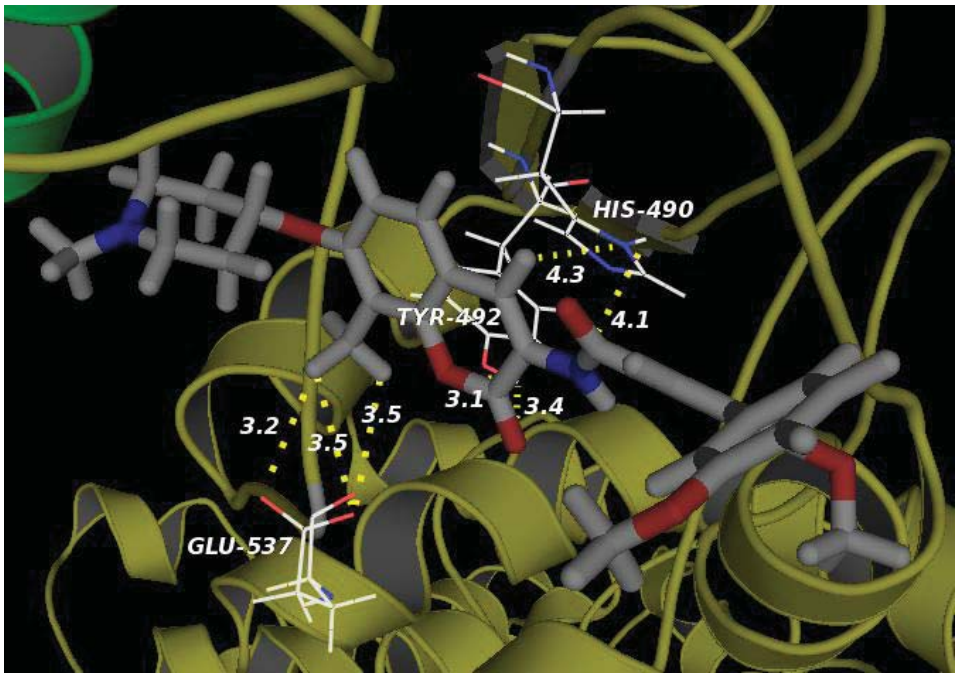

Figure 36. 60 bound to the model.

B. Rational design of coumarin-core replacements

For many reasons, including difficulty of synthesis, limited solubility, and potential rapid metabolism by cytochromes P450, there was interest in moving away from the coumarin ring as the core structure of novobiocin analogues. A suitable replacement ring system would maintain the same essential interactions as the most promising coumarin cores, while improving upon the aforementioned shortcomings. Although two potential substitute cores were explored during the initial studies described in Section I, neither the quinoline nor the naphthalene matched the activity of the coumarins.[170] Moreover, elucidation of the binding model has enabled the rational design of alternative ring systems, while more comprehensive sugar and benzamide studies have elucidated the most promising.

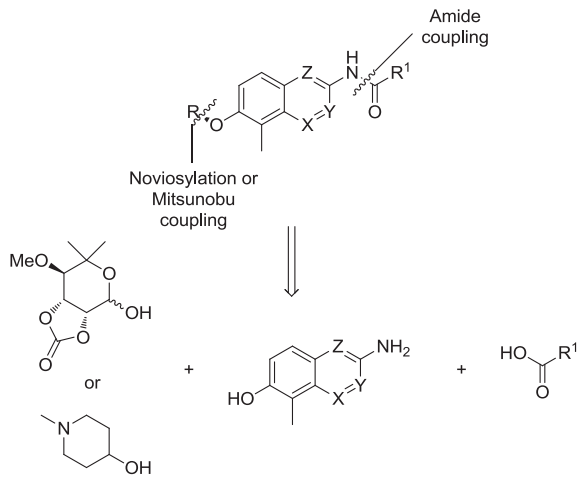

Scheme 14. Retrosynthesis coumarin-replacement analogues.

1. Design of novobiocin-derived analogues lacking a coumarin core

Based on molecular modeling studies, we envisioned construction of novobiocin analogues that contain modified core structures. As shown in Scheme 14, the derivatives were designed for assembly in modular fashion, allowing for the sequential coupling of either noviose or an *N*-methylated piperidine, sugar surrogate and a series of benzoic acids with the modified nuclei.[170] We previously demonstrated that the trichloroacetimidate of noviose carbonate couples readily to coumarin phenols in good yields, to afford the corresponding α-anomer.[171] It was proposed that this same chemistry could be employed on the new ring systems to afford the noviosylated scaffolds. In addition, the *N*-methyl piperidine shown, installed via Mitsunobu etherification, was chosen as a suitable sugar replacement.[194] The benzoic acids were selected based upon previously obtained SAR for the amide side chain as described by Burlison and co-workers and Zhao and co-workers.[102,195]

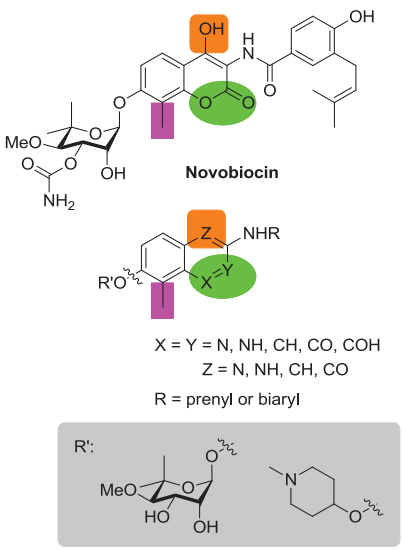

Figure 37. Complementarity of novobiocin and proposed analogues.

The coumarin replacement scaffolds were selected to complement interactions made by novobiocin and optimized analogues with the desired sugar and benzamide side chains in molecular modeling studies. While the western portion of the bicyclic core was explored in detail as part of the initial coumarin study, the eastern portion is being examined herein. In designing analogues that probe the eastern hemisphere, the exact left-hand ring from novobiocin was maintained. The 8-methyl group has been shown to make essential interactions with Glu-537 in molecular modeling studies. Moreover, this finding has been confirmed by the 10-fold improvement in activity when comparing the 8-desmethyl to the same 8-methyl and 8-methoxy analogues.[102] The potential introduction of additional hydrogen bonds, capable of producing 1-2 kcal/mol of binding energy and thus increasing binding by 10-fold, were incorporated into the design strategy.[172] Within the modified eastern portion, hydrogen bond donors and acceptors were placed in positions X, Y, and Z (Figure 37). It is envisioned that while position X and Y would reside proximal to the lactone binding region, Z would extend into the area where the 4-hydroxyl group of novobiocin is located. With this rationale, X and Y have the potential to interact with Tyr-492 while Z can make contacts with His-490. The activity of such compounds

is likely to provide insight into which additional interactions lead to favorable increases in binding affinity.[170]

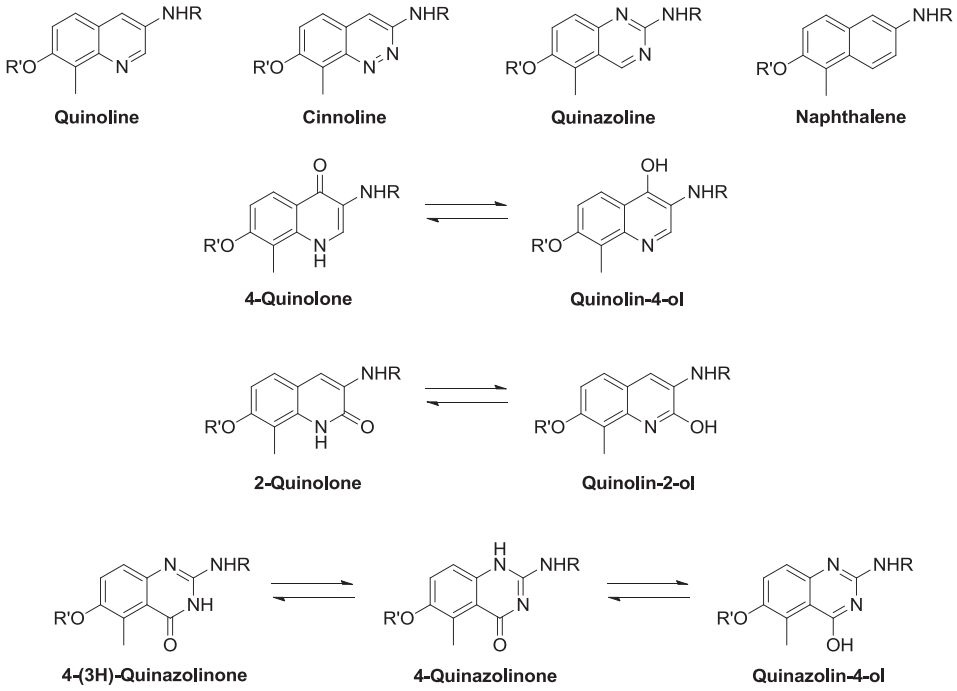

Figure 38. Coumarin ring replacement core structures.

A quinoline, cinnoline, and quinazoline were proposed as core structures that would place hydrogen-bond accepting nitrogens at X, Y, and Z around the ring. 4-quinolone, 2-quinolone, and 4-(3H)-quinazolinone structures exist in multiple tautomeric forms, offering the possibility to hydrogen bond via donating or accepting groups at the same three positions. These ring systems would be compared to a naphthalene nucleus that would fill the same space without offering heteroatoms capable of creating additional hydrogen bonds. These seven different ring systems, shown in Figure 38, would probe the impact of introducing additional hydrogen bonds at various positions around the ring. In contrast, a naphthalene core would investigate whether hydrophobic bulk was sufficient. Overall, these ring systems would identify those interactions that are essential and which replacement ring systems maintain them.

Sugars and benzamide side chains were prepared based upon prior studies. Molecular modeling studies, as discussed in the previous section, confirmed that replacement of the noviose sugar with the *N*-methyl piperidine sugar surrogate did not perturb interactions made by the coumarin core. Likewise, the coumarin interactions were maintained despite replacement of the prenylated side chain with the biaryl acid **27**. Finally, structural modifications at both termini were also well tolerated. The noviose sugar and *N*-methyl piperidine will be appended as sugars, while the prenylated and biaryl side chains will serve as the choices of benzamide side chains. As shown in Figure 39, the rationale for these choices of sugars and benzamides are based upon favorable gains in activity associated with their prior incorporation. Moreover, through incorporation of a noviose sugar and prenylated side chain to each of the ring replacement systems, it can be compared directly with the parent natural product, novobiocin.

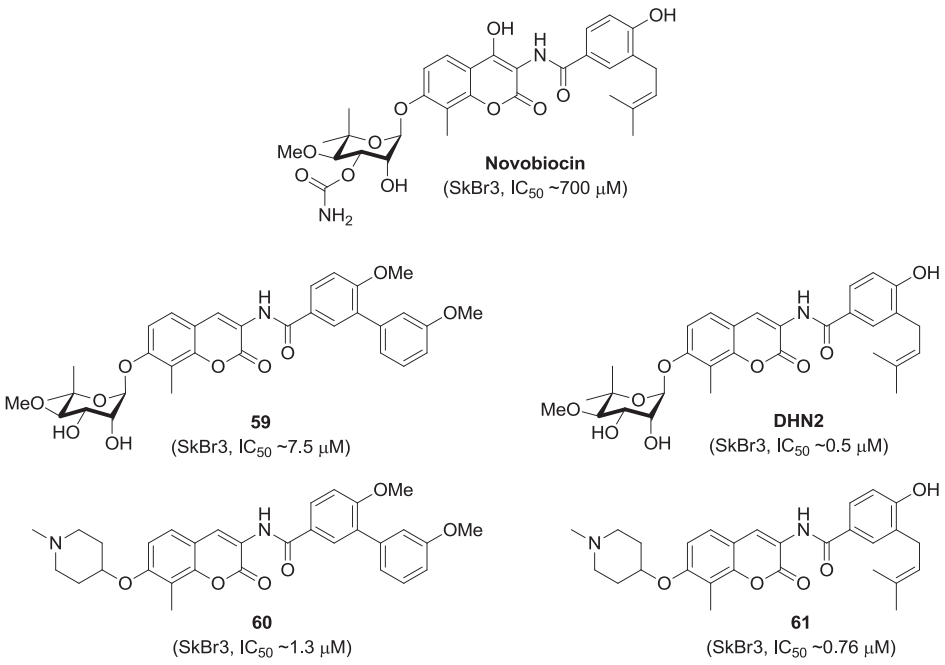

Figure 39. Structures of novobiocin, **59**, **60** and **61**.

2. Efforts toward ring system precursors

As seen in Scheme 15, it was envisioned that four of seven ring systems could be accessed through a common precursor. Since making this intermediate was a priority, several routes have been designed and attempted.

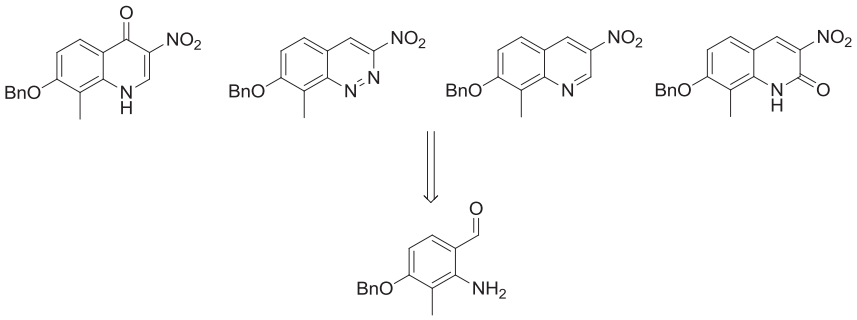

Scheme 15. Common intermediate for several ring systems.

As seen in Scheme 16, phenol **61** was protected as the corresponding methoxy methyl ether in good yield. Nitroarene **62** was quantitatively reduced to the corresponding aniline. Attempts to brominate aniline **63** were not selective for the desired regioisomer and most often led to bromination at multiple sites. It was proposed that incorporation of a bulkier phenolic protecting group would preclude ortho bromination and allow access to the desired regioisomer.

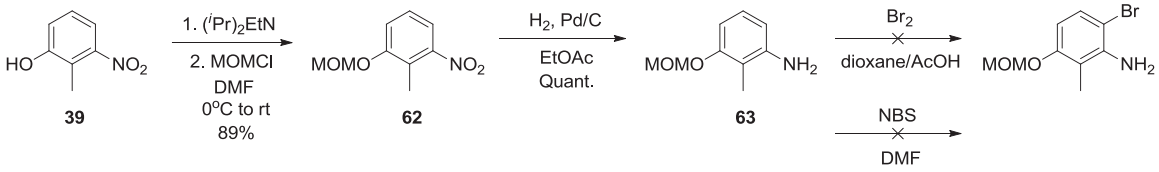

Scheme 16. Synthesis of MOM-protected precursor.

To this end, benzyl-protected aniline **41** was prepared once again from the nitroarene **40** synthesized in making the purine-like coumarin. As shown in Scheme 17, prior to reduction, an unsuccessful Vilsmeier-Haack reaction was attempted to formylate the deactivated system.[196] Next, much simpler reducing conditions were employed than previously described, using platinum on carbon and hydrogen, to afford aniline **41** in nearly quantitative yield. Although it

was proposed that a Vilsmeier-Haack reaction could be exploited for regioselective formylation of this intermediate aniline, the only product observed in this reaction was due to *N*-formylation, yielding the formamide adduct.[196] Simultaneous efforts to brominate ortho to the aniline were based upon literature precedence.[197] *N*-bromosuccinimide was used to install the desired bromine group, leading to one major product in good yield. Attempts to characterize product **64** by ^{1}HNMR, ^{13}CNMR, COSY, HSQC, NOESY and HMBC NMR spectroscopy experiments were not definitive, as either compound would yield nearly indistinguishable perturbations to the spectra. It was believed that conversion of the aryl bromide to the corresponding benzaldehyde would provide definitive spectral characteristics that would enable identification of the product obtained. Despite literature reports, initial efforts to convert the brominated aniline directly to the desired benzaldehyde through lithium–halogen exchange were unsuccessful, exclusively leading to the formamide instead.[198]

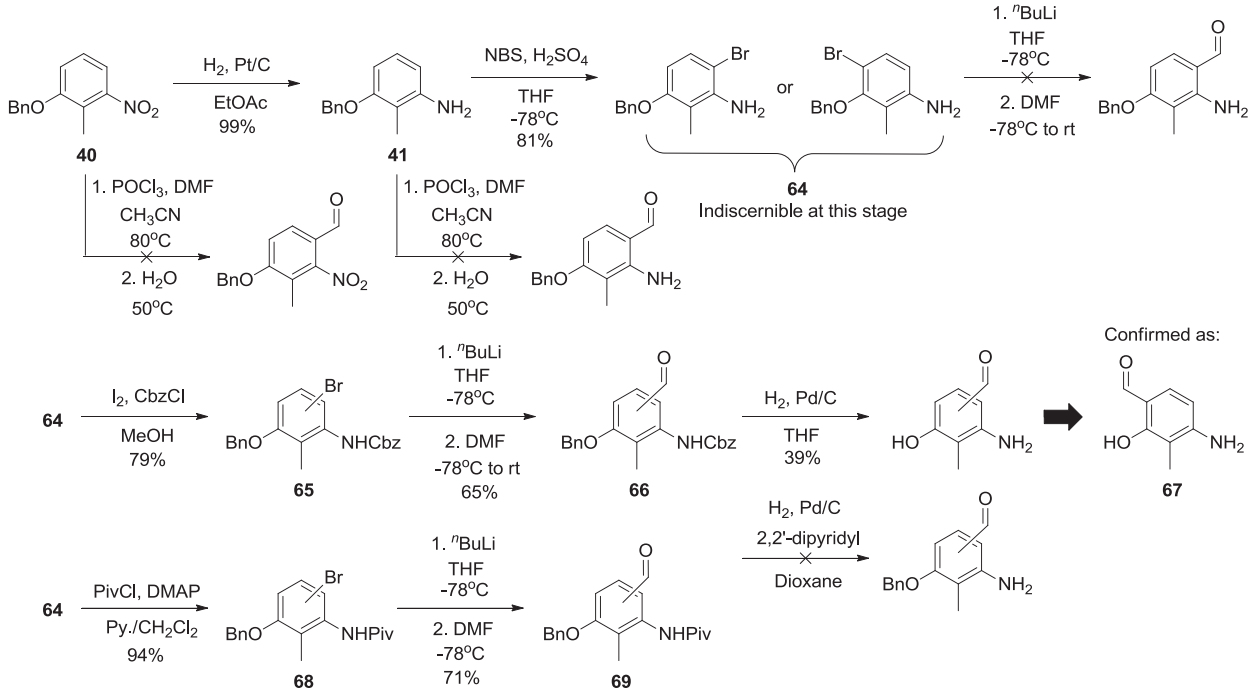

Scheme 17. Synthesis of benzyl-protected precursor.

Two parallel approaches were undertaken toward the benzaldehyde product. Firstly, aniline **64** was protected as the corresponding benzyl carbamate as previously described.[191] The protected aniline **65** was then exposed to lithium–halogen exchange conditions, quenching with *N*,*N*-dimethylformamide. An attempt to selectively cleave the benzyl carbamate while maintaining the benzyl ether group through poisoning the palladium catalyst with 2,2-dipyridyl did not allow for cleavage of either group.[199] Hydrogen and palladium on carbon were used to simultaneously cleave both groups of benzaldehyde **66**, affording compound **67** in modest yield. Simultaneously, a pivaloyl group was used to protect aniline **64**, generating protected aniline **68** in good yield. The pivaloyl group was chosen based upon its known directing ability in *ortho*-lithiations. Lithium–halogen exchange, as previously described, was employed to yield protected benzaldehyde **69**. With compound **67** in hand, there was no need to go through the steps to deprotect **69** until after ^{1}HNMR, ^{13}CNMR, COSY, HSQC, NOESY and HMBC NMR spectroscopy experiments were used to characterize compound **67**. These experiments, namely correlation between the phenolic carbon and the aldehyde proton in the HMBC spectrum and correlation between the aromatic proton and adjacent aniline protons in the NOESY spectrum, identified **67** as the undesired regioisomer.

Subsequent efforts toward this common precursor once again employed the known directing ability of the pivaloyl group in *ortho*-lithiations. As seen in Scheme 18, aniline **41** was protected as the corresponding pivaloyl amide **70** in good yield. It was proposed that the pivaloyl group would guide formylation at the desired position through directed *ortho*-lithiation and subsequent quenching with *N*,*N*-dimethylformamide. Although several organolithium bases, solvents and temperatures were tried, the desired product was not obtained in appreciable yield. It is likely that the desired reaction competed with abstraction of a benzylic proton from the

methyl group ortho to the pivaloyl amide. This route was abandoned in favor of installing the methyl group, rather than the formyl group, as the last substituent, analogous to the approach used in the initial coumarin study.

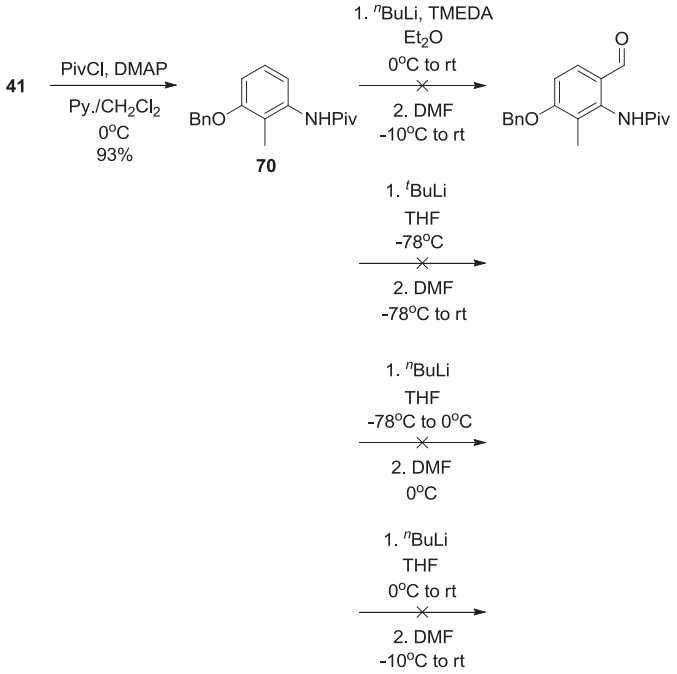

Scheme 18. Efforts to exploit a pivaloyl amide as an *ortho*-lithiation directing group.

To facilitate installation of the methyl group as the final step, attempts to attach the other three groups on the ring were undertaken. As seen in Scheme 19, benzaldehyde **71** was treated with phosphorus pentoxide mixed with silica in the presence of nitric acid, but the desired nitration did not take place.[200] Next, phenol **72** was treated with dimethyl amine and formaldehyde to try and install the dimethyl amine group, which could be reduced to the methyl group through subsequent steps.[201] This reaction was also unsuccessful, as only starting material remained after several hours. Attempted bromination of phenol **72** between the nitro and phenol groups was not selective, yielding many undesired inseparable products. Subsequently, phenol **72** was quantitatively protected as the corresponding methoxy methyl ether **73**. Next, *N*,*N*-dimethylformamide dimethyl acetal (DMF-DMA) in the presence of pyrrolidine was used to

convert the methyl group to an eneamine, which was subsequently oxidized to benzaldehyde **74** in good yield.[202,203] Although the DMF-DMA would mediate formation of an eneamine intermediate, the addition of pyrrolidine reduced reaction temperature and time through formation of a more stable pyrrolidine-containing eneamine. Benzaldehyde **74** was subsequently reduced to aniline **75** using hydrogen in the presence of palladium on carbon. An attempt to brominate aniline **75** between the protected phenol and aniline was unsuccessful. Finally, the same aniline was deprotected through heating with 3M HCl and the procedure to install a dimethyl amine group on phenol **76** was repeated unsuccessfully. Since late-stage methylation proved problematic, focus was redirected toward the preparation of other precursors.

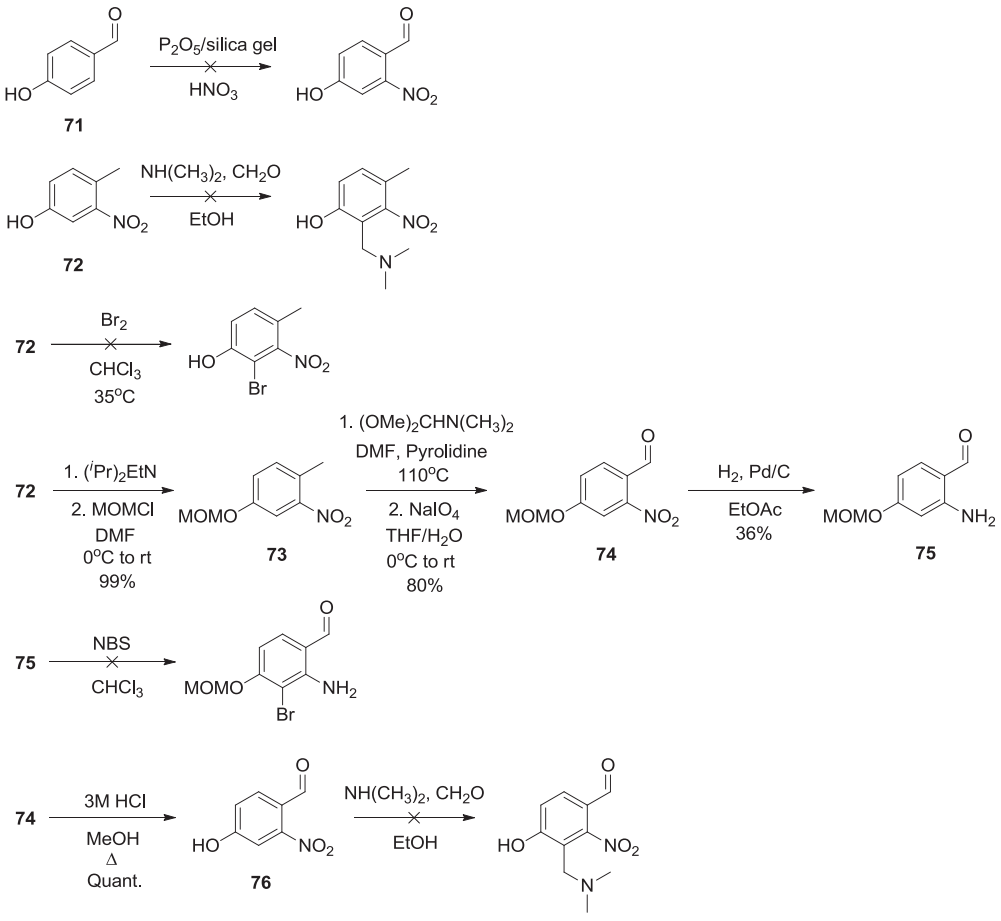

Scheme 19. Efforts toward late-stage methylation.

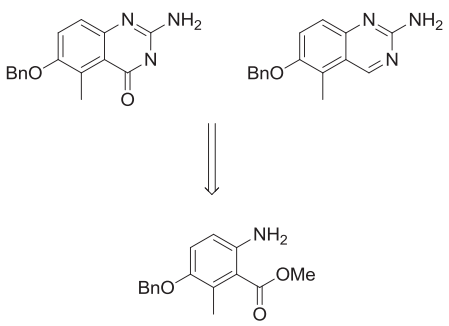

Scheme 20. Common intermediate for remaining heteroaromatic ring systems.

As seen in Scheme 20, a second precursor was designed to represent a common intermediate towards the syntheses of the remaining heteroaromatic ring systems. Initial attempts aimed at installing the fourth functionality with the other three in place were pursued. As seen in Scheme 21, nitration of carboxylic acid **77** did not proceeding the conditions provided. With the goal of late-stage methylation, benzaldehyde **78** was protected as the corresponding methoxy methyl ether in good yield. Next, a Pinnick oxidation was employed to afford carboxylic acid **80**. Despite the known directing effect of both the methoxy methyl ether and carboxylic acid groups, methylation did not occur. Rather, the ^{t}Bu ketone was the sole product isolated from this reaction.

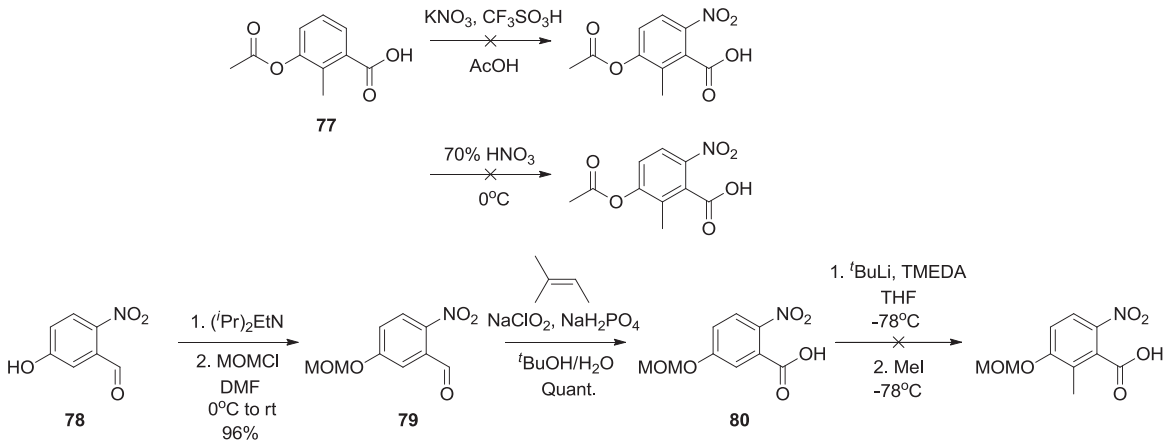

Scheme 21. Efforts toward second common precursor.

Attempts to make the second precursor were not fruitful, and led to a unified route toward all heteroaromatic systems through common intermediate **83**/**89**. It was proposed that preparation of this common ring system would be rather straightforward, allowing for late-stage diversification to several core structures in relatively few steps overall. As shown in Scheme 22, a fully functionalized intermediate was designed to allow access to each synthon required for cyclization in order to access the corresponding heteroaromatic ring system.

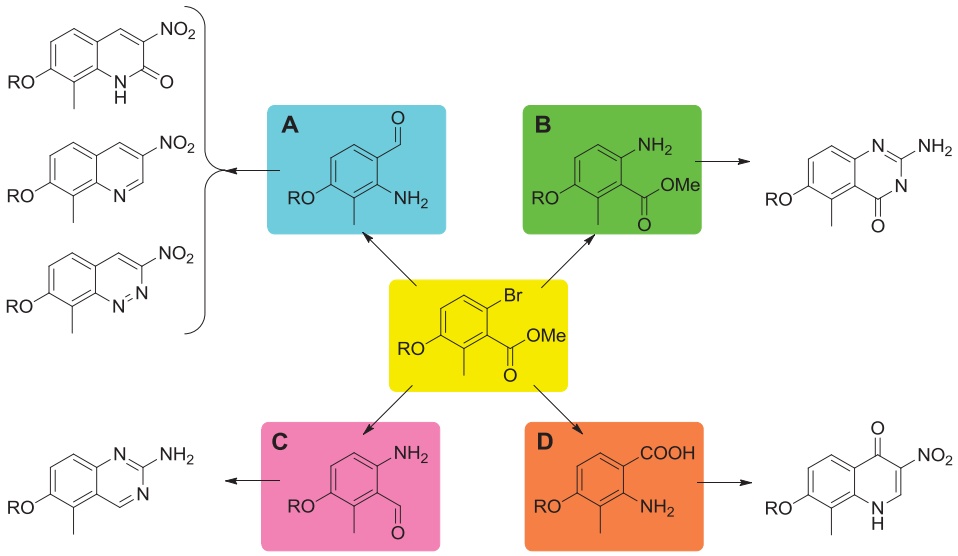

Scheme 22. Utility of common intermediate **83**/**89**.

Synthesis of the MOM-protected precursor is outlined in Scheme 23. Carboxylic acid **77** was converted to the methyl ester using thionyl chloride in methanol. Simultaneous acetate cleavage was observed to yield the phenolic methyl ester, **81**. Next, bromination was carried out at -42°C using a 0.75M solution of bromine in methylene chloride.[204-206] The bromine solution was added portionwise, over more than an hour, to avoid over bromination of the ring. Functionalized intermediate **82** was next protected as the methoxy methyl ether, yielding ester **83** in good yield. Attempts to hydrolyze methyl ester **83** with lithium hydroxide were unsuccessful and it was soon discovered that more harsh conditions were required. Carboxylic acid **84** was

quantitatively obtained through treatment of the aforementioned ester with a 40% potassium hydroxide solution in refluxing ethanol.[207]

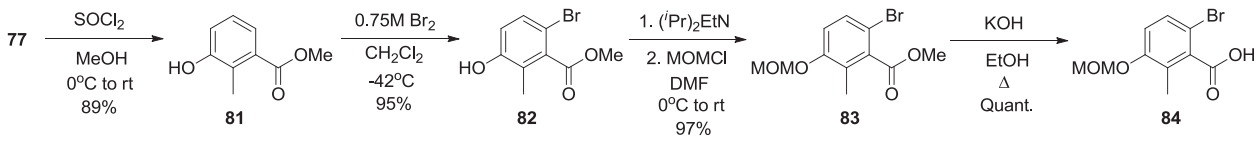

Scheme 23. Synthesis of functionalized universal precursor **83**.

Intermediate **83** could be envisioned to undergo a number of palladium-mediated cross-coupling reactions would furnish the desired synthons for cyclization (Scheme 24). Coupling of a vinyl group or substituted alkene was attempted to furnish the benzaldehyde (synthon **A**) or carboxylic acid (synthon **D**) at the position of the aryl bromide. However, Stille cross-coupling conditions with tributyl(vinyl) tin and tetrakis(triphenyl-phosphine)palladium in toluene or DMF, failed to convert the aryl bromide to the desired olefinic product. Moreover, dehalogenation did not occur, but rather unreacted starting material remained. Simultaneously, a Suzuki cross-coupling reaction was attempted using (E)-styrylboronic acid and the same palladium catalyst, yielding only undesired side products and recovered starting material. Several different Buchwald-Hartwig cross-coupling reactions were attempted with the goal of converting the aryl bromide to a protected aniline species toward preparation of synthons **B** and **C**. Initial attempts to couple (4-methoxyphenyl)methanamine utilized various bases, ligands and palladium sources, but none resulted in successful product formation. Likewise, attempts to couple benzyl carbamate to aryl bromide **86** did not occur, despite changes in the palladium source and ligand.

It was proposed that since unrecovered starting material was recovered in nearly every cross-coupling attempted, that the palladium did not insert into the carbon-halogen bond. In an attempt to facilitate insertion, a more robust palladium source was employed. In addition to being air and water stable, the PEPPSI (**p**yridine-**e**nhanced **p**recatalyst **p**reparation **s**tabilization and

initiation) catalyst is known to improve reductive elimination, increase turnover numbers, and bind the metal more tightly than traditional phosphines and thus prevent metal dissociation.[208] A PEPPSI-catalyzed Stille coupling with tributyl(vinyl) tin was attempted, along with two different PEPPSI-catalyzed Suzuki coupling reactions with (E)-styrylboronic acid. Unfortunately, use of this improved catalyst did not furnish the desired products. It was proposed that an alternative strategy would be required to convert aryl bromide **83** to the desired synthons.

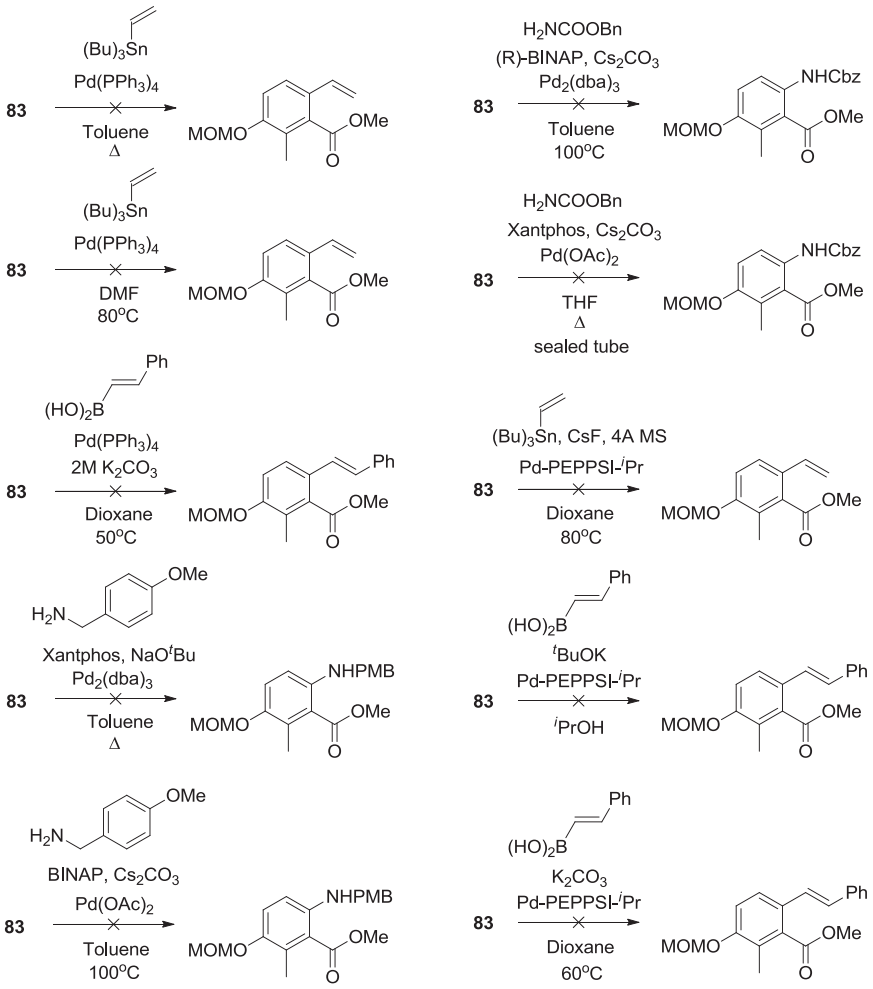

Scheme 24. Attempted Pd-catalyzed cross-coupling reactions with **83**.

Due to the problems encountered with palladium-catalyzed cross-coupling reactions, copper catalysis was employed to prepare the desired synthons. As seen in Scheme 25, it was first proposed that the aryl bromide could be converted to the corresponding nitrile, which would

then be reduced to the corresponding aldehyde (synthons **A** and **D** after oxidation) or aniline (synthons **B** and **C**). Attempted copper-catalyzed cyanations were not successful. Despite different copper sources, additives, solvents and temperatures, starting material remained largely unchanged after these reactions. Based on work done by Paul Knochel, it was proposed that vinylmagnesium bromide could be added to a THF-soluble copper salt CuI•2LiI at low temperature to convert it to the corresponding organocuprate. Next, the aryl bromide would be displaced by the organocuprate to yield the desired vinyl product.[209] Although this reaction was unsuccessful it is believed that the age of the vinyl Grignard reagent may have contributed to its failure. In contrast, a copper-mediated reductive amination of aryl bromide **83** with trimethylsilyl azide yielded aniline **85** in good yield.[210] With a robust reaction to convert the bromide to aniline, efforts were directed at strategies to convert carboxylic acid **84** to an aniline, an important reaction toward synthons A and D.

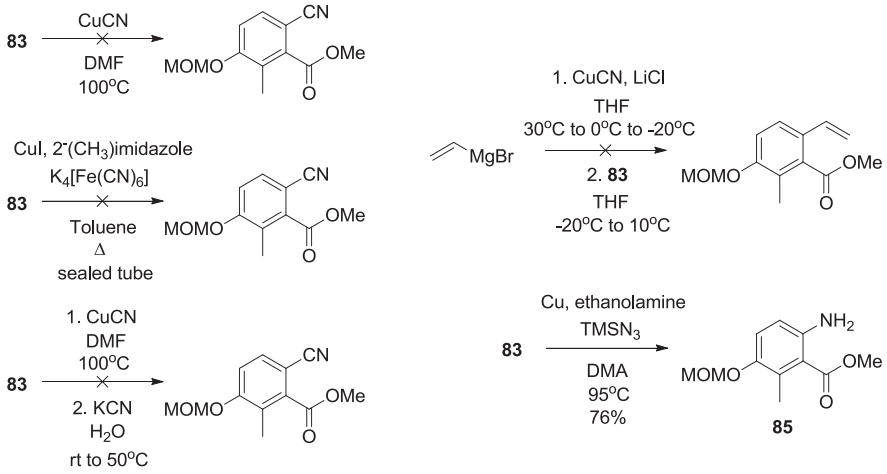

Scheme 25. Attempted copper-catalyzed conversions with **83**.

As part of the original design strategy to use a universal precursor to all synthons, a Curtius rearrangement was planned for conversion of the carboxylic acid to an aniline. Toward this end, several conditions (as seen in Scheme 26), were explored to effect this transformation.

Conversion directly to benzyl carbamate was attempted using a literature protocol that reports a mechanism involving azidoformate formation.[211] Simultaneously, an attempt to quench the isocyanate formed in the first step of the Curtius rearrangement with benzyl alcohol was also attempted toward formation of the Cbz-protected aniline. While the first trial yielded residual starting material, the second reaction demonstrated limited conversion to the desired product, **86**. The modest yield observed for the latter reaction was partially due to a difficult separation.

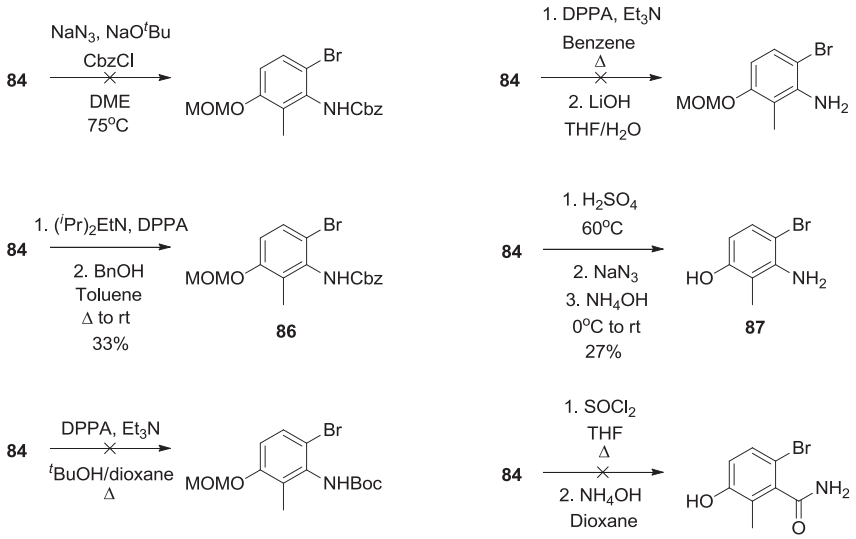

Scheme 26. Curtius and Hofmann rearrangements and Schmidt chemistry with acid **84**.

Next, conversion to the *t*butyloxy carbamate (Boc) was attempted through the addition of *t*butanol to trap the isocyanate intermediate, much like that described previously. This attempt was not as effective and did not yield the desired product. Conversion directly to the aniline was attempted through formation of the isocyanate intermediate, followed by hydrolysis. The basic conditions in the second step were chosen over the often utilized acidic conditions to preserve the methoxy methyl protecting group, however the desired product was not formed. In contrast, harsh Schmidt conditions were employed as another method to elicit conversion from the acid to the aniline, knowing that cleavage of the ether would likely take place as well. Although these

reagents formed aniline **87** in modest yield, the reaction was not reproducible, and unreacted starting material often dominated these conditions. Finally, conversion to the precursor of the Hofmann rearrangement was attempted through conversion to the acid chloride, followed by treatment with ammonium hydroxide. This reaction, however, did not lead to the desired amide and thus, the rearrangement could not be attempted. It was proposed that the environment in which the carboxylic acid resides, ortho to a large and electron-withdrawing bromine, could be contributing to the observed failures. Focus was again returned to replacing the bromine, with intensions of returning to Curtius/Schmidt/Hofmann reactions on a different substrate.

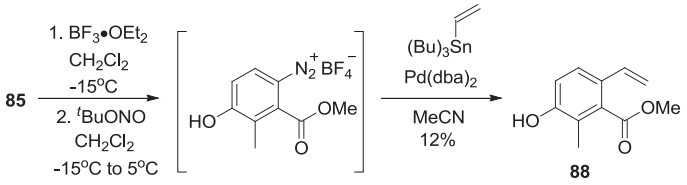

Scheme 27. Conversion to aryl vinyl group via diazonium salt intermediate.

Since conversion of aryl bromide **83** to aniline **85** was robust, this aniline was looked at as a possible handle for the incorporation of desired functionalities. As seen in Scheme 27, the aniline was converted to a diazonium tetrafluoroborate salt through treatment with boron trifluoride etherate, followed by addition of ^{t}Bu nitrite.[212,213] Although the reaction was kept below 5^{o}C throughout, aromatic diazonium tetrafluoroborates are know to be much more stable than typical diazonium salts, and have even been reported stable at room temperature. The conditions employed, while much less harsh than those typically used in diazotization of aromatic amines, were predicted to cleave the methoxy methyl ether *in situ*. After removal of solvents, the crude salt was taken into a Stille coupling using bis(dibenzylideneacetone)-palladium and tributyl(vinyl) tin. Albeit in a very modest yield, conversion of the aryl aniline to vinyl ester **88** was confirmed. It was proposed that liberation of the phenol due to the reaction

conditions may impede the reaction due to consumption of the boron trifluoride etherate or presence of a competing nucleophile. To test this hypothesis, a protecting group that is stable to these conditions was employed.

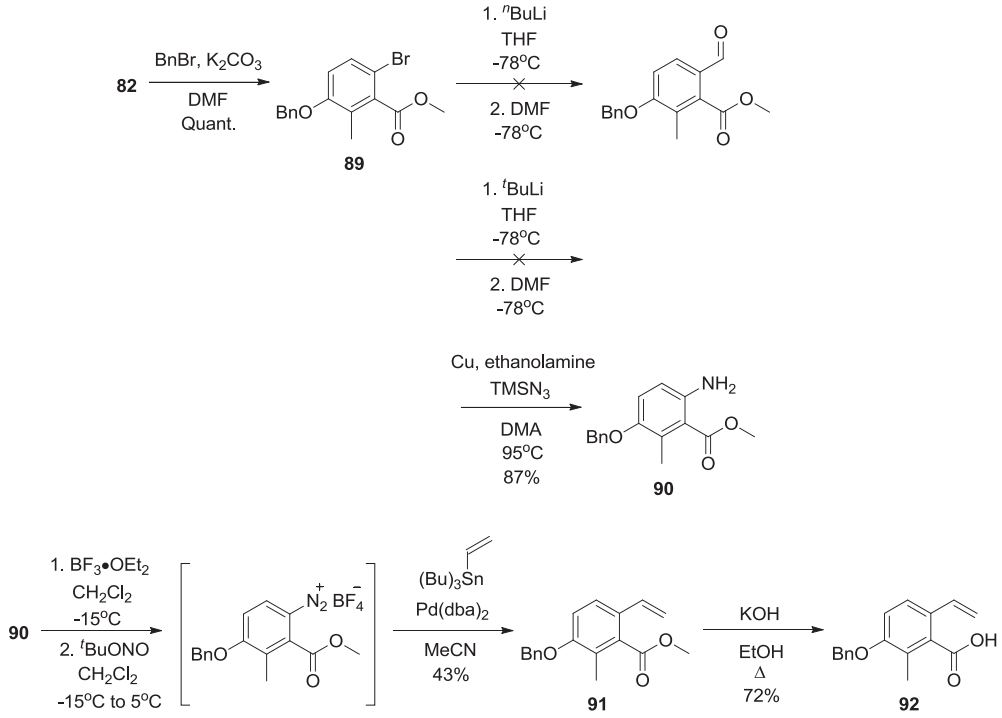

Scheme 28. Preparation of universal intermediate **89**.

A benzyl ether was proposed as a more stable protecting group that would survive the diazotization conditions. As seen in Scheme 28, functionalized phenol **82** was quantitatively protected as the corresponding benzyl ether to afford compound **89**. Like its MOM-protected precursor, this intermediate was labeled as a universal predecessor of the desired synthons. This intermediate allows for direct conversion to the desired benzaldehyde was attempted. Despite trials with both *n*butyllithium and *t*butyllithium, the reaction exhibited the same fate, which was nucleophilic addition of the organolithium base to afford the corresponding ketones. Rather than attempt the same chemical transformations that had failed with the MOM-protected aryl bromide, high-yielding conversion directly to aniline **90** was employed as described

previously.[210] Next, the same conversion from the aniline to vinyl ester through a diazonium tetrafluoroborate salt intermediate was attempted with aniline **90**. As predicted, the benzyl ether survived the required conditions, yielding the desired product **91** in higher yield than previously observed.[212,213] In order to explore conversion to the desired aniline, as required for synthons **A** and **D**, hydrolysis of ester **91** was carried out. Although lithium hydroxide was initially employed to convert to carboxylic acid **92**, these conditions did not work. Just as before, treatment of the ester with a 40% potassium hydroxide solution in refluxing ethanol resulted in conversion to acid **92** in good yield.[207]

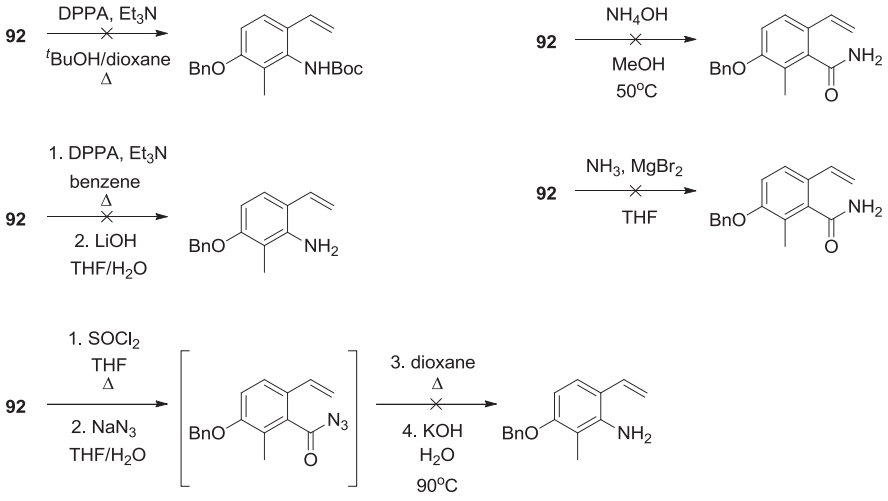

Scheme 29. Attempted Curtius and Hofmann rearrangements on vinyl precursor.

Several of the same conditions as discussed earlier with acid **84** were attempted for conversion of vinyl acid **92** to the corresponding aniline (Scheme 29). As before, conversion to the Boc-protected aniline through trapping of the isocyanate intermediate with *t*butanol was unsuccessful. Likewise, direct conversion to the desired aniline through conventional conditions was also not fruitful. Next, a more lengthy series of steps was employed to furnish the acid chloride, then substitute for the acyl azide, rearrange to the isocyanate and finally hydrolyze to the free aniline. Like the other attempted reactions, this series of transformations did not yield

the desired aniline product. Finally, two different reaction conditions were used toward preparation of the precursor for a Hofmann rearrangement. Unfortunately, neither attempt was successful so this route was not pursued further. While some of the conversions to aniline attempted with the MOM-protected aryl bromide were successful, none with vinyl acid **92** yielded product.

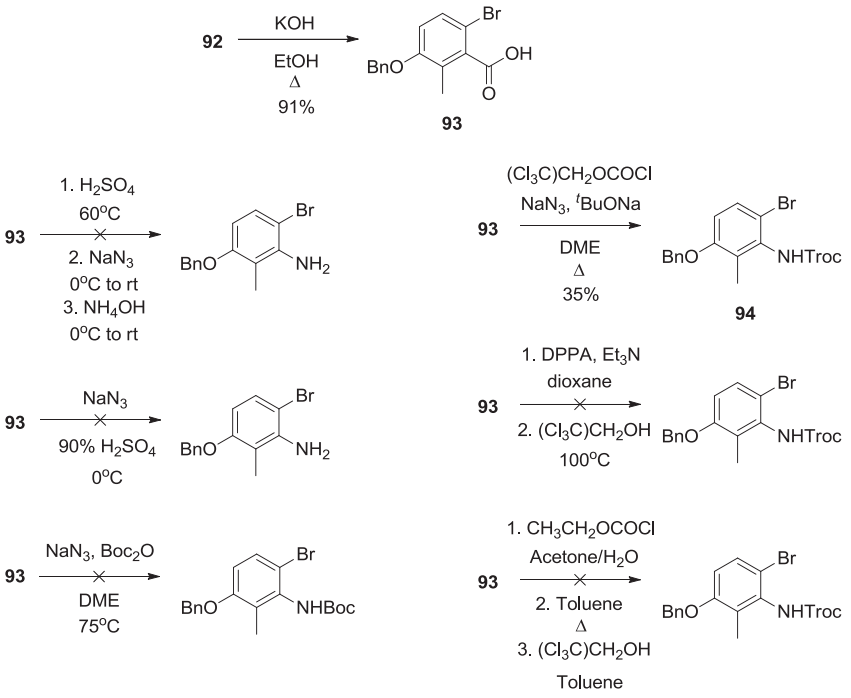

Scheme 30. Attempted Curtius and Schmidt reactions on acid **93**.

It was envisioned that benzyl-protected aryl bromide **89** may be more fruitful than reactions with the corresponding vinyl acid. As seen in Scheme 30, ester **89** was hydrolyzed with a 40% potassium hydroxide solution in refluxing ethanol to yield acid **93** in good yield. Next, the Schmidt chemistry that was somewhat successful with MOM-protected intermediate **84** was employed, but proved to be inconsistent, once again. A slightly different procedure was also tried, involving low temperature (0°C) throughout the course of the reaction, but it too, failed to convert the acid to desired aniline. Next, the opportunity to convert directly to a protected aniline

was once again considered. The same paper that described conversion of the acid to the Cbz-protected aniline through an azidoformate intermediate, also described using di-*tert*-butyl dicarbonate and 2,2,2-trichloroethyl (Troc) chloroformate in place of benzyl chloroformate. Moreover, examples involving an ortho-bromo substituent were included in the discussion.[211] While attempted conversion directly to the Boc-protected aniline was not successful, the Troc-protected aniline **94** was produced in modest yield. Attempts to repeat this reaction on larger scale were unsuccessful, despite changes in order and method of reagent addition, proving it to be an unreliable method for the preparation of the desired synthons. Other attempted methods to prepared Troc-protected aniline **94** included trapping the isocyanate intermediate with 2,2,2-trichloroethanol and preparation of the ethyl anhydride, rearrangement to the isocyanate and another attempt to trap with 2,2,2-trichloroethanol. While the first reaction gave a new undesired side product, the second failed to react at all.

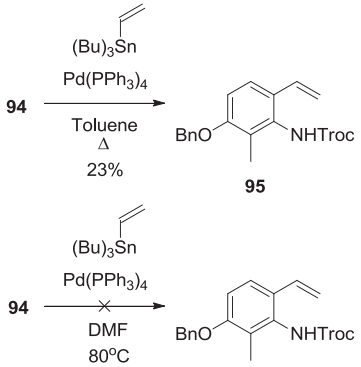

Scheme 31. Endgame toward final functionalized precursor.

Despite its inconsistency, small-scale conversions to protected aniline **94** afforded enough material to carry on toward synthons **A** and **D**. As seen in Scheme 31, an attempted Stille coupling on a small amount of aniline **94** in toluene provided installation of the desired vinyl group in modest yield. In contrast, coupled product **95** was not obtained using the same

conditions when *N*,*N*-dimethylformamide was used as the solvent. A more reproducible route toward synthons **A** and **D** was required to complete its synthesis.

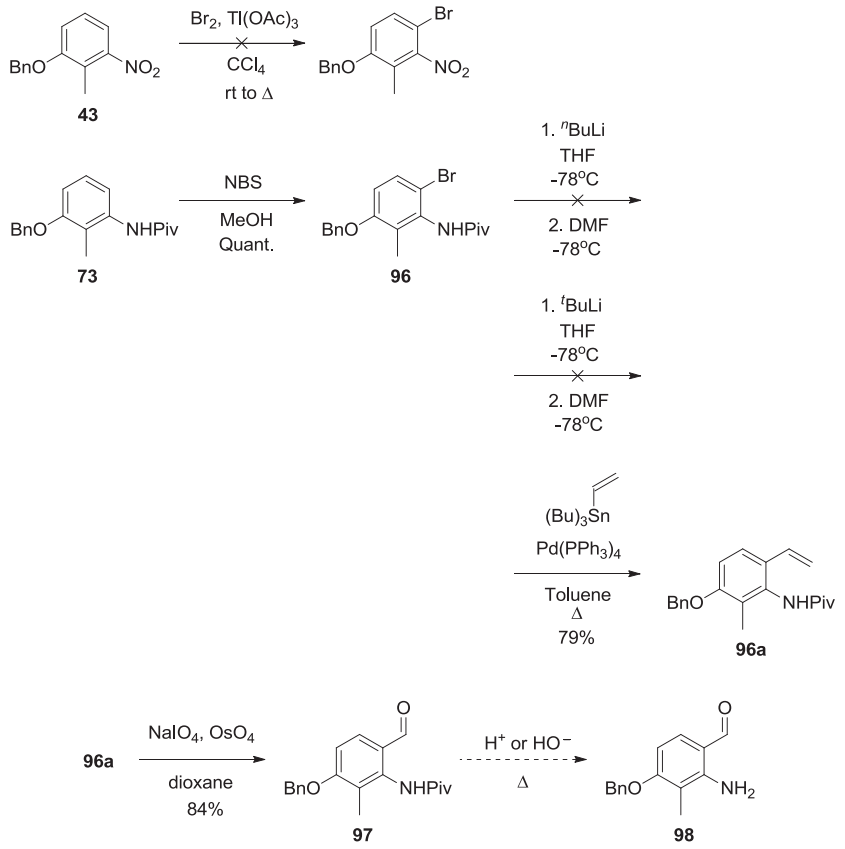

Scheme 32. Bromination and subsequent steps toward synthons **A** and **D**.

As a final attempt to access the desired precursors, bromination of previously prepared intermediates was reconsidered as an option. As shown in Scheme 32, bromination was initially attempted ortho to the nitro group on nitroarene **40**. According to a literature protocol, thallic acetate and bromine were employed to effect the desired transformation, but this method led to multiple brominated products.[214] Diprotected aniline **70**, originally prepared with the goal of executing *ortho*-lithiation, was treated with *N*-bromosuccinimide in methanol, leading to conversion to the desired product in good yield within 15 minutes.[215] Confirmation that the desired regioisomer was obtained through comparison with the spectra associated with the

undesired regioisomer, as prepared before, and through spectral analysis of its own. After ^{1}HNMR, ^{13}CNMR, COSY, HSQC, NOESY and HMBC NMR spectroscopy experiments, namely a correlation between the aromatic proton adjacent to the benzyl ether and the benzylic protons in both COSY and NOESY, it was confirmed that the desired regioisomer was obtained. Next, chemistry that was useful for conversion of the undesired regioisomer to the corresponding benzaldehyde proved unsuccessful for this system. Attempts to convert aryl bromide **96** to the corresponding benzaldehyde **97** using various organolithium bases were not fruitful, leaving only residual starting material as the major reaction component. As an alternative strategy executed by a co-worker, a Stille cross-coupling reaction proved to be a robust method for installation of the vinyl group, which was subsequently oxidized to benzaldehyde **97** using sodium periodate and osmium tetroxide. Finally, cleavage of the pivaloyl group in the presence of the benzyl ether could be accomplished by heating under either acidic or basic conditions to furnish the desired precursor that allows access to synthons **A** and **D**. This common intermediate is pivotal, as it can be used in cyclization reactions to form four of the desired ring systems, as shown back in Scheme 22.

3. Cyclization attempts

With the desired precursors in hand, known cyclization procedures were employed to gain access to the proposed core systems. The quinazoline core (Scheme 33), ester **93** was reduced to the corresponding benzyl alcohol using lithium aluminum hydride to afford compound **99** in nearly quantitative yield. Next, activated manganese oxide was used to oxidize **99** to benzaldehyde **100** in good yield. Finally, cyclization to quinazoline **101**, in modest yield, was accomplished using guanidine hydrochloride in decalin at high temperature.[216]

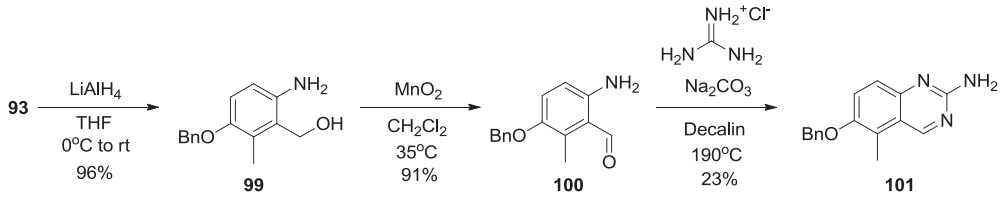

Scheme 33. Synthesis of quinazoline core.

As seen in Scheme 34, several possible routes were attempted toward the 4-(3H)-quinazolinone core. Firstly, using a known procedure, cyanamide (**102**) was converted to chloroformamide hydrochloride and used without further characterization.[217] A mixture of ester **93** and salt **103** were heated at reflux in digylme to yield the desired ring system by crude ^{1}HNMR spectroscopy and mass spectrometry.[218,219]

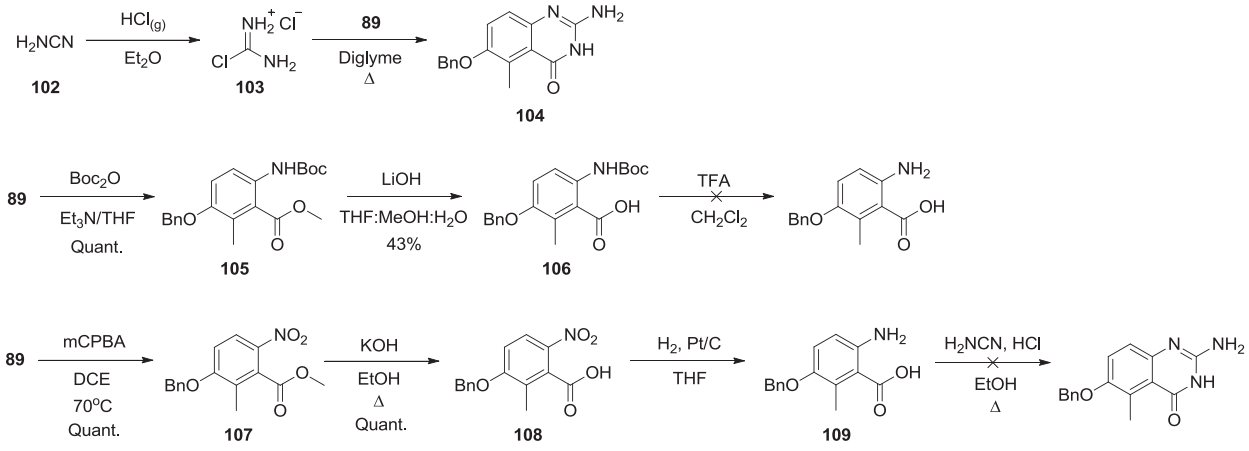

Scheme 34. Synthesis of 4-(3H)-quinazolinone core.

Conversion of aniline **89** to the corresponding acid for use in another 4-(3H)-quinazolinone ring-forming reaction was attempted through two routes. First, the aniline was Boc-protected in quantitative yield, then hydrolyzed to afford acid **105** in modest yield.[220] An attempt to cleave the Boc protecting group using trifluoroacetic acid in methylene chloride was unsuccessful. A second attempt to gain access to this desired precursor began with quantitative oxidation of aniline **89** to nitroarene **107**. Next, 40% potassium hydroxide solution in refluxing ethanol was used to hydrolyze the ester to produce acid **108**.[207] Subsequent reduction of the

nitroarene using platinum on carbon and hydrogen yielded the aniline **109**, which was subjected to cyclization conditions without further purification. Cyanamide and aniline **109** were heated to reflux under acidic conditions, according to literature protocol, but the desired product was not obtained.[221] The strongly acidic conditions at high temperatures likely cleaved the benzyl ether group, leading to undesired competing reactions.

An attempt to employ the conditions used in coumarin ring formation toward synthesis of the 2-quinolone nucleus is shown in Scheme 35. Rather than forming the desired ring system, the reaction conditions led to formation of the product shown in good yield. Although the aniline attacked the eneamine, cyclization to the desired 2-quinolone did not take place.

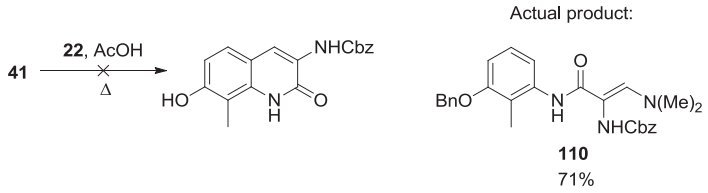

Scheme 35. Efforts toward 2-quinolone core.

A rather straightforward method for synthesizing 4-quinolone derivatives was reported in a recent patent. This method involves heating cyclo-*iso*propylidene malonate with triethylorthoformate for several hours to yield compound **112** (Scheme 36). Dione **112** was carried on without further purification and mixed with aniline **41** in refluxing ethanol to afford intermediate **113** in good yield over two steps. Conjugated dione **113** was cyclized to 4-quinolone in the presence of diphenyl ether and biphenyl over the course of an hour.[222] Although an attempt was made to nitrate 4-quinolone **114**, the desired reaction did not take place.

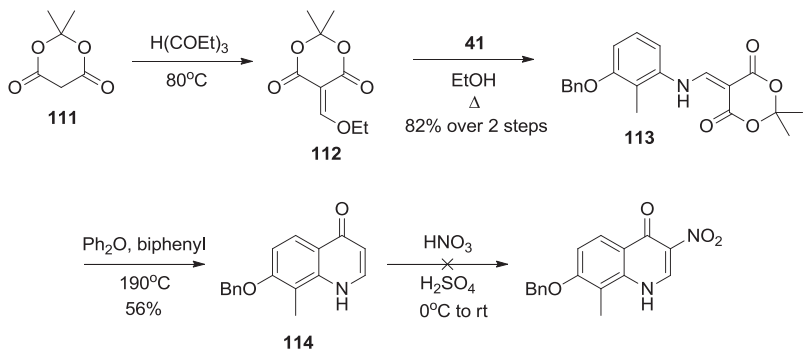

Scheme 36. Efforts toward 4-quinolone system.

Like with the 4-quinolone, a patented procedure was crucial in the development of a route toward the methylated naphthalene core. Following the patented protocol (Scheme 37), naphthol **115** was treated with dimethylamine in the presence of formaldehyde to afford intermediate **116** in nearly quantitative yield within 2 hours. Naphthol **116** was next acetylated, and then sodium borohydride in refluxing ethanol was used to reductively eliminate the dimethylamino group, furnishing the desired methyl substituent.[201] Methylated naphthol **118** was exposed to Mitsunobu conditions to install the desired sugar surrogate, in accordance with modeling studies and toward the final proposed analogues.[193] Next, Buchwald-Hartwig coupling conditions were employed to convert aryl bromide **119** to the corresponding PMB-protected aniline. Although a diverse set of conditions was utilized in an attempt to cleave the PMB group, none proved effective. While the customary oxidative removal using DDQ resulted in a messy mixture of various products, reductive conditions failed completely, leaving predominantly starting material after several days. Since PMB cleavage proved problematic, an alternative route was sought to avoid this transformation.

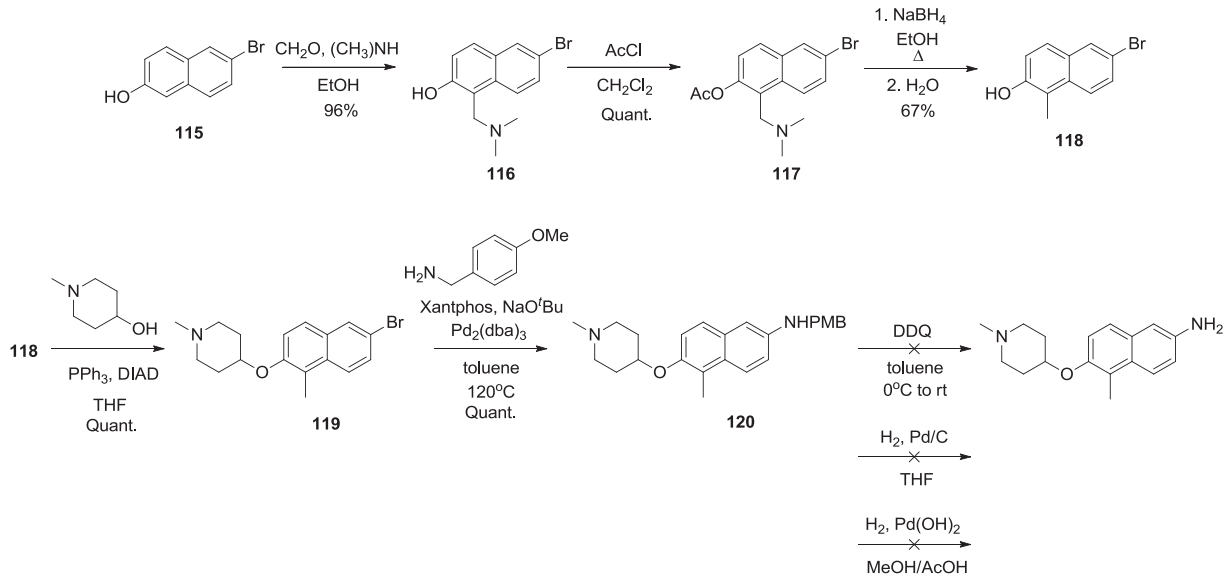

Scheme 37. Efforts toward methylated naphthalene analogues.

As a more unified approach to all desired naphthalene-containing derivatives, allowing the incorporation of various sugars after coupling of desired benzamides, naphthol **118** was protected as the methoxy methyl ether (Scheme 38). Rather than introducing a PMB-protected aniline, it was proposed that chemistry used in constructing the ring system precursors could be applied toward the desired aniline product. To this end, naphthalyl bromide **121** was successfully converted to the corresponding aniline using the copper-mediated reductive amination with trimethylsilyl azide.[210] Next, aniline **122** was readily coupled with either biaryl acid **27** or prenylated acid **126** in the presence of EDCI and pyridine. To explore the potential of sugar attachment to the functionalized biaryl scaffold **123**, the MOM group was cleaved under acidic conditions. Attempted coupling reactions with the *N*-methyl piperidine sugar mimic proved problematic with this late-stage analogue and were not pursued further. Rather, this phenol was envisioned as a handle for noviosylation, leading to two of the four proposed naphthalene-containing derivatives. Intermediate **119** was used as a means toward the piperidine-containing analogues and the copper-mediated reductive amination has since been successfully employed to

access the desired aniline, which can be readily coupled to furnish the last two naphthalene-containing analogues.

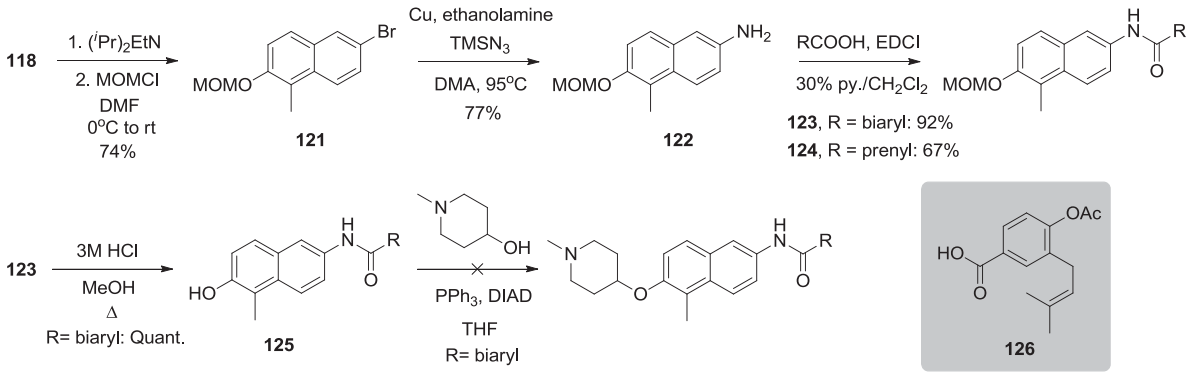

Scheme 38. Late-stage diversification of methylated naphthalene analogues.

With synthon **98** in hand, the four remaining ring systems can be accessed in relatively few steps. As shown in Scheme 39, synthon **98** can be used diazotized and then treated with nitromethane under basic conditions to afford the corresponding phenylhydrazone, which would also exist as its azo tautomer. Exposure to basic conditions, once again, has been reported to induce cyclization to the 3-nitrocinnoline in modest yield.[223] Synthon **98** can also be utilized directly towards the formation of the desired quinoline scaffold. As previously described, freshly prepared methazonic acid and amino benzaldehyde **98** can be condensed in the presence of acid to form the desired 3-nitroquinoline in modest yield.[224] Likewise, common precursor **98** can be heated with ethyl-2-nitroacetate in *N*,*N*-dimethylformamide overnight to form the desired 3-nitro-2-quinolone.[225] Finally, the 3-nitro-4-quinolone scaffold can be accessed from pivaloyl amide **97**. This benzaldehyde can be oxidized to the corresponding carboxylic acid using Pinnick conditions prior to pivaloyl cleavage. Much like the protocol used with the quinoline core, condensation of the amino carboxylic with methazonic acid should yield the phenylhydrazone intermediate, which can be subsequently dehydrated to the desired scaffold using acetic anhydride in the presence of sodium acetate.[226,227]

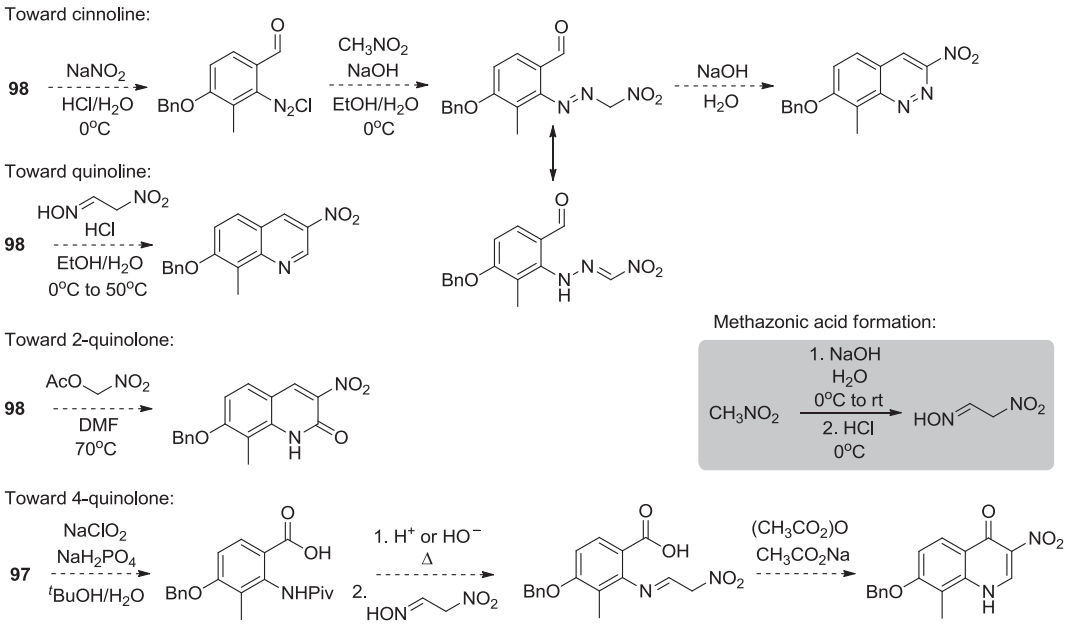

Scheme 39. Proposed preparations of four remaining ring systems.

Through the chemistry developed and shown in Scheme 33 and Scheme 34, the quinazoline and 4-(3H)-quinazolinone core systems can be prepared and coupled to the desired sugars and side chains. Moreover, the synthetic steps developed toward the naphthalene-containing scaffold have enabled the preparation of final analogues with relatively few manipulations. Finally, from key intermediate **98** and its predecessor **97**, these final ring systems can be each be prepared in less than four steps. The proposed intermediate of each core can be easily diversified through sequential coupling of the desired sugars and benzoic acids to afford the final proposed analogues. The desired outcome of these studies is to identify a rationally designed replacement of the coumarin core that manifests equivalent or improved potency over the corresponding coumarin-containing analogue, but lacks its detrimental attributes. Thus, with these final analogues in hand, anti-proliferation assays and subsequent Western blot analyses will examine their potency and specificity for Hsp90, respectively. A potently cytotoxic novobiocin

analogue that lacks a coumarin core will represent a novel contribution to the Hsp90 field and a promising new lead scaffold in the development of *C*-terminal Hsp90 modulators.

V. Conclusion

The studies discussed herein have focused on modifications to the novobiocin coumarin core. Rational design of coumarin cores that mimic GTP resulted in several new potent novobiocin analogues with unique substitution about the coumarin ring system. Likewise, these coumarins inspired the development of other uniquely substituted coumarins and structurally related neuroprotective analogues. Quinoline and naphthalene cores, also examined as part of the initial study, proved that the coumarin core can be replaced with retention of anti-Hsp90 activity. Moreover, these non-coumarin ring systems provided a foundation on which to begin the final study involving the design of other rationally designed coumarin ring surrogates. Overall these research endeavors have elucidated much SAR for the largely unexamined coumarin core of the novobiocin structure, leading to the development of several promising compounds that have moved into advanced studies.

VI. Experimental Protocols

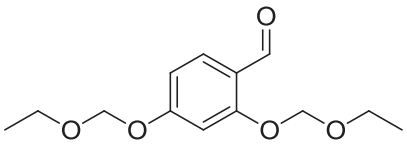

2a

2,4-Bis(ethoxymethoxy)benzaldehyde (2a):[173] *N,N*-diisopropylethylamine (25.3 mL, 145 mmol) was slowly added to 2,4-dihydroxybenzaldehyde (5.00 g, 36.2 mmol) in anhydrous *N,N*-dimethylformamide (100 mL) over 5 min at rt. After 30 min, the solution was cooled to 0°C and chloromethyl ethyl ether (14.2 mL, 145 mmol) was added and the mixture warmed to rt over 12 h. The reaction was quenched by the addition of saturated aqueous NH_4Cl solution and extracted with EtOAc (3 × 50 mL). The combined organic fractions were washed with saturated aqueous NaCl, dried (Na_2SO_4), filtered, and concentrated. The residue was purified via column chromatography (SiO_2, 5:1 → 1:1 Hexane:EtOAc) to give **2a** as a brown amorphous solid (9.10 g, 99%): ^{1}H NMR ($CDCl_3$, 400 MHz) δ 10.34 (d, *J* = 2.4 Hz, 1H), 7.81 (dd, *J* = 8.7, 2.8 Hz, 1H), 6.89 (t, *J* = 2.5 Hz, 1H), 6.74 (s, 1H), 5.34 (d, *J* = 2.8, 2H), 5.28 (d, *J* = 2.8, 2H), 3.81–3.71 (m, 4H), 1.28–1.22 (m, 6H).

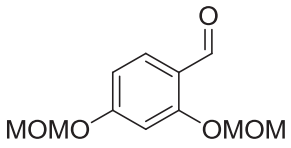

2b

2,4-bis(methoxymethoxy)benzaldehyde (2b).[228] 2,4-dihydroxybenzaldehyde (5.00 g, 36.2 mmol) in anhydrous *N,N*-dimethylformamide (101 mL) was treated with NaH (3.48 g, 145 mmol), portionwise over several minutes at 0°C. After 30 minutes had elapsed, the mixture was cooled to 0°C and methoxy methyl ether (11.0 mL, 145 mmol) was added slowly, and then the mixture was allowed to warm to rt and stir for 12 h. The mixture was quenched with saturated $NaHCO_3$ at 0°C and extracted with ethyl acetate (3 × 50 mL). The combined organic fractions were washed with saturated NaCl, dried (Na_2SO_4), filtered and concentrated. The residue was purified by chromatography (5:1 → 3:1; Hexane:EtOAc) to afford **2b** (6.45 g, 80%) as a white

solid: ^{1}H NMR ($CDCl_3$, 400 MHz) δ ^{1}H NMR ($CDCl_3$, 400 MHz) δ 11.37 (s, 1H), 7.45 (d, J = 8.6 Hz, 1H), 6.65 (dd, J = 8.6, 2.2 Hz, 1H), 6.60 (d, J = 2.0 Hz, 1H), 5.22 (s, 4H), 3.47 (s, 6H).

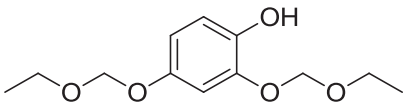

3a

2,4-Bis(ethoxymethoxy)phenol (3a): A solution of **2a** (3.78 g, 12.0 mmol) in anhydrous CH_2Cl_2 (4.0 mL) was slowly added to *m*CPBA (70%) (3.26 g, 13.2 mmol) in anhydrous CH_2Cl_2 (16.3 mL) at 0°C. The resulting solution was warmed to rt, then refluxed for 12 h. After cooling to rt, the resulting solution was washed with saturated aqueous $NaHCO_3$ solution (3 × 20 mL) and 10% aqueous $Na_2S_2O_3$ (30 mL). Combined organic fractions were dried (Na_2SO_4), filtered, and concentrated. The residue was re-dissolved in MeOH (5 mL) and stirred with excess 10% aqueous NaOH for 3 h at rt. The pH was adjusted to 2 with 6M HCl and the solution was extracted with CH_2Cl_2 (3 × 10 mL). Combined organic fractions were dried (Na_2SO_4), filtered, and concentrated to give **3a** as an orange oil (8.21 g, 94%): ^{1}H NMR ($CDCl_3$, 500 MHz) δ 6.89–6.85 (m, 2H), 6.67 (dd, J = 8.8, 2.7 Hz, 1H), 5.81 (d, J = 6.6 Hz, 1H), 5.23 (s, 2H), 5.15 (s, 2H), 3.80–3.73 (m, 4H), 1.29–1.24 (m, 6H); ^{13}C NMR ($CDCl_3$, 125 MHz) δ 151.0, 145.0, 141.5, 115.2, 110.6, 106.0, 94.9, 94.2, 64.8, 64.1, 15.1, 15.1; IR (film) ν_{max} 3362, 2887, 1460, 1286, 1162, 735 cm^{-1}; HRMS (ESI$^+$) *m/z*: [M + Na]$^+$ calcd for $C_{12}H_{18}NaO_5$, 265.1052; found, 265.1045.

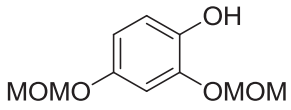

3b

2,4-Bis(methoxymethoxy)phenol (3b):[175] Benzaldehyde **2b** (700 mg, 3.11 mmol) in $CHCl_3$ (1.80 mL) at 0°C was treated with *m*CPBA (70% w/w, 1.61 g, 9.33 mmol). After 10 min, the solution was warmed to rt, then refluxed for 12 h. Upon cooling to rt, the solution was washed with saturated aqueous $NaHCO_3$ (3 × 10 mL), saturated aqueous Na_2SO_3 (20 mL), saturated aqueous NaCl, was dried (Na_2SO_4), filtered, and concentrated. The residue was dissolved in MeOH (5 mL) and stirred with excess triethylamine for 3 h at rt. The solvent was concentrated and the residue purified by column chromatography (SiO_2, 4:1 → 3:1 Hexane:EtOAc) to afford **3b** as a yellow oil (320 mg, 50%): ^{1}H NMR ($CDCl_3$, 400 MHz) δ 6.87 (d, J = 8.9 Hz, 1H), 6.86 (s, 1H), 6.67 (dd, J = 11.5, 2.8 Hz, 1H), 5.21 (s, 2H), 5.11 (s, 2H), 3.54 (s, 3H), 3.50 (s, 3H).

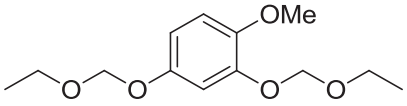

4a

2,4-Bis(ethoxymethoxy)-1-methoxybenzene (4a): Potassium carbonate (14.3 g, 103 mmol) was added to **3a** (2.50 g, 10.3 mmol) in *N,N*-dimethylformamide (103 mL). After 10 min, methyl iodide (6.43 mL, 103 mmol) was added and the solution was heated to reflux for 12 h. Upon cooling to rt, the solution was extracted with EtOAc (3 × 50 mL); combined organic fractions were washed with saturated aqueous NaCl, dried (Na_2SO_4), and concentrated. The residue was purified by column chromatography (SiO_2, 4:1 Hexane:EtOAc) to afford **4a** as a yellow oil (2.40 g, 91%): ^{1}H NMR ($CDCl_3$, 500 MHz) δ 6.87 (d, J = 2.8 Hz, 1H), 6.72 (d, J = 8.9 Hz, 1H), 6.60 (dd, J = 13.3, 1.7 Hz, 1H), 5.18 (s, 2H), 5.07 (s, 2H), 3.76 (s, 3H), 3.72–3.69 (m, 2H), 3.68–3.63 (m, 2H), 1.17–1.13 (m, 6H); ^{13}C NMR ($CDCl_3$, 125 MHz) δ 150.7, 146.2, 143.9, 111.2, 107.9, 105.8, 93.2, 93.0, 63.3, 63.0, 55.4, 14.1, 14.0; IR (film) ν_{max} 2976, 2932, 2899, 2835, 1595, 1508,

1393, 1227, 1153, 1103, 1080, 1009, 847 cm^{-1}; HRMS (ESI^+) *m/z*: $[M + Na]^+$ calcd for $C_{13}H_{20}NaO_5$, 279.1208; found, 279.1181.

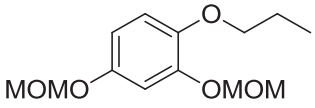

4b

2,4-Bis(methoxymethoxy)-1-propoxybenzene (4b): Potassium carbonate (322 mg, 2.33 mmol) was added to **3b** (50 mg, 0.233 mmol) in *N,N*-dimethylformamide (2.33 mL) at rt. After 10 min, iodopropane (226 μL, 2.33 mmol) was added and the solution was heated to reflux for 12 h. Upon cooling to rt, the solution was extracted with EtOAc (3 × 10 mL); combined organic fractions were washed with saturated aqueous NaCl, dried (Na_2SO_4), filtered, and concentrated. The residue was purified by column chromatography (SiO_2, 5:1 Hexane:EtOAc) to afford **4b** as a yellow oil (36.4 mg, 61%): ^1H NMR (CD_2Cl_2, 400 MHz) δ 6.87 (s, 1H), 6.84 (d, *J* = 2.9 Hz, 1H), 6.68 (dd, *J* = 11.7, 2.8 Hz, 1H), 5.19 (s, 2H), 5.12 (s, 2H), 3.93 (t, *J* = 6.6 Hz, 2H), 3.53 (s, 3H), 3.49 (s, 3H), 1.86–1.78 (m, 2H), 1.06 (t, *J* = 7.5 Hz, 3H); ^{13}C NMR ($CDCl_3$, 125 MHz) δ 150.6, 146.5, 143.8, 113.7, 108.5, 106.6, 94.7, 94.2, 70.3, 55.2, 54.9, 21.6, 9.5; IR (film) ν_{max} 2961, 2826, 1595, 1506, 1400, 1261, 1154, 1013, 1076, 924, 800 cm^{-1}; HRMS (ESI^+) *m/z*: $[M + H]^+$ calcd for $C_{13}H_{20}O_5$, 257.1389; found, 257.1410; $[M + Na]^+$ calcd for $C_{13}H_{20}NaO_5$, 279.1208; found, 279.1165.

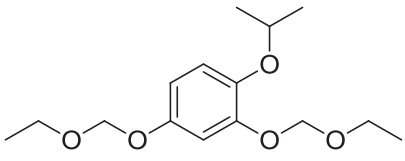

4c

2,4-Bis(ethoxymethoxy)-1-isopropoxybenzene (4c): Potassium carbonate (2.85 g, 20.7 mmol) was added to **3a** (500 mg, 2.07 mmol) in *N,N*-dimethylformamide (4.10 mL) at rt. After

10 min, 2-iodopropane (2.06 mL, 20.7 mmol) was added and the solution was heated to reflux for 12 h. Upon cooling to rt, the solution was extracted with EtOAc (3 × 20 mL); combined organic fractions were washed with saturated aqueous NaCl, dried (Na_2SO_4), filtered, and concentrated. The residue was purified via column chromatography (SiO_2, 5:1 → 1:1 Hexane:EtOAc) to afford **4c** as a yellow oil (0.32 g, 55%): ^{1}H NMR (CD_2Cl_2, 400 MHz) δ 6.87 (s, 1H), 6.86 (d, *J* = 4.9 Hz, 1H), 6.66 (dd, *J* = 11.6, 3.4 Hz, 1H), 5.23 (s, 2H), 5.17 (s, 2H), 4.44–4.38 (m, 1H), 3.83–3.72 (m, 4H), 1.33 (s, 3H), 1.31 (s, 3H), 1.27–1.23 (m, 6H); ^{13}C NMR ($CDCl_3$, 125 MHz) δ 152.4, 149.1, 143.2, 118.6, 109.5, 107.5, 94.4, 93.9, 72.8, 64.3, 64.1, 22.2 (2C), 15.1, 15.1; IR (film) ν_{max} 2976, 1591, 1504, 1528, 1391, 1258, 1217, 1107, 1011, 847 cm^{-1}; HRMS (ESI$^+$) *m/z*: $[M + H]^+$ calcd for $C_{15}H_{24}O_5$, 285.1702; found, 285.1746; $[M + Na]^+$ calcd for $C_{15}H_{24}NaO_5$, 307.1522; found, 307.1310.

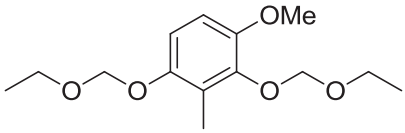

5a

1,3-Bis(ethoxymethoxy)-4-methoxy-2-methylbenzene (5a): A solution of **4a** (632 mg, 2.27 mmol) in anhydrous THF (1.94 mL) was added dropwise to a solution of ^{n}BuLi (2.5 M in hexanes, 1.48 mL, 3.70 mmol) in anhydrous THF (1.62 mL) at rt. After 1 h, the solution was cooled to -78° C and methyl iodide (620 μL, 9.87 mmol) was added. The resulting solution was warmed to rt over 12 h, and the reaction was quenched by the addition of saturated aqueous NH_4Cl. Water (5 mL) was added and the solution was extracted with CH_2Cl_2 (3 × 10 mL). Combined organic fractions were dried (Na_2SO_4), filtered, and concentrated. The residue was purified via column chromatography (SiO_2, 8:1 → 5:1 Hexane:EtOAc) to afford **5a** as a yellow

oil (353 mg, 53%): ^{1}H NMR ($CDCl_3$, 500 MHz) δ 6.74 (d, *J* = 9.0 Hz, 1H), 6.60 (d, *J* = 9.0 Hz, 1H) 5.10 (s, 2H), 5.05 (s, 2H), 3.78 (q, *J* = 7.1 Hz, 2H), 3.72 (s, 3H), 3.67 (q, *J* = 7.1 Hz, 2H), 2.14 (s, 3H), 1.18–1.15 (m, 6H); ^{13}C NMR ($CDCl_3$, 125 MHz) δ 149.1, 146.5, 121.7, 109.0, 108.4, 96.2, 93.0, 64.3, 63.1, 55.1, 28.7, 14.2, 14.1, 8.8; IR (film) ν_{max} 2918, 2359, 1487, 1260, 1248, 1082, 1055, 945, 798 cm^{-1}; HRMS (ESI^{+}) *m/z*: [M + Na]$^{+}$ calcd for $C_{14}H_{22}NaO_5$, 293.1365; found, 293.1357.

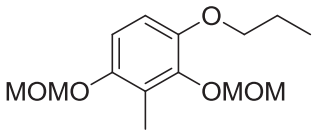

5b

1,3-Bis(methoxymethoxy)-2-methyl-4-propoxybenzene (5b): A solution of **4b** (165 mg, 0.64 mmol) in anhydrous THF (520 μL) was added dropwise to a solution of ^{n}BuLi (2.5 M in hexanes, 390 μL, 0.97 mmol) in anhydrous THF (420 μL) at rt. After 1 h, the solution was cooled to -78° C and methyl iodide (160 μL, 2.58 mmol) was added. The resulting solution was warmed to rt over 12 h, and the reaction was quenched by the addition of saturated aqueous NH_4Cl. Water (5 mL) was added and the solution was extracted with CH_2Cl_2 (3 × 10 mL). Combined organic fractions were dried (Na_2SO_4), filtered, and concentrated. The residue was purified via column chromatography (SiO_2, 6:1 Hexane:EtOAc) to afford **5b** as a yellow oil (166 mg, 95%): ^{1}H NMR ($CDCl_3$, 500 MHz) δ 6.66 (d, *J* = 9.0 Hz, 1H), 6.60 (d, *J* = 9.0 Hz, 1H), 5.02 (s, 2H), 5.00 (s, 2H), 3.80–3.77 (m, 2H), 3.49 (s, 3H), 3.47 (s, 3H), 2.14 (d, *J* = 7.1 Hz, 3H), 1.73–1.69 (m, 2H), 0.94 (t, *J* = 7.5 Hz, 3H); ^{13}C NMR ($CDCl_3$, 125 MHz) δ 148.5, 148.5, 147.3, 145.6, 126.7, 123.0, 112.8, 110.8, 110.4, 99.2, 57.7, 57.6, 21.2, 10.9, 10.0; IR (film) ν_{max} 2957, 2924, 2853, 1738, 1597, 1487, 1468, 1391, 1335, 1231, 1157, 974, 798 cm^{-1}; HRMS (ESI^{+}) *m/z*: [M + H]$^{+}$ calcd for $C_{14}H_{23}O_5$, 271.1545; found, 271.1558.

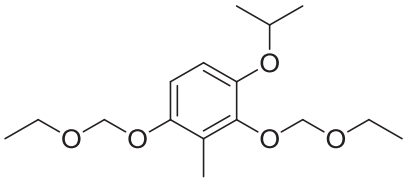

5c

1,3-Bis(ethoxymethoxy)-4-isopropoxy-2-methylbenzene (5c): A solution of **4c** (190 mg, 0.67 mmol) in anhydrous THF (530 μL) was added dropwise to a solution of ^{n}BuLi (2.5 M in hexanes, 410 μL, 1.00 mmol) in anhydrous THF (440 μL) at rt. After 1 h, the solution was cooled to -78° C and methyl iodide (170 μL, 2.67 mmol) was added. The resulting solution was warmed to rt over 12 h, and the reaction was quenched by the addition of saturated aqueous NH_4Cl. Water (5 mL) was added and the solution was extracted with CH_2Cl_2 (3 × 10 mL). Combined organic fractions were dried (Na_2SO_4), filtered, and concentrated. The residue was purified via column chromatography (SiO_2, 6:1 Hexane:EtOAc) to afford **5c** as a yellow oil (157 mg, 79%): ^{1}H NMR ($CDCl_3$, 500 MHz) δ 6.70 (d, *J* = 9.0 Hz, 1H), 6.61 (d, *J* = 9.0 Hz, 1H), 5.10 (s, 2H), 5.08 (s, 2H),4.34 (quintet, *J* = 6.1 Hz, 1H), 3.78 (q, *J* = 7.1 Hz, 2H), 3.67 (q, *J* = 7.1 Hz, 2H), 2.13 (s, 3H), 1.23 (d, *J* = 6.1 Hz, 6H), 1.24–1.15 (m, 6H); ^{13}C NMR ($CDCl_3$, 125 MHz) δ 150.3, 146.6, 145.3, 122.7, 113.7, 110.1, 97.3, 94.0, 71.5, 65.4, 64.2, 29.4, 22.2, 15.2, 15.2, 9.9; IR (film) ν_{max} 2924, 2853, 2359, 2339, 1591, 1483, 1113, 1057, 974 cm^{-1}; HRMS (ESI$^+$) *m/z*: [M + H]$^+$ calcd for $C_{16}H_{27}O_5$, 299.1858; found, 299.1909.

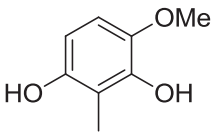

6a

4-Methoxy-2-methylbenzene-1,3-diol (6a): A solution of **5a** (910 mg, 3.37 mmol) in MeOH (28.0 mL) at rt was treated dropwise with 3M HCl (9.00 mL, 26.9 mmol), then heated to reflux

for 1 h. Water (30 mL) was added and the solution was extracted with EtOAc (3 × 30 mL). Combined organic fractions were washed with saturated aqueous NaCl, dried (Na_2SO_4), filtered, and concentrated. The residue was purified via column chromatography (SiO_2, 6:1 Hexane:EtOAc) to afford **6a** as a red amorphous solid (509 mg, 98%): ^{1}H NMR (Acetone-d_6, 500 MHz) δ 7.68 (s, 1H), 7.24 (s, 1H), 6.60 (d, J = 11 Hz, 1H), 6.29 (d, J = 11 Hz, 1H), 3.74 (s, 3H), 2.09 (s, 3H); ^{13}C NMR ($CDCl_3$, 125 MHz) δ 144.7, 142.1, 139.7, 115.6, 110.2, 108.6, 55.6, 7.6; IR (film) ν_{max} 3583, 2920, 2359, 1616, 1259, 1090, 1020, 798 cm^{-1}. HRMS (ESI$^+$) *m/z*: [M + Na]$^+$ calcd for $C_8H_{11}NaO_3$, 177.0528; found, 177.0522.

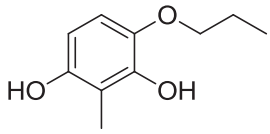

6b

2-Methyl-4-propoxybenzene-1,3-diol (6b): A solution of **5b** (580 mg, 2.15 mmol) in MeOH (17.9 mL) was treated dropwise with 3M HCl (630 μL, 17.2 mmol), then heated to reflux for 1 h. Water (20 mL) was added and the solution was extracted with EtOAc (3 × 20 mL). Combined organic fractions were washed with saturated aqueous NaCl, dried (Na_2SO_4), and concentrated to afford **6b** as a red amorphous solid (387 mg, 99%). ^{1}H NMR ($CDCl_3$, 500 MHz) δ 6.51 (d, J = 8.7 Hz, 1H), 6.21 (d, J = 8.6 Hz, 1H), 5.74 (s, 1H), 4.36 (s, 1H), 3.87–3.85 (m, 2H), 2.09 (s, 3H), 1.75–1.71 (m, 2H), 0.96 (t, J = 7.5 Hz, 3H); ^{13}C NMR ($CDCl_3$, 125 MHz) δ 147.5, 143.8, 139.0, 109.8, 108.4, 103.8, 70.2, 21.6, 9.5, 7.3; IR (film) ν_{max} 3520, 3360, 2966, 2880, 2359, 2341, 1636, 1236, 1068, 785, 750 cm^{-1}. HRMS (ESI$^+$) *m/z*: [M + H]$^+$ calcd for $C_{10}H_{15}O_3$, 183.1021; found, 183.0950.

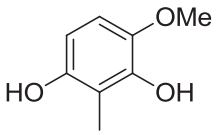

6c

4-methoxy-2-methylbenzene-1,3-diol (6c): A solution of **5c** (157 mg, 0.53 mmol) in MeOH (4.40 mL) at rt was treated dropwise with 3M HCl (1.40 mL, 4.21 mmol), then heated to reflux for 1 h. Water (5 mL) was added and the solution was extracted with EtOAc (3 × 10 mL). Combined organic fractions were washed with saturated aqueous NaCl, dried (Na_2SO_4), filtered, and concentrated to afford **6c** as a red amorphous solid (95 mg, 99%): ^{1}H NMR ($CDCl_3$, 500 MHz) δ 6.54 (d, *J* = 8.7 Hz, 1H), 6.21 (d, *J* = 8.7 Hz, 1H), 5.78 (s, 1H), 4.37–4.32 (m, 1H), 2.09 (s, 3H), 1.25 (d, *J* = 6.1 Hz, 6H); ^{13}C NMR ($CDCl_3$, 125 MHz) δ 147.7, 144.9, 137.5, 110.8, 109.8, 104.0, 71.7, 21.3 (2C); IR (film) ν_{max} 3526, 2974, 2924, 2853, 1717, 1607, 1475, 1238, 1113, 1067, 928, 887, 791 cm^{-1}. HRMS (ESI$^+$) *m/z*: $[M + H]^+$ calcd for $C_{10}H_{11}O_3$, 183.1021; found, 183.0963.

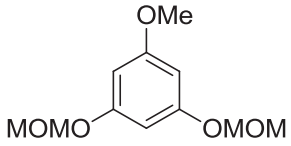

8

1-Methoxy-3,5-bis(methoxymethoxy)benzene (8): *N,N*-diisopropylethylamine (3.15 mL, 18.1 mmol) was added to 5-methoxybenzene-1,3-diol (634 mg, 4.52 mmol) in anhydrous *N,N*-dimethylformamide (12.6 mL) over 5 min at rt. After 30 min, the solution was cooled to 0°C, methoxy methylchloride (3.02 mL, 18.1 mmol) was added, and the solution was warmed to rt over 12 h. The reaction was quenched by the addition of saturated aqueous $NaHCO_3$ at 0°C and extracted with EtOAc (3 × 10 mL). Combined organic fractions were washed with saturated aqueous NaCl, dried (Na_2SO_4), filtered, and concentrated. The residue was purified via column

chromatography (SiO_2, 6:1→ 4:1 Hexane:EtOAc) to afford **8** as a yellow amorphous solid (441 mg, 43%): ^{1}H NMR ($CDCl_3$, 500 MHz) δ 6.29 (t, *J* = 2.2 Hz, 1H), 6.21 (d, *J* = 2.2 Hz, 2H), 5.07 (s, 4H), 3.69 (s, 3H), 3.40 (s, 6H); ^{13}C NMR ($CDCl_3$, 125 MHz) δ 161.394, 159.0 (2C), 97.2, 96.2 (2C), 94.5 (2C), 56.1, 55.4 (2C); IR (film) ν_{max} 2997, 2955, 2903, 2827, 1601, 1475, 1400, 1215, 1194, 1146, 1032, 991, 924, 829, 685 cm^{-1}; HRMS (ESI$^+$) *m/z*: $[M + Na]^+$ calcd for $C_{11}H_{16}NaO_5$, 251.0895; found, 251.0910.

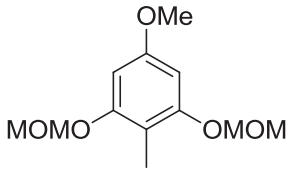

9

5-methoxy-1,3-bis(methoxymethoxy)-2-methylbenzene (9): A solution of **8** (441 mg, 1.93 mmol) in anhydrous THF (1.55 mL) was added dropwise to a solution of ^{n}BuLi (2.5 M in hexanes, 1.16 mL, 2.90 mmol) in anhydrous THF (1.26 mL) at rt. After 1 h, the solution was cooled to -78° C and methyl iodide (480 μL, 7.73 mmol) was added. The resulting solution was warmed to rt over 12 h, and the reaction was quenched by the addition of saturated aqueous NH_4Cl. Water (5 mL) was added and the solution was extracted with CH_2Cl_2 (3 × 10 mL). Combined organic fractions were dried (Na_2SO_4), filtered, and concentrated. The residue was purified via column chromatography (SiO_2, 6:1 → 4:1; Hexane:EtOAc) to afford **9** as a yellow oil (314 mg, 67%): ^{1}H NMR ($CDCl_3$, 500 MHz) δ 6.38 (d, *J* = 2.2 Hz, 1H), 6.24 (d, *J* = 2.1 Hz, 1H), 5.08 (d, *J* = 3.6 Hz, 2H), 5.06 (d, *J* = 2.6 Hz, 2H), 3.72 (s, 3H), 3.40 (s, 6H), 1.97 (s, 3H); ^{13}C NMR ($CDCl_3$, 125 MHz) δ 160.3, 157.8, 155.4, 108.2, 93.9, 93.8, 93.7, 92.9, 55.0, 55.0, 54.6, 7.0; IR (film) ν_{max} 2953, 2934, 2905, 1597, 1497, 1396, 1215, 1144, 1126, 1074, 1059,

1028, 922, 822 cm^{-1}; HRMS (ESI^+) *m/z*: $[M + H]^+$ calcd for $C_{12}H_{19}O_5$, 243.1233; found, 243.1223.

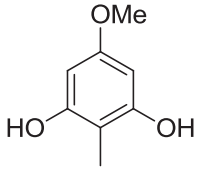

10

5-Methoxy-2-methylbenzene-1,3-diol (10): A solution of **9** (314 mg, 1.30 mmol) in MeOH (10.8 mL) at rt was treated dropwise with 3M HCl (3.46 mL, 10.3 mmol), then heated to reflux for 1 h. Water (11 mL) was added and the solution was extracted with EtOAc (3 × 15 mL). Combined organic fractions were washed with saturated aqueous NaCl, dried (Na_2SO_4), filtered, and concentrated to afford **10** as a red amorphous solid (177 mg, 99%): ^1H NMR ($CDCl_3$, 500 MHz) δ 8.17 (s, 1H), 6.09 (d, *J* = 1.6 Hz, 1H), 6.04 (s, 1H), 3.67 (d, *J* = 9.9 Hz, 3H), 2.08 (d, *J* = 4.1 Hz, 3H); ^{13}C NMR ($CDCl_3$, 125 MHz) δ 160.3, 157.8, 155.4, 108.4, 93.9, 93.8, 55.0, 7.0; IR (film) ν_{max} 3445, 2924, 2853, 2359, 2332, 1653, 1636, 1456, 1080, 1022, 798, 669 cm^{-1}; HRMS (ESI^+) *m/z*: [\M + H]$^+$ calcd for $C_8H_{11}O_3$, 309.1338 found, 309.1332.

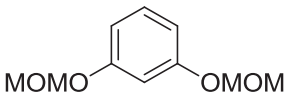

12

1,3-Bis(methoxymethoxy)benzene (12):[229] Sodium hydride (872 mg, 36.3 mmol) was added to resorcinol (1.00 g, 9.08 mmol) in anhydrous *N,N*-dimethylformamide (25.4 mL) at 0°C. After 30 min, methoxy methylchloride (2.76 mL, 36.3 mmol) was added and the resulting solution was warmed to rt over 12 h. The reaction was cooled to 0°C, quenched by the addition of saturated aqueous $NaHCO_3$, and extracted with EtOAc (3 × 30 mL). Combined organic fractions were washed with saturated aqueous NaCl, dried (Na_2SO_4), filtered, and concentrated. The residue

was purified via column chromatography (SiO_2, 4:1 Hexane:EtOAc) to afford **12** as a yellow oil (1.75 g, 97%): ^{1}H NMR ($CDCl_3$, 400 MHz) δ 7.25–7.20 (m, 1H), 6.80 (d, J = 2.3 Hz, 1H), 6.75 (dd, J = 8.2, 2.4 Hz, 2H), 5.20 (s, 4H), 3.51 (s, 6H).

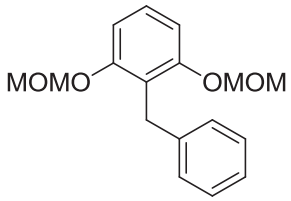

13

2-Benzyl-1,3-bis(methoxymethoxy)benzene (13): A solution of **12** (500 mg, 2.52 mmol) in anhydrous THF (2.02 mL) was added dropwise to a solution of ^{n}BuLi (2.5 M in hexanes, 1.51 mL, 3.78 mmol) in anhydrous THF (1.65 mL) at rt. After 1 h, the solution was cooled to -40°C and benzyl bromide (1.22 mL, 10.10 mmol) was added. The resulting solution was warmed to rt over 12 h, and the reaction was quenched by the addition of saturated aqueous NH_4Cl. Water (5 mL) was added and the solution was extracted with CH_2Cl_2 (3 × 10 mL). Combined organic fractions were dried (Na_2SO_4), filtered, and concentrated. The residue was purified via column chromatography (SiO_2, 4:1; Hexane:EtOAc) to afford **13** as a yellow oil (214 mg, 30%): ^{1}H NMR ($CDCl_3$, 500 MHz) δ 7.17 (d, J = 7.9 Hz, 2H), 7.17–7.12 (m, 2H), 7.06–7.02 (m, 2H), 6.71 (d, J = 8.3 Hz, 2H), 5.09 (s, 4H), 4.00 (s, 2H), 3.29 (s, 6H); ^{13}C NMR ($CDCl_3$, 125 MHz) δ 155.9 (2C), 141.6, 128.5 (2C), 128.0 (2C), 127.5, 125.4, 119.4, 107.7 (2C), 94.3 (2C), 56.0 (2C), 29.1; IR (film) ν_{max} 2953, 2930, 1595, 1470, 1452, 1254, 1153, 1097, 1043, 941, 922, 727, 698 cm^{-1}; HRMS (ESI$^+$) *m/z*: $[M + Na]^+$ calcd for $C_{17}H_{20}NaO_4$, 311.1259; found, 311.1201.

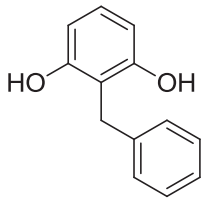

14

2-Benzylbenzene-1,3-diol (14):[230] A solution of **13** (214 mg, 0.74 mmol) in MeOH (6.20 mL) was treated dropwise with 3M HCl (0.22 mL, 5.92 mmol), then heated to reflux for 1 h. Water (10 mL) was added and the solution was extracted with EtOAc (3 × 15 mL). Combined organic fractions were washed with saturated aqueous NaCl, dried (Na_2SO_4), and concentrated to afford **14** as a red amorphous solid (149 mg, 99%). ^{1}H NMR ($CDCl_3$, 400 MHz) δ 7.31 (d, J = 6.6 Hz, 4H), 7.25–7.19 (m, 1H), 7.01 (t, J = 8.1 Hz, 1H), 6.44 (d, J = 8.1 Hz, 2H), 4.82 (s, 2H), 4.09 (s, 2H).

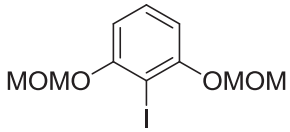

15

2-Iodo-1,3-bis(methoxymethoxy)benzene (15): *n*-Butyllithium (^{n}BuLi, 2.5M in hexanes, 0.22 mL, 0.56 mmol) was added to a solution of **12** (100 mg, 0.50 mmol) in anhydrous THF (790 μL) at 0°C. After 5 min, iodine (141 mg, 0.56 mmol) in anhydrous THF (320 μL) was added. After 2 h at rt, the reaction was quenched via dropwise addition of MeOH and the solvent was concentrated. Water (5 mL) was added and the solution was extracted with EtOAc (3 × 10 mL). Combined organics were washed with saturated aqueous $Na_2S_2O_3$, saturated aqueous NaCl, dried (Na_2SO_4), filtered, and concentrated to afford **15** as a brown oil (129 mg, 79%): ^{1}H NMR ($CDCl_3$, 100 MHz) δ 7.25–7.18 (m, 1H), 6.79–6.71 (m, 2H), 5.27 (s, 2H), 5.18 (s, 2H), 3.54 (s, 3H), 3.50 (s, 3H); ^{13}C NMR ($CDCl_3$, 125 MHz) δ 160.3, 160.2, 130.2, 108.2 (2C), 93.9, 93.8,

74.0, 55.0 (2C); IR (film) ν_{max} 2953, 2924, 2853, 1458, 1377 cm^{-1}. HRMS (ESI^+) *m/z*: $[M + H]^+$ calcd for $C_{10}H_{14}IO_4$, 324.9937; found, 325.0054.

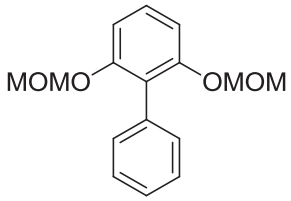

16

2,6-Bis(methoxymethoxy)biphenyl (16): Anhydrous toluene (2.0 mL) was added to a flask charged with tris(dibenzylideneacetone)dipalladium (56.3 mg, 0.062 mmol), dicyclohexyl(2',6'-dimethoxybiphenyl-2-yl)phosphine (50.5 mg, 0.12 mmol), phenylboronic acid (281 mg, 2.31 mmol), and potassium phosphate (979 mg, 4.61 mmol) at rt. After 15 min, a solution of **15** (500 mg, 1.54 mmol) in anhydrous toluene (1.0 mL) was added and the resulting solution was heated to reflux for 12 h. Upon cooling to rt, ether was added, the solution was filtered through SiO_2 and concentrated to give **16** as a colorless amorphous solid (418 mg, 99%): ^1H NMR ($CDCl_3$, 500 MHz) δ 7.35–7.28 (m, 2H), 7.28–7.25 (m, 2H), 7.18–7.15 (m, 2H), 6.83 (d, *J* = 8.3 Hz, 2H), 4.96 (s, 4H), 3.24 (s, 6H); ^{13}C NMR ($CDCl_3$, 125 MHz) δ 155.3, 155.0, 134.3, 130.8, 129.5, 128.7, 128.0, 127.6, 126.8, 122.6, 109.4 (2C), 94.9 (2C), 56.0 (2C); IR (film) ν_{max} 2955, 2928, 2901, 2359, 2341, 1587, 1466, 1439, 1400, 1244, 1153, 1099, 1080, 1041, 922, 764, 733, 700 cm^{-1}; HRMS (ESI^+) *m/z*: $[M + Na]^+$ calcd for $C_{16}H_{18}NaO_4$, 297.1103; found, 297.1052.

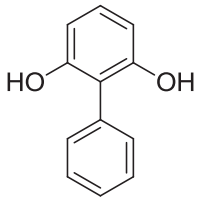

17

Biphenyl-2,6-diol (17):[231] A solution of **16** (400 mg, 1.46 mmol) in MeOH (12.0 mL) at rt was treated dropwise with 3M HCl (430 μL, 11.7 mmol), then heated to reflux for 1 h. Water (15 mL) was added and the solution was extracted with EtOAc (3 × 20 mL). Combined organic fractions were washed with saturated aqueous NaCl, dried (Na_2SO_4), filtered, and concentrated to afford **17** as an orange amorphous solid (269 mg, 99%): ^{1}H NMR ($CDCl_3$, 400 MHz) δ 7.60 (d, *J* = 7.6 Hz, 2H), 7.53–7.49 (m, 1H), 7.46–7.44 (m, 2H), 7.18 (t, *J* = 8.2 Hz, 1H), 6.62 (d, *J* = 8.2 Hz, 2H), 4.84 (s, 1H), 4.83 (s, 1H).

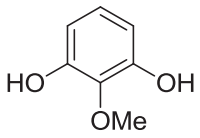

19

2-Methoxybenzene-1,3-diol (19):[232] Lithium carbonate (281 mg, 1.98 mmol) was added to pyrogallol (100 mg, 0.79 mmol) in *N,N*-dimethylformamide (3.0 mL) at rt. After 5 min, methyl iodide (130 μL, 1.98 mmol) was added and the resulting solution was heated to 50°C for 48 h. Upon cooling to rt, water (20 mL) was added and the solution was extracted with EtOAc (3 × 20 mL). Combined organic fractions were dried (Na_2SO_4), filtered, and concentrated. The residue was purified via column chromatography (SiO_2, 5:1 → 1:1 Hexane:EtOAc) to afford **19** as a colorless amorphous solid (44.2 mg, 34%): ^{1}H NMR ($CDCl_3$, 400 MHz) δ 6.89 (td, *J* = 8.0, 0.9 Hz, `H), 6.53 (dd, *J* = 8.2, 0.8 Hz, 2H), 5.83 (bs, 2H), 3.90 (s, 3H).

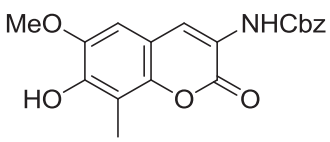

23a

Benzyl 7-hydroxy-6-methoxy-8-methyl-2-oxo-2*H*-chromen-3-ylcarbamate (23a): A solution of **6a** (183 mg, 1.19 mmol) and eneamine **22**[102] (331 mg, 1.19 mmol) in glacial acetic

acid (7.40 mL) was heated to reflux for 40 h. Upon cooling to rt, the solution was extracted with EtOAc (3 × 20 mL); combined organic fractions were dried (Na_2SO_4), filtered, and concentrated. The residue was purified via column chromatography (SiO_2, 100:1 CH_2Cl_2:Acetone) to afford **23a** as a yellow amorphous solid (195 mg, 46%): ^{1}H NMR ($CDCl_3$, 400 MHz) δ 8.27 (s, 1H), 7.54 (s, 1H), 7.43–7.37 (m, 4H), 6.77 (s, 1H), 6.07 (s, 1H), 5.25 (s, 2H), 3.96 (s, 3H), 2.37 (s, 3H); ^{13}C NMR ($CDCl_3$, 125 MHz) δ 159.0, 153.3 (2C), 145.7, 144.1, 144.0, 135.7, 128.7, 128.5, 128.2 (2C), 122.5, 121.6, 112.1, 111.6, 104.5, 67.4, 56.3, 8.2; IR (film) ν_{max} 2910, 2359, 2339, 1693, 1537, 1354, 1209, 1078, 1024 cm^{-1}; HRMS (ESI$^+$) *m/z*: $[M + Na]^+$ calcd for $C_{19}H_{17}NNaO_6$, 378.0954; found, 378.0936.

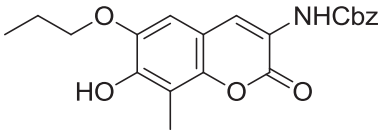

23b

Benzyl 7-hydroxy-8-methyl-2-oxo-6-propoxy-2*H*-chromen-3-ylcarbamate (23b): A solution of **6b** (390 mg, 2.14 mmol) and eneamine **22** (596 mg, 2.14 mmol) in glacial acetic acid (13.4 mL) was heated to reflux for 36 h. Upon cooling to rt, the precipitated yellow solid was collected by filtration, washed with water, recrystallized from MeOH/water, and extracted with EtOAc (3 × 20 mL). Combined organic fractions were washed with saturated aqueous NaCl, dried (Na_2SO_4), filtered, and concentrated. The residue was purified via column chromatography (SiO_2, 100:1 CH_2Cl_2:Acetone) and recrystallized from MeOH/water to afford **23b** as a yellow amorphous solid (278 mg, 34%): ^{1}H NMR (CD_2Cl_2, 400 MHz) δ 8.26 (s, 1H), 7.56 (s, 1H), 7.47–7.38 (m, 5H), 6.84 (s, 1H), 6.28 (s, 1H), 5.25 (s, 2H), 4.09 (t, *J* = 6.6 Hz, 2H), 2.36 (s, 3H), 1.93–1.88 (m, 2H), 1.10 (t, *J* = 7.4 Hz, 3H); ^{13}C NMR ($CDCl_3$, 125 MHz) δ 158.0, 152.2, 144.9, 142.9, 142.3, 134.6, 129.0, 127.6, 127.5 (2C), 127.2 (2C), 121.5, 120.5, 110.9, 110.5, 104.4,

69.8, 66.3, 21.4, 9.4, 7.1; IR (film) ν_{max} 2957, 2920, 2851, 2359, 2341, 1693, 1537, 1358, 1277, 1080, 1024, 910 cm^{-1}; HRMS (ESI^+) *m/z*: $[M + H]^+$ calcd for $C_{21}H_{22}NO_6$, 384.1447; found, 384.1447.

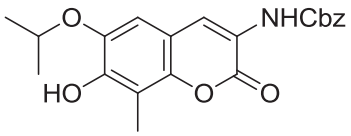

23c

Benzyl 7-hydroxy-6-isopropoxy-8-methyl-2-oxo-2*H*-chromen-3-ylcarbamate (23c): A solution of **6c** (142 mg, 0.78 mmol) and eneamine **22** (217 mg, 0.78 mmol) in glacial acetic acid (4.90 mL) was heated to reflux for 40 h. Upon cooling to rt, the solution was extracted with EtOAc (3 × 10 mL); combined organic fractions were dried (Na_2SO_4), filtered, and concentrated. The residue was purified via column chromatography (SiO_2, 40:1 CH_2Cl_2:Acetone) to afford **23c** as a yellow amorphous solid (159 mg, 53%): ^1H NMR (CD_2Cl_2, 400 MHz) δ 8.26 (s, 1H), 7.56 (s, 1H), 7.44–7.38 (m, 5H), 6.85 (s, 1H), 6.31 (s, 1H), 5.25 (s, 2H), 4.66 (quintet, *J* = 6.1 Hz, 1H), 2.35 (s, 3H), 1.42 (d, *J* = 6.0 Hz, 6H); ^{13}C NMR ($CDCl_3$, 125 MHz) δ 159.1, 154.9, 146.7, 143.9 (2C), 142.0, 135.7, 128.7 (2C), 128.5 128.2 (2C), 122.6 (2C), 111.6, 107.0, 72.3, 67.4, 22.1 (2C), 8.2; IR (film) ν_{max} 3400, 2924, 2853, 2359, 1817, 1699, 1524, 1412, 1354, 1300, 1221, 1204, 1113, 1076, 1022, 824 cm^{-1} ; HRMS (ESI^+) *m/z*: $[M + H]^+$ calcd for $C_{21}H_{22}NO_6$, 384.1447; found, 384.1452.

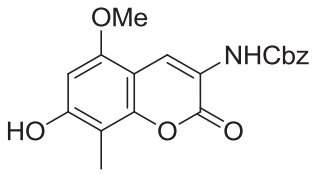

23d

Benzyl 7-hydroxy-5-methoxy-8-methyl-2-oxo-2*H*-chromen-3-ylcarbamate (23d): A solution of **10** (251 mg, 1.63 mmol) and eneamine **22** (680 mg, 2.44 mmol) in glacial acetic acid (10.2 mL) was heated to reflux for 40 h. Upon cooling to rt, the solution was extracted with EtOAc (3 × 15 mL); combined organic fractions were dried (Na_2SO_4), filtered, and concentrated. The residue was purified via column chromatography (SiO_2, 40:1 → 20:1; CH_2Cl_2:Acetone) to afford **23d** as a yellow amorphous solid (204 mg, 35%): ^{1}H NMR (CD_2Cl_2, 400 MHz) δ 8.48 (s, 1H), 7.46–7.38 (m, 6H), 6.38 (s, 1H), 5.25 (s, 2H), 5.15 (s, 1H), 3.87 (s, 3H), 2.23 (s, 3H); ^{13}C NMR ($CDCl_3$, 125 MHz) δ 159.1, 155.8, 154.3, 153.2, 149.8, 137.0, 128.7, 128.6, 128.6, 128.2, 128.2, 109.3, 109.0, 108.5, 105.6, 96.9, 70.8, 60.2, 7.3; IR (film) ν_{max} 3406, 2935, 2837, 1713, 1670, 1607, 1529, 1501, 1364, 1242, 1101, 1051, 991, 966, 735 cm^{-1}; HRMS (ESI$^+$) *m/z*: [M + Na]$^+$ calcd for $C_{19}H_{17}NNaO_6$, 378.0954; found, 378.0974.

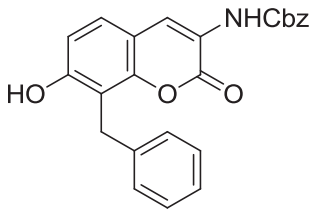

23e

Benzyl 8-benzyl-7-hydroxy-2-oxo-2*H*-chromen-3-ylcarbamate (23e): A solution of **14** (115 mg, 0.57 mmol) and eneamine **22** (160 mg, 0.57 mmol) in glacial acetic acid (4.00 mL) was heated to reflux for 40 h. Upon cooling to rt, the solution was extracted with EtOAc (3 × 10 mL); combined organic fractions were dried (Na_2SO_4), filtered, and concentrated. The residue was purified via column chromatography (SiO_2, 100:1; CH_2Cl_2:Acetone), followed by recrystallization from MeOH to afford **23e** as an orange amorphous solid (296 mg, 48%): ^{1}H NMR (CD_2Cl_2, 400 MHz) δ 8.29 (s, 1H), 7.53 (s, 1H), 7.46–7.38 (m, 4H), 7.37–7.27 (m, 4H), 7.23–7.19 (m, 2H), 7.01 (t, *J* = 8.1 Hz, 1H), 6.86 (d, *J* = 8.4 Hz, 1H), 6.46 (d, *J* = 8.1 Hz, 1H),

5.25 (s, 2H), 4.25 (s, 2H), 4.06 (s, 1H); ^{13}C NMR ($CDCl_3$, 125 MHz) δ 157.7, 154.3, 153.9, 152.2, 148.0, 137.9, 134.5, 127.6, 127.6, 127.6, 127.6, 127.5, 127.3, 127.2, 127.4, 126.6, 125.4, 125.3, 121.4, 120.4, 114.0, 112.6, 66.5, 27.5; IR (film) ν_{max} 3381, 2957, 2928, 2359, 2341, 1693, 1607, 1526, 1466, 1454, 1383, 1366, 1219, 1204, 1076, 1045, 764, 737, 700 cm^{-1}; HRMS (ESI$^+$) *m/z*: $[M + H]^+$ calcd for $C_{24}H_{20}NO_5$, 402.1341; found, 402.1341.

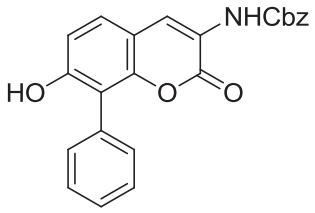

23f

Benzyl 7-hydroxy-2-oxo-8-phenyl-2*H*-chromen-3-ylcarbamate (23f): A solution of **17** (400 mg, 2.15 mmol) and eneamine **22** (598 mg, 2.15 mmol) in glacial acetic acid (14.3 mL) was heated to reflux for 40 h. Upon cooling to rt, the solution was extracted with EtOAc (3 × 30 mL); combined organic fractions were dried (Na_2SO_4), filtered, and concentrated. The residue was purified via column chromatography (SiO_2, 100:1; CH_2Cl_2:Acetone), then recrystallized from MeOH to afford **23f** as an orange amorphous solid (264 mg, 27%): ^{1}H NMR ($CDCl_3$, 500 MHz) δ 8.25 (s, 1H), 7.51–7.48 (m, 2H), 7.43–7.40 (m, 2H), 7.35–7.29 (m, 8H), 6.94 (d, *J* = 8.6 Hz, 1H), 5.16 (s, 2H); ^{13}C NMR ($CDCl_3$,125 MHz) δ 158.5 (2C), 154.3, 153.2, 147.7, 135.6, 130.9, 130.6, 130.5, 129.8, 129.4, 129.2 (2C), 128.7 (2C), 128.6, 128.3, 127.8, 122.2, 121.6, 113.3, 113.5, 67.5; IR (film) ν_{max} 3398, 2957, 2926, 2854, 1815, 1699, 1601, 1524, 1383, 1366, 1308, 1215, 1045, 1009, 764, 750, 698 cm^{-1}; HRMS (ESI$^+$) *m/z*: $[M + H]^+$ calcd for $C_{24}H_{18}NO_5$, 388.1185; found, 388.1214.

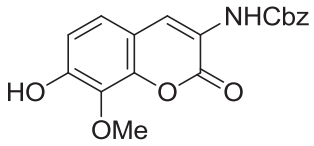

23g

Benzyl 7-hydroxy-8-methoxy-2-oxo-2*H*-chromen-3-ylcarbamate (23g): A solution of **19** (1.10 g, 7.86 mmol) and eneamine **22** (2.18 g, 7.86 mmol) in glacial acetic acid (60.0 mL) was heated to reflux for 90 h. Upon cooling to rt, the solution was extracted with EtOAc (3 × 50 mL); combined organic fractions were washed with saturated aqueous NaCl, dried (Na_2SO_4), filtered, and concentrated. The residue was purified via column chromatography (SiO_2, 11:1; Hexane:EtOAc → EtOAc) then recrystallized from MeOH/water to afford **23g** as a colorless amorphous solid (207 mg, 7.7%): ^{1}H NMR ($CDCl_3$, 400 MHz) δ 8.30 (s, 1H), 7.50 (s, 1H), 7.43–7.36 (m, 5H), 7.13 (d, *J* = 8.6 Hz, 1H), 6.97 (d, *J* = 7.9 Hz, 1H), 6.04 (s, 1H), 5.21 (s, 2H), 4.13 (s, 3H); ^{13}C NMR (Acetone-d_6, 100 MHz) δ 157.3, 153.3, 151.5 (2C), 144.1, 136.5, 134.4, 128.4 (2C), 128.1, 128.0 (2C), 122.7, 121.6, 113.6, 113.2, 66.7, 60.7; IR (film) ν_{max} 2920, 2851, 2405, 2357, 1707, 1605, 1522, 1458, 1385, 1364, 1275, 1259, 1213, 1088, 1047, 750 cm^{-1}; HRMS (ESI$^+$) *m/z*: $[M + Na]^+$ calcd for $C_{18}H_{15}NNaO_6$, 364.0797; found, 364.0776.

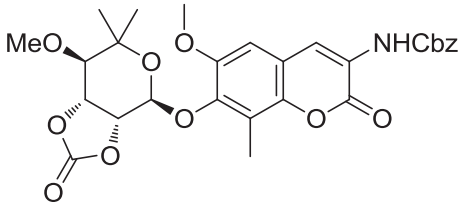

25a

Benzyl 6-methoxy-7-((3*aR*,4*S*,7*R*,7*aR*)-7-methoxy-6,6-dimethyl-2-oxotetrahydro-3*aH*-[1,3]dioxolo[4,5-*c*]pyran-4-yloxy)-8-methyl-2-oxo-2*H*-chromen-3-ylcarbamate (25a): Boron trifluoride etherate (5.30 μL, 0.042 mmol) was added to **23a** (50.0 mg, 0.14 mmol) and

(3*aR*,4*S*,7*R*,7*aR*)-7-methoxy-6,6-dimethyl-2-oxo-tetrahydro-3*aH*-[1.3]dioxolo[4,5-*c*]pyran-4-yl 2,2,2-trichloroacetimidate (171 mg, 0.47 mmol) in anhydrous CH_2Cl_2 (3.00 mL). After stirring at rt for 14 h, triethylamine (150 μL) was added and the solvent was concentrated. The residue was purified via column chromatography (SiO_2, 40:1 CH_2Cl_2:Acetone) to give **25a** as a colorless foam (74.0 mg, 95%): ^{1}H NMR (CD_2Cl_2, 400 MHz) δ 8.29 (s, 1H), 7.64 (s, 1H), 7.47–7.39 (m, 5H), 6.91 (s, 1H), 5.52 (d, *J* = 3.4 Hz, 1H), 5.26 (s, 2H), 5.23 (dd, *J* = 8.4, 3.5 Hz, 1H), 4.95 (t, *J* = 8.2 Hz, 1H), 3.92 (s, 3H), 3.60 (s, 3H), 3.33 (d, *J* = 8.0 Hz, 1H), 2.42 (s, 3H), 1.38 (s, 3H), 1.33 (s, 3H); ^{13}C NMR ($CDCl_3$, 125 MHz) δ 157.6, 152.7, 152.1, 148.1, 144.8, 141.8, 134.5, 127.8, 127.7, 127.5, 127.3, 122.3, 120.2, 119.8, 115.1. 109.6, 105.2, 98.3, 82.0, 77.1, 66.5, 65.5, 59.4, 57.4, 55.1, 26.0, 20.9, 8.9; IR (film) ν_{max} 2957, 2928, 2854, 2359, 2341, 1817, 1709, 1522, 1464, 1389, 1371, 1205, 1174, 1111, 1072, 1034, 957, 800 cm^{-1}; HRMS (ESI$^+$) *m/z*: $[M + H]^+$ calcd for $C_{28}H_{30}NO_{11}$, 556.1819; found, 556.1822.

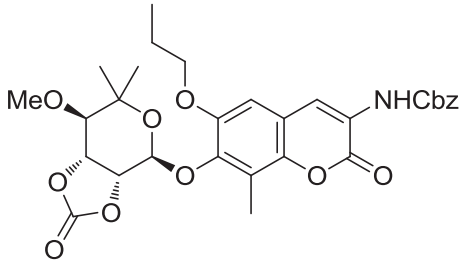

25b

Benzyl 7-((3*aR*,4*S*,7*R*,7*aR*)-7-methoxy-6,6-dimethyl-2-oxotetrahydro-3*aH*-[1,3]dioxolo[4,5-*c*]pyran-4-yloxy)-8-methyl-2-oxo-6-propoxy-*2H*-chromen-3-ylcarbamate (25b): Boron trifluoride etherate (16.7 μL, 0.13 mmol) was added to **23b** (170 mg, 0.44 mmol) and (3*aR*,4*S*,7*R*,7*aR*)-7-methoxy-6,6-dimethyl-2-oxo-tetrahydro-3*aH*-[1.3]dioxolo[4,5-*c*]pyran-4-yl 2,2,2-trichloroacetimidate (643 mg, 1.77 mmol) in anhydrous CH_2Cl_2 (11.1 mL). After stirring at rt for 48 h, triethylamine (150 μL) was added and the solvent was concentrated. The

residue was purified via column chromatography (SiO_2, 100:1 → 40:1 CH_2Cl_2:Acetone) to give **25b** as a colorless foam (246 mg, 95%): ^{1}H NMR ($CDCl_3$, 500 MHz) δ 8.17 (s, 1H), 7.35–7.27 (m, 5H), 6.84 (s, 1H), 5.96 (s, 1H), 5.15 (s, 2H), 4.99 (d, *J* = 7.5 Hz, 1H), 4.59 (d, *J* = 9.7 Hz, 1H), 4.23 (d, *J* = 9.6 Hz, 1H), 3.97 (t, *J* = 6.6 Hz, 1H), 3.82–3.75 (m, 2H), 3.37 (s, 3H), 1.84–1.79 (m, 2H), 1.51 (s, 3H), 1.41 (s, 3H), 1.18 (s, 3H), 1.00 (t, *J* = 7.5 Hz, 3H); ^{13}C NMR ($CDCl_3$, 125 MHz) δ 157.8, 154.3, 152.2, 151.8, 146.7, 144.2, 142.9, 134.6, 127.8, 127.6, 127.5, 127.5, 127.2, 121.0, 120.9, 111.1, 105.3, 101.7, 91.6, 85.7, 82.8, 80.0, 69.8, 58.1, 54.8, 28.3, 28.2, 22.4, 21.3, 9.4; IR (film) ν_{max} 2961, 2939, 2906, 2359, 2341, 1811, 1757, 1726, 1522, 1445, 1371, 1267, 1175, 1113, 1086, 825, 768 cm^{-1}; HRMS (ESI$^+$) *m/z*: $[M + Na]^+$ calcd for $C_{30}H_{33}NNaO_{11}$, 606.1952; found, 606.1950.

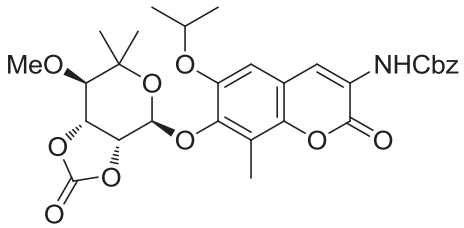

25c

Benzyl 6-isopropoxy-7-((3*aR*,4*S*,7*R*,7*aR*)-7-methoxy-6,6-dimethyl-2-oxotetrahydro-3*aH*-[1,3]dioxolo[4,5-*c*]pyran-4-yloxy)-8-methyl-2-oxo-*2H*-chromen-3-ylcarbamate (25c): Boron trifluoride etherate (1.30 μL, 0.010 mmol) was added to **23c** (13.0 mg, 0.034 mmol) and (3*aR*,4*S*,7*R*,7*aR*)-7-methoxy-6,6-dimethyl-2-oxo-tetrahydro-3*aH*-[1.3]dioxolo[4,5-*c*]pyran-4-yl 2,2,2-trichloroacetimidate (83.0 mg, 0.23 mmol) in anhydrous CH_2Cl_2 (1.30 mL). After stirring at rt for 1.5 h, triethylamine (150 μL) was added and the solvent was concentrated. The residue was purified via column chromatography (SiO_2, 40:1 CH_2Cl_2:Acetone) to give **25c** as a colorless foam (19.0 mg, 95%): ^{1}H NMR ($CDCl_3$, 500 MHz) δ 8.17 (s, 1H), 7.51 (s, 1H), 7.35 (s, 1H), 7.34–7.33 (m, 4H), 6.74 (s, 1H), 5.54 (dd, *J* = 9.2, 1.2 Hz, 1H), 5.16 (s, 2H), 4.87–4.84 (m, 1H),

4.73 (dd, *J* = 7.9, 1.9 Hz, 1H), 4.51 (quintet, *J* = 6.0 Hz, 1H), 3.52 (s, 3H), 3.28 (d, *J* = 4.8 Hz, 1H), 2.33 (s, 3H), 1.80–1.77 (m, 6H), 1.30 (s, 3H), 1.27 (s, 3H); ^{13}C NMR ($CDCl_3$, 125 MHz) δ 161.6, 158.6, 153.2 153.1, 147.1, 146.8, 142.5, 135.5, 128.7, 128.6, 128.3, 123.3, 121.4, 121.1, 116.2, 108.6, 99.4, 83.1, 79.9, 76.1, 74.7, 72.2, 68.0, 60.5, 27.1, 25.6, 21.9, 21.6, 21.0, 10.1; IR (film) ν_{max} 2955, 2922, 2853, 2359, 2339, 1819, 1711, 1520, 1464, 1375, 1171, 1111, 1034, 962, 822, 766 cm^{-1}; HRMS (ESI$^+$) *m/z*: $[M + H]^+$ calcd for $C_{30}H_{34}NO_{11}$, 584.2132; found, 584.2111.

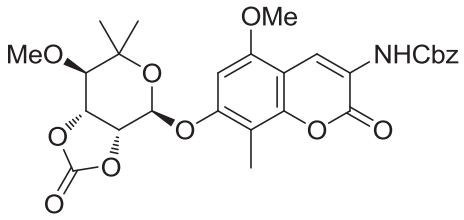

25d

Benzyl 5-methoxy-7-((3*aR*,4*R*,7*R*,7*aR*)-7-methoxy-6,6-dimethyl-2-oxotetrahydro-3*aH*-[1,3]dioxolo[4,5-*c*]pyran-4-yloxy)-8-methyl-2-oxo-*2H*-chromen-3-ylcarbamate (25d): Boron trifluoride etherate (18.5 μL, 0.15 mmol) was added to **23d** (174 mg, 0.49 mmol) and (3*aR*,4*S*,7*R*,7*aR*)-7-methoxy-6,6-dimethyl-2-oxo-tetrahydro-3*aH*-[1.3]dioxolo[4,5-*c*]pyran-4-yl 2,2,2-trichloroacetimidate (621 mg, 1.71 mmol) in anhydrous CH_2Cl_2 (11.0 mL). After stirring at rt for 14 h, triethylamine (150 μL) was added and the solvent was concentrated. The residue was purified via column chromatography (SiO_2, 40:1 CH_2Cl_2:Acetone) to give **25d** as a colorless foam (200 mg, 74%): ^{1}H NMR ($CDCl_3$, 500 MHz) δ 8.49 (s, 1H), 7.34–7.27 (m, 5H), 6.67 (s, 1H), 6.60 (s, 1H), 5.69 (s, 2H), 5.16 (d, *J* = 5.3 Hz, 1H), 4.89 (t, *J* = 7.8 Hz, 1H), 4.63 (dd, *J* = 7.9, 2.4 Hz, 1H), 3.83 (s, 3H), 3.37 (s, 3H), 3.15 (d, *J* = 8.0 Hz, 1H), 2.16 (s, 3H), 2.16 (s, 3H), 2.12 (s, 3H); ^{13}C NMR ($CDCl_3$, 125 MHz) δ 158.9, 156.0, 155.2, 154.2, 153.1 (2C), 149.4, 135.7, 128.7 (2C), 128.5, 128.2 (2C), 120.8, 117.4, 106.6, 105.4, 94.6, 94.1, 82.9, 67.4, 60.6, 60.6, 56.1, 56.0, 22.2, 22.0, 7.9; IR (film) ν_{max} 2955, 2924, 2853, 1817, 1713, 1526, 1209, 1105,

1072, 1034, 976, 808 cm^{-1}; HRMS (ESI^+) *m/z*: $[M + H]^+$ calcd for $C_{28}H_{30}NO_{11}$, 556.1819; found, 556.1826.

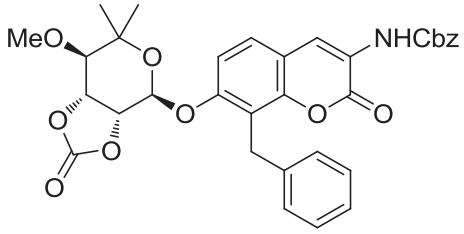

25e

Benzyl 8-benzyl-7-((3*aR*,4*R*,7*R*,7*aR*)-7-methoxy-6,6-dimethyl-2-oxotetrahydro-3*aH*-[1,3]dioxolo[4,5-*c*]pyran-4-yloxy)-2-oxo-*2H*-chromen-3-ylcarbamate (25e): Boron trifluoride etherate (7.80 μL, 0.062 mmol) was added to **23e** (80.0 mg, 0.21 mmol) and (3*aR*,4*S*,7*R*,7*aR*)-7-methoxy-6,6-dimethyl-2-oxo-tetrahydro-3*aH*-[1.3]dioxolo[4,5-*c*]pyran-4-yl 2,2,2-trichloroacetimidate (299 mg, 0.83 mmol) in anhydrous CH_2Cl_2 (5.20 mL). After stirring at rt for 48 h, triethylamine (150 μL) was added and the solvent was concentrated. The residue was purified via column chromatography (SiO_2, 40:1 CH_2Cl_2:Acetone) to give **25e** as a colorless foam (47.0 mg, 39%): ^1H NMR ($CDCl_3$, 500 MHz) δ 8.22 (s, 1H), 7.46 (s, 1H), 7.35–7.27 (m, 5H), 7.17–7.06 (m, 5H), 6.86 (d, *J* = 10 Hz, 1H), 6.01 (d, *J* = 10 Hz, 1H), 5.65 (d, *J* = 1.6 Hz, 1H), 5.23 (s, 2H), 5.16 (s, 2H), 4.77–4.70 (m, 1H), 4.10 (s, 1H), 3.50 (s, 3H), 3.28 (s, 1H), 3.16 (d, *J* = 7.4 Hz, 1H), 1.25 (s, 3H), 1.18 (s, 3H); ^{13}C NMR ($CDCl_3$, 125 MHz) δ 155.1, 153.2 (2C), 153.1, 148.6 (2C), 139.6 (2C), 128.7, 128.6 (2C), 128.4 (2C), 128.3 (2C), 128.3 (2C), 126.5, 126.2, 123.1, 122.4, 121.7, 117.6, 114.9, 111.5, 94.7, 82.8, 67.6, 60.6 (2C), 29.7, 27.6, 21.9; IR (film) ν_{max} 2926, 2854, 2359, 2341, 1811, 1709, 1607, 1522, 1456, 1381, 1366, 1259, 1209, 1171, 1078, 1049, 968, 766, 700 cm^{-1}; HRMS (ESI^+) *m/z*: $[M + H]^+$ calcd for $C_{33}H_{32}NO_{10}$, 602.2026; found, 602.2053.

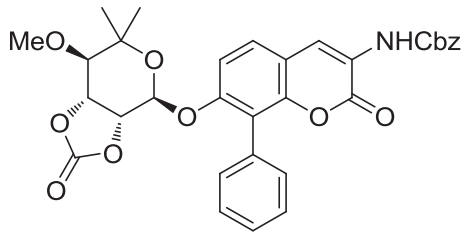

25f

Benzyl 7-((3*aR*,4*R*,7*R*,7*aR*)-7-methoxy-6,6-dimethyl-2-oxotetrahydro-3*aH*-[1,3]dioxolo[4,5-*c*]pyran-4-yloxy)-2-oxo-8-phenyl-*2H*-chromen-3-ylcarbamate (25f): Boron trifluoride etherate (14.6 μL, 0.12 mmol) was added to **23f** (155 mg, 0.39 mmol) and (3*aR*,4*S*,7*R*,7*aR*)-7-methoxy-6,6-dimethyl-2-oxo-tetrahydro-3*aH*-[1.3]dioxolo[4,5-*c*]pyran-4-yl 2,2,2-trichloroacetimidate (560 mg, 1.55 mmol) in anhydrous CH_2Cl_2 (9.70 mL). After stirring at rt for 48 h, triethylamine (150 μL) was added and the solvent was concentrated. The residue was purified via column chromatography (SiO_2, 100:1 → 40:1 CH_2Cl_2:Acetone) to give **25f** as a colorless foam (225 mg, 99%): ^{1}H NMR (CD_2Cl_2, 400 MHz) δ 8.37 (s, 1H), 7.75–7.73 (m, 2H), 7.60–7.36 (m, 10H), 7.32 (d, *J* = 8.8 Hz, 1H), 5.77 (d, *J* = 1.7 Hz, 1H), 5.26 (s, 2H), 4.76–4.68 (m, 1H), 4.36–4.28 (m, 1H), 3.56 (s, 3H), 3.28 (d, *J* = 7.2 Hz, 1H), 1.37 (s, 3H), 1.31 (s, 3H); ^{13}C NMR ($CDCl_3$, 125 MHz) δ 157.2, 153.0 (2C), 152.1 (2C), 152.1, 134.4, 129.9, 129.8, 129.4, 127.7 (2C), 127.5, 127.2 (2C), 127.1 (2C), 127.0, 126.3, 121.5 (2C), 120.3, 111.2 (2C), 93.9, 81.9, 66.5, 59.4 (3C), 20.9 (2C); IR (film) ν_{max} 3400, 2959, 2926, 2853, 2359, 2341, 1819, 1715, 1601, 1522, 1381, 1366, 1261, 1215, 1173, 1111, 1059, 970, 800, 700 cm^{-1}; HRMS (ESI$^+$) *m/z*: $[M + H]^+$ calcd for $C_{32}H_{30}NO_{10}$, 588.1870; found, 588.1846.

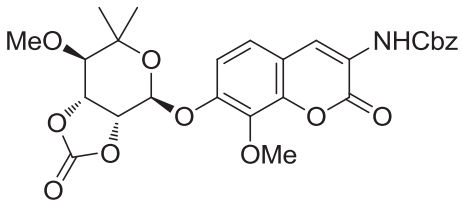

25g

Benzyl 8-methoxy-7-((3*aR*,4*S*,7*R*,7*aR*)-7-methoxy-6,6-dimethyl-2-oxotetrahydro-3*aH*-[1,3]dioxolo[4,5-*c*]pyran-4-yloxy)-2-oxo-*2H*-chromen-3-ylcarbamate (25g): Boron trifluoride etherate (17.3 μL, 0.14 mmol) was added to **23g** (157 mg, 0.46 mmol) and (3*aR*,4*S*,7*R*,7*aR*)-7-methoxy-6,6-dimethyl-2-oxo-tetrahydro-3*aH*-[1.3]dioxolo[4,5-*c*]pyran-4-yl 2,2,2-trichloroacetimidate (665 mg, 1.83 mmol) in anhydrous CH_2Cl_2 (11.5 mL). After stirring at rt for 24 h, triethylamine (150 μL) was added and the solvent was concentrated. The residue was purified via column chromatography (SiO_2, 40:1 → 10:1 CH_2Cl_2:Acetone) to give **25g** as a colorless foam (237 mg, 95%): ^{1}H NMR ($CDCl_3$, 500 MHz) δ 8.20 (s, 1H), 7.48 (s, 1H), 7.33–7.29 (m, 5H), 7.09 (dd, *J* = 14.2, 8.8 Hz, 2H), 5.72 (d, *J* = 1.8 Hz, 1H), 5.16 (s, 2H), 5.02 (dd, *J* = 7.8, 1.8 Hz, 1H), 4.89 (t, *J* = 7.8 Hz, 1H), 3.88 (s, 3H), 3.52 (s, 3H), 3.21 (d, *J* = 7.8 Hz, 1H), 1.27 (s, 3H) 1.17 (s, 3H); ^{13}C NMR ($CDCl_3$, 125 MHz) δ 158.0, 153.3, 153.2, 153.1, 149.8, 143.8, 137.1, 135.5, 128.7 (2C), 128.6, 128.3 (2C), 122.7, 122.2, 121.4, 116.1, 113.7, 95.3, 74.7, 72.9, 67.6, 61.9, 60.7, 60.6, 29.7, 29.4; IR (film) ν_{max} 3400, 3319, 2984, 2935, 2359, 1815, 1715, 1609, 1526, 1464, 1383, 1364, 1285, 1213, 1175, 1111, 1063, 968, 764, 737, 700 cm^{-1}; HRMS (ESI$^+$) *m/z*: $[M + Na]^+$ calcd for $C_{27}H_{27}NNaO_{11}$, 564.1482; found, 564.1455.

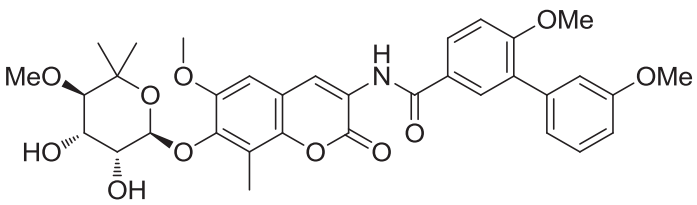

26a

***N*-(7-((2*S*,3*R*,4*S*,5*R*)-3,4-dihydroxy-5-methoxy-6,6-dimethyltetrahydro-*2H*-pyran-2-yloxy)-6-methoxy-8-methyl-2-oxo-*2H*-chromen-3-yl)-3',6-dimethoxybiphenyl-3-carboxamide (26a):** Palladium on carbon (20%, 20.0 mg) was added to **25a** (100 mg, 0.18 mmol) in anhydrous THF (5.00 mL) and the solution was placed under an atmosphere of H_2. After 6.5 h, the solution was filtered through SiO_2 (1:1 CH_2Cl_2:Acetone) and the eluent was concentrated to afford a yellow solid, which was used without further purification (56.0 mg, 75%).

EDCI (21.4 mg, 0.11 mmol) and 3',6-dimethoxybiphenyl-3-carboxylic acid (23.1 mg, 0.089 mmol) were added to the amine (18.7 mg, 0.045 mmol) in 30% pyridine/CH_2Cl_2 (0.70 mL). After 12 h, the solvent was concentrated and the residue purified via column chromatography (SiO_2, 40:1 CH_2Cl_2:Acetone) to afford a colorless solid, which was used without further purification (10.5 mg, 36%).

Triethylamine (250 μL) was added to the carbonate (10.4 mg, 0.016 mmol) in MeOH (2.50 mL). After 12 h, the solvent was concentrated and the residue purified via column chromatography (SiO_2, 20:1; CH_2Cl_2:MeOH) to afford **26a** as a colorless amorphous solid (2.00 mg, 20%, 5% over 3 steps): ^{1}H NMR ($CDCl_3$, 500 MHz) δ 8.73 (s, 1H), 8.70 (d, *J* = 5.4 Hz, 1H), 7.84 (td, *J* = 6.2, 2.4 Hz, 1H), 7.82 (s, 1H), 7.30 (t, *J* = 8.0 Hz, 1H), 7.06 (d, *J* = 7.8 Hz, 1H), 7.03–7.00 (m, 2H), 6.88–6.86 (m, 1H), 6.81 (s, 1H), 4.99 (d, *J* = 6.6 Hz, 1H), 4.24 (t, *J* = 4.2 Hz, 1H), 4.00 (dd, *J* = 6.5, 3.7 Hz, 1H), 3.90 (s, 3H), 3.86 (s, 3H), 3.83 (s, 3H), 3.80 (d, J = 7.4 Hz, 1H), 3.45 (s, 3H), 3.08 (d, *J* = 4.7 Hz, 1H), 2.67 (s, 1H), 2.42 (s, 3H), 1.28 (d, *J* = 8.1 Hz, 3H), 1.18 (s, 3H); ^{13}C NMR ($CDCl_3$, 125 MHz) δ 164.6, 158.9, 158.3, 158.2, 148.2, 145.6, 142.5, 137.5, 130.1, 129.0, 128.2, 127.2, 124.9, 122.5, 122.2, 121.2, 121.0, 115.1, 144.2, 112.1, 110.0, 105.4, 101.3, 81.7, 76.8, 69.0, 68.0, 59.1, 55.3, 54.9, 54.3, 28.3, 28.2, 9.1; IR (film) ν_{max} 2961,

2928, 1713, 1670, 1601, 1464, 1383, 1261, 1094, 1022, 798, 700 cm^{-1}; HRMS (ESI^+) *m/z*: $[M + H]^+$ calcd for $C_{34}H_{38}NO_{11}$, 636.2445; found, 636.2477.

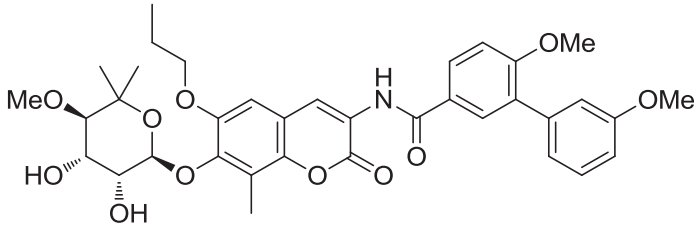

26b

***N*-(7-((2*S*,3*R*,4*S*,5*R*)-3,4-dihydroxy-5-methoxy-6,6-dimethyltetrahydro-*2H*-pyran-2-yloxy)-8-methyl-2-oxo-6-propoxy-*2H*-chromen-3-yl)-3',6-dimethoxybiphenyl-3-carboxamide (26b):** Palladium on carbon (20%, 85.0 mg) was added to **25b** (425 mg, 0.7283 mmol) in anhydrous THF (4.90 mL) and the solution was placed under an atmosphere of H_2. After 6.5 h, the solution was filtered through SiO_2 (1:1 CH_2Cl_2:Acetone) and the eluent was concentrated to afford a yellow solid, which was used without further purification (325 mg, 99%).

EDCI (116 mg, 0.60 mmol) and 3',6-dimethoxybiphenyl-3-carboxylic acid (125 mg, 0.48 mmol) were added to the amine (108 mg, 0.24 mmol) in 30% pyridine/CH_2Cl_2 (6.70 mL). After 12 h, the solvent was concentrated and the residue purified via column chromatography (SiO_2, 3:1 Hexane:Ether → 20:1 CH_2Cl_2:Acetone) to afford a colorless solid, which was used without further purification (51.0 mg, 31%).

Triethylamine (250 μL) was added to the carbonate (51.0 mg, 0.074 mmol) in MeOH (2.50 mL). After 48 h, the solvent was concentrated and the residue purified via column chromatography (SiO_2, 40:1 CH_2Cl_2:Acetone) to afford **26b** as a colorless amorphous solid (22.8 mg, 47%, 14% over 3 steps): ^1H NMR (CD_2Cl_2, 400 MHz) δ 8.79 (s, 1H), 8.78 (s, 1H), 7.96 (dd, *J* = 8.6, 2.4 Hz, 1H), 7.91 (d, *J* = 2.4 Hz, 1H), 7.39 (t, *J* = 7.9 Hz, 1H), 7.16–7.11 (m, 2H), 6.97–

6.94 (m, 2H), 5.97 (s, 1H), 5.14 (d, J = 6.5 Hz, 1H), 4.31 (t, J = 3.5 Hz, 1H), 4.12–4.06 (m, 2H), 4.03 (dd, J = 6.8, 1.8 Hz, 1H), 3.93 (s, 3H), 3.88 (s, 3H), 3.65 (s, 1H), 3.53 (s, 3H), 3.17 (d, J = 4.8 Hz, 1H), 2.80 (s, 1H), 2.48 (s, 3H), 1.95–1.90 (m, 2H), 1.37 (s, 3H), 1.35 (s, 3H), 1.11 (t, J = 7.4 Hz, 3H); ^{13}C NMR ($CDCl_3$, 125 MHz) δ 165.0, 164.6, 158.8, 158.3, 147.7, 145.7, 142.3, 137.8, 137.5, 131.3, 129.0, 128.2, 127.2, 124.9, 122.3, 121.2, 121.0, 115.111, 114.2, 112.1, 110.0, 106.2, 101.1, 81.7, 70.0, 69.0, 68.0, 64.8, 59.1, 54.9, 54.3, 24.7, 24.0, 21.3, 9.5, 9.1; IR (film) ν_{max} 3398, 3196, 2964, 2935, 2359, 2330, 1705, 1580, 1526, 1504, 1381, 1242, 1124, 1094, 939, 808, 760, 735 cm^{-1}; HRMS (ESI$^+$) *m/z*: $[M + H]^+$ calcd for $C_{36}H_{42}NO_{11}$, 664.2758; found, 664.2754.

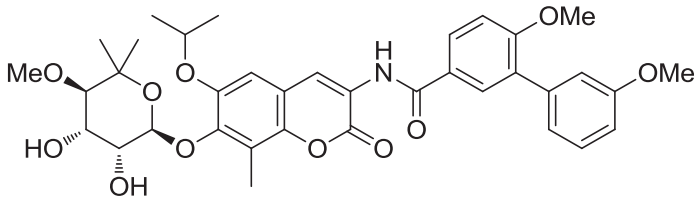

26c

***N*-(7-((2*S*,3*R*,4*S*,5*R*)-3,4-dihydroxy-5-methoxy-6,6-dimethyltetrahydro-*2H*-pyran-2-yloxy)-6-isopropoxy-8-methyl-2-oxo-*2H*-chromen-3-yl)-3',6-dimethoxybiphenyl-3-carboxamide (26c):** Palladium on carbon (20%, 11 mg) was added to **25c** (54.5 mg, 0.093 mmol) in anhydrous THF (600 μL) and the solution was placed under an atmosphere of H_2. After 12 h, the solution was filtered through SiO_2 (1:1 CH_2Cl_2:Acetone) and the eluent was concentrated to afford a yellow solid, which was used without further purification (42.0 mg, 99%).

EDCI (14.9 mg, 0.078 mmol) and 3',6-dimethoxybiphenyl-3-carboxylic acid (16 mg, 0.062 mmol) were added to the amine (14.0 mg, 0.031 mmol) in 30% pyridine/CH_2Cl_2 (900 μL). After 12 h, the solvent was concentrated and the residue purified via column chromatography (SiO_2,

3:1 Hexane:Ether → 40:1 CH_2Cl_2:Acetone) to afford a colorless solid, which was used without further purification (17.5 mg, 82%).

Triethylamine (250 μL) was added to the carbonate (17.5 mg, 0.025 mmol) in MeOH (2.50 mL) and CH_2Cl_2 (2.50 mL). After 12 h, the solvent was concentrated and the residue purified via column chromatography (SiO_2, 10:1 CH_2Cl_2:Acetone) to afford **26c** as a colorless amorphous solid (6.0 mg, 35%, 28% over 3 steps): ^{1}H NMR (CD_2Cl_2, 500 MHz) δ 8.69 (s, 1H), 8.67 (s, 1H), 7.84 (dd, *J* = 8.6, 2.4 Hz, 1H), 7.80 (d, *J* = 2.4 Hz, 1H), 7.29 (d, *J* = 8.0 Hz, 1H), 7.25 (t, *J* = 7.9 Hz, 1H), 7.03–7.01 (m, 2H), 6.87 (s, 1H), 6.87–6.83 (m, 1H), 4.96 (d, *J* = 6.8 Hz, 1H), 4.61–4.56 (m, 1H), 4.19 (t, *J* = 4.0 Hz, 1H), 3.89 (dd, *J* = 6.8, 3.7 Hz, 1H), 3.82 (s, 3H), 3.76 (s, 3H), 3.75 (s, 1H), 3.41 (s, 3H), 3.34 (s, 1H), 3.03 (d, *J* = 4.5 Hz, 1H), 2.36 (s, 3H), 1.33 (t, *J* = 6.2 Hz, 6H), 1.25 (s, 3H), 1.23 (s, 3H); ^{13}C NMR (CD_2Cl_2, 125 MHz) δ 164.6, 159.1, 158.6, 158.3, 146.7, 146.3, 142.5, 138.1, 130.2, 129.1, 128.3, 127.4, 125.2, 122.8, 122.2, 121.2, 121.1, 115.5, 144.5, 112.1, 110.2, 108.4, 101.4, 81.9, 77.0, 71.1, 69.2, 68.3, 59.1, 55.1, 54.5, 28.7, 28.6, 20.8, 20.8, 9.1; IR (film) ν_{max} 2924, 2854, 2359, 2341, 1734, 1684, 1653, 1558, 1541, 1522, 1506, 1458, 1387, 1339, 1286, 1244, 1113, 912, 797 cm^{-1}; HRMS (ESI$^+$) *m/z*: [M + Na]$^+$ calcd for $C_{36}H_{41}NNaO_{11}$, 686.2578; found, 686.2610.

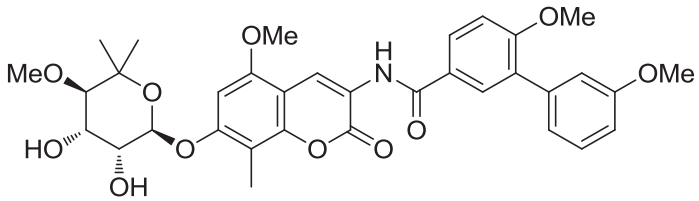

26d

***N*-(7-((2*R*,3*R*,4*S*,5*R*)-3,4-dihydroxy-5-methoxy-6,6-dimethyltetrahydro-*2H*-pyran-2-yloxy)-5-methoxy-8-methyl-2-oxo-*2H*-chromen-3-yl)-3',6-dimethoxybiphenyl-3-carboxamide (26d):** Palladium on carbon (20%, 40 mg) was added to **25d** (200 mg, 0.36 mmol)

in anhydrous THF (2.40 mL) and the solution was placed under an atmosphere of H_2. After 12 h, the solution was filtered through SiO_2 (1:1 CH_2Cl_2:Acetone) and the eluent was concentrated to afford a yellow solid, which was used without further purification (150 mg, 99%).

EDCI (57.5 mg, 0.30 mmol) and 3',6-dimethoxybiphenyl-3-carboxylic acid (62 mg, 0.24 mmol) were added to the amine (50.6 mg, 0.12 mmol) in 30% pyridine/CH_2Cl_2 (3.30 mL). After 12 h, the solvent was concentrated and the residue purified via column chromatography (SiO_2, 3:1 Hexane:Ether → 40:1 → 10:1 CH_2Cl_2:Acetone) to afford a colorless solid, which was used without further purification (25.2 mg, 32%).

Triethylamine (200 μL) was added to the carbonate (25.2 mg, 0.038 mmol) in MeOH (2.0 mL) and CH_2Cl_2 (2.0 mL). After 48 h, the solvent was concentrated and the residue purified via column chromatography (SiO_2, 40:1 CH_2Cl_2:Acetone) to afford **26d** as a colorless amorphous solid (17.0 mg, 70%, 22% over 3 steps): ^{1}H NMR (CD_2Cl_2, 400 MHz) δ 9.02 (s, 1H), 8.97 (s, 1H), 8.66 (s, 1H), 7.96 (dd, *J* = 8.6, 2.4 Hz, 1H), 7.91–7.90 (m, 1H), 7.39 (t, *J* = 7.9 Hz, 1H), 7.16–7.11 (m, 2H), 6.96 (dd, *J* = 8.3, 2.6 Hz), 6.85 (d, *J* = 5.5 Hz, 1H), 5.70 (d, *J* = 2.1 Hz, 1H), 4.36–4.33 (m, 1H), 4.27 (m, 1H), 3.99 (s, 3H), 3.93 (s, 3H), 3.88 (s, 3H), 3.62 (s, 3H), 3.41–3.38 (m, 1H), 2.24 (s, 3H), 1.41 (s, 3H), 1.19 (s, 3H); ^{13}C NMR ($CDCl_3$, 125 MHz) δ 164.2, 158.7, 158.6, 158.3, 155.3, 153.5, 148.6, 137.6, 129.9, 128.9, 128.1, 127.1, 125.1, 121.0, 119.4, 118.9, 114.2, 114.2, 112.1, 110.0, 104.9, 103.7, 96.7, 92.9, 83.2, 70.1, 67.5, 60.9, 60.8, 54.8, 54.3, 21.9, 21.4, 6.8; IR (film) ν_{max} 3405, 2986, 2934, 1713, 1609, 1528, 1383, 1250, 1213, 1053, 999, 914, 878, 737 cm^{-1}; HRMS (ESI$^+$) *m/z*: $[M + H]^+$ calcd for $C_{34}H_{38}NO_{11}$, 636.2445; found, 636.2482.

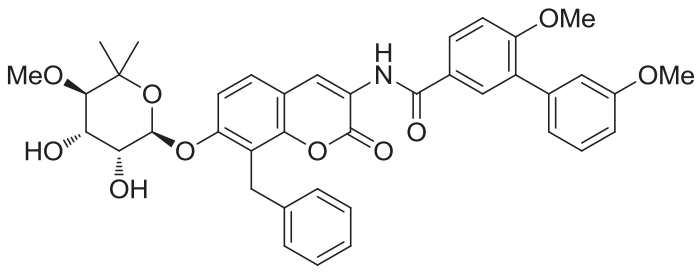

26e

***N*-(8-benzyl-7-((2*R*,3*R*,4*S*,5*R*)-3,4-dihydroxy-5-methoxy-6,6-dimethyltetrahydro-*2H*-pyran-2-yloxy)-2-oxo-*2H*-chromen-3-yl)-3',6-dimethoxybiphenyl-3-carboxamide (26e):** Palladium on carbon (20%, 46 mg) was added to **25e** (230 mg, 0.38 mmol) in anhydrous THF (2.50 mL) and the solution was placed under an atmosphere of H_2. After 12 h, the solution was filtered through SiO_2 (1:1 CH_2Cl_2:Acetone) and the eluent was concentrated to afford a yellow solid, which was used without further purification (177 mg, 99%).

EDCI (61.5 mg, 0.32 mmol) and 3',6-dimethoxybiphenyl-3-carboxylic acid (66.3 mg, 0.26 mmol) were added to the amine (60.0 mg, 0.13 mmol) in 30% pyridine/CH_2Cl_2 (3.50 mL). After 12 h, the solvent was concentrated and the residue purified via column chromatography (SiO_2, 3:1 Hexane:Ether → 20:1 CH_2Cl_2:Acetone) to afford a colorless solid, which was used without further purification (12.3 mg, 14%).

Triethylamine (150 μL) was added to the carbonate (12.3 mg, 0.017 mmol) in MeOH (1.5 mL) and CH_2Cl_2 (1.5 mL). After 48 h, the solvent was concentrated and the residue purified via column chromatography (SiO_2, 40:1 CH_2Cl_2:Acetone) to afford **26e** as a colorless amorphous solid (6.00 mg, 51%, 7.1% over 3 steps): ^{1}H NMR (CD_2Cl_2, 400 MHz) δ 8.84 (s, 1H), 8.72 (s, 1H), 7.96 (dd, J = 10, 2.4 Hz, 1H), 7.91 (d, J = 2.4 Hz, 1H), 7.50 (d, J = 8.8 Hz, 1H), 7.39 (t, J = 7.9 Hz, 1H), 7.31 (d, J = 8.8 Hz, 1H), 7.28–7.25 (m, 5H), 7.21–7.18 (m, 1H), 7.15–7.11 (m, 2H), 6.97–6.94 (m, 1H), 5.54 (d, J = 2.7 Hz, 1H), 4.25 (t, J = 15.1 Hz, 2H), 4.17–4.11 (m, 1H), 4.05

(d, J = 2.6 Hz, 1H), 3.93 (s, 3H), 3.88 (s, 3H), 3.58 (s, 3H), 3.31 (d, J = 8.7 Hz, 1H), 2.64 (s, 1H), 2.04 (s, 1H), 1.40 (s, 3H), 1.03 (s, 3H); ^{13}C NMR ($CDCl_3$, 125 MHz) δ 165.5, 159.8, 159.3, 159.3, 156.4, 148.9, 140.0 (2C), 138.6, 131.1, 130.0, 129.2, 128.5, 128.3, 128.2, 127.0, 126.2 (2C), 126.0 (2C), 124.1, 122.2, 122.0, 117.2, 115.2, 114.4, 113.2, 111.7, 111.0, 98.0, 70.6 (2C), 68.6, 61.6, 55.9, 55.4, 29.3, 28.9, 28.3; IR (film) ν_{max} 3404, 2930, 2359, 2341, 1713, 1670, 1605, 1526, 1502, 1367, 1244, 1180, 1134, 1076, 1026, 960 cm^{-1}; HRMS (ESI$^+$) *m/z*: $[M + H]^+$ calcd for $C_{39}H_{40}NO_{10}$, 682.2652; found, 682.2653.

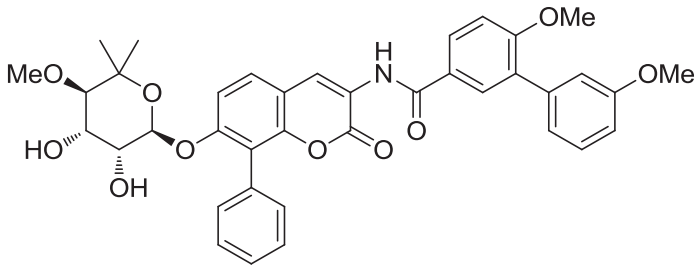

26f

***N*-(7-((2*R*,3*R*,4*S*,5*R*)-3,4-dihydroxy-5-methoxy-6,6-dimethyltetrahydro-*2H*-pyran-2-yloxy)-2-oxo-8-phenyl-*2H*-chromen-3-yl)-3',6-dimethoxybiphenyl-3-carboxamide (26f):** Palladium on carbon (20%, 14 mg) was added to **25f** (68.0 mg, 0.12 mmol) in anhydrous THF (800 μL) and the solution was placed under an atmosphere of H_2. After 12 h, the solution was filtered through SiO_2 (1:1 CH_2Cl_2:Acetone) and the eluent was concentrated to afford a yellow solid, which was used without further purification (52.0 mg, 99%).

EDCI (18.5 mg, 0.096 mmol) and 3',6-dimethoxybiphenyl-3-carboxylic acid (19.9 mg, 0.077 mmol) were added to the amine (17.5 mg, 0.039 mmol) in 30% pyridine/CH_2Cl_2 (1.10 mL). After 12 h, the solvent was concentrated and the residue purified via column chromatography (SiO_2, 40:1 CH_2Cl_2:Acetone) to afford a colorless solid, which was used without further purification (14.0 mg, 52%).

Triethylamine (150 μL) was added to the carbonate (14.0 mg, 0.020 mmol) in MeOH (1.5 mL) and CH_2Cl_2 (1.5 mL). After 48 h, the solvent was concentrated and the residue purified via column chromatography (SiO_2, 40:1 CH_2Cl_2:Acetone) to afford **26f** as a colorless amorphous solid (5.20 mg, 39%, 20% over 3 steps): ^{1}H NMR (CD_2Cl_2, 500 MHz) δ 8.85 (s, 1H), 8.65 (s, 1H), 7.92 (d, *J* = 2.4 Hz, 1H), 7.90 (d, *J* = 2.4 Hz, 1H), 7.86 (d, *J* = 2.4 Hz, 1H), 7.57–7.43 (m, 3H), 7.36–7.33 (m, 4H), 7.11–7.06 (m, 3H), 6.92 (d, *J* = 0.8 Hz, 1H), 5.52 (d, *J* = 2.4 Hz, 1H), 4.08 (q, *J* = 7.2, Hz, 1H), 3.89 (s, 3H), 3.83 (s, 3H), 3.74 (dd, *J* = 9.0, 3.5 Hz, 1H), 3.50 (s, 3H), 3.23 (d, *J* = 9.0 Hz, 1H), 2.12 (s, 1H), 2.00 (s, 1H), 1.33 (s, 3H), 1.04 (s, 3H); ^{13}C NMR (CD_2Cl_2, 125 MHz) δ 164.5, 159.0 (2C), 158.6, 158.1, 154.4, 147.2, 138.0 (2C), 130.7, 130.1, 129.7, 129.1, 128.7, 128.3, 127.4, 127.2, 127.0, 127.0, 125.2, 122.6, 121.6, 121.1, 118.6, 114.5, 113.8, 112.1, 111.3, 110.2, 97.5, 70.1 (2C), 67.4, 60.8, 55.0, 54.5, 21.9, 21.6; IR (film) ν_{max} 3402, 2932, 2359, 2341, 1713, 1603, 1524, 1500, 1367, 1267, 1086, 1040, 964, 750 cm^{-1}; HRMS (ESI$^+$) *m/z*: $[M + H]^+$ calcd for $C_{38}H_{38}NO_{10}$, 668.2496; found, 668.2485.

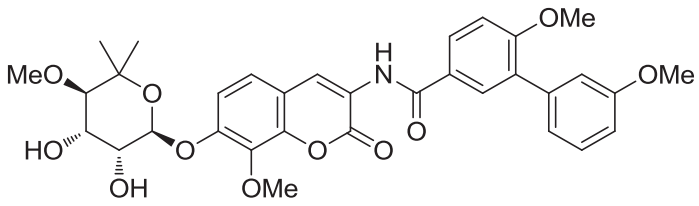

26g

***N*-(7-((2*S*,3*R*,4*S*,5*R*)-3,4-dihydroxy-5-methoxy-6,6-dimethyltetrahydro-*2H*-pyran-2-yloxy)-8-methoxy-2-oxo-*2H*-chromen-3-yl)-3',6-dimethoxybiphenyl-3-carboxamide (26g):** Palladium on carbon (20%, 47 mg) was added to **25g** (237 mg, 0.44 mmol) in anhydrous THF (2.93 mL) and the solution was placed under an atmosphere of H_2. After 12 h, the solution was filtered through SiO_2 (1:1 CH_2Cl_2:Acetone) and the eluent was concentrated to afford a yellow solid, which was used without further purification (177 mg, 99%).

EDCI (69.4 mg, 0.36 mmol) and 3',6-dimethoxybiphenyl-3-carboxylic acid (74.8 mg, 0.29 mmol) were added to the amine (59.0 mg, 0.14 mmol) in 30% pyridine/CH_2Cl_2 (4.00 mL). After 12 h, the solvent was concentrated and the residue purified via column chromatography (SiO_2, 3:1 Hexane:Ether → 40:1 CH_2Cl_2:Acetone) to afford a colorless solid, which was used without further purification (26.0 mg, 28%).

Triethylamine (200 μL) was added to the carbonate (26.0 mg, 0.040 mmol) in MeOH (2.0 mL) and CH_2Cl_2 (2.0 mL). After 48 h, the solvent was concentrated and the residue purified via column chromatography (SiO_2, 40:1 CH_2Cl_2:Acetone) to afford **26g** as a colorless amorphous solid (15.7 mg, 63%, 18% over 3 steps): ^{1}H NMR (CD_2Cl_2, 400 MHz) δ 8.82 (s, 1H), 8.73 (s, 1H), 7.96 (dd, *J* = 8.6, 2.4 Hz, 1H), 7.91 (d, *J* = 2.4 Hz, 1H) 7.39 (t, *J* = 7.9 Hz, 1H), 7.30 (s, 2H), 7.14 (d, *J* = 8.6 Hz, 2H), 7.12 (d, *J* = 2.2 Hz, 1H), 6.96 (dd, *J* = 8.3, 2.5 Hz, 1H), 5.61 (d, *J* = 2.4 Hz, 1H), 4.29 (t, *J* = 4.0 Hz, 1H), 4.27–4.25 (m, 1H), 3.98 (s, 3H), 3.93 (s, 3H), 3.88 (s, 3H), 3.62 (s, 3H), 3.47 (s, 1H), 3.37 (d, *J* = 8.8 Hz, 1H), 2.62 (s, 1H), 1.30 (s, 3H), 1.24 (s, 3H); ^{13}C NMR ($CDCl_3$, 125 MHz) δ 164.5, 158.8, 158.3, 157.8, 150.2 (2C), 142.9, 137.5, 135.6, 130.0, 128.9, 128.2, 127.2, 127.2, 124.9, 122.8, 121.6, 121.0, 114.3, 114.2, 112.3, 112.1, 110.0, 97.7, 70.0 (2C), 67.5, 60.8 (2C), 54.9, 54.3, 28.7, 28.3; IR (film) ν_{max}3402, 2961, 2928, 2853, 1713, 1672, 1607, 1526, 1504, 1462, 1367, 1263, 1248, 1086, 1040, 953, 798, 735, 700 cm^{-1}; HRMS (ESI$^+$) *m/z*: $[M + H]^+$ calcd for $C_{33}H_{36}NO_{11}$, 622.2288; found, 622.2307.

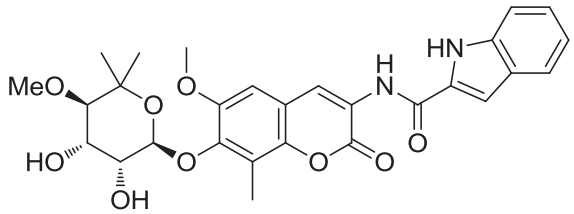

26i

***N*-(7-((2*S*,3*R*,4*S*,5*R*)-3,4-dihydroxy-5-methoxy-6,6-dimethyltetrahydro-*2H*-pyran-2-yloxy)-6-methoxy-8-methyl-2-oxo-*2H*-chromen-3-yl)-*1H*-indole-2-carboxamide (26i):** Palladium on carbon (20%, 15 mg) was added to **25a** (74.0 mg, 0.13 mmol) in anhydrous THF (5.00 mL) and the solution was placed under an atmosphere of H_2. After 12 h, the solution was filtered through SiO_2 (1:1 CH_2Cl_2:Acetone) and the eluent was concentrated to afford a yellow solid, which was used without further purification (60.0 mg, 99%).

EDCI (69.0 mg, 0.36 mmol) and *1H*-indole-2-carboxylic acid (46.4 mg, 0.29 mmol) were added to the amine (60.0 mg, 0.14 mmol) in 30% pyridine/CH_2Cl_2 (3.50 mL). After 12 h, the solvent was concentrated and the residue purified via column chromatography (SiO_2, 3:1 Hexane:Ether → 40:1 CH_2Cl_2:Acetone) to afford a colorless solid, which was used without further purification (68.0 mg, 85%).

Triethylamine (250 μL) was added to the carbonate (68.0 mg, 0.12 mmol) in MeOH (2.5 mL) and CH_2Cl_2 (2.50 mL). After 12 h, the solvent was concentrated and the residue purified via column chromatography (SiO_2, 40:1 CH_2Cl_2:Acetone) to afford **26i** as a colorless amorphous solid (12.6 mg, 19%, 16% over 3 steps): ^{1}H NMR (CD_2Cl_2, 400 MHz) δ 8.29 (s, 1H), 7.63 (s, 1H), 7.45–7.39 (m, 3H), 6.92 (s, 1H), 6.85 (s, 1H), 6.19 (s, 1H), 5.09 (d, *J* = 6.5 Hz, 1H), 4.31–4.28 (m, 1H), 4.01–3.97 (m, 1H), 3.94 (s, 3H), 3.62 (s, 1H), 3.56 (s, 3H), 3.15 (d, *J* = 4.9 Hz, 1H), 2.46 (s, 3H), 2.36 (s, 1H), 1.38 (d, *J* = 11.5 Hz, 3H), 1.32 (s, 3H); ^{13}C NMR ($CDCl_3$, 125 MHz) δ 157.6, 152.1, 148.2, 145.4, 142.2, 134.5, 129.9, 127.8, 127.7, 127.5, 127.3, 122.3, 121.2, 120.2, 115.0, 105.3, 105.1, 101.3, 81.7, 69.0, 68.0, 66.5, 59.1, 55.2, 28.7, 24.6, 24.1, 9.1; IR (film) ν_{max} 2926, 1707, 1526, 1464, 1391, 1340, 1296, 1231, 1207, 1086, 1024, 943, 739, 700, 623 cm^{-1}; HRMS (ESI$^+$) *m/z*: $[M + Na]^+$ calcd for $C_{28}H_{30}N_2NaO_9$, 561.1849; found, 561.1781.

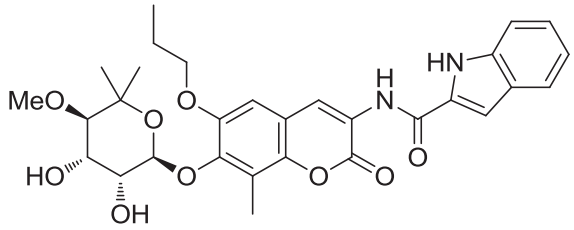

26j

***N*-(7-((2*S*,3*R*,4*S*,5*R*)-3,4-dihydroxy-5-methoxy-6,6-dimethyltetrahydro-*2H*-pyran-2-yloxy)-8-methyl-2-oxo-6-propoxy-*2H*-chromen-3-yl)-*1H*-indole-2-carboxamide (26j):** Palladium on carbon (20%, 85 mg) was added to **25b** (425 mg, 0.729 mmol) in anhydrous THF (4.90 mL) and the solution was placed under an atmosphere of H_2. After 12 h, the solution was filtered through SiO_2 (1:1 CH_2Cl_2:Acetone) and the eluent was concentrated to afford a yellow solid, which was used without further purification (325 mg, 99%).

EDCI (116 mg, 0.6026 mmol) and *1H*-indole-2-carboxylic acid (77.7 mg, 0.4821 mmol) were added to the amine (108 mg, 0.2410 mmol) in 30% pyridine/CH_2Cl_2 (6.70 mL). After 12 h, the solvent was concentrated and the residue purified via column chromatography (SiO_2, 3:1 Hexane:Ether → 40:1 CH_2Cl_2:Acetone) to afford a colorless solid, which was used without further purification (91.0 mg, 64%).

Triethylamine (250 μL) was added to the carbonate (91.0 mg, 0.1536 mmol) in MeOH (2.5 mL) and CH_2Cl_2 (2.50 mL). After 48 h, the solvent was concentrated and the residue purified via column chromatography (SiO_2, 40:1 CH_2Cl_2:Acetone) to afford **26j** as a colorless amorphous solid (17.5 mg, 20%, 13% over 3 steps): ^{1}H NMR (CD_2Cl_2, 400 MHz) δ 9.32 (s, 1H), 8.80 (s, 1H), 8.76 (s, 1H), 7.77 (d, *J* = 8.0 Hz, 1H), 7.53 (d, *J* = 7.5 Hz, 1H), 7.40–7.36 (m, 1H), 7.24–7.20 (m, 1H), 6.98 (s, 1H), 6.01 (s, 1H), 5.15 (d, *J* = 6.5 Hz, 1H), 4.32–4.25 (m, 1H), 4.11–4.04, (m, 1H), 3.62–3.59 (m, 2H), 3.53 (s, 3H), 3.18–3.12 (m, 1H), 2.64 (s, 1H), 2.49 (s, 3H), 2.18 (s, 1H), 1.95–1.91 (m, 2H), 1.36 (d, *J* = 9.6 Hz, 3H), 1.29 (d, *J* = 9.8 Hz, 3H), 1.12 (t, *J* = 7.4 Hz,

3H); ^{13}C NMR ($CDCl_3$, 125 MHz) δ 160.1, 159.0, 148.8, 146.9, 143.4, 136.9, 129.8, 127.6, 125.5, 123.5, 123.0, 122.6, 122.3, 121.2, 116.0, 112.0, 107.3, 104.3, 102.2, 82.8, 71.0, 70.1, 69.1, 60.2, 59.7, 25.7, 23.1, 23.4, 10.5, 10.2; IR (film) ν_{max} 3630, 3304, 2926, 2854, 2359, 2332, 1713, 1705, 1539, 1387, 1240, 1103, 947, 930, 822, 739 cm^{-1}; HRMS (ESI^+) *m/z*: $[M + H]^+$ calcd for $C_{30}H_{35}N_2O_9$, 567.2342; found, 567.2367.

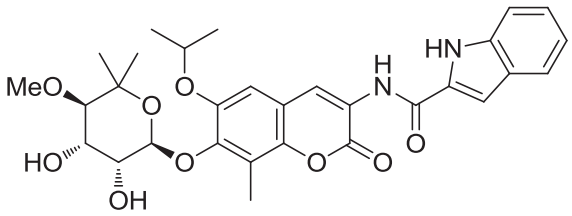

26k

***N*-(7-((2*S*,3*R*,4*S*,5*R*)-3,4-dihydroxy-5-methoxy-6,6-dimethyltetrahydro-*2H*-pyran-2-yloxy)-6-isopropoxy-8-methyl-2-oxo-*2H*-chromen-3-yl)-*1H*-indole-2-carboxamide (26k):** Palladium on carbon (20%, 4 mg) was added to **25c** (19.0 mg, 0.033 mmol) in anhydrous THF (220 μL) and the solution was placed under an atmosphere of H_2. After 12 h, the solution was filtered through SiO_2 (1:1 CH_2Cl_2:Acetone) and the eluent was concentrated to afford a yellow solid, which was used without further purification (14.5 mg, 99%).

EDCI (15.6 mg, 0.081 mmol) and *1H*-indole-2-carboxylic acid (10.5 mg, 0.065 mmol) was added to the amine (14.5 mg, 0.033 mmol) in 30% pyridine/CH_2Cl_2 (1.00 mL). After 12 h, the solvent was concentrated and the residue purified via column chromatography (SiO_2, 40:1 CH_2Cl_2:Acetone) to afford a colorless solid, which was used without further purification (10.0 mg, 50%).

Triethylamine (250 μL) was added to the carbonate (10.0 mg, 0.017 mmol) in MeOH (2.5 mL) and CH_2Cl_2 (2.50 mL). After 12 h, the solvent was concentrated and the residue purified via column chromatography (SiO_2, 10:1 CH_2Cl_2:Acetone) to afford **26k** as a colorless amorphous

solid (6.00 mg, 46%, 23% over 3 steps): ^{1}H NMR ($CDCl_3$, 500 MHz) δ 8.16 (s, 1H), 7.52 (s, 1H), 7.34–7.30 (m, 5H), 6.75 (s, 1H), 4.93 (d, *J* = 5.0 Hz, 1H), 4.56–4.51 (m, 1H), 4.23 (t, *J* = 4.0 Hz, 1H), 3.98–3.96 (m, 1H), 3.76 (s, 1H), 3.43 (s, 3H), 3.06 (d, *J* = 4.3 Hz, 1H), 2.65 (s, 1H), 2.38 (s, 3H), 1.33 (dd, *J* = 11.2, 6.1 Hz, 6H), 1.29 (s, 3H), 1.27 (s, 3H); ^{13}C NMR ($CDCl_3$, 125 MHz) δ 157.6, 152.1, 146.6, 146.0, 142.1, 134.5, 127.7, 127.5, 127.2, 122.2, 121.3 (2C), 120.2 (2C), 115.0 (2C), 108.1 (2C), 101.2, 81.6, 71.2, 68.9, 68.1, 66.5, 59.0, 24.8, 23.6, 20.8 (2C), 9.1; IR (film) ν_{max} cm^{-1} 3406, 2930, 2375, 1705, 1522, 1394, 1229, 1205, 1111, 1078, 1049, 933, 793, 739, 698; HRMS (ESI^{+}) *m/z*: $[M + Na]^{+}$ calcd for $C_{30}H_{34}N_2NaO_9$, 589.2162; found, 589.2111.

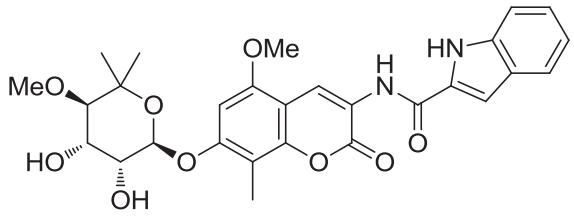

26l

***N*-(7-((2*R*,3*R*,4*S*,5*R*)-3,4-dihydroxy-5-methoxy-6,6-dimethyltetrahydro-*2H*-pyran-2-yloxy)-5-methoxy-8-methyl-2-oxo-*2H*-chromen-3-yl)-*1H*-indole-2-carboxamide (26l):** Palladium on carbon (20%, 40 mg) was added to **25d** (200 mg, 0.36 mmol) in anhydrous THF (2.40 mL) and the solution was placed under an atmosphere of H_2. After 12 h, the solution was filtered through SiO_2 (1:1 CH_2Cl_2:Acetone) and the eluent was concentrated to afford a yellow solid, which was used without further purification (150 mg, 99%).

EDCI (57.5 mg, 0.30 mmol) and *1H*-indole-2-carboxylic acid (38.7 mg, 0.24 mmol) were added to the amine (50.6 mg, 0.12 mmol) in 30% pyridine/CH_2Cl_2 (3.30 mL). After 12 h, the solvent was concentrated and the residue purified via column chromatography (SiO_2, 40:1 CH_2Cl_2:Acetone) to afford a colorless solid, which was used without further purification (26.3 mg, 39%).

Triethylamine (200 μL) was added to the carbonate (26.3 mg, 0.047 mmol) in MeOH (2.00 mL) and CH_2Cl_2 (2.00 mL). After 48 h, the solvent was concentrated and the residue purified via column chromatography (SiO_2, 40:1 CH_2Cl_2:Acetone) to afford **26l** as a colorless amorphous solid (6.60 mg, 26%, 10% over 3 steps): ^{1}H NMR (CD_2Cl_2, 400 MHz) δ 9.26 (s, 1H), 8.96 (s, 1H), 8.68 (s, 1H), 7.74 (d, *J* = 8.1 Hz, 1H), 7.52 (d, *J* = 8.3 Hz, 1H), 7.38–7.34 (m, 1H), 7.22–7.16 (m, 1H), 6.84 (s, 1H), 6.00 (s, 1H), 5.65 (d, *J* = 1.7 Hz, 1H), 4.26–4.21 (m, 2H), 3.96 (s, 3H), 3.59 (s, 3H), 3.35 (d, *J* = 8.6 Hz, 1H), 2.25 (s, 3H), 1.53 (s, 3H), 1.20 (s, 3H); ^{13}C NMR ($CDCl_3$, 125 MHz) δ 165.1, 157.4, 156.5, 149.7, 136.7, 134.7, 127.7, 125.3, 122.5, 121.1, 120.0, 111.9, 104.6, 103.8, 97.7, 94.0, 84.3, 84.2, 82.6, 69.6, 69.1, 66.1, 62.2, 62.0, 59.7, 23.1, 22.7, 14.2; IR (film) ν_{max} 3389, 2924, 2853, 1697, 1605, 1535, 1460, 1340, 1211, 1101, 1088, 962, 729 cm^{-1}; HRMS (ESI$^+$) *m/z*: $[M + H]^+$ calcd for $C_{28}H_{31}N_2O_9$, 539.2030; found, 539.2056.

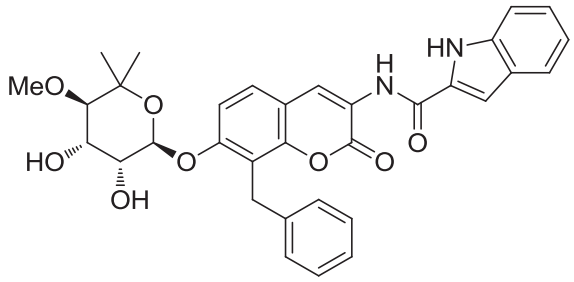

26m

***N*-(8-benzyl-7-((2*R*,3*R*,4*S*,5*R*)-3,4-dihydroxy-5-methoxy-6,6-dimethyltetrahydro-*2H*-pyran-2-yloxy)-2-oxo-*2H*-chromen-3-yl)-*1H*-indole-2-carboxamide (26m):** Palladium on carbon (20%, 46 mg) was added to **25e** (230 mg, 0.38 mmol) in anhydrous THF (2.50 mL) and the solution was placed under an atmosphere of H_2. After 12 h, the solution was filtered through SiO_2 (1:1 CH_2Cl_2:Acetone) and the eluent was concentrated to afford a yellow solid, which was used without further purification (177 mg, 99%).

EDCI (61.5 mg, 0.32 mmol) and *1H*-indole-2-carboxylic acid (41.4 mg, 0.26 mmol) were added to the amine (60.0 mg, 0.13 mmol) in 30% pyridine/CH_2Cl_2 (3.50 mL). After 12 h, the solvent was concentrated and the residue purified via column chromatography (SiO_2, 3:1 Hexane:Ether → 40:1 CH_2Cl_2:Acetone) to afford a yellow solid, which was used without further purification (66.2 mg, 85%).

Triethylamine (250 μL) was added to the carbonate (66.2 mg, 0.11 mmol) in MeOH (2.50 mL) and CH_2Cl_2 (2.50 mL). After 12 h, the solvent was concentrated and the residue purified via column chromatography (SiO_2, 40:1 CH_2Cl_2:Acetone) to afford **26m** as a colorless amorphous solid (6.50 mg, 10%, 8.4% over 3 steps): ^{1}H NMR (CD_2Cl_2, 500 MHz) δ 8.68 (s, 1H), 8.62 (s, 1H), 7.63–7.61 (m, 1H), 7.47 (dd, *J* = 5.7, 3.3 Hz, 1H), 7.16–7.10 (m, 4H), 7.10–7.04 (m, 4H), 6.99 (t, *J* = 8.2 Hz, 1H), 6.74 (d, *J* = 8.0 Hz, 1H), 6.43 (dd, *J* = 8.1, 0.7 Hz, 1H), 5.31 (d, *J* = 2.9 Hz, 1H), 4.17 (t, *J* = 6.8 Hz, 1H), 4.01 (dd, *J* = 8.5, 2.9 Hz, 1H), 3.90 (d, *J* = 13.1 Hz, 2H), 3.45 (s, 3H), 3.16 (d, *J* = 8.6 Hz, 1H), 2.43 (s, 1H), 2.21 (s, 1H), 1.25 (s, 3H), 0.95 (s, 3H); ^{13}C NMR ($CDCl_3$, 125 MHz) δ 166.8, 155.4, 153.8, 140.2, 131.6, 130.2, 128.0, 127.6, 127.5 (2C), 127.4 (2C), 126.9, 125.1 (2C), 115.2, 108.3 (2C), 105.8 (2C), 97.1 (2C), 83.3 (2C), 77.2, 70.2, 67.9 (2C), 65.0, 60.6, 21.9, 13.1, 13.0; IR (film) ν_{max} 3333, 2961, 2926, 2854, 1717, 1601, 1466, 1261, 1090, 1076, 1041, 800, 750 cm^{-1}; HRMS (ESI$^+$) *m/z*: $[M + Na]^+$ calcd for $C_{33}H_{32}N_2NaO_8$, 607.2056; found, 607.2056.

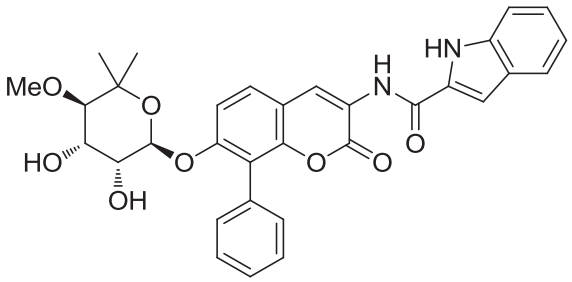

26n

***N*-(7-((2*R*,3*R*,4*S*,5R)-3,4-dihydroxy-5-methoxy-6,6-dimethyltetrahydro-*2H*-pyran-2-yloxy)-2-oxo-8-phenyl-*2H*-chromen-3-yl)-*1H*-indole-2-carboxamide (26n):** Palladium on carbon (20%, 14 mg) was added to **25f** (68.0 mg, 0.12 mmol) in anhydrous THF (800 μL) and the solution was placed under an atmosphere of H_2. After 12 h, the solution was filtered through SiO_2 (1:1 CH_2Cl_2:Acetone) and the eluent was concentrated to afford a yellow solid, which was used without further purification (52.0 mg, 99%).

EDCI (18.5 mg, 0.096 mmol) and *1H*-indole-2-carboxylic acid (12.4 mg, 0.077 mmol) were added to the amine (17.5 mg, 0.039 mmol) in 30% pyridine/CH_2Cl_2 (1.10 mL). After 12 h, the solvent was concentrated and the residue purified via column chromatography (SiO_2, 40:1 CH_2Cl_2:Acetone) to afford a colorless solid, which was used without further purification (8.20 mg, 36%).

Triethylamine (100 μL) was added to the carbonate (8.2 mg, 0.014 mmol) in MeOH (1.00 mL) and CH_2Cl_2 (1.00 mL). After 48 h, the solvent was concentrated and the residue purified via column chromatography (SiO_2, 40:1 CH_2Cl_2:Acetone) to afford **26n** as a colorless amorphous solid (4.00 mg, 51%, 18% over 3 steps): ^{1}H NMR (CD_2Cl_2, 500 MHz) δ 9.23 (s, 1H), 8.80 (s, 1H), 8.67 (s, 1H), 7.71 (dd, *J* = 8.0, 0.7 Hz, 1H), 7.57 (d, *J* = 8.8 Hz, 1H), 7.51–7.48 (m, 3H), 7.46–7.44 (m, 1H), 7.37–7.32 (m, 4H), 7.19–7.17 (m, 2H), 5.53 (d, *J* = 2.4 Hz, 1H), 3.86 (s, 1H), 3.76–3.73 (m, 2H), 3.51 (s, 3H), 3.23 (d, *J* = 9.1 Hz, 1H), 2.41 (s, 1H), 1.34 (s, 3H), 1.05 (s, 3H); ^{13}C NMR (CD_2Cl_2, 125 MHz) δ 159.1, 157.9, 154.5, 147.3, 136.0 (2C), 130.7 (2C), 129.8, 129.2,. 127.3, 127.1, 127.0, 126.9, 124.5, 122.8, 121.6, 121.2, 120.3, 113.7, 111.4, 111.1, 103.1 (2C), 97.5, 83.2, 77.7, 70.1, 67.5, 60.8, 21.9, 21.7; IR (film) ν_{max} 3427, 2961, 2924, 2853, 2062, 1643, 1614, 1537, 1362, 1236, 1094, 1041, 962, 791, 739, 698 cm^{-1}; HRMS (ESI$^+$) *m/z*: [M + Na]$^+$ calcd for $C_{32}H_{30}N_2NaO_8$, 593.1900; found, 593.1890.

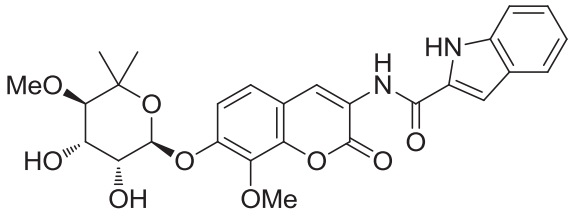

26o

***N*-(7-((2*S*,3*R*,4*S*,5*R*)-3,4-dihydroxy-5-methoxy-6,6-dimethyltetrahydro-*2H*-pyran-2-yloxy)-8-methoxy-2-oxo-*2H*-chromen-3-yl)-*1H*-indole-2-carboxamide (26o):** Palladium on carbon (20%, 47 mg) was added to **25g** (237 mg, 0.44 mmol) in anhydrous THF (2.93 mL) and the solution was placed under an atmosphere of H_2. After 12 h, the solution was filtered through SiO_2 (1:1 CH_2Cl_2:Acetone) and the eluent was concentrated to afford a yellow solid, which was used without further purification (177 mg, 99%).

EDCI (69.4 mg, 0.36 mmol) and *1H*-indole-2-carboxylic acid (46.7 mg, 0.29 mmol) were added to the amine (59.0 mg, 0.14 mmol) in 30% pyridine/CH_2Cl_2 (4.00 mL). After 12 h, the solvent was concentrated and the residue purified via column chromatography (SiO_2, 3:1 Hexane:Ether → 40:1 CH_2Cl_2:Acetone) to afford a colorless solid, which was used without further purification (32.0 mg, 49%).

Triethylamine (200 μL) was added to the carbonate (32.0 mg, 0.071 mmol) in MeOH (2.00 mL) and CH_2Cl_2 (2.00 mL). After 48 h, the solvent was concentrated and the residue purified via column chromatography (SiO_2, 3:1 CH_2Cl_2:Acetone) to afford **26o** as a colorless amorphous solid (22.1 mg, 73%, 35% over 3 steps): ^{1}H NMR (CD_2Cl_2, 400 MHz) δ 9.28 (s, 1H), 8.78 (s, 1H), 7.77 (d, *J* = 8.1 Hz, 1H), 7.53 (dd, *J* = 8.3, 0.8 Hz, 1H), 7.38 (m, 1H), 7.31 (s, 2H), 7.24 (d, *J* = 0.9 Hz, 1H), 7.22–7.20 (m, 1H), 6.02 (s, 1H), 5.62 (d, *J* = 2.3 Hz, 1H), 4.25 (t, *J* = 3.5 Hz, 1H), 3.99 (s, 3H), 3.75 (dd, *J* = 9.0, 3.6 Hz, 1H), 3.62 (s, 3H), 3.13 (d, *J* = 3.6 Hz, 1H), 1.30 (s, 3H), 1.27 (s, 3H); ^{13}C NMR ($CDCl_3$, 125 MHz) δ 163.8, 159.1, 157.7, 150.6, 143.3, 136.0,

135.8, 129.2, 126.9, 124.6, 122.8, 121.8, 121.6, 121.4, 120.3, 114.4, 112.5, 111.2, 103.1, 98.0, 83.2, 77.9, 74.0, 60.9, 58.7, 22.3, 21.8; IR (film) ν_{max} 3420, 2957, 2924, 2854, 2359, 1653, 1558, 1541, 1246, 1001, 798 cm^{-1}; HRMS (ESI^+) *m/z*: $[M + H]^+$ calcd for $C_{27}H_{29}N_2O_9$, 525.1873; found, 525.1875.

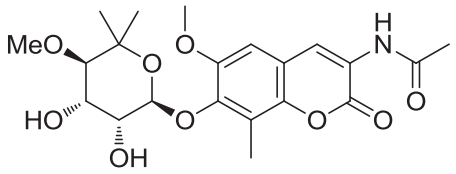

30a

N-(7-(((2S,3R,4S,5R)-3,4-dihydroxy-5-methoxy-6,6-dimethyltetrahydro-2H-pyran-2-yl)oxy)-6-methoxy-8-methyl-2-oxo-2H-chromen-3-yl)acetamide (30a): Palladium on carbon (20%, 20.0 mg) was added to **25a** (100 mg, 0.18 mmol) in anhydrous THF (5.00 mL) and the solution was placed under an atmosphere of H_2. After 6.5 h, the solution was filtered through SiO_2 (1:1 CH_2Cl_2:Acetone) and the eluent was concentrated to afford a yellow solid, which was used without further purification (56.0 mg, 74%).

Acetic anhydride (8.4 μL, 0.089 mmol) was added to the amine (18.7 mg, 0.045 mmol) in 50% pyridine/CH_2Cl_2 (0.70 mL). After 12 h, the solvent was concentrated and the residue purified via column chromatography (SiO_2, 40:1 CH_2Cl_2:Acetone) to afford a colorless solid, which was used without further purification (11.2 mg, 54%).

Triethylamine (250 μL) was added to the carbonate (10.4 mg, 0.016 mmol) in MeOH (2.50 mL). After 12 h, the solvent was concentrated and the residue purified via column chromatography (SiO_2, 20:1; CH_2Cl_2:MeOH) to afford **30a** as a colorless amorphous solid (2.0 mg, 19%, 8% over 3 steps): ^1H NMR ($CDCl_3$, 500 MHz) δ 8.54 (s, 1H), 7.98 (s, 1H), 6.77 (s, 1H), 4.98 (d, *J* = 6.6 Hz, 1H), 4.24 (t, *J* = 4.2 Hz, 1H), 3.99 (dd, *J* = 6.5, 3.7 Hz, 1H), 3.84 (s, 3H), 3.61 (s, 1H), 3.44 (s, 3H), 3.08 (d, *J* = 4.7 Hz, 1H), 2.67 (s, 1H), 2.39 (s, 3H), 2.17 (s, 3H),

1.28 (d, J = 8.1 Hz, 6H); ^{13}C NMR ($CDCl_3$, 125 MHz) δ 169.4, 159.0, 149.3, 146.7, 143.5, 123.4, 123.2, 122.2, 116.0, 106.4, 102.3, 82.8, 77.9, 70.0, 69.1, 60.1, 56.3, 25.7, 25.1, 24.8, 10.1; IR (film) ν_{max} 2930, 1710, 1660, 1516, 1464, 1385, 1270, 1090, 1026, 750, 700 cm^{-1}; HRMS (ESI$^+$) *m/z*: $[M + Na]^+$ calcd for $C_{21}H_{27}NNaO_9$, 460.1584; found, 460.1524.

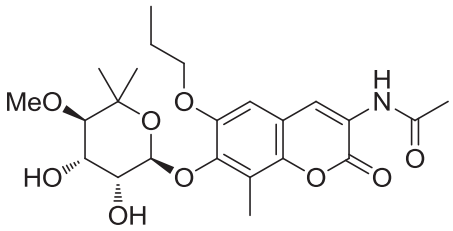

30b

N-(7-(((2S,3R,4S,5R)-3,4-dihydroxy-5-methoxy-6,6-dimethyltetrahydro-2H-pyran-2-yl)oxy)-8-methyl-2-oxo-6-propoxy-2H-chromen-3-yl)acetamide (30b): Palladium on carbon (20%, 85.0 mg) was added to **25b** (425 mg, 0.73 mmol) in anhydrous THF (4.90 mL) and the solution was placed under an atmosphere of H_2. After 6.5 h, the solution was filtered through SiO_2 (1:1 CH_2Cl_2:Acetone) and the eluent was concentrated to afford a yellow solid, which was used without further purification (325 mg, 99%).

Acetic anhydride (46.0 μL, 0.48 mmol) was added to the amine (108 mg, 0.24 mmol) in 50% pyridine/CH_2Cl_2 (6.70 mL). After 12 h, the solvent was concentrated and the residue purified via column chromatography (SiO_2, 3:1 Hexane:Ether → 40:1 CH_2Cl_2:Acetone) to afford a colorless solid, which was used without further purification (23.0 mg, 20%).

Triethylamine (300 μL) was added to the carbonate (23.0 mg, 0.047 mmol) in 50% MeOH/CH_2Cl_2 (3.00 mL). After 48 h, the solvent was concentrated and the residue purified via column chromatography (SiO_2, 40:1 CH_2Cl_2:Acetone) to afford **30b** as a colorless amorphous solid (7.70 mg, 35%, 7% over 3 steps): ^{1}H NMR (CD_2Cl_2, 400 MHz) δ 8.62 (s, 1H), 8.08, (s, 1H), 6.91 (s, 1H), 5.12 (d, J = 6.5 Hz, 1H), 4.30 (t, J = 3.6 Hz, 1H), 4.10–3.98 (m, 3H), 3.62 (s,

1H), 3.52 (s, 3H), 3.15 (d, J = 4.7 Hz, 1H), 2.76 (s, 1H), 2.46 (s, 3H), 2.23 (s, 3H), 1.94–1.89 (m, 2H), 1.36 (s, 3H), 1.34 (s, 3H), 1.10 (t, J = 7.3 Hz, 3H); ^{13}C NMR ($CDCl_3$, 125 MHz) δ 169.4, 159.0, 148.7, 146.8, 143.3, 123.5, 123.1, 122.2, 116.0, 107.2, 102.1, 82.7, 77.8, 71.0, 70.0, 69.1, 60.1, 25.8, 24.9, 24.8, 22.4, 10.5, 10.2; IR (film) ν_{max} 2964, 2918, 2359, 2343, 1707, 1684, 1533, 1437, 1383, 1292, 1244, 1124, 1082, 941, 771 cm^{-1}; HRMS (ESI$^+$) *m/z*: [M + Na]$^+$ calcd for $C_{23}H_{31}NNaO_9$, 488.1897; found, 488.1873.

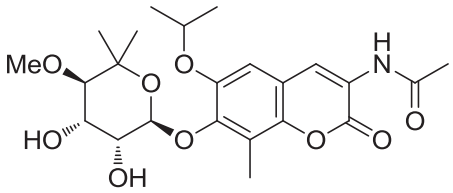

30c

N-(7-(((2S,3R,4S,5R)-3,4-dihydroxy-5-methoxy-6,6-dimethyltetrahydro-2H-pyran-2-yl)oxy)-6-isopropoxy-8-methyl-2-oxo-2H-chromen-3-yl)acetamide (30c): Palladium on carbon (20%, 35 mg) was added to **25c** (175 mg, 0.31 mmol) in anhydrous THF (2.10 mL) and the solution was placed under an atmosphere of H_2. After 12 h, the solution was filtered through SiO_2 (1:1 CH_2Cl_2:Acetone) and the eluent was concentrated to afford a yellow solid, which was used without further purification (133 mg, 99%).

Acetic anhydride (20.0 μL, 0.21 mmol) was added to the amine (44.0 mg, 0.10 mmol) in 50% pyridine/CH_2Cl_2 (900 μL). After 12 h, the solvent was concentrated and the residue purified via column chromatography (SiO_2, 3:1 Hexane:Ether → 40:1 → 5:1 CH_2Cl_2:Acetone) to afford a colorless solid, which was used without further purification (20.0 mg, 41%).

Triethylamine (7.1 μL) was added to the carbonate (3.5 mg, 0.0071 mmol) in 50% MeOH/CH_2Cl_2 (71 μL). After 12 h, the solvent was concentrated and the residue purified via column chromatography (SiO_2, 10:1 CH_2Cl_2:Acetone) to afford **30c** as a colorless amorphous

solid (1.6 mg, 48%, 19% over 3 steps): ^{1}H NMR (CD_2Cl_2, 500 MHz) δ 8.50 (s, 1H), 7.96 (s, 1H), 6.81 (s, 1H), 4.94 (d, *J* = 6.9 Hz, 1H), 4.57 (dd, *J* = 12.2, 6.1 Hz, 1H), 4.19–4.16 (m, 1H), 3.87 (dd, *J* = 6.8, 3.7 Hz, 1H), 3.67 (s, 1H), 3.40 (s, 3H), 3.34 (s, 1H), 3.02 (d, *J* = 4.5 Hz, 1H), 2.34 (s, 3H), 2.12 (s, 3H), 1.30 (t, *J* = 6.0 Hz, 6H), 1.24 (s, 3H), 1.22 (s, 3H); ^{13}C NMR (CD_2Cl_2, 125 MHz) δ 168.5, 158.0, 146.7, 146.3, 142.4, 122.6, 122.1, 121.1, 115.3, 108.3, 101.4, 81.8, 77.0, 71.1, 69.2, 68.3, 59.0, 28.9, 28.6, 20.8 (2C), 23.8, 23.7; IR (film) ν_{max} 2955, 2926, 2854, 1717, 1697, 1684, 1522, 1437, 1387, 1375, 1339, 1292, 1259, 1113, 929, 766, 750 cm^{-1}; HRMS (ESI^{+}) *m/z*: $[M + Na]^{+}$ calcd for $C_{23}H_{31}NNaO_9$, 488.1897; found, 488.1861.

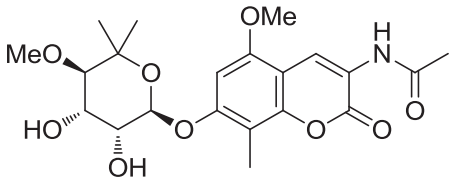

30d

N-(7-(((2R,3R,4S,5R)-3,4-dihydroxy-5-methoxy-6,6-dimethyltetrahydro-2H-pyran-2-yl)oxy)-5-methoxy-8-methyl-2-oxo-2H-chromen-3-yl)acetamide (30d): Palladium on carbon (20%, 40 mg) was added to **25d** (200 mg, 0.36 mmol) in anhydrous THF (2.40 mL) and the solution was placed under an atmosphere of H_2. After 12 h, the solution was filtered through SiO_2 (1:1 CH_2Cl_2:Acetone) and the eluent was concentrated to afford a yellow solid, which was used without further purification (150 mg, 99%).

Acetic anhydride (23 μL, 0.24 mmol) was added to the amine (50.6 mg, 0.12 mmol) in 50% pyridine/CH_2Cl_2 (3.30 mL). After 12 h, the solvent was concentrated and the residue purified via column chromatography (SiO_2, 40:1 CH_2Cl_2:Acetone) to afford a colorless solid, which was used without further purification (16.0 mg, 29%).

Triethylamine (35 μL) was added to the carbonate (16.0 mg, 0.035 mmol) in 50% MeOH/CH_2Cl_2 (0.35 mL). After 48 h, the solvent was concentrated and the residue purified via column chromatography (SiO_2, 40:1 CH_2Cl_2:Acetone) to afford **30d** as a colorless amorphous solid (13.5 mg, 89%, 26% over 3 steps): ^{1}H NMR (CD_2Cl_2, 400 MHz) δ 8.82 (s, 1H), 7.94 (s, 1H), 6.82 (s, 1H), 5.64 (d, *J* = 1.9 Hz, 1H), 4.28–4.24 (m, 2H), 3.96 (s, 3H), 3.62 (s, 3H), 3.38 (d, *J* = 6.4 Hz, 1H), 2.20 (s, 6H), 1.41 (s, 3H), 1.18 (s, 3H); ^{13}C NMR ($CDCl_3$, 125 MHz) δ 168.9, 159.4, 156.4, 154.5, 149.6, 120.1, 105.9, 104.6, 97.7, 94.0, 84.3, 78.6, 71.1, 68.6, 62.0, 56.0, 53.5, 29.4, 29.1, 24.7, 22.5; IR (film) ν_{max} 3398, 2974, 2930, 2910, 2840, 1717, 1605, 1528, 1367, 1344, 1250, 1103, 1051, 991, 966, 926, 802 cm^{-1}; HRMS (ESI$^+$) *m/z*: $[M + Na]^+$ calcd for $C_{21}H_{27}NNaO_9$, 460.1584; found, 460.1530.

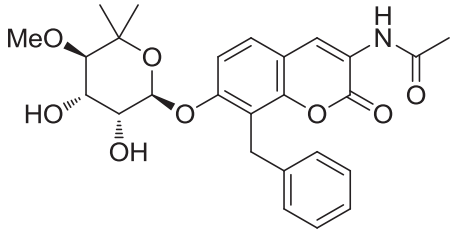

30e

N-(8-benzyl-7-(((2R,3R,4S,5R)-3,4-dihydroxy-5-methoxy-6,6-dimethyltetrahydro-2H-pyran-2-yl)oxy)-2-oxo-2H-chromen-3-yl)acetamide (30e): Palladium on carbon (20%, 46 mg) was added to **25e** (230 mg, 0.38 mmol) in anhydrous THF (2.50 mL) and the solution was placed under an atmosphere of H_2. After 12 h, the solution was filtered through SiO_2 (1:1 CH_2Cl_2:Acetone) and the eluent was concentrated to afford a yellow solid, which was used without further purification (177 mg, 99%).

Acetic anhydride (24.3 μL, 0.26 mmol) was added to the amine (60.0 mg, 0.13 mmol) in 50% pyridine/CH_2Cl_2 (3.50 mL). After 12 h, the solvent was concentrated and the residue purified via

column chromatography (SiO_2, 3:1 Hexane:Ether → 20:1 → 4:1 CH_2Cl_2:Acetone) to afford a colorless solid, which was used without further purification (10.4 mg, 16%).

Triethylamine (20 μL) was added to the carbonate (10.4 mg, 0.020 mmol) in 50% MeOH/CH_2Cl_2 (0.20 mL). After 48 h, the solvent was concentrated and the residue purified via column chromatography (SiO_2, 40:1 CH_2Cl_2:Acetone) to afford **30e** as a colorless amorphous solid (7.50 mg, 76%, 12% over 3 steps): ^{1}H NMR (CD_2Cl_2, 500 MHz) δ 8.60 (s, 1H), 7.96 (s, 1H), 7.38 (d, *J* = 8.5 Hz, 1H), 7.23–7.13 (m, 6H), 5.46 (d, *J* = 2.5 Hz, 1H), 4.17 (d, *J* = 14.5 Hz, 1H), 4.11 (d, *J* = 14.5 Hz, 1H), 4.08 (dd, *J* = 8.5, 3.5 Hz, 1H), 3.99 (t, *J* = 3.0 Hz, 1H), 3.52 (s, 3H), 3.25 (d, *J* = 8.5 Hz, 1H), 2.58 (s, 3H), 1.33 (s, 3H), 0.97 (s, 3H); ^{13}C NMR (CD_2Cl_2, 125 MHz) δ 168.4, 158.0, 155.4, 148.1, 139.3, 127.5, 126.0, 125.3, 122.8, 121.3, 116.2, 113.5, 110.8, 97.5, 83.2, 77.7, 70.1, 67.8, 60.7, 30.8, 28.9, 28.3, 27.9, 27.6, 23.7, 21.7; IR (film) ν_{max} 3391, 3329, 2976, 2932, 2359, 2332, 1715, 1684, 1605, 1526, 1375, 1259, 1130, 1113, 1076, 1036, 960, 746 cm^{-1}; HRMS (ESI$^+$) *m/z*: [M + Na]$^+$ calcd for $C_{26}H_{29}NNaO_8$, 506.1791; found, 506.1792.

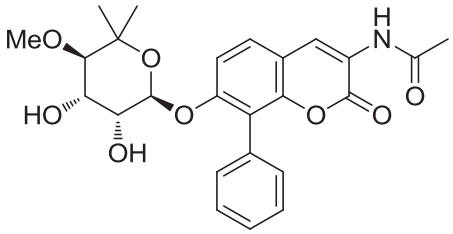

30f

N-(7-(((2R,3R,4S,5R)-3,4-dihydroxy-5-methoxy-6,6-dimethyltetrahydro-2H-pyran-2-yl)oxy)-2-oxo-8-phenyl-2H-chromen-3-yl)acetamide (30f): Palladium on carbon (20%, 14 mg) was added to **25f** (68.0 mg, 0.12 mmol) in anhydrous THF (0.80 mL) and the solution was placed under an atmosphere of H_2. After 12 h, the solution was filtered through SiO_2 (1:1

CH_2Cl_2:Acetone) and the eluent was concentrated to afford a yellow solid, which was used without further purification (52.0 mg, 99%).

Acetic anhydride (7.30 μL, 0.077 mmol) was added to the amine (17.5 mg, 0.039 mmol) in 50% pyridine/CH_2Cl_2 (1.10 mL). After 12 h, the solvent was concentrated and the residue purified via column chromatography (SiO_2, 40:1 CH_2Cl_2:Acetone) to afford a colorless solid, which was used without further purification (12.1 mg, 63%).

Triethylamine (24 μL) was added to the carbonate (12.1 mg, 0.024 mmol) in 50% MeOH/CH_2Cl_2 (0.24 mL). After 48 h, the solvent was concentrated and the residue purified via column chromatography (SiO_2, 40:1 CH_2Cl_2:Acetone) to afford **30f** as a colorless amorphous solid (9.0 mg, 79%, 49% over 3 steps): ^{1}H NMR (CD_2Cl_2, 400 MHz) δ 8.70 (s, 1H), 7.98 (s, 1H), 7.55–7.45 (m, 3H), 7.37 (dd, *J* = 6.9, 1.6 Hz, 2H), 5.54 (d, *J* = 2.5 Hz, 1H), 3.88 (t, *J* = 1.6 Hz, 1H), 3.77 (dd, *J* = 9.0, 3.4 Hz, 1H), 3.54 (s, 3H), 3.25 (d, *J* = 9.0 Hz, 1H), 2.22 (s, 3H), 1.32 (s, 3H), 1.30 (s, 3H), 1.07 (s, 3H); ^{13}C NMR ($CDCl_3$, 125 MHz) δ 169.3, 158.7, 155.2, 148.0, 131.1, 130.4, 128.1, 127.9, 127.7, 123.9, 122.0, 119.7, 114.6, 112.4, 98.3, 84.0, 78.5, 70.8, 68.3, 61.8, 29.7, 28.8, 24.8, 22.7, 14.2; IR (film) ν_{max} 3369, 3331, 2924, 2853, 2359, 2332, 1713, 1682, 1599, 1524, 1375, 1261, 1177, 1115, 1045 cm^{-1}; HRMS (ESI$^+$) *m/z*: [M + H]$^+$ calcd for $C_{25}H_{28}NO_8$, 470.1815; found, 470.1806.

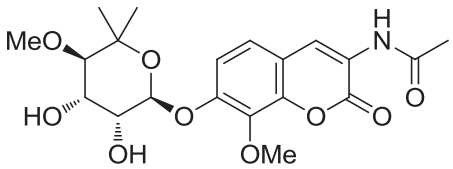

30g

N-(7-(((2S,3R,4S,5R)-3,4-dihydroxy-5-methoxy-6,6-dimethyltetrahydro-2H-pyran-2-yl)oxy)-8-methoxy-2-oxo-2H-chromen-3-yl)acetamide (30g): Palladium on carbon (20%, 50

mg) was added to **25g** (249 mg, 0.46 mmol) in anhydrous THF (3.1 mL) and the solution was placed under an atmosphere of H_2. After 12 h, the solution was filtered through SiO_2 (1:1 CH_2Cl_2:Acetone) and the eluent was concentrated to afford a yellow solid, which was used without further purification (187 mg, 99%).

Acetic anhydride (29.0 μL, 0.31 mmol) was added to the amine (62.4 mg, 0.15 mmol) in 50% pyridine/CH_2Cl_2 (4.20 mL). After 12 h, the solvent was concentrated and the residue purified via column chromatography (SiO_2, 3:1 Hexane:Ether → 40:1 → 10:1 CH_2Cl_2:Acetone) to afford a colorless solid, which was used without further purification (32.0 mg, 47%).

Triethylamine (71 μL) was added to the carbonate (26.0 mg, 0.040 mmol) in 50% MeOH/CH_2Cl_2 (0.71 mL). After 48 h, the solvent was concentrated and the residue purified via column chromatography (SiO_2, 3:1 CH_2Cl_2:Acetone) to afford **30g** as a colorless amorphous solid (22.1 mg, 73%, 34% over 3 steps): ^{1}H NMR ($CDCl_3$, 500 MHz) δ 8.54 (s, 1H), 7.94 (s, 1H), 7.16 (d, *J* = 8.5 Hz, 1H), 7.10 (d, *J* = 9.0 Hz, 1H), 5.50 (s, 1H), 5.23 (s, 1H), 4.20 (d, *J* = 10.5 Hz, 1H), 3.87 (s, 3H), 3.53 (s, 3H), 3.29 (d, *J* = 8.5 Hz, 1H), 2.82 (s, 1H), 2.63 (s, 1H), 2.16 (s, 3H), 1.32 (s, 3H), 1.14 (s, 3H); ^{13}C NMR ($CDCl_3$, 125 MHz) δ 169.3, 158.5, 151.2, 143.9, 136.6, 124.0, 122.6, 122.1, 115.2, 113.3, 98.7, 84.1, 78.7, 71.0, 68.5, 61.8 (2C), 28.9, 24.7, 22.9; IR (film) ν_{max} 3391, 3323, 3273, 2934, 2359, 2332, 1607, 1458, 1375, 1275, 1254, 1132, 1088, 1040, 951, 798 cm^{-1}; HRMS (ESI$^+$) *m/z*: $[M + Na]^+$ calcd for $C_{20}H_{25}NNaO_9$, 446.1427; found, 446.1430.

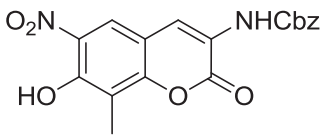

32

Benzyl (7-hydroxy-8-methyl-6-nitro-2-oxo-2H-chromen-3-yl)carbamate (32): Zirconyl nitrate (35%) (0.63 mL, 1.36 mmol) was added to a solution of coumarin **31**[102] (448 mg, 1.36 mmol) in acetone (2.0 mL), then heated to reflux for 12 h. Once cool, the solution was concentrated, then water (30 mL) was added and the solution was extracted with EtOAc (3 × 30 mL). Combined organic fractions were dried (Na_2SO_4), filtered, and concentrated to afford **32** as a yellow amorphous solid (411 mg, 81%): ^{1}H NMR ($CDCl_3$, 400 MHz) δ 11.13 (s, 1H), 8.29 (s, 1H), 8.20 (s, 1H), 7.54 (bs, 1H), 7.44–7.39 (m, 5H), 5.27 (s, 2H), 2.43 (s, 3H); ^{13}C NMR ($CDCl_3$, 125 MHz) δ 155.8, 152.3, 151.3, 151.2, 133.6, 129.4, 127.1, 127.1, 126.8, 121.7, 119.7, 118.5, 114.6, 111.4, 66.2, 28.1, 27.8, 6.7; HRMS (ESI$^+$) *m/z*: [M + Na]$^+$ calcd for $C_{18}H_{14}N_2NaO_7$, 393.0699; found, 393.0652.

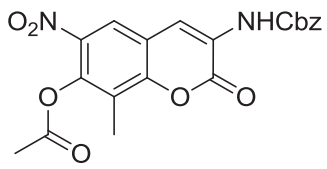

33

3-(((Benzyloxy)carbonyl)amino)-8-methyl-6-nitro-2-oxo-2H-chromen-7-yl acetate (33):): A solution of coumarin **32** (150 mg, 0.41 mmol) in pyridine (3.0 mL) was treated with acetic anhydride (1.0 mL). After 12 h, the solvent was concentrated and the residue purified via column chromatography (SiO_2, 100:1 CH_2Cl_2:Acetone) to afford **33** as a yellow amorphous solid (140 mg, 84%): ^{1}H NMR ($CDCl_3$, 400 MHz) δ 8.35 (s, 1H), 8.15 (s, 1H), 7.65 (s, 1H), 7.43–7.37 (m, 5H), 5.27 (s, 2H), 2.46 (s, 3H), 2.37 (s, 3H); ^{13}C NMR ($CDCl_3$, 125 MHz) δ 168.2, 157.1, 152.8, 150.6, 143.0, 139.0, 135.1, 128.8, 128.7, 128.5, 128.4, 125.3, 122.8, 122.0, 119.1, 117.6, 68.0, 29.7, 20.6, 9.5; HRMS (ESI$^+$) *m/z*: [M + Na]$^+$ calcd for $C_{20}H_{16}N_2NaO_8$, 435.0804; found, 435.0841.

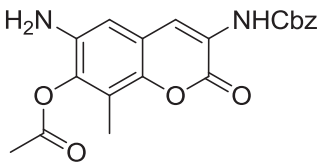

34

6-amino-3-(((benzyloxy)carbonyl)amino)-8-methyl-2-oxo-2H-chromen-7-yl acetate (34): Tin (II) chloride dihydrate (137 mg, 0.61 mmol) was added to was added to a solution of coumarin **33** (25 mg, 0.061 mmol) in MeOH (1.20 mL), then heated to reflux for 30 min. Once cool, the solution was concentrated, then saturated $NaHCO_3$ (10 mL) and EtOAc (10 mL) and the biphasic solution was filtered through Celite. Next, the filtrate was extracted with EtOAc (3 x 30 mL) and the combined organic fractions were dried (Na_2SO_4), filtered, and concentrated to afford **34** as a yellow amorphous solid (21.5 mg, 93%): ^{1}H NMR (Acetone-d_6, 400 MHz) δ 9.74 (bs, 1H), 8.17 (s, 1H), 8.12 (bs, 1H), 7.43–7.39 (m, 2H), 7.37–7.32 (m, 5H), 5.25 (s, 2H), 2.29 (s, 3H), 2.26 (s, 3H); ^{13}C NMR ($CDCl_3$, 125 MHz) δ 171.2, 158.7, 153.2., 149.3, 147.2, 135.5 (2C), 128.7 (2C), 128.6 (2C), 128.2, 123.6, 122.0, 121.4, 116.9, 112.4, 56.0, 29.8, 8.8; HRMS (ESI$^+$) *m/z*: $[M + H]^+$ calcd for $C_{20}H_{19}N_2O_6$, 383.1243; found, 383.1286.

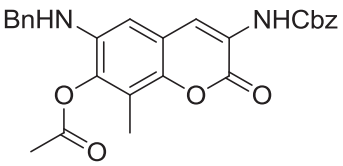

35

6-(benzylamino)-3-(((benzyloxy)carbonyl)amino)-8-methyl-2-oxo-2H-chromen-7-yl acetate (35): A solution of benzyl chloride, in 42 μL anhydrous *N,N*-dimethylformamide, was added dropwise to a solution of cesium carbonate (34 mg, 0.10 mmol), potassium iodide (35 mg, 0.21 mmol), and coumarin **34** (40 mg, 0.10 mmol) in anhydrous *N,N*-dimethylformamide (0.17 mL), then heated to 95^{o}C for 4 h. Water (30 mL) was added and the solution was extracted with

EtOAc (3 × 10 mL). Combined organic fractions were washed with saturated aqueous NaCl, dried (Na_2SO_4), filtered, and concentrated. The residue was purified via column chromatography (SiO_2, 40:1; CH_2Cl_2:Acetone) to afford **35** as a yellow amorphous solid (44 mg, 90%): ^{1}H NMR ($CDCl_3$, 400 MHz) δ 8.37 (s, 1H), 8.33 (s, 1H), 7.57 (s, 1H), 7.46–7.42 (m, 10H), 7.33 (s, 1H), 5.26 (s, 2H), 4.95 (s, 2H), 2.48 (s, 3H), 1.91 (s, 3H); ^{13}C NMR ($CDCl_3$, 125 MHz) δ 168.1, 158.6, 153.0, 147.5, 144.7, 136.2, 135.5, 129.3, 129.2 (2C), 129.0, 128.7 (2C), 128.5 (3C), 128.4, 127.8, 123.3, 122.0, 118.9, 116.2, 115.2, 67.6, 29.7, 24.5, 9.6; HRMS (ESI$^+$) *m/z*: $[M + H]^+$ calcd for $C_{27}H_{25}N_2O_6$, 473.1713; found, 473.1723.

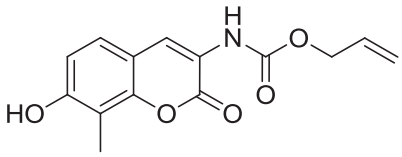

36

Allyl (7-hydroxy-8-methyl-2-oxo-2H-chromen-3-yl)carbamate (36): Palladium on carbon (20%, 50 mg) was added to coumarin **31**[102] (250 mg, 0.77 mmol) in anhydrous THF (5.0 mL) and the solution was placed under an atmosphere of H_2. After 12 h, the solution was filtered through SiO_2 (40:1 CH_2Cl_2:Acetone) and the eluent was concentrated to afford a yellow solid, which was used without further purification (147 mg, 99%).

A solution of allyl chloroformate (0.10 mL, 0.96 mmol), in anhydrous THF (0.37 mL), was added dropwise to a solution of the aminocoumarin (147 mg, 0.77 mmol) and pyridine (77 μL, 0.96 mmol) in anhydrous THF (2.8 mL) at 0^{o}C, then warmed to rt slowly over 2 h. The reaction mixture was filtered to remove insoluble salts, eluting with EtOAc, and then water (30 mL) was added to the filtrate and the solution was extracted with EtOAc (3 x 30 mL) and the combined organic fractions were washed with saturated aqueous NaCl, dried (Na_2SO_4), filtered, and concentrated. The residue was purified via column chromatography (SiO_2, 40:1 → 20:1

CH_2Cl_2:Acetone) to afford **36** as a colorless amorphous solid (175 mg, 83%): ^{1}H NMR ($CDCl_3$, 400 MHz) δ 8.27 (s, 1H), 7.49 (s, 1H), 7.22 (d, *J* = 8.4 Hz, 1H), 6.82 (d, *J* = 8.4 Hz, 1H), 6.04–5.94 (m, 1H), 5.72 (s, 1H), 5.43–5.29 (m, 2H), 4.72–4.71 (m, 2H), 2.36 (s, 3H); ^{13}C NMR ($CDCl_3$, 125 MHz) δ 160.1, 157.3, 153.0, 151.8, 149.5, 135.0, 128.0, 122.3, 120.1, 115.2, 112.6, 111.0, 67.0, 9.1; HRMS (ESI$^+$) *m/z*: $[M + Na]^+$ calcd for $C_{14}H_{13}NNaO_5$, 298.0691; found, 298.0706.

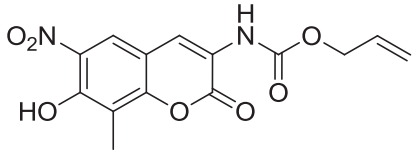

37

Allyl (7-hydroxy-8-methyl-6-nitro-2-oxo-2H-chromen-3-yl)carbamate (37): Zirconyl nitrate (35%) (21.7 μL, 0.054 mmol) was added to a solution of coumarin **36** (15.0 mg, 0.054 mmol) in acetone (0.27 mL), then heated to reflux for 1 h. Once cool, the solution was concentrated, then water (10 mL) was added and the solution was extracted with EtOAc (3 × 10 mL). Combined organic fractions were dried (Na_2SO_4), filtered, and concentrated to afford **37** as a yellow amorphous solid (17.5 mg, 99%): ^{1}H NMR ($CDCl_3$, 400 MHz) δ 11.12 (s, 1H), 8.28 (s, 1H), 8.19 (s, 1H), 7.51 (bs, 1H), 6.04–5.94 (m, 1H), 5.44–5.40 (m, 1H), 5.33 (dd, *J* = 10.4, 1.2 Hz, 1H), 4.74 (dd, *J* = 9.7, 1.2 Hz, 2H), 2.43 (s, 3H); ^{13}C NMR ($CDCl_3$, 125 MHz) δ 156.4, 152.9, 151.8, 130.6, 122.3, 120.3, 119.1, 118.0, 115.2, 112.0, 65.6, 7.3; HRMS (ESI$^+$) *m/z*: $[M + H]^+$ calcd for $C_{14}H_{13}N_2O_7$, 321.0723; found, 321.0707.

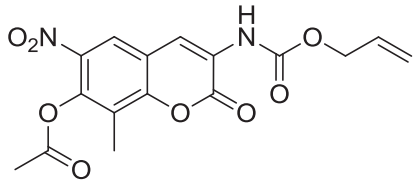

38

3-(((Allyloxy)carbonyl)amino)-8-methyl-6-nitro-2-oxo-2H-chromen-7-yl acetate (38): A solution of coumarin **37** (17.5 mg, 0.055 mmol) in pyridine (0.5 mL) was treated with acetic anhydride (0.17 mL). After 12 h, the solvent was concentrated and the residue purified via column chromatography (SiO_2, 100:1 CH_2Cl_2:Acetone) to afford **38** as a yellow amorphous solid (9.9 mg, 50%): ^{1}H NMR ($CDCl_3$, 400 MHz) δ 8.28 (s, 1H), 8.19 (s, 1H), 7.54 (s, 1H), 6.03–5.95 (m, 1H), 5.42 (d, *J* = 16.0 Hz, 1H), 5.33 (d, *J* = 8.0 Hz, 1H), 4.73 (d, *J* = 8.0 Hz, 2H), 2.42 (s, 3H) 2.12 (s, 3H); ^{13}C NMR ($CDCl_3$, 125 MHz) δ 167.1, 155.5, 151.7, 149.6, 141.9, 130.8, 124.2, 122.1, 121.9, 121.7, 118.2, 118.1, 117.7, 67.3, 22.0, 9.9; HRMS (ESI^+) *m/z*: $[M + Na]^+$ calcd for $C_{16}H_{14}N_2NaO_8$, 385.0648; found, 385.0655.

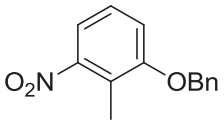

40

1-(Benzyloxy)-2-methyl-3-nitrobenzene (40):[233] Benzyl bromide (4.70 mL, 39.2 mmol) was added dropwise to a solution of 2-methyl-3-nitrophenol (2.0 g, 13.1 mmol) and potassium carbonate (9.0 g, 65.3 mmol) in anhydrous *N,N*-dimethylformamide (26.0 mL), then stirred for 12 h. Water (50 mL) was added and the solution was extracted with EtOAc (3 × 50 mL). Combined organic fractions were washed with saturated aqueous NaCl, dried (Na_2SO_4), filtered, and concentrated. The residue was purified via column chromatography (SiO_2, 100% Hexane, 8:1 → 3:1 Hexane:EtOAc) to afford **40** as a yellow oil (3.07 g, 97%): ^{1}H NMR ($CDCl_3$, 500

MHz) δ 7.40–7.37 (m, 6H), 7.27 (t, *J* = 8.0 Hz, 1H), 7.13 (d, *J* = 8.0 Hz, 1H), 5.16 (s, 2H), 2.46 (s, 3H).

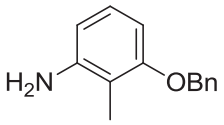

41

3-(Benzyloxy)-2-methylaniline (41):[234] **Preparation 1:** 2-bromoethanol (0.29 mL, 4.11 mmol) was added to a solution of nitroarene **40** (1.0 g, 4.11 mmol) and phthalocyanatoiron (47 mg, 0.082 mmol) in diglyme (23 mL). After several minutes, sodium borohydride (311 mg, 8.22 mmol) was added and the solution was stirred for 12 h. Water (30 mL) was added and the solution was extracted with EtOAc (3 x 30 mL). Combined organic fractions were dried (Na_2SO_4), filtered, and concentrated. The residue was purified via column chromatography (SiO_2, 6:1 Hexane:EtOAc) to afford **41** as a red oil (262 mg, 79%).

Preparation 2: Platinum on carbon (20%, 200 mg) was added to nitroarene **40** (1.0 g, 4.11 mmol) in anhydrous THF (27.0 mL) and the solution was placed under an atmosphere of H_2. After 12 h, the solution was filtered through SiO_2 (40:1 CH_2Cl_2:Acetone) and the eluent was concentrated to afford **41** as a red oil (864 mg, 99%): ^{1}H NMR ($CDCl_3$, 400 MHz) δ 7.48–7.32 (m, 5H), 6.99 (t, *J* = 8.0 Hz, 1H), 6.44 (d, *J* = 8.0 Hz, 1H), 6.40 (d, *J* = 8.0 Hz, 1H), 5.08 (s, 2H), 3.65 (bs, 2H), 2.15 (s, 3H).

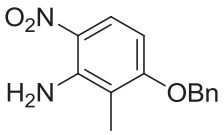

42

3-(Benzyloxy)-2-methyl-6-nitroaniline (42): Zirconyl nitrate (35%) (7.44 mL, 14.0 mmol) was added to a solution of aniline **41** (2.0 g, 9.33 mmol) in acetone (47.0 mL), then heated to

reflux for 12 h. Once cool, the solution was concentrated, then water (30 mL) was added and the solution was extracted with EtOAc (3 × 30 mL). Combined organic fractions were dried (Na_2SO_4), filtered, and concentrated. The crude solid residue was washed with hexanes, allowing collection of **42** as a gray amorphous solid (2.0 g, 83%): ^{1}H NMR (Acetone-d_6, 400 MHz) δ 7.54 (s, 1H), 7.52 (s, 1H), 7.42 (t, J = 7.2 Hz, 1H), 7.35 (t, J = 7.2 Hz, 1H), 7.31 (d, J = 8.0 Hz, 1H), 7.16 (d, J = 8.0 Hz, 1H), 6.86 (d, J = 8.0 Hz, 1H), 5.22 (s, 2H), 2.07 (s, 3H); ^{13}C NMR ($CDCl_3$, 125 MHz) δ 155.7, 141.3, 136.8, 127.5, 127.4, 126.6, 126.2, 126.1, 125.7, 124.9, 120.4, 99.5, 69.0, 7.6; HRMS (ESI$^+$) *m/z*: [M + Na]$^+$ calcd for $C_{14}H_{14}N_2NaO_3$, 281.0902; found, 281.0933.

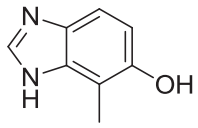

43

7-Methyl-1H-benzo[d]imidazol-6-ol (43): Tin (II) chloride dihydrate (41.5 mg, 0.18 mmol) was added to was added to a solution of aniline **42** (10.3 mg, 0.061 mmol) in 88% formic acid (0.20 mL), then heated to 130^{o}C for 30 min in the microwave. Once cool, water (5 mL) was added and the solution was neutralized using 50% aqueous NaOH. Next, the solution was extracted with EtOAc (3 x 15 mL), and then the combined organic fractions were dried (Na_2SO_4), filtered, and concentrated. The residue was purified via column chromatography (SiO_2, 5:1 Hexane:EtOAc) to afford **43** as a red oil (7.0 mg, 77%): ^{1}H NMR ($CDCl_3$, 400 MHz) δ 6.89 (t, J = 8.0 Hz, 1H), 6.34 (d, J = 8.0 Hz, 1H), 6.25 (d, J = 8.0 Hz, 1H), 4.66 (bs, 1H), 3.66 (bs, 1H), 2.09 (s, 3H); ^{13}C NMR ($CDCl_3$, 125 MHz) δ 154.2, 146.1, 128.6, 126.7, 122.8, 107.9, 105.6, 9.2; HRMS (ESI$^+$) *m/z*: [M + Na]$^+$ calcd for $C_8H_8N_2NaO$, 171.0534; found, 171.0586.

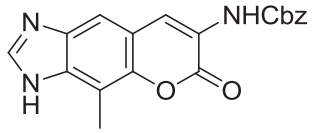

44

Benzyl (4-methyl-6-oxo-3,6-dihydrochromeno[6,7-d]imidazol-7-yl)carbamate (44): A solution of **43** (387 mg, 2.61 mmol) and eneamine **22** (1.09 g, 3.92 mmol) in glacial acetic acid (16.3 mL) was heated to reflux for 40 h. Upon cooling to rt, the yellow precipitate was collected by vacuum filtration and recrystallized from MeOH/H_2O. The filtrate was extracted with EtOAc (3 x 15 mL), and then the combined organic fractions were dried (Na_2SO_4), filtered, and concentrated. The residue was recrystallized as described above and combined with the previous obtained product, to afford **44** as a yellow amorphous solid (171 mg, 19%): ^{1}H NMR ($CDCl_3$, 400 MHz) δ 10.15 (s, 1H), 7.97 (d, *J* = 8.7 Hz, 1H), 7.45–7.39 (m, 5H), 7.12 (dd, *J* = 8.7, 1.8 Hz, 1H), 6.97 (d, *J* = 2.0 Hz, 1H), 5.19 (s, 2H), 1.59 (s, 3H); ^{13}C NMR ($CDCl_3$, 125 MHz) δ 159.3, 154.2, 148.0, 146.4, 141.3, 138.8, 134.2 (2C), 128.7 (4C), 128.3, 122.0, 121.9, 119.9, 113.0, 68.0, 10.1; $[M + Na]^+$ calcd for $C_{19}H_{15}N_3NaO_4$, 372.0960; found, 372.0953.

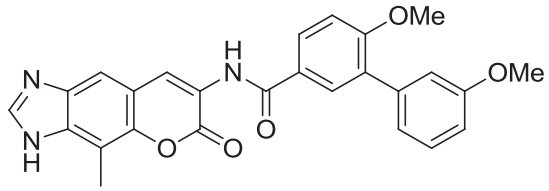

45

3',6-Dimethoxy-N-(4-methyl-6-oxo-3,6-dihydrochromeno[6,7-d]imidazol-7-yl)-[1,1'-biphenyl]-3-carboxamide (45): Palladium on carbon (20%, 12 mg) was added to **44** (60 mg, 0.17 mmol) in anhydrous THF (4.0 mL) and the solution was placed under an atmosphere of H_2. After 12 h, the system was evacuated and an Ar atmosphere was introduced. EDCI (82.3 mg, 0.43 mmol), pyridine (1.7 mL), and 3',6-dimethoxybiphenyl-3-carboxylic acid (88.7 mg, 0.34

mmol) were added and the solution was stirred for 12 h. Next, solvent was removed and the residue purified via column chromatography (SiO_2, 40:1 CH_2Cl_2:Acetone) to afford **45** as a yellow amorphous solid (15.6 mg, 20%): ^{1}H NMR ($CDCl_3$, 400 MHz) δ 8.86 (s, 1H), 8.77 (s, 1H), 8.03 (d, *J* = 8.5 Hz, 1H), 7.96–7.92 (m, 1H), 7.87 (d, *J* = 12.5 Hz, 1H), 7.46 (d, *J* = 8.5 Hz, 1H), 7.39 (t, *J* = 8.0 Hz, 1H), 7.16–7.09 (m, 3H), 6.95 (d, *J* = 8.3 Hz, 1H), 3.93 (s, 3H), 3.88 (d, *J* = 2.2 Hz, 3H), 3.81 (s, 1H), 2.46 (s, 3H); ^{13}C NMR ($CDCl_3$, 125 MHz) δ 165.6, 165.2, 159.8, 159.3, 148.4, 138.6, 137.6, 129.8, 129.2 (2C), 128.3, 125.8, 123.7, 122.0 (2C), 120.0, 116.8, 115.4, 115.2, 113.2, 113.0, 111.1, 111.0, 55.9, 55.3, 29.7; HRMS (ESI$^+$) *m/z*: $[M + H]^+$ calcd for $C_{26}H_{22}N_3O_5$, 456.1559; found, 456.1627.

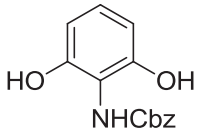

48

Benzyl (2,6-dihydroxyphenyl)carbamate (48): Palladium on carbon (5%, 50 mg) was added to 2-nitroresorcinol (1.0 g, 6.45 mmol) in EtOAc (65 mL) and the solution was placed under an atmosphere of H_2. After 12 h, the solution was filtered through SiO_2 (1:3 Hexane:EtOAc) and the eluent was concentrated to afford **47**[225] as a brown amorphous solid (800 mg, 99%), which was used without further purification.

Benzyl chloroformate (28 μL, 0.20 mmol) was added dropwise to a solution of aniline **47** (25 mg, 0.20 mmol) in MeOH (0.40 mL). After several minutes, iodine (1 mg, 0.0040 mmol) was added and the solution was stirred for 1.5 h. Et_2O (30 mL) was added and the organic layer was washed with saturated aqueous $Na_2S_2O_3$, saturated aqueous $NaHCO_3$, dried (Na_2SO_4), filtered, and concentrated. The residue was purified via column chromatography (SiO_2, 2:1 Hexane:EtOAc) to afford **48** as a brown amorphous solid (33 mg, 64%): ^{1}H NMR ($CDCl_3$, 400

MHz) δ 7.45–7.38 (m, 5H), 7.16 (bs, 1H), 6.92 (t, J = 8.0 Hz, 1H), 6.52 (d, J = 8.0 Hz, 2H), 5.26 (s, 2H); ^{13}C NMR ($CDCl_3$, 125 MHz) δ 154.5, 146.4 (2C), 133.5, 127.1 (3C), 127.0 (3C), 112.2, 108.0 (2C), 66.9; HRMS (ESI^+) *m/z*: $[M + H]^+$ calcd for $C_{14}H_{14}NO_4$, 260.0923; found, 260.0939.

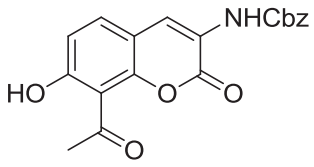

50

Benzyl (8-acetyl-7-hydroxy-2-oxo-2H-chromen-3-yl)carbamate (50): A solution of 1-(2,6-dihydroxyphenyl)ethanone (500 mg, 3.29 mmol) and eneamine **22** (915 mg, 3.29 mmol) in glacial acetic acid (22.0 mL) was heated to reflux for 48 h. Upon cooling to rt, the orange precipitate was collected by vacuum filtration and recrystallized from MeOH/H_2O. The filtrate was extracted with EtOAc (3 x 15 mL), and then the combined organic fractions were dried (Na_2SO_4), filtered, and concentrated. The residue was recrystallized as described above and combined with the previous obtained product, to afford **50** as a yellow amorphous solid (450 mg, 40%): ^{1}H NMR ($CDCl_3$, 500 MHz) δ 8.23 (bs, 1H), 7.47 (d, J = 9.0 Hz, 1H), 7.37–7.29 (m, 6H), 6.88 (d, J = 8.5 Hz, 1H), 5.17 (s, 2H), 2.88 (s, 3H); ^{13}C NMR ($CDCl_3$, 125 MHz) δ 203.7, 165.2, 157.3, 153.1, 150.4, 135.4, 134.4, 128.7 (2C), 128.6 (2C), 128.3, 122.4, 121.3, 116.5, 111.6, 109.2, 67.7, 33.8; HRMS (ESI^+) *m/z*: $[M + Na]^+$ calcd for $C_{19}H_{15}NNaO_6$, 376.0797; found, 376.0821.

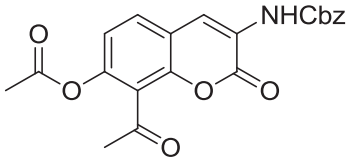

52

8-Acetyl-3-(((benzyloxy)carbonyl)amino)-2-oxo-2H-chromen-7-yl acetate (52): A solution of coumarin **50** (50 mg, 0.15 mmol) in pyridine (2.25 mL) was treated with acetic anhydride (0.75 mL). After 12 h, the solvent was concentrated and the residue purified via column chromatography (SiO_2, 100:1 CH_2Cl_2:Acetone) to afford **52** as a colorless amorphous solid (36.7 mg, 65%): ^{1}H NMR ($CDCl_3$, 400 MHz) δ 8.35 (s, 1H), 7.59 (bs, 1H), 7.57 (d, *J* = 8.5 Hz, 1H), 7.45–7.38 (m, 5H), 7.10 (d, *J* = 8.5 Hz, 1H), 5.27 (s, 2H), 2.70 (s, 3H), 2.31 (s, 3H); ^{13}C NMR ($CDCl_3$, 125 MHz) δ 197.4, 169.0, 157.0, 153.0, 147.5, 146.7, 135.3, 129.2, 128.7 (3C), 128.3, 124.0, 122.9 (2C), 120.3, 120.2, 118.0, 67.8, 32.0, 20.9; HRMS (ESI$^+$) *m/z*: $[M + Na]^+$ calcd for $C_{21}H_{17}NNaO_7$, 418.0903; found, 418.0952.

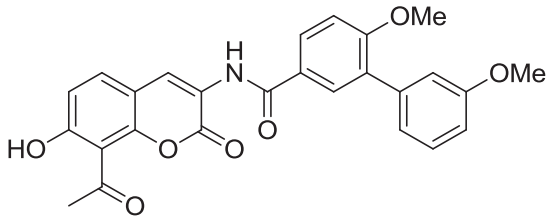

54

N-(8-acetyl-7-hydroxy-2-oxo-2H-chromen-3-yl)-3',6-dimethoxy-[1,1'-biphenyl]-3-carboxamide (54): Palladium on carbon (20%, 30 mg) was added to **52** (149 mg, 0.37 mmol) in anhydrous THF (2.60 mL) and the solution was placed under an atmosphere of H_2. After 12 h, the solution was filtered through SiO_2 (1:1 CH_2Cl_2:Acetone) and the eluent was concentrated to afford a yellow solid, which was used without further purification (97.0 mg, 99%).

EDCI (178 mg, 0.93 mmol) and 3',6-dimethoxybiphenyl-3-carboxylic acid (192 mg, 0.74 mmol) were added to the amine (97 mg, 0.37 mmol) in 30% pyridine/CH_2Cl_2 (5.60 mL). After 12 h, the solvent was concentrated and the residue purified via column chromatography (SiO_2, 40:1 CH_2Cl_2:Acetone) to afford **53** as a colorless solid (51 mg, 27%), which was used without further purification.

A solution of **53** (30 mg, 0.060 mmol) in MeOH (0.6 mL) at rt was treated with triethylamine (60 μL). After 12 h, the solvent was removed and the residue purified via column chromatography (SiO_2, 2:1, Hexane:EtOAc) to afford **54** as a yellow amorphous solid (27 mg, 99%): ^{1}H NMR ($CDCl_3$, 400 MHz) δ 13.46 (s, 1H), 8.85 (s, 1H), 8.62 (s, 1H), 7.95–7.91 (m, 2H), 7.63 (d, *J* = 8.8 Hz, 1H), 7.39 (t, *J* = 8.0 Hz, 1H), 7.15–7.10 (m, 3H), 7.01–6.95 (m, 2H), 3.93 (s, 3H), 3.88 (s, 3H), 3.00 (s, 3H); ^{13}C NMR ($CDCl_3$, 125 MHz) δ 202.4, 164.4, 164.2, 158.7, 158.1, 156.7, 149.5, 137.3, 133.6, 129.9, 128.7, 128.0, 127.0, 124.5, 123.2, 120.7, 120.3, 115.4, 114.1, 111.9, 110.5, 109.9, 108.0, 54.7, 54.1, 32.6; HRMS (ESI$^+$) *m/z*: $[M + H]^+$ calcd for $C_{26}H_{22}NO_7$, 460.1396; found, 460.1346.

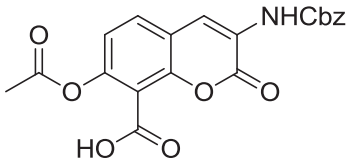

57

7-Acetoxy-3-(((benzyloxy)carbonyl)amino)-2-oxo-2H-chromene-8-carboxylic acid (57): A solution of 2,6-dihydroxybenzoic acid (554 mg, 3.60 mmol) and eneamine **22** (1.0 g, 3.60 mmol) in glacial acetic acid (18.7 mL) was heated to reflux for 48 h. Upon cooling, the solution was extracted with EtOAc (3 × 50 mL); combined organic fractions were washed with saturated aqueous NaCl, dried (Na_2SO_4), filtered, and concentrated to afford a brown solid, which was used without further purification (1.28 g, 99%).

A solution of the crude coumarin (22.0 mg, 0.062 mmol)in pyridine (1.50 mL) was treated with acetic anhydride (0.5 mL). After 12 h, the solvent was concentrated and the residue purified via column chromatography (SiO_2, 40:1 CH_2Cl_2:Acetone) to afford **57** as a yellow amorphous solid (13.0 mg, 53% over 2 steps): ^{1}H NMR ($CDCl_3$, 400 MHz) δ 8.33 (s, 1H), 7.60 (s, 1H), 7.51–7.40 (m, 5H), 7.14 (s, 1H), 7.11–7.07 (m, 2H), 5.26 (s, 2H), 2.37 (s, 3H); ^{13}C NMR

($CDCl_3$, 125 MHz) δ 168.9, 158.2, 153.1, 151.1, 149.9, 135.4, 128.8, 128.7, 128.6, 128.5, 128.3, 128.0, 123.8, 120.6, 119.0, 117.6, 115.5, 110.0, 67.7, 21.1; HRMS (ESI^+) *m/z*: $[M + H]^+$ calcd for $C_{20}H_{16}NO_8$, 398.0876; found, 398.0882.

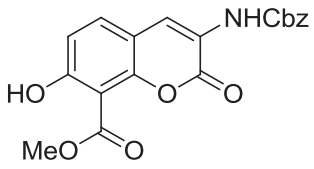

58

Methyl 3-(((benzyloxy)carbonyl)amino)-7-hydroxy-2-oxo-2H-chromene-8-carboxylate (58): Thionyl chloride (3 μL, 0.035 mmol) was added dropwise to a solution of **57** (7.0 mg, 0.018 mmol) and 4Å molecular sieves in anhydrous MeOH (0.18 mL) at 0°C, then warmed to rt slowly over 12 h. The reaction mixture was filtered through SiO_2 (EtOAc) and the eluent was concentrated. The residue purified via column chromatography (SiO_2, 40:1 CH_2Cl_2:Acetone) to afford **58** as a yellow amorphous solid (4.5 mg, 69%): ^1H NMR (Acetone-d_6, 400 MHz) δ 8.26 (s, 1H), 7.53 (d, *J* = 8.5 Hz, 1H), 7.47 (d, *J* = 7.4 Hz, 2H), 7.42–7.35 (m, 3H), 6.89 (dd, *J* = 8.5, 2.4 Hz, 1H), 6.79 (d, *J* = 2.3 Hz, 1H), 5.63 (s, 3H), 5.24 (s, 2H); ^{13}C NMR ($CDCl_3$, 125 MHz) δ 162.9, 159.3, 158.2, 153.1 (2C), 149.9, 135.4, 128.8 (2C), 128.7, 128.6, 128.5, 128.3, 121.9, 113.6 (2C), 103.1, 67.5, 29.7; HRMS (ESI^+) *m/z*: $[M + Na]^+$ calcd for $C_{19}H_{15}NNaO_7$, 392.0746; found, 392.0794.

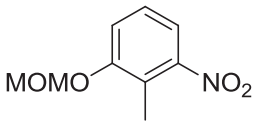

62

1-(Methoxymethoxy)-2-methyl-3-nitrobenzene (62): *N,N*-diisopropylethylamine (2.30 mL, 13.1 mmol) was slowly added to 2-methyl-3-nitrophenol (500 mg, 3.27 mmol) in anhydrous

N,N-dimethylformamide (9.30 mL) over 5 min at rt. After 30 min, the solution was cooled to 0°C and chloromethyl methyl ether (1.0 mL, 13.1 mmol) was added and the mixture warmed to rt over 12 h. The reaction was quenched by the addition of saturated aqueous NH_4Cl solution and extracted with EtOAc (3 × 30 mL). The combined organic fractions were washed with saturated aqueous NaCl, dried (Na_2SO_4), filtered, and concentrated. The residue was purified via column chromatography (SiO_2, 15:1 Hexane:EtOAc) to give **62** as a yellow oil (576 mg, 89%): ^{1}H NMR ($CDCl_3$, 400 MHz) δ 7.49 (d, J = 8.0 Hz, 1H), 7.33 (d, J = 7.6 Hz, 1H), 7.26 (d, J = 8.4 Hz, 1H), 5.27 (s, 2H), 3.52 (s, 3H), 2.42 (s, 3H); ^{13}C NMR ($CDCl_3$, 125 MHz) δ 156.2, 151.1, 126.7, 122.7, 117.8, 117.1, 94.9, 56.3, 11.8; HRMS (ESI$^+$) *m/z*: $[M + H]^+$ calcd for $C_9H_{12}NO_4$, 198.0766; found, 198.0759.

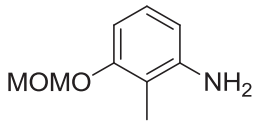

63

3-(Methoxymethoxy)-2-methylaniline (63): Palladium on carbon (5%, 24 mg) was added to nitroarene **62** (482 mg, 2.44 mmol) in EtOAc (31.0 mL) and the solution was placed under an atmosphere of H_2. After 12 h, the solution was filtered through SiO_2 (3:1 Hexane:EtOAc) and the eluent was concentrated to afford **63** as a red oil (415 mg, 99%): ^{1}H NMR ($CDCl_3$, 500 MHz) δ 6.88 (t, J = 8.0 Hz, 1H), 6.46 (d, J = 8.0 Hz, 1H), 6.32 (dd, J = 8.0, 0.5 Hz, 1H), 5.10 (s, 2H), 3.54 (bs, 2H), 3.41 (s, 3H), 2.01 (s, 3H); ^{13}C NMR ($CDCl_3$, 125 MHz) δ 155.8, 145.8, 126.6, 111.6, 109.2, 104.8, 94.8, 56.0, 9.2; HRMS (ESI$^+$) *m/z*: $[M + H]^+$ calcd for $C_9H_{14}NO_2$, 168.1025; found, 168.1015.

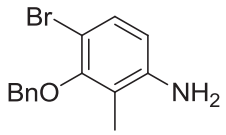

64

3-(Benzyloxy)-4-bromo-2-methylaniline (64): *N*-bromosuccinimide (92 mg, 0.52 mmol) was added to a solution of aniline 41 (100 mg, 0.47 mmol) and H_2SO_4 (2.5 μL, 0.047 mmol) in anhydrous THF (2.30 mL) at -78°C. After 1.5 h, a 1:1 mixture of saturated aqueous $Na_2S_2O_3$:saturated aqueous $NaHCO_3$ (5 mL) was added at -78°C and the solution was extracted with EtOAc (3 x 30 mL). The combined organic fractions were dried (Na_2SO_4), filtered, and concentrated. The residue was purified via column chromatography (SiO_2, 3:1 Hexane:EtOAc) to afford **64** as a yellow oil (110 mg, 81%): ^{1}H NMR ($CDCl_3$, 400 MHz) δ 7.57 (d, J = 7.2 Hz, 2H), 7.45–7.36 (m, 3H), 7.23 (d, J = 8.4 Hz, 1H), 6.43 (d, J = 8.8 Hz, 1H), 4.92 (s, 2H), 3.68 (bs, 2H), 2.13 (s, 3H); ^{13}C NMR ($CDCl_3$, 125 MHz) δ 154.1, 145.5, 137.0, 130.4, 128.6, 128.5, 128.3 (2C), 128.2, 117.9, 112.3, 105.6, 74.8, 10.8; HRMS (ESI$^+$) *m/z*: $[M + H]^+$ calcd for $C_{14}H_{15}BrNO$, 292.0337; found, 292.0349.

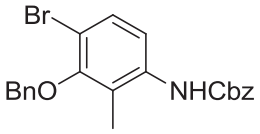

65

Benzyl (3-(benzyloxy)-4-bromo-2-methylphenyl)carbamate (65): Benzyl chloroformate (12 μL, 0.086 mmol) was added dropwise to a solution of aniline **64** (25 mg, 0.086 mmol) in MeOH (0.17 mL). After several minutes, iodine (1 mg, 0.0017 mmol) was added and the solution was stirred for 1.5 h. Et_2O (30 mL) was added and the organic layer was washed with saturated aqueous $Na_2S_2O_3$, saturated aqueous $NaHCO_3$, dried (Na_2SO_4), filtered, and concentrated. The residue was purified via column chromatography (SiO_2, 6:1 Hexane:EtOAc) to afford **65** as a

colorless amorphous solid (29 mg, 79%): ^{1}H NMR ($CDCl_3$, 400 MHz) δ 7.55–7.52 (m, 2H), 7.46–7.36 (m, 10H), 6.44 (bs, 1H), 5.23 (s, 2H), 4.93 (s, 2H), 2.18 (s, 3H); ^{13}C NMR ($CDCl_3$, 125 MHz) δ 153.9, 153.4, 136.6, 136.4, 135.8, 130.8, 128.7 (3C), 128.6 (2C), 128.5 (3C), 128.3 3C), 118.2 (2C), 75.0, 67.4, 11.2; HRMS (ESI$^+$) *m/z*: $[M + Na]^+$ calcd for $C_{22}H_{20}BrNNaO_3$, 448.0524; found, 448.0535.

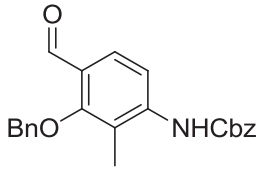

66

Benzyl (3-(benzyloxy)-4-formyl-2-methylphenyl)carbamate (66): ^{n}BuLi (2.5M in hexanes, 0.14 mL, 0.35 mmol) was added to a solution of **65** (100 mg, 0.24 mmol) in anhydrous THF (2.40 mL) at -78° C. After 10 min, anhydrous *N,N*-dimethylformamide (91 μL, 1.18 mmol) was added dropwise over several minutes. After 2 h at rt, the reaction was poured into saturated aqueous NaCl and the solution was extracted with Et_2O (3 × 10 mL). The combined organic extracts were dried (Na_2SO_4), filtered, and concentrated. The residue was purified via column chromatography (SiO_2, 3:1 Hexane:EtOAc) to afford **66** as a colorless amorphous solid (57 mg, 65%): ^{1}H NMR ($CDCl_3$, 400 MHz) δ 10.19 (s, 1H), 8.02 (d, *J* = 8.4 Hz, 1H), 7.78 (d, *J* = 8.8 Hz, 1H), 7.47–7.38 (m, 10H), 6.74 (bs, 1H), 5.26 (s, 2H), 4.96 (s, 2H), 2.19 (s, 3H); ^{13}C NMR ($CDCl_3$, 125 MHz) δ 189.1, 160.3, 152.8, 143.1, 135.8, 135.5, 128.8 (4C), 128.7 (3C), 128.4 (3C), 127.8, 125.0, 119.7, 115.4 (2C), 67.7, 10.0; HRMS (ESI$^+$) *m/z*: $[M + H]^+$ calcd for $C_{23}H_{22}NO_4$, 376.1549; found, 376.1565.

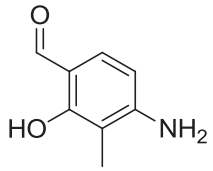

67

4-Amino-2-hydroxy-3-methylbenzaldehyde (67): Palladium on carbon (20%, 17 mg) was added to **67** (83 mg, 0.22 mmol) in anhydrous THF (1.50 mL) and the solution was placed under an atmosphere of H_2. After 12 h, the solution was filtered through SiO_2 (1:1 CH_2Cl_2:Acetone) and the eluent was concentrated. The residue was purified via column chromatography (SiO_2, 3:1 → 2:1 Hexane:EtOAc → 100% EtOAc) to afford **67** as a red amorphous solid (13 mg, 39%): ^{1}H NMR ($CDCl_3$, 400 MHz) δ 11.90 (s, 1H), 9.56 (s, 1H), 7.19 (d, J = 8.4 Hz, 1H), 6.29 (d, J = 8.4 Hz, 1H), 4.37 (bs, 2H), 2.05 (s, 3H); ^{13}C NMR ($CDCl_3$,125 MHz) δ 193.3, 161.8, 152.8, 133.1, 113.1, 107.0, 106.7, 7.7; HRMS (ESI^+) *m/z*: $[M + H]^+$ calcd for $C_8H_{10}NO_2$, 152.0712; found, 152.0703.

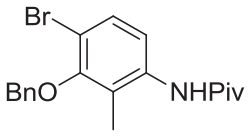

68

N-(3-(benzyloxy)-4-bromo-2-methylphenyl)pivalamide (68): Pivaloyl chloride (0.48 mL, 3.91 mmol) was added dropwise to a solution of aniline **64** (950 mg, 3.26 mmol), pyridine (0.53 mL, 6.52 mmol) and 4-dimethylaminopyridine (DMAP, 4.0 mg, 0.033 mmol) in CH_2Cl_2 (6.50 mL) at 0^{o}C. After stirring for 1 h at 0^{o}C, the reaction mixture was poured into ice-cooled aqueous 1M HCl and the solution was extracted with EtOAc (3 × 30 mL). The combined organic extracts were washed with aqueous 1M HCl, saturated aqueous $NaHCO_3$, saturated aqueous NaCl, dried (Na_2SO_4), filtered, and concentrated. The residue was purified via column chromatography

(SiO_2, 4:1 → 3:1 Hexane:EtOAc → 100% EtOAc) to afford **68** as a colorless amorphous solid (1.15 g, 94%): ^{1}H NMR ($CDCl_3$, 400 MHz) δ 7.63 (d, *J* = 8.8 Hz, 1H), 7.57–7.55 (m, 2H), 7.47–7.37 (m, 4H), 7.22 (bs, 1H), 4.93 (s, 2H), 2.22 (s, 3H), 1.36 (s, 9H); ^{13}C NMR ($CDCl_3$, 125 MHz) δ 176.5, 154.0, 136.7, 136.4, 130.7, 128.6 (2C), 128.3 (3C), 125.0, 120.3, 113.3, 75.0, 39.8, 27.7 (3C), 11.2; HRMS (ESI$^+$) *m/z*: $[M + Na]^+$ calcd for $C_{19}H_{22}BrNNaO_2$, 398.0732; found, 398.0723.

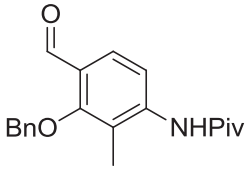

69

N-(3-(benzyloxy)-4-formyl-2-methylphenyl)pivalamide (69): ^{n}BuLi (2.5M in hexanes, 40 μL, 0.10 mmol) was added to a solution of **68** (25 mg, 0.067 mmol) in anhydrous THF (0.70 mL) at -78° C. After 30 min, anhydrous *N,N*-dimethylformamide (51 μL, 0.67 mmol) was added dropwise over several minutes. After 30 min at -78° C, the reaction was quenched with saturated aqueous NH_4Cl at -78° C and then gradually warmed to rt. The solution was extracted with EtOAc (3 × 10 mL), and then the combined organic extracts were dried (Na_2SO_4), filtered, and concentrated. The residue was purified via column chromatography (SiO_2, 6:1 → 3:1 Hexane:EtOAc) to afford **69** as a colorless amorphous solid (15.3 mg, 71%): ^{1}H NMR ($CDCl_3$, 400 MHz) δ 10.19 (s, 1H), 8.08 (d, *J* = 8.4 Hz, 1H), 7.77 (d, *J* = 8.8 Hz, 1H), 7.48–7.42 (m, 6H), 4.97 (s, 2H), 2.24 (s, 3H), 1.39 (s, 9H); ^{13}C NMR ($CDCl_3$, 125 MHz) δ 189.2, 176.2, 160.3, 143.1, 135.8, 128.8 (2C), 128.7, 128.4 (2C), 127.7, 125.7, 121.2, 117.6, 78.5, 40.2, 27.7 (3C), 10.1; HRMS (ESI$^+$) *m/z*: $[M + H]^+$ calcd for $C_{20}H_{24}NO_3$, 326.1756; found, 326.1771.

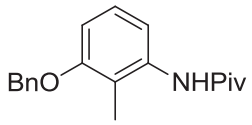

70

N-(3-(benzyloxy)-2-methylphenyl)pivalamide (70): Pivaloyl chloride (0.76 mL, 6.19 mmol) was added dropwise to a solution of aniline **41** (1.10 g, 5.16 mmol), pyridine (0.83 mL, 10.3 mmol) and 4-dimethylaminopyridine (DMAP, 6.0 mg, 0.052 mmol) in CH_2Cl_2 (10.3 mL) at 0°C. After stirring for 1 h at 0°C, the reaction mixture was poured into ice-cooled aqueous 1M HCl and the solution was extracted with EtOAc (3 × 30 mL). The combined organic extracts were washed with aqueous 1M HCl, saturated aqueous $NaHCO_3$, saturated aqueous NaCl, dried (Na_2SO_4), filtered, and concentrated. The residue was purified via column chromatography (SiO_2, 6:1 Hexane:EtOAc) to afford **70** as a colorless amorphous solid (143 g, 93%): ^{1}H NMR ($CDCl_3$, 400 MHz) δ 7.52 (d, *J* = 8.4 Hz, 1H), 7.47–7.39 (m, 4H), 7.37–7.33 (m, 1H), 7.17 (t, *J* = 8.0 Hz, 1H), 6.78 (d, *J* = 8.4 Hz, 1H), 5.10 (s, 2H), 2.20 (s, 3H), 1.37 (s, 9H); ^{13}C NMR ($CDCl_3$,125 MHz) δ 176.5, 156.9, 137.3, 136.8, 128.6 (2C), 127.8, 127.2 (2C), 126.6, 118.3, 116.0, 108.7, 70.4, 39.8, 27.8 (3C), 9.9; HRMS (ESI^+) *m/z*: $[M + H]^+$ calcd for $C_{19}H_{24}NO_2$, 298.1807; found, 298.1815.

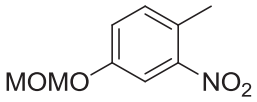

73

4-(Methoxymethoxy)-1-methyl-2-nitrobenzene (73): *N,N*-diisopropylethylamine (4.55 mL, 26.1 mmol) was slowly added to 4-methyl-3-nitrophenol (1.0 g, 6.53 mmol) in anhydrous *N,N*-dimethylformamide (21.8 mL) over 5 min at rt. After 30 min, the solution was cooled to 0°C and chloromethyl methyl ether (1.98 mL, 26.1 mmol) was added and the mixture warmed to rt over

12 h. The reaction was quenched by the addition of saturated aqueous NH_4Cl solution and extracted with EtOAc (3 × 30 mL). The combined organic fractions were washed with saturated aqueous NaCl, dried (Na_2SO_4), filtered, and concentrated. The residue was purified via column chromatography (SiO_2, 40:1 Hexane:EtOAc) to give **73** as a yellow oil (1.28 g, 99%): ^{1}H NMR ($CDCl_3$, 400 MHz) δ 7.68 (d, *J* = 2.4 Hz, 1H), 7.27 (d, *J* = 5.2 Hz, 1H), 7.20 (dd, *J* = 8.8, 2.4 Hz, 1H), 5.22 (s, 2H), 3.50 (s, 3H), 2.55 (s, 3H); ^{13}C NMR ($CDCl_3$, 125 MHz) δ 155.6, 149.4, 133.4, 126.6, 121.4, 112.2, 94.6, 56.2, 19.8; HRMS (ESI$^+$) *m/z*: $[M + H]^+$ calcd for $C_9H_{12}NO_4$, 198.0766; found, 198.0739.

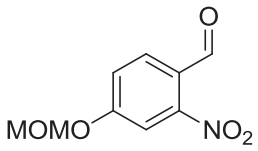

74

4-(Methoxymethoxy)-2-nitrobenzaldehyde (74): *N*,*N*-dimethylformamide dimethyl acetal (0.41 mL, 3.04 mmol) was added to a solution of nitroarene **73** (500 mg, 2.54 mmol) and pyrrolidine (0.25 mL, 3.04 mmol) in anhydrous *N,N*-dimethylformamide (1.40 mL), then heated to 110^{o}C for 4 h. Once cool, the solution was concentrated to remove volatile organics. Next, the residue was dissolved in anhydrous THF (1.70 mL) and added dropwise to a solution of sodium periodate (1.63 g, 7.61 mmol) in 50% aqueous THF (11.3 mL) at 0^{o}C, then warmed slowly to rt over 8 h. The reaction mixture was filtered to remove insoluble salts, eluting with EtOAc, and the filtrate was washed with water, dried (Na_2SO_4), filtered, and concentrated. The residue was purified via column chromatography (SiO_2, 10:1 → 3:1 Hexane:EtOAc) to give **74** as a yellow oil (431 mg, 80%): ^{1}H NMR ($CDCl_3$, 400 MHz) δ 10.32 (s, 1H), 7.99 (d, *J* = 8.8 Hz, 1H), 7.70 (d, *J* = 2.4 Hz, 1H), 7.40 (dd, *J* = 8.8, 2.4 Hz, 1H), 5.33 (s, 2H), 3.53 (s, 3H); ^{13}C NMR ($CDCl_3$,

125 MHz) δ 187.0, 161.3, 151.5, 131.4, 124.3, 120.9, 111.8, 94.6, 56.7; HRMS (ESI^+) *m/z*: $[M + H]^+$ calcd for $C_9H_{10}NO_5$, 212.0559; found, 212.0623.

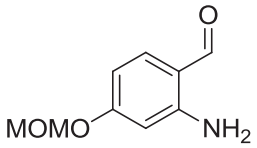

75

2-Amino-4-(methoxymethoxy)benzaldehyde (75): Palladium on carbon (5%, 5 mg) was added to nitroarene **74** (100 mg, 0.47 mmol) in EtOAc (5.90 mL) and the solution was placed under an atmosphere of H_2. After 12 h, the solution was filtered through SiO_2 (1:3 Hexane:EtOAc) and the eluent was concentrated. The residue was purified via column chromatography (SiO_2, 3:1 Hexane:EtOAc) to afford **75** as a red amorphous solid (31 mg, 36%): ^1H NMR ($CDCl_3$, 400 MHz) δ 9.74 (s, 1H), 7.40 (d, *J* = 8.8 Hz, 1H), 6.43 (dd, *J* = 8.8, 2.0 Hz, 1H), 6.28 (d, *J* = 1.6 Hz, 1H), 6.23 (bs, 2H), 5.20 (s, 2H), 3.50 (s, 3H); ^{13}C NMR ($CDCl_3$, 125 MHz) δ 191.2, 157.6, 156.2, 153.1, 120.5, 119.6, 93.0, 92.3, 55.3; HRMS (ESI^+) *m/z*: $[M + H]^+$ calcd for $C_9H_{12}NO_3$, 182.0817; found, 182.0862.

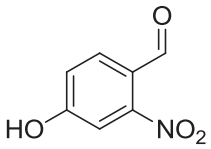

76

4-Hydroxy-2-nitrobenzaldehyde (76):[200] A solution of **74** (100 mg, 0.47 mmol) in MeOH (4.70 mL) was treated dropwise with 3M HCl (1.30 mL, 3.79 mmol), then heated to reflux for 1 h. Water (15 mL) was added and the solution was extracted with EtOAc (3 × 15 mL). Combined organic fractions were washed with saturated aqueous $NaHCO_3$, saturated aqueous NaCl, dried (Na_2SO_4), and concentrated to afford **76** as a red amorphous solid (79 mg, 99%): ^1H NMR

($CDCl_3$, 500 MHz) δ 10.17 (s, 1H), 7.85 (d, J = 9.0 Hz, 1H), 7.37 (d, J = 2.0 Hz, 1H), 7.09 (dd, J = 8.5, 2.0 Hz, 1H).

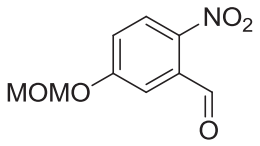

79

5-(Methoxymethoxy)-2-nitrobenzaldehyde (79):[235] *N,N*-diisopropylethylamine (4.20 mL, 23.9 mmol) was slowly added to 5-hydroxy-2-nitrobenzaldehyde (1.0 g, 5.98 mmol) in anhydrous *N,N*-dimethylformamide (20.0 mL) over 5 min at rt. After 30 min, the solution was cooled to 0°C and chloromethyl methyl ether (1.80 mL, 23.9 mmol) was added and the mixture warmed to rt over 12 h. The reaction was quenched by the addition of saturated aqueous NH_4Cl solution and extracted with EtOAc (3 × 50 mL). The combined organic fractions were washed with saturated aqueous NaCl, dried (Na_2SO_4), filtered, and concentrated. The residue was purified via column chromatography (SiO_2, 5:1 Hexane:EtOAc) to give **79** as a yellow amorphous solid (1.21 g, 96%): ^{1}H NMR ($CDCl_3$, 500 MHz) δ 10.40 (s, 1H), 8.09 (d, J = 9.0 Hz, 1H), 7.41 (d, J = 2.5 Hz, 1H), 7.23 (dd, J = 9.0, 3.0 Hz, 1H), 5.23 (s, 2H), 3.42 (s, 3H).

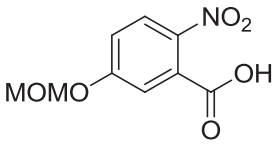

80

5-(Methoxymethoxy)-2-nitrobenzoic acid (80): Monosodium phosphate (NaH_2PO_4, 588 mg, 4.26 mmol) was added to a solution of aqueous 0.4M $NaClO_2$ (8.10 mL, 3.22 mmol). This aqueous solution was subsequently added to a solution of benzaldehyde **79** (100 mg, 0.47 mmol) and 2-methyl-2-butene (1.81 mL, 17.1 mmol) in *tert*-butanol (2.40 mL), then stirred for 12 h.

Saturated aqueous NaH_2PO_4 was added and the solution was extracted with EtOAc (3 x 30 mL). The combined organic fractions were washed with saturated aqueous NaCl, dried (Na_2SO_4), filtered, and concentrated. The residue was then resuspended in CH_2Cl_2 and saturated aqueous $NaHCO_3$ was used to extract the desired product, washing with CH_2Cl_2. The combined aqueous extracts were acidified and extracted with EtOAc (3 x 30 mL), and then dried (Na_2SO_4), filtered, and concentrated to afford **80** as a yellow amorphous solid (106 mg, 99%): ^{1}H NMR ($CDCl_3$, 400 MHz) δ 8.03 (dd, *J* = 8.8, 1.6 Hz, 1H), 7.39 (d, *J* = 2.8 Hz, 1H), 7.28–7.24 (m, 1H), 5.31 (s, 2H), 3.53 (s, 3H); ^{13}C NMR ($CDCl_3$, 125 MHz) δ 170.2, 160.8, 141.2, 129.5, 126.6, 118.4, 116.8, 94.5, 56.6; HRMS (ESI$^+$) *m/z*: $[M + Na]^+$ calcd for $C_9H_9NNaO_6$, 250.0328; found, 250.0345.

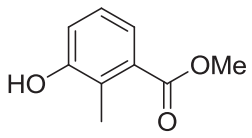

81

Methyl 3-hydroxy-2-methylbenzoate (81):[236] Thionyl chloride (1.44 mL, 19.8 mmol) was added dropwise to a solution of 3-acetoxy-2-methylbenzoic acid (3.50 g, 18.0 mmol) in anhydrous MeOH (77.0 mL) at 0^{o}C, then warmed to rt slowly over 12 h. Solvent was concentrated and the residue was resuspended in EtOAc (50 mL), washed with saturated aqueous $NaHCO_3$, saturated aqueous NaCl, dried (Na_2SO_4), filtered, and concentrated to afford **81** as a colorless amorphous solid (2.67 g, 89%): ^{1}H NMR ($CDCl_3$, 400 MHz) δ 7.45–7.43 (m, 1H), 7.14 (t, *J* = 8.0 Hz, 1H), 6.97–6.95 (m, 1H), 5.02 (bs, 1H), 3.91 (s, 3H), 2.48 (s, 3H).

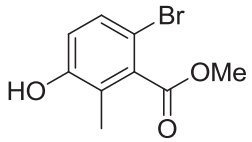

82

Methyl 6-bromo-3-hydroxy-2-methylbenzoate (82):[205] A 0.75 M solution of bromine in CH_2Cl_2 (8.82 mL, 6.62 mmol) was added portionwise to solution of **81** (1.0 g , 6.02 mmol) in CH_2Cl_2 (60.0 mL) at -42°C in a flask wrapped in foil. Initially, 4.0 mL (0.5 eq.) of the 0.75M solution was added, which was followed by another 0.8 mL (0.1 eq) every 10 minutes until addition was complete. Several minutes after addition was complete, saturated aqueous $Na_2S_2O_3$ was added at -42°C. The solution was extracted with CH_2Cl_2 (3 x 50 mL), washed with water, dried (Na_2SO_4), filtered, and concentrated. The residue was purified via column chromatography (SiO_2, 100% Hexane → 6:1 Hexane:EtOAc → 100% EtOAc) to give **82** as a yellow oil (1.39 g, 95%): ^{1}H NMR ($CDCl_3$, 400 MHz) δ 7.24 (d, *J* = 8.4 Hz, 1H), 6.70 (d, *J* = 8.8 Hz, 1H), 5.51 (s, 1H), 3.98 (s, 3H), 2.20 (s, 3H).

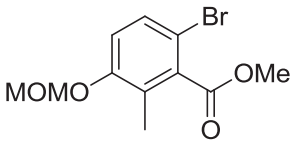

83

Methyl 6-bromo-3-(methoxymethoxy)-2-methylbenzoate (83): *N,N*-diisopropylethylamine (3.28 mL, 18.8 mmol) was slowly added to phenol **82** (1.15 g, 4.71 mmol) in anhydrous *N,N*-dimethylformamide (16.0 mL) over 5 min at rt. After 30 min, the solution was cooled to 0°C and chloromethyl methyl ether (3.14 mL, 18.8 mmol) was added and the mixture warmed to rt over 12 h. The reaction was quenched by the addition of saturated aqueous NH_4Cl solution and extracted with EtOAc (3 × 50 mL). The combined organic fractions were washed with saturated aqueous NaCl, dried (Na_2SO_4), filtered, and concentrated. The residue was purified via column chromatography (SiO_2, 20:1 Hexane:EtOAc) to give **83** as a colorless oil (1.31 g, 97%): ^{1}H NMR ($CDCl_3$, 400 MHz) δ 7.34 (d, *J* = 9.2 Hz, 1H), 7.01 (d, *J* = 8.8 Hz, 1H), 5.21 (s, 2H), 3.97 (s, 3H), 3.48 (s, 3H), 2.22 (s, 3H); ^{13}C NMR ($CDCl_3$, 125 MHz) δ 168.3, 154.5, 137.0, 130.2, 126.6,

116.1, 110.3, 94.5, 56.1, 52.6, 13.6; HRMS (ESI^+) *m/z*: $[M + H]^+$ calcd for $C_{11}H_{14}BrO_4$, 289.0075; found, 289.0089.

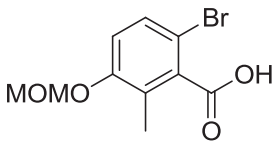

84

6-Bromo-3-(methoxymethoxy)-2-methylbenzoic acid (84): An aqueous solution of 40% KOH (3.16 mL, 22.6 mmol) was added to a solution of **83** (130 mg, 0.45 mmol) in EtOH (11.3 mL), then heated to reflux for 12 h. Once cool, the solution was concentrated and the aqueous residue was acidified, and then extracted with EtOAc (3 x 25 mL). The combined organic layers were next extracted with saturated aqueous $NaHCO_3$ (3 x 30 mL), and then the aqueous extracts were acidified. Finally, EtOAc (3 x 30 mL) was used to extract the acid product, and the combined organic extracts were washed with saturated aqueous NaCl, dried (Na_2SO_4), filtered, and concentrated to afford **84** as a colorless amorphous solid (124 mg, 99%): ^1H NMR ($CDCl_3$, 400 MHz) δ 7.38 (d, *J* = 8.8 Hz, 1H), 7.05 (d, *J* = 8.8 Hz, 1H), 5.23 (s, 2H), 3.50 (s, 3H), 2.33 (s, 3H); ^{13}C NMR ($CDCl_3$, 125 MHz) δ 172.4, 154.5, 136.0, 130.7, 126.6, 116.5, 110.0, 94.5, 56.1, 13.5; HRMS (ESI^+) *m/z*: $[M + H]^+$ calcd for $C_{10}H_{12}BrO_4$, 274.9919; found, 274.9992.

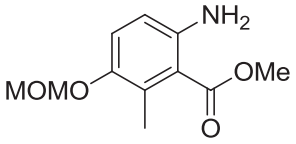

85

Methyl 6-amino-3-(methoxymethoxy)-2-methylbenzoate (85): Trimethylsilyl azide (0.22 mL, 1.70 mmol) was added to a solution of **83** (245 mg, 0.85 mmol), copper (108 mg, 1.70 mmol), and ethanolamine (0.13 mL, 2.13 mmol) in dimethylacetamide (1.70 mL), then heated to

95°C for 12 h. Once cool, the solution was extracted with EtOAc (3 x 30 mL), washing with water, saturated aqueous NaCl, dried (Na_2SO_4), filtered, and concentrated. The residue was purified via column chromatography (SiO_2, 5:1 Hexane:EtOAc) to give **85** as a red oil (145 mg, 76%): ^{1}H NMR ($CDCl_3$, 400 MHz) δ 7.03 (d, *J* = 8.8 Hz, 1H), 6.53 (d, *J* = 8.4 Hz, 1H), 5.08 (s, 2H), 4.52 (bs, 2H), 3.93 (s, 3H), 3.51 (s, 3H), 2.31 (s, 3H); ^{13}C NMR ($CDCl_3$, 125 MHz) δ 169.4, 147.8, 142.2, 128.6, 120.7 (2C), 114.8, 96.1, 56.1, 51.7, 14.2; HRMS (ESI$^+$) *m/z*: $[M + H]^+$ calcd for $C_{11}H_{16}NO_4$, 226.1079; found, 226.1055.

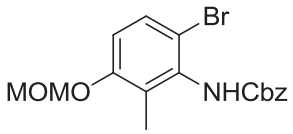

86

Benzyl (6-bromo-3-(methoxymethoxy)-2-methylphenyl)carbamate (86): Diphenylphosphoryl azide (0.10 mL, 0.47 mmol) was added to a solution of **84** (100 mg, 0.36 mmol) and *N,N*-diisopropylethylamine (0.11 mL, 0.62 mmol) in toluene (15.0 mL), then heated at reflux for 3 h. Once cool, benzyl alcohol (64 μL, 0.62 mmol) was added and the solution was stirred for 12 h. Solvent was removed and the residue was purified via column chromatography (SiO_2, 30:1 → 5:1 Hexane:EtOAc) to give **86** as a colorless oil (28 mg, 33%): ^{1}H NMR ($CDCl_3$, 400 MHz) δ 7.40–7.36 (m, 6H), 6.95 (d, *J* = 9.2 Hz, 1H), 5.24 (s, 2H), 5.22 (s, 2H), 3.49 (s, 3H), 2.20 (s, 3H); ^{13}C NMR ($CDCl_3$, 125 MHz) δ 155.3, 154.0, 136.2, 134.3, 129.8, 129.5, 128.8, 128.6, 128.3, 127.8, 120.1, 116.3, 114.1, 94.7, 67.4, 56.1, 12.4; HRMS (ESI$^+$) *m/z*: $[M + Na]^+$ calcd for $C_{17}H_{18}BrNNaO_4$, 402.0317; found, 402.0320.

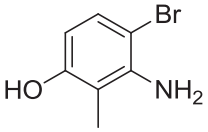

87

3-Amino-4-bromo-2-methylphenol (87): A solution of carboxylic acid **84** (77.0 mg, 0.28 mmol) in H_2SO_4 (0.70 mL) was heated at 60°C for 1.5 h. Once cool, sodium azide (365 mg, 5.62 mmol) was added portionwise over 30 min, and then the solution was stirred for 42 h. Sodium hydroxide was added at 0°C to neutralize and then the solution was extracted with EtOAc (3 x 30 mL), washed with water, saturated aqueous NaCl, dried (Na_2SO_4), filtered, and concentrated. The residue was purified via column chromatography (SiO_2, 8:1 Hexane:EtOAc) to give **87** as a colorless amorphous solid (15 mg, 27%): ^{1}H NMR ($CDCl_3$, 400 MHz) δ 7.15 (d, *J* = 8.8 Hz, 1H), 6.17 (d, *J* = 8.8 Hz, 1H), 4.59 (s, 1H), 4.12 (bs, 2H), 2.13 (s, 3H); ^{13}C NMR ($CDCl_3$, 125 MHz) δ 153.2, 143.3, 129.5, 109.6, 106.4, 101.0, 10.1; HRMS (ESI$^+$) *m/z*: $[M + H]^+$ calcd for C_7H_9BrNO, 201.9868; found, 201.9858.

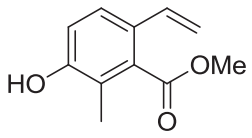

88

Methyl 3-hydroxy-2-methyl-6-vinylbenzoate (88): A solution of aniline **85** (39 mg, 0.17 mmol) in anhydrous CH_2Cl_2 (0.35 mL) was added to a solution of boron trifluoride etherate (32.0 μL, 0.26 mmol) at -15°C in an ice-acetone bath. Next, a solution of *tert*-butyl nitrite (25.0 μL, 0.21 mmol) in anhydrous CH_2Cl_2 (0.18 mL) was added dropwise over several minutes, then stirred at -15°C for 10 min before warming to 5°C over 20 min in an ice-water bath. Solvent was removed under vacuum, without heat, and the crude residue was used without further purification (56 mg, 99%)

Bis(dibenzylideneacetone)palladium (1.0 mg, 0.0017 mmol) was added to a solution of diazonium salt (56 mg, 0.17 mmol) and tributyl(vinyl) tin (100 μL, 0.35 mmol) in anhydrous MeCN (0.70 mL). After gas evolution has ceased, solvent was removed and the residue was

purified via column chromatography (SiO_2, 10:1 Hexane:EtOAc) to give **88** as a colorless oil (4.0 mg, 12%): ^{1}H NMR ($CDCl_3$, 400 MHz) δ 7.34 (d, *J* = 8.4 Hz, 1H), 6.82 (d, *J* = 8.4 Hz, 1H), 6.63 (dd, *J* = 17.2, 10.8 Hz, 1H), 5.60 (dd, *J* = 17.2, 0.8 Hz, 1H), 5.22 (dd, *J* = 10.8, 0.8 Hz, 1H), 4.96 (bs, 1H), 3.95 (s, 3H), 2.20 (s, 3H); ^{13}C NMR ($CDCl_3$, 125 MHz) δ 169.9, 153.3, 133.5, 127.9 (2C), 126.2, 124.2, 120.8, 114.6, 52.3, 12.7; HRMS (ESI$^+$) *m/z*: $[M + H]^+$ calcd for $C_{11}H_{13}O_3$, 193.0865; found, 193.0868.

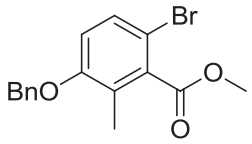

89

Methyl 3-(benzyloxy)-6-bromo-2-methylbenzoate (89): Benzyl bromide (3.02 mL, 25.4 mmol) was added dropwise to a solution of **82** (2.07 g, 8.47 mmol) and potassium carbonate (5.85 g, 42.3 mmol) in anhydrous *N,N*-dimethylformamide (17.0 mL), then stirred for 12 h. Water (50 mL) was added and the solution was extracted with EtOAc (3 × 30 mL). Combined organic fractions were washed with saturated aqueous NaCl, dried (Na_2SO_4), filtered, and concentrated. The residue was purified via column chromatography (SiO_2, 100% Hexane, 30:1 Hexane:EtOAc) to afford **89** as a yellow amorphous solid (2.83 g, 99%): ^{1}H NMR ($CDCl_3$, 400 MHz) δ 7.41–7.35 (m, 5H), 7.34 (d, *J* = 8.8 Hz, 1H), 6.81 (d, *J* = 8.8 Hz, 1H), 5.10 (s, 2H), 3.98 (s, 3H), 2.26 (s, 3H); ^{13}C NMR ($CDCl_3$, 125 MHz) δ 168.3, 155.9, 137.0, 136.5, 130.4, 128.7, 128.2, 128.1, 127.1 (2C), 126.4, 113.8, 109.3, 70.4, 52.6, 13.7; HRMS (ESI$^+$) *m/z*: $[M + Na]^+$ calcd for $C_{16}H_{15}BrNaO_3$, 357.0102; found, 357.0117.

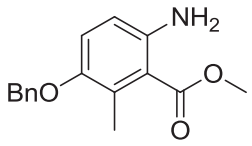

90

Methyl 6-amino-3-(benzyloxy)-2-methylbenzoate (90): Trimethylsilyl azide (0.16 mL, 1.20 mmol) was added to a solution of **89** (200 mg, 0.60 mmol), copper (76 mg, 1.20 mmol), and ethanolamine (90 μL, 1.50 mmol) in dimethylacetamide (1.20 mL), then heated to 95°C for 12 h. Once cool, the solution was extracted with EtOAc (3 x 30 mL), washing with water, saturated aqueous NaCl, dried (Na_2SO_4), filtered, and concentrated. The residue was purified via column chromatography (SiO_2, 5:1 Hexane:EtOAc) to give **90** as a red oil (141 mg, 87%): ^{1}H NMR ($CDCl_3$, 400 MHz) δ 7.40–7.34 (m, 5H), 6.89 (d, *J* = 8.8 Hz, 1H), 6.53 (d, *J* = 8.4 Hz, 1H), 4.99 (s, 2H), 4.45 (bs, 2H), 3.93 (s, 3H), 2.34 (s, 3H); ^{13}C NMR ($CDCl_3$, 125 MHz) δ 169.4, 149.6, 140.8, 137.5, 128.5, 128.3, 128.0, 127.8, 127.5, 127.3, 127.1, 118.3, 114.8, 71.9, 51.8, 14.2; HRMS (ESI^+) *m/z*: $[M + H]^+$ calcd for $C_{16}H_{18}NO_3$, 272.1287; found, 272.1258.

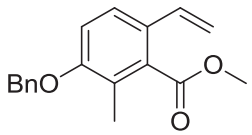

91

Methyl 3-(benzyloxy)-2-methyl-6-vinylbenzoate (91): A solution of aniline **90** (40 mg, 0.15 mmol) in anhydrous CH_2Cl_2 (0.30 mL) was added to a solution of boron trifluoride etherate (27.0 μL, 0.22 mmol) at -15°C in an ice-acetone bath. Next, a solution of *tert*-butyl nitrite (21.0 μL, 0.18 mmol) in anhydrous CH_2Cl_2 (0.15 mL) was added dropwise over several minutes, then stirred at -15°C for 10 min before warming to 5°C over 20 min in an ice-water bath. Solvent was

removed under vacuum, without heat, and the crude residue was used without further purification (55 mg, 99%)

Bis(dibenzylideneacetone)palladium (1.0 mg, 0.0015 mmol) was added to a solution of diazonium salt (55 mg, 0.15 mmol) and tributyl(vinyl) tin (87.0 μL, 0.30 mmol) in anhydrous MeCN (0.60 mL). After gas evolution has ceased, solvent was removed and the residue was purified via column chromatography (SiO_2, 30:1 Hexane:EtOAc) to give **91** as a colorless oil (18.0 mg, 43%): ^{1}H NMR ($CDCl_3$, 400 MHz) δ 7.37–7.35 (m, 6H), 6.93 (d, *J* = 8.8 Hz, 1H), 6.64 (dd, *J* = 17.4, 11.2, 1H), 5.61 (dd, *J* = 17.4, 0.8, 1H), 5.22 (dd, *J* = 10.8, 0.8, 1H), 5.13 (s, 2H), 3.95 (s, 3H), 2.24 (s, 3H); ^{13}C NMR ($CDCl_3$, 125 MHz) δ 168.9, 155.2, 135.9, 133.3, 127.8, 127.9, 127.0 (2C), 126.5, 126.1, 125.3, 122.9, 122.8, 113.6, 111.8, 69.2, 51.2, 12.2; HRMS (ESI^+) *m/z*: $[M + Na]^+$ calcd for $C_{18}H_{18}NaO_3$, 305.1154; found, 305.1184.

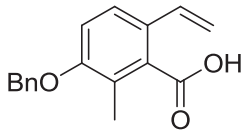

92

3-(Benzyloxy)-2-methyl-6-vinylbenzoic acid (92): An aqueous solution of 40% KOH (1.86 mL, 13.3 mmol) was added to a solution of **91** (75.0 mg, 0.27 mmol) in EtOH (6.60 mL), then heated to reflux for 12 h. Once cool, the solution was concentrated and the aqueous residue was acidified, and then extracted with EtOAc (3 x 15 mL). The combined organic layers were next extracted with saturated aqueous $NaHCO_3$ (3 x 20 mL), and then the aqueous extracts were acidified. Finally, EtOAc (3 x 20 mL) was used to extract the acid product, and the combined organic extracts were washed with saturated aqueous NaCl, dried (Na_2SO_4), filtered, and concentrated to afford **92** as an orange amorphous solid (51.0 mg, 72%): ^{1}H NMR ($CDCl_3$, 400 MHz) δ 7.38–7.34 (m, 6H), 6.97 (d, *J* = 8.4 Hz, 1H), 6.85 (dd, *J* = 17.2, 10.8, 1H), 5.65 (dd, *J* =

17.6, 0.8, 1H), 5.26 (d, J = 11.6, 1H), 5.14 (s, 2H), 2.36 (s, 3H); ^{13}C NMR ($CDCl_3$, 125 MHz) δ 172.9, 156.3, 136.9 (2C), 130.4, 130.0, 128.6 (2C), 128.0, 127.7, 127.2, 127.1, 126.1, 115.0, 113.2, 70.3, 13.3; HRMS (ESI$^+$) *m/z*: $[M + Na]^+$ calcd for $C_{17}H_{16}NaO_3$, 291.0997; found, 291.1006.

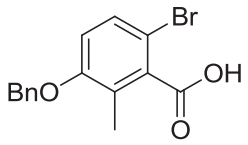

93

3-(Benzyloxy)-6-bromo-2-methylbenzoic acid (93): An aqueous solution of 40% KOH (84.0 mL, 598 mmol) was added to a solution of **89** (2.0 g, 5.98 mmol) in EtOH (150 mL), then heated to reflux for 12 h. Once cool, the solution was concentrated and the aqueous residue was acidified, and then extracted with EtOAc (3 x 50 mL). The combined organic layers were next extracted with saturated aqueous $NaHCO_3$ (3 x 50 mL), and then the aqueous extracts were acidified. Finally, EtOAc (3 x 50 mL) was used to extract the acid product, and the combined organic extracts were washed with saturated aqueous NaCl, dried (Na_2SO_4), filtered, and concentrated to afford **93** as a colorless amorphous solid (1.75 g, 91%): ^{1}H NMR ($CDCl_3$, 500 MHz) δ 7.35–7.26 (m, 6H), 6.75 (d, J = 9.0 Hz, 1H), 5.02 (s, 2H), 2.27 (s, 3H); ^{13}C NMR ($CDCl_3$, 125 MHz) δ 171.5, 155.9, 136.4, 135.8, 130.6, 128.7, 128.3, 128.1, 127.1 (2C), 126.4, 114.1, 108.9, 70.4, 13.8; HRMS (ESI$^+$) *m/z*: $[M + Na]^+$ calcd for $C_{15}H_{13}BrNaO_3$, 342.9946; found, 342.9968.

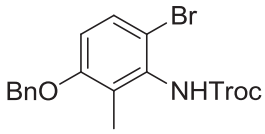

94

2,2,2-Trichloroethyl (3-(benzyloxy)-6-bromo-2-methylphenyl)carbamate (94): ,2,2-trichloroethyl (Troc) chloroformate (46 μL, 0.34 mmol) was added to a solution of carboxylic acid **93** (100 mg, 0.31 mmol), sodium azide (35 mg, 0.53 mmol) and sodium *tert*-butoxide in dimethoxyethane (3.10 mL), then heated at reflux for 12 h. Once cool, solvent was removed and the residue was purified via column chromatography (SiO_2, 20:1 Hexane:EtOAc) to give **94** as a colorless amorphous solid (49.0 mg, 35%): ^{1}H NMR ($CDCl_3$, 500 MHz) δ 7.40–7.37 (m, 6H), 6.89 (d, J = 9.0 Hz, 1H), 5,12 (s, 2H), 4.94 (s, 2H), 2.35 (s, 3H); ^{13}C NMR ($CDCl_3$, 125 MHz) δ 160.5, 156.0, 147.6, 136.2, 133.7, 130.8, 128.7 (2C), 128.2, 127.5, 127.1 (2C), 115.0, 109.1, 93.5, 70.5, 13.7; HRMS (ESI$^+$) *m/z*: $[M + H]^+$ calcd for $C_{17}H_{16}BrCl_3NO_3$, 465.9379; found, 465.9367.

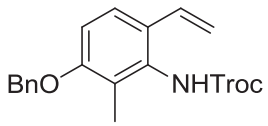

95

2,2,2-Trichloroethyl (3-(benzyloxy)-2-methyl-6-vinylphenyl)carbamate (95): A flame-dried flask was charged with **94** (20 mg, 0.044 mmol), tributyl(vinyl) tin (14 μL, 0.049 mmol) and tetrakis(triphenyl-phosphine)palladium (3.0 mg, 0.0022 mmol), then degassed. Anhydrous toluene (2.20 mL) was added and the solution was heated at reflux for 2 h. Once cool, solvent was removed and the residue was purified via column chromatography (SiO_2, 20:1 Hexane:EtOAc) to give **95** as a colorless oil (4.0 mg, 23%): ^{1}H NMR ($CDCl_3$, 400 MHz) δ 7.40–7.37 (m, 5H), 6.89 (d, J = 10.4 Hz, 1H), 6.60 (dd, J = 35.2, 10.4 Hz, 1H), 6.14 (dd, J = 10.4, 0.8 Hz, 1H), 5.93 (dd, J = 17.6, 0.8 Hz, 1H), 5.57 (d, J = 17.6 Hz, 1H), 5.14 (s, 2H), 4.88 (s, 2H), 2.13 (s, 3H); ^{13}C NMR ($CDCl_3$, 125 MHz) δ 156.3 (2C), 138.3 (2C), 133.5 (2C), 128.6 (2C),

128.0, 127.6, 127.1 (2C), 123.8 (2C), 114.4, 112.3, 76.7, 70.2, 12.9; HRMS (ESI^+) *m/z*: $[M + H]^+$ calcd for $C_{19}H_{19}Cl_3NO_3$, 414.0431; found, 414.0461.

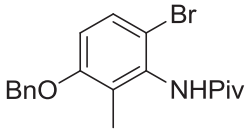

96

N-(3-(benzyloxy)-6-bromo-2-methylphenyl)pivalamide (96): *N*-bromosuccinimide (15 mg, 0.084 mmol) was added to a solution of amide **73** (25 mg, 0.080 mmol) in MeOH (0.16 mL). After 15 min, the reaction was poured into a 1:1 mixture of saturated aqueous $Na_2S_2O_3$:saturated aqueous $NaHCO_3$ (10 mL) and the solution was extracted with EtOAc (3 x 15 mL). The combined organic extracts were dried (Na_2SO_4), filtered, and concentrated to afford **96** as a yellow amorphous solid (31 mg, 99%): ^1H NMR ($CDCl_3$, 400 MHz) δ 7.52 (d, *J* = 8.4 Hz, 1H), 7.47–7.33 (m, 5H), 7.15 (s, 1H), 6.72 (d, *J* = 6.8 Hz, 1H), 5.07 (s, 2H), 2.17 (s, 3H), 1.38 (s, 9H); ^{13}C NMR ($CDCl_3$, 125 MHz) δ 156.7, 154.0, 136.7, 134.6, 129.3, 128.6, 128.3, 127.9, 127.8, 127.1, 113.3, 112.7, 111.7, 70.5, 39.5, 27.7 (3C), 12.5; HRMS (ESI^+) *m/z*: $[M + Na]^+$ calcd for $C_{19}H_{22}BrNNaO_2$, 398.0732; found, 398.0726.

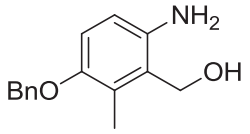

99

(6-Amino-3-(benzyloxy)-2-methylphenyl)methanol (99): A solution of ester **90** (150 mg, 0.55 mmol) in anhydrous THF (2.00 mL) was added to a solution of lithium aluminum hydride (42 mg, 1.11 mmol) in anhydrous THF (3.50 mL) at 0°C, then warmed to rt over 1.5 h. Water (5 mL) was added dropwise to quench, and then Na_2SO_4 was added. The reaction mixture was filtered through Celite (2:1, Hexane:EtOAc) and the eluent was concentrated to afford **99** as a

yellow amorphous solid (130 mg, 96%): ^{1}H NMR ($CDCl_3$, 400 MHz) δ 7.42–7.34 (m, 5H), 6.78 (d, *J* = 8.8 Hz, 1H), 6.57 (d, *J* = 8.8 Hz, 1H), 5.00 (s, 2H), 4.80 (s, 2H), 2.32 (s, 3H); ^{13}C NMR ($CDCl_3$, 125 MHz) δ 150.2, 150.1, 140.2, 128.5 (2C), 127.7, 127.3, 126.5, 126.4, 125.5, 114.2, 114.0, 71.4, 59.2, 11.7; HRMS (ESI^+) *m/z*: $[M + H]^+$ calcd for $C_{15}H_{18}NO_2$, 244.1338; found, 244.1335.

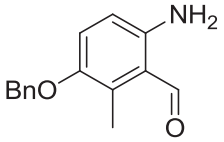

100

6-Amino-3-(benzyloxy)-2-methylbenzaldehyde (100): Activated magnesium oxide (455 mg) was added to a solution of alcohol **99** (130 mg, 0.53 mmol) in CH_2Cl_2 (3.80 mL), then warmed to 35°C for 12 h. Once cool, the reaction mixture was filtered through Celite (Acetone) and the eluent was concentrated to afford **100** as a red amorphous solid (113 mg, 91%): ^{1}H NMR ($CDCl_3$, 400 MHz) δ 10.42 (s, 1H), 7.47–7.33 (m, 5H), 7.07 (d, *J* = 9.2 Hz, 1H), 6.48 (d, *J* = 9.2 Hz, 1H), 6.12 (bs, 2H), 4.98 (s, 2H), 2.53 (s, 3H); ^{13}C NMR ($CDCl_3$, 125 MHz) δ 192.9, 147.2, 146.2, 137.4, 131.4, 128.6 (2C), 128.0, 127.6, 127.2, 124.9, 116.9, 114.8, 73.1, 10.6; HRMS (ESI^+) *m/z*: $[M + H]^+$ calcd for $C_{15}H_{16}NO_2$, 242.1181; found, 242.1187.

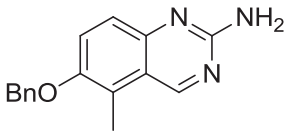

101

6-(Benzyloxy)-5-methylquinazolin-2-amine (101): Guanidine hydrochloride (80.0 mg, 0.84 mmol) was added to a solution of benzaldehyde **100** (100 mg, 0.41 mmol) and sodium carbonate (89 mg, 0.84 mmol) in decalin (0.92 mL), then heated at 190°C for 2.5 h. Once cool, solvent was

removed and the residue was purified via column chromatography (SiO_2, 10:1 CH_2Cl_2:MeOH) to afford **101** as a brown amorphous solid (25 mg, 23%): ^{1}H NMR ($CDCl_3$, 400 MHz) δ 9.25 (d, *J* = 4.0 Hz, 1H), 7.53 (d, *J* = 9.2 Hz, 1H), 7.48–7.36 (m, 6H), 5.17 (s, 2H), 2.58 (s, 3H); ^{13}C NMR ($CDCl_3$, 125 MHz) δ 159.2, 158.8, 153.0, 151.4, 137.1, 128.6, 128.3, 128.0, 127.4, 127.8, 127.2, 124.9, 120.1, 114.8, 77.0, 9.8; HRMS (ESI^+) *m/z*: $[M + H]^+$ calcd for $C_{16}H_{16}N_3O$, 266.1293; found, 266.1285.

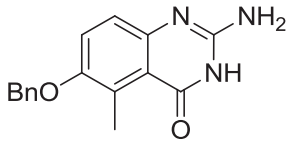

104

2-Amino-6-(benzyloxy)-5-methylquinazolin-4(3H)-one (104): HCl gas was bubbled through a solution of cyanamide (1.0 g, 23.8 mmol) in Et_2O (75.0 mL) for 10 min, and then the resultant solution was capped and stirred for 12 h. The white precipitate was collected by filtration, washing with Et_2O, to afford chloroformamide hydrochloride **103** (1.59 g, 58%), which was used without further purification.

Chloroformamide hydrochloride (21 mg, 0.18 mmol) was added to a solution of ester **90** (50 mg, 0.18 mmol) in anhydrous diglyme (0.37 mL), then heated at reflux for 1 h. After time had elapsed, the solution was cooled to 0^{o}C and insoluble salts were removed by filtration, washing with Et_2O. Concentration of the filtrate revealed crude **104** by ^{1}HNMR. ^{1}H NMR ($CDCl_3$, 400 MHz) δ 7.43–7.34 (m, 5H), 6.89 (d, *J* = 8.8 Hz, 1H), 6.53 (d, *J* = 8.8 Hz, 1H), 5.11 (s, 2H), 4.99 (s, 2H), 3.41 (s, 1H), 2.34 (s, 3H); HRMS (ESI^+) *m/z*: $[M + Na]^+$ calcd for $C_{16}H_{15}N_3NaO_2$, 304.1062; found, 304.1064.

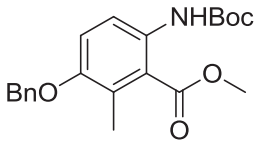

105

Methyl 3-(benzyloxy)-6-((*tert*-butoxycarbonyl)amino)-2-methylbenzoate (105): Di-*tert*-butyl dicarbonate (84 mg, 0.39 mmol) was added to a solution of aniline **90** (100 mg, 0.37 mmol) in 1% Et_3N/THF (7.47 mL), and then stirred for 12 h. Solvent was removed, then the residue was diluted with water (20 mL), and then extracted with EtOAc (3 x 30 mL), dried (Na_2SO_4), filtered, and concentrated. The residue was purified via column chromatography (SiO_2, 15:1 → 10:1 → 5:1 Hexane:EtOAc) to afford **105** as a colorless amorphous solid (139 mg, 99%): ^{1}H NMR ($CDCl_3$, 400 MHz) δ 7.80 (d, *J* = 8.8 Hz, 1H), 7.75 (bs, 1H), 7.43–7.32 (m, 5H), 6.99 (d, *J* = 8.8 Hz, 1H), 5.08 (s, 2H), 3.97 (s, 3H), 2.32 (s, 3H), 1.52 (s, 9H); ^{13}C NMR ($CDCl_3$, 125 MHz) δ 169.1, 153.2, 152.7, 137.1 (2C), 128.6 (3C), 127.9, 127.2 (3C), 115.2 (2C), 80.3, 70.8, 52.3, 28.3 (3C), 14.2; HRMS (ESI$^+$) *m/z*: $[M + Na]^+$ calcd for $C_{21}H_{25}NNaO_5$, 394.1630; found, 394.1628.

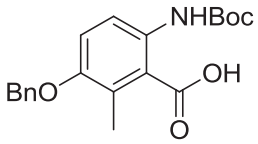

106

3-(Benzyloxy)-6-((*tert*-butoxycarbonyl)amino)-2-methylbenzoic acid (106): Lithium hydroxide (157 mg, 1.87 mmol) was added to a solution of **105** (139 mg, 0.37 mmol) in 3:1:1 THF:MeOH:H_2O (3.70 mL). After 12 h, the solution was concentrated and the aqueous residue was acidified, and then extracted with EtOAc (3 x 15 mL). The combined organic layers were next extracted with saturated aqueous $NaHCO_3$ (3 x 15 mL), and then the aqueous extracts were acidified. Finally, EtOAc (3 x 15 mL) was used to extract the acid product, and the combined

organic extracts were washed with saturated aqueous NaCl, dried (Na_2SO_4), filtered, and concentrated to afford **106** as a colorless amorphous solid (57 mg, 43%): ^{1}H NMR ($CDCl_3$, 400 MHz) δ 8.01 (bs, 1H), 7.43–7.35 (m, 6H), 7.02 (d, *J* = 8.8 Hz, 1H), 5.09 (s, 2H), 2.43 (s, 3H), 1.53 (s, 9H); ^{13}C NMR ($CDCl_3$, 125 MHz) δ 169.1, 153.1 (2C), 137.0 (2C), 128.6 (3C), 128.0, 127.2 (3C), 115.2 (2C), 80.3, 70.8, 28.3 (3C), 14.2; HRMS (ESI$^+$) *m/z*: [M + Na]$^+$ calcd for $C_{20}H_{23}NNaO_5$, 380.1474; found, 380.1441.

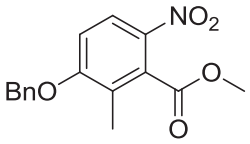

107

Methyl 3-(benzyloxy)-2-methyl-6-nitrobenzoate (107): *m*CPBA (70%) (102 mg, 0.44 mmol) was added to a solution of aniline **90** (30 mg, 011 mmol) in dichloroethane (0.22 mL), then heated at 70^{o}C for 2 h in a flask wrapped in foil. Once cool, EtOAc (20 mL) was added and the organic layer was washed with aqueous 0.1M NaOH until the aqueous layer was nearly colorless, followed by saturated aqueous NaCl. The combined organic extracts were dried (Na_2SO_4), filtered, and concentrated to afford **107** as a yellow amorphous solid (34 mg, 99%): ^{1}H NMR ($CDCl_3$, 400 MHz) δ 8.10 (d, *J* = 9.2 Hz, 1H), 7.44–7.38 (m, 5H), 6.99 (d, *J* = 9.2 Hz, 1H), 5.23 (s, 2H), 4.01 (s, 3H), 2.29 (s, 3H); ^{13}C NMR ($CDCl_3$, 125 MHz) δ 167.1, 161.5, 138.5, 135.4, 131.7, 128.9 (2C), 128.5, 127.2 (2C), 126.2, 124.5, 111.1, 70.9, 53.2, 13.1; HRMS (ESI$^+$) *m/z*: [M + Na]$^+$ calcd for $C_{16}H_{15}NNaO_5$, 324.0848; found, 324.0847.

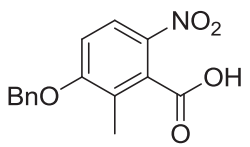

108

3-(Benzyloxy)-2-methyl-6-nitrobenzoic acid (108): An aqueous solution of 40% KOH (0.75 mL, 5.31 mmol) was added to a solution of **107** (32.0 mg, 0.11 mmol) in EtOH (2.66 mL), then heated to reflux for 12 h. Once cool, the solution was concentrated and the aqueous residue was acidified, and then extracted with EtOAc (3 x 10 mL). The combined organic layers were next extracted with saturated aqueous $NaHCO_3$ (3 x 10 mL), and then the aqueous extracts were acidified. Finally, EtOAc (3 x 10 mL) was used to extract the acid product, and the combined organic extracts were washed with saturated aqueous NaCl, dried (Na_2SO_4), filtered, and concentrated to afford **108** as a colorless amorphous solid (30.5 mg, 99%): ^{1}H NMR (Acetone-d_6, 400 MHz) δ 7.85 (d, J = 7.5 Hz, 1H), 7.35 (d, J = 7.5 Hz, 1H), 7.27 (t, J = 7.5 Hz, 1H), 7.23–7.17 (m, 2H), 7.07 (d, J = 8.5 Hz, 1H), 6.96 (d, J = 8.5 Hz, 1H), 6.54 (dd, J = 9.0, 4.5 Hz, 1H), 3.84 (d, J = 7.0 Hz, 2H), 2.37 (s, 3H); ^{13}C NMR (Acetone-d_6, 125 MHz) δ 167.6, 162.9, 131.3, 130.2, 129.1 (2C), 128.5 (2C), 127.4, 125.2 (2C), 115.5, 111.8, 65.8, 14.8; HRMS (ESI$^+$) *m/z*: $[M + Na]^+$ calcd for $C_{15}H_{13}NNaO_5$, 310.0691; found, 310.0625.

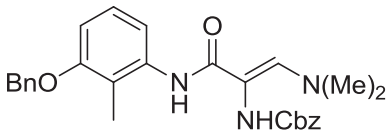

110

(Z)-methyl 3-(4-amino-2-(benzyloxy)-3-methylphenyl)-2-(((benzyloxy)carbonyl)-amino)-3-(dimethylamino)acrylate (110): A solution of **41** (27 mg, 0.13 mmol) and eneamine **22** (42 mg, 0.15 mmol) in glacial acetic acid (0.84 mL) was heated to reflux for 40 h. Upon cooling to rt, the solution was extracted with EtOAc (3 × 15 mL); combined organic fractions were dried (Na_2SO_4), filtered, and concentrated. The residue was purified via column chromatography (SiO_2, 3:1 Hexane:EtOAc) to afford **110** as a gray amorphous solid (40 mg, 71%): ^{1}H NMR ($CDCl_3$, 400 MHz) δ 8.02 (bs, 1H), 7.79–7.71 (m, 1H), 7.48–7.34 (m, 10H), 7.15 (t, J = 8.0 Hz,

1H), 6.78–6.72 (m, 1H), 6.68 (t, J = 8.0 Hz, 1H), 5.95 (bs, 1H), 5.22 (s, 2H), 5.11 (s, 2H), 3.80 (s, 6H), 2.28 (s, 3H); ^{13}C NMR ($CDCl_3$, 125 MHz) δ 166.2, 157.4, 154.9, 137.3, 137.2, 136.0, 128.6 (2C), 128.4 (2C), 128.3, 128.2, 128.1, 128.0, 127.9, 127.2 (3C), 114.5, 107.2, 106.2, 102.1, 70.4, 67.7, 51.9 (2C), 9.3; HRMS (ESI$^+$) *m/z*: $[M + H]^+$ calcd for $C_{27}H_{30}N_3O_4$, 460.2236; found, 460.2215.

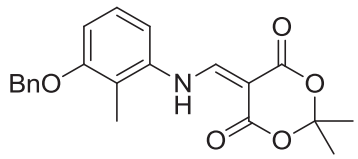

113

5-(((3-(Benzyloxy)-2-methylphenyl)amino)methylene)-2,2-dimethyl-1,3-dioxane-4,6-dione (113): A solution of 2,2-dimethyl-1,3-dioxane-4,6-dione (100 mg, 0.69 mmol) in triethylorthoformate (0.35 mL, 2.08 mmol) was heated at 80°C for 3 h. Once cool, solvent was removed to afford dione **112** as a yellow solid (139 mg, 99%), which was used without further purification.

A solution of aniline **41** (148 mg, 0.69 mmol) and dione **112** (139 mg, 0.69 mmol) in EtOH (1.50 mL) was heated at reflux for 2 h. Once cool, the precipitate was collected and washed with EtOH to afford **113** as a yellow amorphous solid (210 mg, 82% over 2 steps): ^{1}H NMR ($CDCl_3$, 400 MHz) δ 11.49 (d, J = 12.4 Hz, 1H), 8.66 (d, J = 12.4 Hz, 1H), 7.47–7.37 (m, 5H), 7.25 (d, J = 8.0 Hz, 1H), 6.97 (d, J = 8.0 Hz, 1H), 6.88 (d, J = 8.0 Hz, 1H), 5.14 (s, 2H), 2.35 (s, 3H), 1.79 (s, 6H); ^{13}C NMR ($CDCl_3$, 125 MHz) δ 165.9, 163.7, 157.6, 153.4 (2C), 137.6, 136.7, 128.7 (2C), 128.1, 127.7, 127.2 (2C), 117.7, 110.0, 109.3, 105.2, 70.5, 27.1 (2C), 9.8; HRMS (ESI$^+$) *m/z*: $[M + Na]^+$ calcd for $C_{21}H_{21}NNaO_5$, 390.1317; found, 390.1341.

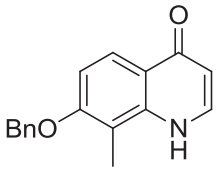

114

7-(Benzyloxy)-8-methylquinolin-4(1H)-one (114): Biphenyl (764 mg, 4.95 mmol) was added to a solution of dione **114** (182 mg, 0.50) in phenyl ether (1.96 mL, 12.4 mmol), then heated at 190°C for 1 h. After cooling to 60°C, the reaction mixture was poured into heptane and the precipitate was collected by filtration, washing with heptane and Et_2O. The solid collected was purified via column chromatography (SiO_2, 20:1 → 10:1 CH_2Cl_2:MeOH) to afford **114** as a yellow amorphous solid (73 mg, 56%): ^{1}H NMR ($CDCl_3$, 400 MHz) δ 8.55 (bs, 1H), 8.27 (d, *J* = 9.2 Hz, 1H), 7.65 (t, *J* = 7.2 Hz, 1H), 7.48–7.35 (m, 5H), 7.10 (d, *J* = 9.2 Hz, 1H), 6.26 (d, *J* = 7.2 Hz, 1H), 5.23 (s, 2H), 2.40 (s, 3H); ^{13}C NMR ($CDCl_3$, 125 MHz) δ 179.0, 158.7, 139.6, 137.7, 136.6, 128.7, 128.2, 127.8, 127.6, 127.3, 125.5, 120.9, 113.9, 110.8, 109.7, 70.7, 8.9; HRMS (ESI^+) *m/z*: $[M + H]^+$ calcd for $C_{17}H_{16}NO_2$, 266.1181; found, 266.1183.

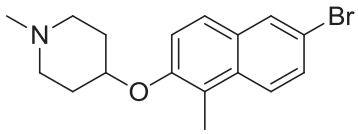

119

4-((6-Bromo-1-methylnaphthalen-2-yl)oxy)-1-methylpiperidine (119): Diisopropylazodicarboxylate (1.29 mL, 6.67 mmol) was added to a solution of 1-methylpiperidin-4-ol (768 mg, 6.67 mmol), phenol **118**[201] (790 mg, 3.33 mmol) and triphenylphosphine (1.75 g, 6.67 mmol) in anhydrous THF (33.0 mL). After 2 h, the solvent was removed and the residue was purified via column chromatography (SiO_2, 10:1 CH_2Cl_2:MeOH) to afford compound **119** as a yellow amorphous solid (1.11 g, 99%): ^{1}H NMR ($CDCl_3$, 500 MHz) δ

7.94 (dd, J = 5.0, 2.0 Hz, 1H), 7.82 (dd, J = 9.0, 5.0 Hz, 1H), 7.62–7.55 (m, 2H), 7.25 (dd, J = 9.0, 5.0 Hz, 1H), 4.51 (bs, 1H), 2.89 (bs, 2H), 2.66 (s, 2H), 2.58 (s, 3H), 2.49 (bs, 2H), 2.20 (s, 3H), 2.03 (bs, 2H); ^{13}C NMR ($CDCl_3$, 125 MHz) δ 152.4, 132.4, 130.5, 130.1, 129.3, 126.2, 125.5, 121.7, 118.0, 117.4, 73.6, 52.6 (2C), 46.1, 31.1 (2C), 11.1; HRMS (ESI$^+$) *m/z*: $[M + Na]^+$ calcd for $C_{17}H_{20}BrNNaO$, 356.0626; found, 356.0612.

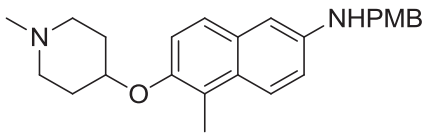

120

N-(4-methoxybenzyl)-5-methyl-6-((1-methylpiperidin-4-yl)oxy)naphthalen-2-amine (120): A solution of Xantphos (4.0 mg, 0.0064 mmol) and tris(dibenzylideneacetone)dipalladium (6.0 mg, 0.0064 mmol) in anhydrous toluene (0.17 mL) was stirred at rt. After several minutes, naphthalene **119** (43 mg, 0.13 mmol), (4-methoxyphenyl)methanamine (18 μL, 0.14 mmol), sodium *tert*-butoxide (17.0 mg, 0.18 mmol), and an additional portion of anhydrous toluene (0.17 mL) were added, and the solution was heated at reflux for 12 h. Once cool, water (20 mL) was added and the solution was extracted with EtOAc (3 x 20 mL), then dried (Na_2SO_4), filtered, and concentrated. The residue was purified via column chromatography (SiO_2, 20:1 → 10:1, CH_2Cl_2:MeOH) to afford compound **120** as a yellow amorphous solid (45 mg, 99%): ^{1}H NMR ($CDCl_3$, 400 MHz) δ 7.78 (d, J = 9.2 Hz, 1H), 7.45 (d, J = 8.8 Hz, 1H), 7.35 (d, J = 8.4 Hz, 1H), 7.14 (d, J = 9.2 Hz, 1H), 6.97 (dd, J = 8.8, 2.4 Hz, 1H), 6.91 (d, J = 8.4 Hz, 1H), 6.85 (d, J = 2.0 Hz, 1H), 4.37 (s, 2H), 4.26 (bs, 1H), 3.83 (s, 3H), 2.79 (bs, 2H), 2.61 (s, 3H), 2.54 (s, 3H), 2.36 (bs, 5H), 1.96–1.91 (bs, 4H); ^{13}C NMR ($CDCl_3$, 125 MHz) δ 158.9, 149.6, 144.3, 133.9, 131.3, 131.2, 129.5, 129.4, 128.9, 127.6, 125.0, 124.8, 123.7, 118.1, 114.1 (2C), 105.6, 55.3, 53.8, 52.7,

48.0, 46.0, 31.1, 31.0, 11.3; HRMS (ESI^+) *m/z*: $[M + H]^+$ calcd for $C_{25}H_{31}N_2O_2$, 391.2386; found, 391.2326.

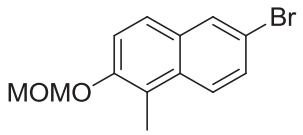

121

6-Bromo-2-(methoxymethoxy)-1-methylnaphthalene (121): *N,N*-diisopropylethylamine (2.90 mL, 16.9 mmol) was slowly added to phenol **118** (1.0 g, 4.22 mmol) in anhydrous *N,N*-dimethylformamide (14.0 mL) over 5 min at rt. After 30 min, the solution was cooled to 0°C and chloromethyl methyl ether (2.8 mL, 16.9 mmol) was added and the mixture warmed to rt over 12 h. The reaction was quenched by the addition of saturated aqueous NH_4Cl solution and extracted with EtOAc (3 × 30 mL). The combined organic fractions were washed with saturated aqueous NaCl, dried (Na_2SO_4), filtered, and concentrated. The residue was purified via column chromatography (SiO_2, 50:1 Hexane:EtOAc → 100% EtOAc) to give **121** as a colorless amorphous solid (871 mg, 74%): ^1H NMR ($CDCl_3$, 500 MHz) δ 7.86 (d, *J* = 2.0 Hz, 1H), 7.75 (d, *J* = 9.0 Hz, 1H), 7.53–7.46 (m, 2H), 7.33 (d, *J* = 9.0 Hz, 1H), 5.21 (s, 2H), 3.47 (s, 3H), 2.49 (s, 3H); ^{13}C NMR ($CDCl_3$, 125 MHz) δ 152.4, 132.2, 130.8, 130.2, 129.3, 126.3, 125.6, 121.0, 117.7, 117.6, 95.5, 56.3, 10.9; HRMS (ESI^+) *m/z*: $[M + Na]^+$ calcd for $C_{13}H_{13}BrNaO_2$, 302.9997; found, 303.0040.

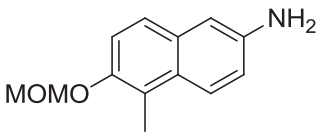

122

6-(Methoxymethoxy)-5-methylnaphthalen-2-amine (122): Trimethylsilyl azide (0.10 mL, 0.79 mmol) was added to a solution of **121** (110 mg, 0.39 mmol), copper (50 mg, 0.79 mmol),

and ethanolamine (59 μL, 0.99 mmol) in dimethylacetamide (0.79 mL), then heated to 95°C for 12 h. Once cool, the solution was extracted with EtOAc (3 x 30 mL), washing with water, saturated aqueous NaCl, dried (Na_2SO_4), filtered, and concentrated. The residue was purified via column chromatography (SiO_2, 5:1 Hexane:EtOAc) to give **122** as a red oil (66.0 mg, 77%): ^{1}H NMR ($CDCl_3$, 500 MHz) δ 7.82 (d, *J* = 6.8 Hz, 1H), 7.47 (d, *J* = 7.2 Hz, 1H), 7.30 (d, *J* = 9.2 Hz, 1H), 7.01 (d, *J* = 8.8 Hz, 2H), 5.24 (s, 2H), 3.78 (bs, 2H), 3.57 (s, 3H), 2.56 (s, 3H); ^{13}C NMR ($CDCl_3$, 125 MHz) δ 150.0, 142.4, 131.3, 128.0, 125.0 (2C), 121.3, 118.6, 118.1, 109.5, 96.2, 56.2, 11.0; HRMS (ESI$^+$) *m/z*: $[M + H]^+$ calcd for $C_{13}H_{16}NO_2$, 218.1181; found, 218.1163.

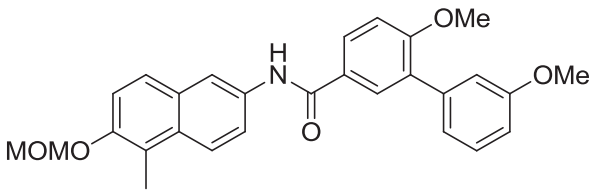

123

3',6-Dimethoxy-N-(6-(methoxymethoxy)-5-methylnaphthalen-2-yl)-[1,1'-biphenyl]-3-carboxamide (123): EDCI (180 mg, 0.94 mmol) and 3',6-dimethoxybiphenyl-3-carboxylic acid (194 mg, 0.75 mmol) were added to aniline **122** (81 mg, 0.37 mmol) in 30% pyridine/CH_2Cl_2 (5.60 mL). After 12 h, the solvent was concentrated and the residue purified via column chromatography (SiO_2, 5:1 → 3:1 Hexane:EtOAc) to afford **123** as a colorless amorphous solid (158 mg, 92%): ^{1}H NMR ($CDCl_3$, 400 MHz) δ 8.29 (s, 1H), 8.00–7.96 (m, 2H), 7.91 (s, 1H), 7.88 (d, *J* = 2.0 Hz, 1H), 7.69 (d, *J* = 8.8 Hz, 1H), 7.63 (dd, J = 9.2, 2.0 Hz, 1H), 7.42 (t, *J* = 8.0 Hz, 2H), 7.13–7.10 (m, 2H), 7.11 (d, *J* = 8.8 Hz, 1H), 6.96 (dd, *J* = 8.0, 2.4 Hz, 1H), 5.30 (s, 2H), 3.93 (s, 3H), 3.89 (s, 3H), 3.57 (s, 3H), 2.61 (s, 3H); ^{13}C NMR ($CDCl_3$, 125 MHz) δ 165.2, 159.4 (2C), 151.8, 138.9, 133.9, 130.9, 130.7, 130.1, 129.5, 129.2, 128.4, 127.2, 126.9, 124.7,

122.0, 120.9, 120.3, 117.7, 117.5, 115.3, 113.0, 111.1, 95.7, 56.3, 55.9, 55.4, 10.9; HRMS (ESI^+) *m/z*: $[M + H]^+$ calcd for $C_{28}H_{28}NO_5$, 458.1967; found, 458.1986.

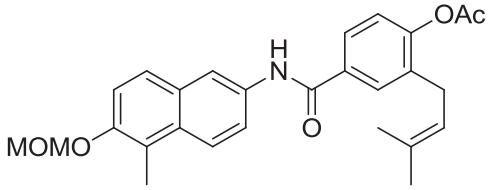

124

4-((6-(Methoxymethoxy)-5-methylnaphthalen-2-yl)carbamoyl)-2-(3-methylbut-2-en-1-yl)phenyl acetate (124): EDCI (146 mg, 0.76 mmol) and 4-acetoxy-3-(3-methylbut-2-en-1-yl)benzoic acid (152 mg, 0.61 mmol) were added to aniline **122** (66 mg, 0.31 mmol) in 30% pyridine/CH_2Cl_2 (4.60 mL). After 12 h, the solvent was concentrated and the residue purified via column chromatography (SiO_2, 6:1 Hexane:EtOAc) to afford **124** as a colorless amorphous solid (92.0 mg, 67%): ^1H NMR ($CDCl_3$, 400 MHz) δ 8.28 (s, 1H), 7.98 (d, *J* = 9.2 Hz, 1H), 7.88 (s, 1H), 7.83 (s, 1H), 7.76 (d, *J* = 8.4 Hz, 1H), 7.70 (d, *J* = 8.8 Hz, 1H), 7.60 (d, *J* = 9.2 Hz, 1H), 7.41 (d, *J* = 9.2 Hz, 1H), 7.19 (d, *J* = 8.4 Hz, 1H), 5.30 (s, 2H), 5.27 (s, 1H), 3.58 (s, 3H), 3.34 (d, *J* = 6.8 Hz, 2H), 2.61 (s, 3H), 2.37 (s, 3H), 1.78 (s, 3H), 1.75 (s, 3H); ^{13}C NMR ($CDCl_3$, 125 MHz) δ 169.1, 165.3, 151.8, 151.6, 134.6, 134.1, 133.6, 133.0, 131.0, 130.1, 129.4, 127.0, 125.6, 124.7, 122.7, 120.9, 120.8, 120.2, 117.7, 117.6, 95.7, 56.3, 29.3, 25.8, 20.9, 17.9, 10.9; HRMS (ESI^+) *m/z*: $[M + Na]^+$ calcd for $C_{27}H_{29}NNaO_5$, 470.1943; found, 470.1937.

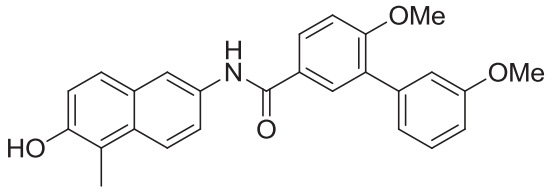

125

N-(6-Hydroxy-5-methylnaphthalen-2-yl)-3',6-dimethoxy-[1,1'-biphenyl]-3-carboxamide (125): A solution of **123** (30.0 mg, 0.066 mmol) in MeOH (0.70 mL) at rt was treated dropwise with 3M HCl (0.18 mL, 0.53 mmol), then heated to reflux for 1 h. Water (15 mL) was added and the solution was extracted with EtOAc (3 × 20 mL). Combined organic fractions were washed with saturated aqueous NaCl, dried (Na_2SO_4), filtered, and concentrated to afford **125** as gray amorphous solid (30 mg, 99%): ^{1}H NMR ($CDCl_3$, 400 MHz) δ 8.24 (s, 1H), 7.98 (dd, *J* = 8.8, 2.4 Hz, 1H), 7.92 (s, 1H), 7.90–7.88 (m, 2H), 7.61–7.58 (m, 2H), 7.39 (t, *J* = 8.0 Hz, 1H), 7.16 (d, *J* = 8.0 Hz, 1H), 7.13 (t, *J* = 2.0 Hz, 1H), 7.09 (t, *J* = 8.4 Hz, 2H), 6.97–6.94 (m, 1H), 5.05 (bs, 1H), 3.92 (s, 3H), 3.88 (s, 3H), 2.54 (s, 3H); ^{13}C NMR ($CDCl_3$, 125 MHz) δ 164.3, 158.3, 149.1, 137.8, 132.1, 130.5, 130.1, 129.8, 129.7, 128.5, 128.4, 128.2, 127.4, 126.1, 123.1, 121.0, 119.6, 117.4, 117.1, 114.4, 114.3, 112.0, 110.1, 54.8, 54.3, 9.5; HRMS (ESI^+) *m/z*: $[M + Na]^+$ calcd for $C_{26}H_{23}NNaO_4$, 436.1525; found, 436.1515.

VII. Common biological evaluation procedures:

A. Anti-proliferation assays

Cells were maintained in a 1:1 mixture of Advanced DMEM/F12 (Gibco) supplemented with non-essential amino acids, L-glutamine (2 mM), streptomycin (500 μg/mL), penicillin (100 units/mL), and 10% FBS. Cells were grown to confluence in a humidified atmosphere (37° C, 5% CO_2), seeded (2000/well, 100 μL) in 96-well plates, and allowed to attaché overnight. Compound or GDA at varying concentrations in DMSO (1% DMSO final concentration) was added, and cells were returned to the incubator for 72 h. At 72 h, the number of viable cells was

determined using an MTS/PMS cell proliferation kit (Promega) per the manufacturer's instructions. Cells incubated in 1% DMSO were used at 100% proliferation, and values were adjusted accordingly. IC_{50} values were calculated from separate experiments performed in triplicate using GraphPad Prism.

B. Western blot analyses

MCF-7 cells were cultured as described above and treated with various concentrations of drug, GDA in DMSO (1% DMSO final concentration), or vehicle (DMSO) for 24 h. Cells were harvested in cold PBS and lysed in RIPA lysis buffer containing 1 mM PMSF, 2 mM sodium orthovanadate, and protease inhibitors on ice for 1 h. Lysates were clarified at 14000g for 10 min at 4° C. Protein concentrations were determined using the Pierce BCA protein assay kit per the manufacturer's instructions. Equal amounts of protein (20 μg) were electrophoresed under reducing conditions, transferred to a nitrocellulose membrane, and immunoblotted with the corresponding specific antibodies. Membranes were incubated with an appropriate horseradish peroxidase-labeled secondary antibody, developed with a chemiluminescent substrate, and visualized.

Chapter III

Examination of the Sugar Appendage on Novobiocin

I. Introduction

Although many novobiocin analogues have been synthesized, the noviose sugar requires the most synthetic steps, as the assembly of this complex pyranose is not trivial. Even the most efficient syntheses of noviose require more than 10 synthetic procedures, and the overall yield is less than desirable.[237] It was proposed that while the sugar moiety plays a critical role in the presentation of binding interactions to Hsp90, not all functionalities of the complex sugar are essential.[15,18] To further elucidate structure–activity relationships and identify key interactions, while simplifying the overall inhibitor synthesis, a library of sugar and non-sugar analogues was prepared.

Simplified sugars and related azasugars were designed to conserve structural motifs present in noviose, while allowing identification of essential interactions with the putative binding pocket. These analogues were designed to probe potential hydrogen bonds as well as to identify spatial constraints. In addition to these simplified or modified sugars, alternative groups were explored at the 7-position of the coumarin ring wherein noviose is typically attached. These non-sugar analogues incorporate heteroatoms alongside steric bulk, to probe both the hydrogen bonding capabilities and pocket dimensions, respectively. Exploration of these diverse compounds provides the opportunity to simplify the novobiocin scaffold, while maintaining or improving solubility, absorption and activity.[238-240] Identification of a simplified noviose surrogate will enable the expeditious synthesis of novobiocin-derived Hsp90 inhibitors.

II. Identification of KU135 (128a) as a potential lead

A. 7-Acetyl Analogues

A series of analogues derived from the initial coumarin study was designed to probe the tolerance of the sugar binding pocket for non-sugar moieties. Rather than substituting the noviose sugar for another complex sugar or similar surrogate, an acetyl group was installed at the 7-position of the coumarin ring. It was proposed that an acetylated phenol would be capable of participating in hydrogen bonding, but lack complexity of the noviose.

1. Syntheses of 5-, 6-, and 8-alkyl(oxy) 7-acetyl novobiocin analogues

Preparation of the previously described acetylated compounds is outlined in Scheme 40. Coumarin phenols **23a–g** were treated with acetic anhydride in pyridine to furnish acetylated scaffolds **127a–g**. Next, the benzyl carbamate was removed via hydrogenolysis to produce the corresponding aminocoumarin, which was readily coupled with biaryl acid **27** in the presence of EDCI and pyridine.

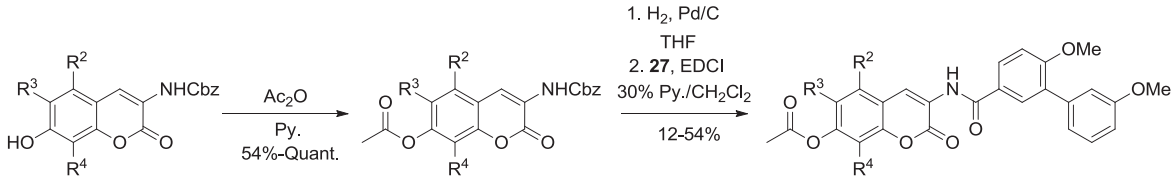

23a: R^2 = H; R^3 = OMe; R^4 = Me
23b: R^2 = H; R^3 = OPr; R^4 = Me
23c: R^2 = H; R^3 = O^{i}Pr; R^4 = Me
23d: R^2 = OMe; R^3 = H; R^4 = Me
23e: R^2 = H; R^3 = H; R^4 = Bn
23f: R^2 = H; R^3 = H; R^4 = Ph
23g R^2 = H; R^3 = H; R^4 = OMe

127a: R^2 = H; R^3 = OMe; R^4 = Me (Quant.)
127b: R^2 = H; R^3 = OPr; R^4 = Me (Quant.)
127c: R^2 = H; R^3 = O^{i}Pr; R^4 = Me (87%)
127d: R^2 = OMe; R^3 = H; R^4 = Me (54%)
127e: R^2 = H; R^3 = H; R^4 = Bn (87%)
127f: R^2 = H; R^3 = H; R^4 = Ph (83%)
127g: R^2 = H; R^3 = H; R^4 = OMe (Quant.)

128a: R^2 = H; R^3 = OMe; R^4 = Me (54%)
128b: R^2 = H; R^3 = OPr; R^4 = Me (49%)
128c: R^2 = H; R^3 = O^{i}Pr; R^4 = Me (45%)
128d: R^2 = OMe; R^3 = H; R^4 = Me (39%)
128e: R^2 = H; R^3 = H; R^4 = Bn (22%)
128f: R^2 = H; R^3 = H; R^4 = Ph (12%)
128g: R^2 = H; R^3 = H; R^4 = OMe (50%)

Scheme 40. Synthesis of 7-acetyl biaryl analogues.[194]

2. Biological evaluation of 5-, 6-, and 8-alkyl(oxy) 7-acetyl novobiocin analogues

Upon construction of this library of acetylated novobiocin analogues, the compounds were evaluated for anti-proliferative activity against SKBr3 and MCF-7 breast cell lines. As shown in Table 3, the binding pocket was very exclusive, only tolerating specific modifications to the coumarin ring system. With respect to the 6-position, groups larger than a methoxy group were not tolerated when the 7-position is acetylated. The 6-methoxy 7-acetyl compound **128a** (KU135) manifested notable activity, representing the most active compound from the study and a 10-fold improved potency over its noviosylated counterpart (**26a**). Although its activity was modest, the 5-position analogue showed some selectivity for SKBr3 cells over MCF-7 cells. This difference in activity could be the result of isoform selectivity, but would require further studies to confirm this hypothesis. Finally, like with the 6-position analogues, the 8-position was only tolerant of the methoxy group, as all other groups resulted in completely inactive compounds. The SAR trends observed are consistent with the noviosylated scaffolds, implying that binding orientation may not be perturbed.

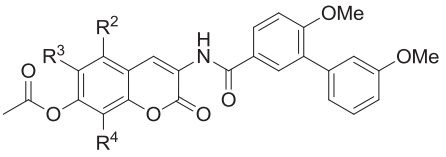

Table 3. Anti-proliferative activities of 7-acetyl biaryl analogues.

Compound	R^2	R^3	R^4	SKBr3 (IC_{50}, μM)	MCF-7 (IC_{50}, μM)
128a	H	OMe	Me	5.72 ± 0.03[a]	1.5 ± 0.3
128b	H	OPr	Me	>100	>100
128c	H	O^{i}Pr	Me	>100	>100
128d	OMe	H	Me	48.0 ± 0.4	>100

128e	H	H	Bn	>100	>100
128f	H	H	Ph	>100	1.79 ± 0.7
128g	H	H	OMe	20.5 ± 1.6	8.62 ± 2.5

[a] Values represent mean ± standard deviation for at least two separate experiments performed in triplicate.

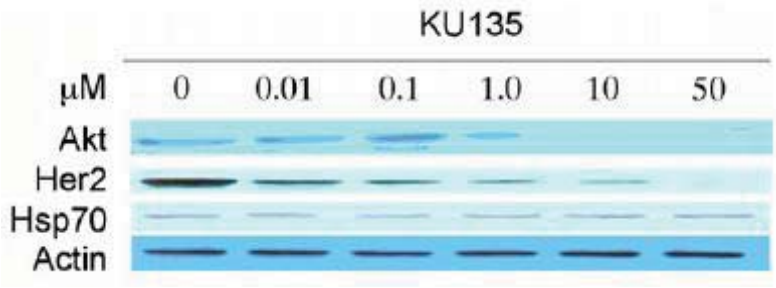

Figure 40. Western blot analyses of Hsp90 client protein degradation assays against MCF-7 cells after 48 h incubation with **128a**. Concentrations (in μM) of **128a** (KU135) are indicated above each lane. GDA (geldanamycin, 500 nM) and DMSO were respectively employed as positive and negative controls.[241]

As the 6-methoxy containing compound was the most intriguing, it was taken on into subsequent studies. To confirm that the observed anti-proliferative activities exhibited by **128a** (KU135) results from Hsp90 inhibition, it was evaluated through Western blot analyses in MCF-7 cells by a co-worker in the laboratory. As seen in Figure 40, the ability of **128a** to induce degradation of Hsp90-dependent client proteins Akt and Her2 in a concentration-dependent manner was confirmed. Moreover, this degradation correlates well with the observed anti-proliferative IC_{50} value of 1.5 μM against MCF-7 cells, clearly linking Hsp90 inhibition to cell viability. In addition, Hsp70 levels remained constant at all concentrations tested, which is a hallmark of *C*-terminal Hsp90 inhibition and in contrast to the induction observed upon treatment with *N*-terminal inhibitors. Finally, since actin, a non-Hsp90-dependent protein, is not

affected by this compound, anti-proliferative activity correlates directly with Hsp90-client protein degradation.

3. Novobiocin versus 128a

Confirmation that the anti-proliferative activity of **128a** was due to Hsp90 inhibition, generated interest in pursuing other simplified sugars. Although the binding model was not in existence at the onset of this project, **128a** has since been docked into the Hsp90α model.[192] The conformation exhibited by novobiocin versus that which **128a** adopts is shown in Figure 41. Although the two compounds assume similar orientations within the binding pocket, the simplified acetyl group allows **128a** to fit much deeper into the cleft where the noviose portion of novobiocin extends. Due to this shift, it is perceived that many important interactions with the coumarin and benzamide portions may be sacrificed.

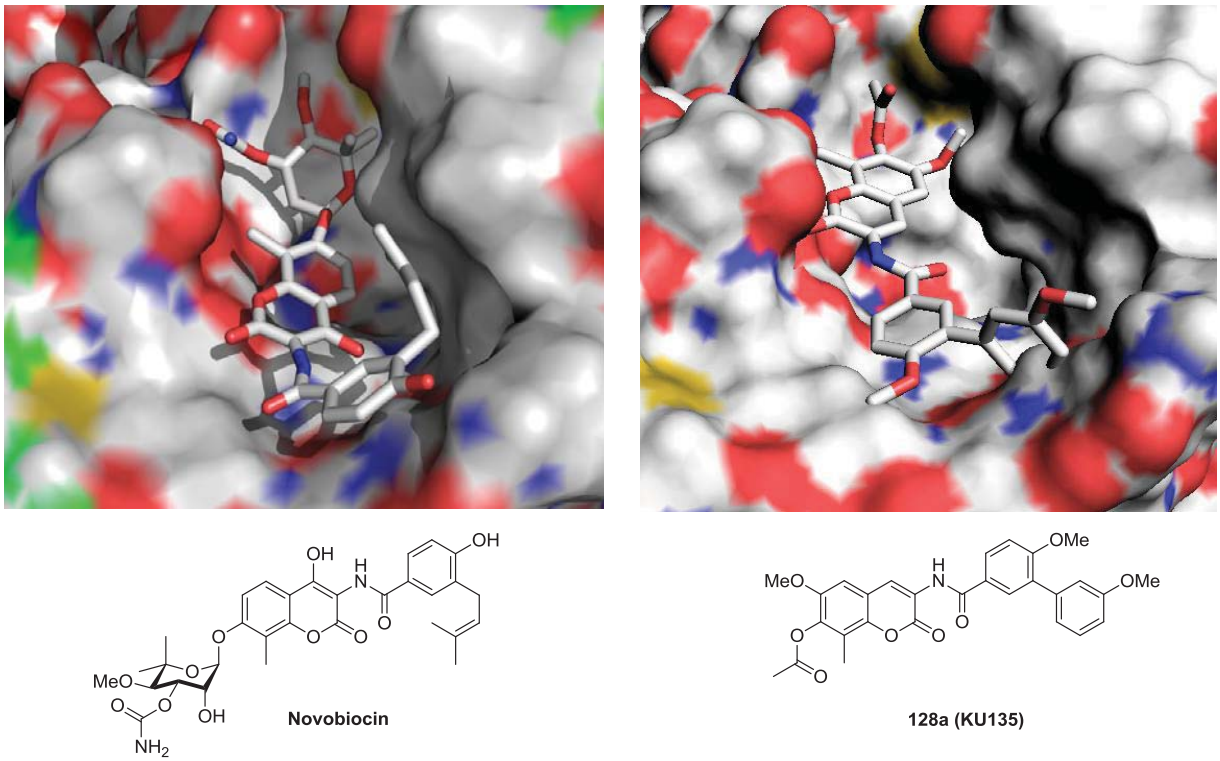

Figure 41. Novobiocin versus **128a** bound to Hsp90α model.

It was proposed that **128a** may exert its anti-Hsp90 through a distinct mechanism, potentially involving acetylation of a key residue on Hsp90. Studies using ^{14}C-labeled **128a**, and incorporation of the ^{14}C within the acetyl group, to examine potential Hsp90 acetylation through 2D-gel electrophoresis and subsequent mass spectrometry are under investigation. Although these studies have not been executed, a synthetic variant of **128a** was designed to probe the specific mechanism by which **128a** inhibits Hsp90.

B. 7-homologated analogue of 128a

To explore the possibility that **128a** was not exhibiting its activity due to acetylation, but rather was making important interactions and binding in the pocket much like other novobiocin analogues, several congeners were designed. The first **128a** analogue was designed to add a single methylene unit between the coumarin 7-position and the oxygen to which the acetyl group would be attached. This derivative would reduce the lability of the acetyl group and could potentially extend the group back into the sugar binding region, allowing the analogue to adopt a similar binding orientation as other novobiocin analogues.

1. Synthesis of 7-alcohol-containing coumarin

Attempted synthesis of the desired coumarin scaffold is shown in Scheme 41. Starting from benzaldehyde **129**, a known procedure was followed to install the chloromethyl group using formaldehyde, zinc (II) chloride and bubbling HCl gas. Formation of the undesired regioisomer, due to installation of the chloromethyl group at both positions ortho to the methoxy group, explains the ~50% yield.[242] Next, calcium carbonate in aqueous medium was used to displace the

benzyl chloride and install the desired benzyl alcohol functionality. Benzaldehyde **131** was next converted, to phenol **132** using Dakin oxidation conditions in good yield. An attempt to cyclize intermediate **132** using a modified Pechmann condensation led to formation of an undesired side product, caused by transesterification of the benzyl alcohol. Although this reaction is reversible, the desired product was not formed. It was proposed that oxidation directly to the corresponding acid would eliminate the potential for the competing reaction in coumarin ring formation. Thus, two oxidation conditions were employed, but neither yielded the desired product. Likewise, attempted oxidation to the corresponding aldehydes using Dess Martin periodinane was not fruitful. It is proposed that hydrogen bonding between the methoxy and alcohol groups may lock this system into a stable six-membered hydrogen-bonding ring, making it unreactive to typical oxidation conditions. Alternative routes toward this important analogue were sought.

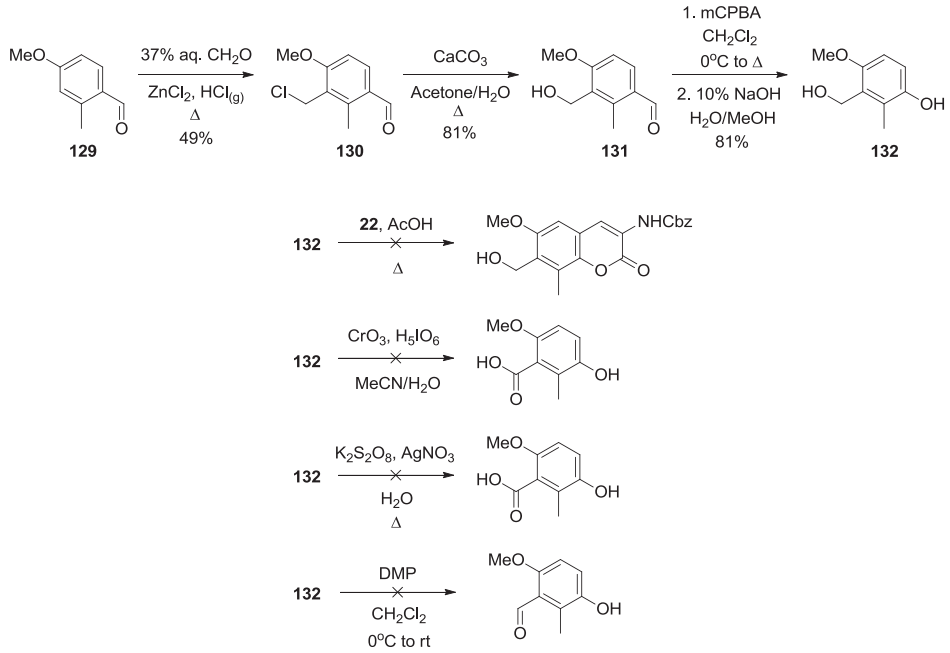

Scheme 41. Attempts to homologate the 7-position of 6-methoxy coumarin scaffold.

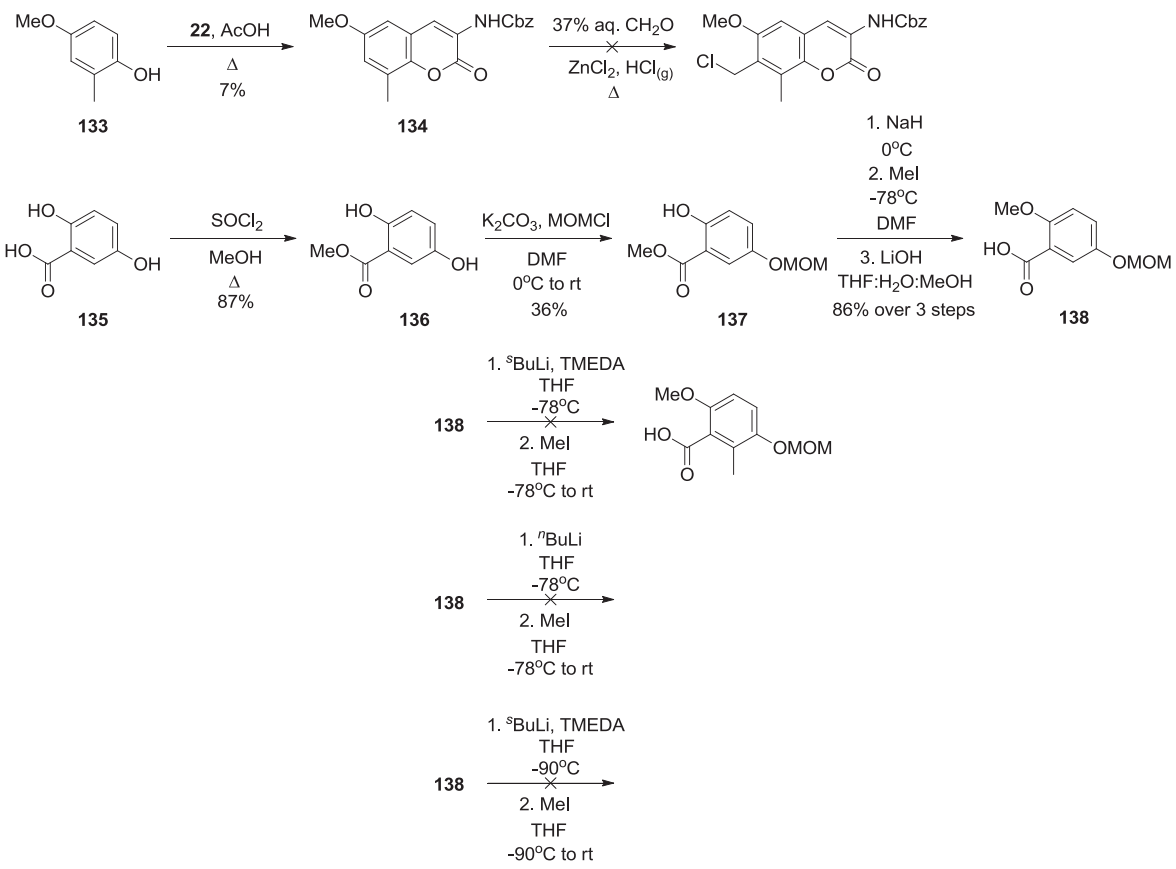

Scheme 42. Other efforts to homologate the 7-position of 6-methoxy coumarin scaffold.

Other strategies to install the desired functionality at the 7-position are outlined in Scheme 42. Starting from phenol **133**, a modified Pechmann condensation was attempted to construct a coumarin lacking functionality at the 7-position. Although it was envisioned that this coumarin ring, **134**, could then be functionalized to install the chloromethyl group, an attempt to do so did not lead to desired product. As part of an alternative strategy, hydroquinone **135** was converted to methyl ester **136** using a known procedure.[243] Next, exclusively one phenol was protected as the methoxy methyl ether. Phenol **137** was next methylated and the crude intermediate was taken on to hydrolysis, furnishing carboxylic acid **138** in good yield over three steps. Next, *ortho*-lithiation conditions were employed to install the requisite methyl group

between the directing MOM group and acid. Several attempts using different organolithium bases, with and without the addition of TMEDA, were unsuccessful. Although efforts to make this homologated coumarin did not continue, it is perceived that this compound would be instrumental in understanding the unique activity exhibited by analogue **128a**.

C. Excision of 7-position oxygen

As another strategy to explore the activity exhibited by **128a**, analogues that lack the 7-position oxygen were proposed. While the carbonyl oxygen would still be available for hydrogen bonding, these proposed analogues would not contain a labile acetyl. Thus, simple 7-ester and 7-acid analogues of 8-methyl coumarins were constructed.

1. Synthesis of 7-ester and 7-acid coumarins

Starting from acid **139**, modified Pechmann condensation conditions were employed to produce coumarin **140** (Scheme 43). Due to difficulty in isolation and purification, this coumarin was taken on crude to functionalization attempts. Esterification of the 7-position acid proceeded with partial cleavage of the benzyl carbamate *in situ*, to yield aminocoumarin **142**. Alternatively, the benzyl carbamate was cleaved prior to esterification, to afford esterified coumarin **142** in better yield than observed using the former strategy. Aminocoumarin **142** was next coupled with biaryl acid **27** in the presence of EDCI to afford ester **143**. While some of ester **143** could be isolated, separation from the biproduct formed due to self condensation of the acid was difficult. Purification was eased greatly by hydrolysis to acid-containing coumarin, **144**. Upon preparation, both coumarins **143** and **144** were subjected to anti-proliferation assays.

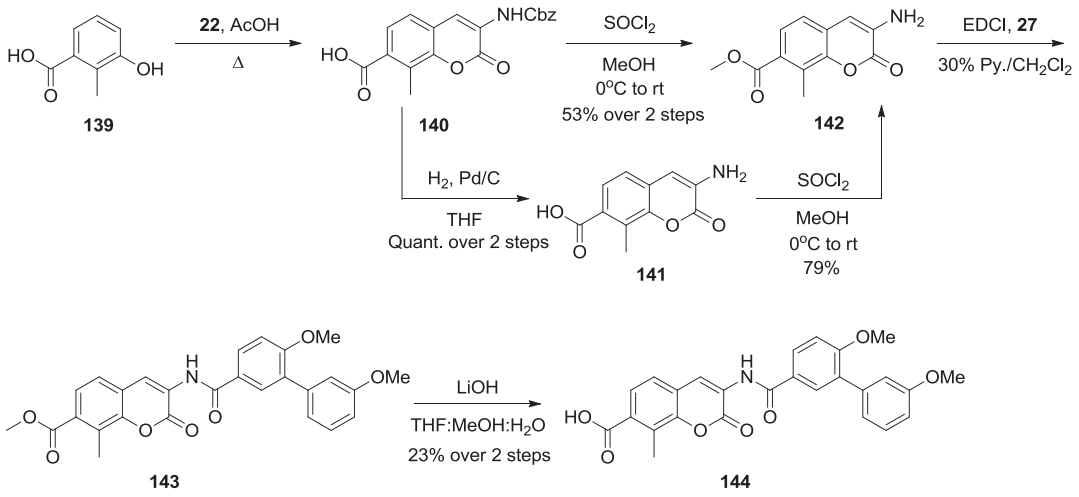

Scheme 43. Synthesis of 7-position analogues.

2. Biological evaluation of analogues 143 and 144

Upon construction of compounds lacking the 7-position oxygen linkage, they were evaluated for anti-proliferative activity against SKBr3 and MCF-7 breast cancer cell lines. While free acid **144** proved inactive against both cell lines, ester 143 showed specificity for one cell line, exhibiting an IC_{50} of 9.39 ± 0.31 μM against MCF-7 cells and proving inactive against SKBr3 cells. Thus, while the acid is not tolerated, potentially due to solubility issues, the ester demonstrates modest, and potentially isoform-specific, activity. However, neither is as active as **128a** and this oxygen linkage may be important to its observed potency. Moreover, these analogues do not discount the possibility of acetylation as the mechanism through which **128a** exerts its activity. Further studies into the mechanism of **128a** are discussed in the next chapter.

III. Survey of potential sugar surrogates on simple coumarin

Because of the novel and exciting activity of **128a**, it was proposed that complementary analogues, built upon an optimized novobiocin scaffold, could lead to more efficacious

compounds. Because it has been extensively studied and prepared in relatively few steps, the 8-methyl coumarin scaffold outfitted with the biaryl benzamide side chain, as is found in compound **59**, was selected as the scaffold upon which to append various sugar replacements (Figure 42). The design and synthesis of these non-sugar analogues are discussed in the following sections, as well as the anti-proliferative activities manifested by such compounds.[194]

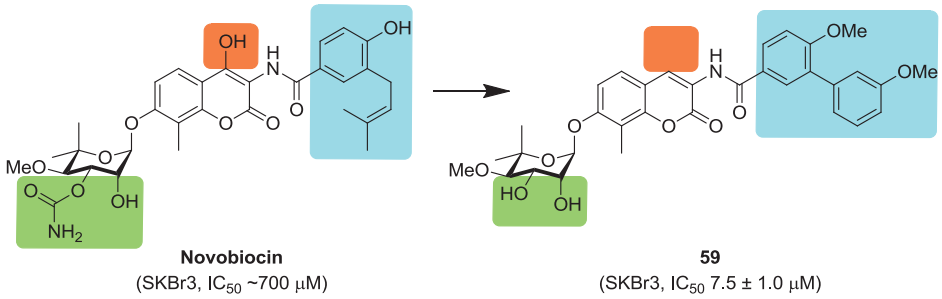

Figure 42. Summary of sugar surrogate strategy.[194]

A. Design of sugar analogues of novobiocin

To extend upon our knowledge of **128a** and its SAR, several simplified non-sugar moieties were appended to the 7-position of the coumarin ring. Chemistry developed by our lab was used to construct the coumarin core and attach the desired biaryl benzamide side chain, while acetylation protected the phenol until subsequent modification.[170] Phenol **148** was chosen as the scaffold upon which to build these analogues, because of its expeditious synthesis and to explore whether the activity of **128a** can be further attenuated.[102] Most analogues were designed with a sugar replacement that maintained interactions proposed to be manifested by noviose. In addition to probing the dimensions and electronic environment, functionalities that exhibit improved solubility profiles were incorporated. Denoviosylated phenol **148**, which lacks the sugar functionality and corresponds to a potential metabolite upon cleavage of the glycosidic bond, was also evaluated. Many bioactive natural products bearing carbohydrates are often

rendered inactive upon removal of their sugar moieties.[244-249] However, Le Bras and co-workers recently reported that disruption of the Hps90 heteroprotein complexes occurs by a compound bearing a free phenol at the 7-position of a novobiocin-derived scaffold.[105] Although this compound did not demonstrate remarkable activity, it was notable that it maintained Hsp90 inhibition despite removal of noviose.[194]

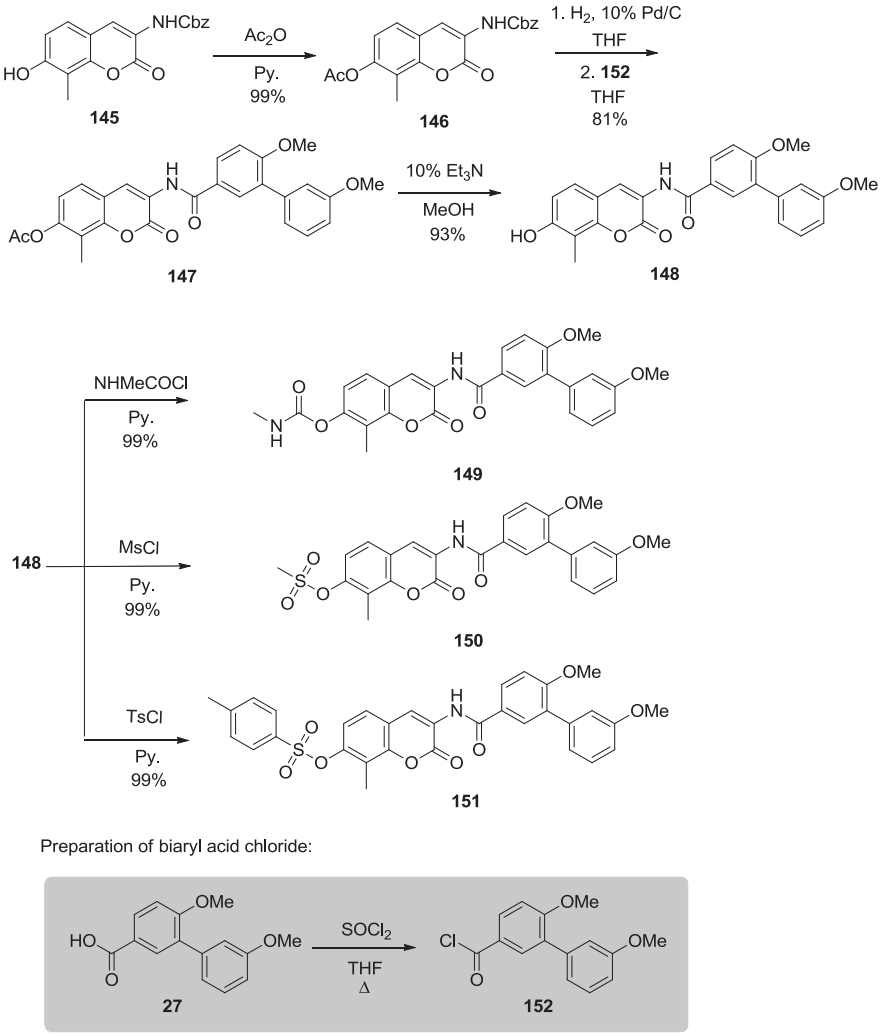

Scheme 44. Synthesis of phenol **148** and non-sugar analogues **149–151**.[102,170,194]

1. Synthesis of derivatives with sugar replacement

Previously reported coumarin **145** was acetylated, and then the benzyl carbamate was cleaved and the aminocoumarin was coupled to biaryl acid chloride **157**, prepared from biaryl acid **27**, in good yield (Scheme 44).[102,170] For direct comparison to **128a**, acetylated scaffold **147** was also evaluated. Next, **147** was hydrolyzed to phenol **148**, which acted as the precursor used in all subsequent coupling reactions. A methylated carbamate was chosen to compliment the size of the acetate group, while providing additional stability, as carbamates are not readily cleaved *in vivo*. The methylated carbamate was installed on phenol **148** via the carbamoyl chloride to further probe dimensions of the pocket. Methyl and toluene sulfonic esters were also appended to the 7-position to explore both hydrogen bonding interactions, while simultaneously probing pocket dimensions. It was envisioned that the sulfonic ester is capable of participating as a hydrogen bond acceptor, while the alkyl/aryl appendages probe the ability of the pocket to encapsulate hydrophobic bulk. Moreover, the 7-tolylsulfonate ester has been shown by the Renoir group to maintain Hsp90 inhibition and demonstrate modest potency when attached to a novobiocin-derived scaffold.[106] The desired functional group was installed onto the 7-phenol using the requisite sulfonyl chloride, in the presence of pyridine.[194]

While the planar aromatic tolyl group offers a rigid six-membered ring, the pyranose of noviose represents a flexible ring system. Thus, heterocyclic six-membered rings were investigated to serve as simplified mimics of noviose. Substituted piperidines were synthesized by a co-worker as simplified azasugars to probe essential substituents on the noviose ring. Azasugars were selected due to the prevalence of N-heterocycles in a wide variety of bioactive compounds with diverse therapeutic applications.[250-252] An unsubstituted 3-piperidine (**153**) represents an aza-surrogate to probe essential hydrogen bonds, such as those potentially made by

the noviose diol. In contrast, the acetylated 3-piperidine (**154**), while still capable of maintaining hydrogen bonds, introduces steric bulk. It is proposed that this acetylated amine, which introduces bulk into the gem-dimethyl region on noviose, should be tolerated. Finally, a methylated 4-piperidine (**154**) was introduced to replace the sugar. The methylated amine was introduced to project this moiety into the same cavity as the 4'-methoxy group on noviose. Synthesis of the piperidine-containing analogues shown in Figure 43 was accomplished using Mitsunobu conditions.[194]

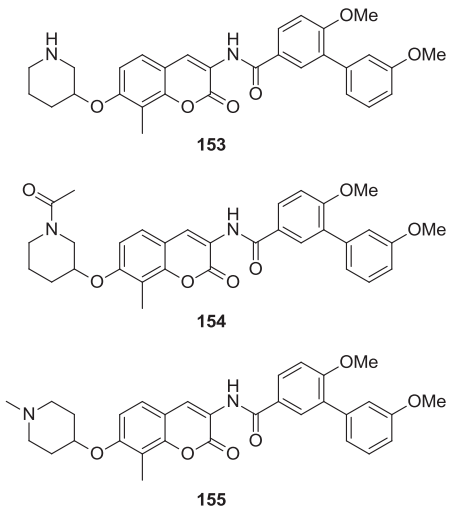

Figure 43. Structures of piperidine-containing analogues.[194]

In addition to the piperidines, simplified pyranoses were appended in lieu of noviose. Pyranoses are attached to several clinically prescribed anticancer drugs, such as bleomycin, doxorubicin and etoposide, in addition to novobiocin.[253] The simple 2- and 3-hydroxy pyranoses were chosen as each could maintain similar hydrogen bonds as found in noviose. Through systematic removal of each hydroxyl, identification of which hydroxy group is essential could be ascertained. Once attached, the α anomer of each of the pyranoses was evaluated (**156** and **157**), as this is the anomer present in novobiocin.[254,255] Finally, a syn-diol-containing cyclohexane was chosen as the final non-sugar moiety (**158**). This sugar alternative maintains the diol of noviose,

but does not contain the labile hemi-acetal linkage. These final pyranose- and cyclohexyl-containing analogues, shown in Figure 44, were prepared by colleagues using Mitsunobu conditions.[194]

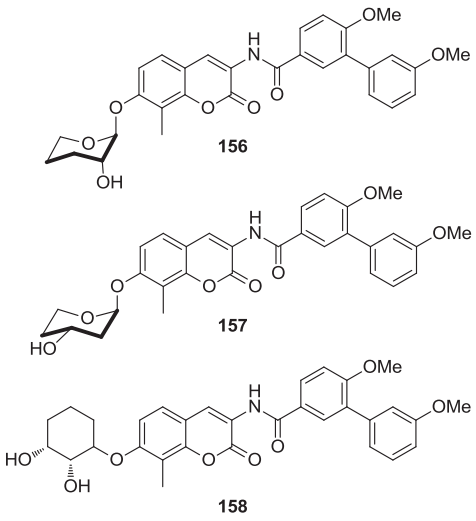

Figure 44. Structures of pyranose- and cyclohexyl-containing analogues.[194]

2. Biological evaluation of sugar analogues of 59

Upon construction of the non-sugar and modified sugar analogues of novobiocin, the compounds were evaluated for anti-proliferative activity against SKBr3 and MCF-7 breast cancer cells. Compounds with an asymmetric center were tested as a mixture of compounds to explore general trends in activity, with plans to resolve the two compounds and test them individually if promising results were obtained. Results of these assays are presented in Table 4, along with values for acetylated **128a** and noviosylated **59** as comparisons.[194]

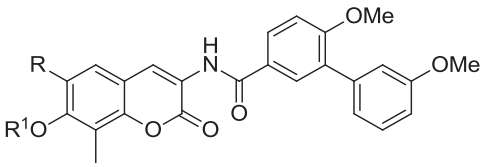

Table 4. Anti-proliferative activities of non-sugar and modified sugar analogues.[194]

Compound	R	R^1	SKBr3 (IC_{50}, μM)	MCF-7 (IC_{50}, μM)
128a	OMe	Ac	5.72	1.50 ± 0.3
59	H	Noviose	7.50 ± 1.0	18.70 ± 1.8
147	H	Ac	0.98	1.40 ± 0.0
148	H	H	8.88 ± 0.6	6.93 ± 0.6
149	H	Me carbamate	2.40 ± 0.2	1.72 ± 0.2
150	H	Ms	7.33 ± 1.2	8.85 ± 1.1
151	H	Ts	>100	>100
153	H	3-NH piperidine	1.16 ± 0.2	1.63 ± 0.4
154	H	3-NAc piperidine	10.79 ± 0.1	9.18 ± 0.8
155	H	4-NMe piperidine	1.34 ± 0.2	1.51 ± 0.3
156	H	2'-OH pyranose	>100	>100
157	H	3'-OH pyranose	9.28 ± 0.1	11.20 ± 0.6
158	H	Cyclohexyl diol	>100	>100

[a] Values represent mean ± standard deviation for at least two separate experiments performed in triplicate.

Upon examination of the non-sugar analogues, some interesting trends were observed. Despite complete excision of the noviose sugar, the free phenol **148** demonstrated comparable activity to the corresponding noviosylated scaffold (**59**). Also, the acetylated and methylated carbamate scaffolds, **147** and **149**, respectively, demonstrated comparable activity to **128a**, and the latter represents an exciting analogue that maintains activity without the labile acetate group.

While the methyl sulfonic ester **150** maintained similar activity to its noviosylated counterpart, the toluene sulfonic ester **151** was inactive, indicating the toluene-containing compound exceeded the limits tolerated by the binding pocket.

Much like the non-sugar analogues, the piperidine scaffolds manifested a broad range of activities. While the unsubstituted 3-piperidine **153** demonstrated low-micromolar activity, acetylation (**154**) compromised its activity. Transposition of the amine to the 4-position and subsequent methylation (**155**) returned low-micromolar activity. The various hydroxylated pyranoses demonstrated intriguing activity. While the 3'-hydroxylated pyranose **157** maintained the activity of noviosylated **59**, the 2'-hydroxylated pyranose **156** was completely inactive. Similarly, the syn-diol-containing cyclohexane **158** did not display measurable activity in the anti-proliferation assay, indicating a hydrogen-bond acceptor adjacent to the phenolic oxygen is needed.

The SAR trends observed for the non-sugar analogues offer insight into the nature of the binding pocket. As mentioned previously, sugars are known to play important roles in both solubility and transport.[254,255] The potency of compounds containing a hydrogen bond donor, such as the carbamate and unsubstituted piperidine, affirms the need for hydrogen bonds with the pocket. Furthermore, activity of the 3-piperidine correlates well with the data from the set of pyranoses, supporting an essential hydrogen bond donor at the 3-position of the ring, while a hydrogen-bond at the 2-position is dispensable. In contrast, it appears that within this hydrogen bonding network, a simple syn-diol cyclohexane system cannot take advantage of such interactions, suggesting an essential role of the hemi-acetal linkage made by the pyranose systems. It is possible that the endocyclic oxygen of the pyranose ring provides interactions with the binding pocket that properly orients the hydroxy groups. Another important observation from

this series of sugar mimics is that steric bulk is selectively tolerated. When comparing the methylated 4-piperidine and acetylated 3-piperidine, it becomes clear that bulk is much better tolerated at the 4-position than the 3-position. Moreover, when comparing the methyl and toluene sulfonic ester, the methyl-containing compound, despite its poor solubility, maintains activity, while the corresponding toluene derivative does not. SAR for this series of compounds is summarized in Figure 45.

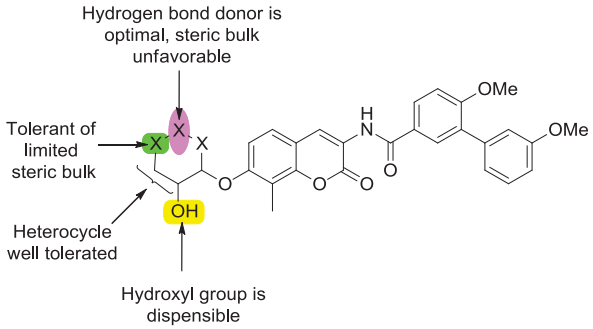

Figure 45. SAR summary for non-sugar analogues.

To confirm that the anti-proliferative activities exhibited by the sugar and non-sugar analogues result from Hsp90 inhibition, analogues **149** and **155** were evaluated by Western blot analyses. It was essential that these analogues demonstrate selective Hsp90-dependent client protein degradation, versus a loading control. Figure 46 shows that in MCF-7 cells, the Hsp90-dependent client proteins Akt, Raf, and Her2 were degraded in a concentration-dependent manner upon treatment with the compounds. Hsp90 client protein degradation occurred at concentrations that paralleled the observed anti-proliferative IC_{50} values of 1.72 ± 0.2 μM, for **149**, and 1.51 ± 0.30 μM, for **155**, confirming that Hsp90-dependent client protein degradation is causative for inhibition of cell growth. Moreover, Hsp90 remained constant at all concentrations tested, which is a hallmark of *C*-terminal Hsp90 inhibition. Since the non-Hsp90-dependent

protein, actin, was not affected by these analogues, selective degradation of Hsp90-dependent proteins occurred directly through Hsp90 inhibition.

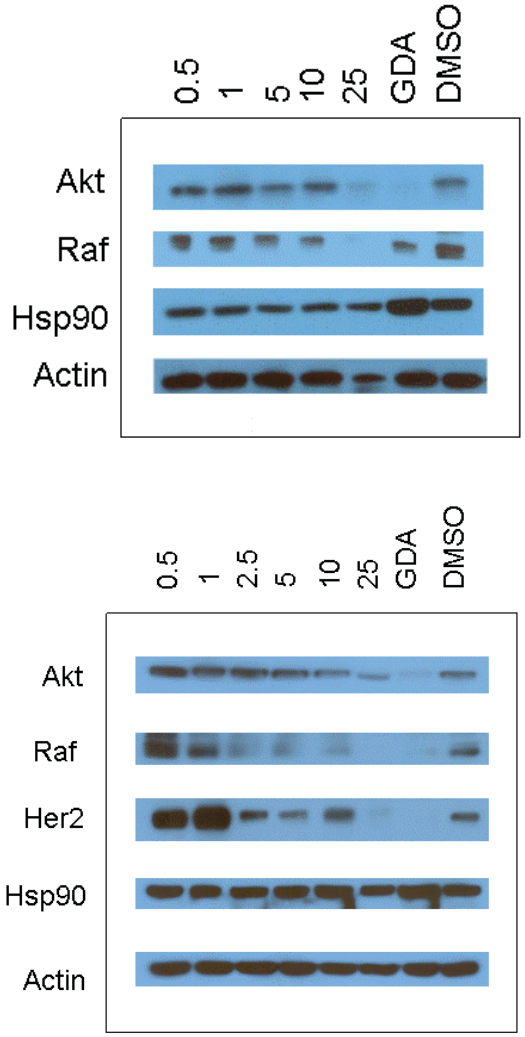

Figure 46. Western blot analyses of Hsp90 client protein degradation assays against MCF-7 cells after 24 hours incubation with non-sugar analogues. Concentrations (in μM) of **149** (top blot) and **155** (lower blot) are indicated above each lane. GDA (geldanamycin, 500 nM) and DMSO were respectively employed as positive and negative controls.

The studies described sought to elucidate the potential role of the noviose sugar in the binding of novobiocin-derived compounds to Hsp90. SAR for the noviose appendage has been presented and important interactions highlighted. Essential interactions, which can be maintained by simplified scaffolds, as well as those that are dispensable were identified. In addition, the steric environment into which the sugar is presented was explored and insight was gained into which groups are best tolerated. Small changes in substitution resulted in significant changes in activity, reflecting a sensitive steric environment within this binding pocket. Capitalization on key interactions and steric bulk resulted in the preparation of several low-micromolar Hsp90 inhibitors that exhibit improved activity versus the parent noviosylated compounds and lack complexity. The analogues described benefit from facile preparation, and offer the potential for the more efficient synthesis of Hsp90 *C*-terminal inhibitors.

IV. Survey of potential sugar surrogates on optimized coumarin scaffolds

A. Molecular modeling

Since completion of the study in Section II, development of the Hsp90α model has enabled a better understanding of how noviosylated compounds bind the *C*-terminal site. Moreover, through docking of compounds similar to **59**, the SAR trends have been confirmed and can be rationalized.

1. Specific interactions made by the sugar of 59

Since it represented the basis for comparison of the compounds described in Section II, key interactions made by noviose when **59** is docked into the model were examined. As seen in Figure 47, the noviose sugar sits in a hydrogen bond rich portion of the binding pocket, flanked by several polar amino acids. Key interactions are made with several residues from each of the two monomers that make up the Hsp90α homodimer. Hydrogen bonds are proposed between Thr-540 and the 2'-OH of the noviose ring system. The secondary alcohol on the threonine side chain is within 4 Å of two potential hydrogen bonds, involving the oxygen and hydrogen of the 2'-OH on the noviose sugar. Likewise, it is proposed that the nitrogen from the Asn-686 amide backbone hydrogen bonds to the 2'- and 3'-hydroxyls. This aspartic acid residue offers a hydrogen bond acceptor, capable of interacting with the proton on each of these two hydroxyl groups as well.

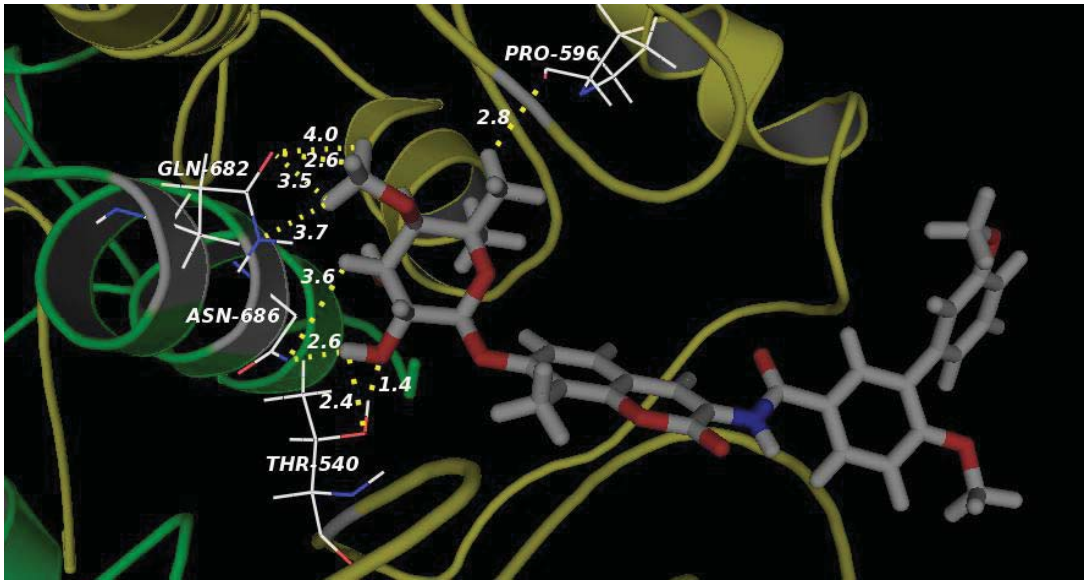

Figure 47. 59 bound to the model.

Moreover, Gln-682 is another polar residue that provides several hydrogen bonds with the pyranose system. Like with the previously discussed aspartic acid residue, the amide

backbone nitrogen of the glutamine residue is within distance to elicit hydrogen bonds with the hydrogens of the 4'-methoxy group. In addition, the adjacent amide carbonyl can act as a hydrogen bond acceptor. The *gem*-dimethyl group on the noviose ring appears to interact with Pro-596 at the top of the pocket.

These key hydrogen bonds made between noviose and the putative binding pocket correlate well with the SAR trends determined through the study in Section II (Figure 45). Although the orientation may be slightly altered when the non-sugar derivatives bind, several trends are explained by this model. Firstly, the highly charged nature of this pocket would likely favor the incorporation of a heterocycle. Next, the analogues in the prior section including the simplified pyranose systems, which revealed the 2'-OH to be dispensable, are likely to bind in a different orientation because they lack the bulky *gem*-dimethyl functionality. This slightly altered or potentially flipped conformation would not allow the 2'-OH to make favorable contacts with Thr-540. The proximity of Gln-682 to the putative 4'-position explains the favorable contacts made by the methyl group of the *N*-methyl piperidine. Finally, it is proposed that, depending on the analogue, the 5'-position could flip and become the putative 3'-position in order to capitalize on hydrogen bonding with Asn-686. This is likely the case with the unsubstituted 3-piperidine. In contrast, the acetylated 3-piperidine is too bulky and likely clashes with either Asn-686 or Pro-596. Validation through modeling of the trends observed experimentally, the focus was moved to optimization of these non-sugar containing analogues through subsequent studies.

B. Rational design of optimized non-sugar containing novobiocin scaffolds

As discussed in Section I of this chapter, incorporation of a non-sugar group at the 7-position was only synergistic with installation of a 6- or 8-methoxy group on the coumarin ring. As shown in Section II, several non-sugar surrogates can be installed in lieu of the noviose sugar to improve activity, while simplifying analogue synthesis, and these derivatives still maintain Hsp90 as their target.[194] Combination of the results derived from each of these initial studies provided the rationale needed for the subsequent design of optimized non-sugar novobiocin analogues (Figure 48).

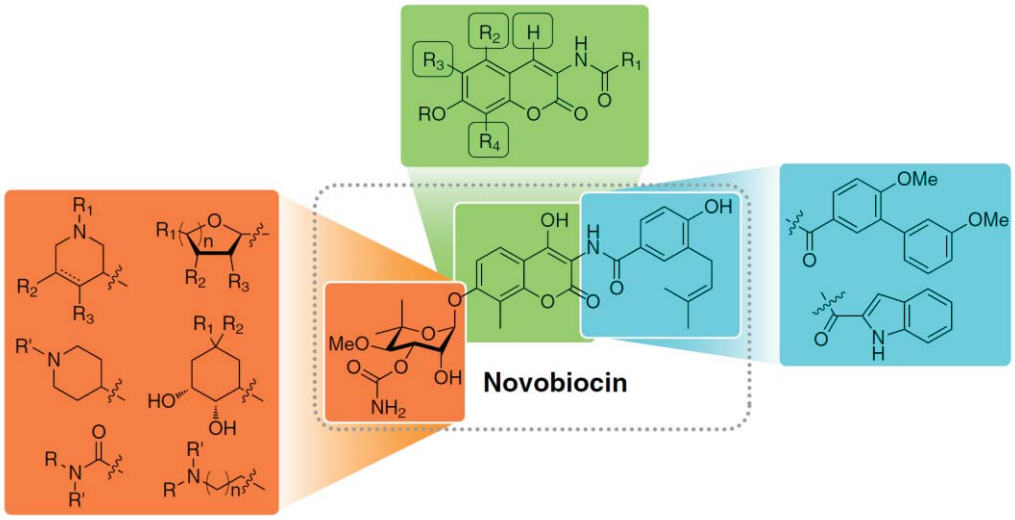

Figure 48. Summary of optimized non-sugar novobiocin scaffolds.[193]

The most potent coumarin scaffolds obtained from the coumarin studies were coupled with the optimal biaryl side chain to yield a scaffold upon which sugar surrogates were appended.[102,170] Based on the inhibitory activity manifested by the biaryl analogues, the most promising sugar surrogates were coupled with coumarins containing the 2-indole side chain.[102] The simplified sugars and related azasugars were found to conserve structural units present in noviose, but lacked the complexity of multi-step synthesis. These and several other sugar

surrogates were designed to probe potential hydrogen bonds as well as to determine the dimensions of the pocket. In addition to simplified sugars, several surrogates containing heteroatoms and various appendages were also explored. These diverse sugar and non-sugar analogues simplify the preparation of novobiocin analogues, while providing a handle to improve both solubility and efficacy.[193]

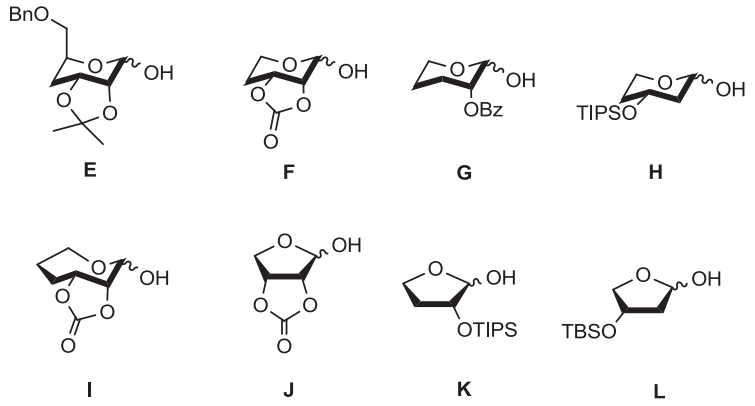

Figure 49. 5-, 6-, and 7-membered noviose alternatives.[193]

1. Design and synthesis of modified sugar and cyclohexyl analogues

Numerous biologically active natural products contain carbohydrates appended to their scaffolds that serve to increase solubility and provide interactions with their cognate receptor. In many cases, removal of the carbohydrate moiety renders the aglycon inactive, whereas alteration of the sugar ring size can drastically alter affinity of the compounds toward specific targets.[256-258] Modifications to the noviose pyranose ring were proposed to elucidate functionalities required for inhibitory activity, as well as to determine whether different sized sugars can be utilized as replacements for noviose. Thus, 5-, 6- and 7-membered sugars were synthesized and coupled to the aforementioned scaffolds to determine optimal interactions. When available, the α- and β-anomers were also evaluated. A set of protected mono-, di- and trihydroxylated furanoses,

pyranoses and oxepanose sugars previously synthesized by Yu and coworkers[240] (**E-L**, Figure 49) was chosen based on these considerations.[193]

The analogues were assembled in modular fashion, allowing sequential coupling of sugars and the biaryl acid side chain with the desired scaffold. As shown in the retrosynthetic analysis (Scheme 45), the biaryl acid side chain was assembled through a Suzuki coupling reaction, as described previously.[170] Next, the biaryl acid was converted to its corresponding acid chloride (**152**) and then, following hydrogenolysis, coupled with protected coumarins, **147**, **128a**, and **128g**. Finally, Mitsunobu etherification between coumarin phenols **148**, **159** and **160** and sugars **E–L** yielded the desired analogues in good yields.[193]

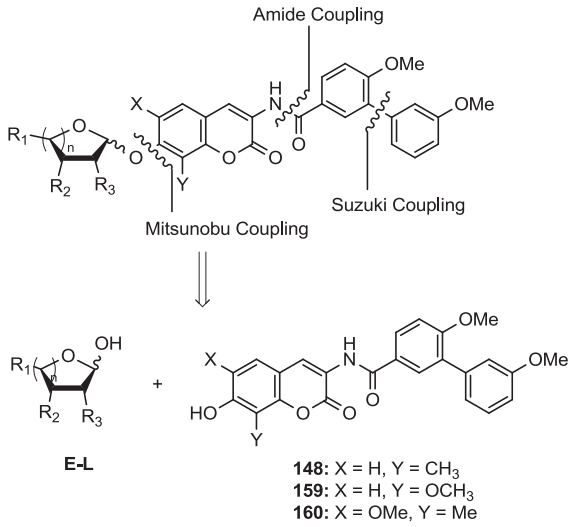

Scheme 45. Retrosynthesis of novobiocin biaryl analogues with sugars **E–L**.[193]

Synthesis of the scaffolds required for these and related analogues, as described in Scheme 47, began via protection of phenols **145**, **23a** and **23g**[102,170] as the corresponding esters, **146**, **127a** and **127g**. Next, hydrogenolysis was employed to liberate the corresponding vinylogous amides, which were subsequently coupled with biaryl acyl chloride, **152**. The biaryl acid chloride was generated from the corresponding biaryl acid **27**, as described previously

(Scheme 46).[170] Finally, solvolysis of esters **147**, **128a**, and **128g** afforded phenols **148**, **159** and **160** in good yield.[193]

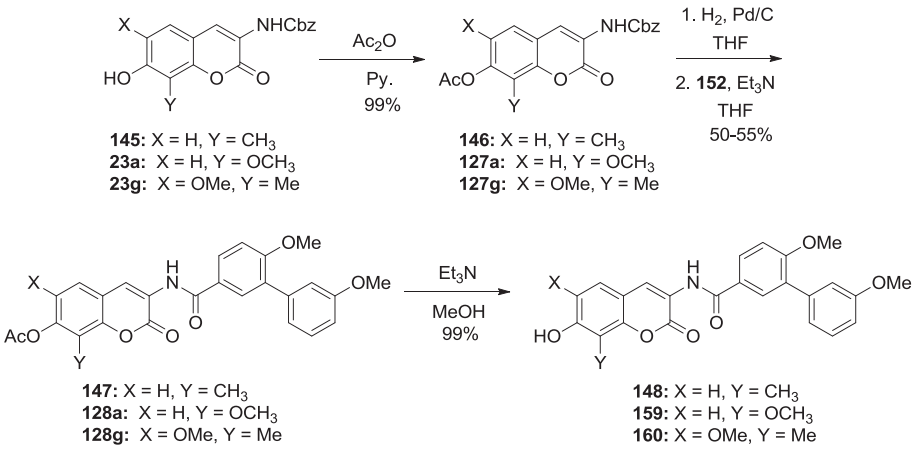

Scheme 46. Synthesis of phenols **148**, **159**, and **160**.[193]

The various coumarin phenols (**148**, **159**, and **160**) and protected pyranoses **E–H** were coupled via a Mitsunobu etherification and subsequently submitted to deprotection protocols to afford the analogues shown in Figure 50. Preparation of these compounds was carried out by a co-worker as part of this study.[193]

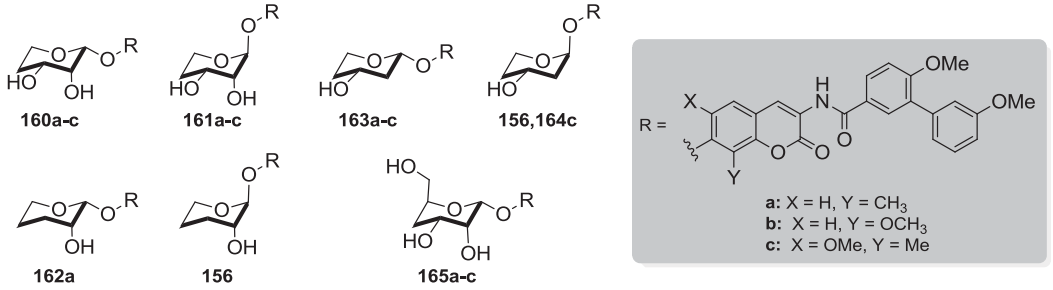

Figure 50. Pyranose-containing compounds prepared.[193]

As with the pyranose-containing analogues, Mitsunobu etherification was enlisted to couple coumarin phenols **148**, **159**, and **160** to protected sugars **I–L**. These couplings and subsequent deprotections were executed by a co-worker to afford compounds **166–171** (Figure 51).[193]

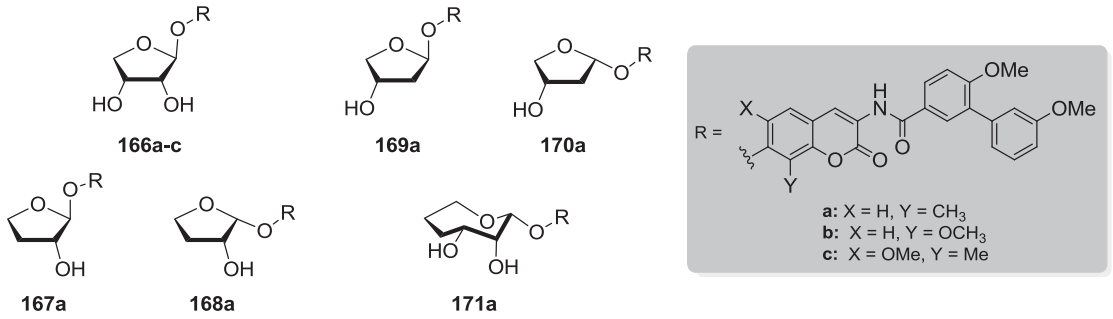

Figure 51. Furanose- and oxepanose-containing compounds prepared.[193]

In addition to the variable-sized sugar-containing analogues, cyclohexyl analogues were designed to examine if a sugar was necessary. Additionally, to probe the tolerance of steric bulk, analogues with and without alkyl substituents were pursued. Many of the simplified cyclohexyl sugar mimics were accessed using common procedures, then coupled via Mitsunobu conditions and further functionalized by a co-worker (Figure 52).[193]

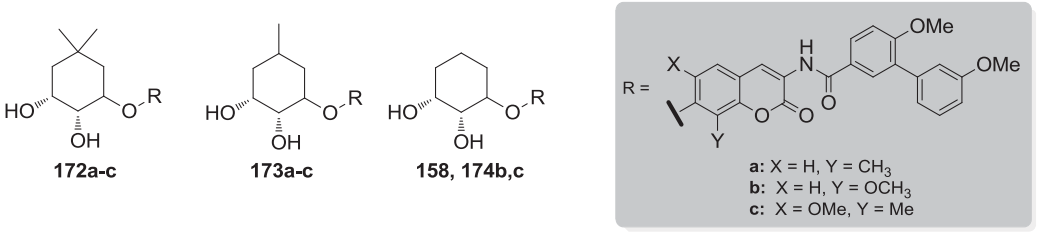

Figure 52. Cyclohexyl-containing compounds prepared.[193]

2. Biological evaluation of modified sugar and cyclohexyl analogues

Upon construction of the sugar and cyclohexyl sugar analogues of novobiocin, the compounds were evaluated for anti-proliferative activity against SKBr3, MCF-7, LNCaP-LN3 (androgen-dependent human prostate cancer cells) and PC3-MM2 (androgen-independent prostate cancer cells) cell lines. As shown in Table 5, analogues containing six-membered pyranose moieties (scaffold **A**) were found to be the most active compounds against the two breast cancer cell lines. Analogues containing dihydroxyl groups consistently exhibited good to

modest anti-proliferative activities against both breast cancer cell lines. In contrast, analogues that contained a single hydroxyl at the 2'-position proved inactive, while most analogues with a 3'-hydroxyl exhibited modest activity. These data indicate that the 3'-position hydroxy group is essential for anti-proliferative activity. Interestingly, the natural substrate for the *C*-terminal pocket of Hsp90, ATP/ADP, also contains a 3'-hydroxyl. Although the β epimer exhibited better activity than its α counterpart (**160a–c** vs. **161a–c**) for most analogues, this was not a general trend observed throughout the series (**156, 163b,c** vs. **164a–c**). In addition, the majority of the compounds from this series demonstrated modest activity against the prostate cancer cell lines. Notably, however, some compounds (**163a**) that were completely inactive against both breast cancer cells lines were efficacious against prostate cancer.[193]

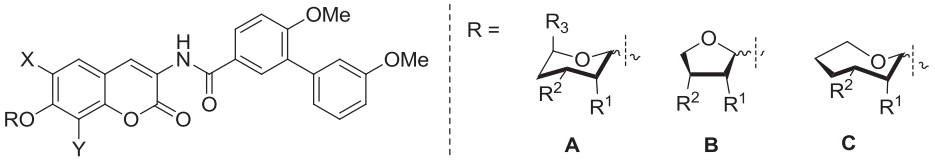

a: X = H, Y = CH_3
b: X = H, Y = OCH_3
c: X = OMe, Y = Me

Table 5. Anti-proliferative activities of various sugar analogues.[193]

Compound	R	R^1	R^2	R^3	Anomer	SKBr3 (IC_{50}, μM)	MCF7 (IC_{50}, μM)	LNCaP-LN3 (IC_{50}, μM)	PC3-MM2 (IC_{50}, μM)
160a	**A**	OH	OH	H	β	6.23 ± 0.52[a,c]	2.56 ± 0.08[a]	3.59 ± 3.40[b]	NT[b]
161a	**A**	OH	OH	H	α	6.71± 0.80	42.56 ± 2.48	1.20 ± 0.83	12.88 ± 9.30
160b	**A**	OH	OH	H	β	1.46 ± 0.46	17.46 ± 1.22	2.29 ± 1.25	10.72 ± 10.85
161b	**A**	OH	OH	H	α	11.10 ± 0.43	10.85 ± 0.18	NT	NT
160c	**A**	OH	OH	H	β	7.18 ± 0.20	9.50 ± 0.16	12.76 ± 5.12	24.03 ± 17.14
161c	**A**	OH	OH	H	α	12.52 ± 0.54	64.51 ± 3.52	14.93 ± 9.24	25.37 ± 7.26
162a	**A**	OH	H	H	β	>100	>100	3.75 ± 0.01[d]	10.05 ± 0.01[d]
156[194]	**A**	OH	H	H	α	>100	>100	7.34 ± 11.82	NT

163a	**A**	H	OH	H	β	>100	>100	3.11 ± 2.58	>100
157[194]	**A**	H	OH	H	α	9.28 ± 0.04	11.20 ± 0.49	8.56 ± 9.00	NT
163b	**A**	H	OH	H	β	8.75 ± 0.49	95.77 ± 3.21	11.50 ± 5.66	NT
163c	**A**	H	OH	H	β	>100	>100	1.49 ± 0.51	1.24[d]
164c	**A**	H	OH	H	α	1.37 ± 0.14	>100	3.27 ± 0.09[d]	2.35 ± 1.11
165a	**A**	OH	OH	CH_2OH	β	9.59 ± 0.42	11.07 ± 0.47	3.23 ± 3.76	4.58 ± 2.78
165b	**A**	OH	OH	CH_2OH	β	11.76 ± 0.06	14.34 ± 0.16	6.78 ± 2.25	17.94 ± 10.33
165c	**A**	OH	OH	CH_2OH	β	9.45 ± 0.19	3.37 ± 0.06	4.66 ± 1.48	5.90 ± 2.58
166a	**B**	OH	OH	H	β	12.46 ± 0.52	37.17 ± 1.68	3.65 ± 2.83	NT
166b	**B**	OH	OH	H	β	7.57 ± 1.05	11.73 ± 0.78	2.60 ± 1.51	10.64 ± 20.83
166c	**B**	OH	OH	H	β	9.45 ± 0.19	3.37 ± 0.07	4.72 ± 1.48	9.56 ± 2.58
167a	**B**	OH	H	--	β	>100	>100	NT	NT
168a	**B**	OH	H	--	α	>100	>100	5.34 ± 4.76	NT
169a	**B**	H	OH	--	β	35.24 ± 1.76	>100	3.72[d]	10.05 ± 6.75[d]
170a	**B**	H	OH	--	α	>100	>100	4.96 ± 10.58	26.79 ± 58.24
171a	**C**	OH	OH	--	β	2.38 ± 0.06	>100	>100	NT

[a] Values represent mean ± standard deviation for at least two separate experiments performed in triplicate.

[b] Values represent mean ± standard deviation from dose response curves for at least two separate experiments performed in duplicate.

[c] All error values listed represent 95% confidence intervals throughout the manuscript except where indicated

[d] Error values listed as standard deviations

As shown in Table 6, analogues containing a cyclohexyl moiety in lieu of the sugar demonstrated a range of activities. While analogues containing an 8-methyl group (**172a**, **173a**, **158**) were inactive against breast cancer, those with an 8-methoxy group (**172b**, **173b**, **174b**) exhibited an IC_{50} value of ~10 μM, which is comparable to its noviosylated counterpart.[170]

Interestingly, the *gem*-dimethyl group is well tolerated in the case of the 8-methoxy coumarin (**172b**), but detrimental in the case of the 6-methoxy coumarin (**172c**). This finding suggests a mutually exclusive orientation between the *gem*-dimethyl group and substituents on the coumarin, which may preclude proper binding orientation.[193]

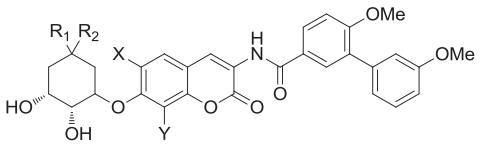

a: X = H, Y = CH_3
b: X = H, Y = OCH_3
c: X = OMe, Y = Me

Table 6. Anti-proliferative activities of cyclohexyl analogues.[193]

Compound	R^1	R^2	SKBr3 (IC_{50}, μM)	MCF-7 (IC_{50}, μM)	LNCaP-LN3 (IC_{50}, μM)	PC3-MM2 (IC_{50}, μM)
172a	CH_3	CH_3	>100[a]	>100[a]	1.24 ± 0.17[b,d]	2.49 ± 1.70[b]
172b	CH_3	CH_3	3.45 ± 1.73	1.56 ± 0.03	NT	NT
172c	CH_3	CH_3	>100	>100	NT	NT
173a	H	CH_3	>100	>100	1.14 ± 0.67	4.09 ± 1.63
173b	H	CH_3	6.38 ± 0.71	8.52 ± 0.36	NT	NT
173c	H	CH_3	>100	>100	NT	NT
158[194]	H	H	>100[a]	>100	1.58 ± 0.75	4.04 ± 0.38[d]
174b	H	H	7.44 ± 0.36	5.46 ± 0.36	NT	NT
174c	H	H	8.18 ± 0.79	10.13± 1.04	NT	NT

[a] Values represent mean ± standard deviation for at least two separate experiments performed in triplicate.

[b] Values represent mean ± standard deviation from dose response curves for at least two separate experiments performed in duplicate.

Overall, this library containing sugar surrogates and cyclohexyl groups confirmed the 3'-hydroxy as the most important functional group. Moreover, the 4'-methoxy, 5'-*gem*-dimethyl

and anomeric oxygen found in noviose were identified as dispensable moieties. Several analogues exhibited low micromolar anti-proliferative activity against SKBr3 cells, which makes them ~500-fold more active than novobiocin.[193] Moreover, subsequent studies have been proposed to examine the role that stereochemistry plays since several of the cyclohexyl-containing analogues contain an asymmetric center.

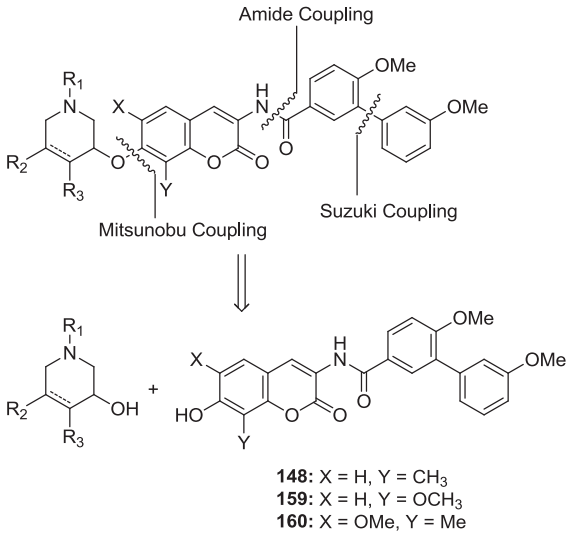

Scheme 47. Retrosynthesis of azasugar-containing biaryl analogues.[193]

3. Design and synthesis of azasugar analogues

After evaluation of the initial library, it was proposed that other six-membered heteroatom-containing ring systems may serve as replacements for noviose. N-heterocycles are found in a wide variety of biologically active compounds, imparting solubility to otherwise insoluble aglycons. Several heterocycles were designed to probe hydrogen-bonding interactions with the binding pocket as well as to improve solubility.[193]

The analogues were assembled similarly to those described previously, in modular fashion, allowing sequential coupling of various sugar surrogates and the biaryl side chain. As shown in the retrosynthetic analysis depicted in Scheme 47, following hydrogenolysis, the biaryl

acid chloride was coupled with coumarins **147**, **128a**, and **128g**. Following solvolysis, coumarin phenols **148**, **159** and **160** were etherified using Mitsunobu conditions.[193]

Through application of Mitsunobu conditions, protected piperidines were coupled to the coumarin phenols. After subsequent deprotections and appropriate functionalization, where applicable, the 1,3-azasugar-containing compounds shown in Figure 53 were prepared by a colleague.[193]

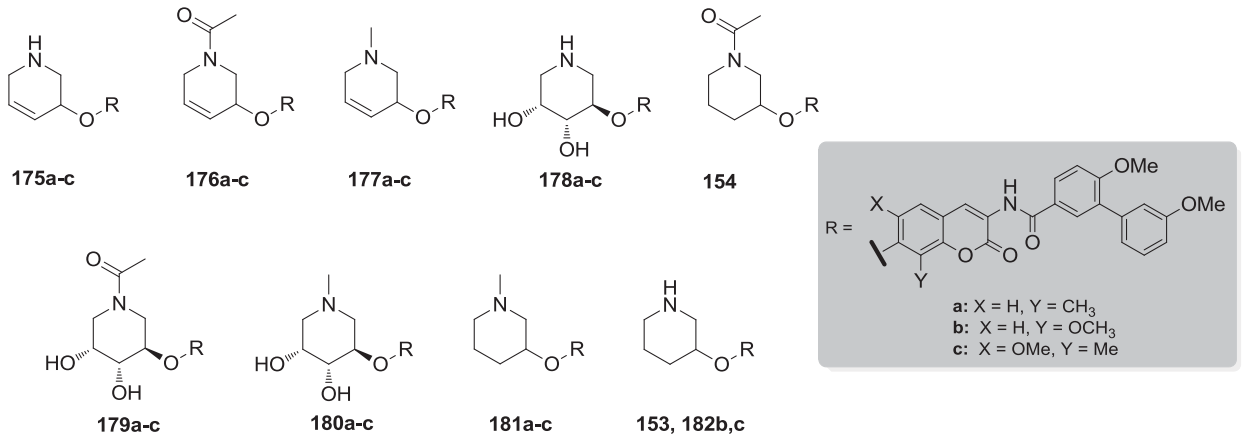

Figure 53. 1,3-azasugar-containing analogues prepared.[193]

In addition, compounds lacking the diol functionality and containing a transposed nitrogen within the heterocycle were selected for investigation. A co-worker coupled, then deprotected 1,4-azasugars as described previously to yield the compounds shown in Figure 54.[193]

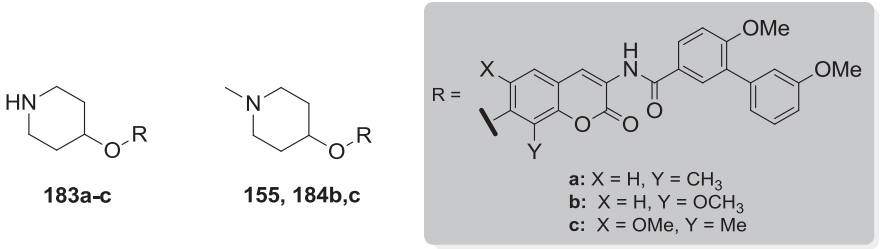

Figure 54. 1,4-azasugar-containing analogues prepared.[193]

4. Biological evaluation of azasugar analogues

Upon construction of the azasugar-containing analogues, they were evaluated for anti-proliferative activity against two breast and two prostate cancer cell lines. As shown in Table 7, the activity against breast cancer cells exhibited by the majority of these secondary and tertiary amines varied between 1-3 μM, making them ~700-fold more active than novobiocin. Although dihydroxylation of the piperidine ring is well-tolerated when appended to the 8-methyl scaffold (**178a**), this is not the case for the other two scaffolds (**178b** and **178c**). These data suggest that dihydroxylation of the piperidine ring is not essential for anti-proliferative activity. Inclusion of unsaturation within the piperidine ring is also well tolerated (scaffold **A** vs. **C** and **D**, Table 7) while methylation of the amine within this unsaturated ring decreases activity (**175** vs. **177**). It was observed that acetylation of the amine functionality (**176a**, **154**, **179a**) severely decreased solubility in organic solvents, and produced inactive compounds. Although insolubility can be overcome through dihydroxylation of the piperidine ring (**179a**), the resulting compound is ~5-fold less active than secondary or tertiary amines. There is no significant effect when the nitrogen is transposed within the piperidine ring, as all of the analogues exhibited activity between ~1-3 μM. In addition, secondary amines exhibited comparable activity to methylated tertiary amines (**181** vs. **183**, **153**/**182** vs. **155**/**184**). Overall, these azasugar analogues consistently exhibited low micromolar anti-proliferative activity, representing an improved sugar mimic.[193] Subsequent studies that probe the influence of fixed stereochemistry on the activity of these piperidine-containing compounds have been proposed.

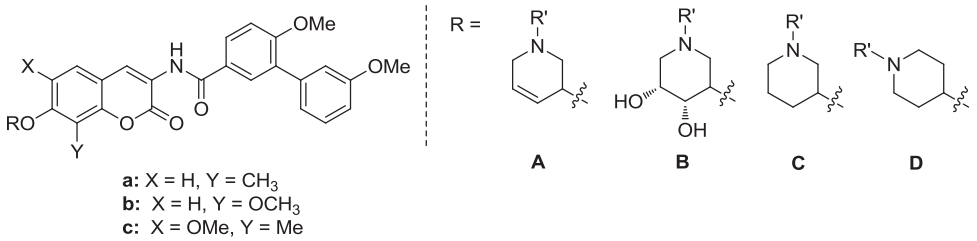

a: X = H, Y = CH_3
b: X = H, Y = OCH_3
c: X = OMe, Y = Me

Table 7. Anti-proliferative activities of azasugar analogues.[193]

Compound	R	R'	SKBr3 (IC_{50}, μM)	MCF-7 (IC_{50}, μM)	LNCaP-LN3 (IC_{50}, μM)	PC3-MM2 (IC_{50}, μM)
175a	**A**	H	1.61 ± 0.05[a]	1.73[a]	4.27 ± 0.05[b,d]	4.40 ± 0.06[b,d]
175b	**A**	H	3.07 ± 0.78	1.43 ± 0.37	6.45 ± 2.70[d]	4.88 ± 2.20
175c	**A**	H	1.21 ± 0.07	1.68 ± 0.04	5.40 ± 9.99	3.57 ± 0.71[d]
176a	**A**	Ac	>50	>50	0.90 ± 0.59	3.73 ± 0.67
177a	**A**	CH_3	2.92 ± 1.33	5.29 ± 0.23	1.22[d]	1.73 ± 1.80
177b	**A**	CH_3	3.42 ± 0.45	1.65 ± 0.28	0.36 ± 0.14	0.98 ± 0.40
177c	**A**	CH_3	1.96 ± 0.48	5.27 ± 0.22	4.49 ± 0.17[d]	3.87 ± 0.03[d]
178a	**B**	H	2.91 ± 0.90	2.07 ± 0.86	4.90 ± 9.16	6.33 ± 4.12
178b	**B**	H	8.98 ± 0.44	10.17 ± 0.02	12.19 ± 6.30	14.43 ± 7.39
178c	**B**	H	3.65 ± 0.22	3.34	9.45 ± 5.90	6.84 ± 2.80
154[194]	**C**	Ac	>50	>50	1.23 ± 0.67	3.42 ± 1.24
179a	**B**	Ac	10.79 ± 0.08	9.18 ± 0.60	0.71 ± 0.54	2.22 ± 1.04
180a	**B**	CH_3	3.92 ± 0.32	1.85 ± 0.02	0.59 ± 0.54	2.99 ± 1.27
180b	**B**	CH_3	6.64 ± 0.54	11.02 ± 1.12	1.50 ± 0.62	3.52 ± 1.43
180c	**B**	CH_3	2.77 ± 0.90	2.01 ± 0.46	4.69 ± 0.57[d]	4.17 ± 0.16[d]
181a	**C**	H	1.16 ± 0.16	1.63 ± 0.28	3.02 ± 0.97[d]	2.57 ± 1.13
181b	**C**	H	2.61 ± 0.37	3.29 ± 0.42	12.72 ± 3.25	10.43 ± 2.15
181c	**C**	H	2.27 ± 0.61	2.90 ± 0.67	3.66[d]	2.59 ± 13.91
153[194]	**D**	H	1.19 ± 0.06	1.47 ± 0.02	3.38 ± 1.25	4.12 ± 1.29

182b	**D**	H	1.79	3.23 ± 0.20	10.85 ± 5.92	8.47 ± 4.28
182c	**D**	H	1.20 ± 0.08	2.82 ± 1.10	5.27 ± 22.18	4.02 ± 2.13
183a	**C**	CH_3	2.06 ± 0.57	5.04 ± 0.02	1.22 ± 0.17[d]	4.23 ± 1.68
183b	**C**	CH_3	1.40 ± 0.14	1.38 ± 0.14	1.78 ± 0.80	2.16 ± 1.28
183c	**C**	CH_3	1.49 ± 0.06	1.41 ± 0.13	10.48 ± 5.46[d]	6.86 ± 2.92[d]
155[194]	**D**	CH_3	1.34 ± 0.18	1.51 ± 0.24	4.12 ± 0.16[d]	3.13 ± 0.67
184b	**D**	CH_3	0.97 ± 0.07	1.39 ± 0.28	4.75 ± 2.03	3.71 ± 1.27
184c	**D**	CH_3	1.19 ± 0.17	1.79 ± 0.09	4.17 ± 0.15[d]	2.84 ± 1.88

[a] Values represent mean ± standard deviation for at least two separate experiments performed in triplicate.

[b] Values represent mean ± standard deviation from dose response curves for at least two separate experiments performed in duplicate.

5. Design and synthesis of novobiocin analogues with acyclic sugar replacements

The promising results obtained when azasugars were appended to these scaffolds encouraged the synthesis of acyclic nitrogen-containing replacements. To probe the importance of a constrained ring system, a library of ring-opened, amine-containing sugar surrogates was designed. A series of heteroatom-containing aliphatic chains were synthesized to impart flexibility and explore the potential of additional interactions with the binding pocket.[193]

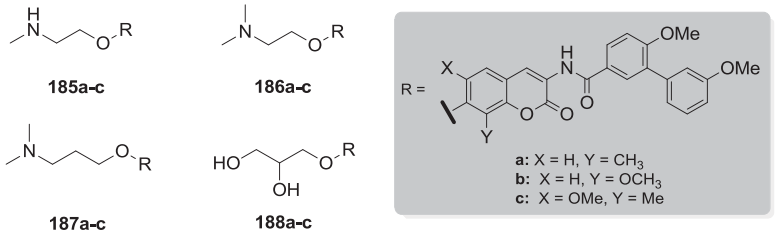

Figure 55. Alkyl sugar analogues prepared.[193]

Aliphatic amines, either commercially available or prepared over a modest number of steps, were appended to the biaryl coumarin cores through standard Mitsunobu coupling to yield compounds **185**–**188**. These compounds, prepared by a colleague, are depicted in Figure 55.[193]

In addition to the aliphatic amine analogues synthesized, several simplified non-sugar molecules were appended in lieu of the noviose sugar. These non-sugars include simplified functionalities based upon **128a**, a recently described inhibitor of the Hsp90 *C*-terminus.[259] Substitutions were selected to probe hydrogen-bonding interactions and pocket dimensions, with the aim of increasing favorable interactions with residues within the binding pocket. Carbamates with variable substitution were installed through Lewis acid catalysis. A phosphate ester (**192**) was introduced through an esterification reaction to increase the hydrophilicity of the inhibitor and finally, methyl and toluene sulfonic esters were incorporated using the corresponding sulfonic chlorides to explore potential interactions within the pocket, like those reported by Renoir and co-workers (Scheme 48).[105,193]

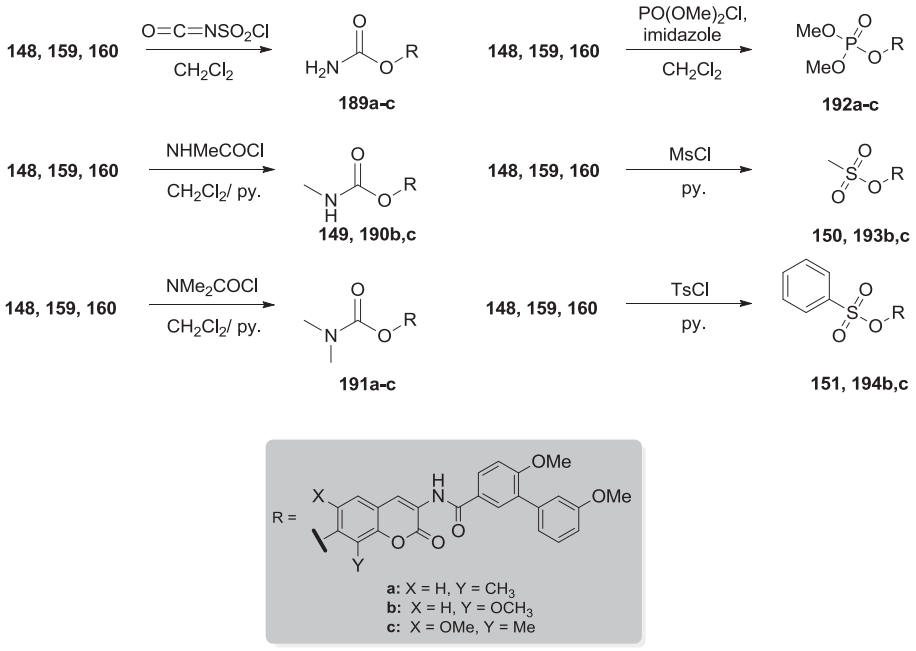

Scheme 48. Synthesis of non-sugar biaryl analogues.[193]

6. Biological evaluation of novobiocin analogues with acyclic sugar replacements

Upon construction of these alkyl and non-sugar compounds, they were evaluated for anti-proliferative activity against various cancer cell lines. The anti-proliferative data are summarized in Table 8 and Table 9. All of the tertiary amine analogues demonstrated notable anti-proliferative activity of ~1 μM, while the secondary amine analogues maintained activity of ~3–5 μM against both breast cancer cell lines. The tertiary amine analogues homologated by two methylene groups (**186a–c**) exhibited activity of 1–3 μM, which is comparable to the piperidine analogues. Moreover, homologation by three methylene groups (**187a–c**) resulted in compounds that manifested anti-proliferative activity in the mid-nanomolar range, a finding that is consistent with the piperidine ring analogues. In contrast, the diol-containing analogues, when appended to the 8-methyl (**188a**) or 8-methoxy (**188b**) coumarin scaffolds were inactive, but resulted in modest activity when appended to the 6-methoxy coumarin (**188c**). Furthermore, the aliphatic amine and corresponding dihydroxylated analogues manifested modest activities against the prostate cancer cell lines.[193] As discussed previously, plans to prepare promising analogues as single stereoisomers will reveal the role that stereochemistry plays in dictating the activity of these compounds.

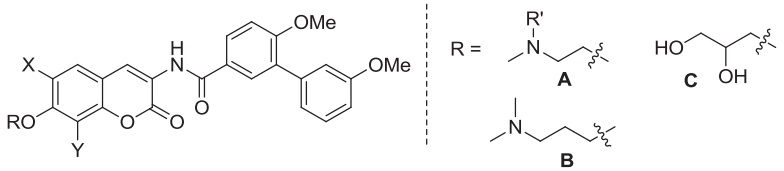

a: X = H, Y = CH_3
b: X = H, Y = OCH_3
c: X = OMe, Y = Me

Table 8. Anti-proliferative activities of analogues with acyclic sugar replacements.[193]

Compound	R	R'	SKBr3 (IC_{50}, μM)	MCF-7 (IC_{50}, μM)	LNCaP-LN3 (IC_{50}, μM)	PC3-MM2 (IC_{50}, μM)

185a	A	H	5.36 ± 0.08[a]	9.80 ± 0.11[a]	>100[b]	14.01 ± 0.28[b,d]
185b	A	H	3.60 ± 0.28	4.32 ± 0.32	15.24 ± 7.96	9.12 ± 5.92
185c	A	H	3.15 ± 0.54	6.23 ± 0.14	>100	11.77 ± 5.94
186a	A	CH_3	1.02 ± 0.13	1.46 ± 0.08	6.65 ± 12.43	4.17 ± 19.64
186b	A	CH_3	1.77 ± 0.12	3.08 ± 0.08	5.22 ± 3.25	6.20 ± 2.22
186c	A	CH_3	1.42 ± 0.21	1.29 ± 0.17	6.28 ± 2.22[d]	4.87 ± 2.91
187a	B	--	0.60 ± 0.01	0.50 ± 0.03	37.51 ± 54.24	12.85 ± 11.42
187b	B	--	0.91 ± 0.14	1.53 ± 0.14	8.03 ± 7.93	4.08 ± 1.83
187c	B	--	0.49 ± 0.20	0.70 ± 0.15	4.71 ± 0.21[d]	5.40 ± 3.15
188a	C	--	>50	>50	NT	0.19 ± 0.33
188b	C	--	>50	>50	0.96 ± 1.20	1.66 ± 6.05
188c	C	--	>50	>50	NT	NT

[a] Values represent mean ± standard deviation for at least two separate experiments performed in triplicate.

[b] Values represent mean ± standard deviation from dose response curves for at least two separate experiments performed in duplicate.

The anti-proliferative data for the non-sugar analogues revealed several interesting trends. The free phenol of each scaffold was nearly equal in activity to its noviosylated counterpart. Moreover, the acetylated phenols, in the case of the 8-methyl (**147**) and 6-methoxy coumarins (**128a**), displayed activities of ~1 μM against breast cancer cells. Similarly, the carbamate and methylated carbamate were well tolerated when appended to 8-methyl and 6-methoxy coumarins, resulting in low micromolar analogues. Addition of another methyl group to the carbamate severely compromised activity. The methyl sulfonic ester was only tolerated when appended to the 8-methyl scaffold (**150**), while the toluene sulfonic ester was not tolerated by any analogue. Likewise, addition of the phosphate ester decreased activity of the analogues.

Overall, it was concluded that hydrogen bonding and limited hydrophobic bulk govern optimal binding.[193]

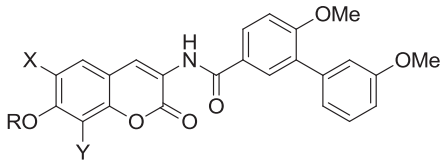

a: X = H, Y = CH_3
b: X = H, Y = OCH_3
c: X = OMe, Y = Me

Table 9. Anti-proliferative activity of non-sugar analogues.[193]

Compound	R	SKBr3 (IC_{50}, μM)	MCF-7 (IC_{50}, μM)	LNCaP-LN3 (IC_{50}, μM)	PC3-MM2 (IC_{50}, μM)
148[194]	H	8.88 ± 0.48[a]	6.93 ± 0.48[a]	3.21 ± 1.78[b]	5.36 ± 2.71[b]
147[194]	$COCH_3$	0.98 ± 0.02	1.40	1.50 ± 1.00	2.85 ± 1.66
59[102]	Noviose	7.50 ± 0.80	18.70 ± 1.44	NT	NT
150[194]	Ms	7.33 ± 0.96	8.85 ± 0.88	19.96 ± 42.67	>100
151[194]	Ts	> 100	> 100	0.58 ± 1.34	>100
189a	$CONH_2$	3.02 ± 0.56	1.16 ± 0.08	2.61 ± 1.09	6.37 ± 4.31
149[194]	CONHMe	2.40 ± 0.16	1.72 ± 0.16	3.75 ± 0.76	5.22 ± 2.16
191a	$CONMe_2$	39.85 ± 0.48	74.35 ± 3.92	5.40 ± 6.58	>100
192a	$PO(OMe)_2$	> 100	> 100	3.65 ± 5.73	>100
159	H	3.23 ± 1.20	11.70 ± 1.92	15.79 ± 32.60	11.23 ± 30.70
128a	$COCH_3$	5.72 ± 0.02	1.50 ± 0.24	1.05 ± 0.59	1.69 ± 2.05
26a[170]	Noviose	58.80 ± 1.04	> 100	26.57 ± 67.44	>100
193b	Ms	> 100	> 100	>100	NT
194b	Ts	> 100	> 100	NT	>100
189b	$CONH_2$	6.83 ± 0.24	6.29 ± 0.88	3.55 ± 3.44	2.62 ± 2.04
190b	CONHMe	1.53 ± 0.16	7.78 ± 1.68	4.77 ± 8.37	3.13 ± 2.34
191b	$CONMe_2$	6.17 ± 1.68	34.4 ± 7.20	12.75 ± 0.32[d]	4.04 ± 16.68

192b	$PO(OMe)_2$	26.48 ± 0.80	24.22 ± 2.40	1.36 ± 2.80	31.32 ± 54.87
160	H	> 100	5.32 ± 0.08	6.18 ± 7.43	>100
128g	$COCH_3$	20.50 ± 1.28	8.62 ± 2.00	14.62 ± 23.63	19.33 ± 50.90
26g[170]	Noviose	13.90 ± 0.96	9.00 ± 4.32	0.11 ± 0.02	1.44 ± 0.32
193c	Ms	>100	>100	0.87 ± 1.32	NT
194c	Ts	>100	>100	0.11 ± 4.68	NT
189c	$CONH_2$	76.83 ± 1.84	5.56 ± 0.24	4.83 ± 3.87	>100
190c	CONHMe	>100	6.54 ± 1.84	2.37 ± 1.44	1.68 ± 1.89
191c	$CONMe_2$	>100	>100	15.73 ± 14.09	11.57 ± 10.04
192c	$PO(OMe)_2$	18.07 ± 2.88	>100	6.58 ± 4.14	11.46 ± 6.54

[a] Values represent mean ± standard deviation for at least two separate experiments performed in triplicate.

[b] Values represent mean ± standard deviation from dose response curves for at least two separate experiments performed in duplicate.

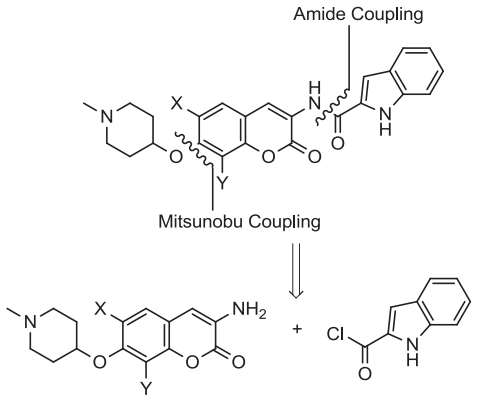

Scheme 49. Retrosynthesis of azasugar indole novobiocin analogues.[193]

7. Design and synthesis of optimized scaffolds using most promising surrogates

Based on the biological evaluation discussed thus far, we identified the *N*-methyl-4-hydroxy-piperidine and 3-(dimethylamino)propan-1-ol as optimal noviose replacements. Therefore, these surrogates were appended to three previously identified and optimized coumarin scaffolds, containing either the 2-indole or prenylated benzamide side chain in lieu of the biaryl

system.[102,195] As detailed earlier, the analogues were assembled in a modular fashion, allowing sequential coupling of sugar mimics and the indole acid chloride or prenylated acid chloride with the desired scaffold (Scheme 49). Unlike previously discussed scaffolds, the Mitsunobu ether coupling was performed prior to amide coupling due to solubility issues arising from the indole-containing free phenol. These optimized analogues, shown in Figure 56, were synthesized by a co-worker.[193]

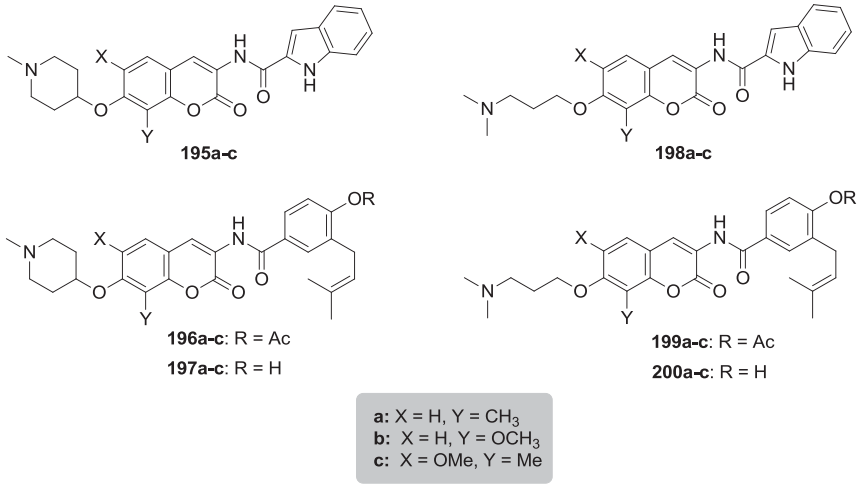

Figure 56. Optimized compounds prepared.[193]

8. Biological evaluation of optimized scaffolds

As described previously, these compounds were evaluated for their anti-proliferative activities against a panel of breast and prostate cancer cell lines (Table 10). The piperidine-containing analogues with an indole side chain (**195a–c**) exhibited increased anti-proliferative activity when attached to the 8-methyl and 6-methoxy coumarin (**195a** and **195c**). **195c** was notably 10-fold more active against SKBr3 cells when compared to its biaryl counterpart **184c**. In contrast, attachment of this sugar surrogate to the 8-methoxy coumarin (**195b**) compromised its activity versus the biaryl-containing analogue **184b**. In the case of the prenylated benzamide side chain (**196a–c** and **197a–c**), attachment of the azasugar increased activity against both cell

lines, with the 6-methoxy coumarin manifesting superior activity (**196c** and **196c**). In addition, the intermediate acetylated phenols **196a–c** demonstrated comparable activity to the hydrolyzed phenol products **197a–c**. Based on the results obtained with the biaryl containing analogues, it was proposed that appendage of the aliphatic amine to the coumarins with an indole side chain would result in increased activity. However, the anti-proliferative activity of these indole analogues (**198a–c**) was maintained or slightly decreased in nearly every case. When these alkyl sugars were attached to the coumarins containing a prenylated benzamide side chain, the compounds manifested anti-proliferative activity in the mid-nanomolar range against SKBr3 cells. Moreover, compounds built upon the 6-methoxy coumarin scaffold (**199c** and **200c**) exhibited the best activity against both cell lines.[193] Future plans involving these optimized scaffolds will focus on examining the role that stereochemistry plays in dictating their activity.

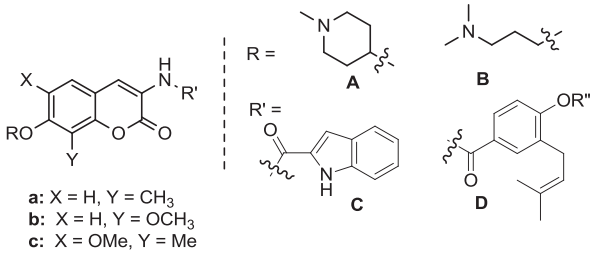

Table 10. Anti-proliferative activity of optimized analogues.[193]

Compound	R	R'	R"	SKBr3 (IC_{50}, μM)	MCF-7 (IC_{50}, μM)	LNCAP-LN3 (IC_{50}, μM)	PC3-MM2 (IC_{50}, μM)
195a	**A**	**C**	--	0.48 ± 0.09[a]	0.57 ± 0.03[a]	11.83 ± 0.54[b]	11.40 ± 5.25[b]
195b	**A**	**C**	--	2.58 ± 0.28	1.86 ± 0.08	12.64 ± 0.32[d]	7.93 ± 4.18
195c	**A**	**C**	--	0.11 ± 0.01	0.52 ± 0.04	1.47 ± 0.53	0.87 ± 0.46
196a	**A**	**D**	Ac	0.58 ± 0.04	1.18 ± 0.16	NT	2.12 ± 3.32
196b	**A**	**D**	Ac	1.07 ± 0.14	1.64 ± 0.24	NT	3.98 ± 0.06[d]
196c	**A**	**D**	Ac	0.42 ± 0.01	0.58 ± 0.02	NT	1.41 ± 0.04[d]
197a	**A**	**D**	H	0.76 ± 0.14	1.09 ± 0.08	NT	1.37 ± 1.42

197b	**A**	**D**	H	0.92 ± 0.01	1.54 ± 0.21	NT	3.53 ± 0.01[d]
197c	**A**	**D**	H	0.42 ± 0.01	0.54 ± 0.02	NT	2.26 ± 1.43
198a	**B**	**C**	--	1.13 ± 0.01	5.23 ± 0.22	NT	13.69 ± 0.18[d]
198b	**B**	**C**	--	1.50 ± 0.13	1.41 ± 0.09	4.71 ± 1.23[d]	8.95 ± 6.11
198c	**B**	**C**	--	0.57 ± 0.09	0.56	NT	2.58 ± 4.47
199a	**B**	**D**	Ac	0.46 ± 0.15	1.18 ± 0.02	NT	1.42 ± 0.05[d]
199b	**B**	**D**	Ac	0.78 ± 0.17	2.14 ± 0.22	NT	4.59 ± 4.23
199c	**B**	**D**	Ac	0.36 ± 0.03	0.70 ± 0.03	NT	1.46 ± 0.03[d]
200a	**B**	**D**	H	0.44 ± 0.02	1.35 ± 0.30	NT	1.81 ± 1.22
200b	**B**	**D**	H	0.77 ± 0.08	3.26 ± 0.26	NT	9.24 ± 17.79
200c	**B**	**D**	H	0.39 ± 0.06	0.80 ± 0.07	NT	1.38 ± 0.02[d]

[a] Values represent mean ± standard deviation for at least two separate experiments performed in triplicate.

[b] Values represent mean ± standard deviation from dose response curves for at least two separate experiments performed in duplicate.

To confirm that the anti-proliferative activities exhibited by the optimized sugar analogues result from Hsp90 inhibition, analogues **197c** and **199c** were evaluated by Western blot analyses (Figure 57). It was essential that these optimized derivatives demonstrate selective Hsp90-dependent client protein degradation, versus a loading control, to confirm the compounds reported herein also manifest Hsp90 inhibition. Figure 57 shows that in MCF-7 cells, the Hsp90-dependent client proteins Akt, Raf-1, and Her2 were degraded in a concentration-dependent manner upon treatment with the compounds. Hsp90 client protein degradation occurred at concentrations that paralleled the observed anti-proliferative IC_{50} values of 0.54 ± 0.03 μM, for **197c** and 0.70 ± 0.04 μM for **199c** confirming that Hsp90-dependent client protein degradation is causative for inhibition of cell growth. Furthermore, Hsp90 protein levels remained constant at

all concentrations tested, which is consistent with *C*-terminal Hsp90 inhibition. Since the non-Hsp90-dependent protein, actin, was not affected by these analogues, it was concluded that selective degradation of Hsp90-dependent proteins occurred.[193]

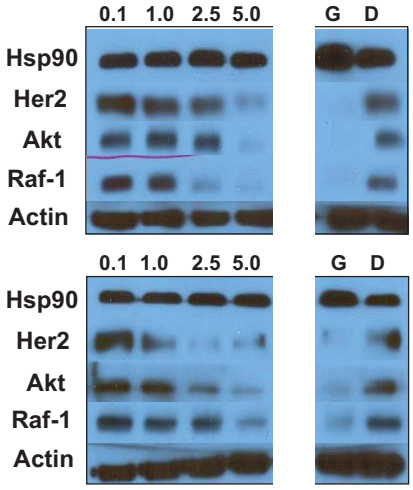

Figure 57. Western blot analyses of Hsp90 client protein degradation assays against MCF-7 cells following treatment with **197c** and **199c**. Concentrations (in μM) of **197c** (top) and **199c** (bottom) are indicated above each lane. G (geldanamycin, 500 nM) and D (DMSO) were respectively employed as positive and negative controls.[193]

C. Subsequent biological testing

Due to the promise of several compounds from this study of optimized scaffolds, subsequent studies were designed to test their promise against other cancer cell lines. It was proposed that these rationally designed analogues may demonstrate efficacy against tumors that were not examined in the previously described studies. Moreover, efforts were undertaken to better understand the mechanism through which these compounds act.

1. Biological evaluation against melanoma and HNSCC

Finally, several analogues from each of the libraries were selected for testing against a panel of melanoma and head and neck squamous cell carcinoma cell lines (Table 11). In preliminary studies, *C*-terminal Hsp90 inhibitors have demonstrated modest activity against melanoma cells and have shown promise in treating head and neck cancers as well. Unpublished *in vivo* data produced by the Cohen lab at the KU Medical Center has demonstrated tumor regression upon sustained treatment with a *C*-terminal Hsp90 inhibitor previously synthesized.[170] Analogues were selected that exhibited diverse structural features to probe the efficacy of these analogues against these cancers. B16F10 (murine melanoma), SKMEL28 (human melanoma), MDA1986 (human head and neck squamous cell carcinoma (HNSCC)), and JMAR (human oral squamous cell carcinoma) were selected for this panel of testing. The majority of the analogues tested manifested mid to low micromolar activity against these cell lines. While some of the compounds exhibited better activity against melanoma than head and neck cancers (**184b**), others were potent in a specific melanoma (**181b**) or a specific head and neck (**162a**) cell line. The low micromolar activity of **195c** and **198c** against all of the cell lines warrants further investigation.[193]

Table 11. Anti-proliferative activity of selected analogues against melanoma and HNSCC.[193]

Compound	B16F10 (IC_{50}, μM)	SKMEL28 (IC_{50}, μM)	MDA1986 (IC_{50}, μM)	JMAR (IC_{50}, μM)
159	5.77 ± 0.96[a]	12.40 ± 0.64[a]	6.70 ± 1.20[a]	24.60 ± 1.92[a]
147[194]	2.30 ± 0.32	2.14 ± 0.08	1.67 ± 0.16	12.60 ± 0.40
160a	37.50 ± 6.56	14.90 ± 2.88	13.40 ± 4.24	2.79 ± 0.64
161a	8.56 ± 2.16	15.80 ± 0.48	3.70 ± 0.64	6.14 ± 1.28

162a	1.01 ± 0.48	1.47 ± 0.24	0.81 ± 0.40	16.10 ± 2.16
156[194]	10.40 ± 1.20	19.60 ± 2.48	18.80 ± 3.68	3.60 ± 0.40
165a	9.60 ± 1.12	10.65 ± 0.40	5.70 ± 0.56	5.80 ± 1.04
166a	4.55 ± 1.20	5.74 ± 2.08	1.94 ± 0.40	12.64 ± 1.28
166b	1.30 ± 0.16	6.41 ± 0.56	5.73 ± 0.96	2.71 ± 0.32
167a	42.70 ± 3.36	18.40 ± 2.96	21.40 ± 3.12	14.90 ± 3.68
169a	12.70 ± 1.44	21.40 ± 3.28	6.90 ± 2.08	24.10 ± 3.28
170a	9.37 ± 1.04	12.40 ± 2.48	18.80 ± 3.76	6.19 ± 2.48
171a	>50	18.50 ± 5.76	22.90 ± 4.96	7.40 ± 1.68
172a	15.90 ± 2.16	3.47 ± 1.20	18.80 ± 0.64	8.50 ± 1.68
173a	2.50 ± 0.48	11.41 ± 1.28	6.74 ± 2.08	2.73 ± 0.32
158[194]	14.10 ± 2.08	2.94 ± 1.20	17.90 ± 1.44	13.90 ± 2.00
175a	2.94 ± 0.08	5.41 ± 0.08	6.54 ± 0.56	3.40 ± 0.16
175b	3.41 ± 0.32	5.49 ± 1.12	5.97 ± 0.40	6.71 ± 0.24
175c	2.86 ± 0.24	5.41 ± 0.16	5.90 ± 0.40	11.60 ± 0.32
176c	21.40 ± 1.28	27.60 ± 1.20	25.10 ± 2.08	35.10 ± 1.20
177a	6.40 ± 1.92	10.79 ± 0.64	7.70 ± 0.56	11.40 ± 1.20
177b	6.47 ± 2.80	1.48 ± 0.48	2.36 ± 0.08	1.94 ± 0.16
177c	6.14 ± 0.64	31.50 ± 1.84	16.40 ± 1.68	18.40 ± 2.56
178a	2.80 ± 0.40	6.14 ± 1.28	5.60 ± 1.04	5.89 ± 0.48
178b	11.75 ± 0.40	11.40 ± 2.56	21.70 ± 1.12	11.60 ± 1.92
178c	5.04 ± 0.32	13.80 ± 2.56	13.80 ± 3.44	11.50 ± 0.72
154[194]	12.40 ± 2.00	20.9 ± 2.56	22.40 ± 1.36	15.14 ± 1.84
179c	23.90 ± 2.88	29.40 ± 3.36	36.40 ± 1.20	32.80 ± 3.36
179b	6.58 ± 0.48	5.90 ± 1.68	5.90 ± 0.48	6.70 ± 0.24
180c	2.81 ± 0.32	5.73 ± 0.32	12.80 ± 1.28	24.50 ± 0.72
181a	1.90 ± 0.24	2.79 ± 0.96	23.60 ± 2.88	>50

181b	0.64 ± 0.08	14.67 ± 0.40	12.80 ± 1.92	12.70 ± 1.44
181c	1.84 ± 0.08	7.19 ± 0.24	6.40 ± 0.96	5.70 ± 0.32
153[194]	2.76 ± 0.32	5.19 ± 0.16	2.74 ± 0.08	5.91 ± 0.40
182b	2.14 ± 0.08	16.45 ± 1.36	10.90 ± 0.64	12.60 ± 0.32
182c	1.84 ± 0.16	5.75 ± 0.24	14.60 ± 1.20	10.90 ± 0.48
183a	2.60 ± 0.32	6.14 ± 0.56	4.50 ± 0.08	12.60 ± 0.32
183b	1.51 ± 0.24	7.14 ± 0.40	11.40 ± 2.56	7.50 ± 0.64
183c	2.67 ± 0.32	5.86 ± 1.20	13.20 ± 0.72	19.10 ± 2.56
184b	0.41 ± 0.08	6.14 ± 0.32	13.10 ± 1.68	13.10 ± 0.64
184c	36.73 ± 0.64	3.74 ± 0.24	1.54 ± 0.08	1.84 ± 0.08
185a	37.40 ± 2.16	25.60 ± 2.96	21.90 ± 2.56	35.10 ± 2.16
186a	15.70 ± 4.56	14.70 ± 1.92	17.50 ± 3.28	18.40 ± 2.00
195c	1.19 ± 0.32	1.47 ± 0.08	1.42 ± 0.16	1.24 ± 0.24
198c	2.03 ± 0.08	1.35 ± 0.08	1.81 ± 0.32	2.65 ± 0.24

[a] Values represent mean ± standard deviation for at least two separate experiments performed in triplicate.

2. NCI 60 cell line screen of most promising compounds

Results from these initial studies led to our interest in submitting these compounds to more thorough analyses, involving cancer cell lines not previously examined. This goal was accomplished through submitting **147**, **195a**, and **195b** to the NCI 60 human tumor cell line screen. Testing of these compounds was reported against leukemia, non-small cell lung, colon, CNS, melanoma, ovarian, renal, prostate, and breast cancers.

147 was shown to demonstrate broad efficacy against these cell lines, with values consistently in the nanomolar to low micromolar range (Figure 58). This compound was most potent, with some high-nanomolar GI_{50} values towards the inhibition of leukemia and colon

cancer cells. The most remarkable activity this compound exhibited was a mid-nanomolar value against MDA-MB-435 melanoma cancer cells. These melanoma cells were thought to be metastatic human breast cancer cells until recent advances in gene expression analysis proved otherwise.

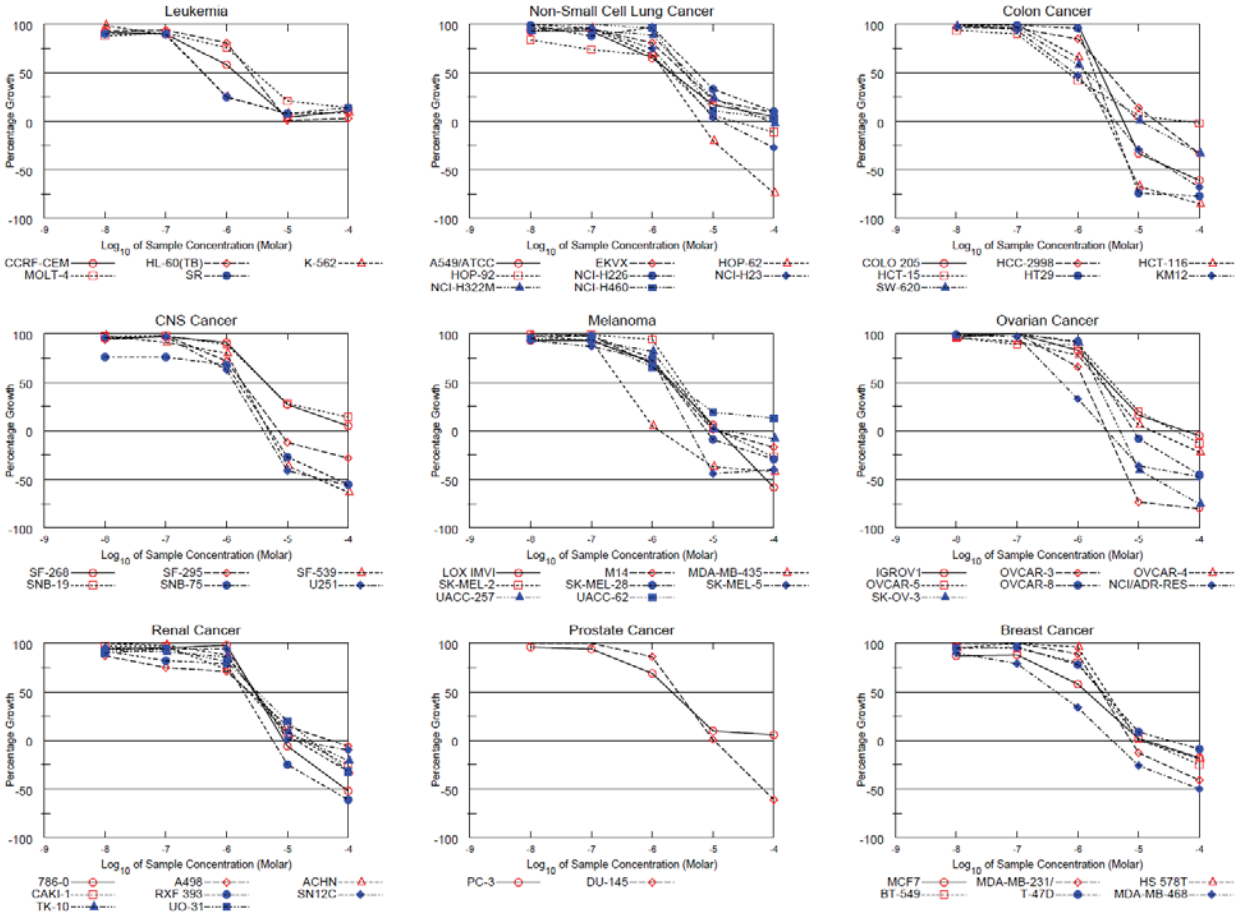

Figure 58. Results of testing **147** against NCI 60 human tumor cell line screen.

When the results from the screen of analogue **195a** were examined, some trends become apparent (Figure 59). Firstly, while this compound exhibited consistent GI_{50} values in the low micromolar range for all cancer cell lines tested, it was significantly more active against leukemia than other cancers. Notably, this compound exhibited mid- to low-nanomolar activity against the CCRF-CEM (human acute T-cell lymphoblastic leukemia cells), K-562 (erythroleukamia, the first human immortalized myelogenous leukemia line) and SR (acute

lymphoblastic leukemia cells) leukemia cancer cell lines. Due to its consistent efficacy, this compound warrants further study in the area of leukemia.

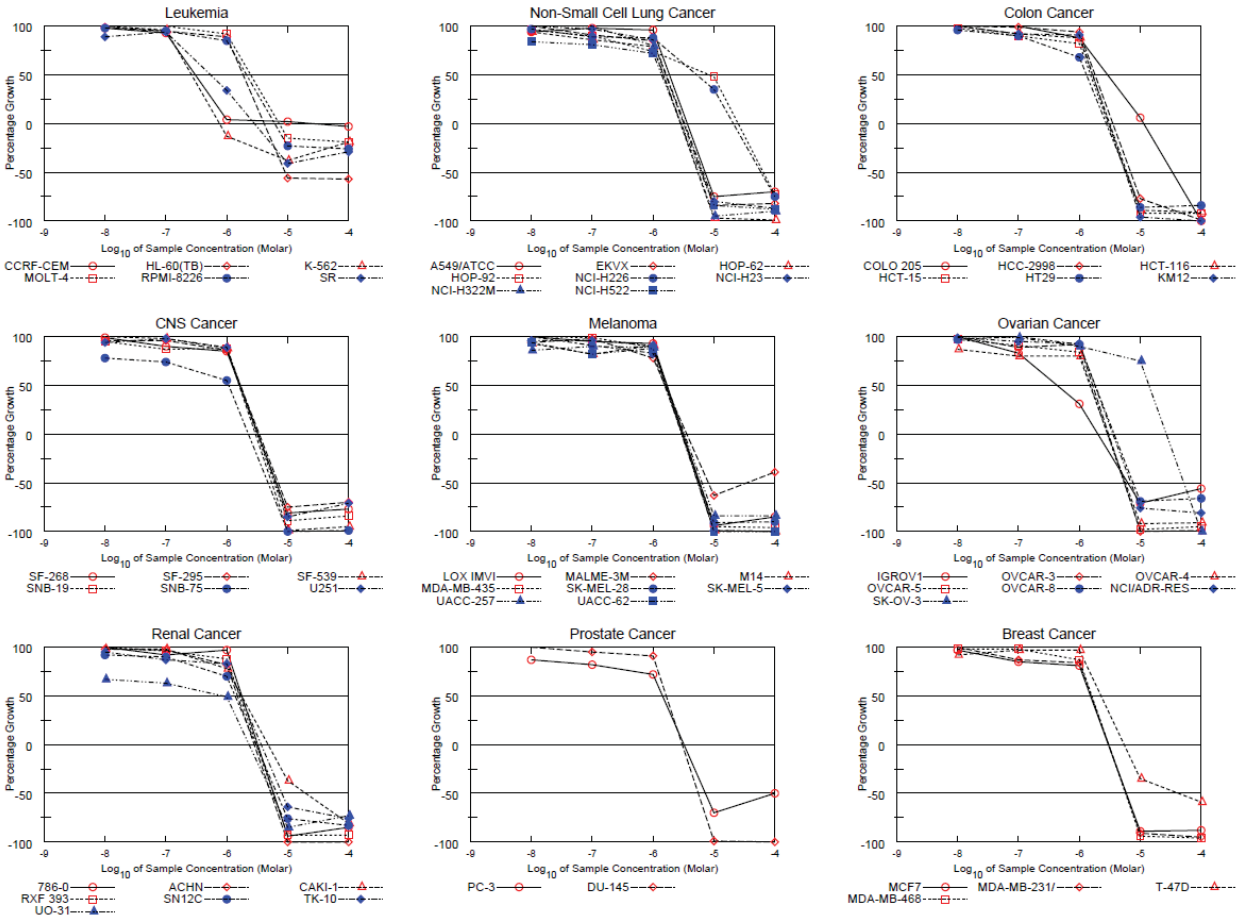

Figure 59. Results of testing **195a** against NCI 60 human tumor cell line screen.

Finally, compound **195b**, like its predecessors, exhibited consistently remarkable potency against several of the cancer cell lines tested (Figure 60). Notably, **195b** manifested mid-nanomolar GI_{50} values against several leukemia, colon, melanoma, and ovarian cancer cell lines. Although this compound demonstrates broad applicability to a range of cancers, like **147**, it is most consistently potent against melanoma cell lines with GI_{50} values ranging from ~190 nM–1.8 μM against the panel of melanomas tested.

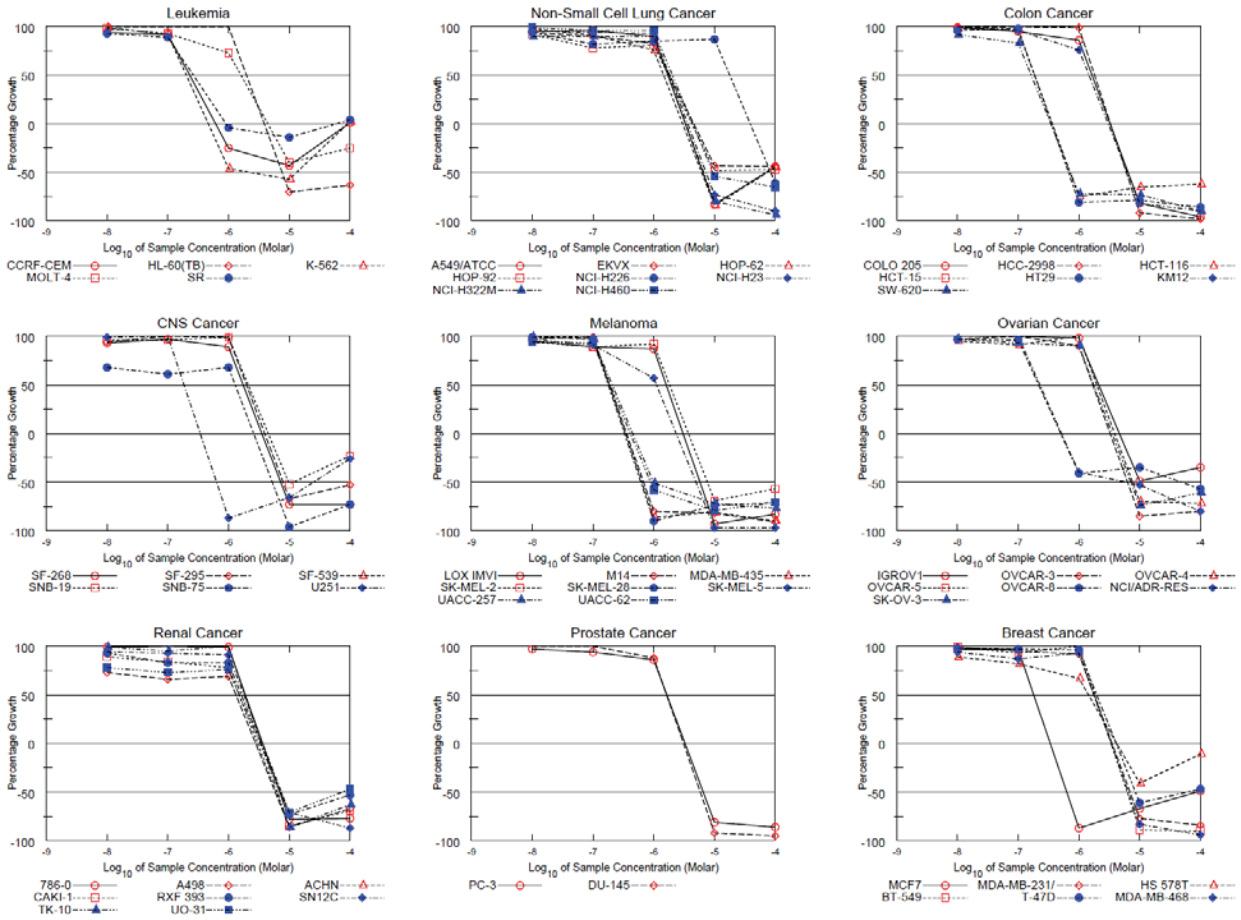

Figure 60. Results of testing **195b** against NCI 60 human tumor cell line screen.

3. Mechanistic studies

Since **197a** represented one of the most potent compounds evaluated as part of the study in Section III, there was interest in further probing its mechanism of action. It was proposed that synthesis of a TAMRA-based probe linked to the **197a** scaffold would enable visualization of where this compound localizes. TAMRA was selected as the fluorophore based upon a recent collaborative study, involving our laboratory and several others at KU, that identified the most uniform intracellular distribution and best cytosolic diffusivity when a TAMRA probe was employed.[260] Through visualization of specific compound localization, potential Hsp90 isoforms

targeted by this compound could be identified and a better understanding of its mechanism of action would be gained.

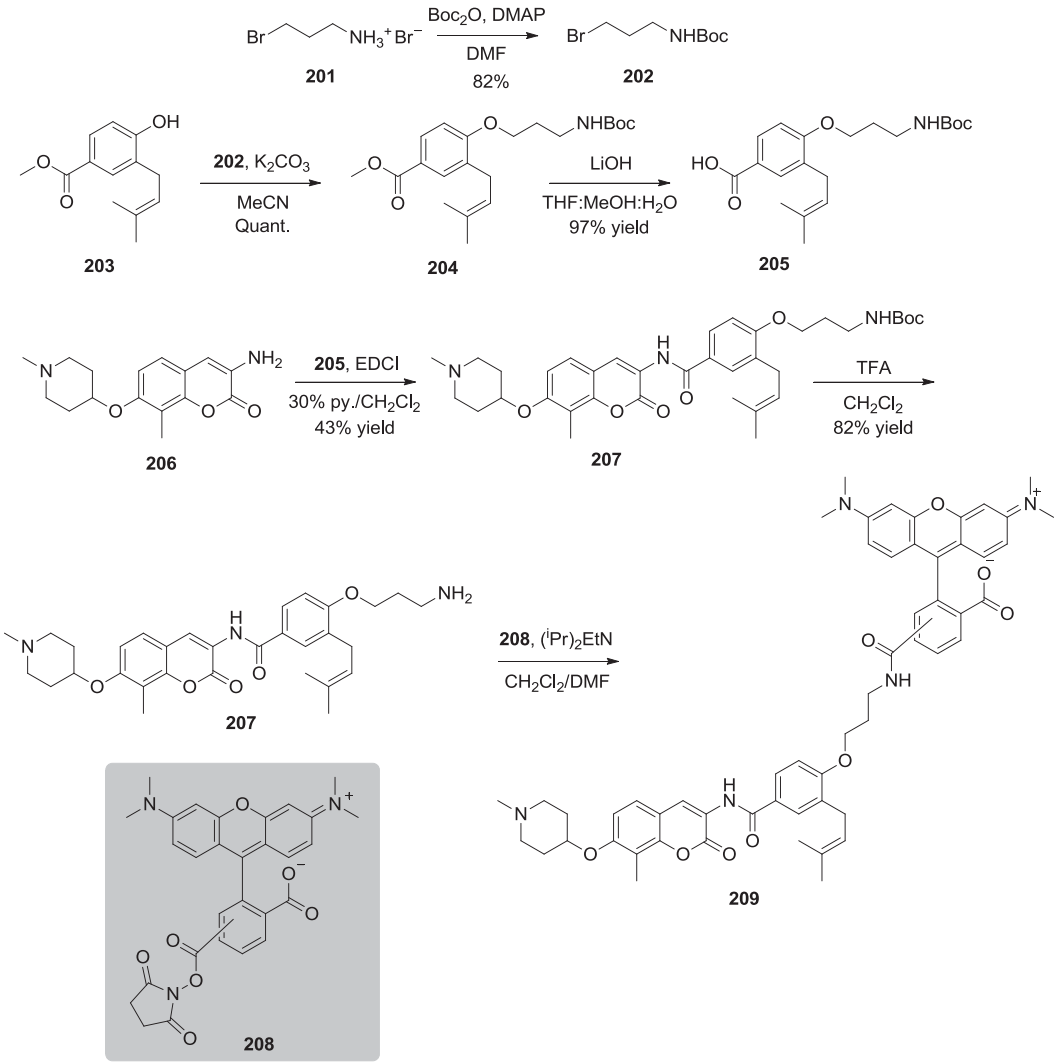

Scheme 50. Synthesis of fluorescent probe.

4. Synthesis of TAMRA-197a

As seen in Scheme 50, alkyl bromide salt **201** was treated with di-*tert*-butyl dicarbonate with catalytic 4-dimethylaminopyridine (DMAP) to afford compound **202** in good yield. Next, prenylated ester **203**, prepared as previously described by Burlison and co-workers,[18] was quantitatively alkylated with protected alkyl bromide **202**.[261] Hydrolysis of ester **204** furnished

the desired acid precursor that was readily coupled with functionalized aminocoumarin **206**.[193] Coupled product **207** was treated with trifluoroacetic acid to liberate the amine used for coupling with commercially available TAMRA probe **208**. Although coupling proceeded, as confirmed by mass spectrometry studies, **209** could not be isolated in a pure form. Silica column chromatography and a variety of HPLC conditions were employed in an attempt to isolate pure compound, but neither proved successful due to the zwitterionic and extremely polar nature of this analogue. Without the ability to obtain **209** in its pure form, the intended localization studies could not be executed. Studies similar to the one designed herein have great potential in understanding the involvement of promising compounds with cellular targets and will be pursued in the future.

V. Conclusion

Several libraries of novobiocin analogues with various structural features were designed, synthesized and evaluated. From the library of sugar mimics, we identified the pyranose as optimal and that a 2'-hydroxy group is indispensable. Several low micromolar analogues containing modified sugars were also identified. From the series of azasugar-containing analogues, we concluded that replacement of noviose with a piperidine ring resulted in consistent low micromolar anti-proliferative activities. The piperidine sugars confirmed that interactions made between noviose and the binding pocket could also be maintained with azasugars. In addition, the acyclic library produced several aliphatic sugar surrogates that manifested mid-nanomolar activity. This library confirmed that flexibility is tolerated and that noviose can be replaced with a simple acyclic moiety to maximize the potency of novobiocin analogues. Finally,

the synthesis of optimized scaffolds with various cytotoxic benzamide side chains identified several novobiocin analogues that exhibited low nanomolar anti-proliferative activity. These analogues confirmed that results obtained from earlier studies could be applied to these appendages and produce compounds that warrant further study.[193]

VI. Experimental Protocols

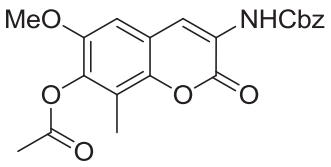

127a

3-(((Benzyloxy)carbonyl)amino)-6-methoxy-8-methyl-2-oxo-2H-chromen-7-yl acetate (127a): A solution of **23a**[14] (195 mg, 0.55 mmol) in anhydrous pyridine (3.0 mL) was treated with acetic anhydride (1.0 mL). After 12 h, the solvent was removed and the residue purified via column chromatography (SiO_2, 100:1, CH_2Cl_2:Acetone) to afford **127a** as a colorless amorphous solid (216 mg, 99%): ^{1}H NMR ($(CD_3)_2CO$, 400 MHz) δ 8.31 (s, 1H), 8.22 (bs, 1H), 7.48 (d, J = 8.0 Hz, 2H), 7.42–7.33 (m, 3H), 7.25 (s, 1H), 5.26 (s, 2H), 3.89 (s, 3H), 2.33 (s, 3H), 2.22 (s, 3H); ^{13}C NMR ($CDCl_3$, 125 MHz) δ 168.6, 158.5, 153.2, 148.8, 142.6, 139.7, 135.6, 128.8 (2C), 128.7, 128.4 (2C), 124.0, 121.3, 120.6, 117.6, 106.2, 67.7, 56.3, 20.5, 9.3; IR (film) ν_{max} 3306, 2924, 2853, 1759, 1703, 1531, 1393, 1205, 1088, 1026, 914, 764, 698 cm^{-1}; HRMS (ESI$^+$) *m/z*: $[M + H]^+$ calcd for $C_{21}H_{20}NO_7$, 398.1240; found, 398.1258.

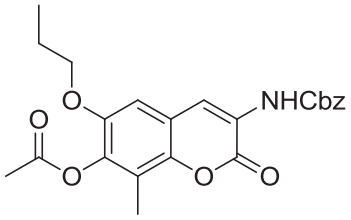

127b

3-(((Benzyloxy)carbonyl)amino)-8-methyl-2-oxo-6-propoxy-2H-chromen-7-yl acetate (127b): A solution of **23b** (50 mg, 0.13 mmol) in anhydrous pyridine (0.75 mL) was treated with acetic anhydride (0.25 mL). After 12 h, the solvent was removed and the residue purified via column chromatography (SiO_2, 100:1, CH_2Cl_2:Acetone) to afford **127b** as a colorless amorphous solid (55 mg, 99%): ^{1}H NMR ($CDCl_3$, 500 MHz) δ 8.19 (s, 1H), 7.53 (s, 1H), 7.34–7.29 (m, 5H), 6.75 (s, 1H), 5.16 (s, 2H), 3.88 (t, J = 6.5 Hz, 2H), 2.29 (s, 3H), 2.22 (s, 3H), 1.76–1.72 (m, 2H), 0.96 (t, J = 7.5 Hz, 3H); ^{13}C NMR ($CDCl_3$, 125 MHz) δ 168.5, 158.4, 153.1, 148.1, 142.3, 139.9, 135.5, 128.7 (2C), 128.6, 128.3 (2C), 123.8, 121.2, 120.3, 117.4, 107.0, 70.5, 67.6, 22.5, 20.3, 10.4, 9.1; IR (film) ν_{max} 3315, 2964, 2930, 1767, 1713, 1526, 1406, 1371, 1231, 1192, 1084, 1024, 903, 752 cm^{-1}; HRMS (ESI$^+$) *m/z*: $[M + H]^+$ calcd for $C_{23}H_{24}NO_7$, 426.1553; found, 426.1549.

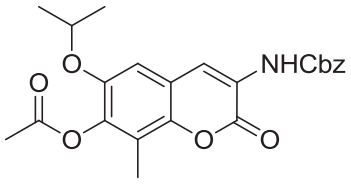

127c

3-(((Benzyloxy)carbonyl)amino)-6-isopropoxy-8-methyl-2-oxo-2H-chromen-7-yl acetate (127c): A solution of **23c** (30.0 mg, 0.078 mmol) in anhydrous pyridine (0.75 mL) was treated with acetic anhydride (0.25 mL). After 12 h, the solvent was removed and the residue purified via column chromatography (SiO_2, 40:1, CH_2Cl_2:Acetone) to afford **127c** as a colorless

amorphous solid (29.0 mg, 87%): ^{1}H NMR (CD_2Cl_2, 400 MHz) δ 8.29 (s, 1H), 7.65 (s, 1H), 7.47–7.39 (m, 5H), 6.94 (s, 1H), 5.26 (s, 2H), 4.58–4.53 (m, 1H), 2.36 (s, 3H), 2.29 (s, 3H), 1.36 (s, 3H), 1.35 (s, 3H); ^{13}C NMR ($CDCl_3$, 125 MHz) δ 168.5, 158.4, 153.1, 146.9, 142.3, 140.8, 135.5, 128.7 (2C), 128.6, 128.3 (2C), 123.7, 121.3, 120.5, 117.4, 108.7, 71.7, 67.6, 21.9 (2C), 20.4, 9.17; IR (film) ν_{max} 2978, 2930, 2359, 2341, 1767, 1711, 1524, 1398, 1232, 1192, 1080, 1022, 903 cm^{-1}; HRMS (ESI^{+}) *m/z*: $[M + H]^{+}$ calcd for $C_{23}H_{24}NO_7$, 426.1553; found, 426.1549.

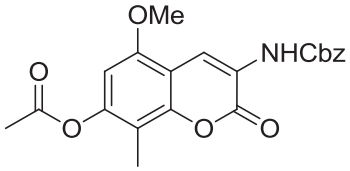

127d

3-(((Benzyloxy)carbonyl)amino)-5-methoxy-8-methyl-2-oxo-2H-chromen-7-yl acetate (127d): A solution of **23d** (30.0 mg, 0.084 mmol) in anhydrous pyridine (0.75 mL) was treated with acetic anhydride (0.25 mL). After 12 h, the solvent was removed and the residue purified via column chromatography (SiO_2, 40:1, CH_2Cl_2:Acetone) to afford **127d** as a colorless amorphous solid (18.2 mg, 54%): ^{1}H NMR ($CDCl_3$, 500 MHz) δ 7.47 (s, 1H), 7.36–7.28 (m, 5H), 6.61 (s, 1H), 6.42 (s, 1H), 5.16 (s, 2H), 3.81 (s, 3H), 2.29 (s, 3H), 2.11 (s, 3H); ^{13}C NMR ($CDCl_3$, 125 MHz) δ 168.9, 158.5, 153.0, 150.1, 149.1, 144.9, 135.6, 128.7, 128.6, 128.5, 128.3, 128.2, 122.1, 116.8, 110.7, 67.5, 56.0, 29.7, 21.0, 20.8, 8.5; IR (film) ν_{max} 3402, 3319, 2953, 2926, 1767, 1715, 1524, 1360, 1204, 1095, 1022, 765 cm^{-1}; HRMS (ESI^{+}) *m/z*: $[M + H]^{+}$ calcd for $C_{21}H_{20}NO_7$, 398.1240; found, 398.1263.

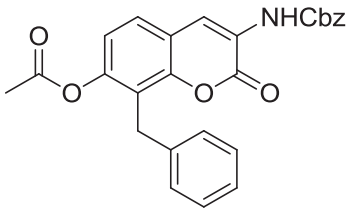

127e

8-Benzyl-3-(((benzyloxy)carbonyl)amino)-2-oxo-2H-chromen-7-yl acetate (127e): A solution of **23e** (50.0 mg, 0.12 mmol) in anhydrous pyridine (0.75 mL) was treated with acetic anhydride (0.25 mL). After 12 h, the solvent was removed and the residue purified via column chromatography (SiO_2, 100:1, CH_2Cl_2:Acetone) to afford **127e** as a colorless amorphous solid (48.0 mg, 87%): ^{1}H NMR ($CDCl_3$, 500 MHz) δ 8.23 (bs, 1H), 7.49 (s, 1H), 7.34–7.24 (m, 5H), 7.23–7.15 (m, 2H), 7.11–7.08 (m, 1H), 7.04–7.02 (m, 2H), 7.00 (d, J = 8.5, 1H), 6.94 (d, J = 8.5, 1H), 5.23 (s, 2H), 5.16 (s, 2H), 2.19 (s, 3H); ^{13}C NMR ($CDCl_3$, 125 MHz) δ 168.9, 158.1, 153.1, 150.1, 148.3, 139.2, 138.7, 135.4, 128.6, 128.5 (2C), 128.3, 128.2, 127.4, 126.2, 125.9, 123.6, 121.5, 121.1, 120.4, 120.0, 67.7, 30.7, 29.5, 20.9, 20.8; IR (film) ν_{max} 3400, 3285, 3030, 2939, 2359, 2341, 1767, 1710, 1693, 1522, 1366, 1198, 1173, 1038, 1030, 696 cm^{-1}; HRMS (ESI$^+$) *m/z*: $[M + H]^+$ calcd for $C_{26}H_{22}NO_6$, 444.1447; found, 444.1476.

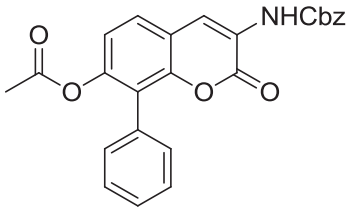

127f

3-(((Benzyloxy)carbonyl)amino)-2-oxo-8-phenyl-2H-chromen-7-yl acetate (127f): A solution of **23f** (50.0 mg, 0.13 mmol) in anhydrous pyridine (0.75 mL) was treated with acetic anhydride (0.25 mL). After 12 h, the solvent was removed and the residue purified via column chromatography (SiO_2, 100:1, CH_2Cl_2:Acetone) to afford **127f** as a yellow amorphous solid

(46.0 mg, 83%): ^{1}H NMR (CD_2Cl_2, 400 MHz) δ 8.40 (s, 1H), 7.61 (s, 1H), 7.58 (d, *J* = 8.5 Hz, 1H), 7.55–7.37 (m, 5H), 7.26–7.24 (m, 2H), 7.17 (d, *J* = 8.5 Hz, 1H), 7.11 (d, *J* = 8.2 Hz, 1H), 5.27 (s, 2H), 2.03 (s, 3H), 1.98 (s, 3H); ^{13}C NMR ($CDCl_3$, 125 MHz) δ 169.2, 158.1, 153.1, 150.1, 149.1, 130.4, 130.0, 129.6, 128.7, 128.6 (2C), 128.3, 128.0, 127.8, 127.0, 123.7, 120.8, 120.5 (2C), 120.0, 118.2, 67.7, 29.5, 20.5 (2C); IR (film) ν_{max} 2920, 2851, 2359, 1767, 1717, 1520, 1366, 1196, 1043, 750 cm^{-1}; HRMS (ESI^{+}) *m/z*: [M + Na]$^{+}$ calcd for $C_{25}H_{19}NNaO_6$, 452.1110; found, 452.1111.

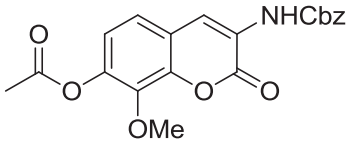

127g

3-(((Benzyloxy)carbonyl)amino)-8-methoxy-2-oxo-2H-chromen-7-yl acetate (127g): A solution of **23g**[14] (60 mg, 0.18 mmol) in anhydrous pyridine (2.25 mL) was treated with acetic anhydride (0.75 mL). After 12 h, the solvent was removed and the residue purified via column chromatography (SiO_2, 40:1, CH_2Cl_2:Acetone) to afford **127g** as a colorless amorphous solid (67 mg, 99%): ^{1}H NMR ($CDCl_3$, 500 MHz) δ 8.29 (s, 1H), 7.59 (s, 1H), 7.42–7.34 (m, 5H), 7.18 (d, *J* = 8.5 Hz, 1H), 7.00 (d, *J* = 8.5 Hz, 1H), 5.23 (s, 2H), 4.01 (s, 3H), 2.36 (s, 3H); ^{13}C NMR ($CDCl_3$, 125 MHz) δ 168.9, 157.6, 153.2, 144.0, 143.5, 139.5, 135.5, 128.8 (2C), 128.7, 128.4 (2C), 123.8, 121.8, 121.2, 119.8, 119.2, 67.8, 61.8, 20.8; IR (film) ν_{max} 3409, 3352, 3312, 3088, 3038, 2945, 2837, 2359, 2332, 1765, 1710, 1533, 1383, 1366, 1238, 1202, 1045, 698 cm^{-1}; HRMS (ESI^{+}) *m/z*: [M + Na]$^{+}$ calcd for $C_{20}H_{17}NNaO_7$, 406.0903; found, 406.0928.

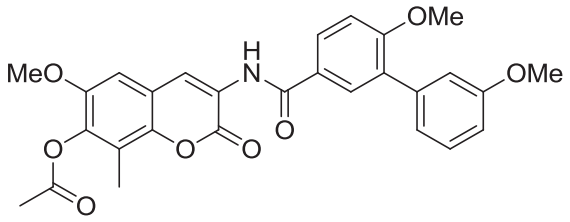

128a

3-(3',6-Dimethoxy-[1,1'-biphenyl]-3-ylcarboxamido)-6-methoxy-8-methyl-2-oxo-2H-chromen-7-yl acetate (128a): Palladium on carbon (10%, 43 mg) was added to **127a** (216 mg, 0.54 mmol) in anhydrous THF (3.6 mL) and the solution was placed under an atmosphere of H_2. After 12 h, the solution was filtered through SiO_2 (40:1, CH_2Cl_2:Acetone) and the eluent was concentrated to afford a yellow solid, which was used without further purification (142 mg, 99%).

A solution of 3',6-dimethoxy-[1,1'-biphenyl]-3-carbonyl chloride[170] (130 mg, 0.47 mmol), in anhydrous THF (2.7 mL), was added to a solution of the amine (123 mg, 0.47 mmol) and anhydrous triethylamine (0.13 mL, 0.94 mmol) in anhydrous THF (2.7 mL). After 12 h, the solvent was removed and the residue purified via column chromatography (SiO_2, 40:1, CH_2Cl_2:Acetone) to afford **128a** as a colorless amorphous solid (129 mg, 55%): ^{1}H NMR (CD_2Cl_2, 400 MHz) δ 8.84 (s, 1H), 8.80 (s, 1H), 7.97 (dd, J = 8.5, 2.5 Hz, 1H), 7.92 (d, J = 2.5 Hz, 1H), 7.39 (t, J = 8.0 Hz, 1H), 7.16–7.11 (m, 3H), 7.01 (s, 1H), 6.97–6.95 (m, 1H), 3.94 (s, 3H), 3.90 (s, 3H), 3.88 (s, 3H), 2.38 (s, 3H), 2.32 (s, 3H); ^{13}C NMR ($CDCl_3$, 125 MHz) δ 168.6, 165.8, 160.0, 159.5, 159.2, 148.9, 142.8, 140.0, 138.7, 131.2, 130.2, 129.3, 128.4, 126.0, 124.2, 123.3, 122.2, 120.6, 117.8, 115.4, 113.3, 111.2, 106.6, 56.4, 56.1, 55.5, 20.6, 9.3; IR (film) ν_{max} 3404, 2926, 2853, 1765, 1713, 1670, 1603, 1522, 1385, 1242, 1204, 1180, 1094, 1022, 571 cm^{-1}; HRMS (ESI$^+$) *m/z*: $[M + H]^+$ calcd for $C_{28}H_{26}NO_8$, 504.1658; found, 504.1625.

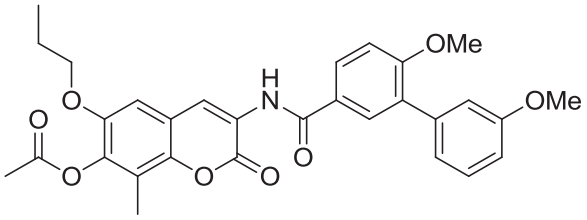

128b

3-(3',6-Dimethoxy-[1,1'-biphenyl]-3-ylcarboxamido)-8-methyl-2-oxo-6-propoxy-2H-chromen-7-yl acetate (128b): Palladium on carbon (20%, 11 mg) was added to **127b** (56 mg, 0.13 mmol) in anhydrous THF (0.90 mL) and the solution was placed under an atmosphere of H_2. After 12 h, the solution was filtered through SiO_2 (40:1, CH_2Cl_2:Acetone) and the eluent was concentrated to afford a yellow solid, which was used without further purification (38.0 mg, 99%).

EDCI (62.5 mg, 0.33 mmol) and 3',6-dimethoxybiphenyl-3-carboxylic acid (67.4 mg, 0.26 mmol) were added to the amine (38.0 mg, 0.13 mmol) in 30% pyridine/CH_2Cl_2 (2.00 mL). After 12 h, the solvent was concentrated and the residue purified via column chromatography (SiO_2, 100:1 CH_2Cl_2:Acetone) to afford a **128b** as a colorless solid (34.0 mg, 49%): ^{1}H NMR (CD_2Cl_2, 400 MHz) δ 8.82 (s, 1H), 8.80 (s, 1H), 7.96 (dd, *J* = 8.6, 2.4 Hz, 1H), 7.91 (d, *J* = 2.3 Hz, 1H), 7.39 (t, *J* = 7.8 Hz, 1H), 7.15–7.11 (m, 3H), 6.99–6.95 (m, 2H), 4.02 (t, *J* = 8.0 Hz, 2H), 3.94 (s, 3H), 3.83 (s, 3H), 2.38 (s, 3H), 2.33 (s, 3H), 1.86–1.81 (m, 2H), 1.07 (t, *J* = 7.4 Hz, 3H); ^{13}C NMR ($CDCl_3$, 125 MHz) δ 167.4, 164.5, 158.8, 158.3, 158.0, 147.1, 141.5, 139.1, 137.5, 130.0, 129.0, 128.2, 127.2, 124.9, 122.8, 122.2, 121.0, 119.3, 116.5, 114.2, 112.1, 110.0, 106.2, 69.4, 54.9, 54.3, 21.4, 19.3, 9.4, 8.1; IR (film) ν_{max} 3404, 2964, 2935, 2837, 1765, 1711, 1672, 1603, 1526, 1501, 1443, 1242, 1204, 1180, 1094, 1022, 906, 735 cm^{-1}; HRMS (ESI$^+$) *m/z*: $[M + H]^+$ calcd for $C_{30}H_{30}NO_8$, 532.1971; found, 532.1970.

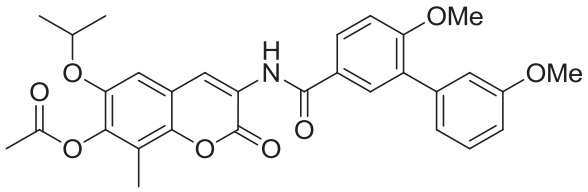

128c

3-(3',6-Dimethoxy-[1,1'-biphenyl]-3-ylcarboxamido)-6-isopropoxy-8-methyl-2-oxo-2H-chromen-7-yl acetate (128c): Palladium on carbon (20%, 5.80 mg) was added to **127c** (29.0 mg, 0.068 mmol) in anhydrous THF (0.50 mL) and the solution was placed under an atmosphere of H_2. After 12 h, the solution was filtered through SiO_2 (40:1, CH_2Cl_2:Acetone) and the eluent was concentrated to afford a yellow solid, which was used without further purification (20.0 mg, 99%).

EDCI (32.7 mg, 0.17 mmol) and 3',6-dimethoxybiphenyl-3-carboxylic acid (35.3 mg, 0.14 mmol) were added to the amine (20.0 mg, 0.068 mmol) in 30% pyridine/CH_2Cl_2 (1.00 mL). After 12 h, the solvent was concentrated and the residue purified via column chromatography (SiO_2, 40:1 CH_2Cl_2:Acetone) to afford a **128c** as a colorless solid (16.4 mg, 45%): ^{1}H NMR (CD_2Cl_2, 400 MHz) δ 8.82 (s, 1H), 8.80 (s, 1H), 7.96 (dd, *J* = 8.8, 2.4 Hz, 1H), 7.91 (d, *J* = 2.4 Hz, 1H), 7.41–7.36 (m, 2H), 7.14 (d, *J* = 8.8 Hz, 1H), 7.12 (d, *J* = 2.4 Hz, 1H), 7.01 (s, 1H), 6.96 (dd, *J* = 8.8, 2.4 Hz, 1H), 4.62–4.56 (m, 1H), 3.94 (s, 3H), 3.88 (s, 3H), 2.37 (s, 3H), 2.32 (s, 3H), 1.38 (s, 3H), 1.36 (s, 3H); ^{13}C NMR ($CDCl_3$, 125 MHz) δ 167.5, 164.6, 158.9, 158.3, 145.9, 141.5, 140.0, 137.5, 131.9, 130.6, 130.1, 129.0, 128.2, 127.2, 124.9, 122.8, 122.3, 121.0, 119.5, 116.5, 114.2, 112.1, 111.9, 110.0, 70.6, 54.9, 54.3, 20.9, 19.3, 8.2; IR (film) ν_{max} 2976, 2932, 2837, 2359, 1767, 1713, 1674, 1603, 1526, 1501, 1391, 1242, 1204, 1182, 908, 735 cm^{-1}; HRMS (ESI$^+$) *m/z*: $[M + H]^+$ calcd for $C_{30}H_{30}NO_8$, 532.1971; found, 532.1982.

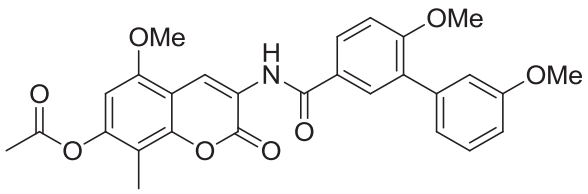

128d

3-(3',6-Dimethoxy-[1,1'-biphenyl]-3-ylcarboxamido)-5-methoxy-8-methyl-2-oxo-2H-chromen-7-yl acetate (128d): Palladium on carbon (20%, 3.64 mg) was added to **127d** (18.2 mg, 0.046 mmol) in anhydrous THF (0.31 mL) and the solution was placed under an atmosphere of H_2. After 12 h, the solution was filtered through SiO_2 (40:1, CH_2Cl_2:Acetone) and the eluent was concentrated to afford a yellow solid, which was used without further purification (12.1 mg, 99%).

EDCI (22.0 mg, 0.11 mmol) and 3',6-dimethoxybiphenyl-3-carboxylic acid (23.7 mg, 0.092 mmol) were added to the amine (12.1 mg, 0.046 mmol) in 30% pyridine/CH_2Cl_2 (1.00 mL). After 12 h, the solvent was concentrated and the residue purified via column chromatography (SiO_2, 40:1 CH_2Cl_2:Acetone) to afford a **128d** as a colorless solid (9.0 mg, 39%): ^{1}H NMR (CD_2Cl_2, 400 MHz) δ 9.06 (s, 1H), 8.73 (s, 1H), 7.96 (dd, *J* = 8.5, 2.4, 1H), 7.93–7.89 (m, 1H), 7.39 (t, *J* = 8.0, 1H), 7.18–7.12 (m, 3H), 6.97–6.95 (m, 1H), 6.60 (s, 1H), 3.97 (s, 3H), 3.95 (s, 3H), 3.88 (s, 3H), 2.38 (s, 3H), 2.22 (s, 3H); ^{13}C NMR ($CDCl_3$, 125 MHz) δ 167.9, 164.3, 158.8, 158.1, 153.0, 149.3, 148.3, 144.2, 137.5, 130.1, 130.0, 128.9, 128.2, 127.1, 125.0, 121.0, 117.8, 114.2, 112.2, 110.8, 100.0, 55.0, 54.9, 54.3, 54.2, 28.7, 19.8, 7.5; IR (film) ν_{max} 3404, 2961, 2934, 2841, 2359, 2332, 1767, 1717, 1605, 1526, 1362, 1240, 1204, 1095, 1022 cm^{-1}; HRMS (ESI$^+$) *m/z*: $[M + Na]^+$ calcd for $C_{28}H_{25}NNaO_8$, 526.1478; found, 526.1468.

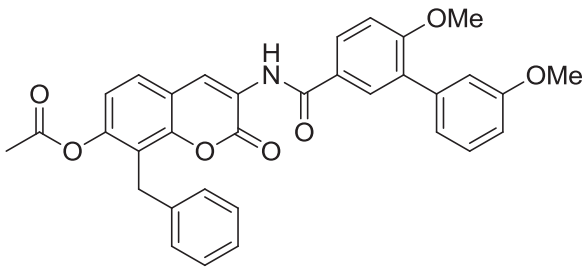

128e

8-Benzyl-3-(3',6-dimethoxy-[1,1'-biphenyl]-3-ylcarboxamido)-2-oxo-2H-chromen-7-yl acetate (128e): Palladium on carbon (20%, 9.6 mg) was added to **127e** (48.0 mg, 0.11 mmol) in anhydrous THF (1.30 mL) and the solution was placed under an atmosphere of H_2. After 12 h, the solution was filtered through SiO_2 (40:1, CH_2Cl_2:Acetone) and the eluent was concentrated to afford a yellow solid, which was used without further purification (33.5 mg, 99%).

EDCI (51.9 mg, 0.27 mmol) and 3',6-dimethoxybiphenyl-3-carboxylic acid (55.9 mg, 0.22 mmol) were added to the amine (33.5 mg, 0.11 mmol) in 30% pyridine/CH_2Cl_2 (2.00 mL). After 12 h, the solvent was concentrated and the residue purified via column chromatography (SiO_2, 100:1 CH_2Cl_2:Acetone) to afford a **128e** as a colorless solid (13.1 mg, 22%): ^{1}H NMR (Acetone-d_6, 400 MHz) δ 8.87 (s, 1H), 8.68 (s, 1H), 8.04 (dd, J = 8.6, 2.2, 1H), 7.98 (d, J = 2.2, 2H), 7.59 (d, J = 8.5, 1H), 7.35 (t, J = 8.0, 1H), 7.29–7.08 (m, 7H), 6.95–6.92 (m, 2H), 4.14 (s, 2H), 3.92 (s, 3H), 3.84 (s, 3H), 2.26 (s, 3H); ^{13}C NMR (500, 125 MHz) δ 168.3, 167.8, 157.4, 148.8, 147.5, 137.6, 129.9 (2C), 127.8 (2C), 127.5 (2C), 127.4 (4C), 125.4 (4C), 125.2 (4C), 122.4, 122.2, 120.5, 119.0, 116.8, 28.7, 28.4, 23.7, 19.8; IR (film) ν_{max} 3339, 3084, 3030, 2959, 2359, 2330, 1749, 1713, 1674, 1599, 1531, 1364, 1209, 1184, 1028, 798 cm^{-1}; HRMS (ESI$^+$) *m/z*: [M + Na]$^+$ calcd for $C_{33}H_{27}NNaO_7$, 572.1685; found, 550.1738.

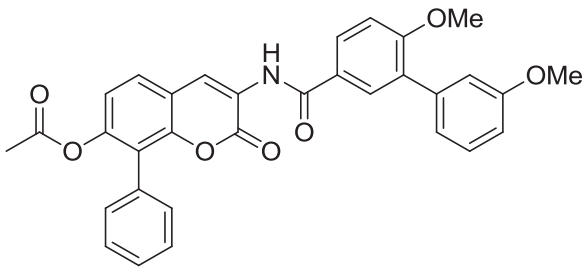

128f

3-(3',6-Dimethoxy-[1,1'-biphenyl]-3-ylcarboxamido)-2-oxo-8-phenyl-2H-chromen-7-yl acetate (128f): Palladium on carbon (20%, 9.20 mg) was added to **127f** (46 mg, 0.11 mmol) in anhydrous THF (0.72 mL) and the solution was placed under an atmosphere of H_2. After 12 h, the solution was filtered through SiO_2 (40:1, CH_2Cl_2:Acetone) and the eluent was concentrated to afford a yellow solid, which was used without further purification (31.6 mg, 99%).

EDCI (51.3 mg, 0.27 mmol) and 3',6-dimethoxybiphenyl-3-carboxylic acid (55.3 mg, 0.21 mmol) were added to the amine (31.6 mg, 0.11 mmol) in 30% pyridine/CH_2Cl_2 (2.00 mL). After 12 h, the solvent was concentrated and the residue purified via column chromatography (SiO_2, 100:1 CH_2Cl_2:Acetone) to afford a **128f** as a colorless solid (6.70 mg, 12%): ^{1}H NMR (Acetone-d_6, 400 MHz) δ 9.12 (s, 1H), 8.83 (s, 1H), 8.03 (dd, J = 8.6, 2.4, 1H), 7.95 (d, J = 2.4, 1H), 7.79 (d, J = 8.6, 1H), 7.52–7.34 (m, 8H), 7.27 (dd, J = 8.6, 3.2, 2H), 6.95–6.91 (m, 1H), 3.91 (s, 3H), 3.83 (s, 3H), 1.99 (s, 3H); ^{13}C NMR ($CDCl_3$, 125 MHz) δ 168.1, 164.7, 158.9, 158.3, 157.6, 148.1, 146.6, 137.5, 130.1 (2C), 129.4 (2C), 129.0, 128.2, 127.8, 127.3 (2C), 127.2, 126.3, 124.8, 123.0, 122.9, 121.8, 121.0, 119.0, 117.4, 114.2, 112.2, 110.0, 54.9, 54.3, 19.5; IR (film) ν_{max} 2961, 2930, 2359, 2341, 1765, 1717, 1672, 1601, 1522, 1501, 1366, 1259, 1202, 1180, 1080, 1020, 908, 698 cm^{-1}; HRMS (ESI$^+$) *m/z*: [M + Na]$^+$ calcd for $C_{32}H_{25}NNaO_7$, 558.1529; found, 558.1538.

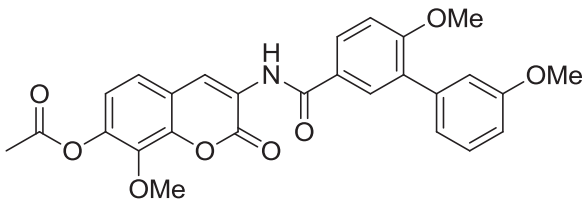

128g

3-(3',6-Dimethoxy-[1,1'-biphenyl]-3-ylcarboxamido)-8-methoxy-2-oxo-2H-chromen-7-yl acetate (128g): Palladium on carbon (10%, 5 mg) was added to **127g** (25 mg, 0.065 mmol) in anhydrous THF (0.44 mL) and the solution was placed under an atmosphere of H_2. After 12 h, the solution was filtered through SiO_2 (40:1, CH_2Cl_2:Acetone) and the eluent was concentrated to afford a yellow solid, which was used without further purification (16 mg, 99%).

A solution of 3',6-dimethoxy-[1,1'-biphenyl]-3-carbonyl chloride[170] (18 mg, 0.064 mmol), in anhydrous THF (0.37 mL), was added to a solution of the amine (16 mg, 0.064 mmol) and anhydrous triethylamine (18 μL, 0.13 mmol), dissolved in anhydrous THF (0.37 mL). After 12 h, the solvent was removed and the residue purified via column chromatography (SiO_2, 40:1, CH_2Cl_2:Acetone) to afford **128g** as a colorless amorphous solid (16 mg, 50%): ^{1}H NMR ($CDCl_3$, 500 MHz) δ 8.83 (s, 1H), 8.75 (s, 1H), 7.92 (dd, *J* = 8.5, 2.5 Hz, 1H), 7.89 (d, *J* = 2.5 Hz, 1H), 7.36 (t, *J* = 8.0 Hz, 1H), 7.26 (d, *J* = 8.0 Hz, 1H), 7.13–7.02 (m, 4H), 6.94–6.92 (m, 1H), 4.04 (s, 3H), 3.90 (s, 3H), 3.86 (s, 3H), 2.37 (s, 3H); ^{13}C NMR ($CDCl_3$, 125 MHz) δ 169.0, 165.8, 160.1, 159.5, 158.3, 144.3, 143.7, 139.6, 138.6, 131.3, 130.2, 129.4, 128.4, 125.9, 124.0, 123.2, 122.3, 122.1, 120.0, 119.4, 115.4, 113.3, 111.2, 61.8, 56.0, 55.5, 20.9; IR (film) ν_{max} 3398, 3097, 2993, 2926, 2853, 2357, 2339, 1765, 1666, 1599, 1520, 1456, 1362, 1244, 1202, 1078, 1022, 905, 802, 734 cm^{-1}; HRMS (ESI$^+$) *m/z*: $[M + 2H]^+$ calcd for $C_{27}H_{25}NO_8$, 491.1580; found, 491.1537.

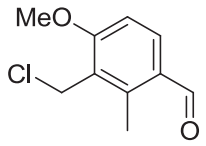

130

3-(Chloromethyl)-4-methoxy-2-methylbenzaldehyde (130): Zinc (II) chloride (219 mg, 1.61 mmol) was added to a solution of 4-methoxy-2-methylbenzaldehyde (161 mg, 1.07 mmol) in 37% formaldehyde (2.0 mL), then heated at reflux, while bubbling HCl gas into the solution, for 10 min. Once cool, the reaction mixture was poured into ice and Et_2O (3 x 15 mL) was used to extract the solution. The combined organic extracts were washed with saturated aqueous $NaHCO_3$, saturated aqueous NaCl, dried (Na_2SO_4), filtered, and concentrated. The residue was purified via column chromatography (SiO_2, 6:1 Hexane: EtOAc) to afford **130** as a colorless amorphous solid (105 mg, 49%): ^{1}H NMR ($CDCl_3$, 400 MHz) δ 10.12 (s, 1H), 7.80 (s, 1H), 6.74 (s, 1H), 4.63 (s, 2H), 3.95 (s, 3H), 2.67 (s, 3H); ^{13}C NMR ($CDCl_3$, 125 MHz) δ 191.3, 161.7, 135.2, 134.0, 128.3, 125.7, 108.4, 56.0, 37.0, 14.0; HRMS (ESI$^+$) *m/z*: $[M + H]^+$ calcd for $C_{10}H_{12}ClO_2$, 199.0526; found, 199.0560.

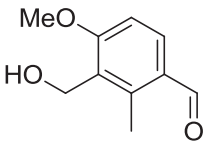

131

3-(Hydroxymethyl)-4-methoxy-2-methylbenzaldehyde (131): Calcium carbonate (459 mg, 4.58 mmol) was added to a solution of benzaldehyde 130 (455 mg, 2.29 mmol) in 40% aqueous acetone (10.2 mL), then heated at reflux for 1 h. Once cool, solvent was removed and the residue was resuspended in Et_2O, washed with water, dried (Na_2SO_4), filtered, and concentrated. The residue was purified via column chromatography (SiO_2, 6:1 → 1:1 Hexane: EtOAc) to afford

131 as a colorless amorphous solid (333 mg, 81%): ^{1}H NMR ($CDCl_3$, 400 MHz) δ 10.21 (s, 1H), 7.82 (d, *J* = 8.6 Hz, 1H), 6.92 (d, *J* = 8.6 Hz, 1H), 4.84 (s, 2H), 3.97 (s, 3H), 2.76 (s, 3H); ^{13}C NMR ($CDCl_3$, 125 MHz) δ 191.6, 162.1, 141.5, 134.6 (2C), 128.4, 108.1, 56.2, 55.8, 14.2; HRMS (ESI^+) *m/z*: $[M + H]^+$ calcd for $C_{10}H_{13}O_3$, 181.0865; found, 181.0864.

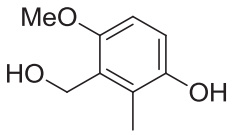

132

3-(Hydroxymethyl)-4-methoxy-2-methylphenol (132): A solution of **131** (1.54 g, 10.3 mmol) in anhydrous CH_2Cl_2 (3.30 mL) was slowly added to *m*CPBA (70%) (3.79 g, 15.4 mmol) in anhydrous CH_2Cl_2 (19.2 mL) at 0°C. The resulting solution was warmed to rt, then refluxed for 12 h. After cooling to rt, the resulting solution was washed with saturated aqueous $NaHCO_3$ solution (3 × 30 mL) and 10% aqueous $Na_2S_2O_3$ (30 mL). Combined organic fractions were dried (Na_2SO_4), filtered, and concentrated. The residue was re-dissolved in MeOH (10.0 mL) and stirred with excess 10% aqueous NaOH for 3 h at rt. The pH was adjusted to 2 with 6M HCl and the solution was extracted with CH_2Cl_2 (3 × 30 mL). Combined organic fractions were dried (Na_2SO_4), filtered, and concentrated. The residue was purified via column chromatography (SiO_2, 3:1 → 1:1 Hexane: EtOAc) to afford **132** as a colorless amorphous solid (1.15 g, 81%): ^{1}H NMR ($CDCl_3$, 400 MHz) δ 6.71 (d, *J* = 8.7 Hz, 1H), 6.63 (d, *J* = 8.7 Hz, 1H), 5.18 (bs, 1H), 4.78 (s, 2H), 3.82 (s, 3H), 2.28 (s, 3H); ^{13}C NMR ($CDCl_3$, 125 MHz) δ 152.3, 147.9, 127.6, 124.4, 114.5, 108.6, 57.6 (2C), 11.5; HRMS (ESI^+) *m/z*: $[M + Na]^+$ calcd for $C_9H_{12}O_3$, 191.0684; found, 191.0694.

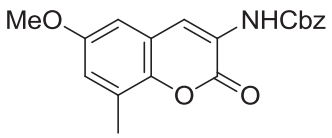

134

Benzyl (6-methoxy-8-methyl-2-oxo-2H-chromen-3-yl)carbamate (134): A solution of 4-methoxy-2-methylphenol (584 mg, 4.22 mmol) and eneamine **22** (1.47 g, 5.28 mmol) in glacial acetic acid (26.3 mL) was heated to reflux for 40 h. Upon cooling to rt, the solution was extracted with EtOAc (3 × 30 mL); combined organic fractions were dried (Na_2SO_4), filtered, and concentrated. The residue was purified via column chromatography (SiO_2, 40:1 CH_2Cl_2:Acetone) to afford **134** as a red amorphous solid (106 mg, 7.0%): ^{1}H NMR ($CDCl_3$, 400 MHz) δ 7.41–7.36 (m, 5H), 6.73 (d, *J* = 8.7 Hz, 2H), 6.66–6.63 (m, 1H), 5.13 (s, 2H), 4.45 (s, 1H), 3.77 (s, 3H), 2.26 (s, 3H); ^{13}C NMR ($CDCl_3$, 125 MHz) δ 160.2, 158.2, 152.1, 151.0, 146.8, 138.1, 136.0, 127.7, 127.5, 127.4, 127.3, 127.2, 123.9, 121.6, 114.5, 100.1, 66.6, 54.6, 13.1; HRMS (ESI$^+$) *m/z*: $[M + Na]^+$ calcd for $C_{19}H_{17}NNaO_5$, 362.1004; found, 362.0995

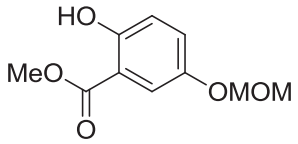

137

Methyl 2-hydroxy-5-(methoxymethoxy)benzoate (137):[243] Chloromethyl methyl ether (0.18 mL, 2.38 mmol) was added dropwise to a solution of **136**[262] (200 mg, 1.19 mmol) and potassium carbonate (164 mg, 1.19 mmol) in anhydrous *N,N*-dimethylformamide (3.30 mL) at 0^{o}C, then warmed to rt over 12 h. The reaction was quenched by the addition of saturated aqueous NH_4Cl solution and extracted with EtOAc (3 × 20 mL). The combined organic fractions were washed with saturated aqueous NaCl, dried (Na_2SO_4), filtered, and concentrated. The residue was purified via column chromatography (SiO_2, 3:1 Hexane:EtOAc) to give **137** as a colorless oil (92

mg, 36%): ^{1}H NMR ($CDCl_3$, 400 MHz) δ 10.46 (s, 1H), 7.51 (d, *J* = 3.0 Hz, 1H), 7.20 (dd, *J* = 9.0, 3.0 Hz, 1H), 6.93 (d, *J* = 9.0 Hz, 1H), 5.14 (s, 2H), 3.96 (s, 3H), 3.50 (s, 3H).

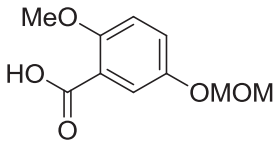

139

2-Methoxy-5-(methoxymethoxy)benzoic acid (139): Sodium hydride (121 mg, 3.02 mmol) was added to phenol **137** (320 mg, 1.51 mmol) in anhydrous *N,N*-dimethylformamide (4.20 mL) at 0°C. After 30 min, iodomethane (0.19 mL, 3.02 mmol) was added at -78^{o}C and the resulting solution was warmed to rt over 12 h. The reaction was cooled to 0°C, quenched by the addition of saturated aqueous $NaHCO_3$, and extracted with EtOAc (3 × 30 mL). Combined organic fractions were washed with saturated aqueous NaCl, dried (Na_2SO_4), filtered, and concentrated. The residue was purified via column chromatography (SiO_2, 4:1 Hexane:EtOAc) to afford the benzoate as a yellow oil (312 mg, 91%), which was used without further purification.

Lithium hydroxide (154 mg, 6.41 mmol) was added to a solution of benzoate (290 mg, 1.28 mmol) in 3:1:1 THF:MeOH:H_2O (12.9 mL). After 12 h, the solution was concentrated and the aqueous residue was acidified, and then extracted with EtOAc (3 x 15 mL). The combined organic layers were next extracted with saturated aqueous $NaHCO_3$ (3 x 15 mL), and then the aqueous extracts were acidified. Finally, EtOAc (3 x 15 mL) was used to extract the acid product, and the combined organic extracts were washed with saturated aqueous NaCl, dried (Na_2SO_4), filtered, and concentrated to afford **139** as a colorless amorphous solid (255 mg, 94%, 86% over 3 steps): ^{1}H NMR ($CDCl_3$, 400 MHz) δ 7.84 (d, *J* = 3.0 Hz, 1H), 7.27 (dd, *J* = 9.0, 3.0 Hz, 1H), 7.01 (d, *J* = 9.0 Hz, 1H), 5.17 (s, 2H), 4.06 (s, 3H), 3.49 (s, 3H); ^{13}C NMR ($CDCl_3$, 125

MHz) δ 165.0, 153.0, 151.9, 123.4, 119.7, 118.3, 112.7, 95.2, 57.2, 56.0; HRMS (ESI^+) *m/z*: [M + Na]$^+$ calcd for $C_{10}H_{12}NaO_5$, 235.0582; found, 235.0596.

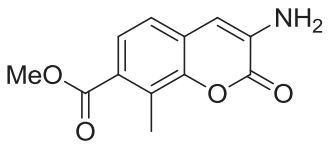

143

Methyl 3-amino-8-methyl-2-oxo-2H-chromene-7-carboxylate (143): A solution of 3-hydroxy-2-methylbenzoic acid (547 mg, 3.59 mmol) and eneamine **22** (1.0 g, 3.59 mmol) in glacial acetic acid (18.7 mL) was heated to reflux for 40 h. Upon cooling to rt, the solution was extracted with EtOAc (3 × 30 mL); combined organic fractions were dried (Na_2SO_4), filtered, and concentrated to afford a brown solid, which was used without further purification (1.27 g, 99%).

Thionyl chloride (10.3 μL, 0.14 mmol) was added dropwise to a solution of crude coumarin (25 mg, 0.071 mmol) in anhydrous MeOH (0.7 mL) at 0^{o}C, then warmed to rt slowly over 12 h. Solvent was concentrated and the residue was resuspended in EtOAc (15 mL), washed with saturated aqueous $NaHCO_3$, saturated aqueous NaCl, dried (Na_2SO_4), filtered, and concentrated. The residue was purified via column chromatography (SiO_2, 3:1 Hexane: EtOAc) to afford **143** as a colorless amorphous solid (10.3 mg, 52% over 2 steps): ^{1}H NMR (CDCl3, 400 MHz) δ 7.41 (d, *J* = 6.7 Hz, 1H), 7.10 (s, 1H), 6.99 (s, 1H), 6.09 (bs, 2H), 3.92 (s, 3H), 2.47 (s, 3H); ^{13}C NMR ($CDCl_3$, 125 MHz) δ 167.0, 152.7, 130.1, 124.6 (2C), 123.9, 121.0 (2C), 116.8, 50.5, 11.0; HRMS (ESI^+) *m/z*: [M + Na]$^+$ calcd for $C_{12}H_{11}NNaO_4$, 256.0586; found, 256.0570.

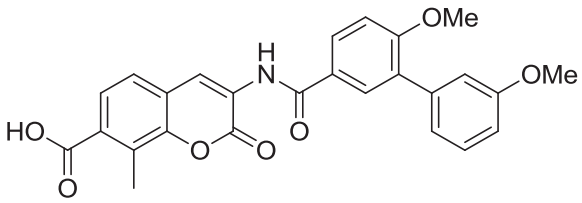

145

3-(3',6-Dimethoxy-[1,1'-biphenyl]-3-ylcarboxamido)-8-methyl-2-oxo-2H-chromene-7-carboxylic acid (145): EDCI (821 mg, 4.28 mmol) and 3',6-dimethoxybiphenyl-3-carboxylic acid (1.11 g, 4.28 mmol) were added to aniline **142** (397 mg, 1.43 mmol) in 30% pyridine/CH_2Cl_2 (28.5 mL). After 12 h, the solvent was concentrated to afford **144** as a colorless amorphous solid (732 mg, 99%), which was used without further purification.

Lithium hydroxide (704 mg, 9.40 mmol) was added to a solution of benzoate (975 mg, 1.88 mmol) in 3:1:1 THF:MeOH:H_2O (18.8 mL). After 12 h, the solution was concentrated and the aqueous residue was acidified, and then extracted with EtOAc (3 x 25 mL). The combined organic layers were next extracted with saturated aqueous $NaHCO_3$ (3 x 25 mL), and then the aqueous extracts were acidified. Finally, EtOAc (3 x 25 mL) was used to extract the acid product, and the combined organic extracts were washed with saturated aqueous NaCl, dried (Na_2SO_4), filtered, and concentrated to afford **145** as a colorless amorphous solid (151 mg, 23% over 2 steps): ^{1}H NMR ($CDCl_3$, 400 MHz) δ 7.43 (d, *J* = 7.8 Hz, 1H), 7.17–7.11 (m, 3H), 6.96 (d, *J* = 7.8 Hz, 1H), 6.53–6.50 (m, 2H), 6.47–6.45 (m, 3H), 3.92 (s, 3H), 3.80 (s, 3H), 2.48 (s, 3H); ^{13}C NMR ($CDCl_3$, 125 MHz) δ 168.6. 160.9, 156.8, 154.3, 131.8 (3C), 130.1, 126.2, 125.5, 122.7, 118.4, 107.8 (4C), 106.4 (4C), 101.5 (3C), 55.3 (2C), 12.6; HRMS (ESI^+) *m/z*: $[M + H]^+$ calcd for $C_{26}H_{22}NO_7$, 460.1396; found, 460.1376.

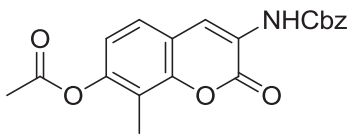

146

3-(((Benzyloxy)carbonyl)amino)-8-methyl-2-oxo-2H-chromen-7-yl acetate (146): A solution of coumarin **31**[102] (182 mg, 0.56 mmol) in pyridine (4.2 mL) was treated with acetic anhydride (1.4 mL). After 12 h, the solvent was concentrated and the residue purified via column chromatography (SiO_2, 40:1 CH_2Cl_2:Acetone) to afford **146** as a colorless amorphous solid (203 mg, 99%): ^{1}H NMR ($CDCl_3$, 400 MHz) δ 8.32 (s, 1H), 7.61 (s, 1H), 7.43–7.34 (m, 6H) 7.03 (d, *J* = 8.8 Hz, 1H), 5.26 (s, 2H), 2.39 (s, 3H), 2.30 (s, 3H); ^{13}C NMR ($CDCl_3$, 125 MHz) δ 168.9, 158.3, 153.1, 149.8 (2C), 148.5, 135.4, 128.7, 128.6, 128.3 (2C), 125.1, 123.4, 121.1, 119.2, 119.0, 117.6, 67.6, 20.8, 9.0; HRMS (ESI$^+$) *m/z*: $[M + Na]^+$ calcd for $C_{20}H_{17}NNaO_6$, 390.0954; found, 390.0957.

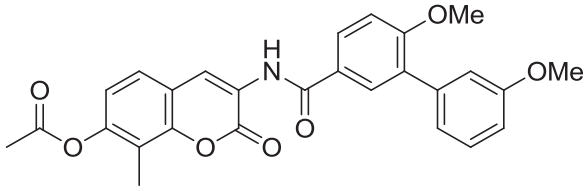

147

3-(3',6-Dimethoxy-[1,1'-biphenyl]-3-ylcarboxamido)-8-methyl-2-oxo-2H-chromen-7-yl acetate (147): Palladium on carbon (10%, 160 mg) was added to **146** (1.6 g, 4.36 mmol) in anhydrous THF (50 mL) and the solution was placed under an atmosphere of H_2. After 12 h, the solution was filtered through SiO_2 (40:1 CH_2Cl_2:Acetone) and the eluent was concentrated to afford a yellow solid, which was used without further purification (1.01 g, 99%).

A solution of 3',6-dimethoxy-[1,1'-biphenyl]-3-carbonyl chloride[170] (1.2 g, 4.36 mmol), in anhydrous THF (25 mL), was added to a solution of the amine (1.01 g, 4.31 mmol) and

anhydrous triethylamine (6.0 mL, 8.72 mmol) in anhydrous THF (25 mL). After 12 h, the solvent was concentrated and the residue purified via column chromatography (SiO_2, 40:1 CH_2Cl_2:Acetone) to afford **147** as a colorless amorphous solid (1.68 g, 81%): ^{1}H NMR ($CDCl_3$, 500 MHz) δ 8.84 (s, 1H), 8.76 (s, 1H), 7.93 (dd, *J* = 8.5, 2.5 Hz, 1H), 7.90 (d, *J* = 2.5 Hz, 1H), 7.41 (d, *J* = 8.5 Hz, 1H), 7.37 (t, *J* = 8.0 Hz, 1H), 7.14–7.12 (m, 1H), 7.10–7.09 (m, 2H), 7.07–7.03 (m, 1H), 6.95–6.93 (m, 1H) 3.91 (s, 3H), 3.86 (s, 3H), 2.37 (s, 3H), 2.31 (s, 3H); ^{13}C NMR ($CDCl_3$, 125 MHz) δ 168.9, 165.6, 159.9, 159.3, 159.0, 150.0, 148.7, 138.5, 131.1, 130.0, 129.2, 128.3, 125.8, 125.5, 123.6, 123.2, 122.0, 119.3, 119.0, 117.8, 115.2, 113.2, 111.0, 55.9, 55.3, 20.8, 9.1; HRMS (ESI$^+$) *m/z*: $[M + Na]^+$ calcd for $C_{27}H_{23}NNaO_7$, 496.1372; found, 496.1338.

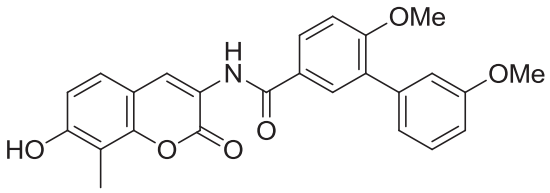

148

N-(7-hydroxy-8-methyl-2-oxo-2H-chromen-3-yl)-3',6-dimethoxy-[1,1'-biphenyl]-3-carboxamide (148): A solution of **147** (1.68 g, 3.55 mmol) in MeOH (36 mL) at rt was treated with triethylamine (3.6 mL, 10%). After 12 h, the solvent was concentrated and the residue purified via column chromatography (SiO_2, 10:1 CH_2Cl_2:Acetone) to afford **148** as a yellow amorphous solid (1.45 g, 93%): ^{1}H NMR ($CDCl_3$, 500 MHz) δ 8.80 (s, 1H), 8.69 (s, 1H), 7.92 (dd, *J* = 8.5, 2.0 Hz, 1H), 7.89 (d, *J* = 2.5 Hz, 1H), 7.37 (t, *J* = 8.5 Hz, 1H), 7.28 (s, 1H), 7.12 (d, *J* = 8.5 Hz, 1H), 7.10–7.07 (m, 2H), 6.93 (dd, *J* = 8.5, 2.0 Hz, 1H), 6.82 (d, *J* = 8.5 Hz, 1H), 5.31 (s, 1H), 3.90 (s, 3H), 3.86 (s, 3H), 2.36 (s, 3H); ^{13}C NMR ($CDCl_3$, 125 MHz) δ 165.6, 159.8, 159.5, 159.3, 155.5, 149.5, 138.6, 131.0, 130.0, 129.2, 128.2, 126.0, 125.9, 124.6, 122.0, 121.5, 115.2, 113.4, 113.2, 113.0, 111.7, 111.0, 55.9, 55.3, 7.9; HRMS (ESI$^+$) *m/z*: $[M + H]^+$ calcd for

$C_{25}H_{22}NO_6$, 432.1447; found, 432.1443. $[M + Na]^+$ calcd for $C_{25}H_{21}NNaO_6$, 454.1267; found, 454.1232.

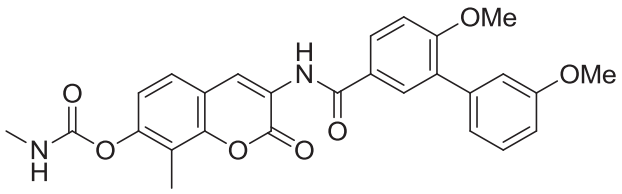

149

3-(3',6-Dimethoxy-[1,1'-biphenyl]-3-ylcarboxamido)-8-methyl-2-oxo-2H-chromen-7-yl methylcarbamate (149): A solution of **148** (30 mg, 0.070 mmol) in a 1:1 mixture of anhydrous CH_2Cl_2 (1.6 mL) and anhydrous pyridine (1.6 mL) at rt was treated with methylcarbamic chloride (9.8 mg, 0.10 mmol). After 12 h, the solvent was concentrated and the residue purified via column chromatography (SiO_2, 40:1 CH_2Cl_2:Acetone) to afford **149** as a yellow amorphous solid (33 mg, 99%): ^{1}H NMR ($CDCl_3$, 500 MHz) δ 8.80 (s, 1H), 8.69 (s, 1H), 7.92 (dd, *J* = 2.5, 8.8 Hz, 1H), 7.89 (d, *J* = 2.5 Hz, 1H), 7.37 (t, *J* = 8.0 Hz, 1H), 7.27 (d, *J* = 8.5 Hz, 1H), 7.12 (dd, *J* = 1.0, 7.5 Hz, 1H) 7.10–7.07 (m, 2H), 6.94 (td, *J* = 0.5, 2.5 Hz, 1H), 6.82 (d, *J* = 8.5 Hz, 1H), 5.32 (bs, 1H), 3.90 (s, 3H), 3.86 (s, 3H), 3.37 (s, 3H), 2.36 (s, 3H); ^{13}C NMR ($CDCl_3$, 125 MHz) δ 165.6, 159.8, 159.5, 159.3, 155.5, 149.5, 138.6, 131.0, 130.0, 129.2, 128.2, 126.0, 125.9, 124.5, 122.0, 121.5, 115.2, 113.4, 113.2, 113.0, 111.7 (2C), 111.0, 55.9, 55.3, 29.7, 7.9; HRMS (ESI^+) *m/z*: $[M + H]^+$ calcd for $C_{27}H_{25}N_2O_7$, 489.1662; found, 489.1674.

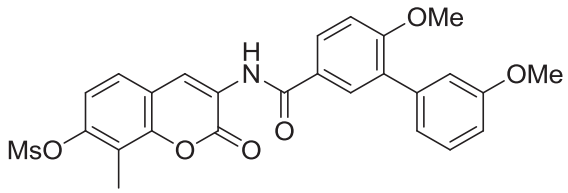

150

3-(3',6-Dimethoxy-[1,1'-biphenyl]-3-ylcarboxamido)-8-methyl-2-oxo-2H-chromen-7-yl methanesulfonate (150): Methanesulfonyl chloride (22 μL, 0.28 mmol) was added to **148** (30 mg, 0.070 mmol) in anhydrous pyridine (0.4 mL) at 0°C. The resulting solution was warmed to rt and stirred overnight, then diluted with H_2O. The desired product was extracted with EtOAc (3 × 10 mL); combined organic fractions were dried (Na_2SO_4), filtered, and concentrated. The residue was purified via column chromatography (SiO_2, 40:1 CH_2Cl_2:Acetone) to afford **150** as a yellow amorphous solid (35 mg, 99%): ^{1}H NMR ($CDCl_3$, 500 MHz) δ 8.85 (s, 1H), 8.78 (s, 1H), 7.93 (dd, *J* = 8.5, 2.5 Hz, 1H), 7.89 (d, *J* = 2.5 Hz, 1H), 7.44 (d, *J* = 8.5 Hz, 1H), 7.38 (t, *J* = 8.0 Hz, 1H), 7.31 (d, *J* = 8.5 Hz, 1H), 7.13 (dd, *J* = 1.5, 1.0 Hz, 1H), 7.12–7.08 (m, 2H), 6.95 (dd, *J* = 2.5, 0.5 Hz, 1H), 3.91 (s, 3H), 3.86 (s, 3H), 3.27 (s, 3H), 2.49 (s, 3H); ^{13}C NMR ($CDCl_3$, 125 MHz) δ 165.7, 160.0, 159.3, 158.7, 148.7, 147.7, 138.5, 131.1, 130.0, 129.2, 128.3, 125.8, 125.6, 124.2, 122.5, 122.0, 120.4, 119.3, 118.9, 115.3, 113.1, 111.0, 55.9, 55.3, 38.5, 9.7; HRMS (ESI$^+$) *m/z*: $[M + Na]^+$ calcd for $C_{26}H_{23}NNaO_8S$, 532.1042; found, 532.1031.

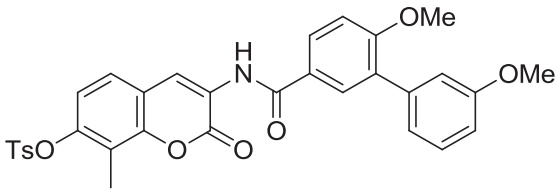

151

3-(3',6-Dimethoxy-[1,1'-biphenyl]-3-ylcarboxamido)-8-methyl-2-oxo-2H-chromen-7-yl 4-methylbenzenesulfonate (151): 4-methylbenzene-1-sulfonyl chloride (53 mg, 0.28 mmol) was added to **148** (30 mg, 0.070 mmol) in anhydrous pyridine (0.4 mL) at 0°C. The resulting solution was warmed to rt and stirred overnight, then diluted with H_2O. The desired product was extracted with EtOAc (3 × 10 mL); combined organic fractions were dried (Na_2SO_4), filtered, and concentrated. The residue was purified via column chromatography (SiO_2, 40:1

CH_2Cl_2:Acetone) to afford **151** as a colorless amorphous solid (40 mg, 99%): ^{1}H NMR ($CDCl_3$, 500 MHz) δ 8.81 (s, 1H), 8.75 (s, 1H), 7.92 (dd, *J* = 9.0, 2.5 Hz, 1H), 7.88 (d, *J* = 2.0 Hz, 1H), 7.75 (dd, *J* = 6.5, 1.5 Hz, 2H), 7.39–7.33 (m, 4H), 7.13–7.11 (m, 1H), 7.09–7.05 (m, 3H), 6.95–6.93 (m, 1H), 3.91 (s, 3H), 3.86 (s, 3H), 2.48 (s, 3H), 2.15 (s, 3H); ^{13}C NMR $CDCl_3$, 500 MHz) δ ; 165.6, 160.0, 159.3, 158.8, 148.5 (2C), 145.9, 138.5, 132.5, 131.1, 130.1, 130.0, 129.2, 128.5, 128.3, 125.6, 125.4, 124.0, 122.7, 122.0, 120.6, 119.6, 118.6, 115.3 (2C), 113. 1 (2C), 111.0, 55.9, 55.3, 21.8, 9.3; HRMS (ESI^+) *m/z*: $[M + H]^+$ calcd for $C_{32}H_{28}NO_8S$, 586.1536; found, 586.1500. $[M + Na]^+$ calcd for $C_{32}H_{27}NNaO_8S$, 608.1355; found, 608.1345.

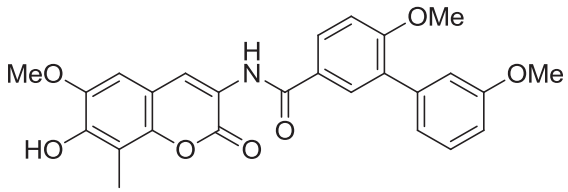

159

N-(7-hydroxy-6-methoxy-8-methyl-2-oxo-2H-chromen-3-yl)-3',6-dimethoxy-[1,1'-biphenyl]-3-carboxamide (159): A solution of **128a** (174 mg, 0.35 mmol) in MeOH (3.5 mL) was treated with triethylamine (0.35 mL). After 12 h, the solvent was removed and the residue purified via column chromatography (SiO_2, 10:1, CH_2Cl_2:Acetone) to afford **159** as a yellow amorphous solid (158 g, 99%): ^{1}H NMR ($CDCl_3$, 500 MHz) δ 8.79 (s, 1H), 8.71 (s, 1H), 7.92 (dd, *J* = 8.5, 2.5 Hz, 1H), 7.89 (d, *J* = 2.5 Hz, 1H), 7.37 (t, *J* = 8.0 Hz, 1H), 7.14–7.06 (m, 3H), 6.94–6.92 (m, 1H), 6.81 (s, 1H), 6.11 (s, 1H), 3.96 (s, 3H), 3.90 (s, 3H), 3.86 (s, 3H), 2.37 (s, 3H); ^{13}C NMR ($CDCl_3$, 125 MHz) δ 165.7, 159.9, 159.7, 159.5, 146.2, 144.5, 144.2, 138.8, 131.1, 130.1, 129.3, 128.3, 126.3, 124.7, 122.2, 122.0, 115.4, 113.3, 112.3, 111.9, 111.1, 104.5, 56.5, 56.0, 55.5, 8.3; IR (film) ν_{max} 3408, 2980, 2843, 2359, 2341, 1636, 1533, 1356, 1244, 1015, 918; HRMS (ESI^+) *m/z*: $[M + H]^+$ calcd for $C_{26}H_{24}NO_7$, 462.1553; found, 462.1529.

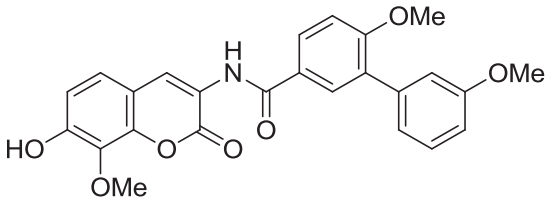

160

N-(7-hydroxy-8-methoxy-2-oxo-2H-chromen-3-yl)-3',6-dimethoxy-[1,1'-biphenyl]-3-carboxamide (160): A solution of **128g** (63 mg, 0.13 mmol) in MeOH (1.3 mL) at rt was treated with triethylamine (0.13 mL). After 12 h, the solvent was removed and the residue purified via column chromatography (SiO_2, 10:1, CH_2Cl_2:Acetone) to afford **160** as a yellow amorphous solid (57 mg, 99%): ^{1}H NMR ($CDCl_3$, 500 MHz) δ 8.82 (s, 1H), 8.66 (s, 1H), 7.92 (dd, *J* = 8.5, 2.5 Hz, 1H), 7.88 (d, *J* = 2.5 Hz, 1H), 7.37 (t, *J* = 8.0 Hz, 1H), 7.19 (d, *J* = 8.5 Hz, 1H), 7.13–7.07 (m, 3H), 6.97–6.92 (m, 2H), 6.03 (bs, 1H), 4.13 (s, 3H), 3.90 (s, 3H), 3.86 (s, 3H); ^{13}C NMR ($CDCl_3$, 125 MHz) δ 165.7, 160.0, 159.5, 158.7, 150.4, 143.1, 138.7, 133.7, 131.2, 130.1, 129.4, 128.3, 126.1, 124.8, 123.3, 122.1, 121.7, 115.4, 114.1, 113.3, 113.1, 111.2, 62.1, 56.1, 55.5; IR (film) ν_{max} 3348, 3038, 2970, 2847, 2093, 1643, 1014, 795; HRMS (ESI$^+$) *m/z*: [M + H]$^+$ calcd for $C_{25}H_{22}NO_7$, 448.1396; found, 448.1381.

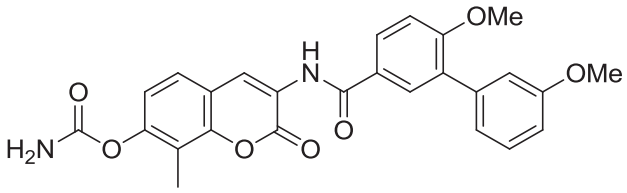

189a

3-(3',6-dimethoxy-[1,1'-biphenyl]-3-ylcarboxamido)-8-methyl-2-oxo-2H-chromen-7-yl carbamate (189a): A solution of sulfurisocyanatidic chloride (6.0 μL, 0.070 mmol), dissolved in anhydrous CH_2Cl_2 (0.20 mL), was slowly added to **148** (30 mg, 0.070 mmol) in anhydrous CH_2Cl_2 (1.20 mL) at rt. After 2 h, the solvent was removed and the residue was stirred with cold

H_2O overnight. The solid was collected by filtration, washing with H_2O, and thoroughly dried to afford **189a** as a yellow amorphous solid (19 mg, 56%): ^{1}H NMR (DMSO-d_6, 500 MHz) δ 9.77 (s, 1H), 8.59 (s, 1H), 8.01 (dd, J = 9.0, 2.5 Hz, 1H), 7.93 (d, J = 2.5 Hz, 1H), 7.62 (d, J = 8.5 Hz, 1H), 7.43 (bs, 1H), 7.37 (t, J = 8.0 Hz, 1H), 7.27 (d, J = 9.0 Hz, 1H), 7.14–7.09 (m, 4H), 6.97–6.94 (m, 1H), 3.87 (s, 3H), 3.80 (s, 3H), 2.21 (s, 3H); ^{13}C NMR (DMSO-d_6, 125 MHz) δ 168.5, 165.3, 159.2, 159.0, 154.2, 149.1, 138.7, 136.7, 130.1, 129.4, 129.3, 129.2, 127.9, 125.7, 125.6, 123.2, 121.8, 119.8, 118.4, 116.6, 115.3, 112.6, 111.6, 56.0, 55.2, 8.7; IR (film) ν_{max} 3053, 2986, 2305, 1713, 1603, 1522, 1421, 1367, 1265, 897, 748; HRMS (ESI$^+$) *m/z*: $[M + 2H]^+$ calcd for $C_{26}H_{24}N_2O_7$, 476.1584; found, 476.1514.

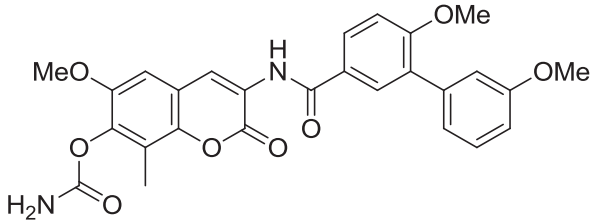

189b

3-(3',6-dimethoxy-[1,1'-biphenyl]-3-ylcarboxamido)-6-methoxy-8-methyl-2-oxo-2H-chromen-7-yl carbamate (189b): A solution of sulfurisocyanatidic chloride (3.8 μL, 0.043 mmol), dissolved in anhydrous CH_2Cl_2 (0.12 mL), was slowly added to **159** (20 mg, 0.043 mmol) in anhydrous CH_2Cl_2 (0.75 mL) at rt. After 2 h, the solvent was removed and the residue was stirred with cold H_2O overnight. The solid was collected by filtration, washing with H_2O, and thoroughly dried to afford **189b** as a yellow amorphous solid (11 mg, 50%): ^{1}H NMR ($CDCl_3$, 500 MHz) δ 8.81 (s, 1H), 8.78 (s, 1H), 7.92 (dd, J = 8.5, 2.5 Hz, 1H), 7.90 (d, J = 2.5 Hz, 1H), 7.37 (t, J = 8.0 Hz, 1H), 7.14–7.07 (m, 4H), 6.95–6.93 (m, 1H), 6.91 (s, 1H), 3.90 (s, 6H), 3.86 (s, 3H), 2.36 (s, 3H); ^{13}C NMR ($CDCl_3$, 125 MHz) δ 165.8, 160.0, 159.5, 159.2, 153.8, 149.6, 142.8, 139.7, 138.7, 131.2, 130.2, 129.3, 128.4, 126,1, 124.1, 123.3, 122.1, 121.3, 117.8,

115.4, 113.3, 111.1, 106.6, 56.5, 56.0, 55.5, 9.2; IR (film) ν_{max} 3053, 2986, 2684, 2305, 1421, 1265, 895, 750, 706; HRMS (ESI^+) *m/z*: $[M + 2H]^+$ calcd for $C_{27}H_{26}N_2O_8$, 506.1689; found, 506.1637.

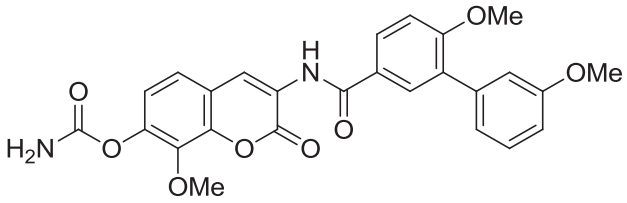

189c

3-(3',6-dimethoxy-[1,1'-biphenyl]-3-ylcarboxamido)-8-methoxy-2-oxo-2H-chromen-7-yl carbamate (189c): A solution of sulfurisocyanatidic chloride (11 μL, 0.13 mmol), dissolved in anhydrous CH_2Cl_2 (0.4 mL), was slowly added to **160** (30 mg, 0.066 mmol) in anhydrous CH_2Cl_2 (1.6 mL) at rt. After 2 h, the solvent was removed and the residue was stirred with cold H_2O overnight. The solid was collected by filtration, washing with H_2O, and thoroughly dried to afford **189c** as a colorless amorphous solid (22 mg, 68%): ^1H NMR (DMSO-d_6, 500 MHz) δ 9.78 (s, 1H), 8.58 (s, 1H), 8.01 (dd, *J* = 8.5, 2.5 Hz, 1H), 7.93 (d, *J* = 2.5 Hz, 1H), 7.49 (d, *J* = 8.5 Hz, 1H), 7.46 (bs, 1H), 7.37 (t, *J* = 8.0 Hz, 1H), 7.27 (d, *J* = 8.5 Hz, 1H), 7.16–7.10 (m, 4H), 6.97–6.94 (m, 1H), 3.91 (s, 3H), 3.87 (s, 3H), 3.80 (s, 3H); ^{13}C NMR ($CDCl_3$, 125 MHz) δ 165.8, 160.1, 159.5, 158.4, 154.1, 144.3, 143.7, 140.0, 138.7, 131.3, 130.1, 129.3, 128.4, 125.9, 123.9, 123.2, 122.2, 122.1, 120.3, 119.3, 115.4, 113.3, 111.2, 62.0, 56.1, 55.5; IR (film) ν_{max} 3406, 3271, 3053, 2986, 2359, 2339, 1715, 1672, 1603, 1531, 1502, 1366, 1265, 1082, 897, 737, 704; HRMS (ESI^+) *m/z*: $[M + H]^+$ calcd for $C_{26}H_{23}N_2O_8$, 491.1454; found, 491.1432.

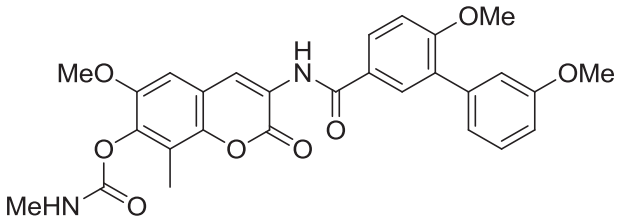

190b

3-(3',6-dimethoxy-[1,1'-biphenyl]-3-ylcarboxamido)-6-methoxy-8-methyl-2-oxo-2H-chromen-7-yl methylcarbamate (190b): A solution of **159** (20 mg, 0.043 mmol) in anhydrous pyridine (2.1 mL) was treated with methylcarbamic chloride (4.4 mg). After 12 h, the solvent was removed and the residue purified via column chromatography (SiO_2, 40:1, CH_2Cl_2:Acetone) to afford **190b** as a yellow amorphous solid (21 mg, 95%): ^{1}H NMR ($CDCl_3$, 500 MHz) δ 8.79 (s, 1H), 8.71 (s, 1H), 7.92 (dd, *J* = 8.5, 2.5 Hz, 1H), 7.89 (d, *J* = 2.5 Hz, 1H), 7.37 (t, *J* = 8.0 Hz, 1H), 7.13–7.06 (m, 3H), 6.95–6.92 (m, 1H), 6.81 (s, 1H), 6.11 (s, 1H), 3.96 (s, 3H), 3.90 (s, 3H), 3.86 (s, 3H), 3.37 (s, 3H), 2.37 (s, 3H); ^{13}C NMR ($CDCl_3$, 125 MHz) δ 165.7, 159.9, 159.7, 159.4, 146.1, 144.5, 144.2, 138.7 (2C), 131.1, 130.1, 129.3, 128.3, 126.3, 124.7, 122.1, 122.0, 115.4, 113.3, 112.2, 111.9, 111.1, 105.0, 56.4, 56.0, 55.5, 29.6, 8.3; IR (film) ν_{max} 3053, 2986, 2685, 2359, 2341, 2307, 1684, 1421, 1265, 1022, 897, 746, 704; HRMS (ESI$^+$) *m/z*: $[M + H]^+$ calcd for $C_{28}H_{27}N_2O_8$, 519.1767; found, 519.1839.

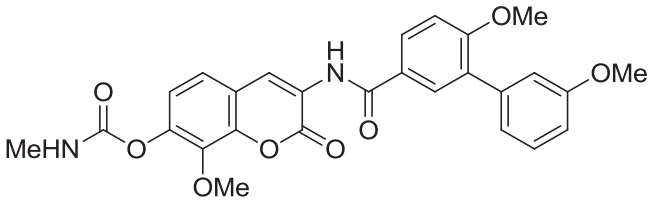

190c

3-(3',6-dimethoxy-[1,1'-biphenyl]-3-ylcarboxamido)-8-methoxy-2-oxo-2H-chromen-7-yl methylcarbamate (190c): A solution of **160** (33 mg, 0.074 mmol) in anhydrous pyridine (3.5

mL) was treated with methylcarbamic chloride (7.4 mg). After 12 h, the solvent was removed and the residue purified via column chromatography (SiO_2, 40:1, CH_2Cl_2:Acetone) to afford **190c** as a yellow amorphous solid (34 mg, 90%): ^{1}H NMR ($CDCl_3$, 500 MHz) δ 8.81 (s, 1H), 8.65 (bs, 1H), 7.97 (bs, 1H), 7.92 (dd, *J* = 8.5, 2.5 Hz, 1H), 7.88 (d, *J* = 2.5 Hz, 1H), 7.37 (t, *J* = 8.0 Hz, 1H), 7.18 (d, *J* = 8.5 Hz, 1H), 7.13–7.07 (m, 3H), 6.96 (d, *J* = 8.5 Hz, 1H), 6.95–6.93 (m, 1H), 4.12 (s, 3H), 3.90 (s, 3H), 3.86 (s, 3H); ^{13}C NMR ($CDCl_3$, 125 MHz) δ 165.7, 160.0, 159.5, 158.7, 150.4, 143.1, 141.6, 138.7, 133.7, 131.2, 130.1, 129.3, 128.3, 126.1, 124.8, 123.3, 122.1, 121.7, 115.4, 114.1, 113.3, 113.1, 111.2, 62.1, 56.0, 55.5, 29.9; IR (film) ν_{max} 3030, 2851, 2284, 1693, 1668, 1599, 1520, 1495, 1487, 1371, 1342, 1231, 1161, 1078, 964, 901, 856, 795; HRMS (ESI$^+$) *m/z*: $[M + Na]^+$ calcd for $C_{27}H_{24}N_2NaO_8$, 527.1430; found, 527.1403.

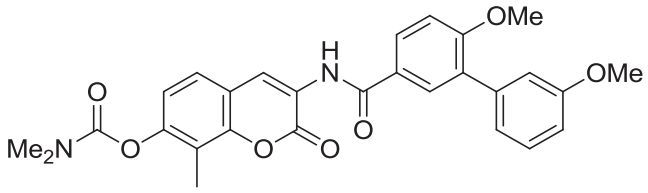

191a

3-(3',6-dimethoxy-[1,1'-biphenyl]-3-ylcarboxamido)-8-methyl-2-oxo-2H-chromen-7-yl dimethylcarbamate (191a): A solution of **148** (30 mg, 0.070 mmol) in pyridine (3.0 mL) at rt was treated with dimethylcarbamyl chloride (1.0 mL). After 12 h, the solvent was removed and the residue purified via column chromatography (SiO_2, 40:1, CH_2Cl_2:Acetone) to afford **191a** as a colorless amorphous solid (31 mg, 89%): ^{1}H NMR ($CDCl_3$, 500 MHz) δ 8.84 (s, 1H), 8.75 (s, 1H), 7.93 (dd, *J* = 8.5, 2.5 Hz, 1H), 7.90 (d, *J* = 2.0 Hz, 1H), 7.40–7.35 (m, 2H), 7.14–7.07 (m, 4H), 6.95–6.92 (m, 1H), 3.91 (s, 3H), 3.86 (s, 3H), 3.17 (s, 3H), 3.05 (s, 3H), 2.34 (s, 3H); ^{13}C NMR ($CDCl_3$, 125 MHz) δ 165.8, 160.0, 159.5, 159.3, 154.2, 151.0, 148.9, 138.7, 131.2, 130.1, 129.3, 128.4, 126.1, 125.5, 123.6, 123.5, 122.2, 119.9, 119.3, 117.4, 115.4, 113.3, 111.2, 56.1.

55.5, 37.0, 36.7, 9.1; IR (film) ν_{max} 3053, 2986, 2305, 1724, 1421, 1265, 1163, 895, 746, 706; HRMS (ESI^+) *m/z*: $[M + 2H]^+$ calcd for $C_{28}H_{28}N_2O_7$, 504.1897; found, 504.1822.

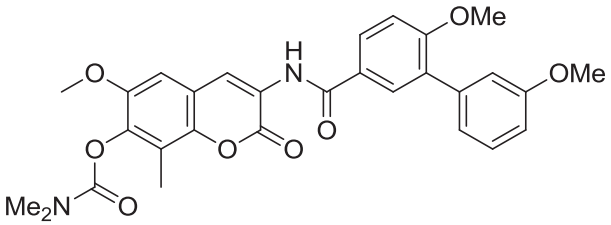

191b

3-(3',6-dimethoxy-[1,1'-biphenyl]-3-ylcarboxamido)-6-methoxy-8-methyl-2-oxo-2H-chromen-7-yl dimethylcarbamate (191b): A solution of **159** (25 mg, 0.054 mmol) in pyridine (2.25 mL) at rt was treated with dimethylcarbamyl chloride (0.75 mL). After 12 h, the solvent was removed and the residue purified via column chromatography (SiO_2, 40:1, CH_2Cl_2:Acetone) to afford **191b** as a yellow amorphous solid (25 mg, 85%): ^1H NMR ($CDCl_3$, 500 MHz) δ 8.81 (s, 1H), 8.77 (s, 1H), 7.92 (dd, *J* = 8.5, 2.5 Hz, 1H), 7.90 (d, *J* = 2.5 Hz, 1H), 7.37 (t, *J* = 8.0 Hz, 1H), 7.14–7.07 (m, 3H), 6.95–6.92 (m, 1H), 6.89 (s, 1H), 3.90 (s, 3H), 3.88 (s, 3H), 3.86 (s, 3H), 3.18 (s, 3H), 3.04 (s, 3H), 2.34 (s, 3H); ^{13}C NMR ($CDCl_3$, 125 MHz) δ 165.7, 160.0, 159.5, 159.3, 154.0, 149.7, 143.0, 140.8, 138.7, 131.2, 130.2, 129.3, 128.4, 126.1, 123.9, 123.6, 122.2, 121.1, 117.3, 115.4, 113.3, 111.1, 106.5, 56.5, 56.0, 55.5, 37.1, 36.8, 9.3; IR (film) ν_{max} 3053, 2986, 2305, 1724, 1713, 1672, 1603, 1522, 1501, 1421, 1383, 1267, 1163, 897, 739, 704; HRMS (ESI^+) *m/z*: $[M + H]^+$ calcd for $C_{29}H_{29}N_2O_8$, 533.1924; found, 533.1841.

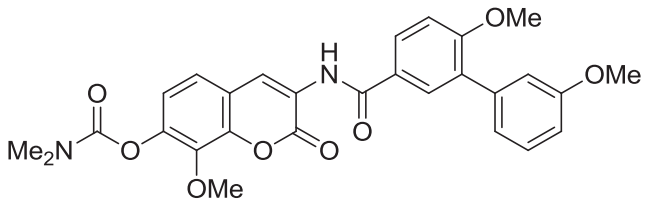

191c

3-(3',6-dimethoxy-[1,1'-biphenyl]-3-ylcarboxamido)-8-methoxy-2-oxo-2H-chromen-7-yl dimethylcarbamate (191c): A solution of **160** (25 mg, 0.056 mmol) in pyridine (2.25 mL) at rt was treated with dimethylcarbamyl chloride (0.75 mL). After 12 h, the solvent was removed and the residue purified via column chromatography (SiO_2, 40:1, CH_2Cl_2:Acetone) to afford **191c** as a colorless amorphous solid (19 mg, 65%): ^{1}H NMR ($CDCl_3$, 500 MHz) δ 8.84 (s, 1H), 8.74 (s, 1H), 7.92 (dd, *J* = 8.5, 2.5 Hz, 1H), 7.90 (d, *J* = 2.5 Hz, 1H), 7.38–7.35 (m, 2H), 7.13–7.07 (m, 4H), 6.95–6.93 (m, 1H), 4.05 (s, 3H), 3.91 (s, 3H), 3.86 (s, 3H), 3.16 (s, 3H), 3.05 (s, 3H); ^{13}C NMR ($CDCl_3$, 125 MHz) δ 165.8, 160.0, 158.6, 156.5, 153.0, 149.9, 145.5, 144.0, 142.6, 140.0, 135.6, 130.1, 129.3, 128.4 (2C), 126.0, 123.5, 122.1, 120.5, 118.9, 115.4, 113.3, 111.2, 61.9, 56.0, 55.5, 36.8 (2C); IR (film) ν_{max} 3053, 2986, 2930, 2685, 2305, 1603, 1421, 1265, 1157, 1024, 895, 737, 704; HRMS (ESI$^+$) *m/z*: $[M + H]^+$ calcd for $C_{28}H_{27}N_2O_8$, 519.1767; found, 519.1750.

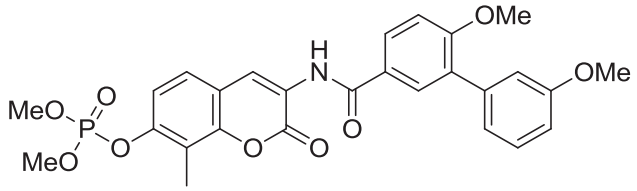

192a

3-(3',6-dimethoxy-[1,1'-biphenyl]-3-ylcarboxamido)-8-methyl-2-oxo-2H-chromen-7-yl dimethyl phosphate (192a): Dimethyl phosphorochloridate (6.3 μL, 0.058 mmol) was slowly added to **148** (25 mg, 0.058 mmol) and 4-dimethylaminopyridine (7.1 mg, 0.058 mmol) in anhydrous CH_2Cl_2 (1.2 mL) at rt. After 12 h, the solvent was removed and the residue purified via column chromatography (SiO_2, 40:1 → 10:1 CH_2Cl_2:Acetone) to afford **192a** as a colorless amorphous solid (17 mg, 54%): ^{1}H NMR ($CDCl_3$, 500 MHz) δ 8.83 (s, 1H), 8.74 (s, 1H), 7.93 (dd, *J* = 8.5, 2.5 Hz, 1H), 7.89 (d, *J* = 2.0 Hz, 1H), 7.39–7.36 (m, 2H), 7.32 (d, *J* = 9.0 Hz, 1H),

7.13–7.07 (m, 3H), 6.95–6.93 (m, 1H), 3.92 (s, 3H), 3.91 (s, 3H), 3.90 (s, 3H), 3.86 (s, 3H), 2.44 (s, 3H); ^{13}C NMR ($CDCl_3$, 125 MHz) δ 165.7, 160.0, 159.5, 159.1, 149.9, 149.8, 149.0, 138.7, 131.2, 130.1, 129.3, 128.4, 125.9, 125.8, 123.5, 123.3, 122.1, 118.1, 117.2, 115.4, 113.3, 111.2, 56.0, 55.5, 55.3 (2C), 9.0; IR (film) ν_{max} 3404, 3053, 2986, 2930, 2854, 2305, 1715, 1674, 1605, 1522, 1501, 1421, 1366, 1265, 1055, 897, 725, 704; HRMS (ESI$^+$) *m/z*: $[M + 2H]^+$ calcd for $C_{27}H_{28}NO_9P$, 541.1502; found, 541.1454.

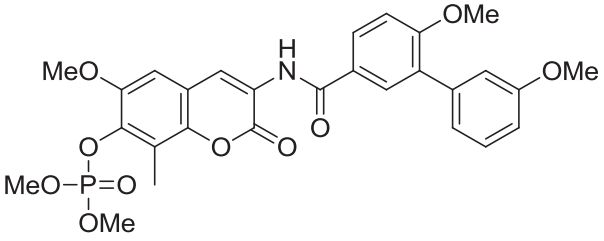

192b

3-(3',6-dimethoxy-[1,1'-biphenyl]-3-ylcarboxamido)-6-methoxy-8-methyl-2-oxo-2H-chromen-7-yl dimethyl phosphate (192b): Dimethyl phosphorochloridate (7.0 μL, 0.065 mmol) was slowly added to **159** (30 mg, 0.065 mmol) and 4-dimethylaminopyridine (8 mg, 0.065 mmol) in anhydrous CH_2Cl_2 (1.3 mL) at rt. After 12 h, the solvent was removed and the residue purified via column chromatography (SiO_2, 40:1 → 10:1 CH_2Cl_2:Acetone) to afford **192b** as a colorless amorphous solid (14 mg, 41%): ^{1}H NMR ($CDCl_3$, 500 MHz) δ 8.79 (s, 1H), 8.77 (s, 1H), 7.92 (dd, *J* = 8.5, 2.5 Hz, 1H), 7.89 (d, *J* = 2.5 Hz, 1H), 7.37 (t, *J* = 8.0 Hz, 1H), 7.13–7.06 (m, 3H), 6.94–6.92 (m, 1H), 6.90 (s, 1H), 3.95 (s, 3H), 3.93 (s, 3H), 3.93 (s, 3H), 3.90 (s, 3H), 3.86 (s, 3H), 2.46 (s, 3H); ^{13}C NMR ($CDCl_3$, 125 MHz) δ 165.8, 160.0, 159.5, 159.2, 148.9 (2C), 138.7, 131.2, 130.2, 129.3, 128.4, 126.0, 124.0, 123.2, 122.1, 120.4, 117.1 (2C), 115.4, 113.3, 111.1, 106.9, 56.5, 56.0, 55.5, 55.3, 55.2, 9.7; IR (film) ν_{max} 3053, 2986, 2685,

2305, 1713, 1522, 1501, 1421, 1385, 1265, 897, 746, 704; HRMS (ESI^+) *m/z*: $[M + Na]^+$ calcd for $C_{28}H_{28}NNaO_{10}P$, 592.1349; found, 592.1341.

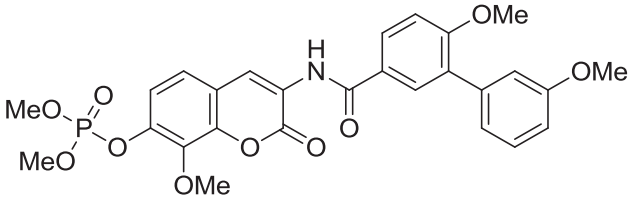

192c

3-(3',6-dimethoxy-[1,1'-biphenyl]-3-ylcarboxamido)-8-methoxy-2-oxo-2H-chromen-7-yl dimethyl phosphate (192c): Dimethyl phosphorochloridate (4.0 μL, 0.038 mmol) was slowly added to **1c** (17 mg, 0.038 mmol) and 4-dimethylaminopyridine (5 mg, 0.038 mmol) in anhydrous CH_2Cl_2 (0.8 mL) at rt. After 12 h, the solvent was removed and the residue purified via column chromatography (SiO_2, 40:1) to afford **192c** as a yellow amorphous solid (6.0 mg, 30%): ^1H NMR ($CDCl_3$, 500 MHz) δ 8.82 (s, 1H) 8.74 (s, 1H), 7.92 (dd, *J* = 8.5, 2.5 Hz, 1H), 7.88 (d, *J* = 2.5 Hz, 1H), 7.37 (t, *J* = 8.0 Hz, 1H), 7.29 (dd, *J* = 8.5, 1.0 Hz, 1H), 7.25–7.23 (m, 1H), 7.13–7.07 (m, 3H), 6.95–6.93 (m, 1H) 4.09 (s, 3H), 3.94 (s, 3H), 3.92 (s, 3H), 3.91 (s, 3H), 3.86 (s, 3H); ^{13}C NMR ($CDCl_3$, 125 MHz) δ 165.7, 160.1, 159.5, 158.4, 144.4, 144.0, 138.6, 131.3, 130.1, 129.3, 128.4, 125.8, 123.8, 123.1, 122.4, 122.1, 118.6, 118.5, 118.4, 115.4, 113.3, 111.2, 62.2, 56.0, 55.5, 55.3 (2C); IR (film) ν_{max} 3053, 2959, 2928, 2854, 2361, 2307, 1718, 1674, 1605, 1522, 1501, 1462, 1366, 1265, 1207, 1180, 1038, 1024, 916, 858, 735, 704; HRMS (ESI^+) *m/z*: $[M + Na]^+$ calcd for $C_{27}H_{26}NNaO_{10}P$, 578.1192; found, 578.1147.

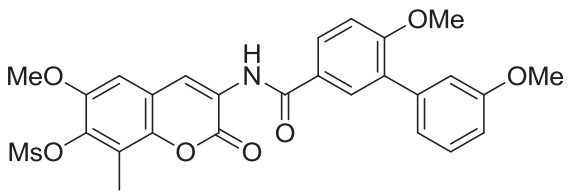

193b

3-(3',6-dimethoxy-[1,1'-biphenyl]-3-ylcarboxamido)-6-methoxy-8-methyl-2-oxo-2H-chromen-7-yl methanesulfonate (193b): Methanesulfonyl chloride (10 μL, 0.13 mmol) was added to **159** (15 mg, 0.033 mmol) in anhydrous pyridine (0.20 mL) at 0°C. The resulting solution was warmed to rt and stirred overnight, then diluted with H_2O. The desired product was extracted with EtOAc (3 × 10 mL); combined organic fractions were dried (Na_2SO_4), filtered, and concentrated. The residue was purified via column chromatography (SiO_2, 40:1, CH_2Cl_2:Acetone) to afford **193b** as a yellow amorphous solid (13 mg, 97%): ^{1}H NMR (DMSO-d_6, 500 MHz) δ 9.77 (s, 1H), 8.64 (s, 1H), 8.01 (dd, J = 8.5, 2.5 Hz, 1H), 7.92 (d, J = 2.5 Hz, 1H), 7.49 (s, 1H), 7.37 (t, J = 8.0 Hz, 1H), 7.27 (d, J = 9.0 Hz, 1H), 7.12–7.10 (m, 2H), 6.97–6.95 (m, 1H), 3.91 (s, 3H), 3.87 (s, 3H), 3.80 (s, 3H), 3.54 (s, 3H), 2.36 (s, 3H); ^{13}C NMR (DMSO-d_6, 125 MHz) δ 165.4, 159.3, 159.0, 157.7, 149.2, 148.9, 139.1, 138.7, 130.1, 129.3, 129.2, 128.9, 126.2, 124.6, 121.8, 121.2, 118.1, 115.3 (2C), 112.6, 111.5, 108.0, 55.1 (2C), 54.8, 29.1, 10.0; IR (film) ν_{max} 3053, 2986, 2928, 2685, 2305, 1717, 1601, 1421, 1383, 1265, 1153, 895, 737, 704; HRMS (ESI$^+$) *m/z*: $[M + H]^+$ calcd for $C_{27}H_{26}NO_9S$, 540.1328; found, 540.1395.

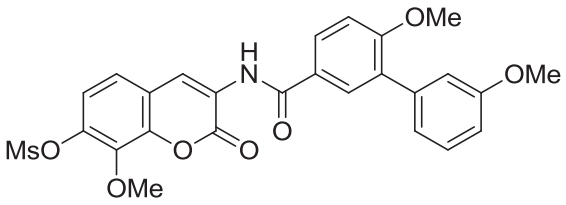

193c

3-(3',6-dimethoxy-[1,1'-biphenyl]-3-ylcarboxamido)-8-methoxy-2-oxo-2H-chromen-7-yl methanesulfonate (193c): Methanesulfonyl chloride (17 μL, 0.22 mmol) was added to **160** (25 mg, 0.056 mmol) in anhydrous pyridine (0.40 mL) at 0°C. The resulting solution was warmed to rt and stirred overnight, then diluted with H_2O. The desired product was extracted with EtOAc (3 × 10 mL); combined organic fractions were dried (Na_2SO_4), filtered, and concentrated. The

residue was purified via column chromatography (SiO_2, 40:1, CH_2Cl_2:Acetone) to afford **193c** as a yellow amorphous solid (29 mg, 99%): ^{1}H NMR ($CDCl_3$, 500 MHz) δ 8.80 (s, 1H), 8.73 (s, 1H), 7.88 (dd, *J* = 8.5, 2.0 Hz, 1H), 7.85 (d, *J* = 2.5 Hz, 1H), 7.34 (t, *J* = 8.0 Hz, 1H), 7.26–7.23 (m, 2H), 7.09–7.04 (m, 3H), 6.91–6.89 (m, 1H), 4.09 (s, 3H), 3.87 (s, 3H), 3.83 (s, 3H), 3.23 (s, 3H); ^{13}C NMR ($CDCl_3$, 125 MHz) δ 165.7, 160.2, 159.5, 158.0, 143.6, 142.4, 140.0, 138.6, 131.2, 130.1, 129.3, 128.4, 125.7, 124.6, 122.5 (2C), 122.1, 121.1, 120.6, 115.4, 113.2, 111.2, 62.6, 56.0, 55.4, 38.6; IR (film) ν_{max} 2928, 2359, 2341, 1720, 1676, 1603, 1521, 1501, 1464, 1364, 1242, 1180, 1078, 970, 860; HRMS (ESI$^+$) *m/z*: $[M + H]^+$ calcd for $C_{26}H_{24}NO_9S$, 526.1172; found, 526.1179.

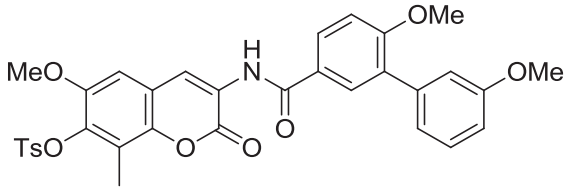

194b

3-(3',6-dimethoxy-[1,1'-biphenyl]-3-ylcarboxamido)-6-methoxy-8-methyl-2-oxo-2H-chromen-7-yl 4-methylbenzenesulfonate (194b): 4-methylbenzene-1-sulfonyl chloride (50 μL, 0.26 mmol) was added to **159** (30 mg, 0.065 mmol) in anhydrous pyridine (0.40 mL) at 0°C. The resulting solution was warmed to rt and stirred overnight, then diluted with H_2O (10 mL). The desired product was extracted with EtOAc (3 × 10 mL); combined organic fractions were dried (Na_2SO_4), filtered, and concentrated. The residue was purified via column chromatography (SiO_2, 40:1, CH_2Cl_2:Acetone) to afford **194b** as a yellow amorphous solid (39 mg, 98%): ^{1}H NMR ($CDCl_3$, 500 MHz) δ 8.79 (s, 1H), 8.78 (s, 1H), 7.92 (dd, *J* = 8.5, 2.5 Hz, 1H), 7.89 (d, *J* = 2.5 Hz, 1H), 7.86 (d, *J* = 8.5 Hz, 1H), 7.39–7.36 (m, 3H), 7.13–7.07 (m, 3H), 6.95–6.93 (m, 1H), 6.81 (s, 1H), 3.91 (s, 3H), 3.86 (s, 3H), 3.59 (s, 3H), 2.49 (s, 3H), 2.37 (s, 3H); ^{13}C NMR

($CDCl_3$, 125 MHz) δ 165.8, 160.0, 159.4, 159.0, 149.8, 145.3, 142.6, 138.7, 138.6, 134.3, 131.2, 130.2, 129.7 (2C), 129.3, 128.5 (2C), 128.4, 125.8, 124.6, 123.0, 122.7, 122.1, 118.6, 115.4, 113.2, 111.1, 106.6, 56.0, 55.9, 55.4, 21.9, 10.4; IR (film) ν_{max} 3053, 2986, 2685, 2305, 1713, 1601, 1421, 1383, 1265, 1163, 895, 739, 706; HRMS (ESI^+) *m/z*: $[M + H]^+$ calcd for $C_{33}H_{30}NO_9S$, 616.1641; found, 616.1676.

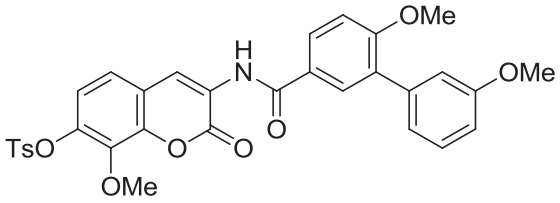

194c

3-(3',6-dimethoxy-[1,1'-biphenyl]-3-ylcarboxamido)-8-methoxy-2-oxo-2H-chromen-7-yl 4-methylbenzenesulfonate (194c): 4-methylbenzene-1-sulfonyl chloride (43 μL, 0.22 mmol) was added to **160** (25 mg, 0.056 mmol) in anhydrous pyridine (0.40 mL) at 0°C. The resulting solution was warmed to rt and stirred overnight, then diluted with H_2O (10 mL). The desired product was extracted with EtOAc (3 × 10 mL); combined organic fractions were dried (Na_2SO_4), filtered, and concentrated. The residue was purified via column chromatography (SiO_2, 40:1, CH_2Cl_2:Acetone) to afford **194c** as a colorless amorphous solid (33 mg, 99%): ^1H NMR ($CDCl_3$, 500 MHz) δ 8.80 (s, 1H), 8.74 (s, 1H), 7.91 (dd, *J* = 8.5, 2.5 Hz, 1H), 7.88 (d, *J* = 2.5 Hz, 1H), 7.81–7.79 (m, 2H), 7.38–7.34 (m, 3H), 7.19 (d, *J* = 8.5 Hz, 1H), 7.12–7.07 (m, 4H), 6.95–6.92 (m, 1H), 3.91 (s, 3H), 3.90 (s, 3H), 3.86 (s, 3H), 2.47 (s, 3H); ^{13}C NMR ($CDCl_3$, 125 MHz) δ 165.7, 160.2, 159.5, 158.1, 145.9, 143.5, 142.6, 140.5, 138.6, 132.9, 131.3, 130.1, 130.0 (2C), 129.3, 128.6 (2C), 128.4, 125.7, 124.4, 122.7, 122.1, 121.9, 120.5, 120.2, 115.4, 113.3, 111.2, 62.1, 56.0, 55.5, 21.9; IR (film) ν_{max} 3053, 2927, 2359, 2341, 1720, 1676, 1603, 1522,

1501, 1462, 1364, 1265, 1178, 1078, 1007, 858, 818, 737, 706; HRMS (ESI^+) *m/z*: $[M + H]^+$ calcd for $C_{32}H_{28}NO_9S$, 602.1485; found, 602.1494.

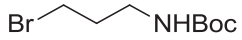

202

***Tert*-butyl (3-bromopropyl)carbamate (202):**[263] Di-*tert*-butyl dicarbonate (1.25 g, 5.71 mmol) was added to a solution of 3-bromopropan-1-aminium bromide (500 mg, 2.28 mmol) and DMAP (279 mg, 2.28 mmol) in anhydrous *N,N*-dimethylformamide (22.8 mL), and then stirred for 12 h. Water (50 mL) was added and the solution was extracted with EtOAc (3 x 30 mL), washed with saturated aqueous NaCl, dried (Na_2SO_4), filtered, and concentrated. The residue was purified via column chromatography (SiO_2, 6:1 Hexane:EtOAc) to afford **202** as a yellow oil (448 mg, 82%): ^{1}H NMR ($CDCl_3$, 400 MHz) δ 4.68 (bs, 1H), 3.46 (t, *J* = 6.4 Hz, 2H), 3.29 (d, *J* = 6.0 Hz, 2H), 2.07 (t, *J* = 6.4 Hz, 2H), 1.46 (s, 9H).

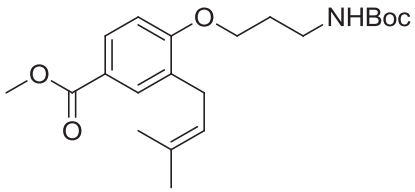

204

Methyl 4-(3-((*tert*-butoxycarbonyl)amino)propoxy)-3-(3-methylbut-2-en-1-yl)benzoate (204): Alkyl bromide **202** (257 mg, 1.08 mmol) was added to a solution of methyl 4-hydroxy-3-(3-methylbut-2-en-1-yl)benzoate[18] (100 mg, 0.45 mmol) and potassium carbonate (188 mg, 1.36 mmol) in MeCN (2.30 mL), then heated at reflux for 12 h. Once cool, solvent was removed and the residue was resuspended in EtOAc, washed with saturated aqueous NaCl, dried (Na_2SO_4), filtered, and concentrated. The residue was purified via column chromatography (SiO_2, 3:1 Hexane:EtOAc) to afford **204** as a yellow oil (171 mg, 99%): ^{1}H NMR ($CDCl_3$, 500 MHz) δ 8.5

(d, J = 8.5 Hz, 1H), 7.85 (s, 1H), 6.87–6.85 (m, 1H), 5.30 (d, J = 4.0 Hz, 1H), 4.78 (bs, 2H), 3.90 (d, J = 5.5 Hz, 3H), 3.35 (d, J = 6.5 Hz, 4H), 2.07–2.05 (m, 2H), 1.77 (s, 3H), 1.74 (s, 3H), 1.46 (s, 9H); ^{13}C NMR ($CDCl_3$, 125 MHz) δ 167.1, 160.2, 156.0, 133.0, 130.9, 130.1, 129.4, 122.3, 121.8, 110.2, 79.3, 66.0, 51.8, 38.0, 29.7, 29.5, 29.3, 28.6, 28.4, 25.8, 17.9; HRMS (ESI$^+$) *m/z*: $[M + Na]^+$ calcd for $C_{21}H_{31}NNaO_5$, 400.2100; found, 400.2091.

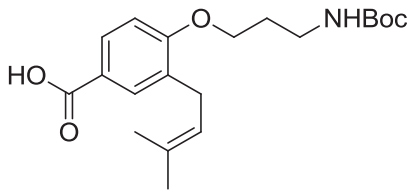

205

4-(3-((*Tert*-butoxycarbonyl)amino)propoxy)-3-(3-methylbut-2-en-1-yl)benzoic acid (205): Lithium hydroxide (14.0 mg, 0.17 mmol) was added to a solution of **204** (15.0 mg, 0.040 mmol) in 3:1:1 THF:MeOH:H_2O (0.34 mL). After 12 h, the solution was concentrated and the aqueous residue was acidified, and then extracted with EtOAc (3 x 10 mL). The combined organic layers were next extracted with saturated aqueous $NaHCO_3$ (3 x 10 mL), and then the aqueous extracts were acidified. Finally, EtOAc (3 x 10 mL) was used to extract the acid product, and the combined organic extracts were washed with saturated aqueous NaCl, dried (Na_2SO_4), filtered, and concentrated to afford **205** as a colorless amorphous solid (14.0 mg, 97%): ^{1}H NMR ($CDCl_3$, 400 MHz) δ 7.94 (s, 1H), 7.89 (s, 1H), 6.97 (d, J = 8.0 Hz, 1H), 5.31 (t, J = 7.6 Hz, 1H), 4.82 (bs, 1H), 4.13 (t, J = 5.6 Hz, 2H), 3.35 (d, J = 7.2 Hz, 4H), 2.07 (bs, 2H), 1.77 (s, 3H), 1.73 (s, 3H), 1.46 (s, 9H); ^{13}C NMR ($CDCl_3$, 125 MHz) δ 171.5, 160.9, 156.0, 133.2 (2C), 131.5, 130.2, 121.6, 121.4, 110.2, 79.4, 66.1, 38.0, 29.5 (4C), 28.4, 25.8, 17.9; HRMS (ESI$^+$) *m/z*: $[M + H]^+$ calcd for $C_{20}H_{30}NO_5$, 364.2124; found, 364.2126.

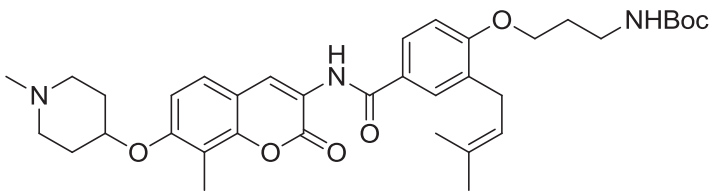

207

***Tert*-butyl (3-(4-((8-methyl-7-((1-methylpiperidin-4-yl)oxy)-2-oxo-2H-chromen-3-yl)-carbamoyl)-2-(3-methylbut-2-en-1-yl)phenoxy)propyl)carbamate (207):** EDCI (80 mg, 0.42 mmol) and **205** (110 mg, 0.30 mmol) were added to aminocoumarin **206** (48 mg, 0.17 mmol), freshly prepared from hydrogenolysis of **210**, in 30% pyridine/CH_2Cl_2 (2.10 mL). After 12 h, the solvent was concentrated and the residue was purified via column chromatography (SiO_2, 10:1 CH_2Cl_2:MeOH) to afford **207** as a colorless oil (45 mg, 43%): ^{1}H NMR ($CDCl_3$, 400 MHz) δ 8.81 (s, 1H), 8.70 (s, 1H), 7.77 (d, *J* = 8.8 Hz, 1H), 7.74 (s, 1H), 7.35 (d, *J* = 8.8 Hz, 1H), 6.93 (d, *J* = 8.8 Hz, 1H), 6.89 (d, *J* = 8.8 Hz, 1H), 5.33 (t, *J* = 7.6 Hz, 1H), 4.80 (bs, 1H), 4.59 (bs, 1H), 4.14 (t, *J* = 5.6 Hz, 2H), 3.39 (d, *J* = 7.2 Hz, 4H), 2.84 (bs, 2H), 2.71 (bs, 2H), 2.50 (bs, 3H), 2.37 (s, 3H), 2.20 (bs, 2H), 2.06 (bs, 4H), 1.79 (s, 3H), 1.75 (s, 3H), 1.46 (s, 9H); ^{13}C NMR ($CDCl_3$, 125 MHz) δ 165.9, 159.9, 159.5, 156.0, 149.4, 133.2, 130.7, 128.6, 126.6 (2C), 125.7, 125.6, 124.0, 121.9, 121.4, 115.1, 113.7, 110.5, 110.3, 79.5 (2C), 66.2, 52.1 (2C), 45.1, 38.0, 29.7, 29.5, 28.5, 28.4 (3C), 25.8, 17.9, 14.1, 8.4; HRMS (ESI^+) *m/z*: $[M + Na]^+$ calcd for $C_{36}H_{47}N_3NaO_7$, 656.3312; found, 656.3330.

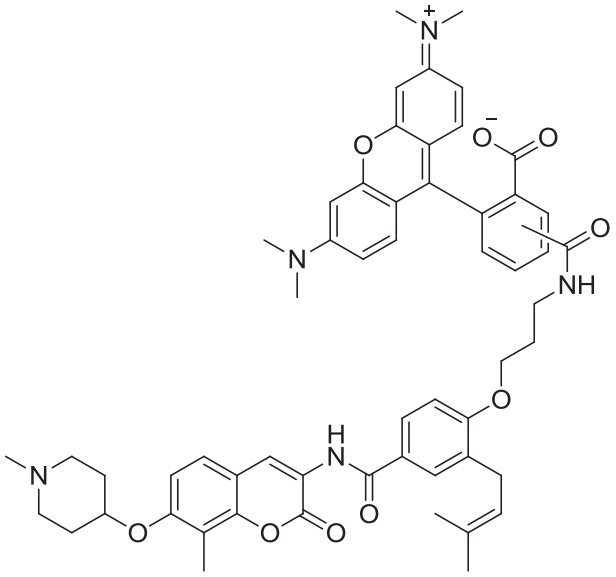

209

2-(3,6-Bis(dimethylamino)-3H-xanthen-9-yl)-5-((3-(4-((8-methyl-7-((1-methylpiperidin-4-yl)oxy)-2-oxo-2H-chromen-3-yl)carbamoyl)-2-(3-methylbut-2-en-1-yl)phenoxy)propyl)carbamoyl)benzoate, and **2-(3,6-bis(dimethylamino)-3H-xanthen-9-yl)-6-((3-(4-((8-methyl-7-((1-methylpiperidin-4-yl)oxy)-2-oxo-2H-chromen-3-yl)carbamoyl)-2-(3-methylbut-2-en-1-yl)phenoxy)propyl)carbamoyl)benzoate (209):** Trifluoroacetic acid (10 μL) was added to a solution of **207** (8.0 mg, 0.013 mmol) in CH_2Cl_2 (0.1 mL) and stirred for 12 h. Solvent was removed and the residue was purified via column chromatography (SiO_2, 10:1 CH_2Cl_2:MeOH) to afford amine (5.50 mg, 82%), which was used without further purification.

N,N-diisopropylethylamine (1 μL) was added to a solution of 5-(and-6)-carboxytetramethylrhodamine, succinimidyl ester **208** (4.9 mg, 0.0094 mmol) and amine (5.50 mg, 0.010 mmol) in 10:1 CH_2Cl_2:DMF (94 μL) at rt for 12 h. Water (10 mL) was added and the solution was extracted with EtOAc (3 x 15 mL), dried (Na_2SO_4), filtered, and concentrated to afford **209** as confirmed by mass spectrometry. HRMS (ESI^+) *m/z*: $[M + H]^+$ calcd for $C_{56}H_{60}N_5O_9$, 946.4391; found, 946.4355.

Chapter IV

Studies on the Novobiocin Benzamide Side Chain

I. Introduction

Modifications to the benzamide side chain of novobiocin analogues have yielded some of the most remarkable improvements in activity. While various analogues have explored important interactions (Figure 61), none have probed the limits of the site into which this side chain extends. Although no co-crystal structure of the *C*-terminal binding site has been reported, recent collaborative studies have yielded a C-terminal Hsp90 binding model. Examination of this model revealed a number of hydrophobic residues surrounding the cavity into which the benzamide portion projects. Using this model, in addition to previously determined SAR for the coumarin and sugar portions, several rationally designed compounds that manifest low micromolar antiproliferative activity have been produced.

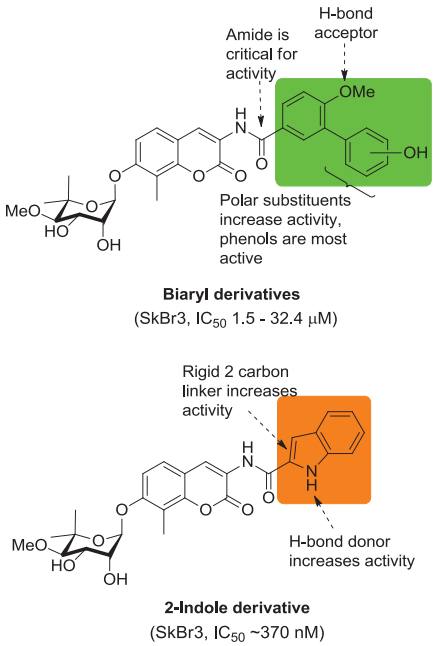

Figure 61. Key SAR from benzamide study.[102]

II. Rational design of ^{t}Bu and O^{t}Bu benzamide-containing novobiocin analogues

As previously discussed, elucidation of a binding model for the Hsp90 C-terminal nucleotide binding site has enabled the rational design of novobiocin analogues. Due to the importance of the benzamide side chain, such as the ability to inter convert between non-toxic and cytotoxic agents through simple modification, it was believed that further studies are needed to further probe its nature. Rather than taking advantage of the hydrogen bonding network, these analogues sought to probe the hydrophobicity of the region into which the prenyl side chain of novobiocin extends.

A. Molecular modeling studies with novobiocin

As seen in Figure 62, the novobiocin prenyl side chain sits in a pocket flanked with residues of diverse nature. While the region of the pocket wherein the amide and phenol bind is largely dominated by polar and charged residues, whereas the prenyl group folds back into a hydrophobic region. The predominance of polar and charged residues in this benzamide binding portion explains the success of compounds like those shown in Figure 61, which are capable of producing key hydrogen bonds. In contrast, it is proposed that favorable interactions between the prenyl group with Leu-714 and Val-715, two amino acids with hydrophobic side chains found in its vicinity, contribute to the binding affinity of novobiocin. Moreover, it is hypothesized that hydrophobic groups installed on the benzamide side chain would increase the affinity of novobiocin analogues for this binding pocket, allowing the analogues to interact with this hydrophobic cleft similar to the prenyl group on novobiocin.

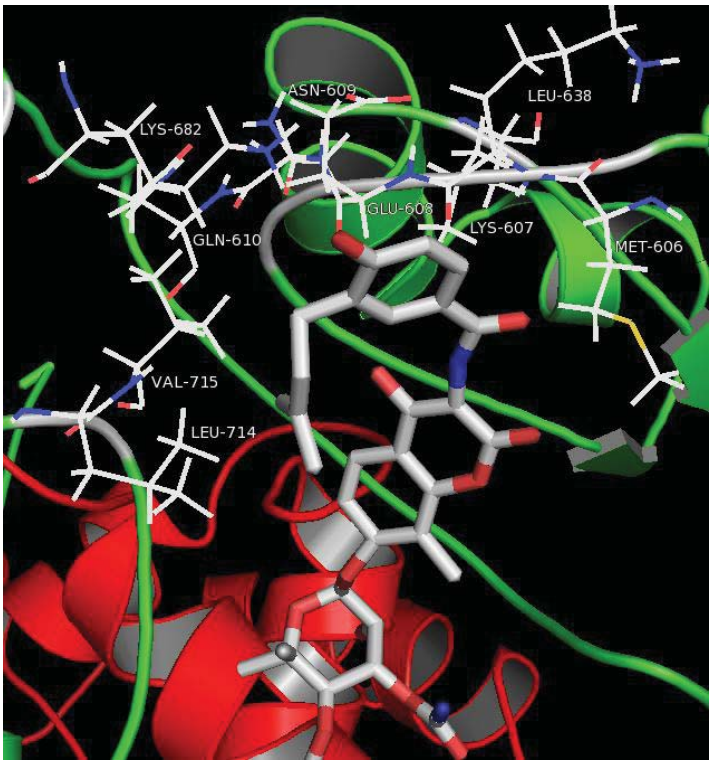

Figure 62. Examination of novobiocin prenyl side chain docked in Hsp90α model.

B. Design of aryl ^{t}Bu benzamide-containing novobiocin analogues

In order to capitalize on interactions with these key hydrophobic residues, a ^{t}Bu group was installed at various positions around the aryl ring. Based on the molecular modeling studies with novobiocin, it was proposed that placement of the hydrophobic ^{t}Bu substituent would be most favorable at the meta and para positions. The 8-methyl coumarin was chosen as the scaffold upon which to append these side chains because of its ease of synthesis and the many studies in which it has been used, offering several compounds for comparison. Moreover, since the coumarin core and benzamide side chain remained largely unperturbed by variation of the sugar (Section II-3.A), the optimal sugar surrogates from the studies outlined in Chapter III were installed on the final analogues.

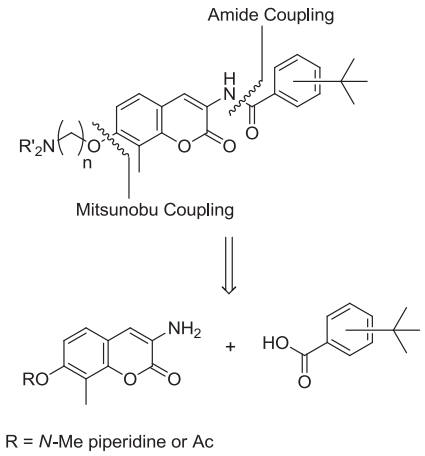

Scheme 51. Retrosynthetic analysis of aryl tBu analogues.

The coumarin and acids were prepared independently, and then coupled as shown in Scheme 51. While the piperidine-containing analogues could be readily obtained by coupling with the aminocoumarin functionalized at the 7-position piperidine ring, the alkyl sugar was installed after amide coupling. These 3-(dimethylamino)propane-containing analogues were accessed through coupling the desired sugars to the 7-acetate protected aminocoumarin, then solvolysis and subsequent Mitsunobu coupling to the coumarin phenol. The preparation protocols were employed due to difficulties encountered during purification.

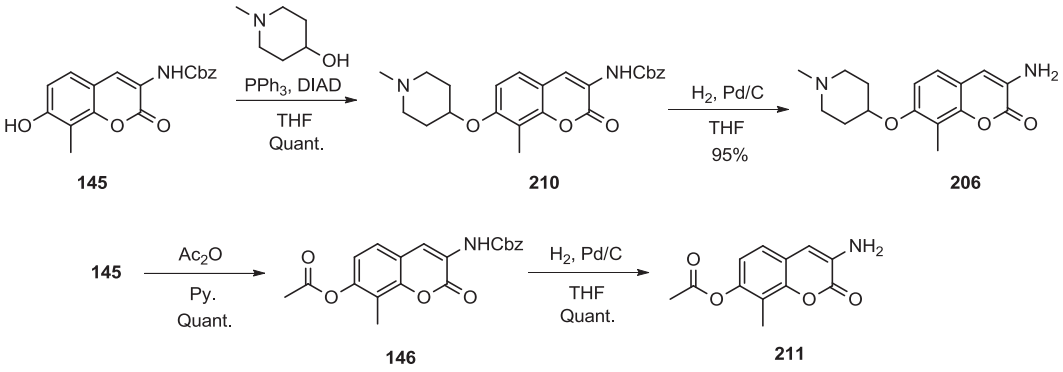

Scheme 52. Synthesis of 7-piperidine and 7-acetyl aminocoumarins.

1. Synthesis of aryl ^{t}Bu benzamide-containing novobiocin analogues

As seen in Scheme 52, 8-methyl coumarin phenol **145** was subjected to Mitsunobu etherification to afford functionalized coumarin **210** in good yield. Next, cleavage of the benzyl carbamate liberated aminocoumarin **206** for use in coupling reactions. As previously described, coumarin phenol **145** was also quantitatively protected as the corresponding acetylated phenol, and then the aminocoumarin was liberated to furnish scaffold **211**. While aminocoumarin **206** has proven to be stable upon benzyl carbamate cleavage, vinylogous amide **211** was always carried on without purification into subsequent coupling reactions.

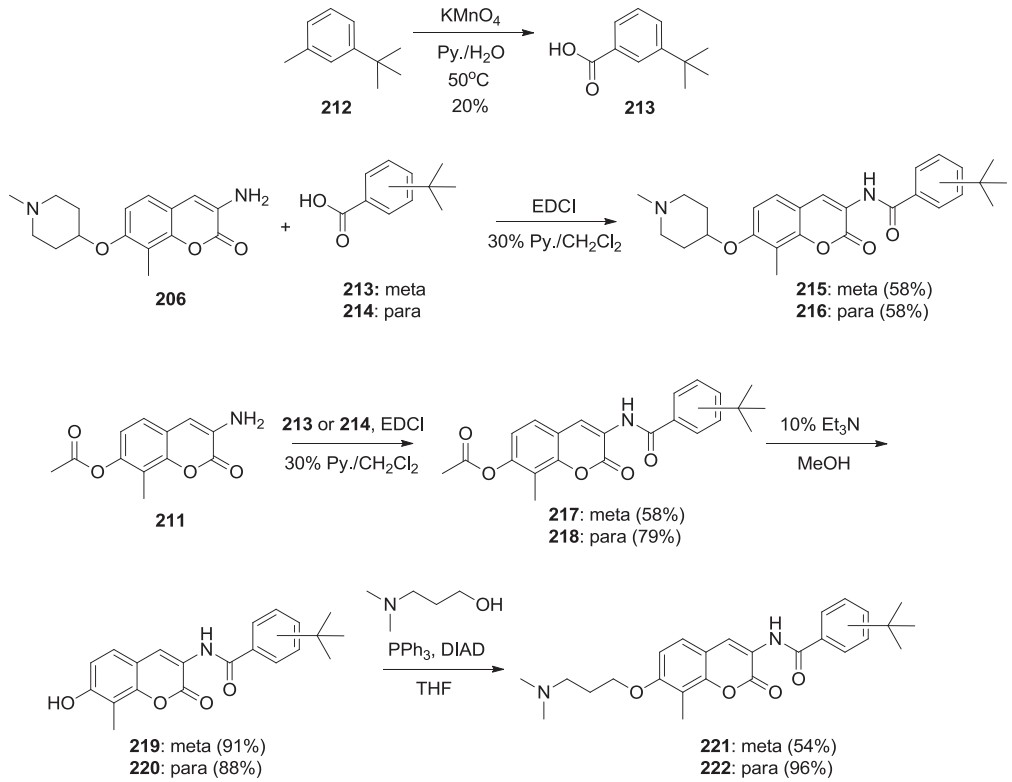

Scheme 53. Synthesis of meta- and para-tBu analogues.

While the desired para-^{t}Bu acid was commercially available, the meta-^{t}Bu acid required preparation prior to coupling. As seen in Scheme 53, the meta-^{t}Bu acid **213** was prepared from the corresponding methyl group through oxidation with potassium permanganate. Subsequent

coupling with piperidine-containing aminocoumarin **206** proceeded in good yield using both acids in the presence of EDCI and pyridine to afford analogues **215** and **216**. Likewise, EDCI-mediated coupling of the two ^{t}Bu acids with freshly prepared acetate-protected aminocoumarin **211** was high yielding. Intermediate esters **217** and **218** were subjected to solvolysis to afford the requisite coumarin phenols, which were then etherified with 3-(dimethylamino)propan-1-ol using Mitsunobu conditions to afford final compounds **221** and **222** in good yields.

2. Biological evaluation of aryl ^{t}Bu benzamide-containing novobiocin analogues

Upon construction of these aryl ^{t}Bu-containing compounds, they were evaluated for anti-proliferative activities against MCF-7 and SKBr3 breast cancer cell lines. The IC_{50} values manifested by these analogues are outlined in Table 12. Examination of the data generated by these compounds suggests several conclusions.

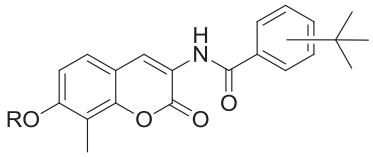

Table 12. Biological evaluation of aryl tBu analogues.

Compound	R	Substitution	MCF-7 (IC_{50}, μM)	SKBr3 (IC_{50}, μM)
219	H	*m*-^{t}Bu	17.11 ± 3.56[a]	40.09 ± 1.39
217	OAc	*m*-^{t}Bu	18.19 ± 1.13	40.22 ± 0.81
215	Piperidine	*m*-^{t}Bu	1.94 ± 0.26	1.81 ± 0.51
221	Alkyl amine	*m*-^{t}Bu	1.91 ± 0.23	1.73 ± 0.15
220	H	*p*-^{t}Bu	9.42 ± 0.43	12.72 ± 2.1

218	OAc	*p*-^{t}Bu	>100	>100
216	Piperidine	*p*-^{t}Bu	1.34 ± 0.27	1.65 ± 0.08
222	Alkyl amine	*p*-^{t}Bu	1.62	1.28 ± 0.12

[a] Values represent mean ± standard deviation for at least two separate experiments performed in triplicate.

Along with the proposed final analogues, functionalized intermediates with variable substitution at the 7-position were also tested. While these phenolic and acetylated compounds were modestly active, the designed analogues were significantly more potent. When considering the designed compounds with meta substitution, variation between the piperidine and alkyl amine sugars did not result in statistical differences in activity. Likewise, this same observation was seen with the para substituted compounds, which both showed activity between 1-2 μM regardless of the azasugar at the 7-position. Moreover, when considering para versus meta substitution, it was concluded that the pocket was tolerant of either attachment at either location on the aryl ring. When compared to the analogous compounds containing the biaryl side chain, these analogues closely mimicked the activity of the piperidine-containing compound (**155)** but lost ~3-4-fold activity versus the acyclic biaryl analogue. Overall, hydrophobic substitution was well tolerated, producing compounds that manifested low micromolar activity against both cancer cell lines.

To confirm that the anti-proliferative activity exhibited by the most promising compound from the series, **216**, was due to Hsp90 inhibition, it was evaluated by Western blot analyses (Figure 63). Selective Hsp90-dependent client protein degradation, versus a loading control, would confirm that this compound also causes Hsp90 inhibition. Figure 63 shows that in MCF-7 cells, the Hsp90-dependent client proteins Her2, Akt and Raf were degraded in a concentration-dependent manner upon treatment with the analogue. Although at a concentration slightly higher

than the observed anti-proliferative IC_{50} value, Hsp90 client protein degradation was observed. Furthermore, Hsp90 protein levels remained constant at all concentrations tested, which is consistent with *C*-terminal Hsp90 inhibition. Since the non-Hsp90-dependent protein, actin, was not affected by these analogues, it was concluded that selective degradation of Hsp90-dependent proteins occurred.

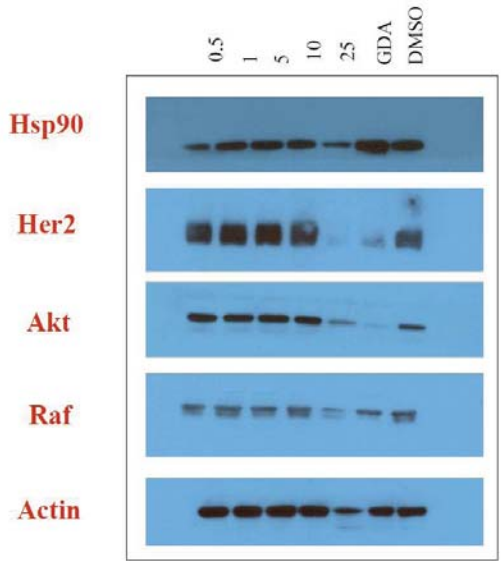

Figure 63. Western blot analyses of Hsp90 client protein degradation assay against MCF-7 cells following treatment with **216**. Concentrations (in μM) of **216** are indicated above each lane. GDA (500 nM) and DMSO were respectively employed as positive and negative controls.

3. Molecular modeling of 216

Due to its promising activity against both breast cancer cell lines and confirmation of Hsp90 inhibitory activity, there was interest in examining the conformation that analogue **216** adopts in the binding model. This compound was selected due to its consistent activity and because the piperidine-containing compounds more closely mimicked the activity observed with

the benzamide and biaryl side chain, suggesting a similar binding orientation. As seen in Figure 64, the sugar and coumarin cores of novobiocin and compound **216** fit into the same general regions of the binding pocket, although the two compounds have adopted inverted conformations. As a result, instead of extending into the same region as the prenyl side chain of novobiocin, the ^{t}Bu group bends away from the intended residues, opting to interact with a hydrophobic methionine (Met-606) instead. This binding orientation is perceived unlikely, due to an expected loss of key interactions with the sugar and coumarin core that would be associated with this inversion that is not consistent with the observed potency. This modeling does, however, demonstrate that a single aryl ring containing a ^{t}Bu group does not have the potential to extend and make contacts with the proposed residues or effectively fill the space. Thus, two libraries of compounds were proposed, one built with a *tert*-butoxy rather than *tert*-butyl group to impart flexibility, and the second with biaryl ^{t}Bu-containing benzamide side chains to better fill the space.

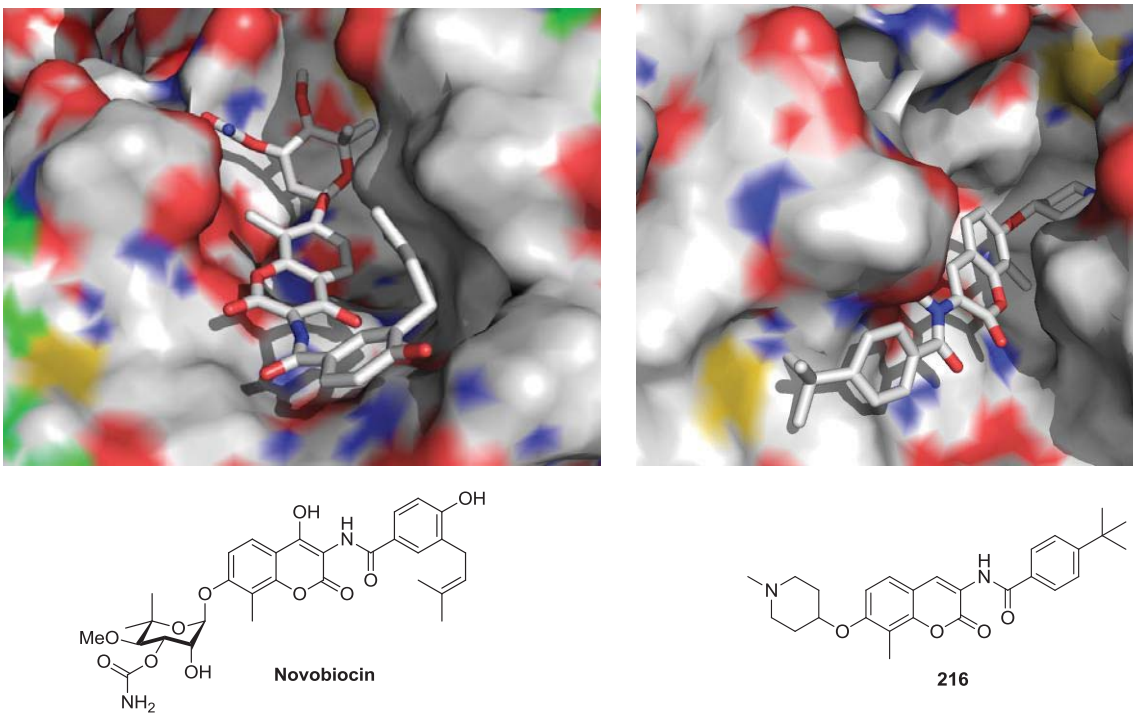

Figure 64. Novobiocin versus **216** bound to Hsp90α model.

C. Design of aryl O^{t}Bu benzamide-containing novobiocin analogues

Based upon the rationale derived from docking analogue **216** to the model, it was proposed that insertion of an oxygen between the aryl ring and ^{t}Bu group would impart conformational flexibility. This added flexibility enables the hydrophobic ^{t}Bu group to freely rotate, allowing it to properly orient itself in the pocket and make favorable hydrophobic interactions with Leu-714 and Val-715. As with the aryl systems, the butoxy group was placed at the meta and para positions on the ring to determine which position was better tolerated.

Similar to the preparation of the aryl ^{t}Bu analogues, the coumarins and acids were prepared independently, and then coupled to the corresponding O^{t}Bu acids (Scheme 54). The order of amide coupling and Mitsunobu etherification varied for the piperidine- and acyclic amine-containing analogues, as described previously. While Mitsunobu coupling was executed to install the piperidine prior to amide coupling, amide coupling with the protected aminocoumarin **211** preceded etherification in the case of those analogues.

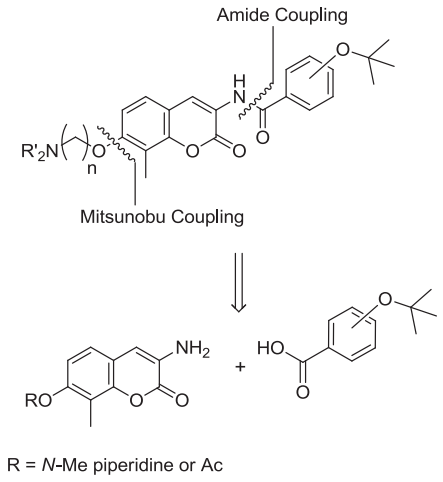

Scheme 54. Retrosynthetic analysis of aryl OtBu analogues.

1. Synthesis of aryl O^{t}Bu benzamide-containing novobiocin analogues

As seen in Scheme 55, commercially available phenols **223** and **224** can be converted to the corresponding ^{t}Bu ethers using a recently reported mild methodology. Through a potential mechanism involving magnesium perchlorate chelation and resultant loss of carbon dioxide, addition of di-*tert*-butyl dicarbonate to the various phenols in the presence of heat-activated magnesium perchlorate afforded the desired O^{t}Bu ethers in good yields.[264] **225** and **226** were subsequently hydrolyzed to the requisite acids, **227** and **228**. Coupling of the acids with aminocoumarin **206** using EDCI in the presence of pyridine afforded analogues **229** and **230**. Similarly, EDCI was employed to couple the O^{t}Bu acids with freshly prepared aminocoumarin **211**. Coupled **231** and **232** were subsequently hydrolyzed and Mitsunobu etherification was employed to install the desired alkyl amine at the 7-position of each coumarin phenol.

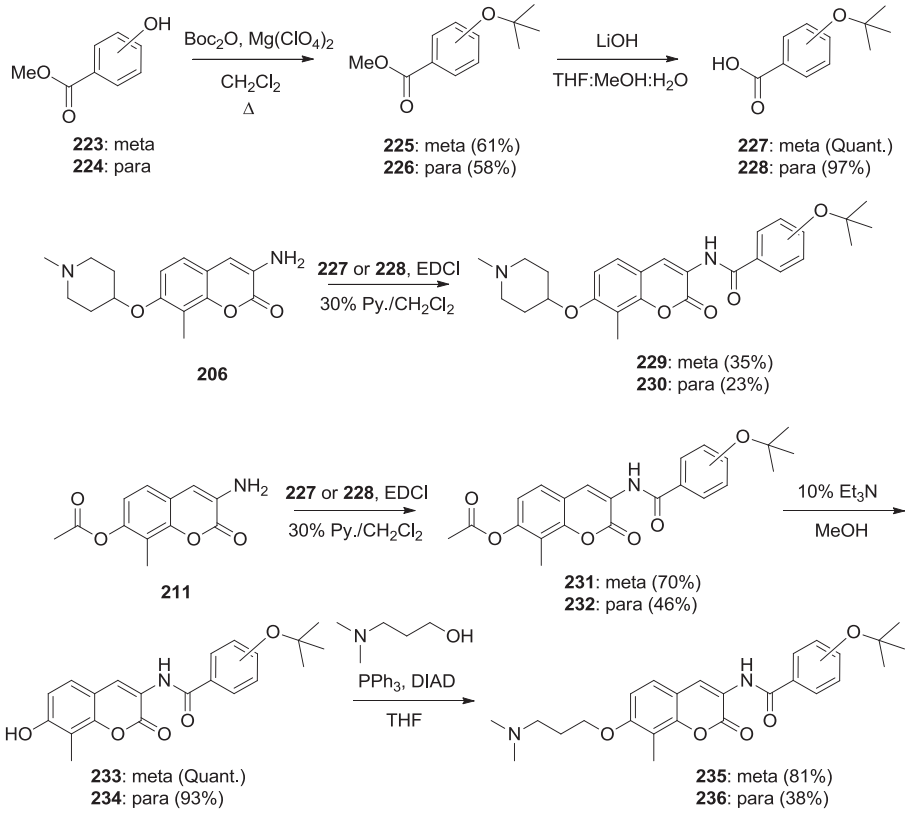

Scheme 55. Synthesis of meta- and para-OtBu analogues.

2. Biological evaluation of aryl O^{t}Bu benzamide-containing novobiocin analogues

Once prepared, the aryl O^{t}Bu-containing analogues were evaluated for anti-proliferative activities against MCF-7 and SKBr3 breast cancer cell lines. The IC_{50} values manifested by these analogues are outlined in Table 13 and analysis follows the table.

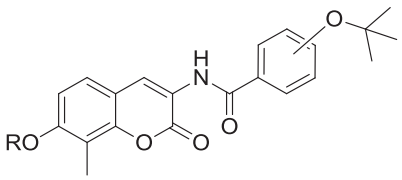

Table 13. Biological evaluation of aryl OtBu analogues.

Compound	R	Substitution	MCF-7 (IC_{50}, μM)	SKBr3 (IC_{50}, μM)
233	H	m-O^{t}Bu	12.28 ± 1.71[a]	23.68 ± 3.18
231	OAc	m-O^{t}Bu	>100	52.93 ± 1.21
229	Piperidine	m-O^{t}Bu	1.94 ± 0.38	2.04 ± 0.16
235	Alkyl amine	m-O^{t}Bu	5.18 ± 0.25	2.41 ± 0.10
234	H	p-O^{t}Bu	8.87 ± 1.29	15.05 ± 0.97
232	OAc	p-O^{t}Bu	48.36 ± 0.41	53.06 ± 1.03
230	Piperidine	p-O^{t}Bu	1.93 ± 0.24	2.44 ± 0.42
236	Alkyl amine	p-O^{t}Bu	1.74 ± 0.32	3.37 ± 0.82

[a] Values represent mean ± standard deviation for at least two separate experiments performed in triplicate.

Like with the aryl ^{t}Bu analogues, functionalized intermediates with variable substitution at the 7-position were tested along with the designed compounds. These phenolic and acetylated compounds were modestly active, manifesting comparable values to the ^{t}Bu analogues with the same 7-position functionality. When considering the designed compounds with meta

substitution, the piperidine analogue was more active than the corresponding acyclic amine analogue against MCF-7 cells. There was no statistical difference between the two against SKBr3 cells. This trend was the same as that observed with the para-O^{t}Bu analogues, which demonstrated better potency against SKBr3 cells when the piperidine azasugar was appended. Once again, the two para-substituted analogues were equally active against MCF-7 cells. When para versus meta substitution was considered with a common piperidine sugar, it became obvious that the pocket was tolerant of either attachment point on the aryl ring system. This is consistent with the trend observed with the ^{t}Bu analogues. In comparing the two libraries, with and without the oxygen inserted, the ^{t}Bu analogues are more consistent in potency despite sugar substitution, and insertion of an oxygen does not significantly change the observed IC_{50} values. The para-^{t}Bu analogues with either sugar were still the most active compounds from these two series, discounting insertion of an oxygen as a potential mechanism through which to access the desired hydrophobic network. A new design strategy was employed to gain access to these hydrophobic residues.

D. Design of biaryl ^{t}Bu benzamide-containing novobiocin analogues

Based upon the rationale derived from docking analogue **216** to the model, it was proposed that a biaryl system would be more capable than a single aryl ring of making the desired hydrophobic interactions. The designed analogues would place a ^{t}Bu substituent at various positions around a second aryl ring, connected meta to the one directly attached to the coumarin core, in an analogous fashion to the biaryl system. This second ring would be placed at the proper distance to extend into the area of Leu-714 and Val-715. Moreover, in accordance

with the novobiocin binding orientation (Figure 62), the ring directly connected to the coumarin core was designed to include a group capable of hydrogen bonding (methoxy group) to the second ring.

As with the aryl systems, the coumarins and acids were prepared independently, and then coupled as shown in Scheme 56. Moreover, the same approach was adopted to prepare the piperidine-containing analogues directly through coupling with functionalized aminocoumarin **206**. In addition, as before, the alkyl sugar was installed during the final step, after amide coupling.

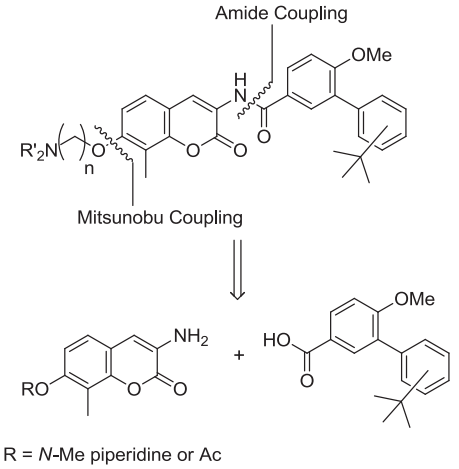

Scheme 56. Retrosynthetic analysis of biaryl tBu analogues.

1. Synthesis of biaryl ^{t}Bu benzamide-containing novobiocin analogues

As outlined in Scheme 57, synthesis of the ^{t}Bu biaryl analogues began with preparation of the requisite acids. Starting from aryl halide **237**, Suzuki coupling with either the meta or para boronic acid yielded the desired biaryl systems. Since separation of **240** and **241** from residual boronic acid proved difficult, the crude esters were directly subjected to hydrolysis conditions, affording the desired acids in good yields over two steps. EDCI-mediated coupling of acids **242** and **243** with piperidine-containing aminocoumarin **206** in the presence of pyridine was

employed toward the synthesis of analogues **244** and **245**. Similarly, coupling to freshly prepared aminocoumarin **211** using the same conditions proceeded in good yield. Intermediate esters **246** and **247** were subjected to solvolysis, and the resulting phenol coupled via Mitsunobu conditions to the appropriate alkyl amine, to afford final analogues **250** and **251**.

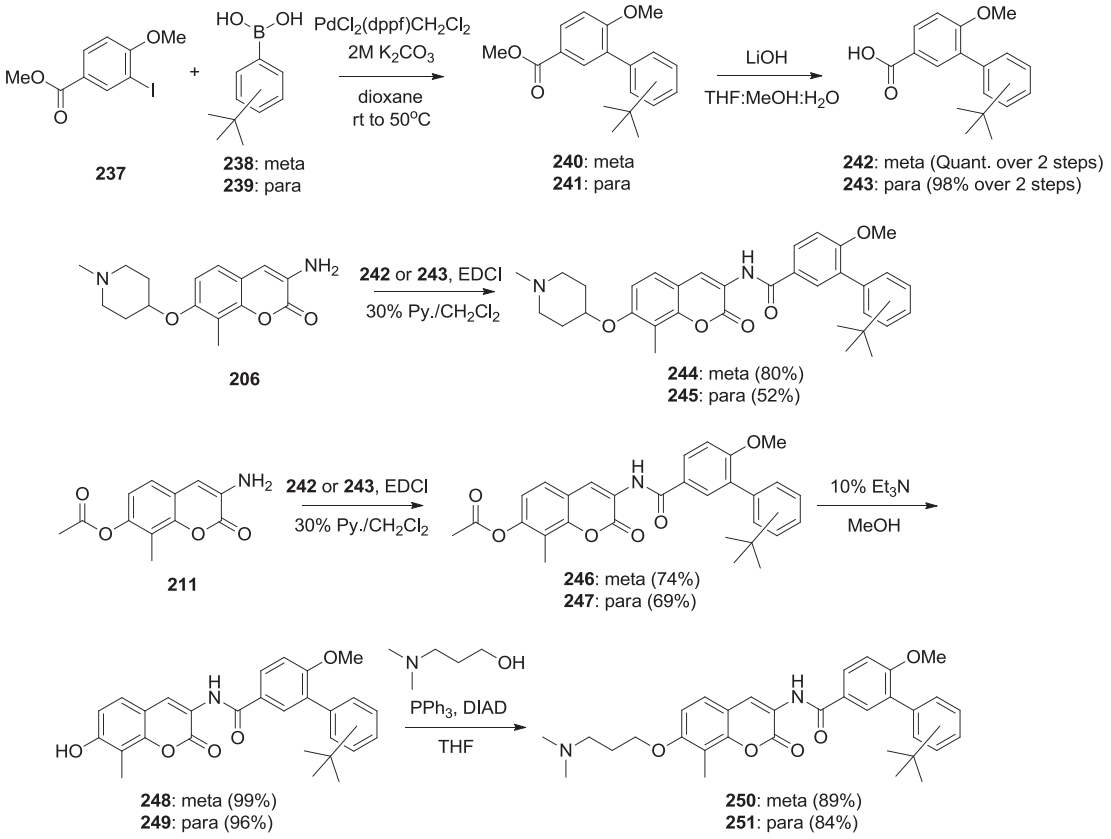

Scheme 57. Synthesis of meta- and para-tBu biaryl analogues.

In addition to the meta and para ^{t}Bu-containing biaryl analogues, ortho-^{t}Bu biaryl systems were sought. It was proposed that, according to the model, an ortho ^{t}Bu group on the second aryl ring would orient interactions with hydrophobic residues. Attempts make the requisite ortho-substituted ^{t}Bu biaryl acid are outlined in Scheme 58. Starting from aniline **252**, 1-bromo-2-tert-butylbenzene was prepared via Sandmeyer chemistry, specifically employing *tert*-butyl nitrite and copper (II) bromide. Next, a previously reported protocol was used to

convert aryl bromide **253** to the corresponding boronic acid, through a lithium–halogen exchange followed by trapping of the anion with triisopropylborate.[265]

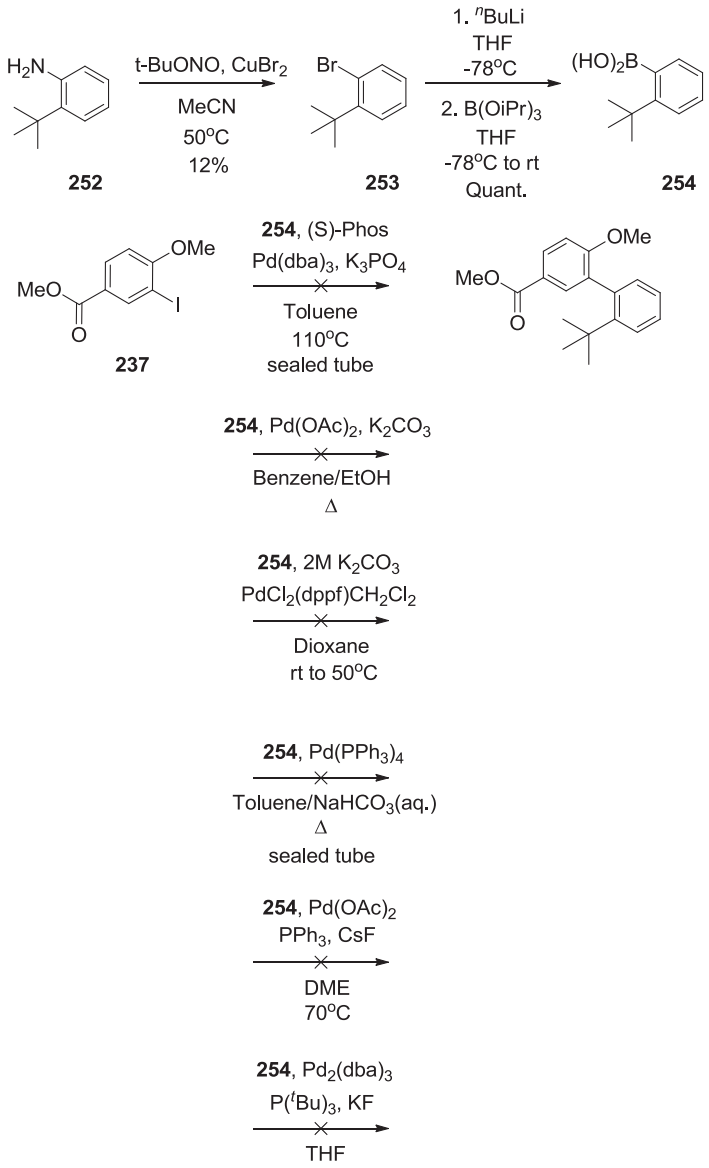

Scheme 58. Attempted reactions toward ortho-tBu biaryl analogues.

Several Suzuki coupling reaction protocols were attempted between boronic acid **254** and aryl iodide **237**. Despite the use of different palladium catalysts, solvents, ligands, additives and temperatures, the desired coupling reaction did not take place. It was proposed that steric repulsion between the two ortho substituted rings prevented the aryl iodide and boronic acid

from coupling with one another. Moreover, dehalogenation often occurred during these Suzuki reaction trials, which reveals oxidative addition into the palladium source occurs, but transmetallation does not.

2. Biological evaluation of biaryl ^{t}Bu benzamide-containing novobiocin analogues

Upon preparation, the biaryl ^{t}Bu-containing analogues were evaluated for anti-proliferative activities against MCF-7 and SKBr3 breast cancer cell lines. The IC_{50} values generated in these assays are summarized in Table 14.

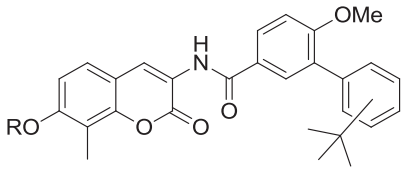

Table 14. Biological evaluation of biaryl analogues.

Compound	R	Substitution	MCF-7 (IC_{50}, μM)	SKBr3 (IC_{50}, μM)
248	H	m-^{t}Bu	19.54 ± 4.73[a]	44.53 ± 1.13
246	OAc	m-^{t}Bu	3.72 ± 1.66	6.18 ± 0.19
244	Piperidine	m-^{t}Bu	3.57 ± 0.48	1.77
250	Alkyl amine	m-^{t}Bu	8.57 ± 1.62	5.28 ± 0.35
249	H	p-^{t}Bu	8.49 ± 2.66	10.24 ± 0.83
247	OAc	p-^{t}Bu	6.10 ± 4.53	12.51 ± 1.21
245	Piperidine	p-^{t}Bu	1.65 ± 0.11	1.35 ± 0.08
251	Alkyl amine	p-^{t}Bu	2.46 ± 0.23	1.90 ± 0.31

[a] Values represent mean ± standard deviation for at least two separate experiments performed in triplicate.

In examining the data generated by this set of biaryl compounds, several trends can be observed. Consistent with the previous libraries, biaryl ^{t}Bu-containing analogues with a 7-position phenol or 7-acetylated phenol demonstrated modest activity. When the meta-^{t}Bu biaryl analogues are considered, it becomes apparent that the piperidine-containing compounds are more active than those with an alkyl amine at the same position. This trend follows in the para series, but is not as pronounced, with only slight differences in potency. When comparing the meta- and para-^{t}Bu biaryl compounds to one another, para-substitution consistently resulted in better potency. Moreover, the activity of the analogue with the para-substituted biaryl ring system and piperidine azasugar (**245**) manifested comparable activity to the most active compound in the initial series (**216**), also with a para-^{t}Bu group and piperidine ring system. Likewise, when compared to the analogous compound containing the biaryl side chain (**155**), **245** closely mimicked its activity against the same cancer cell lines. Addition of this second ring system with a meta-^{t}Bu substituent was not well tolerated, causing significant decreases in potency when compared to the single substituted aryl rings. In contrast, the biaryl system was well tolerated when the ^{t}Bu group was installed at the para position, leading to compounds that exhibited equivalent potency to the aryl ^{t}Bu analogues. However, since no significant potency gains were observed, it was perceived that these biaryl analogues, like their predecessors, were unable to access the hydrophobic residues in the pocket.

Collaborative studies with the Cohen laboratory at the KU Medical Center identified analogue **245** as an interesting lead worth pursuing towards Head and Neck Squamous Cell Carcinoma. A large quantity of compound **245** was prepared for use in an *in vivo* model. Although these studies are in their infancy, promising *in vivo* results are being generated.

E. Design of multifunctional biaryl ^{t}Bu benzamide side chains

It was proposed that other biaryl ring systems containing an O^{t}Bu group on one ring and a hydrogen bond donating phenol on the other could be potentially potent compounds. As part of the benzamide study executed by Burlison and co-workers, phenols were appended on the side chains of some of the most potent analogues.[102] Moreover, a free phenol is present on the prenylated side chain of novobiocin and docking studies have shown that it sits in a portion of the binding pocket that flanked by charged and polar residues (Figure 62). Incorporation of a polar substituent and hydrophobic group on the same biaryl system could potentially enable such a system to capitalize on the diverse interactions offered by the binding pocket.

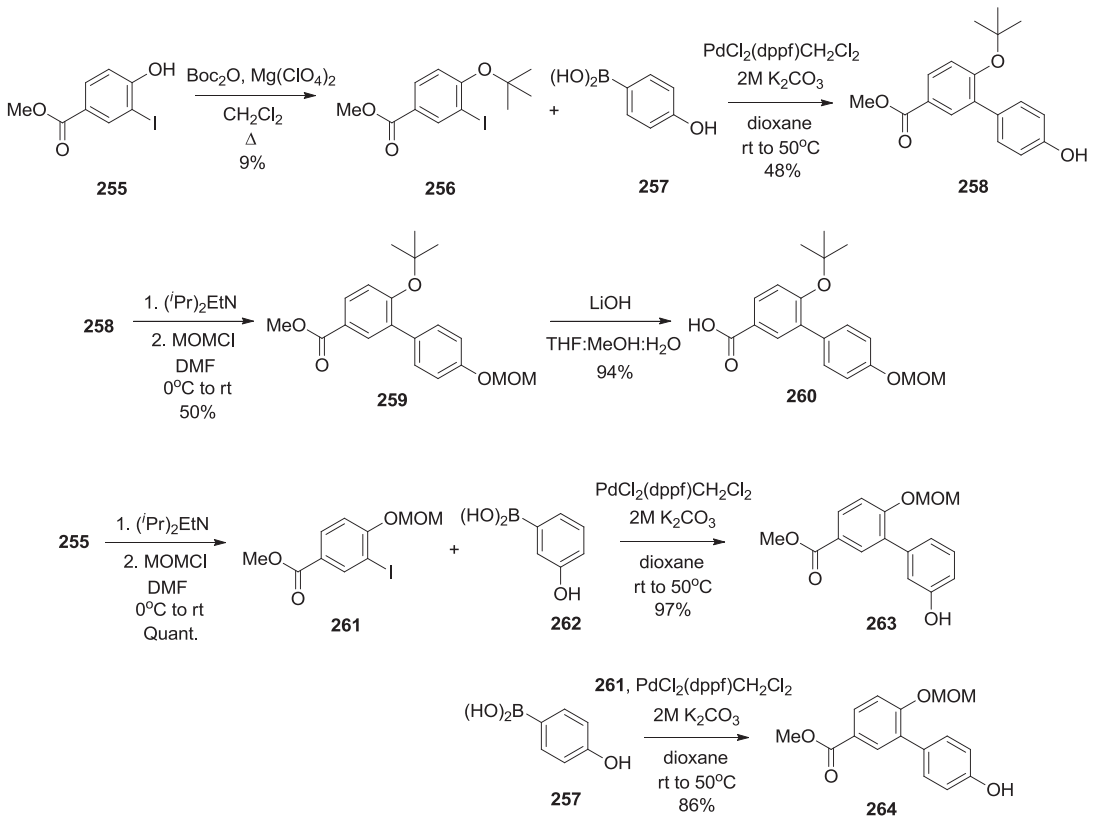

Scheme 59. Efforts toward other biaryl OtBu acids.

1. Synthesis of multifunctional biaryl ^{t}Bu benzamide side chains

As seen in Scheme 59, initial efforts toward the synthesis of the requisite side chains that would allow access to these analogues are described. Addition of di-*tert*-butyl dicarbonate to phenol **255** in the presence of heat-activated magnesium perchlorate afforded the desired O^{t}Bu ester.[264] The resultant aryl iodide was coupled to (4-hydroxyphenyl)boronic acid using Suzuki coupling conditions to afford ester **258**. Following protection of the free phenol as the methoxy methyl ether, ester **259** was subsequently hydrolyzed to acid **260**. It is envisioned that this acid could be coupled to various aminocoumarins and, after cleavage of the MOM group, would represent interesting scaffolds to test for anti-proliferative activity. Likewise, starting from phenol **255**, etherification conditions were used to install a methoxy methyl ether group in good yield. Next, protected aryl iodide **261** was coupled with both meta- and para-hydroxyl phenylboronic acids to yield esters **263** and **264**, respectively. Although these intermediates were not taken on into further development, it was envisioned that the free phenol could be converted to the corresponding O^{t}Bu group and then hydrolyzed to afford the desired acid. Coupling of these acids to selected aminocoumarins would yield several rationally designed analogues with the potential to exhibit promising activity.

III. Conclusion

Several libraries of compounds were designed to explore the potential to capitalize on hydrophobic interactions with residues that line the portion of the binding pocket into which the benzamide side chain extends. Synthesis and testing of these analogues revealed that the binding pocket is tolerant of limited hydrophobic bulk. When a hydrophobic substituent is appended,

analogues bearing a single aryl ring were more potent than those coupled to a biaryl system. Moreover, the pocket was more sensitive to substitution patterns when the larger biaryl system was incorporated. Overall, this study has produced several novel novobiocin analogues with low micromolar activity, including some that have been taken on into advanced studies. Likewise, the compounds described affirm the importance of the benzamide side chain in dictating potency.

IV. Experimental Protocols

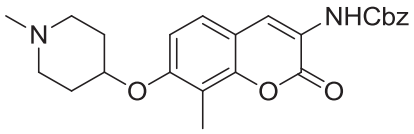

210

Benzyl 8-methyl-7-(1-methylpiperidin-4-yloxy)-2-oxo-2H-chromen-3-ylcarbamate (210). Diisopropylazodicarboxylate (4.17 mL, 21.5 mmol) was added to a solution of 1-methylpiperidin-4-ol (2.48 g, 21.5 mmol), coumarin **145** (3.50 g, 10.8 mmol) and triphenylphosphine (5.64 g, 21.5 mmol) in anhydrous THF (54 mL). After 12 h, the solvent was removed and the residue purified via column chromatography (SiO_2, 10:1, CH_2Cl_2:MeOH) to afford compound **210** as a colorless amorphous solid (4.50 g, 99%). ^{1}H NMR (400 MHz, $CDCl_3$) δ 8.25 (s, 1H), 7.55 (s, 1H), 7.40–7.34 (m, 5H), 7.24 (d, J = 8.0 Hz, 1H), 6.84 (d, J = 8.0 Hz, 1H), 5.22 (s, 2H), 4.48 (bs, 1H), 2.71 (bs, 2H), 2.52–2.49 (m, 2H), 2.38 (s. 3H), 2.11–2.07 (m, 2H), 1.98–1.89 (m, 2H). ^{13}C NMR (100 MHz, $CDCl_3$) δ 158.8, 156.5, 153.2, 149.2, 135.6, 128.7, 128.5, 128.2, 125.1, 122.2, 121.4, 115.2, 113.0, 110.4, 72.4, 67.4, 52.0 (2C), 46.0, 30.3 (2C), 8.4. IR (film) ν_{max} 3406, 3319, 2939, 2849, 2791, 1711, 1609, 1524, 1366, 1271, 1227, 1204, 1103, 1038, 1024 cm^{-1}. HRMS (ESI$^+$) m/z: [M + H$^+$] calcd for $C_{24}H_{27}N_2O_5$, 423.1920; found 423.1920.

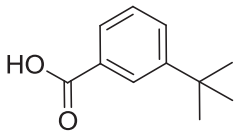

213

3-(*Tert*-butyl)benzoic acid (213):[266] Potassium permanganate (80 mg, 0.51 mmol) was added portionwise to a solution of 1-(*tert*-butyl)-3-methylbenzene (25 mg, 0.17 mmol) and pyridine (68 μL, 0.84 mmol) in water (0.20 mL) at 50°C. After 12 h at 50°C, the solution was cooled, basified with NaOH to pH 12, and washed with EtOAc. The combined aqueous extracts were acidified with 6M HCl to pH 2 and then the solution was extracted with EtOAc (3 x 15 mL), dried (Na_2SO_4), filtered, and concentrated to afford **213** as a colorless amorphous solid (6.0 mg, 20%): ^{1}H NMR ($CDCl_3$, 400 MHz) δ 8.18 (s, 1H), 7.96 (d, *J* = 7.6 Hz, 1H), 7.68 (d, *J* = 7.8 Hz, 1H), 7.44 (t, *J* = 7.8 Hz, 1H), 1.39 (s, 9H).

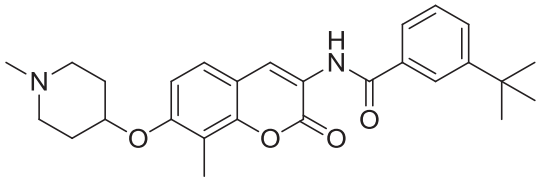

215

3-(*Tert*-butyl)-N-(8-methyl-7-((1-methylpiperidin-4-yl)oxy)-2-oxo-2H-chromen-3-yl)benzamide (215): EDCI (52 mg, 0.27 mmol) and **213** (39 mg, 0.22 mmol) were added to aminocoumarin **206** (32 mg, 0.11 mmol), freshly prepared from hydrogenolysis of **210**, in 30% pyridine/CH_2Cl_2 (1.60 mL). After 12 h, the solvent was concentrated and the residue was purified via column chromatography (SiO_2, 10:1 CH_2Cl_2:MeOH) to afford **215** as a colorless amorphous solid (29.0 mg, 58%): ^{1}H NMR (MeOD, 400 MHz) δ 8.63 (s, 1H), 7.99 (t, *J* = 1.6 Hz, 1H), 7.74–7.72 (m, 1H), 7.70–7.68 (m, 1H), 7.49–7.43 (m, 2H), 7.08 (d, *J* = 8.4 Hz, 1H), 4.73 (bs, 1H), 3.09 (bs, 2H), 2.93 (bs, 2H), 2.65 (bs, 3H), 2.32 (s, 3H), 2.16 (bs, 2H), 2.04 (bs,

2H), 1.39 (s, 9H); ^{13}C NMR (MeOD, 125 MHz) δ 168.9, 160.5, 158.3, 153.3, 151.2, 135.0, 130.7, 129.7, 128.1 (2C), 127.2, 125.6, 125.5, 122.8, 115.7, 114.6, 111.7, 52.8, 45.5, 35.8, 31.6 (5C), 30.7, 8.4; HRMS (ESI$^+$) *m/z*: $[M + H]^+$ calcd for $C_{27}H_{33}N_2O_4$, 449.2440; found, 449.2411.

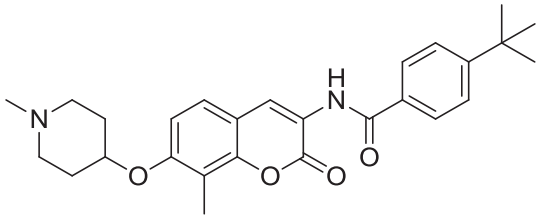

216

4-(*Tert*-butyl)-N-(8-methyl-7-((1-methylpiperidin-4-yl)oxy)-2-oxo-2H-chromen-3-yl)benzamide (216): EDCI (52 mg, 0.27 mmol) and 4-(*tert*-butyl)benzoic acid (39 mg, 0.22 mmol) were added to aminocoumarin **206** (32 mg, 0.11 mmol), freshly prepared from hydrogenolysis of **210**, in 30% pyridine/CH_2Cl_2 (1.60 mL). After 12 h, the solvent was concentrated and the residue was purified via column chromatography (SiO_2, 10:1 CH_2Cl_2:MeOH) to afford **216** as a colorless amorphous solid (29.0 mg, 58%): ^{1}H NMR (MeOD, 400 MHz) δ 8.67 (s, 1H), 7.89 (d, *J* = 8.4 Hz, 2H), 7.60 (d, *J* = 8.4 Hz, 2H), 7.47 (d, *J* = 8.8 Hz, 1H), 7.10 (d, *J* = 8.8 Hz, 1H), 4.79 (bs, 1H), 3.23 (bs, 2H), 3.13 (bs, 2H), 2.78 (bs, 3H), 2.35 (s, 3H), 2.19 (bs, 2H), 2.11 (bs, 2H), 1.37 (s, 9H); ^{13}C NMR (MeOD, 125 MHz) δ 168.2, 160.2, 157.4, 152.1 (2C), 132.2, 128.4 (2C), 127.6, 127.3, 126.9 (2C), 123.0, 115.8, 115.0, 111.6, 54.0, 44.4, 36.0, 31.5 (5C), 29.8, 8.4; HRMS (ESI$^+$) *m/z*: $[M + Na]^+$ calcd for $C_{27}H_{32}N_2NaO_4$, 471.2260; found, 471.2213.

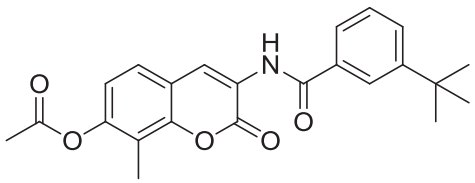

217

3-(3-(*Tert*-butyl)benzamido)-8-methyl-2-oxo-2H-chromen-7-yl acetate (217): EDCI (83 mg, 0.44 mmol) and **213** (62 mg, 0.35 mmol) were added to aminocoumarin **211** (39 mg, 0.17 mmol), freshly prepared from hydrogenolysis of **147**, in 30% pyridine/CH_2Cl_2 (2.60 mL). After 12 h, the solvent was concentrated and the residue was purified via column chromatography (SiO_2, 40:1 CH_2Cl_2:Acetone) to afford **217** as a colorless amorphous solid (59.0 mg, 58%): ^{1}H NMR ($CDCl_3$, 400 MHz) δ 8.87 (s, 1H), 8.81 (s, 1H), 8.00 (s, 1H), 7.71–7.64 (m, 2H), 7.49–7.41 (m, 2H), 7.06 (d, J = 8.4 Hz, 1H), 2.39 (s, 3H), 2.33 (s, 3H), 1.40 (s, 9H); ^{13}C NMR ($CDCl_3$, 125 MHz) δ 168.9, 166.7, 158.9, 152.3, 150.1, 148.8, 133.3, 129.8, 128.7, 125.6, 124.5, 123.8, 123.6, 123.4, 119.3, 119.1, 117.8, 35.0, 31.3 (3C), 20.8, 9.1; HRMS (ESI$^+$) *m/z*: $[M + H]^+$ calcd for $C_{23}H_{24}NO_5$, 394.1654; found, 394.1667.

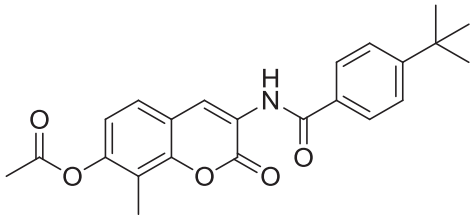

218

3-(4-(*Tert*-butyl)benzamido)-8-methyl-2-oxo-2H-chromen-7-yl acetate (218): EDCI (167 mg, 0.87 mmol) and 4-(*tert*-butyl)benzoic acid (124 mg, 0.70 mmol) were added to aminocoumarin **211** (77 mg, 0.35 mmol), freshly prepared from hydrogenolysis of **147**, in 30% pyridine/CH_2Cl_2 (5.20 mL). After 12 h, the solvent was concentrated and the residue was purified via column chromatography (SiO_2, 40:1 CH_2Cl_2:Acetone) to afford **218** as a colorless amorphous solid (105 mg, 79%): ^{1}H NMR ($CDCl_3$, 400 MHz) δ 8.87 (s, 1H), 8.81 (s, 1H), 7.90–7.87 (m, 2H), 7.57–7.54 (m, 2H), 7.42 (d, J = 8.4 Hz, 1H), 7.06 (d, J = 8.4 Hz, 1H), 2.39 (s, 3H), 2.33 (s, 3H), 1.39 (s, 9H); ^{13}C NMR ($CDCl_3$, 125 MHz) δ 168.9, 166.1, 158.9, 156.3, 150.1,

148.8, 130.7, 127.1, 126.9, 126.1, 125.9, 125.5, 123.6, 123.2, 119.3, 119.2, 117.8, 35.1, 31.1 (3C), 20.8, 9.1; HRMS (ESI^+) *m/z*: $[M + H]^+$ calcd for $C_{23}H_{24}NO_5$, 394.1654; found, 394.1689.

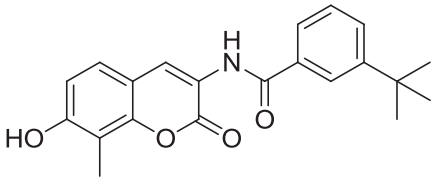

219

3-(*Tert*-butyl)-N-(7-hydroxy-8-methyl-2-oxo-2H-chromen-3-yl)benzamide (219): A solution of **217** (43.0 mg, 0.11 mmol) in MeOH (1.10 mL) was treated with triethylamine (0.11 mL, 10%). After 12 h, the solvent was concentrated and the residue purified via column chromatography (SiO_2, 40:1 CH_2Cl_2:Acetone) to afford **219** as a yellow amorphous solid (35.0 mg, 91%): ^1H NMR (Acetone-d_6, 500 MHz) δ 8.79 (bs, 1H), 8.59 (s, 1H), 7.91 (d, *J* = 1.5 Hz, 1H), 7.66 (dd, *J* = 8.0, 1.0 Hz, 1H), 7.58 (dd, *J* = 8.0, 1.0 Hz, 1H), 7.38 (t, *J* = 8.0 Hz, 1H), 7.28 (d, *J* = 8.0 Hz, 1H), 6.83 (d, *J* = 8.0 Hz, 1H), 2.16 (s, 3H), 1.26 (s, 9H); ^{13}C NMR (Acetone-d_6, 125 MHz) δ 166.7, 159.6, 158.3, 152.7, 150.9, 134.9, 130.1, 129.5, 126.7, 125.8, 125.7, 125.1, 122.1, 113.6, 113.2, 112.3, 35.5, 31.5 (3C), 8.1; HRMS (ESI^+) *m/z*: $[M + H]^+$ calcd for $C_{21}H_{22}NO_4$, 352.1549; found, 352.1566.

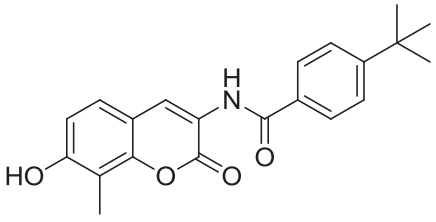

220

4-(*Tert*-butyl)-N-(7-hydroxy-8-methyl-2-oxo-2H-chromen-3-yl)benzamide (220): A solution of **218** (55.0 mg, 0.14 mmol) in MeOH (1.40 mL) was treated with triethylamine (0.14 mL, 10%). After 12 h, the solvent was concentrated and the residue purified via column

chromatography (SiO_2, 40:1 → 10:1 CH_2Cl_2:Acetone) to afford **220** as a yellow amorphous solid (43.0 mg, 88%): ^{1}H NMR (Acetone-d_6, 400 MHz) δ 9.14 (bs, 1H), 8.87 (s, 1H), 8.72 (d, J = 3.2 Hz, 1H), 7.95–7.93 (m, 2H), 7.64–7.62 (m, 2H), 7.42 (d, J = 8.4 Hz, 1H), 6.96 (d, J = 8.4 Hz, 1H), 2.29 (s, 3H), 1.37 (s, 9H); ^{13}C NMR (Acetone-d_6, 125 MHz) δ 164.3, 157.8, 156.4, 154.7, 149.0, 130.4, 126.1, 124.9, 124.8, 123.6, 120.3, 111.8, 111.4, 110.4, 33.8, 30.8, 30.0, 28.9, 21.5, 12.5, 6.3; HRMS (ESI$^+$) *m/z*: $[M + H]^+$ calcd for $C_{21}H_{22}NO_4$, 352.1549; found, 352.1561.

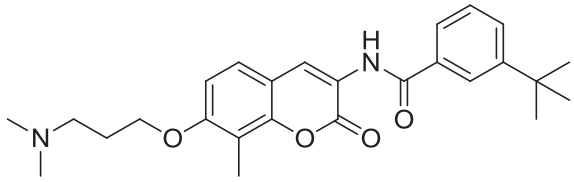

221

3-(*Tert*-butyl)-N-(7-(3-(dimethylamino)propoxy)-8-methyl-2-oxo-2H-chromen-3-yl)benzamide (221): Diisopropylazodicarboxylate (42.0 μL, 0.22 mmol) was added to a solution of 3-(dimethylamino)propan-1-ol (26.0 μL, 0.22 mmol), **219** (37 mg, 0.11 mmol) and triphenylphosphine (57.0 mg, 0.22 mmol) in anhydrous THF (1.10 mL). After 12 h, the solvent was removed and the residue purified via column chromatography (SiO_2, 10:1, CH_2Cl_2:MeOH) to afford compound **221** as a colorless amorphous solid (25.0 mg, 54%): ^{1}H NMR ($CDCl_3$, 400 MHz) δ 8.83 (s, 1H), 8.75 (s, 1H), 7.99 (s, 1H), 7.70 (d, J = 7.6 Hz, 1H), 7.64 (d, J = 7.6 Hz, 1H), 7.46 (t, J = 8.0 Hz, 1H), 7.36 (d, J = 8.4 Hz, 1H), 6.90 (d, J = 8.4 Hz, 1H), 4.15 (t, J = 6.0 Hz, 2H), 2.66 (bs, 2H), 2.41 (bs, 6H), 2.35 (s, 3H), 2.12 (t, J = 6.0 Hz, 2H), 1.40 (s, 9H); ^{13}C NMR ($CDCl_3$, 125 MHz) δ 166.6, 159.5, 158.4, 152.2, 149.2, 133.6, 129.6, 128.6, 125.8, 124.6, 124.5, 123.8, 121.5, 114.1, 113.4, 108.9, 66.7, 56.2 (2C), 45.1, 34.9, 31.2 (3C), 27.1, 8.2; HRMS (ESI$^+$) *m/z*: $[M + H]^+$ calcd for $C_{26}H_{33}N_2O_4$, 437.2440; found, 437.2418.

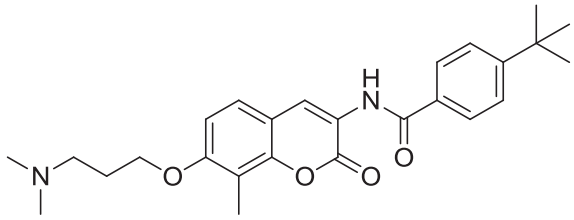

222

4-(*Tert*-butyl)-N-(7-(3-(dimethylamino)propoxy)-8-methyl-2-oxo-2H-chromen-3-yl)benzamide (222): Diisopropylazodicarboxylate (33.0 μL, 0.17 mmol) was added to a solution of 3-(dimethylamino)propan-1-ol (20.0 μL, 0.17 mmol), **220** (29 mg, 0.085 mmol) and triphenylphosphine (45.0 mg, 0.17 mmol) in anhydrous THF (0.85 mL). After 12 h, the solvent was removed and the residue purified via column chromatography (SiO_2, 10:1, CH_2Cl_2:MeOH) to afford compound **222** as a colorless amorphous solid (35.0 mg, 96%): ^{1}H NMR ($CDCl_3$, 400 MHz) δ 8.82 (s, 1H), 8.75 (s, 1H), 7.87 (d, *J* = 8.4 Hz, 2H), 7.55 (d, *J* = 8.4 Hz, 2H), 7.35 (d, *J* = 8.4 Hz, 1H), 6.89 (d, *J* = 8.4 Hz, 1H), 4.15 (t, *J* = 6.0 Hz, 2H), 2.68 (t, *J* = 6.8 Hz, 2H), 2.42 (bs, 6H), 2.34 (s, 3H), 2.13 (t, *J* = 6.8 Hz, 2H), 1.38 (s, 9H); ^{13}C NMR ($CDCl_3$, 125 MHz) δ 166.0, 159.5, 158.3, 156.1, 149.2, 130.9, 127.0 (2C), 125.9 (2C), 125.7, 124.5, 121.5, 114.0, 113.4, 108.9, 66.6, 56.2, 45.1, 35.1, 31.1 (3C), 27.0, 14.2, 8.1; HRMS (ESI$^+$) *m/z*: $[M + H]^+$ calcd for $C_{26}H_{33}N_2O_4$, 437.2440; found, 437.2443

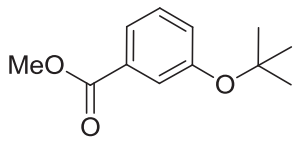

225

Methyl 3-(*tert*-butoxy)benzoate (225): Di-*tert*-butyl dicarbonate (825 mg, 3.78 mmol) was added to a solution of methyl 3-hydroxybenzoate (250 mg, 1.64 mmol) and activated magnesium perchlorate (37 mg, 0.16 mmol, heated at 130^{o}C for 1.5 under vacuum prior to the reaction) in

CH_2Cl_2 (2.50 mL), then heated at reflux for 12 h. Once cool, water (15 mL) was added and CH_2Cl_2 (3 x 15 mL) was used to extract the product. The combined organic extracts were dried (Na_2SO_4), filtered, and concentrated and the residue was purified via column chromatography (SiO_2, 12:1, Hexane:EtOAc) to afford compound **225** as a colorless amorphous solid (209 mg, 61%): ^{1}H NMR ($CDCl_3$, 400 MHz) δ 7.78 (dt, *J* = 7.6, 1.2 Hz, 1H), 7.68 (t, *J* = 2.0 Hz, 1H), 7.35 (t, *J* = 8.0 Hz, 1H), 7.20 (ddd, *J* = 8.0, 2.4, 1.2 Hz, 1H), 3.93 (s, 3H), 1.39 (s, 9H); ^{13}C NMR ($CDCl_3$, 125 MHz) δ 166.9, 155.5, 131.0, 128.9, 128.8, 125.0, 124.5, 79.1, 52.2, 28.8 (3C); HRMS (ESI^+) *m/z*: $[M + Na]^+$ calcd for $C_{12}H_{16}NaO_3$, 231.0997; found, 231.0958.

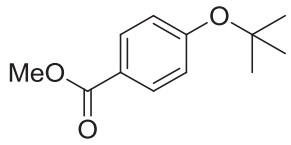

226

Methyl 4-(*tert*-butoxy)benzoate (226):[267] Di-*tert*-butyl dicarbonate (825 mg, 3.78 mmol) was added to a solution of methyl 4-hydroxybenzoate (250 mg, 1.64 mmol) and activated magnesium perchlorate (37 mg, 0.16 mmol, heated at 130^{o}C for 1.5 under vacuum prior to the reaction) in CH_2Cl_2 (2.50 mL), then heated at reflux for 12 h. Once cool, water (15 mL) was added and CH_2Cl_2 (3 x 15 mL) was used to extract the product. The combined organic extracts were dried (Na_2SO_4), filtered, and concentrated and the residue was purified via column chromatography (SiO_2, 12:1, Hexane:EtOAc) to afford compound **226** as a colorless amorphous solid (197 mg, 58%): ^{1}H NMR ($CDCl_3$, 500 MHz) δ 7.98 (dd, *J* = 7.0, 1.5 Hz, 2H), 7.04 (dd, *J* = 7.0, 1.5 Hz, 2H), 3.91 (s, 3H), 1.43 (s, 9H).

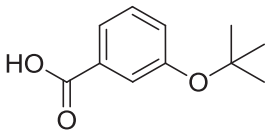

227

3-(*Tert*-butoxy)benzoic acid (227):[268] Lithium hydroxide (399 mg, 4.76 mmol) was added to a solution of **225** (198 mg, 0.95 mmol) in 3:1:1 THF:MeOH:H_2O (9.50 mL). After 12 h, the solution was concentrated and the aqueous residue was acidified, and then extracted with EtOAc (3 x 15 mL). The combined organic layers were next extracted with saturated aqueous $NaHCO_3$ (3 x 15 mL), and then the aqueous extracts were acidified. Finally, EtOAc (3 x 15 mL) was used to extract the acid product, and the combined organic extracts were washed with saturated aqueous NaCl, dried (Na_2SO_4), filtered, and concentrated to afford **227** as a colorless amorphous solid (158 mg, 99%): ^{1}H NMR ($CDCl_3$, 400 MHz) δ 7.86 (dt, *J* = 6.0, 0.8 Hz, 1H), 7.58 (t, *J* = 1.6 Hz, 1H), 7.40 (t, *J* = 6.0 Hz, 1H), 7.28–7.26 (m, 1H), 1.41 (s, 9H).

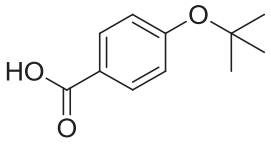

228

4-(*Tert*-butoxy)benzoic acid (228):[269] Lithium hydroxide (399 mg, 4.76 mmol) was added to a solution of **225** (198 mg, 0.95 mmol) in 3:1:1 THF:MeOH:H_2O (9.50 mL). After 12 h, the solution was concentrated and the aqueous residue was acidified, and then extracted with EtOAc (3 x 15 mL). The combined organic layers were next extracted with saturated aqueous $NaHCO_3$ (3 x 15 mL), and then the aqueous extracts were acidified. Finally, EtOAc (3 x 15 mL) was used to extract the acid product, and the combined organic extracts were washed with saturated aqueous NaCl, dried (Na_2SO_4), filtered, and concentrated to afford **228** as a colorless amorphous solid (158 mg, 99%): ^{1}H NMR ($CDCl_3$, 400 MHz) δ 8.05 (dd, *J* = 6.8, 2.0 Hz, 2H), 7.06 (dd, *J* = 6.8, 2.0 Hz, 2H), 1.45 (s, 9H).

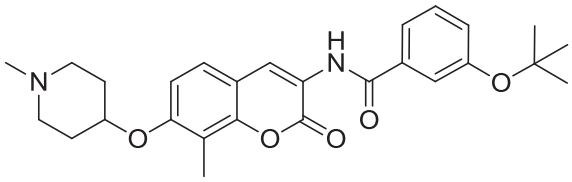

229

3-(*Tert*-butoxy)-N-(8-methyl-7-((1-methylpiperidin-4-yl)oxy)-2-oxo-2H-chromen-3-yl)benzamide (229): EDCI (50.0 mg, 0.26 mmol) and **227** (40.0 mg, 0.21 mmol) were added to aminocoumarin **206** (30.0 mg, 0.10 mmol), freshly prepared from hydrogenolysis of **210**, in 30% pyridine/CH_2Cl_2 (1.60 mL). After 12 h, the solvent was concentrated and the residue was purified via column chromatography (SiO_2, 10:1 CH_2Cl_2:MeOH) to afford **229** as a colorless amorphous solid (17.0 mg, 35%): ^{1}H NMR ($CDCl_3$, 400 MHz) δ 8.83 (s, 1H), 8.74 (s, 1H), 7.62–7.58 (m, 2H), 7.43 (t, J = 8.0 Hz, 1H), 7.36 (d, J = 8.4 Hz, 1H), 7.24 (d, J = 7.6 Hz, 1H), 6.89 (d, J = 8.4 Hz, 1H), 4.60 (bd, 1H), 2.84 (bs, 2H), 2.66 (bs, 2H), 2.52 (bs, 3H), 2.38 (s, 3H), 2.22 (bs, 2H), 2.05 (bs, 2H), 1.42 (s, 9H); ^{13}C NMR ($CDCl_3$, 125 MHz) δ 165.8, 159.4 (2C), 156.1, 149.5, 134.7, 129.4, 128.0, 125.7, 124.5, 122.7 (2C), 121.6, 121.5, 115.2, 113.5, 110.3, 79.4, 51.8 (2C), 45.5, 28.9 (3C), 28.8 (2C), 8.4; HRMS (ESI$^+$) *m/z*: $[M + H]^+$ calcd for $C_{27}H_{33}N_2O_5$, 465.2389; found, 465.2373.

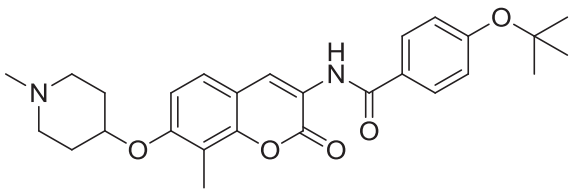

230

4-(*Tert*-butoxy)-N-(8-methyl-7-((1-methylpiperidin-4-yl)oxy)-2-oxo-2H-chromen-3-yl)benzamide (230): EDCI (50.0 mg, 0.26 mmol) and **228** (40.0 mg, 0.21 mmol) were added to aminocoumarin **206** (30.0 mg, 0.10 mmol), freshly prepared from hydrogenolysis of **210**, in 30%

pyridine/CH_2Cl_2 (1.60 mL). After 12 h, the solvent was concentrated and the residue was purified via column chromatography (SiO_2, 10:1 CH_2Cl_2:MeOH) to afford **230** as a colorless amorphous solid (11.0 mg, 23%): ^{1}H NMR ($CDCl_3$, 400 MHz) δ 8.82 (s, 1H), 8.71 (s, 1H), 7.87 (d, *J* = 8.8 Hz, 2H), 7.36 (d, *J* = 8.8 Hz, 1H), 7.12 (d, *J* = 8.4 Hz, 2H), 6.89 (d, *J* = 8.4 Hz, 1H), 4.57 (bs, 1H), 2.82 (bs, 2H), 2.66 (bs, 2H), 2.49 (bs, 3H), 2.39 (s, 3H), 2.20 (bs, 2H), 2.03 (bs, 2H), 1.45 (s, 9H); ^{13}C NMR ($CDCl_3$, 125 MHz) δ 165.7, 159.7, 159.5 (2C), 149.4, 128.4 (2C), 128.0, 125.7, 124.2, 123.1 (2C), 121.7 (2C), 115.2, 113.6, 110.3, 79.7, 51.8 (2C), 45.7, 28.9 (5C), 8.4; HRMS (ESI$^+$) *m/z*: $[M + H]^+$ calcd for $C_{27}H_{33}N_2O_5$, 465.2389; found, 465.2404.

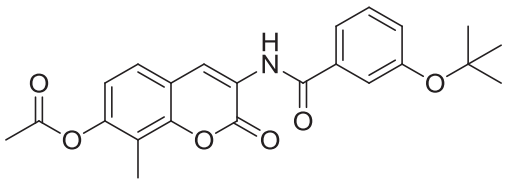

231

3-(3-(*Tert*-butoxy)benzamido)-8-methyl-2-oxo-2H-chromen-7-yl acetate (231): EDCI (82 mg, 0.43 mmol) and **227** (67 mg, 0.34 mmol) were added to aminocoumarin **211** (40 mg, 0.17 mmol), freshly prepared from hydrogenolysis of **147**, in 30% pyridine/CH_2Cl_2 (2.60 mL). After 12 h, the solvent was concentrated and the residue was purified via column chromatography (SiO_2, 40:1 CH_2Cl_2:Acetone) to afford **231** as a colorless amorphous solid (49.0 mg, 70%): ^{1}H NMR ($CDCl_3$, 400 MHz) δ 8.87 (s, 1H), 8.80 (s, 1H), 7.63–7.59 (m, 2H), 7.44 (t, *J* = 8.4 Hz, 2H), 7.24 (dd, *J* = 8.0, 2.4 Hz, 1H), 7.07 (d, *J* = 8.4 Hz, 1H), 2.40 (s, 3H), 2.33 (s, 3H), 1.43 (s, 9H); ^{13}C NMR ($CDCl_3$, 125 MHz) δ 168.9, 165.9, 158.9, 156.2, 150.2, 148.8, 134.5, 129.5, 128.1, 125.6, 123.5 (2C), 122.8, 121.5, 119.4, 119.1, 117.7, 79.4, 28.8 (3C), 20.8, 9.1; HRMS (ESI$^+$) *m/z*: $[M + Na]^+$ calcd for $C_{23}H_{23}NNaO_6$, 432.1423; found, 432.1398.

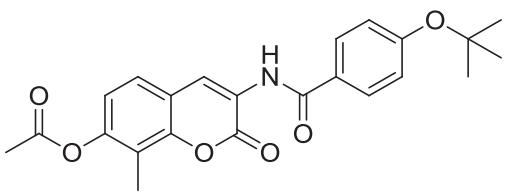

232

3-(4-(*Tert*-butoxy)benzamido)-8-methyl-2-oxo-2H-chromen-7-yl acetate (232): EDCI (82 mg, 0.43 mmol) and **228** (67 mg, 0.34 mmol) were added to aminocoumarin **211** (40 mg, 0.17 mmol), freshly prepared from hydrogenolysis of **147**, in 30% pyridine/CH_2Cl_2 (2.60 mL). After 12 h, the solvent was concentrated and the residue was purified via column chromatography (SiO_2, 40:1 CH_2Cl_2:Acetone) to afford **232** as a colorless amorphous solid (32.5 mg, 46%): ^{1}H NMR ($CDCl_3$, 400 MHz) δ 8.86 (s, 1H), 8.78 (s, 1H), 7.88 (d, *J* = 8.4 Hz, 2H), 7.43 (d, *J* = 8.4 Hz, 1H), 7.13 (d, *J* = 8.4 Hz, 2H), 7.07 (d, *J* = 8.4 Hz, 1H), 2.40 (s, 3H), 2.33 (s, 3H), 1.45 (s, 9H); ^{13}C NMR ($CDCl_3$, 125 MHz) δ 168.9, 165.8, 159.8, 159.0, 150.1, 148.8, 128.5, 127.7 (2C), 125.5, 123.6, 123.2 (2C), 123.1, 119.3, 119.0, 117.8, 79.8, 28.9 (3C), 20.8, 9.1; HRMS (ESI^+) *m/z*: $[M + Na]^+$ calcd for $C_{23}H_{23}NNaO_6$, 432.1423; found, 432.1413.

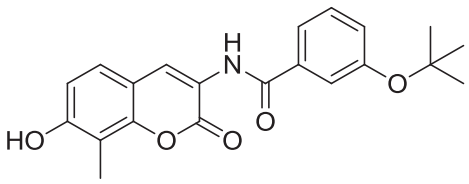

233

3-(*Tert*-butoxy)-N-(7-hydroxy-8-methyl-2-oxo-2H-chromen-3-yl)benzamide (233): A solution of **231** (32.0 mg, 0.078 mmol) in MeOH (0.80 mL) was treated with triethylamine (80 μL, 10%). After 12 h, the solvent was concentrated and the residue purified via column chromatography (SiO_2, 40:1 → 10:1 CH_2Cl_2:Acetone) to afford **233** as a yellow amorphous solid (28.6 mg, 99%): ^{1}H NMR ($CDCl_3$, 400 MHz) δ 8.83 (s, 1H), 8.73 (s, 1H), 7.60 (t, *J* = 8.4 Hz,

2H), 7.43 (t, *J* = 7.6 Hz, 1H), 7.29–7.27 (m, 1H), 7.23 (d, *J* = 7.6 Hz, 1H), 6.84 (d, *J* = 8.4 Hz, 1H), 5.24 (bs, 1H), 2.39 (s, 3H), 1.42 (s, 9H); ^{13}C NMR ($CDCl_3$, 125 MHz) δ 165.9, 159.4, 156.1, 155.6, 134.8, 129.5, 128.0, 125.9 (2C), 124.8, 122.7, 121.5, 121.4, 113.3, 113.0, 111.8, 79.4, 28.8 (3C), 7.9; HRMS (ESI$^+$) *m/z*: $[M + H]^+$ calcd for $C_{21}H_{22}NO_5$, 368.1498; found, 368.1477.

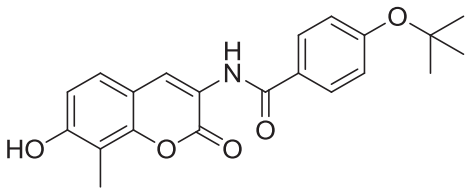

234

4-(*Tert*-butoxy)-N-(7-hydroxy-8-methyl-2-oxo-2H-chromen-3-yl)benzamide (234): A solution of **232** (12.0 mg, 0.029 mmol) in MeOH (0.29 mL) was treated with triethylamine (29 μL, 10%). After 12 h, the solvent was concentrated and the residue purified via column chromatography (SiO_2, 40:1 → 10:1 CH_2Cl_2:Acetone) to afford **234** as a yellow amorphous solid (10.0 mg, 93%): ^{1}H NMR ($CDCl_3$, 400 MHz) δ 8.82 (s, 1H), 8.70 (s, 1H), 7.87 (d, *J* = 8.8 Hz, 2H), 7.29 (d, *J* = 8.8 Hz, 1H), 7.12 (d, *J* = 8.4 Hz, 2H), 6.84 (d, *J* = 8.4 Hz, 1H), 5.27 (s, 1H), 2.39 (s, 3H), 1.45 (s, 9H); ^{13}C NMR ($CDCl_3$, 125 MHz) δ 165.7, 159.7, 159.5, 155.4, 149.5, 128.4 (2C), 127.9, 125.9, 124.5, 123.1 (2C), 113.4, 113.0, 111.7, 28.9 (5C), 7.9; HRMS (ESI$^+$) *m/z*: $[M + H]^+$ calcd for $C_{21}H_{22}NO_5$, 368.1498; found, 368.1484.

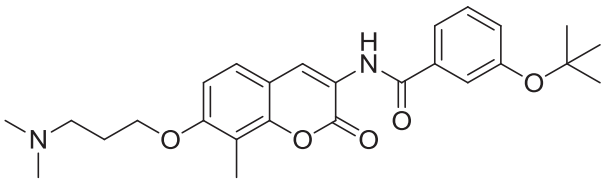

235

3-(*Tert*-butoxy)-N-(7-(3-(dimethylamino)propoxy)-8-methyl-2-oxo-2H-chromen-3-yl)benzamide (235): Diisopropylazodicarboxylate (24.0 μL, 0.13 mmol) was added to a solution of 3-(dimethylamino)propan-1-ol (15.0 μL, 0.13 mmol), **233** (23 mg, 0.063 mmol) and triphenylphosphine (33.0 mg, 0.13 mmol) in anhydrous THF (0.63 mL). After 12 h, the solvent was removed and the residue purified via column chromatography (SiO_2, 10:1, CH_2Cl_2:MeOH) to afford compound **235** as a colorless amorphous solid (23.0 mg, 81%): ^{1}H NMR ($CDCl_3$, 500 MHz) δ 8.83 (s, 1H), 8.74 (s, 1H), 7.62–7.58 (m, 2H), 7.43 (t, *J* = 8.0 Hz, 1H), 7.37 (d, *J* = 8.5 Hz, 1H), 7.24 (dd, *J* = 8.0, 2.0 Hz, 1H), 6.90 (d, *J* = 8.5 Hz, 1H), 4.18 (t, *J* = 6.0 Hz, 2H), 2.84 (bs, 2H), 2.56 (bs, 6H), 2.35 (s, 3H), 2.22 (bs, 2H), 1.43 (s, 9H); ^{13}C NMR ($CDCl_3$, 125 MHz) δ 165.8, 159.4, 156.1, 149.2, 134.8, 129.5 (2C), 128.0, 125.9, 124.6, 122.8, 121.6, 121.5, 114.0 (2C), 108.8, 79.4, 66.2, 56.2, 44.4, 28.9 (5C), 8.2; HRMS (ESI$^+$) *m/z*: $[M + Na]^+$ calcd for $C_{26}H_{32}N_2NaO_5$; 475.2209; found, 475.2218.

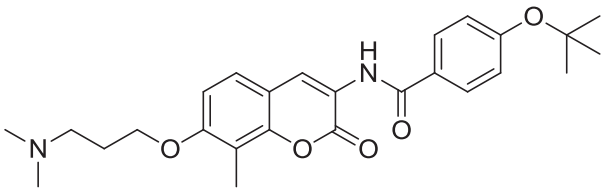

236

4-(*Tert*-butoxy)-N-(7-(3-(dimethylamino)propoxy)-8-methyl-2-oxo-2H-chromen-3-yl)benzamide (236): Diisopropylazodicarboxylate (18.0 μL, 0.093 mmol) was added to a solution of 3-(dimethylamino)propan-1-ol (11.0 μL, 0.093 mmol), **234** (17.0 mg, 0.046 mmol) and triphenylphosphine (24.0 mg, 0.093 mmol) in anhydrous THF (0.50 mL). After 12 h, the solvent was removed and the residue purified via column chromatography (SiO_2, 10:1, CH_2Cl_2:MeOH) to afford compound **236** as a colorless amorphous solid (8.0 mg, 38%): ^{1}H NMR ($CDCl_3$, 400 MHz) δ 8.81 (s, 1H), 8.70 (s, 1H), 7.87 (d, *J* = 8.4 Hz, 2H), 7.37 (d, *J* = 8.4 Hz,

1H), 7.12 (d, *J* = 8.8 Hz, 2H), 6.89 (d, *J* = 8.4 Hz, 1H), 4.18 (t, *J* = 6.0 Hz, 2H), 2.92 (bs, 2H), 2.62 (bs, 6H), 2.34 (s, 3H), 2.26 (bs, 2H), 1.45 (s, 9H); ^{13}C NMR ($CDCl_3$, 125 MHz) δ 165.7, 159.7, 159.5, 157.8, 149.1, 128.4 (2C), 128.0, 125.9, 124.3 (2C), 123.1, 121.7, 114.0, 113.7, 108.8, 79.7, 66.1, 56.1, 44.4, 28.9 (5C), 8.2; HRMS (ESI^+) *m/z*: $[M + Na]^+$ calcd for $C_{26}H_{32}N_2NaO_5$; 475.2209; found, 475.2228.

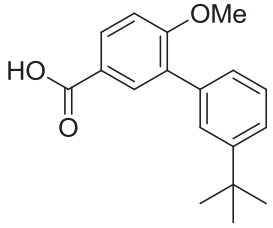

242

3'-(*Tert*-butyl)-6-methoxy-[1,1'-biphenyl]-3-carboxylic acid (242): 1,1'-bis(diphenyl-phosphino)ferrocene-palladium(II)dichloride dichloromethane complex (16.8 mg, 0.021 mmol) was added to a solution of methyl 3-iodo-4-methoxybenzoate (200 mg, 0.68 mmol), (3-(tert-butyl)phenyl)boronic acid (366 mg, 2.05 mmol) and 2M K_2CO_3 (1.0 mL, 2.05 mmol) in dioxane (9.3 mL). After 1 h at rt, the solution was heated to 50^{o}C for 12 h. Once cool, solvent was removed and the residue was resuspended in EtOAc, washed with water, dried (Na_2SO_4), filtered and concentrated. The residue was purified via column chromatography (SiO_2, 6:1, Hexane:EtOAc) to afford benzoate as a colorless oil (204 mg, 99%), which was used without further purification.

Lithium hydroxide (269 mg, 3.20 mmol) was added to a solution of benzoate (191 mg, 0.64 mmol) in 3:1:1 THF:MeOH:H_2O (6.40 mL). After 12 h, the solution was concentrated and the aqueous residue was acidified, and then extracted with EtOAc (3 x 15 mL). The combined organic layers were next extracted with saturated aqueous $NaHCO_3$ (3 x 15 mL), and then the aqueous extracts were acidified. Finally, EtOAc (3 x 15 mL) was used to extract the acid

product, and the combined organic extracts were washed with saturated aqueous NaCl, dried (Na_2SO_4), filtered, and concentrated to afford **242** as a colorless amorphous solid (152 mg, 78%): ^{1}H NMR ($CDCl_3$, 400 MHz) δ 8.13 (s, 1H), 8.11 (s, 1H), 7.56 (s, 1H), 7.44–7.37 (m, 3H), 7.06 (d, *J* = 9.2 Hz, 1H), 3.92 (s, 3H), 1.39 (s, 9H);^{13}C NMR ($CDCl_3$, 125 MHz) δ 170.8, 160.9, 150.9, 136.9, 133.1, 131.4, 131.3, 127.7, 126.7, 126.6, 124.4, 121.5, 110.6, 55.8, 34.8, 31.4 (3C); HRMS (ESI$^+$) *m/z*: $[M + H]^+$ calcd for $C_{18}H_{21}O_3$, 285.1491; found, 285.1494.

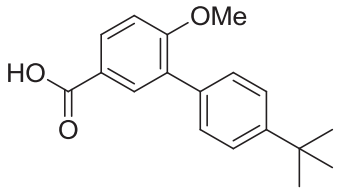

243

4'-(*Tert*-butyl)-6-methoxy-[1,1'-biphenyl]-3-carboxylic acid (243): 1,1'-bis(diphenyl-phosphino)ferrocene-palladium(II)dichloride dichloromethane complex (16.8 mg, 0.021 mmol) was added to a solution of methyl 3-iodo-4-methoxybenzoate (200 mg, 0.68 mmol), (4-(tert-butyl)phenyl)boronic acid (366 mg, 2.05 mmol) and 2M K_2CO_3 (1.0 mL, 2.05 mmol) in dioxane (9.3 mL). After 1 h at rt, the solution was heated to 50^{o}C for 12 h. Once cool, solvent was removed and the residue was resuspended in EtOAc, washed with water, dried (Na_2SO_4), filtered and concentrated. The residue was purified via column chromatography (SiO_2, 6:1, Hexane:EtOAc) to afford benzoate as a colorless oil (204 mg, 99%), which was used without further purification.

Lithium hydroxide (339 mg, 4.53 mmol) was added to a solution of benzoate (270 mg, 0.91 mmol) in 3:1:1 THF:MeOH:H_2O (9.10 mL). After 12 h, the solution was concentrated and the aqueous residue was acidified, and then extracted with EtOAc (3 x 15 mL). The combined organic layers were next extracted with saturated aqueous $NaHCO_3$ (3 x 15 mL), and then the

aqueous extracts were acidified. Finally, EtOAc (3 x 15 mL) was used to extract the acid product, and the combined organic extracts were washed with saturated aqueous NaCl, dried (Na_2SO_4), filtered, and concentrated to afford **243** as a colorless amorphous solid (190 mg, 98%): ^{1}H NMR (Acetone-d_6, 400 MHz) δ 8.03 (d, J = 8.4 Hz, 1H), 7.98 (d, J = 2.0 Hz, 1H), 7.48 (d, J = 1.2 Hz, 4H), 7.21 (d, J = 8.4 Hz, 1H), 3.92 (d, J = 1.6 Hz, 3H), 1.36 (d, J = 1.6 Hz, 9H); ^{13}C NMR (Acetone-d_6, 125 MHz) δ 167.3, 161.3, 150.8, 135.8, 132.9, 131.5, 131.2, 130.0, 127.0, 125.8, 123.8, 112.0, 56.2, 35.1, 31.9, 31.6 (3C); HRMS (ESI$^+$) *m/z*: $[M + H]^+$ calcd for $C_{18}H_{21}O_3$, 285.1491; found, 285.1495.

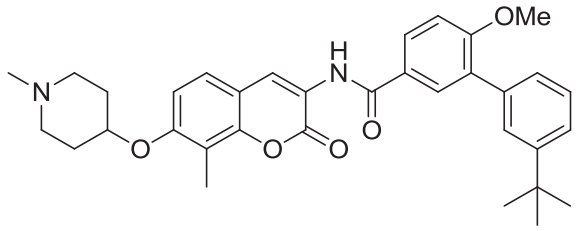

244

3'-(*Tert*-butyl)-6-methoxy-N-(8-methyl-7-((1-methylpiperidin-4-yl)oxy)-2-oxo-2H-chromen-3-yl)-[1,1'-biphenyl]-3-carboxamide (244): EDCI (50.0 mg, 0.26 mmol) and **242** (59 mg, 0.21 mmol) were added to aminocoumarin **206** (30.0 mg, 0.10 mmol), freshly prepared from hydrogenolysis of **210**, in 30% pyridine/CH_2Cl_2 (1.60 mL). After 12 h, the solvent was concentrated and the residue was purified via column chromatography (SiO_2, 10:1 CH_2Cl_2:MeOH) to afford **244** as a colorless amorphous solid (46.0 mg, 80%): ^{1}H NMR ($CDCl_3$, 400 MHz) δ 8.83 (s, 1H), 8.74 (s, 1H), 7.95–7.92 (m, 2H), 7.58 (s, 1H), 7.43–7.35 (m, 4H), 7.10 (d, J = 8.4 Hz, 1H), 6.89 (d, J = 8.8 Hz, 1H), 4.60 (bs, 1H), 3.92 (s, 3H), 2.85 (bs, 2H), 2.72 (bs, 2H), 2.52 (bs, 3H), 2.37 (s, 3H), 2.23 (bs, 2H), 2.05 (bs, 2H), 1.40 (s, 9H); ^{13}C NMR ($CDCl_3$, 125 MHz) δ 165.6, 159.9, 159.5, 156.4, 151.0, 149.4, 136.8, 131.7, 130.1, 127.9, 127.8, 126.7, 126.6, 126.0, 125.7, 124.6, 124.1, 121.8, 115.2, 113.7, 111.0, 110.3, 70.5, 55.9 (2C), 51.6, 45.6,

34.8, 31.8, 31.7, 31.4 (2C), 31.3, 8.4; HRMS (ESI^+) *m/z*: $[M + Na]^+$ calcd for $C_{34}H_{38}N_2NaO_5$; 577.2678; found, 577.2661.

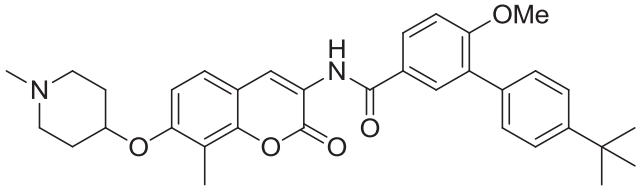

245

4'-(*Tert*-butyl)-6-methoxy-N-(8-methyl-7-((1-methylpiperidin-4-yl)oxy)-2-oxo-2H-chromen-3-yl)-[1,1'-biphenyl]-3-carboxamide (245): EDCI (34.0 mg, 0.18 mmol) and **243** (40 mg, 0.14 mmol) were added to aminocoumarin **206** (20.3 mg, 0.070 mmol), freshly prepared from hydrogenolysis of **210**, in 30% pyridine/CH_2Cl_2 (1.10 mL). After 12 h, the solvent was concentrated and the residue was purified via column chromatography (SiO_2, 10:1 CH_2Cl_2:MeOH) to afford **245** as a colorless amorphous solid (20.0 mg, 52%): ^1H NMR ($CDCl_3$, 400 MHz) δ 8.83 (s, 1H), 8.72 (s, 1H), 7.94 (d, *J* = 2.4 Hz, 1H), 7.93–7.91 (m, 1H), 7.52 (dd, *J* = 14.8, 8.4 Hz, 4H), 7.37 (d, *J* = 8.8 Hz, 1H), 7.09 (d, *J* = 8.8 Hz, 1H), 6.89 (d, *J* = 8.8 Hz, 1H), 4.61 (bs, 1H), 3.93 (s, 3H), 2.87 (bs, 2H), 2.54 (bs, 3H), 2.38 (s, 5H), 2.28 (bs, 2H), 2.08 (bs, 2H), 1.40 (s, 9H); ^{13}C NMR ($CDCl_3$, 125 MHz) δ 165.6, 159.9, 159.4, 150.5, 149.4, 134.2, 131.0, 129.9, 129.2 (4C), 128.0, 126.1, 125.7, 125.2 (4C), 124.1, 121.9, 111.0 (2C), 110.9, 110.3, 55.9 (2C), 34.6, 31.4 (5C), 8.5; HRMS (ESI^+) *m/z*: $[M + H]^+$ calcd for $C_{34}H_{39}N_2O_5$, 555.2859; found, 555.2855.

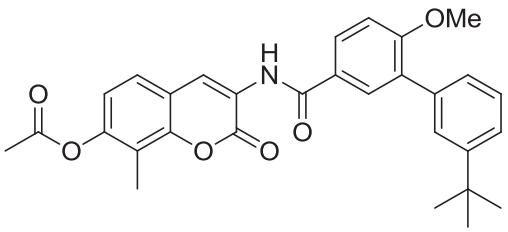

246

3-(3'-(*Tert*-butyl)-6-methoxy-[1,1'-biphenyl]-3-ylcarboxamido)-8-methyl-2-oxo-2H-chromen-7-yl acetate (246): EDCI (152 mg, 0.79 mmol) and **242** (135 mg, 0.47 mmol) were added to aminocoumarin **211** (70 mg, 0.30 mmol), freshly prepared from hydrogenolysis of **147**, in 30% pyridine/CH_2Cl_2 (4.0 mL). After 12 h, the solvent was concentrated and the residue was purified via column chromatography (SiO_2, 40:1 CH_2Cl_2:Acetone) to afford **246** as a colorless amorphous solid (111 mg, 74%): ^{1}H NMR ($CDCl_3$, 400 MHz) δ 8.87 (s, 1H), 8.80 (s, 1H), 7.96–7.92 (m, 2H), 7.58 (s, 1H), 7.44–7.40 (m, 4H), 7.11 (d, *J* = 8.4 Hz, 1H), 7.06 (d, *J* = 8.4 Hz, 1H), 3.93 (s, 3H), 2.40 (s, 3H), 2.33 (s, 3H), 1.40 (s, 9H); ^{13}C NMR ($CDCl_3$, 125 MHz) δ 168.9, 165.7, 160.0, 159.0, 151.0, 150.0, 148.7, 136.8, 131.8, 130.1, 128.0, 127.8, 126.7, 126.6, 125.8, 125.5, 124.6, 123.7, 123.1, 119.3, 119.0, 117.8, 111.0, 55.9, 34.8, 31.4 (3C), 20.8, 9.1; HRMS (ESI$^+$) *m/z*: $[M + Na]^+$ calcd for $C_{30}H_{29}NNaO_6$; 522.1893; found, 522.1905.

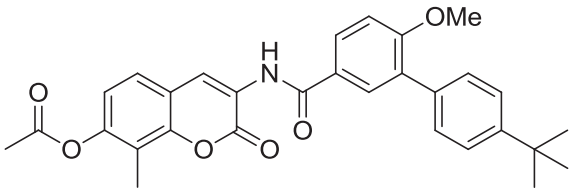

247

3-(4'-(*Tert*-butyl)-6-methoxy-[1,1'-biphenyl]-3-ylcarboxamido)-8-methyl-2-oxo-2H-chromen-7-yl acetate (247): EDCI (152 mg, 0.79 mmol) and **243** (135 mg, 0.47 mmol) were added to aminocoumarin **211** (70 mg, 0.30 mmol), freshly prepared from hydrogenolysis of **147**, in 30% pyridine/CH_2Cl_2 (4.0 mL). After 12 h, the solvent was concentrated and the residue was purified via column chromatography (SiO_2, 40:1 CH_2Cl_2:Acetone) to afford **247** as a colorless amorphous solid (104 mg, 69%): ^{1}H NMR ($CDCl_3$, 400 MHz) δ 8.88 (s, 1H), 8.79 (s, 1H), 7.92 (dd, *J* = 6.0, 2.4 Hz, 2H), 7.55–7.49 (m, 4H), 7.43 (d, *J* = 8.4 Hz, 1H), 7.10 (d, *J* = 8.4 Hz, 1H), 7.06 (d, *J* = 8.4 Hz, 1H), 3.93 (s, 3H), 2.40 (s, 3H), 2.33 (s, 3H), 1.40 (s, 9H); ^{13}C NMR ($CDCl_3$,

125 MHz) δ 168.9, 165.7, 160.0, 158.9, 150.5, 150.0, 148.7, 134.2, 131.0, 129.9, 129.2, 128.1, 125.9, 125.5, 125.2, 123.7, 123.1, 119.7, 119.3, 119.0, 117.8, 111.0, 55.9, 34.6, 31.5 (3C), 31.4, 20.8, 9.1; HRMS (ESI^+) *m/z*: $M + Na]^+$ calcd for $C_{30}H_{29}NNaO_6$; 522.1893; found, 522.1903.

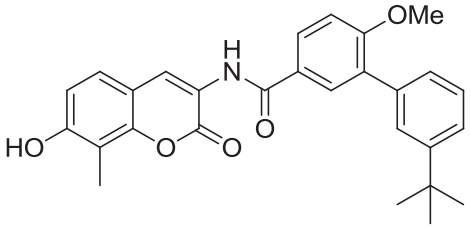

248

3'-(*Tert*-butyl)-N-(7-hydroxy-8-methyl-2-oxo-2H-chromen-3-yl)-6-methoxy-[1,1'-biphenyl]-3-carboxamide (248): A solution of **246** (93.0 mg, 0.19 mmol) in MeOH (1.90 mL) was treated with triethylamine (0.19 mL, 10%). After 12 h, the solvent was concentrated and the residue purified via column chromatography (SiO_2, 40:1 → 10:1 CH_2Cl_2:Acetone) to afford **248** as a yellow amorphous solid (84.0 mg, 99%): ^1H NMR (Acetone-d_6, 400 MHz) δ 9.15 (bs, 1H), 8.91 (s, 1H), 8.73 (s, 1H), 8.02 (dd, *J* = 8.8, 2.4 Hz, 1H), 7.95 (d, *J* = 2.4 Hz, 1H), 7.63 (s, 1H), 7.45–7.38 (m, 4H), 7.92 (d, *J* = 8.8 Hz, 1H), 6.95 (d, *J* = 8.4 Hz, 1H), 3.94 (s, 3H), 2.29 (s, 3H), 1.38 (s, 9H); ^{13}C NMR (Acetone-d_6, 125 MHz) δ 165.8, 160.7, 158.1, 151.5, 138.3, 132.1, 130.8, 129.0, 128.6, 127.6, 127.4 (2C), 127.3, 126.7 (2C), 125.5, 125.0, 122.2, 113.5, 113.3, 112.2 (2C), 56.3, 35.3, 31.7 (3C), 8.1; HRMS (ESI^+) *m/z*: $[M + Na]^+$ calcd for $C_{28}H_{27}NNaO_5$; 480.1787; found, 480.1774.

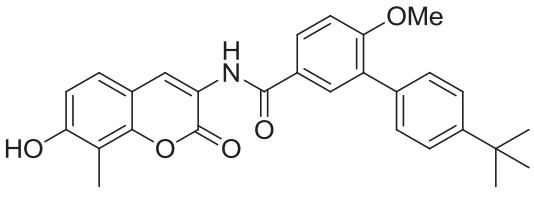

249

4'-(*Tert*-butyl)-N-(7-hydroxy-8-methyl-2-oxo-2H-chromen-3-yl)-6-methoxy-[1,1'-biphenyl]-3-carboxamide (249): A solution of **247** (85.0 mg, 0.17 mmol) in MeOH (1.7 mL) was treated with triethylamine (0.17 mL, 10%). After 12 h, the solvent was concentrated and the residue purified via column chromatography (SiO_2, 40:1 → 10:1 → 5:1 CH_2Cl_2:Acetone) to afford **249** as a yellow amorphous solid (75.0 mg, 96%): ^{1}H NMR (Acetone-d_6, 400 MHz) δ 9.15 (bs, 1H), 8.92 (s, 1H), 8.71 (s, 1H), 8.01 (d, J = 2.4 Hz, 1H), 7.95 (d, J = 2.4 Hz, 1H), 7.55–7.49 (m, 4H), 7.42 (d, J = 8.4 Hz, 1H), 7.28 (d, J = 8.8 Hz, 1H), 6.96 (d, J = 8.4 Hz, 1H), 3.94 (s, 3H), 2.29 (s, 3H), 1.38 (s, 9H); ^{13}C NMR (Acetone-d_6, 125 MHz) δ 165.8, 160.7, 158.1, 150.9, 135.7, 131.5 (2C), 130.6 (2C), 130.0, 129.0, 127.3, 126.7 (2C), 125.8 (2C), 125.5, 122.2, 113.5, 113.3, 112.2 (2C), 56.2, 35.1, 31.6 (3C), 8.1; HRMS (ESI$^+$) *m/z*: $[M + Na]^+$ calcd for $C_{28}H_{27}NNaO_5$; 480.1787; found, 480.1781.

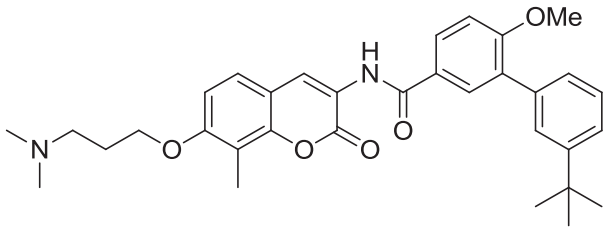

250

3'-(*Tert*-butyl)-N-(7-(3-(dimethylamino)propoxy)-8-methyl-2-oxo-2H-chromen-3-yl)-6-methoxy-[1,1'-biphenyl]-3-carboxamide (250): Diisopropylazodicarboxylate (16.9 μL, 0.087 mmol) was added to a solution of 3-(dimethylamino)propan-1-ol (10.3 μL, 0.087 mmol), **248** (20 mg, 0.044 mmol) and triphenylphosphine (23.0 mg, 0.087 mmol) in anhydrous THF (0.43 mL). After 12 h, the solvent was removed and the residue purified via column chromatography (SiO_2, 10:1, CH_2Cl_2:MeOH) to afford compound **250** as a colorless amorphous solid (21.0 mg, 89%): ^{1}H NMR ($CDCl_3$, 400 MHz) δ 8.83 (s, 1H), 8.74 (s, 1H), 7.95–7.92 (m, 2H), 7.58 (s, 1H), 7.44–7.33 (m, 4H), 7.10 (d, J = 8.0 Hz, 1H), 6.90 (d, J = 8.8 Hz, 1H), 4.16 (t, J = 6.0 Hz, 2H), 3.92 (s,

3H), 2.73 (bs, 2H), 2.47 (s, 3H), 2.35 (bs, 6H), 2.20 (bs, 2H), 1.40 (s, 9H); ^{13}C NMR ($CDCl_3$, 125 MHz) δ 165.6, 159.8, 159.6, 158.2, 151.0, 149.1, 136.9, 131.7, 130.1, 127.9, 127.8, 126.7 (2C), 126.1, 125.7, 124.6, 124.3, 121.6, 114.0, 113.5, 111.0, 108.9, 66.5, 56.2, 55.9, 44.9, 34.8, 31.4 (4C), 29.7, 8.2; HRMS (ESI$^+$) *m/z*: $[M + H]^+$ calcd for $C_{33}H_{39}N_2O_5$, 543.2859; found, 543.2839.

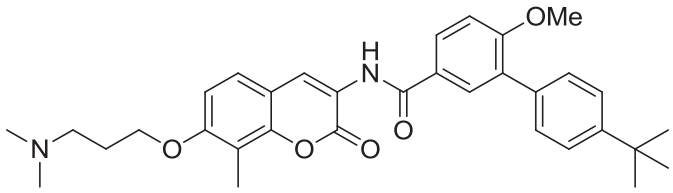

251

4'-(*tert*-butyl)-N-(7-(3-(dimethylamino)propoxy)-8-methyl-2-oxo-2H-chromen-3-yl)-6-methoxy-[1,1'-biphenyl]-3-carboxamide (251): Diisopropylazodicarboxylate (16.9 μL, 0.087 mmol) was added to a solution of 3-(dimethylamino)propan-1-ol (10.3 μL, 0.087 mmol), **249** (20 mg, 0.044 mmol) and triphenylphosphine (23.0 mg, 0.087 mmol) in anhydrous THF (0.43 mL). After 12 h, the solvent was removed and the residue purified via column chromatography (SiO_2, 10:1, CH_2Cl_2:MeOH) to afford compound **251** as a colorless amorphous solid (20.0 mg, 84%): ^{1}H NMR ($CDCl_3$, 400 MHz) δ 8.83 (s, 1H), 8.72 (s, 1H), 7.95–7.91 (m, 2H), 7.53 (d, *J* = 8.4 Hz, 2H), 7.49 (d, *J* = 8.4 Hz, 2H), 7.36 (d, *J* = 8.8 Hz, 1H), 7.09 (d, *J* = 8.8 Hz, 1H), 6.89 (d, *J* = 8.4 Hz, 1H), 4.16 (t, *J* = 6.0 Hz, 2H), 3.93 (s, 3H), 2.73 (bs, 2H), 2.46 (bs, 6H), 2.35 (s, 3H), 2.15 (t, *J* = 6.0 Hz, 2H), 1.40 (s, 9H); ^{13}C NMR ($CDCl_3$, 125 MHz) δ 165.6, 159.8, 159.6, 158.1, 150.5, 149.1, 134.3, 131.0, 129.9, 129.2 (2C), 128.0, 126.1 (2C), 125.7, 125.2, 124.3, 121.6, 114.0, 113.5, 110.9, 108.8, 66.5, 56.2, 55.9, 44.9, 34.6, 31.4 (5C), 8.2; HRMS (ESI$^+$) *m/z*: $[M + H]^+$ calcd for $C_{33}H_{39}N_2O_5$, 543.2859; found, 543.2862.

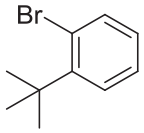

253

1-Bromo-2-(*tert*-butyl)benzene (253):[270] Copper (I) bromide (7.88 g, 35.3 mmol) was slowly added to a solution of 2-(tert-butyl)aniline (5.0 mL, 32.1 mmol) and *tert*-butyl nitrite (6.41 mL, 48.1 mmol) in MeCN (32.0 mL), then heated at 50°C for 1 h. Once cool, saturated aqueous $NaHCO_3$ (30 mL) was added and the solution was extracted with EtOAc (3 x 30 mL). The combined organic layers were dried (Na_2SO_4), filtered, and concentrated. The residue was purified via column chromatography (SiO_2, 100% Hexane → 30:1 Hexane:EtOAc) to give **253** as a red oil (825 mg, 12%): ^{1}H NMR ($CDCl_3$, 500 MHz) δ 7.48 (dd, *J* = 8.5, 1.5 Hz, 1H), 7.30–7.26 (m, 2H), 6.63 (dd, *J* = 8.5, 1.5 Hz, 1H), 1.18 (s, 9H).

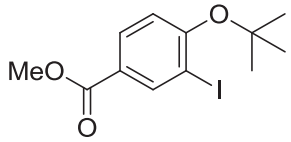

256

Methyl 4-(*tert*-butoxy)-3-iodobenzoate (256): Di-*tert*-butyl dicarbonate (451 mg, 2.07 mmol) was added to a solution of methyl 4-hydroxy-3-iodobenzoate (250 mg, 0.90 mmol) and activated magnesium perchlorate (20 mg, 0.090 mmol, heated at 130°C for 1.5 under vacuum prior to the reaction) in CH_2Cl_2 (1.40 mL), then heated at reflux for 12 h. Once cool, water (15 mL) was added and CH_2Cl_2 (3 x 20 mL) was used to extract the product. The combined organic extracts were dried (Na_2SO_4), filtered, and concentrated and the residue was purified via column chromatography (SiO_2, 12:1, Hexane:EtOAc) to afford compound **256** as a colorless amorphous solid (27 mg, 9.0%): ^{1}H NMR ($CDCl_3$, 500 MHz) δ 8.39 (d, *J* = 2.0 Hz, 1H), 7.85 (dd, *J* = 8.5, 2.5 Hz, 1H), 7.01 (d, *J* = 8.5 Hz, 1H), 3.82 (s, 3H), 1.45 (s, 9H); ^{13}C NMR ($CDCl_3$, 125 MHz) δ

163.7, 158.3, 139.2, 128.8, 123.6, 117.3, 91.3, 80.5, 503., 27.5, 27.4, 27.2; HRMS (ESI^+) *m/z*: $[M + H]^+$ calcd for $C_{12}H_{16}IO_3$, 335.0144; found 335.0162.

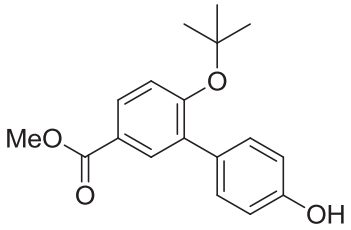

258

Methyl 6-(*tert*-butoxy)-4'-hydroxy-[1,1'-biphenyl]-3-carboxylate (258): 1,1'-bis(diphenylphosphino)ferrocene-palladium(II)dichloride dichloromethane complex (7.3 mg, 0.0090 mmol) was added to a solution of **256** (100 mg, 0.30 mmol), (4-hydroxyphenyl)boronic acid (124 mg, 0.90 mmol) and 2M K_2CO_3 (0.45 mL, 0.90 mmol) in dioxane (4.00 mL). After 1 h at rt, the solution was heated to 50°C for 12 h. Once cool, solvent was removed and the residue was resuspended in EtOAc, washed with water, dried (Na_2SO_4), filtered and concentrated. The residue was purified via column chromatography (SiO_2, 40:1 CH_2Cl_2:Acetone) to afford **258** as a colorless oil (43 mg, 48%): ^1H NMR ($CDCl_3$, 400 MHz) δ 8.08 (d, *J* = 2.4 Hz, 1H), 7.92 (dd, *J* = 8.4, 2.4 Hz, 1H), 7.47 (dd, *J* = 6.8, 2.4 Hz, 2H), 7.16 (d, *J* = 8.8 Hz, 1H), 6.89 (dd, *J* = 6.8, 2.0 Hz, 2H) 5.32 (s, 1H), 3.93 (s, 3H), 1.22 (s, 9H); ^{13}C NMR ($CDCl_3$, 125 MHz) δ 167.0, 157.4, 154.7, 136.0, 132.2 (2C), 131.5, 131.2, 129.0, 124.8, 122.9, 114.8 (2C), 81.0, 52.0, 28.9 (3C); HRMS (ESI^+) *m/z*: $[M + H]^+$ calcd for $C_{18}H_{21}O_4$, 301.1440; found, 301.1462.

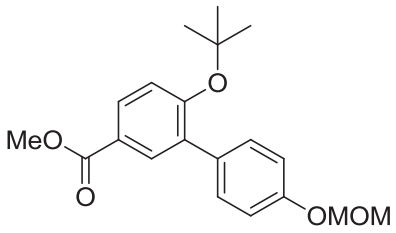

259

Methyl 6-(*tert*-butoxy)-4'-(methoxymethoxy)-[1,1'-biphenyl]-3-carboxylate (259): *N,N*-diisopropylethylamine (55 μL, 0.32 mmol) was slowly added to **258** (19 mg, 0.063 mmol) in anhydrous *N,N*-dimethylformamide (0.21 mL) over 5 min at rt. After 30 min, the solution was cooled to 0°C and chloromethyl ethyl ether (24 μL, 0.32 mmol) was added and the mixture warmed to rt over 12 h. The reaction was quenched by the addition of saturated aqueous NH_4Cl solution and extracted with EtOAc (3 × 10 mL). The combined organic fractions were washed with saturated aqueous NaCl, dried (Na_2SO_4), filtered, and concentrated. The residue was purified via column chromatography (SiO_2, 8:1 → 3:1 Hexane:EtOAc) to give **259** as a yellow oil (11.0 mg, 50%): ^{1}H NMR ($CDCl_3$, 500 MHz) δ 7.96 (d, *J* = 2.0 Hz, 1H), 7.83 (dd, *J* = 8.5, 2.5 Hz, 1H), 7.42 (dd, *J* = 6.5, 2.0 Hz, 2H), 7.08 (d, *J* = 8.5 Hz, 1H), 7.00 (dd, *J* = 6.5, 2.0 Hz, 2H), 5.15 (s, 2H), 3.82 (s, 3H), 3.44 (s, 3H), 1.14 (s, 9H); ^{13}C NMR ($CDCl_3$, 125 MHz) δ 167.0, 157.4, 156.5, 135.9, 132.3, 130.9, 129.1, 124.7, 122.7, 117.5, 115.9, 115.6, 115.3, 94.5, 80.9, 56.1, 52.0, 29.3, 28.9, 28.7; HRMS (ESI$^+$) *m/z*: $[M + H]^+$ calcd for $C_{20}H_{25}O_5$, 345.1702; found, 345.1696.

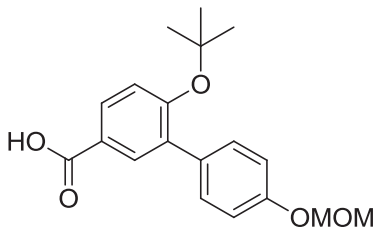

260

6-(*Tert*-butoxy)-4'-(methoxymethoxy)-[1,1'-biphenyl]-3-carboxylic acid (260): Lithium hydroxide (38.0 mg, 0.45 mmol) was added to a solution of **259** (31.0 mg, 0.090 mmol) in 3:1:1 THF:MeOH:H_2O (0.9 mL). After 12 h, the solution was concentrated and the aqueous residue was acidified, and then extracted with EtOAc (3 x 10 mL). The combined organic layers were next extracted with saturated aqueous $NaHCO_3$ (3 x 10 mL), and then the aqueous extracts were

acidified. Finally, EtOAc (3 x 10 mL) was used to extract the acid product, and the combined organic extracts were washed with saturated aqueous NaCl, dried (Na_2SO_4), filtered, and concentrated to afford **260** as a colorless amorphous solid (28.0 mg, 94%): ^{1}H NMR ($CDCl_3$, 400 MHz) δ 8.11 (s, 1H), 7.98 (d, *J* = 8.4 Hz, 1H), 7.52 (d, *J* = 8.8 Hz, 2H), 7.20 (d, *J* = 8.4 Hz, 1H), 7.10 (d, *J* = 8.4 Hz, 2H), 5.25 (s, 2H), 3.54 (s, 3H), 1.27 (s, 9H); ^{13}C NMR ($CDCl_3$, 125 MHz) δ 170.6, 158.2, 156.5, 135.8, 132.9, 132.3, 130.9 (2C), 129.8, 123.5, 122.4, 115.6 (2C), 94.5, 81.1, 56.1, 28.9 (3C); HRMS (ESI$^+$) *m/z*: $[M + Na]^+$ calcd for $C_{19}H_{22}NaO_5$; 353.1365; found, 353.1343.

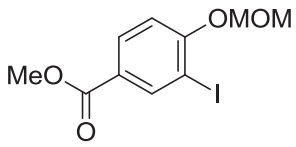

261

Methyl 3-iodo-4-(methoxymethoxy)benzoate (261):[271] *N,N*-diisopropylethylamine (0.50 mL, 2.88 mmol) was slowly added to methyl 4-hydroxy-3-iodobenzoate (200 mg, 0.72 mmol) in anhydrous *N,N*-dimethylformamide (2.10 mL) over 5 min at rt. After 30 min, the solution was cooled to 0°C and chloromethyl ethyl ether (0.22 mL, 2.88 mmol) was added and the mixture warmed to rt over 12 h. The reaction was quenched by the addition of saturated aqueous NH_4Cl solution and extracted with EtOAc (3 × 15 mL). The combined organic fractions were washed with saturated aqueous NaCl, dried (Na_2SO_4), filtered, and concentrated. The residue was purified via column chromatography (SiO_2, 15:1 → 10:1 Hexane:EtOAc) to give **261** as a yellow amorphous solid (234 mg, 99%): ^{1}H NMR ($CDCl_3$, 400 MHz) δ 8.48 (d, *J* = 2.0 Hz, 1H), 8.01–7.98 (m, 1H), 7.10 (dd, *J* = 8.6, 2.8 Hz, 1H), 5.32 (d, *J* = 2.8 Hz, 2H), 3.91 (s, 3H), 3.53 (s, 3H); ^{13}C NMR ($CDCl_3$, 125 MHz) δ 165.5, 159.5, 141.1, 131.4, 125.3, 113.4, 94.7, 86.2, 56.6, 52.2; HRMS (ESI$^+$) *m/z*: $[M + H]^+$ calcd for $C_{10}H_{12}IO_4$, 322.9780; found, 322.9796.

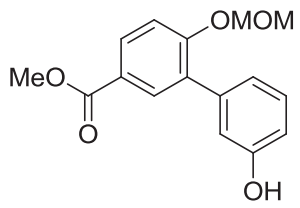

263

Methyl 3'-hydroxy-6-(methoxymethoxy)-[1,1'-biphenyl]-3-carboxylate (263): 1,1'-bis(diphenylphosphino)ferrocene-palladium(II)dichloride dichloromethane complex (5.0 mg, 0.0056 mmol) was added to a solution of **261** (60 mg, 0.19 mmol), (3-hydroxyphenyl)boronic acid (77 mg, 0.56 mmol) and 2M K_2CO_3 (0.28 mL, 0.56 mmol) in dioxane (2.50 mL). After 1 h at rt, the solution was heated to 50^{o}C for 12 h. Once cool, solvent was removed and the residue was resuspended in EtOAc, washed with water, dried (Na_2SO_4), filtered and concentrated. The residue was purified via column chromatography (SiO_2, 40:1 → 10:1 → 1:1 CH_2Cl_2:Acetone) to afford **263** as a colorless oil (52 mg, 97%): ^{1}H NMR ($CDCl_3$, 500 MHz) δ 7.95 (d, *J* = 2.0 Hz, 1H), 7.92 (dd, *J* = 8.5, 2.0 Hz, 1H), 7.24–7.16 (m, 2H), 7.02 (dt, *J* = 7.5, 1.0 Hz, 1H), 6.94 (t, *J* = 2.0 Hz, 1H), 6.78–6.76 (m, 1H), 5.14 (s, 2H), 4.90 (bs, 1H), 3.83 (s, 3H), 3.36 (s, 3H); ^{13}C NMR ($CDCl_3$, 125 MHz) δ 166.8, 157.8, 155.2, 139.2, 132.6, 130.9, 130.6, 129.3, 122.1, 116.5, 114.4, 114.3, 94.6, 56.4, 52.0, 31.0; HRMS (ESI$^+$) *m/z*: $[M + Na]^+$ calcd for $C_{16}H_{16}NaO_5$; 311.0895; found, 311.0913.

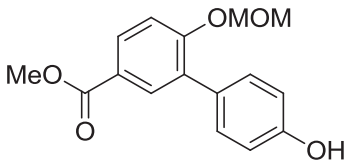

264

Methyl 4'-hydroxy-6-(methoxymethoxy)-[1,1'-biphenyl]-3-carboxylate (264): 1,1'-bis(diphenylphosphino)ferrocene-palladium(II)dichloride dichloromethane complex (5.0 mg,

0.0056 mmol) was added to a solution of **261** (60 mg, 0.19 mmol), (4-hydroxyphenyl)boronic acid (77 mg, 0.56 mmol) and 2M K_2CO_3 (0.28 mL, 0.56 mmol) in dioxane (2.50 mL). After 1 h at rt, the solution was heated to 50°C for 12 h. Once cool, solvent was removed and the residue was resuspended in EtOAc, washed with water, dried (Na_2SO_4), filtered and concentrated. The residue was purified via column chromatography (SiO_2, 40:1 CH_2Cl_2:Acetone) to afford **264** as a colorless oil (46 mg, 86%): ^{1}H NMR ($CDCl_3$, 400 MHz) δ 8.08 (d, *J* = 2.4 Hz, 1H), 7.98 (dd, *J* = 8.6, 2.4 Hz, 1H), 7.46–7.42 (m, 2H), 7.24 (d, *J* = 8.8 Hz, 1H), 6.93–6.90 (m, 2H), 5.23 (s, 2H), 5.00 (bs, 1H), 3.92 (s, 3H), 3.46 (s, 3H); ^{13}C NMR ($CDCl_3$, 125 MHz) δ 166.8, 157.8, 155.2, 139.2, 132.6, 130.9, 130.7, 129.3, 122.1, 116.5, 114.5, 114.4, 94.6, 56.4, 52.1, 29.7; HRMS (ESI^+) *m/z*: $[M + Na]^+$ calcd for $C_{16}H_{16}NaO_5$; 311.0895; found, 311.0893.

Chapter V

Modulation of Hsp90 with Small Molecules

I. Introduction

Studies discussed in Chapters II–III have led to the identification of several novel novobiocin analogues that exhibit significant activity. Interest in examining these compounds further has driven subsequent collaborative studies with laboratories at KU as well as with researchers at the NCI. These efforts have produced notable findings regarding the broad applicability and unique mechanism(s) of action these analogues manifest. Additional collaborative studies with researchers at the NCI resulted in the identification of a novel inhibitor that acts through a unique mechanism to modulate Hsp90 activity. Studies with these novobiocin analogues and this novel inhibitor of Wee1 are presented herein.

II. Follow-up studies using 26g (KU174)

A. *In vitro* assays with 26g

The promising activity of **26g** (KU174) has led to intense interest in studying this compound further. Through studies largely carried out by collaborators, the scope of understanding the activity of this remarkable compound against cancer cells has been expanded.

1. Effect of 26g on more aggressive and resistant cancer cell lines

Although initial studies examined the activity of **26g** against breast and prostate cancer cells, collaborative studies with Dr. Holzbeierlein at the KU Medical Center (KUMC), demonstrated this compound manifests activity against other cancers as well. Notably, it was important to look at the activity of **26g** against cancers that are known to be highly metastatic or resistant to other chemotherapeutics. LNCaP-LN3 (androgen-dependent human prostate cancer cells) and PC3-MM2 (androgen-independent prostate cancer cells) cells, provided by the Holzbeierlein lab at KUMC, were chosen to represent aggressive prostate cancer cells with high metastatic potential. A549 (adenocarcinomic human alveolar basal epithelial cells) cells, provided by the Cohen lab at KUMC, were selected as a result of their previously described resistance to several clinically used anti-cancer agents. The anti-proliferative activity of **26g** against these cells lines is shown in Table 15.

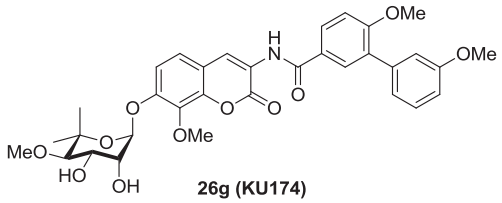

26g (KU174)

Table 15. Anti-proliferative activity of **26g**.

Compound	PC3-MM2 (IC_{50}, μM)	LNCaP-LN3 (IC_{50}, μM)	A549 (IC_{50}, μM)
26g	1.44 ± 0.4[a]	0.11 ± 0.02	4.51 ± 0.1

[a] Values represent mean ± standard deviation for at least two separate experiments performed in triplicate.

The activity manifested by **26g** against these cell lines is very promising, and represents the most significant potency to date against LNCaP-LN3 cells. These consistent low micromolar values have motivated further mechanistic studies. In collaboration with the Holzbeierlein

laboratory, biological studies continue in an effort to identify the specific mechanism which **26g** exhibits its activity, including the potential inhibition of individual Hsp90 isoforms. Moreover, the consistent activity manifested by **26g** against several divergent cancer cell lines prompted further studies.

2. Time-dependent activity of 26g versus 17-AAG

In collaboration with the Holzbeierlein lab, the time course required for this compound to exert its anti-proliferative activity was investigated. **26g** was compared with its parent compound, novobiocin, and the *N*-terminal Hsp90 inhibitor **17-AAG** (Figure 64), which is in advanced clinical trials for cancer. The IC_{50} value of each of these compounds was determined against LN3 prostate cancer cells after 4 h, 12 h, 24 h, and 48 h. Unlike the advanced clinical candidate, **17-AAG**, which took 72 h to reach its reported IC_{50} value, **26g** quickly demonstrated efficacy, reaching its maximum potency after 4 h. Moreover, the **26g** exhibited greater potency than **17-AAG** against LN3 cells. This study demonstrated the fast-acting nature of **26g** and confirmed its remarkable potency over advanced clinical agents. These results support that there would be a large variance in dosing schedules when administering these two compounds. Finally, if total cell death, which corresponds directly with absorbance, is considered, it becomes clear that **17-AAG** never kills more than 60% of the cells while **26g** consistently kills more than 90% of the cells. This finding supports that while **17-AAG** is a cytostatic agent, **26g** is a cytotoxic agent against LN-3 cells.

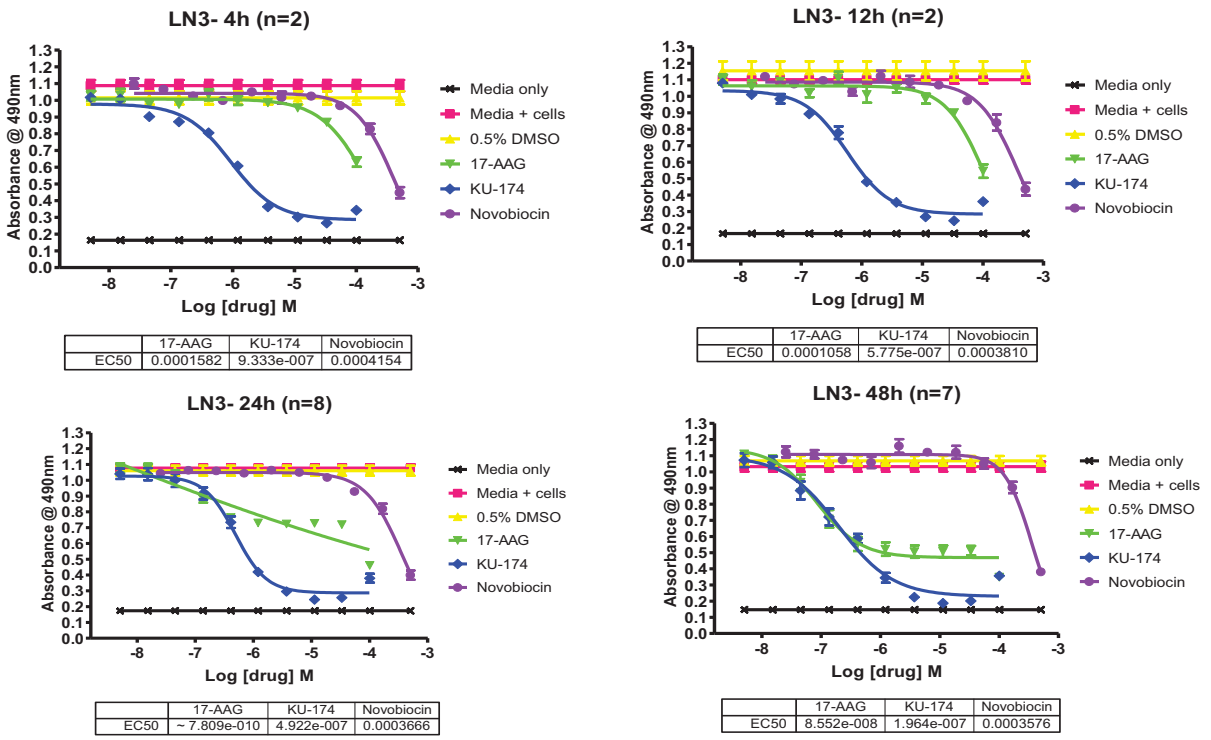

Figure 65. Time-dependent IC_{50} values of **26g** (KU174) versus **17-AAG** against LN3 cells.

3. High-throughput screen (HTS) of 26g against several cancer cell lines

The potency exhibited by **26g** against LN3 cells motivated subsequent examination of its activity against a panel of cancer cell lines. In collaboration with Dr. Chaguturu in the KU HTS laboratory, **26g** alongside several other novobiocin analogues and **17-AAG** were screened against several cancer cell lines. After screening, the compounds were ranked based upon their percent inhibition at the highest concentration tested (30 μM). As seen in Figure 66, **26g** (KU174) was consistently most active, averaging 80% inhibition and exhibiting significant potency against cell lines wherein other compounds failed to kill cells. In line with the study executed by the Holzbeierlein lab, **26g** was once again confirmed to be consistently more active than advanced clinical candidate **17-AAG**.

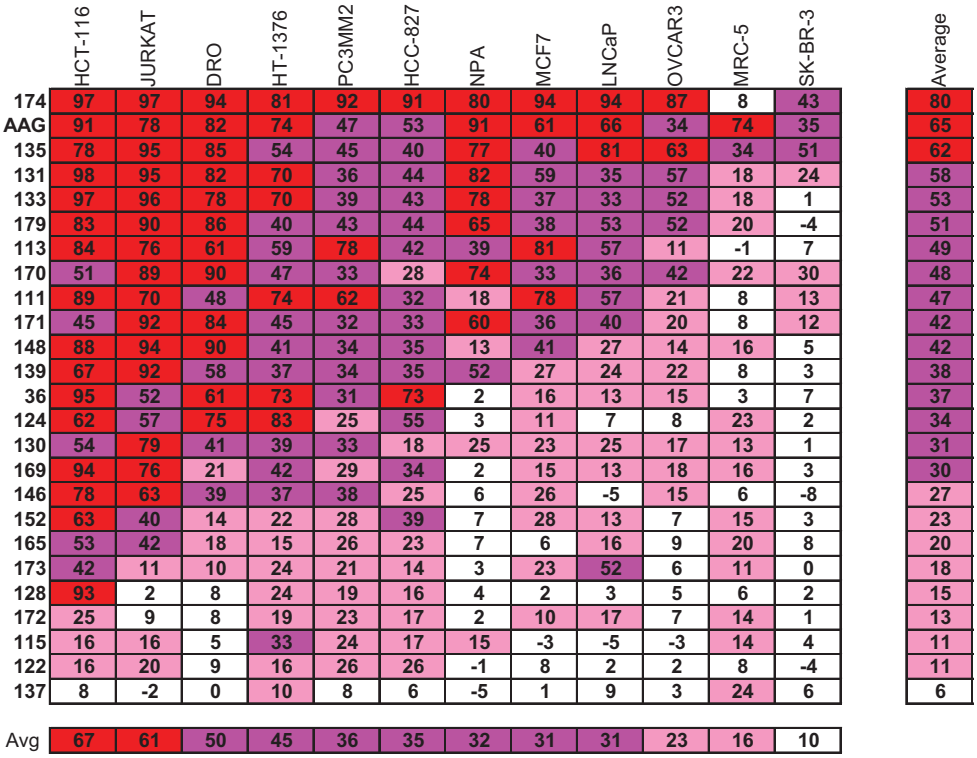

	HCT-116	JURKAT	DRO	HT-1376	PC3MM2	HCC-827	NPA	MCF7	LNCaP	OVCAR3	MRC-5	SK-BR-3	Average
174	97	97	94	81	92	91	80	94	94	87	8	43	80
AAG	91	78	82	74	47	53	91	61	66	34	74	35	65
135	78	95	85	54	45	40	77	40	81	63	34	51	62
131	98	95	82	70	36	44	82	59	35	57	18	24	58
133	97	96	78	70	39	43	78	37	33	52	18	1	53
179	83	90	86	40	43	44	65	38	53	52	20	-4	51
113	84	76	61	59	78	42	39	81	57	11	-1	7	49
170	51	89	90	47	33	28	74	33	36	42	22	30	48
111	89	70	48	74	62	32	18	78	57	21	8	13	47
171	45	92	84	45	32	33	60	36	40	20	8	12	42
148	88	94	90	41	34	35	13	41	27	14	16	5	42
139	67	92	58	37	34	35	52	27	24	22	8	3	38
36	95	52	61	73	31	73	2	16	13	15	3	7	37
124	62	57	75	83	25	55	3	11	7	8	23	2	34
130	54	79	41	39	33	18	25	23	25	17	13	1	31
169	94	76	21	42	29	34	2	15	13	18	16	3	30
146	78	63	39	37	38	25	6	26	-5	15	6	-8	27
152	63	40	14	22	28	39	7	28	13	7	15	3	23
165	53	42	18	15	26	23	7	6	16	9	20	8	20
173	42	11	10	24	21	14	3	23	52	6	11	0	18
128	93	2	8	24	19	16	4	2	3	5	6	2	15
172	25	9	8	19	23	17	2	10	17	7	14	1	13
115	16	16	5	33	24	17	15	-3	-5	-3	14	4	11
122	16	20	9	16	26	26	-1	8	2	2	8	-4	11
137	8	-2	0	10	8	6	-5	1	9	3	24	6	6
Avg	67	61	50	45	36	35	32	31	31	23	16	10	

Figure 66. HTS of novobiocin analogues versus **17-AAG** against a panel of cancer cell lines.

4. NCI 60 cell line screen of 26g

The results from these studies led to our interest in submitting these compounds to a more thorough analysis, utilizing cancer cell lines not previously examined. This goal was accomplished through submitting **26g** to the NCI 60 human tumor cell line screen. Results of testing **26g** against leukemia, non-small cell lung, colon, CNS, melanoma, ovarian, renal, prostate, and breast cancers are shown in Figure 67. **26g** was shown to demonstrate broad efficacy against these cell lines, with values consistently in the nanomolar to low micromolar range. This compound was most potent (mid-nanomolar GI_{50}) at inhibiting growth of SK-MEL-5 metastatic melanoma and MDA-MB-468 estrogen receptor (ER)-negative breast cancer cells, while it was consistently in the nanomolar range against all leukemia cell lines. The promising activity manifested by **26g** in this 60 cell panel screen prompted the NCI to request additional

material for additional biological investigation. Due to its reproducible activity in the *in vitro* screens, **26g** is scheduled to undergo a hollow fiber screen. This assay will be performed by the NCI as they have demonstrated the ability to provide quantitative indices of drug efficacy with minimal expenditures of time and materials. Thus, the hollow fiber assay will act as an initial *in vivo* experience for **26g**.

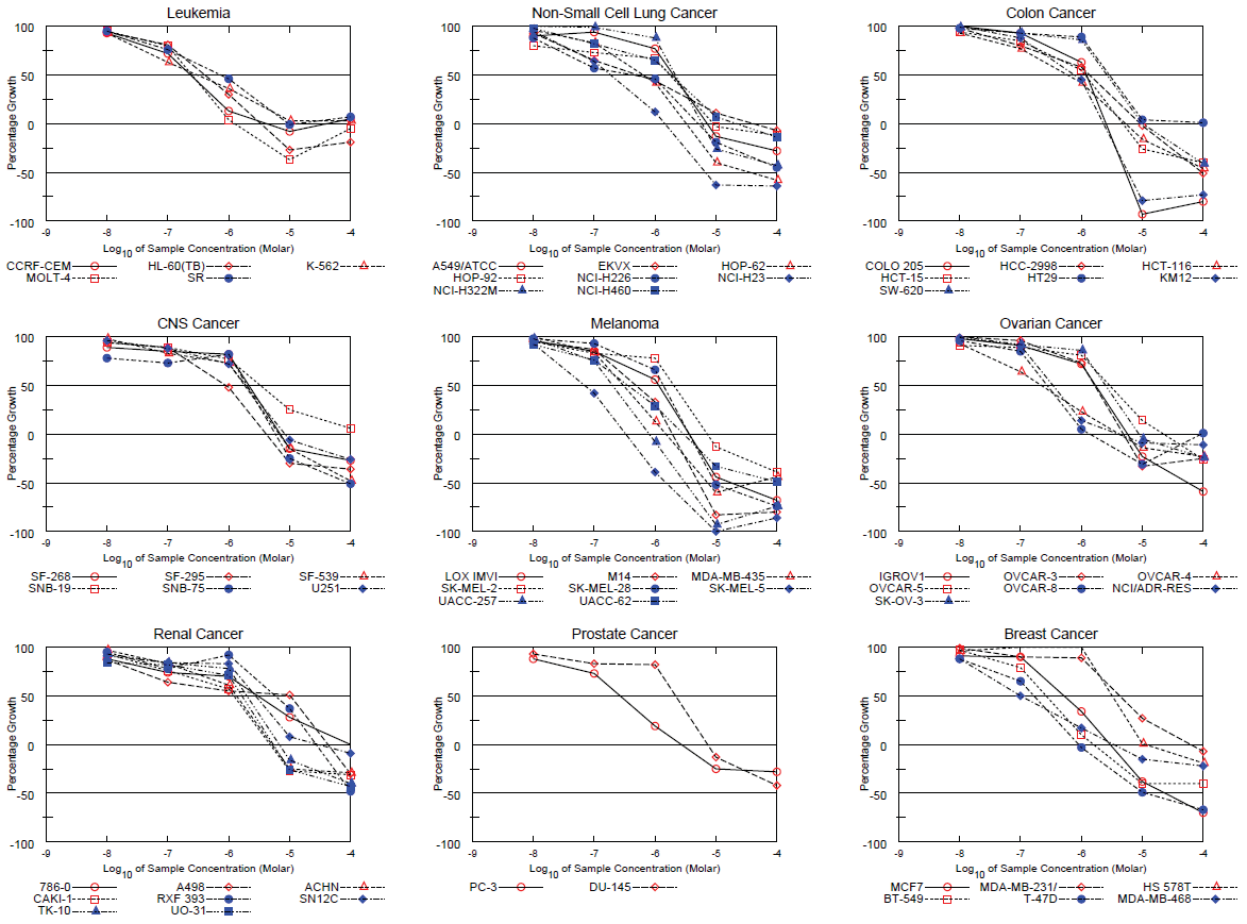

Figure 67. Results of testing **26g** against NCI 60 human tumor cell line screen.

B. *In vivo* assay with 26g

An animal model to examine the efficacy of **26g** was pursued in collaboration with the Cohen lab at KUMC. Head and neck squamous cell carcinomas (HNSCC) were implanted into nude mice and their tumor volumes were monitored over several weeks.

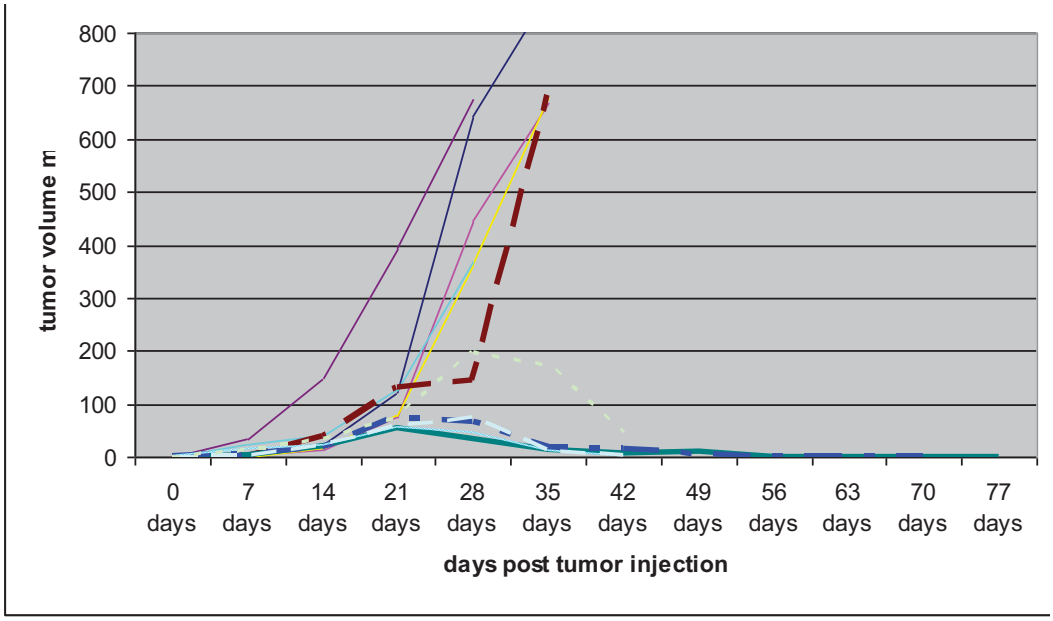

Figure 68. *In vivo* screen of **26g** against HNSCC in mice.

1. Mouse model of 26g against HNSCC

As seen in Figure 68, the solid lines represent control mice that were not dosed with any **26g**, while the dashed lines correspond to those mice that received 5mg/kg of **26g** 5X/week for 3 weeks, starting on day 21. The results obtained from this study demonstrate that **26g** manifests *in vivo* efficacy. In comparison to the control mice with similar tumor volumes (in mm^2) at the start of dosing, all but one mouse showed complete tumor regression. The non-responsive mouse had a markedly larger tumor at the inception of treatment. Of note, upon conclusion of dosing after 3

weeks, none of the treated animals showed a reemergence of the tumor, resulting in a cure for 5 out of 6 mice. This study affirmed that **26g** exhibits promise as an *in vivo* agent and could represent an exciting clinical anti-cancer agent in the future.

III. Follow-up studies using 128a (KU135)

A. *In vitro* assays with 128a

The activity manifested by **128a** (KU135) has also led to subsequent studies with this compound. Collaborative studies with many of the same groups studying **26g** have led to an enhanced understanding of the mechanisms through which **128a** elicits its activity.

1. Effect of 128a on several diverse and aggressive cancer cell lines

Initial anti-proliferative studies examined the activity of **128a** against MCF-7 and SKBr3 breast cancer cells. To explore its applicability to other cancers, HCT-116 colon cancer cells and PL45 pancreatic adenocarcinoma epithelial cells, also available within our laboratory, were screened for their response to **128a**. Next, examination of additional carcinomas was carried out through collaborative screens executed by the Holzbeierlein laboratory at KUMC. As stated before, it was important to look at the activity of **128a** against cancers that are known to be highly metastatic or resistant to other chemotherapeutics. As with **26g**, LNCaP-LN3 (androgen-dependent human prostate cancer cells) and PC3-MM2 (androgen-independent prostate cancer cells) cells, were chosen. In collaboration with the Robertson laboratory at KUMC, immortalized

T-lymphocytic Jurkat cells were used to study acute T-cell leukemia. The anti-proliferative activity of **128a** against these cells lines is shown in Table 16.

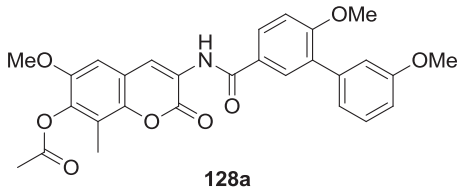

128a

Table 16. Anti-proliferative activity of **128a**.

Compound	HCT-116 (IC_{50}, μM)	PL45 (IC_{50}, μM)	LNCaP-LN3 (IC_{50}, μM)	PC-3-MM2 (IC_{50}, μM)	Jurkat T-cells (IC_{50}, μM)
128a	0.52 ± 0.01	4.1 ± 2.2	0.42 ± 0.27	0.97 ± 0.68	0.42

[a] Values represent mean ± standard deviation for at least two separate experiments performed in triplicate.

The activity manifested by **128a** against these cell lines is very promising, and represents improved activity over its initial values against breast cancer cells in almost every new cell line employed (SKBr3 ~5.7 μM, MCF-7 ~1.5 μM). These nanomolar IC_{50} values demonstrate the broad applicability and efficacy of **128a** against cancer cell types of variable origin. Moreover, this novobiocin analogue manifested submicromolar activity against the metastatic LNCaP-LN3 and PC-3-MM2 cells, making it a promising lead for aggressive prostate cancers. The remarkable and consistent activity of **128a** against several divergent cancer cell lines prompted biological studies in an effort to identify the specific mechanism by which **128a** exhibits its activity.

2. Time-dependent activity of 128a versus novobiocin, 17-AAG and etoposide

As part of a collaborative study with the Robertson laboratory at KUMC, studies were implemented to evaluate the extent to which wild-type Jurkat T-lymphoblastoid leukemia cells (clone E6.1) were sensitive to **128a**. The potency of **128a** was compared to that of novobiocin, as well as **17-AAG** and the anticancer drug, etoposide. As illustrated in Figure 69, all four compounds inhibited cell proliferation in a concentration- and time-dependent manner. The IC_{50} values for **128a**, etoposide, **17-AAG** and novobiocin at 48 h after treatment were found to be 416 nM and 1.3, 4.0, and 252 μM, respectively. Thus, although all four drug treatments inhibited Jurkat cell proliferation, **128a** was ~3, ~10, and ~600 times more potent than the clinically used agent, etoposide, the advanced clinical agent, **17-AAG**, and novobiocin, respectively.[259]

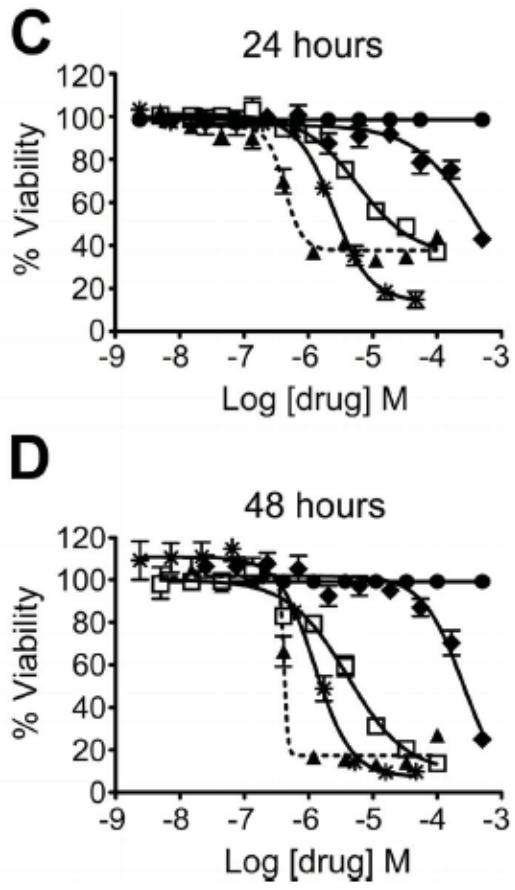

Cells (3 X 10^4) were cultured in a 96-well plate for 24 (C) or 48 h (D) in the absence or presence of:
DMSO (●),
KU135 (2.5 nM to 50 μM) (▲),
17-AAG (0.5 nM to 10 μM) (□),
etoposide (2.4 nM to 47 μM) (∗),
or novobiocin (25 nM to 500 μM) (◆)

Figure 69. Time-dependent IC_{50} values of **128a** (KU135) against Jurkat T-cells.[259]

3. HTS of 128a against several cancer cell lines

The potency exhibited by **128a** against these cancer cells of divergent origin motivated subsequent examination of its activity against a broader panel of cancer cell lines. In collaboration with Dr. Chaguturu in the KU HTS laboratory, **128a** was included with several other novobiocin analogues and **17-AAG** in a screen against several cancer cell lines. After screening, the compounds were ranked based upon their percent inhibition at the highest concentration tested (30 μM). As seen in Figure 66, **128a** (KU135) was in the top three compounds in terms of potency, averaging 62% inhibition overall. Notably, **128a** exhibited nearly equivalent potency when compared to advanced clinical candidate **17-AAG**. Moreover, in agreement with the study executed by Robertson and co-workers, **128a** was notably more potent than **17-AAG** against Jurkat T-cells. This study confirmed the promise of this novel novobiocin analogue and motivated an even broader screen to probe its efficacy.

4. NCI 60 cell line screen of 128a

Results from these led to interest in submitting these compounds to a more thorough analysis, utilizing cancer cell lines not previously examined. This goal was accomplished through submitting **128a** to the NCI 60 human tumor cell line screen. Results of testing **128a** against leukemia, non-small cell lung, colon, CNS, melanoma, ovarian, renal, prostate, and breast cancers are shown in Figure 70. **128a** was shown to demonstrate broad efficacy against these cell lines, with values consistently in the nanomolar to low micromolar range. This compound was most consistently efficacious (mid-nanomolar GI_{50}) against leukemia, CNS and prostate cancer cells. However, the most remarkable activity (~200 nM) that **128a** manifested as part of this screen was against SNB-75 (CNS), MDA-MB-435 (melanoma), and OVCAR-3

(ovarian) cancer cells. Due to its overall potency, **128a** may represent a promising lead compound in treatment of these or many of the other cancer types tested. Moreover, the results of this screen motivated further studies into the exact mechanisms through which this unique scaffold manifests its remarkable activity.

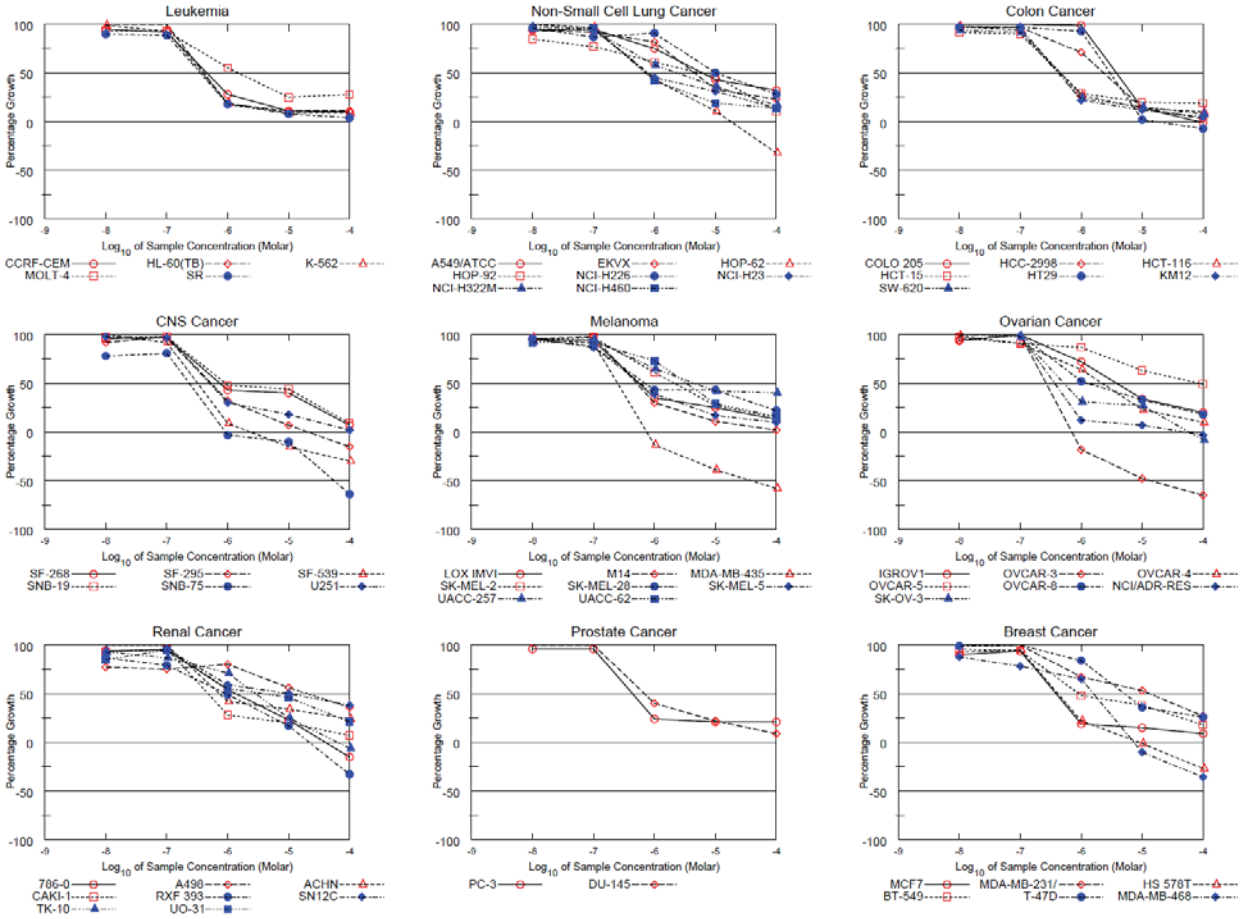

Figure 70. Results of testing **128a** against NCI 60 human tumor cell line screen.

B. Mechanistic studies involving 128a

Several studies utilizing alternate approaches and various cancer cell lines have been used to elucidate mechanisms that explain the activity manifested by **128a**. Selected collaborative studies are presented herein.

1. Western blot analyses against Jurkat cells

As part of the previously discussed collaborative study with the Robertson laboratory at KUMC, Western blot analyses were used to compare the expression profiles of four different Hsp90 proteins in response to **128a** versus **17-AAG**. Moreover, the depletion of associated client proteins and/or the induction of Hsp70 were examined as well. As illustrated in Figure 71, Jurkat cells constitutively express all four isoforms of Hsp90 and incubation with **17-AAG** but not **128a** (KU135) for 24 h led to a considerable increase in of Hsp90α and β. Moreover, both compounds caused significant alterations in the level of known Hsp90 client proteins, especially phospho-Akt (Akt-p). While levels of HIF-1α were decreased upon treatment with either agent, cell cycle regulator cdc2 was only sensitive to treatment with **17-AAG**. Figure 71 illustrates that Hsp70 expression was induced to a far greater extent in cells treated with **17-AAG** than in cells treated with **128a** (KU135). It was proposed that the differential expression profiles of Hsp90α, Hsp90β and Hsp70 might partially explain the increased potency of **128a** versus **17-AAG** against Jurkat T-cells.[259]

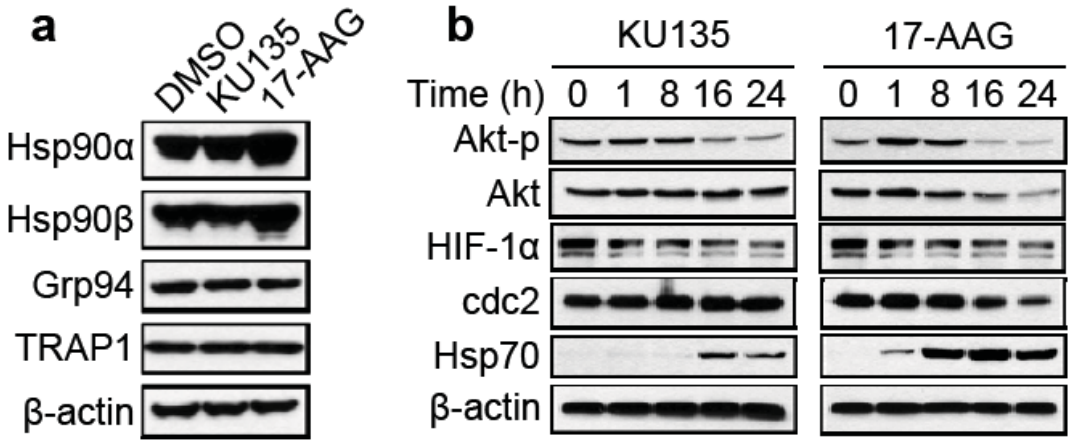

Figure 71. Western blot analyses of **128a** versus **17-AAG**.[259]

2. 128a triggers unique mechanism of apoptosis

As another facet of the previously described study in Jurkat cells, the mechanism of apoptosis induced in response to treatment with **128a** was examined. Apaf-1-deficient Jurkat cells and cells overexpressing Bcl-2 or Bcl-x_L were used to investigate whether the instrinsic (mitochodria-mediated) pathway was responsible for **128a**-induced cell death. While Apaf-1 is strictly required for apoptosome-mediated activation of initiator caspase-9 within the instrinsic pathway, Bcl-2 or Bcl-x_L are well characterized anti-apoptotic proteins whose overexpression is known to inhibit apoptosis by preventing release of pro-apoptotic proteins into the cytosol.

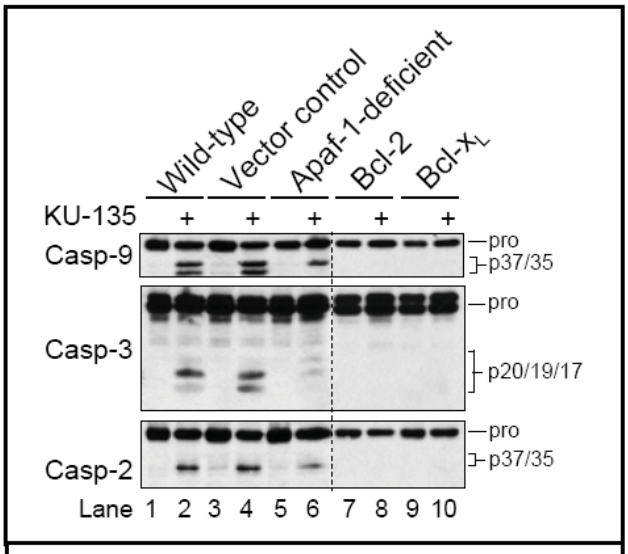

Figure 10: Bcl-2 or Bcl-x_L overexpresion, but not Apaf-1 knockdown, inhibits all caspase processing induced by KU135. Cells (10^6/ml) were cultured with DMSO or 1 μM KU135 for 24 h, harvested and lysed for Western blotting.

Figure 72. 128a exhibits unique apoptotic mechanism.[259]

As seen in Figure 72, Western blot analysis of cell lysates obtained at 24 h after **128a** treatment revealed that cells lacking Apaf-1 or overexpressing Bcl-2/Bcl-x_L were resistant to **128a**-induced apoptosis. This finding is supported by the extensive proteolytic processing of pro-

caspase-9, -3, and -2 in wild-type and control-transfected cells, which did not occur in Bcl-2/Bcl-x_L-overexpressing cells. Some processing, however, was observed in Apaf-1 deficient cells despite their being resistant to **128a**. However, while cleavage of caspase-9 in response to **128a** in the wild-type and control-transfected cells produced two fragments (p37/p35), only one caspase-9 cleavage fragment (p37) was detected in the Apaf-1-deficient cells. This novel finding is significant because it has been reported that apoptosome-dependent activation of caspase-9 yields the p35 fragment, while the p37 form is generally believed to be produced by caspase-3-mediated cleavage and to be catalytically inactive. Since only a trace amount of active caspase-3 was detected, it is proposed that the generation of the p37 fragment of caspase-9 may be caspase-3-independent. Together these data demonstrate that **128a** induces the instrinsic apoptotic pathway through a unique caspase-induced mechanism.[259]

C. *In vivo* examination of 128a activity

Due to the promise of **128a** *in vitro*, it was proposed that subsequent studies with this compound could be accomplished during a research rotation at the NCI with Dr. Leonard Neckers. Yeast was proposed as a suitable model in which to examine the efficacy and identify a potential mechanism through which **128a**, versus structurally related *C*-terminal Hsp90 modulators.

1. Isoform selectivity in yeast

It has been previously demonstrated that Hsp90 is an essential molecular chaperone that is important for activation of many regulatory proteins of eukaryotic cells. Because Hsp90 is

such an extremely conserved protein, heterologous expression of either human Hsp90α or β will provide the essential Hsp90 function in *Saccharomyces cerevisiae* yeast [272,273]

Based upon this knowledge and previous reports, this *in vivo* system was used to assess the sensitivity of yeast cells to Hsp90 C-terminal modulators novobiocin, **KU32** (Figure 27) and **128a** (KU135). The results of these studies are shown in Figure 73. Examination of the yeast colonies reveal that those expressing human Hsp90α are slightly more sensitive to all three inhibitors when compared to yeast cells expressing human Hsp90β. This study, one of the first to examine the isoform-selectivity of *C*-terminal inhibitors, offers insight into the potential involvement of Hsp90α in eliciting the activity of **128a**. Moreover, this study confirms the *in vivo* efficacy of **128a** in yeast.

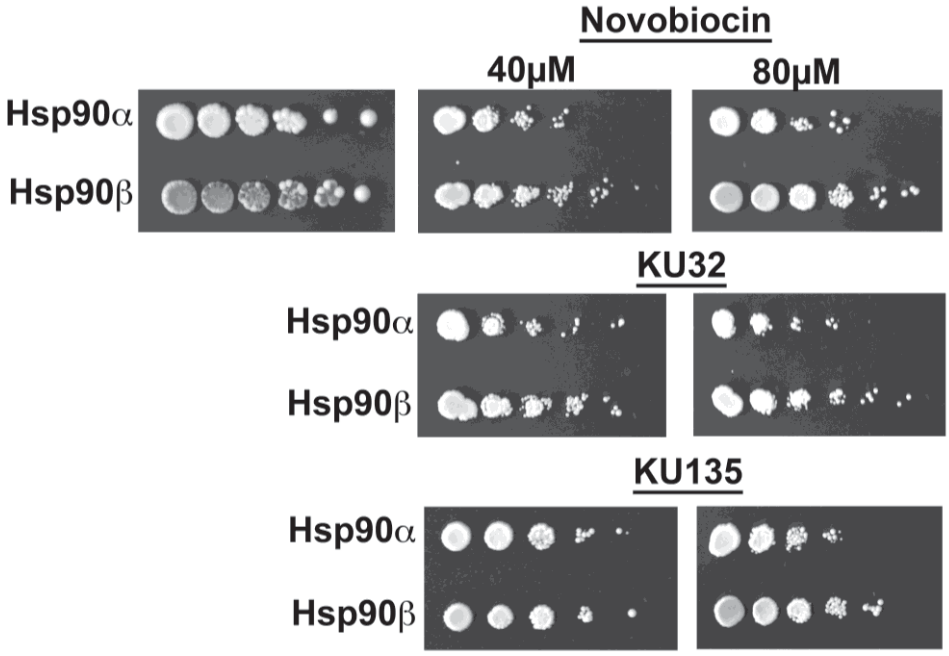

Figure 73. Differential sensitivity of Hsp90 isoforms to *C*-terminal modulators.

2. Effect of 128a is heat shock specific

Heat shock transcription factor (HSF) is an Hsp90-dependent client protein. It is generally accepted that interaction of HSF with Hsp90 downregulates HSF activity through a negative feedback mechanism.[274] Therefore, inhibition of Hsp90 chaperoning activity leads to strong induction in HSF activity even in the absence of heat shock stress. Based on this response and previous work that has demonstrated that human Hsp90 proteins are functional in yeast lacking the endogenous yHsp90 (yeast Hsp90), a β-galactosidase assay in yeast was proposed as a method to quantify the effect of **128a** on heat shock induction (Figure 74).

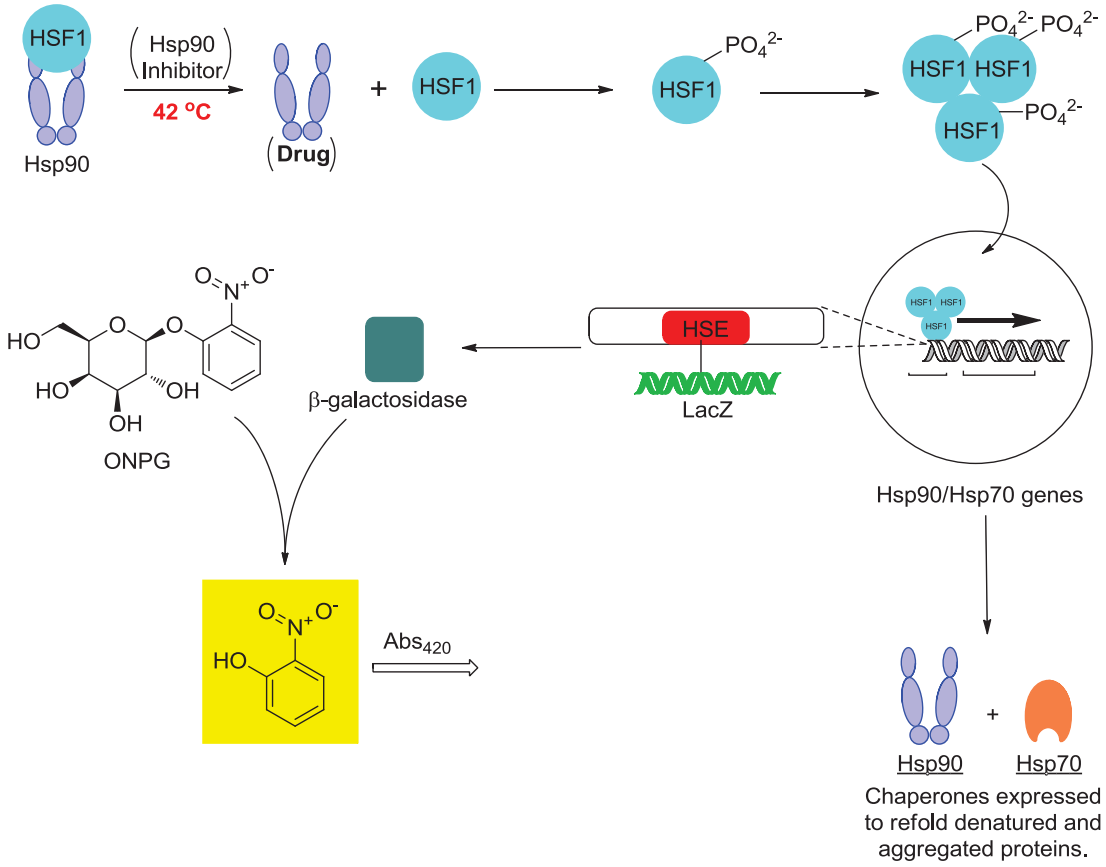

Figure 74. β-galactosidase assay.

Interaction between HSF and Hsp90 were exploited in the design of this assay. As shown in Figure 75, HSF binds to heat shock element (HSE), which is a transcriptional promoter for the

heat shock proteins. By attaching *lac*Z, a reporter that encodes for β-galactosidase, to HSE, the transcriptional activation of heat shock proteins can be monitored via chemiluminescence, because they share production of β-galactosidase mirrors the normal heat shock transcription. Thus, cleavage of added substrate ONPG by the expressed β-galactosidase to a chemiluminescent is reflective of the induction of this gene.

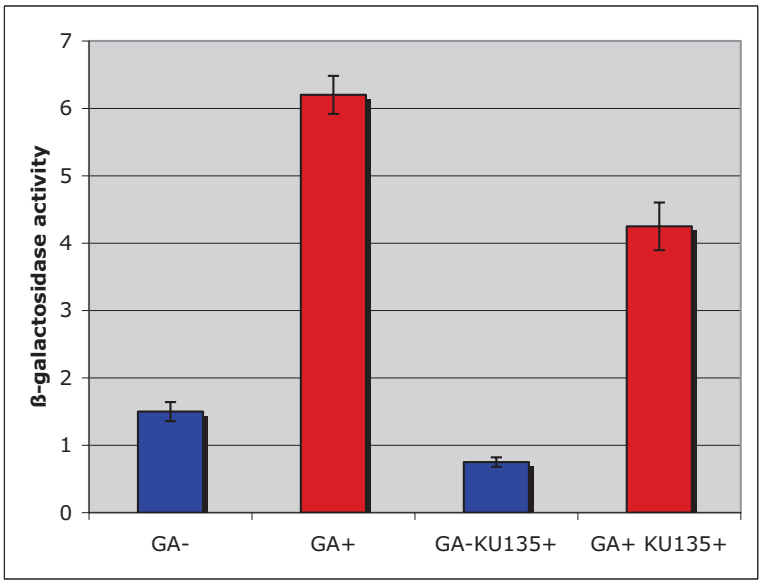

Figure 75. Effect of 128a is heat shock specific.

Next, this assay was used to examine the effect of **128a** on heat shock response in combination with well-studied *N*-terminal Hsp90 inhibitor, geldanamycin (GA, Figure 2). Yeast PP30 cells expressing human Hsp90α as the only Hsp90-isoform and also containing the HSF-*lac*Z reporter (HSE-*lac*Z) were treated with 100μM of the above compounds for 3 hrs. For comparison, these cells were stressed by heat shock (39˚C) for 1 hr and the results observed at ambient temperature were compared to those obtained following heat shock. While the **GA** treated cells at ambient temperature (-, blue) showed basal levels of heat shock response, induction was quite significant upon exposure to elevated temperatures (+, red). In comparison, addition of **128a** (KU135) to already treated with **GA** reduced heat shock response at both

ambient and elevated temperatures. These results suggest that the mechanism through which **128a** acts is heat shock specific and that **128a** interferes with pathways leading to the transcriptional activation of the heat shock response.

3. Inhibition of chaperoning activity by 128a in yeast

The tyrosine kinase v-Src is a well-known Hsp90 client protein.[275] v-Src expression in yeast is Hsp90-dependent and its activation is associated with yeast lethality due to deregulated phosphorylation of yeast proteins. This known activity has transformed v-src into a widely used reporter assay in yeast for analysis of Hsp90 chaperone function.

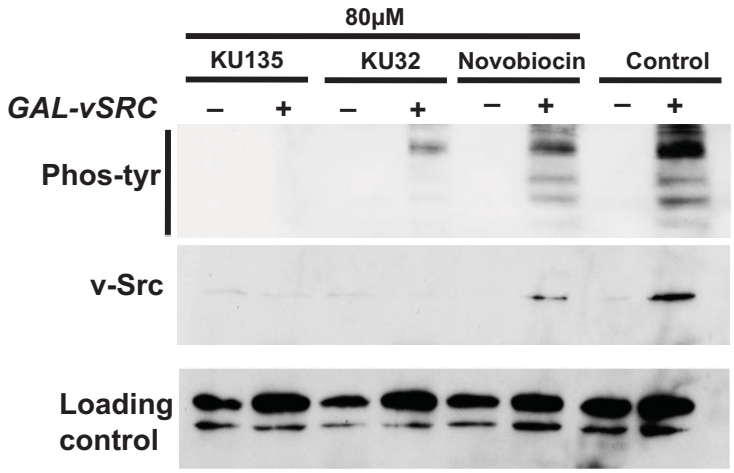

Figure 76. Yeast cells expressing expressing human Hsp90α as the sole Hsp90 and v-Src were grown on media with glucose (–) or galactose (+) and also treated with indicated compounds. Total phosphotyrosine and v-Src expression were analyzed by immunoblotting.

Use of this reporter assay to analyze the effect of *C*-terminal inhibitors **128a**, **KU32**, and novobiocin on yeast expressing human Hsp90α as the sole Hsp90 is shown in Figure 76. v-Src protein and v-Src-mediated phosphorylation of total yeast proteins were clearly detectable in

control yeast expressing human Hsp90α. In contrast, levels of both were significantly reduced in cells treated with 80 μM novobiocin. Moreover, both v-Src and resultant phosphorylation were absent in cells treated with 80 μM **KU32** or **KU135** (Figure 76). Thus, it is proposed that these novobiocin-derived compounds interfere with productive chaperoning of v-Src in yeast. This assay confirms that **128a** acts through an Hsp90-dependent mechanism *in vivo*.

IV. Characterization of 26g (KU174) and 128a (KU135) as Hsp90 inhibitors

A. Synthesis of labeled analogues

Although Western blot analyses with **26g** and **128a** have confirmed Hsp90 inhibition as the mechanism through which both exhibit their anti-proliferative activity, subsequent studies were designed to more specifically define their interactions with Hsp90. Various analogues of these compounds were prepared for subsequent studies that sought to define their interaction with Hsp90.

1. Drug metabolism studies with 128a

To probe potential metabolites formed upon exposure to **128a**, a deuterium-labeled analogue was synthesized (Scheme 60). Starting from phenol **265**, an iodination protocol was employed to furnish carboxylic acid **266**. Next, addition of deuterated iodomethane in the presence of potassium carbonate and subsequent hydrolysis yielded the requisite deuterated acid **267**. Next, EDCI-mediated coupling of freshly prepared aniline **268** to the deuterated acid in the presence of pyridine was used to access intermediate **269**. Subsequent Suzuki coupling with

boronic acid **270** afforded the desired analogue in good yield. Upon preparation of deuterated compound **271**, it was provided to Dr. Roger Rajewski to be placed into metabolism studies. Results of these biological studies are pending.

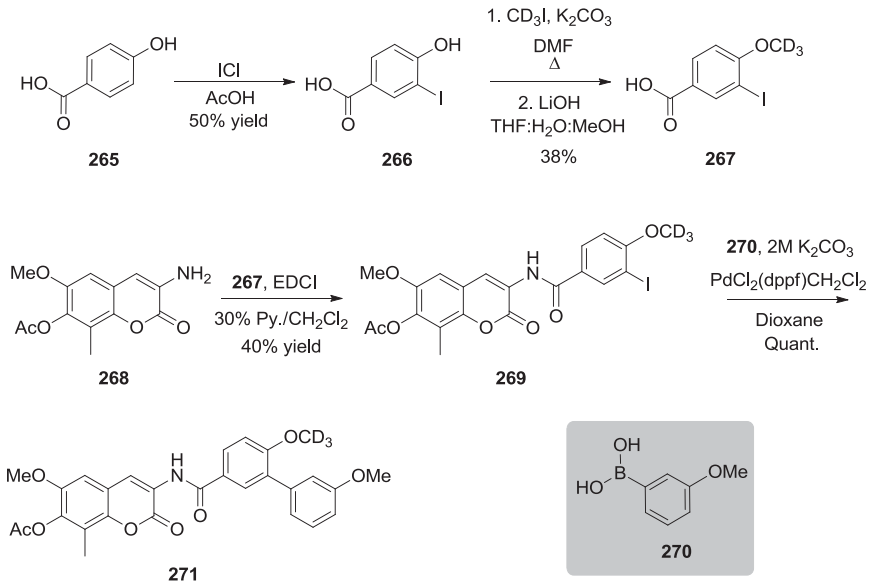

Scheme 60. Synthesis of deuterium-labeled **128a**.

2. ^{13}C NMR studies

Several NMR-based studies were proposed to occur in collaboration with Dr. Robert Matts at Oklahoma State University. Through incorporation of a ^{13}C into the structure of compounds of interest, NMR studies using ^{15}N-labeled Hsp90 and these analogues could be used to identify the protein residues with which they interact.

A ^{13}C-labeled analogue of **26g** was prepared for NMR studies. As seen in Scheme 61, aryl iodide **237** was coupled to meta-hydroxy phenylboronic acid **262** using Suzuki conditions to yield acid **272**. Although not intended, hydrolysis occurred *in situ* upon exposure to the Suzuki coupling protocol. Next, alkylation and esterification proceeded in modest yield using ^{13}C-labeled iodomethane in the presence of potassium carbonate, and then ester **273** was hydrolyzed

to afford the requisite acid. Coupling of acid **274** and freshly prepared aminocoumarin **275**, the product of submitting benzyl carbamate-protected coumarin **25g** to hydrogenolysis, was carried out in the presence of EDCI and pyridine. Finally, the cyclic carbonate on the noviose ring was solvolyzed to afford the final compound, **277**.

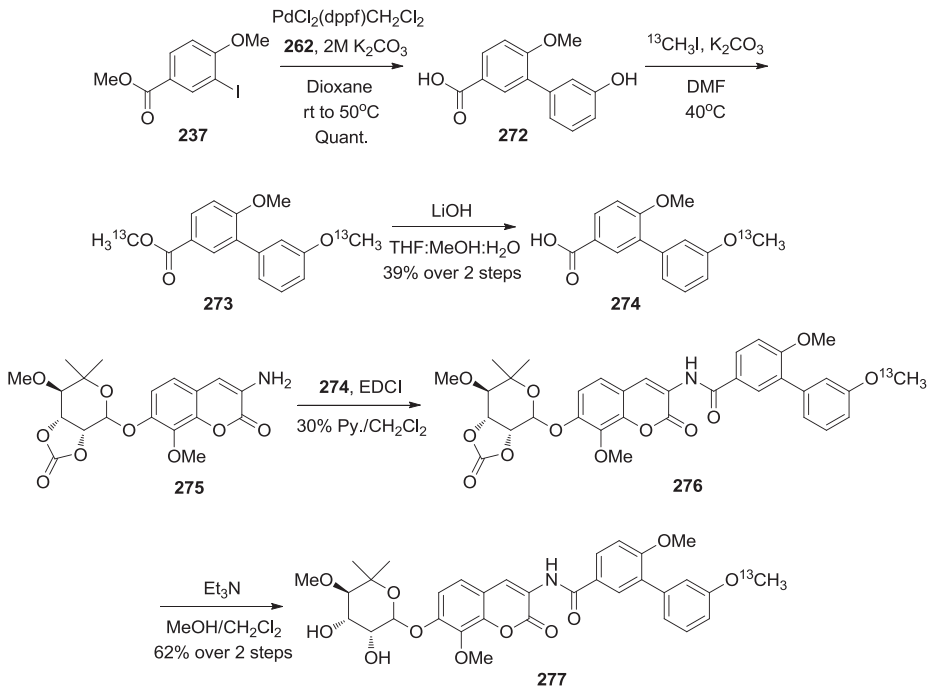

Scheme 61. Synthesis of ^{13}C-labeled **26g**.

Synthesis of a ^{13}C variant of **128a** is outlined in Scheme 62. Addition of ^{13}C-labeled acetic anhydride to biaryl-containing 6-methoxy coumarin phenol **159** in the presence of pyridine afforded the desired analogue **278**. Upon preparation, both ^{13}C-labeled analogues were sent to Dr. Matts and are awaiting subsequent NMR studies. Results of these studies will be reported in due course.

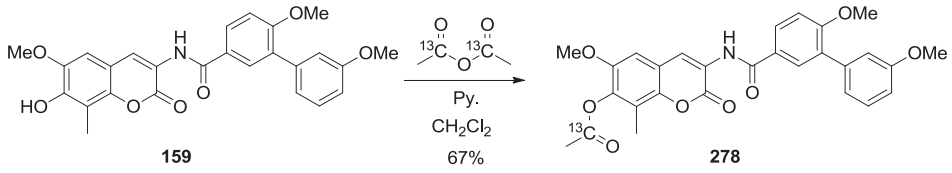

Scheme 62. Synthesis of ^{13}C-labeled **128a**.

3. Biotinylated analogues

As a final method through which binding of **26g** and **128a** to Hsp90 can be examined, a biotinylated analogue of each was prepared. These molecules were designed as probes that would help localize their site(s) of interaction with Hsp90.

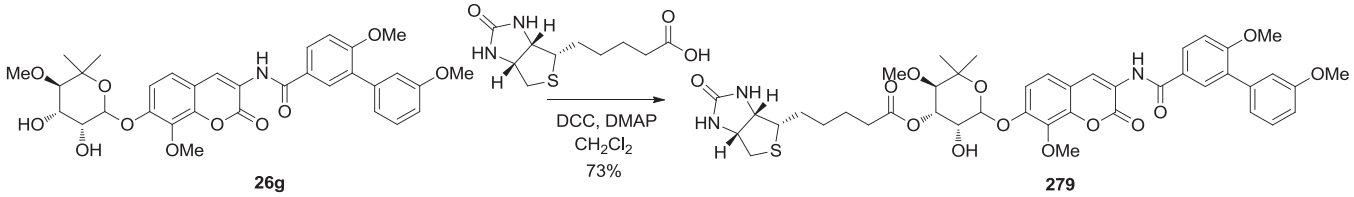

Scheme 63. Synthesis of biotinylated **26g**.

Biotinylation of **26g** was accomplished using *N,N′*-dicyclohexylcarbodiimide in the presence of a catalytic amount of DMAP. These reaction conditions, shown in Scheme 63, afforded the desired compound in good yield.

Like the previous analogue, synthesis of the biotinylated-**128a** variant was carried out in a single step, shown in Scheme 64. Employing the same methodology used for synthesis of biotinylated-**26g**, desired compound **280** was obtained in good yield. Upon preparation of these two designed analogues, they were sent to the Neckers laboratory at the NIH for subsequent binding studies to examine specific interaction of these compounds with their protein target

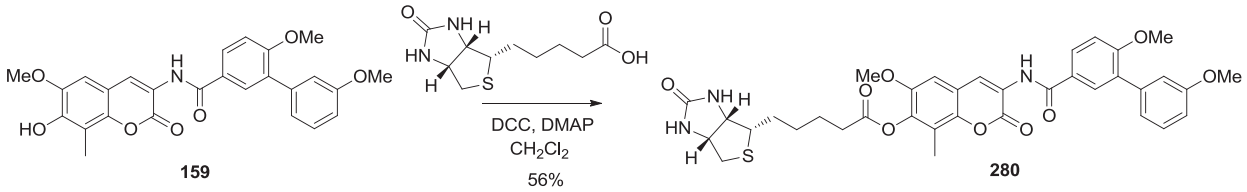

Scheme 64. Synthesis of biotinylated **128a**.

B. Systematic characterization of Hsp90 binding

Co-workers in the Blagg laboratory, in collaboration with Dr. Matts at Oklahoma State University, designed several experiments to examine the binding of **26g** and **128a** to Hsp90. These complementary studies have defined **26g** and **128a** as *C*-terminal Hsp90 inhibitors.

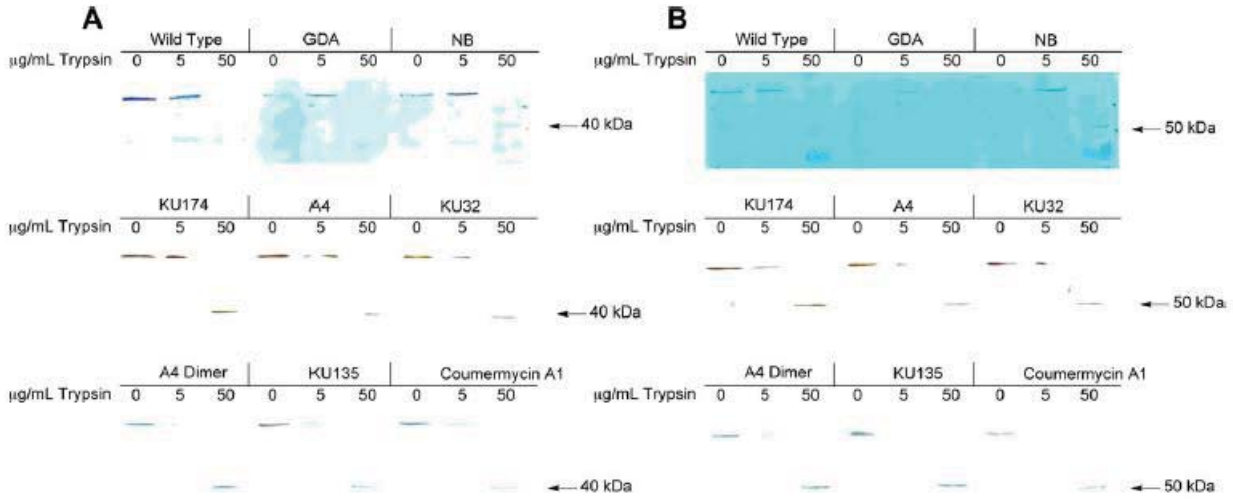

Figure 77. Hsp90 proteolytic fingerprint after incubation with various Hsp90 modulators.[241]

1. Effect of 26g and 128a on the proteolytic fingerprint of Hsp90

As shown in Figure 77, Hsp90 produces a different proteolytic fingerprint upon treatment with the *N*-terminal Hsp90 inhibitor GDA versus *C*-terminal inhibitor novobiocin (NB). These fingerprints, analyzed by SDS-PAGE and Western blotting with antibodies directed against the *N*-terminus (A) and *C*-terminus (B), were in agreement with previously published reports and provided a means for comparison to other Hsp90 modulators. Trypsinolysis of Hsp90 in the presence of **26g** (KU174) and **128a** (KU135) led to a fragment pattern that mimicked those observed upon treatment with novobiocin. Moreover, the most prominent band occurred following immunoblot with the *C*-terminal antibody. Since both analogues blocked trypsinolysis at the same amino acid residue (Arg612) as novobiocin, it was concluded that **26g** and **128a**

induce similar conformational effects on Hsp90, thereby suggesting a similar mode of binding for these compounds.[241]

2. Effect of 26g and 128a on affinity chromatography

Determination that novobiocin interacted with the Hsp90 *C*-terminus was originally confirmed based upon affinity purification experiments.[84] As seen in Figure 78, novobiocin immobilized on sepharose beads demonstrated the retention of an Hsp90 *C*-terminal fragment, but not an *N*-terminal fragment. Also, increasing concentrations of GDA were found to be insufficient for the elution of Hsp90 from NB-sepharose column. In contrast, however, an increasing concentration of NB eluted Hsp90 from GDA-immobilized sepharose beads. Based on these trends, it was proposed that other compounds that manifest similar activity to NB indicate a similar mode of binding to the *C*-terminus of Hsp90.[241]

When increasing concentrations of **26g** and **128a** were used to elute the bound Hsp90 from either the NB- or GDA-sepharose beads, Hsp90 was eluted from the column. Washing the NB- or GDA-sepharose beads with these same compounds produced the same effect as that observed with novobiocin. These data suggest that **26g** and **128a** bind Hsp90 similarly to NB.[241]

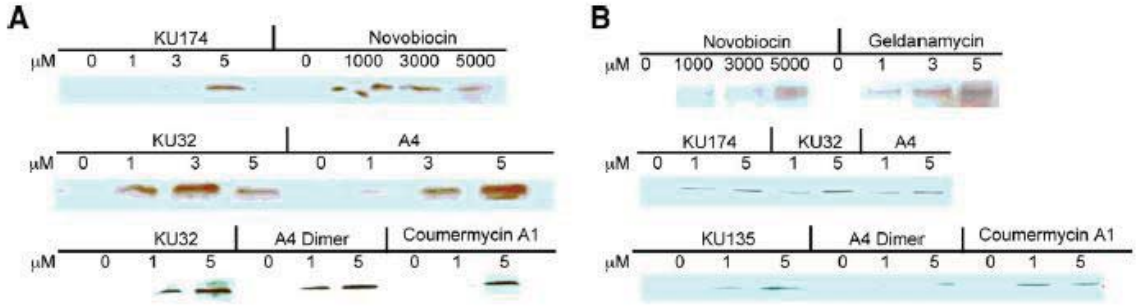

Figure 78. NB-bound- (A) and GDA-bound-sepharose (B) affinity chromatography.[241]

3. Evaluation of the heat shock response induced by Hsp90 modulators

Through application of the β-galactosidase assay described in Section II-B.2, the effect of **26g** and **128a** versus several other novobiocin-derived analogues on HSF activity was examined. As before, PP30 cells expressing human Hsp90α as the only copy of Hsp90 and also containing the HSF-*lac*Z reporter (HSE-*lac*Z) were treated with 100μM of the above compounds for 3 hrs. For comparison purposes, these cells were then further stressed with heat shock (39˚C) for 1 hr and results were compared between ambient and heat-shocked conditions.

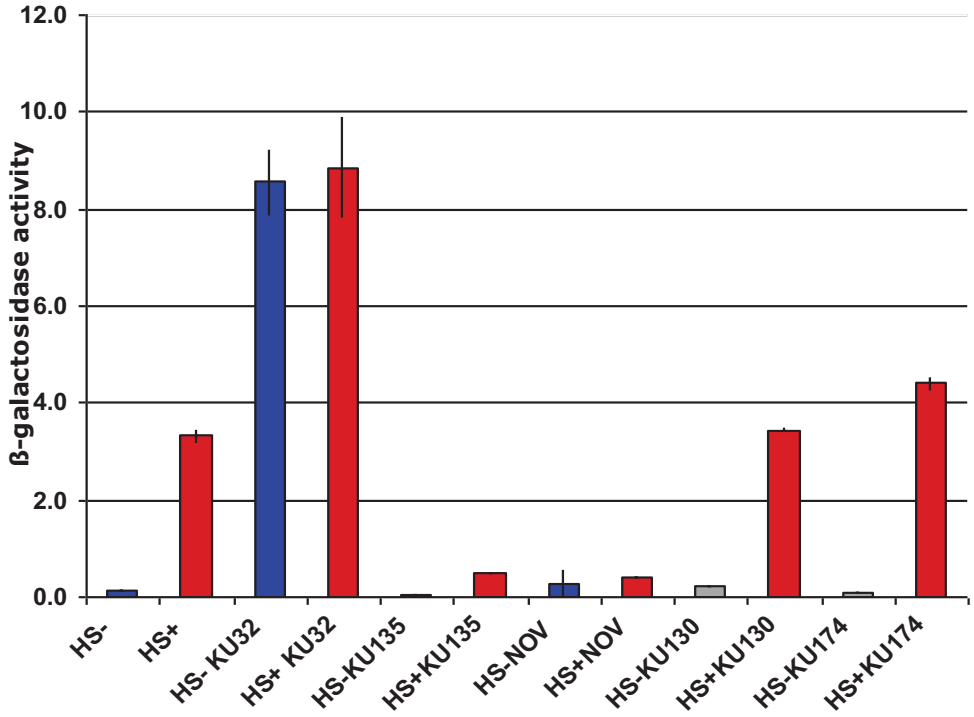

Figure 79. Evaluation of the heat shock response in the presence of Hsp90 modulators.

During examination of the data generated from this study (Figure 79), some obvious trends became apparent. In comparison to **KU32**, which acted much like GDA in this assay (Figure 75) and produced heat shock response with or without added heat, novobiocin and **128a** (KU135) acted distinctly. **128a** demonstrated an ability to block the heat shock response even in

the presence of high temperatures. This finding is consistent with the results observed in the same assay when GDA and **128a** were examined in combination, which supports the hypothesis that **128a** prevents release of HSF-1 from Hsp90. In contrast, **26g** had no effect on heat shock response in yeast. This analogue neither induced nor prevented heat shock, suggesting that interference of the Hsp90/HSF interaction is not the mechanism through which this compound acts. This β-galactosidase assay identified three classes of Hsp90 *C*-terminal modulators, those that induce (**KU32**), those that inhibit (**128a**) and those that do not interfere (**26g**) with the heat shock response. Moreover, this study affirmed that **128a** and **26g** act via distinct mechanisms from one another.

V. Studies of Hsp90 phosphorylation

It was proposed that the dynamics of the Hsp90 chaperone cycle are significantly influenced by epigenetic factors, including post-translational modifications. Moreover, numerous literature reports identify Hsp90 as a phosphoprotein and support that Hsp90 phosphorylation impacts its function.[276] Studies to better understand the details of phosphorylation and potential role that this post-translational modification plays on Hsp90 function were designed. As part of my research rotation at the NCI and in the time since, I contributed to with these efforts.

A. Role of Wee1 in regulating Hsp90 phosphorylation

Saccharomyces WEE1 (Swe1), a tyrosine kinase in budding yeast, is an Hsp90-dependent client protein. Although Swe1 is thought to play a singular role in regulation of Cdc28

in yeast, it was proposed that this kinase might also play a role in Hsp90 phosphorylation. Several studies were designed to probe this potential role, including the one that follows.[276]

1. Western blot analysis of Wee1

Wildtype and mutant forms of yeast and human Hsp90 were required for the intended studies. These proteins and specific mutants, which incorporated a tyrosine to phenylalanine mutation at a proposed Hsp90 phosphorylation site, were bacterially expressed and purified. Following Ni-NTA purification of yHsp90-His_6, yHsp90-His_6-Y2F, hHsp90-His_6, and hHsp90-His_6-Y2F proteins, the quality of the purified proteins was first examined by Coomassie staining of SDS-PAGE gels and then confirmed by Western blot analyses. This quality assessment was executed prior to use of these proteins in *in vitro* kinase assays.[276]

As seen in Figure 80, one such stained Coomassie gel for the yeast Hsp90 and its mutant demonstrate that the ~90 kDa band dominates the total protein content. Moreover, pull-down studies identified the same band, corresponding to the desired pure protein. Finally, Western blot analyses, using the corresponding antibody, confirmed protein identity.[276]

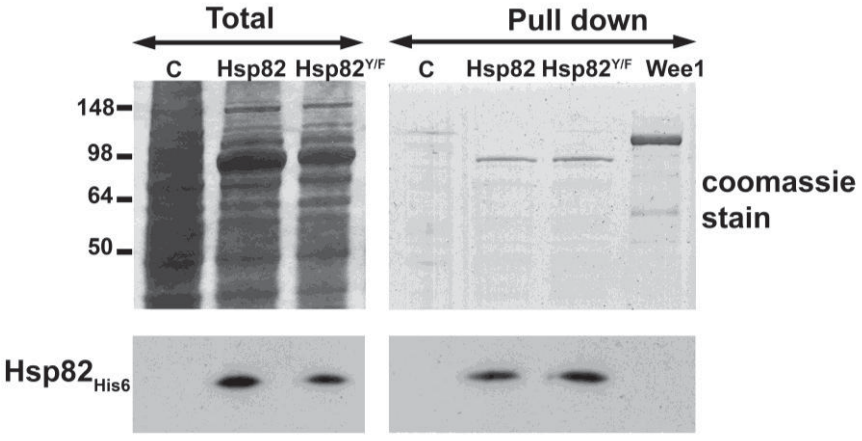

Figure 80. Analysis of protein purity.[276]

Next, use of these pure proteins in the subsequent *in vitro* assay is shown in Figure 81. After several control experiments, it was identified that while phosphorylation of yeast Hsp90 (Hsp82) by Wee1 occurred in its wildtype form, mutation of a specific tyrosine residue abrogated this phosphorylation event. This *in vitro* assay confirmed that Wee1 phosphorylates yeast Hsp90 and that this specific tyrosine residue that was mutated is an essential part of this phosphorylation process.[276]

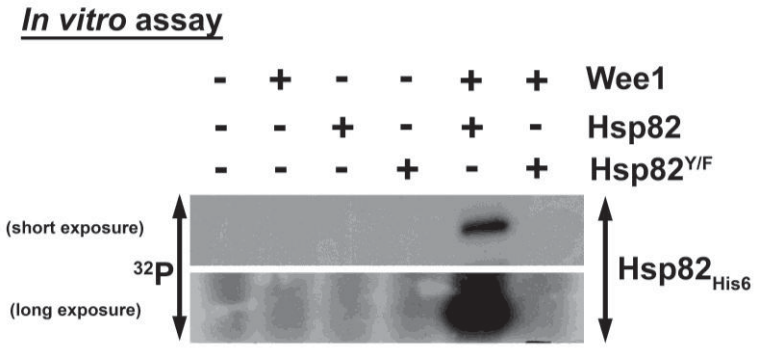

Figure 81. *In vitro* kinase assay.[276]

At the conclusion of this study, it was shown that Swe1 phosphorylates a conserved tyrosine residue (Y24 in yeast Hsp90 and Y38 in human Hsp90α) in the *N*-terminal domain of Hsp90. Moreover, this phosphorylation was found to be cell-cycle associated and to modulate the ability of Hsp90 to chaperone selected proteins, including v-Src and other kinases.[276]

B. Wee1 inhibition

Based on the finding that several Hsp90 clients are differentially regulated due to Hsp90 phosphorylation, it was suggested that Wee1 inhibition might provide a strategy to increase the cellular potency of Hsp90 inhibitors. Likewise, it was shown that deletion of *SWE1* in yeast increases Hsp90 binding to GDA and pharmacologic inhibition/silencing of Wee1 (the human

form of Swe1) sensitizes cancer cells to Hsp90 inhibitor-induced apoptosis.[276] Based on these results, synthesis of a reported selective Wee1 inhibitor was pursued for synergistic use against cancers in combination with known Hsp90 inhibitors.

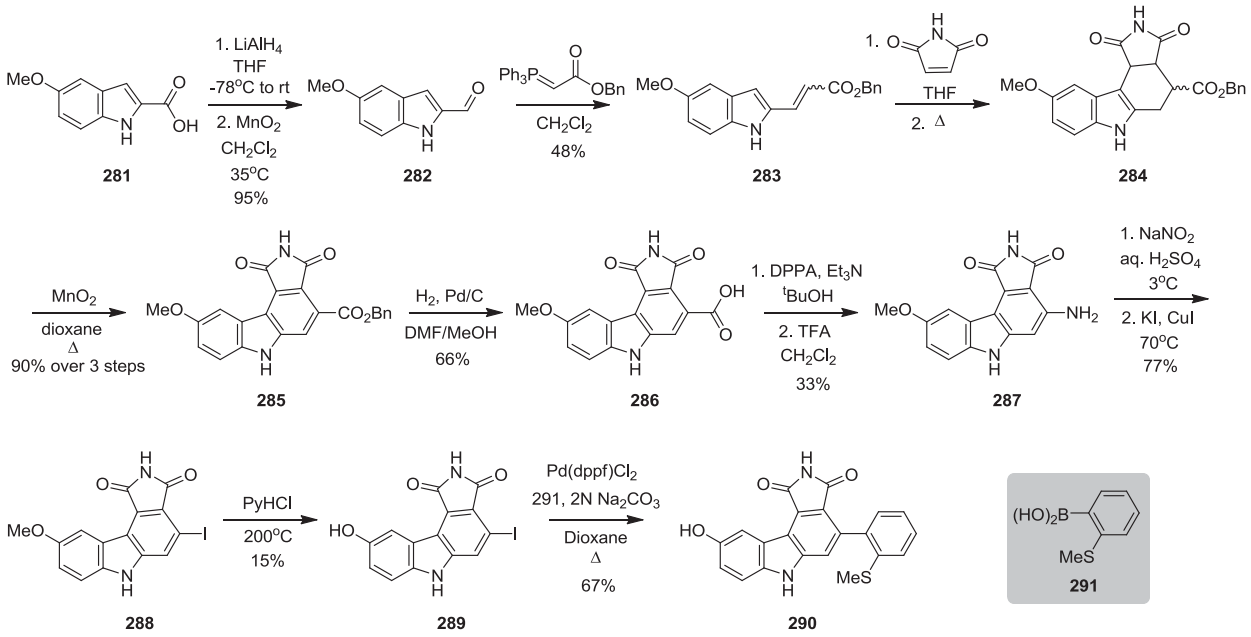

Scheme 65. Synthesis of first Wee1 inhibitor.[277]

1. Synthesis of Wee1 inhibitors

A recent paper reported the synthesis of inhibitors of Wee1. Inhibitory activities of the compounds were reported against Wee1 and related checkpoint kinase Chk1. Examination of the ratio of Chk1 to Wee1 IC_{50} values revealed compound **290** to be most selective and thus, its preparation was pursued. Following the reported route (Scheme 65),[277] carboxylic acid **281** was reduced and subsequently oxidized to the corresponding benzaldehyde. Benzaldehyde **282** was then used in a Wittig reaction with benzyl 2-(triphenylphosphoranylidene)acetate to yield diene **283** as a mixture of the *cis*- and *trans*-isomers. Next, a Diels-Alder reaction was carried out between the prepared diene and maleimide, and then the enantiomeric mixture was aromatized using activated magnesium oxide. Hydrogenolysis of intermediate **285** liberated carboxylic acid

286, which was subsequently submitted to a Curtius rearrangement. Aniline **287** was next converted to aryl iodide **288** using Sandmeyer chemistry and finally pyridine hydrochloride was used to liberate the phenol. Finally, a Suzuki coupling was employed to furnish the desired compound, **290**.[277]

Upon generation, Wee1 inhibitor **290** was sent to the Neckers laboratory for use in biological assays. Despite its reported activity, this compound proved to be inactive against Wee1 in the assays attempted. It was proposed that the sulfoxide or sulfone, rather than the thioether-containing compound, may have exhibited the activity reported in the original publication. Rather than probing this possibility, efforts were directed at synthesizing another promising selective Wee1 inhibitor identified in the same study, on large scale.

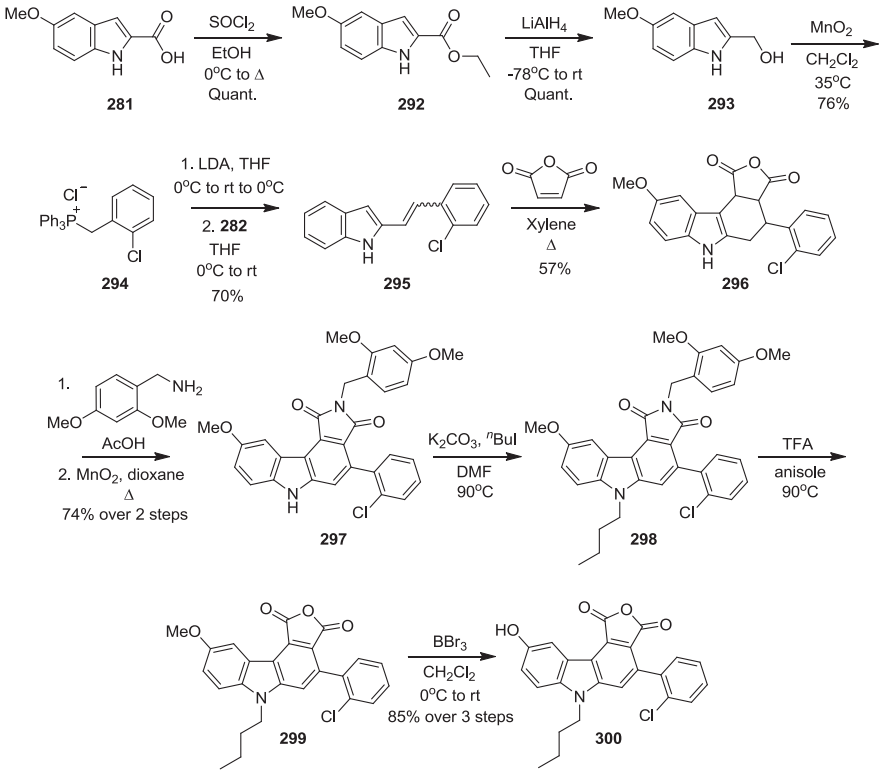

Scheme 66. Synthesis of second Wee1 inhibitor.[277]

As seen in Scheme 66, carboxylic acid **261** was esterified with thionyl chloride in ethanol and then reduced to the corresponding benzyl alcohol in quantitative yield.[278] Alcohol **293** was oxidized to the corresponding benzaldehyde, which was subsequently used in a Wittig reaction to form diene **295**. Diels-Alder chemistry was employed to construct the tetracyclic core **296**. Next, the anhydride was subsequently converted to the protected maleimide and the system was aromatized to afford intermediate **297**. Alkylation of the indole nitrogen, followed by cleavage of the amine protecting group to regenerate the anhydride ring yielded precursor **299**. Demethylation using boron tribromide resulted in generation of the desired final compound.[277]

Since its intended use was in an *in vivo* model, the gram of pure **300** was analyzed via HPLC to ascertain its purity. Once HPLC analysis revealed the compound to be 93-95% pure, it was sent to the NIH for use in subsequent studies. Preliminary results using this compound have been promising and will be reported in due course.

VI. Conclusion

Comprehensive studies involving **26g** and **128a** have confirmed that these compounds are extremely promising anti-cancer agents. The *in vitro* potency exhibited in a variety of assays was mimicked in *in vivo* models, demonstrating the true potential of these novobiocin analogues. Moreover, these studies have elucidated that while both are *C*-terminal inhibitors of Hsp90, they act through distinct mechanisms. Finally, through yet another unique mechanism, Wee1 inhibition has demonstrated promise as a strategy to increase the cellular potency of Hsp90 inhibitors. It is envisioned that these diverse studies could result in synergistic compounds that

would revolutionize the field of Hsp90 modulation and have the potential to transform cancer chemotherapy.

VII. Experimental Protocols

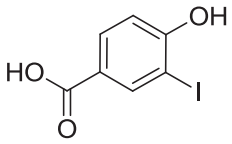

266

4-Hydroxy-3-iodobenzoic acid (266):[279] Iodine monochloride (2.82 g, 17.4 mmol) was added to a solution of 4-hydroxybenzoic acid (2.0 g, 14.5 mmol) in acetic acid (17.8 mL), and then stirred for 4 h at rt. Water was added and the solution was extracted with EtOAc (3 x 30 mL), washed with water, saturated aqueous $Na_2S_2O_3$, dried (Na_2SO_4), filtered and concentrated. The residue was recrystallized from 50% MeCN in toluene to afford **266** as a colorless amorphous solid (1.90 g, 50%): ^{1}H NMR (Acetone-d_6, 500 MHz) δ 7.80–7.77 (m, 2H), 6.92 (d, J = 8.0 Hz, 1H), 6.80–6.78 (m, 1H).

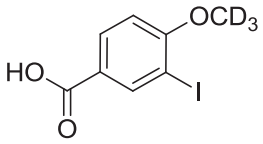

267

3-Iodo-4-(methoxy-d3)benzoic acid (267): Potassium carbonate (5.30 g, 37.9 mmol) was added to **266** (1.0 g, 3.79 mmol) in *N,N*-dimethylformamide (7.60 mL). After 10 min, iodomethane-d3 (2.0 mL, 32.1 mmol) was added and the solution was heated to reflux for 12 h. Upon cooling to rt, the solution was extracted with EtOAc (3 × 50 mL); combined organic fractions were washed with saturated aqueous NaCl, dried (Na_2SO_4), and concentrated. The

residue was purified by column chromatography (SiO_2, 5:1 → 3:1 Hexane:EtOAc) to afford the desired product as a yellow oil (1.05 g, 99%), which was used without further purification.

Lithium hydroxide (454 mg, 18.9 mmol) was added to a solution of aryl halide (1.13 g, 3.79 mmol) in 3:1:1 THF:MeOH:H_2O (37.9 mL). After 12 h, the solution was concentrated and the aqueous residue was acidified, and then extracted with EtOAc (3 x 10 mL). The combined organic layers were next extracted with saturated aqueous $NaHCO_3$ (3 x 10 mL), and then the aqueous extracts were acidified. Finally, EtOAc (3 x 10 mL) was used to extract the acid product, and the combined organic extracts were washed with saturated aqueous NaCl, dried (Na_2SO_4), filtered, and concentrated to afford **267** as a colorless amorphous solid (28.0 mg, 38% over 2 steps): ^{1}H NMR (Acetone-d_6, 500 MHz) δ 8.28 (d, J = 2.0 Hz, 1H), 7.93–7.85 (m, 2H), 6.99–6.88 (m, 2H); ^{13}C NMR (Acetone-d_6, 125 MHz) δ 167.2, 165.9, 141.7, 132.5, 125.5, 114.5, 111.5, 85.6; HRMS (ESI$^+$) *m/z*: $[M + H]^+$ calcd for $C_8H_5D_3IO_3$, 281.9706; found, 281.9730.

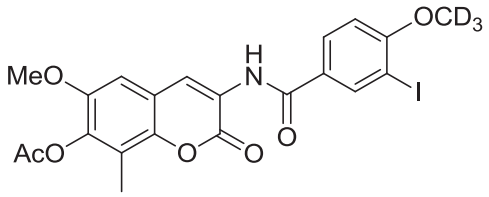

269

3-(3-Iodo-4-(methoxy-d3)benzamido)-6-methoxy-8-methyl-2-oxo-2H-chromen-7-yl acetate (269): EDCI (36.4 mg, 0.19 mmol) and **267** (42.7 mg, 0.15 mmol) were added to aminocoumarin **268** (20 mg, 0.076 mmol), freshly prepared from hydrogenolysis of **127a**, in 30% pyridine/CH_2Cl_2 (1.40 mL). After 12 h, the solvent was concentrated and the residue was purified via column chromatography (SiO_2, 40:1 CH_2Cl_2:Acetone) to afford **269** as a yellow amorphous solid (21.0 mg, 40%): ^{1}H NMR (Acetone-d_6, 400 MHz) δ 9.05 (s, 1H), 8.75 (s, 1H), 8.43 (d, J = 2.2 Hz, 1H), 8.07 (dd, J = 8.6, 2.2 Hz, 1H), 7.16 (d, J = 8.6 Hz, 1H), 6.93 (s, 1H),

3.91 (s, 3H), 2.35 (s, 3H), 2.22 (s, 3H); ^{13}C NMR (Acetone-d_6, 125 MHz) δ 168.7, 165.9, 164.0, 159.2, 149.9, 143.4, 140.7, 130.1 (2C), 126.9, 125.3, 123.5, 123.4, 120.6, 118.5, 114.9 (2C), 107.9, 56.7, 20.3, 9.1; HRMS (ESI$^+$) *m/z*: $[M + Na]^+$ calcd for $C_{21}H_{15}D_3INNaO_7$, 549.0214; found, 549.0231.

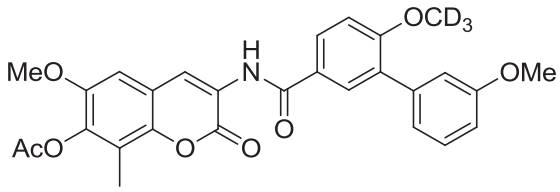

271

3-((6-Methoxy-d3)-3'-methoxy-[1,1'-biphenyl]-3-ylcarboxamido)-6-methoxy-8-methyl-2-oxo-2H-chromen-7-yl acetate (271): 1,1'-bis(diphenylphosphino)ferrocene-palladium(II)dichloride dichloromethane complex (1.0 mg, 0.0012 mmol) was added to a solution of **271** (21.0 mg, 0.040 mmol), (3-methoxyphenyl)boronic acid (18.2 mg, 0.12 mmol) and 2M K_2CO_3 (60.0 μL, 0.12 mmol) in dioxane (0.60 mL). After 1 h at rt, the solution was heated to 50^{o}C for 12 h. Once cool, solvent was removed and the residue was resuspended in EtOAc, washed with water, dried (Na_2SO_4), filtered and concentrated. The residue was purified via column chromatography (SiO_2, 3:1 Hexane:EtOAc) to afford **271** as a colorless amorphous solid (25.3 mg, 99%): ^{1}H NMR (Acetone-d_6, 400 MHz) δ 9.00 (s, 1H), 8.75 (s, 1H), 8.01 (dd, J = 8.6, 2.4 Hz, 1H), 7.95 (d, J = 2.4 Hz, 1H), 7.37 (t, J = 8.0 Hz, 1H), 7.27 (d, J = 8.5 Hz, 2H), 7.14 (d, J = 7.6 Hz, 2H), 6.95 (dt, J = 9.0, 1.6 Hz, 1H), 3.91 (s, 3H), 3.86 (s, 3H), 2.34 (s, 3H), 2.24 (s, 3H); ^{13}C NMR (Acetone-d_6, 125 MHz) δ 168.7, 166.0, 160.8, 160.4, 159.1, 149.9, 143.5, 140.7, 140.0, 131.5, 130.8, 129.9, 129.4, 127.0, 125.3, 123.8, 122.7, 120.6, 118.4, 116.2, 113.6, 112.3, 107.9, 56.7 (2C), 55.6, 20.3, 9.1; HRMS (ESI$^+$) *m/z*: $[M + Na]^+$ calcd for $C_{28}H_{22}D_3NNaO_8$, 529.1666; found, 529.1686.

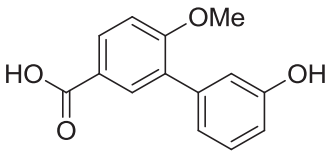

272

3'-Hydroxy-6-methoxy-[1,1'-biphenyl]-3-carboxylic acid (272): 1,1'-bis(diphenyl-phosphino)ferrocene-palladium(II)dichloride dichloromethane complex (84.0 mg, 0.10 mmol) was added to a solution of methyl 3-iodo-4-methoxybenzoate (1.0 g, 3.42 mmol), (3-hydroxyphenyl)boronic acid (1.42 g, 10.3 mmol) and 2M K_2CO_3 (5.1 mL, 10.3 mmol) in dioxane (50.0 mL). After 1 h at rt, the solution was heated to 50^{o}C for 12 h. Once cool, solvent was removed and the residue was resuspended in EtOAc, washed with water, dried (Na_2SO_4), filtered and concentrated. The residue was purified via column chromatography (SiO_2, 5:1 → 2:1 Hexane:EtOAc) to afford **272** as an orange amorphous solid (884 mg, 99%): ^{1}H NMR ($CDCl_3$, 400 MHz) δ 8.07–8.04 (m, 1H), 7.32 (t, *J* = 8.0, 2H), 7.06–7.01 (m, 3H), 6.85 (dd, *J* = 8.0, 2.4 Hz, 1H), 4.85 (bs, 1H), 3.91 (d, *J* = 8.0, 3H); ^{13}C NMR (Acetone-*d*$_6$, 125 MHz) δ 166.9, 161.3, 158.0, 139.9, 132.6, 130.7, 130.0, 123.4, 121.5, 119.0, 117.3, 114.6, 112.1, 56.2; HRMS (ESI$^+$) *m/z*: $[M + Na]^+$ calcd for $C_{14}H_{12}NaO_4$, 267.0633; found, 267.0646.

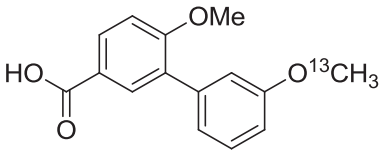

274

(3'-Methoxy-^{13}C)-6-methoxy-[1,1'-biphenyl]-3-carboxylic acid (274): Potassium carbonate (942 mg, 6.82 mmol) was added to **272** (880 mg, 2.56 mmol) in *N,N*-dimethylformamide (6.80 mL). After 10 min, iodomethane-^{13}C (0.43 mL, 6.82 mmol) was added and the solution was heated to reflux for 12 h. Upon cooling to rt, the solution was extracted with EtOAc (3 × 30 mL);

combined organic fractions were washed with saturated aqueous NaCl, dried (Na_2SO_4), and concentrated. The residue was purified by column chromatography (SiO_2, 5:1 Hexane:EtOAc → 100% EtOAc) to afford the desired product as a yellow oil (388 mg, 39%), which was used without further purification.

Lithium hydroxide (21 mg, 0.88 mmol) was added to a solution of benzoate (48 mg, 0.18 mmol) in 3:1:1 THF:MeOH:H_2O (1.80 mL). After 12 h, the solution was concentrated and the aqueous residue was acidified, and then extracted with EtOAc (3 x 10 mL). The combined organic layers were next extracted with saturated aqueous $NaHCO_3$ (3 x 10 mL), and then the aqueous extracts were acidified. Finally, EtOAc (3 x 10 mL) was used to extract the acid product, and the combined organic extracts were washed with saturated aqueous NaCl, dried (Na_2SO_4), filtered, and concentrated to afford **274** as a colorless amorphous solid (46.0 mg, 39% over 2 steps): ^{1}H NMR (Acetone-d_6, 400 MHz) δ 8.04 (d, J = 8.6 Hz, 1H), 7.98 (d, J = 1.9 Hz, 1H), 7.35 (t, J = 8.0 Hz, 1H), 7.22 (d, J = 8.6 Hz, 1H), 7.09 (d, J = 7.4 Hz, 2H), 6.93 (d, J = 8.0 Hz, 1H), 4.02 (s, 1.5H), 3.92 (s, 3H), 3.66 (s, 1.5H); ^{13}C NMR (Acetone-d_6, 125 MHz) δ 167.3, 161.2, 160.4, 140.0, 132.9, 131.8, 131.2, 129.9, 123.7, 122.6, 116.0, 113.5, 112.0, 30.1, 30.0; HRMS (ESI$^+$) *m/z*: $[M + Na]^+$ calcd for $C_{14}{}^{13}CH_{14}NaO_4$, 282.0823; found, 282.0812.

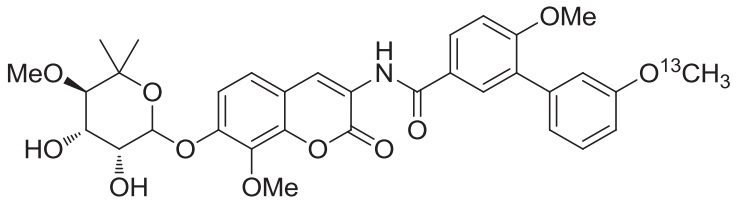

277

N-(7-(((3R,4S,5R)-3,4-dihydroxy-5-methoxy-6,6-dimethyltetrahydro-2H-pyran-2-yl)oxy)-8-methoxy-2-oxo-2H-chromen-3-yl)-(3'-methoxy-^{13}C)-6-methoxy-[1,1'-biphenyl]-3-carboxamide (277): EDCI (23.0 mg, 0.12 mmol) and **274** (24.8 mg, 0.10 mmol) were added to

the amine (20.3 mg, 0.048 mmol), freshly prepared from **25g**, in 30% pyridine/CH_2Cl_2 (0.7 mL). After 12 h, the solvent was concentrated and the residue purified via column chromatography (SiO_2, 40:1 CH_2Cl_2:Acetone) to afford a colorless solid, which was used without further purification (24.7 mg, 77%).

Triethylamine (20 μL) was added to the carbonate (13.0 mg, 0.020 mmol) in 50% MeOH/CH_2Cl_2 (0.20 mL). After 48 h, the solvent was concentrated and the residue purified via column chromatography (SiO_2, 9:1 CH_2Cl_2:Acetone) to afford **277** as a colorless amorphous solid (10.0 mg, 80%, 62% over 2 steps): ^{1}H NMR ($CDCl_3$, 500 MHz) δ 8.81 (s, 1H), 8.73 (s, 1H), 7.94–7.89 (m, 2H), 7.38 (t, *J* = 8.0 Hz, 1H), 7.25 (dd, *J* = 16.5, 8.0 Hz, 2H), 7.14–7.12 (m, 3H), 7.10–6.96 (m, 1H), 5.58 (d, *J* = 2.5 Hz, 1H), 5.13 (s, 1H), 4.28 (t, *J* = 2.5 Hz, 2H), 3.98 (s, 3H), 3.97 (s, 3H), 3.91 (s, 3H), 3.61 (s, 3H), 3.36 (d, *J* = 2.5 Hz, 2H), 1.41 (s, 3H), 1.24 (s, 3H); ^{13}C NMR ($CDCl_3$, 125 MHz) δ 163.3, 157.6, 157.0, 156.5, 148.9 (2C), 141.6, 136.2, 134.3, 128.8, 127.7, 126.9, 125.9, 123.6, 121.5, 121.2, 120.4, 120.1, 119.7, 112.9, 111.0, 110.8, 108.7, 93.6, 76.4 (2C), 68.8, 59.5 (2C), 53.2, 53.0, 27.4 (2C); HRMS (ESI$^+$) *m/z*: $[M + H]^+$ calcd for $C_{32}{}^{13}CH_{36}NO_{11}$, 623.2322; found, 623.2347.

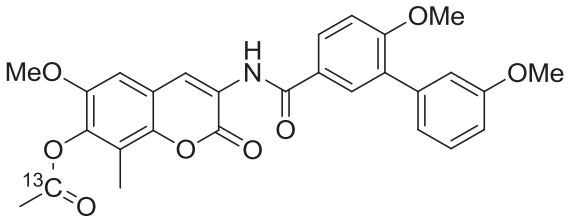

278

3-(3',6-Dimethoxy-[1,1'-biphenyl]-3-ylcarboxamido)-6-methoxy-8-methyl-2-oxo-2H-chromen-7-yl (acetate-^{13}C) (278): A solution of coumarin **159** (27.5 mg, 0.060 mmol) in pyridine (1.50 mL) was treated with acetic anhydride-^{13}C (0.50 mL). After 12 h, the solvent was concentrated and the residue purified via column chromatography (SiO_2, 40:1 CH_2Cl_2:Acetone)

to afford **278** as a colorless amorphous solid (20.2 mg, 67%): ^{1}H NMR ($CDCl_3$, 400 MHz) δ 8.83 (s, 1H), 8.80 (s, 1H), 7.96–7.92 (m, 2H), 7.39 (t, *J* = 8.0 Hz, 1H), 7.15 (d, *J* = 8.0, 1H), 7.12–7.11 (m, 1H), 7.08 (s, 1H), 6.96 (dd, *J* = 8.0, 2.4 Hz, 2H), 3.92 (s, 3H), 3.90 (s, 3H), 3.88 (s, 3H), 2.40 (d, *J* = 7.0 Hz, 3H), 2.33 (s, 3H); ^{13}C NMR ($CDCl_3$, 125 MHz) δ 168.5 (^{13}C), 165.6, 159.9, 159.3, 148.8, 142.7, 139.8 (2C), 138.6, 131.1, 130.0, 129.2, 128.2, 125.9, 124.0, 123.1, 122.0, 120.5, 117.6, 115.3, 113.1, 111.0, 106.4, 56.2, 55.9, 55.3, 20.2, 9.2; HRMS (ESI$^+$) *m/z*: $[M + H]^+$ calcd for $C_{27}{}^{13}CH_{26}NO_8$, 505.1692; found, 505.1675.

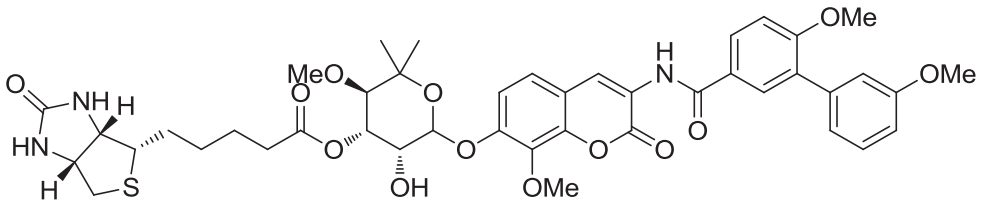

279

(3R,4S,5R)-6-((3-(3',6-dimethoxy-[1,1'-biphenyl]-3-ylcarboxamido)-8-methoxy-2-oxo-2H-chromen-7-yl)oxy)-5-hydroxy-3-methoxy-2,2-dimethyltetrahydro-2H-pyran-4-yl 5-((3aS,4S,6aR)-2-oxohexahydro-1H-thieno[3,4-d]imidazol-4-yl)pentanoate (279): DMAP (7.50 mg, 0.061 mmol) was added to a solution of *N,N'*-dicyclohexylcarbodiimide (12.6 mg, 0.061 mmol), **26g** (19 mg, 0.031 mmol), and 5-((3aS,4S,6aR)-2-oxohexahydro-1H-thieno[3,4-d]imidazol-4-yl)pentanoic acid (biotin, 11.2 mg, 0.046 mmol) in CH_2Cl_2 (2.10 mL), and the solution was stirred for 12 h. Solvent was removed and the residue was recrystallized from EtOAc/Hexane to afford **279** as a yellow amorphous solid (19.0 mg, 73%): ^{1}H NMR ($CDCl_3$, 400 MHz) δ 10.15 (d, *J* = 6.4 Hz, 1H), 8.75 (s, 1H), 8.70 (s, 1H), 8.23 (d, *J* = 6.4 Hz, 2H), 8.85 (s, 1H), 7.26 (d, *J* = 7.0 Hz, 1H), 7.12–7.09 (m, 2H), 6.90 (d, *J* = 7.0 Hz, 1H), 6.57 (d, *J* = 6.7 Hz, 1H), 4.35–4.51 (m, 1H), 4.38–4.41 (m, 1H), 4.07 (s, 3H), 3.93 (s, 1H), 3.88 (s, 1H), 3.59–3.49 (m, 6H), 3.12–3.08 (m, 2H), 3.07 (s, 3H), 2.79–2.82 (m, 2H), 2.72–2.76 (m, 2H), 2.50–2.25

(m, 4H), 1.94 (s, 3H), 1.73 (s, 3H), 1.42–1.27 (m, 2H), 1.22–1.10 (m, 4H); ^{13}C NMR (Acetone-d_6, 125 MHz) δ 174.2, 167.1, 164.8, 162.1 (2C), 157.2, 146.6, 144.2, 141.0, 139.2, 136.4, 130.7 (2C), 128.5, 128.3, 127.1, 121.3 (3C), 114.4, 113.4 (2C), 112.3 (2C), 106.3, 93.1, 71.0, 69.3, 75.8, 66.9, 61.3, 61.1, 60.1, 54.2 (3C), 39.5, 32.9, 27.8, 27.3, 24.3, 22.4, 22.3; HRMS (ESI$^+$) *m/z*: $[M + Na]^+$ calcd for $C_{43}H_{49}N_3NaO_{13}S$, 870.2884; found, 870.2869.

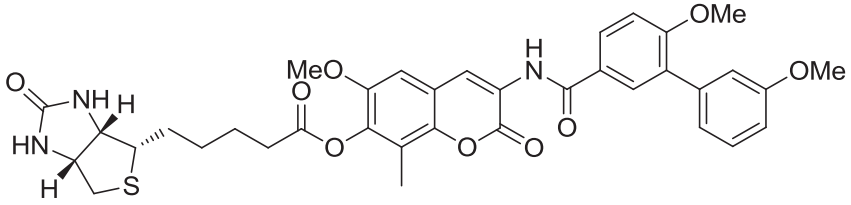

280

3-(3',6-Dimethoxy-[1,1'-biphenyl]-3-ylcarboxamido)-6-methoxy-8-methyl-2-oxo-2H-chromen-7-yl 5-((3aS,4S,6aR)-2-oxohexahydro-1H-thieno[3,4-d]imidazol-4-yl)pentanoate (280): DMAP (10.6 mg, 0.087 mmol) was added to a solution of *N,N'*-dicyclohexylcarbodiimide (17.9 mg, 0. 087 mmol), **159** (20 mg, 0.043 mmol), and 5-((3aS,4S,6aR)-2-oxohexahydro-1H-thieno[3,4-d]imidazol-4-yl)pentanoic acid (biotin, 15.9 mg, 0.065 mmol) in CH_2Cl_2 (2.90 mL), and the solution was stirred for 12 h. Solvent was removed and the residue was recrystallized from EtOAc/Hexane to afford **280** as a colorless amorphous solid (16.8 mg, 56%): ^{1}H NMR ($CDCl_3$, 400 MHz) δ 8.84 (s, 1H), 8.80 (s, 1H), 8.22 (d, J = 6.8 Hz, 1H), 7.96–7.92 (m, 1H), 7.39 (t, J = 8.0 Hz, 1H), 7.15–7.09 (m 2H), 7.00–6.90 (m 2H), 6.62 (d, J = 6.8 Hz, 1H), 4.96 (s, 1H), 4.78 (s, 1H), 4.58–4.55 (m 1H), 4.37–4.35 (m, 1H), 4.10 (d, J = 7.3 Hz, 3H), 3.93 (s, 3H), 3.89 (d, J = 4.9 Hz, 3H), 3.33 (d, J = 3.9 Hz, 1H), 3.00–2.55 (m, 2H), 2.80–2.69 (m, 2H), 2.32 (s, 3H), 1.42–1.32 (m, 2H), 1.21–1.07 (m, 4H); ^{13}C NMR ($CDCl_3$, 125 MHz) δ 168.7, 163.2, 157.4, 156.8, 156.5, 146.2, 140.2, 137.3, 136.1, 128.5, 127.6, 126.7, 125.8, 125.3, 123.3, 121.5, 120.8,

119.5, 117.9, 115.1, 112.8, 110.6, 108.5, 103.9, 69.9 (2C), 59.1 (4C), 38.0, 31.0, 28.5, 27.3, 26.9, 6.8; HRMS (ESI^+) *m/z*: $[M + Na]^+$ calcd for $C_{36}H_{37}N_3NaO_9S$, 710.2148; found, 710.2145.

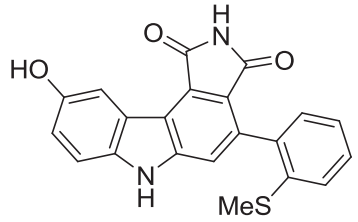

290

9-Hydroxy-4-(2-(methylthio)phenyl)pyrrolo[3,4-c]carbazole-1,3(2H,6H)-dione (290): Compound was prepared according to literature protocol.[277] ^1H NMR (DMSO, 400 MHz) δ 8.10 (s, 1H), 7.97 (d, *J* = 7.3 Hz, 1H), 7.36–7.30 (m, 2H), 7.26 (d, *J* = 7.6 Hz, 1H), 7.18 (d, *J* = 7.9 Hz, 1H), 7.10 (dd, *J* = 15.8, 7.4 Hz, 2H), 2.51 (t, *J* = 1.7 Hz, 3H).

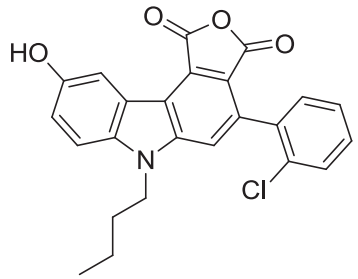

300

6-Butyl-4-(2-chlorophenyl)-9-hydroxy-1H-furo[3,4-c]carbazole-1,3(6H)-dione (300): Compound was prepared according to literature protocol.[277] ^1H NMR (Acetone-d_6, 400 MHz) δ 9.83 (s, 1H), 8.55 (d, *J* = 2.4 Hz, 1H), 8.37 (s, 1H), 7.72 (s, 1H), 7.59 (d, *J* = 8.8 Hz, 1H), 7.55–7.44 (m, 3H), 7.24 (dd, *J* = 8.8, 2.4 Hz, 1H), 4.55 (t, *J* = 7.2 Hz, 2H), 1.91–1.87 (m, 2H), 1.48–1.38 (m, 2H), 0.93 (t, *J* = 7.2 Hz, 3H). This material was determined to be 98% pure (Retention time = 10.78) by HPLC (Phenomenex Luna C-18 10 x 250 mm column eluting with 60% MeCN/40% H_2O, flow rate 5.0 mL/min.

VII. Yeast Protocols

A. General yeast growth conditions

Yeast was grown on YPD (2% [W/V] Bacto peptone, 1% yeast extract, 2% glucose or (YPGal) 2% galactose, 20 mg/L adenine). Selective growth was on dropout 2% glucose (DO) medium supplemented with appropriate amino acids.[280] YPD cultures were diluted to an optical density at 600 nM of 0.5, and 5 μL aliquots of a 10-fold dilution series were spotted onto YPD 2.0% agar plates with or without compounds. Growth was monitored over 3 to 5 days at 25°C.

B. v-Src activity assay *in vivo* (Section II.C.3)

PP30 yeast strain expressing human Hsp90α as its sole copy of Hsp90[273] was transformed with the YpRS316-v-SRC.[281,282] v-SRC is under control of the *GAL1* promoter. Its activity was analyzed as described previously.[282,283] Cells were grown on YPD to mid-log phase and then harvested, washed with sterile dH_2O, and then resuspended in YPGal media for 8 h in order to switch on the *GAL1* promoter. Cells were harvested and washed with dH_2O and then protein was extracted and quantified using Bio-Rad assay. v-Src protein levels were detected with EC10 mouse antibody (Millipore) and v-Src activity with 4G10 mouse anti-phosphotyrosine antibody (Millipore). Hsp90-His_6 was detected with Tetra-His monoclonal antibody (Qiagen).

C. Heat shock response assay (Sections II.C.2 and III.B.3)

PP30 yeast strain expressing Hsp90a as their sole Hsp90[273] was transformed with the centromeric *URA3* vector, pHSE[284] constitutively expressing β-galactosidase (encoded by *lacZ*) as a reporter gene under control of a promoter bearing 3 × Heat Shock Element (HSE) response elements.[284] Transformants were selected by DO medium (dropout 2% glucose medium) supplemented with appropriate amino acids without uracil.[280] Yeast cells were grown overnight to exponential phase with a cell density of 2-3×10^6 cells per mL in 50 mL of the same medium at 30°C. Then, appropriate compounds were added to a final concentration of 30 μM, followed by incubation at 30°C for 2 h. Cells were additionally heat shocked at 39˚C for 1 h, collected by centrifugation (2000 × g; 5 min), washed once with ddH_2O, and frozen at -80°C. The proteins were extracted as previously described,[285] except for exclusion of EDTA in the extraction buffer. β-galactosidase activities of HSE were measured as previously described.[282] Cell lysate (10 μL) was mixed with equal volume of 2 × buffer Z (0.12M Na_2HPO_4•$7H_2O$, 0.08M Na_2HPO_4•H_2O, 0.02M KCl, 0.002M $MgSO_4$, pH 7.0). The mixture was added to 700 μL of 2mg/mL ONPG solution in 1 × buffer Z prewarmed at 30°C and incubated at 30°C for 5-30 min. The reaction was stopped by adding 500 μL of 1M Na_2CO_3. The optical density at 420nM (OD_{420}) of each reaction mixture was determined. The protein concentration of the lysate was determined by the BioRad assay (BioRad). The β-galactosidase activity was calculated using the following formula:

Enzyme Activity = 1000 × OD_{420}/minute/[10 μL × protein concentration (μg/μL)].

Table 17. β-galactosidase assay solutions.

1 x Z buffer (pH 7.0)	Substrate solution	Stop solution
60mM Na_2HPO_4	2mg/mL O-Nitrophenyl-β-D-galactopyranoside (ONPG) dissolved in 1× Z buffer	1M Na_2CO_3
60mM NaH_2PO_4		
5mM KCl		
0.5mM $MgSO_4$		
0.025% β-mercaptoethanol		

D. Yeast protein extraction (Section IV.A.1)

Yeast cells were collected from solid media by a plastic sterile inoculating loop, or from liquid culture by centrifugation and resuspended in 1 mL of protein extraction buffer (PEBY). The cells were vortexed and centrifuged in a microfuge (16000 × g; 3 min). The supernatant was removed and two pellet volumes of acid washed glass beads were added, plus sufficient PEBY to cover both the pellet and the glass beads. To lyse the cells, tubes were agitated using a bead beater (mini-Beadbeater 8, Biospec Products, USA) for 40 seconds at maximum speed. Subsequently, 200 μL PEBY was added and tubes were vortexed to wash protein off of the beads, followed by centrifugation (16000 × g; 15 seconds) to pellet the beads and unbroken cells. The supernatant was transferred to a new microfuge tube and centrifuged (16000 × g; 15 min) to pellet insoluble aggregates. Supernatant was then transferred to a fresh microfuge tube and TWEEN20 (from a 1% stock in ddH_2O) was added to final concentration of 0.1%.

Table 18. Yeast protein extraction buffer.

Protein extraction buffer (PEBY)	**Protease inhibitor cocktail stock (stored at -20°C)**
20mM Tris/HCl pH 8.0	2 inhibitor tablets
1mM EDTA	6 mL ddH_2O
15% glycerol	
1mM PMSF	
2μg/mLPepstatin A	
4μg/mL RNAase	
1% β-mercaptoethanol	
Protease inhibitor cocktail (100 μL of stock to 50 mL of protein extraction buffer)- added just prior to use	

E. High efficiency yeast transformation (Section II.C.1)

A loop of yeast was inoculated into 50 mL of appropriate media and incubated to exponential phase at appropriate temperature. Cells were harvested in 50 mL sterile tubes by centrifugation (2000 x g, 5 min) and resuspended in 100 mM LiAc (lithium acetate) (20 mL). Cells were harvested by centrifugation (2000 x g, 5 min) and washed once again in 100 mM LiAc (20 mL). Cells were harvested again (2000 × g, 5 min) and resuspended in 100 mM LiAc in a volume that gave a final cell density 1×10^{10} cells/mL. Cells were aliquoted to 50 μL per microfuge tube and incubated at 30°C for 30 min. Next, the following were added in the order shown:

1. 240 µL PEG (50% w/v)
2. 36 µL 1.0 M Lithium acetate (LiAc/$LiOOCCH_3$)
3. 25 µL single stranded carrier DNA
4. 50 µL DNA mixture (1.5 µL plasmid + 48.5 µL dH_2O)

After gentle mixing with a pipette, the sample was incubated at 30°C for 30 min, followed by heat shock at 42°C for 20 min. Cells were harvested (2000 × g, 5 min) and resuspended in 1 mL YPD. This mixture was added to 8 mL YPD, followed by incubation with gentle agitation at 30°C for 90 min. Cells were harvested and washed with 6 mL dH_2O to remove YPD media. Following centrifugation (2000 × g, 5 min), cells were resuspended in 600 µL dH_2O and spread on three selective plates and incubated at 30°C for 3 days.

(1) Terasawa, K.; Minami, M.; Minami, Y. *J. Biochem.* **2005**, *137*, 443-447.

(2) Pratt, W. B.; Toft, D. O. *Exp. Biol. Med.* **2003**, *228*, 111-133.

(3) Issacs, J. S.; Xu, W.; Neckers, L. *Cancer Cell* **2003**, *3*, 213-217.

(4) Buchner, J. *Trends Biochem. Sci.* **1999**, *24*, 136-141.

(5) Picard, D. *Cell. Mol. Life Sci.* **2002**, *59*, 1640-1648.

(6) Yonehara, M.; Minami, Y.; Kawata, Y.; Nagai, J.; Yahara, I. *J. Biol. Chem.* **1996**, *271*, 2641-2645.

(7) Xiao, L.; Lu, X.; Ruden, D. M. *Mini Rev. Med. Chem.* **2006**, *6*, 1137-1143.

(8) Zhao, R.; Houry, W. A. *Biochem. Cell Biol.* **2005**, *83*, 703.

(9) Garnier, C.; Lafitte, D.; Tsvetkov, P. O.; Barbier, P.; Leclerc-Devin, J.; Millot, J.-M.; Briand, C.; Makarov, A. A.; Catelli, M. G.; Peyrot, V. *J. Biol. Chem.* **2002**, *277*, 12208-12214.

(10) Chiosis, G.; Huezo, H.; Rosen, N.; Mimnaugh, E.; Whitesell, L.; Neckers, L. *Mol. Cancer Ther.* **2003**, *2*, 123-129.

(11) Hanahan, D.; Weinberg, R. A. *Cell* **2000**, *100*, 57-70.

(12) Neckers, L., Ivy, S. P. *Curr. Opin. Oncol.* **2003**, *15*, 419-424.

(13) Warrick, J. M.; Chan, H. Y.; Chai, G. B. Y.; Paulson, H. L.; Bonin, N. M. *Nat. Genet.* **1999**, *23*, 425-428.

(14) Donnelly, A.; Blagg, B. S. *Curr. Med. Chem.* **2008**, *15*, 2702-2717.

(15) Yu, X. M.; Shen, G.; Neckers, L.; Blake, H.; Holzbeierlein, J.; Cronk, B.; Blagg, B. S. J. *J. Am. Chem. Soc.* **2005**, *127*, 12778-12779.

(16) Zhang, H.; Burrows, F. *J. Mol. Med.* **2004**, *82*, 488.

(17) Chiosis, G., Vilenchik, M., Kim, J., Solit, D. *Drug Discuss. Today* **2004**, *9*, 881.

(18) Burlison, J. A.; Neckers, L.; Smith, A. B.; Maxwell, A.; Blagg, B. S. J. *J. Am. Chem. Soc.* **2006**, *128*, 15529-15536.

(19) Toft, D. O. *Trends Endocrin. Metab.* **1998**, *9*, 238-243.

(20) Walter, S.; Buchner, J. *J. Agnew. Chem., Int. Ed.* **2002**, *41*, 1098-1113.

(21) Chaudhury, S.; Welch, T. R.; Blagg, B. S. J. *ChemMedChem* **2006**, *1*, 1331-1340.

(22) Prodromou, C.; Roe, S. M.; O'Brien, R.; Ladbury, J. E.; Piper, P. W.; Pearl, L. H. *Cell* **1997**, *90*, 65-75.

(23) Roe, S. M.; Prodromou, C.; O'Brien, R.; Ladbury, J. E.; Piper, P. W.; Pearl, L. H. *J. Med. Chem.* **1999**, *42*, 260-266.

(24) Whitesell, L.; Mimnaugh, E. G.; De Costa, B.; Myers, C. E.; Neckers, L. M. *Proc. Natl. Acad. Sci. USA* **1994**, *91*, 8324-8328.

(25) Ali, M. M. U.; Roe, S. M.; Vaughan, C. K.; Meyer, P.; Panaretou, B.; Piper, P. W.; Prodromou, C.; Pearl, L. H. *Nature* **2006**, *440*, 1013-1017.

(26) Panaretou, B.; Prodromou, C.; Roe, S. M.; O'Brien, R.; Ladbury, J. E.; Piper, P. W.; Pearl, L. H. *EMBO J.* **1998**, *17*, 4829-4836.

(27) Obermann, W. M. J.; Sondermann, H.; Russo, A. A.; Pavletich, N. P.; Hartl, F. U. *J. Cell. Biol.* **1998**, *143*, 901-910.

(28) Zhang, W.; Hirshberg, M.; McLaughlin, S. H.; Lazar, G. A.; Grossmann, J. G.; Nielsen, P. R.; Sobott, F.; Robinson, C. V.; Jackson, S. E.; Laue, E. D. *J. Mol. Biol.* **2005**, *340*, 891-907.

(29) Hawl, P.; Siepmann, M.; Harst, A.; Siderius, M.; Reusch, H. P.; Obermann, W. M. J. *Mol. Cell. Biol.* **2006**, *26*, 8385-8395.

(30) Harst, A.; Lin, H.; Obermann, W. M. J. *Biochem. J.* **2005**, *387*, 789-796.

(31) Lotz, G. P.; Lin, H.; Harst, A.; Obermann, W. M. J. *J. Biol. Chem.* **2003**, *278*, 17228-7235.

(32) Matsumoto, S.; Tanaka, E.; Nemoto, T. K.; Ono, T.; Takagi, T.; Imai, J.; Kimura, Y.; Yahara, I.; Kobayakawa, T.; Ayuse, T.; Oi, K.; Mizuno, A. *J. Biol. Chem.* **2002**, *277*, 32959-34966.

(33) Meyer, P.; Prodromou, C.; Hu, B.; Vaughan, C.; Roe, S. M.; Panaretou, B.; Piper, P. W.; Pearl, L. H. *Mol. Cell.* **2003**, *11*, 647-658.

(34) Panaretou, B.; Siligardi, G.; Meyer, P.; Maloney, A.; Sullivan, J. K.; Singh, S.; Millson, S. H.; Clarke, P. A.; Naaby-Hansen, S.; Stein, R.; Cramer, R.; Mollapour, M.; Workman, P.; Piper, P. W.; Pearl, L. H.; Prodromou, C. *Mol. Cell.* **2002**, *10*, 1307-1318.

(35) Sato, S.; Fujita, N.; Tsuruo, T. *Proc. Natl. Acad. Sci. USA* **2000**, *97*, 10832-10837.

(36) Chadli, A.; Bruinsma, E. S.; Stensqard, B.; Toft, D. *Biochemistry* **2008**, *47*, 2850-2857.

(37) Soti, C.; Vermes, A.; Haystead, T. A. J.; Csermely, P. *Eur. J. Biochem.* **2003**, *270*, 2421-2428.

(38) Welch, W. J. *Curr. Opin. Cell Biol.* **1991**, *3*, 1033-1038.

(39) Ferris, D. K.; Harel-Bellan, A.; Morimoto, R. I.; Welch, W. J.; Farrar, W. L. *Proc. Natl. Acad. Sci. USA* **1988**, *85*, 3850-3854.

(40) Sreedhar, A. S.; Kalmar, E.; Csermely, P.; Shen, Y. F. *FEBS Letters* **2004**, *562*, 11-15.

(41) Csermly, P., Schnaider, T., Soiti, C., Prohaszka, Z., Nardi, G. *Pharmacol. Ther.* **1998**, *79*, 129-168.

(42) Felts, S. J.; Owen, B. A. L.; Nguyen, P.; Trepel, J.; Donner, D. B.; Toft, D. O. *J. Biol. Chem.* **2000**, *275*, 3305-3312.

(43) Krishna, P.; Gloor, G. *Cell Stress Chaperones* **2001**, *6*, 238-246.

(44) Pepin, K.; Momose, F.; Ishida, N.; Nagata, K. *J. Vet. Med. Sci.* **2001**, *63*, 115-124.

(45) Millson, S. H.; Truman, A. W.; Racz, A.; Hu, B.; Panaretou, B.; Nuttall, J.; Mollapour, M.; Soti, C.; Piper, P. W. *FEBS J.* **2007**, *274*, 4453-4463.

(46) Sorger, P. K.; Pelham, H. R. B. *J. Mol. Biol.* **1987**, *194*, 341-344.

(47) Csermely, P.; Schnaider, T.; Soti, C.; Prohaszka, Z.; Nardi, G. *Pharmacol. Ther.* **1998**, *79*, 129-168.

(48) Kim, S. H.; Kim, D.; Jung, G. S.; Um, J. H.; Chung, B. S.; Kang, C. D. *Biochem. Biophys. Res. Commun.* **1999**, *262*, 516-522.

(49) Grammatikakis, N.; Vultur, A.; Ramana, C. V.; Siganou, A.; Schweinfest, C. W.; Watson, D. K.; Raptis, L. *J. Biol. Chem.* **2002**, *277*, 8312-8320.

(50) Cunningham, C. N.; Krukenberg, K. A.; Agard, D. A. *J. Biol. Chem.* **2008**, *In press*.

(51) Nemoto, T.; Ohara-Nemoto, Y.; Ota, M.; Takagi, T.; Yokoyama, K. *Eur. J. Biochem.* **1995**, *233*, 1-8.

(52) Kobayakawa, T.; Yamada, S.; Mizuno, A.; Nemoto, T. K. *Cell Stress Chaperones* **2008**, *13*, 97-104.

(53) Vaughan, C. K.; Gohlke, U. S., F.; Good, V. M.; Ali, M. M. U.; Prodromou, C.; Robinson, C. V.; Saibil, H. R.; Pearl, L. H. *Mol. Cell* **2006**, *23*, 697-707.

(54) Bron, P.; Giudice, E.; Rolland, J.-P.; Buey, R. M.; Barbier, P.; Diaz, J. F.; Peyrot, V.; Thomas, D.; Garnier, C. *Biol. Cell* **2008**, *in press*.

(55) Lindquist, S.; Craig, E. A. *Annu. Rev. Genet.* **1988**, *22*, 631-677.

(56) Gallo, K. A. *J. Chem. Biol.* **2006**, *13*, 115-116.

(57) Frydman, J. *Annu. Rev. Biochem.* **2001**, *70*, 603-649.

(58) Kim, S. A.; Yoon, J. H.; Lee, S. H.; Ahn, S. G. *J. Biol. Chem.* **2005**, *280*, 12653-12657.

(59) Guettouche, T.; Boellmann, F.; Lane, W. S.; Voellmy, R. *BMC Biochem.* **2005**, *6*, 4.

(60) Shamovsky, I.; Ivannikov, M.; Kandel, E. S.; Gershon, D.; Nudler, E. *Nature* **2006**, *440*, 556-560.

(61) Soti, C.; Nagy, E.; Giricz, Z.; Vigh, L.; Csermely, P.; Ferdinandy, P. *Br. J. Pharmacol.* **2005**, *146*, 769-780.

(62) Murphy, P. J. M.; Kanelakis, K. C.; Galigniana, M. D.; Morishima, Y.; Pratt, W. B. *J. Biol. Chem.* **2001**, *276*, 30092-30098.

(63) Onuoha, S. C.; Coulstock, E. T.; Grossmann, J. G.; Jackson, S. E. *J. Mol. Biol.* **2008**, *379*, 732-744.

(64) Kosano, H.; Stensgard, B.; Charlesworth, M. C.; McMahon, N.; Toft, D. *J. Biol. Chem.* **1998**, *273*, 32973-32979.

(65) Chen, S.; Sullivan, W. P.; Toft, D. O.; Smith, D. F. *Cell Stress Chaperones* **1998**, *3*, 1118-129.

(66) Forsythe, H. L.; Jarvis, J. L.; Turner, J. W. E., L. W.; Holt, S. E. *J. Biol. Chem.* **2001**, *276*, 15571-15574.

(67) Caplan, A. J. *Cell Stress Chaperones* **2003**, *8*, 105-107.

(68) Blagg, B. S. J.; Kerr, T. D. *Med. Res. Rev.* **2006**, *26*, 310-338.

(69) Prodromou, C.; Panaretou, B.; Chohan, S.; Siligardi, G.; O'Brien, R.; Ladbury, J. E.; Roe, S. M.; Piper, P. W.; Pearl, L. H. *EMBO J.* **2000**, *19*, 4383-4392.

(70) Xu, Z.; Horwich, A. L.; Sigler, P. B. *Nature (London)* **1997**, *388*, 741-750.

(71) Kimura, Y.; Matsumoto, S.; Yahara, I. *Mol. Gen. Genet.* **1994**, *242*, 517-527.

(72) Imai, J.; Maruya, M.; Yashiroda, H.; Yahara, I.; Tanaka, K. *EMBO J.* **2003**, *22*, 3557-3567.

(73) Correia, M. A.; Sadeghi, S.; Mundo-Paredes, E. *Annu. Rev. Pharmacol. Toxicol.* **2005**, *45*, 439-464.

(74) Goetz, M. P.; Toft, D. O.; Ames, M. M.; Erlichman, C. *Ann. Oncol.* **2003**, *14*, 1169-1176.

(75) Xu, W.; Mimnaugh, E. G.; Kim, J.-S.; Trepel, J. B.; Neckers, L. M. *Cell Stress Chaperones* **2002**, *7*, 91-96.

(76) Basso, A. D.; Solit, D. B.; Chiosis, G.; Giri, B.; Tsichlis, P.; Rosen, N. *J. Biol. Chem.* **2002**, *277*, 39858-39866.

(77) Marcu, M. G.; Chadli, A.; Bohouche, I.; Catelli, B.; Neckers, L. M. *J. Biol. Chem.* **2001**, *276*, 37181-37186.

(78) Soti, C.; Racz, A.; Csermely, P. *J. Biol. Chem.* **2002**, *277*, 7066-7075.

(79) Allan, R. K.; Mok, D.; Ward, B. K.; Ratajczak, T. *J. Biol. Chem.* **2006**, *281*, 7161-7171.

(80) Young, J. C.; Obermann, W. M. J.; Hartl, F. U. *J. Biol. Chem.* **1998**, *273*, 18001-18010.

(81) Prodromou, C.; Siligardi, G.; O'Brien, R.; Woolfson, D. N.; Regan, L.; Panaretou, B.; Ladbury, J. E.; Piper, P. W.; Peral, L. H. *EMBO J.* **1999**, *18*, 754-762.

(82) Scheufler, C.; Brinker, A.; Bourenkov, G. P., S.; Moroder, L.; Bartunik, H.; Harl, F. U.; Moarefi, I. *Cell* **2000**, *101*, 199-210.

(83) Louvion, J.-F.; Warth, R.; Picard, D. *Proc. Natl. Acad. Sci. USA* **1996**, *93*, 13937-13942.

(84) Marcu, M. G.; Schulte, T. W.; Neckers, L. *J. Natl. Cancer Inst.* **2000**, *92*, 242-248.

(85) Callebaut, I.; Catelli, M. G.; D., P.; Meng, X.; Cadepond, F.; A., B.; Baulieu, E. E.; Mornon, J. P. *C. R. Acad. Sci. III (Paris)* **1994**, *317*.

(86) Yun, B. G.; Huang, W.; Leach, N.; Hartson, S. D.; Matts, R. L. *Biochemistry* **2004**, *43*, 8217-8229.

(87) Scheibel, T.; Weikl, T.; Buchner, J. *Proc. Natl. Acad. Sci. USA* **1988**, *95*, 1495-1499.

(88) Hartson, S. D.; Thulasiraman, V.; Huang, W.; Whitesell, L.; Matts, R. L. *Biochemistry* **1999**, *38*, 3837-3849.

(89) Jibard, N.; Meng, X.; Leclerc, P.; Rajkowski, K.; Fortin, D.; Schweizer-Groyer, G.; Catelli, M.-G.; Baulieu, E.-E.; Cadepond, F. *Exp. Cell Res.* **1999**, *247*, 461-474.

(90) Scheibel, T.; Siegmund, H. I.; Jaenicke, R.; Ganz, P.; Lilie, H.; Buchner, J. *Proc. Natl. Acad. Sci. USA* **1999**, *96*, 1297-1302.

(91) Reece, R. J.; Maxwell, A. *Crit. Rev. Biochem. Mol. Biol.* **1991**, *26*, 335-375.

(92) Laurin, P.; Ferroud, D.; Schio, L.; Klich, M.; Dupuis-Hamelin, C.; Mauvais, P.; Lassaigne, P.; Bonnefoy, A.; Musicki, B. *Bioorg. Med. Chem. Lett.* **1999**, *9*, 2875-2880.

(93) Lewis, R. J.; Tsai, F. T.; Wigley, D. B. *BioEssays* **1996**, *18*, 661-671.

(94) Ali, J. A.; Jackson, A. P.; Howells, A. J.; Maxwell, A. *Biochemistry* **1993**, *32*.

(95) Holdgate, G. A.; Tunnicliffe, A.; Ward, W. H. J.; Weston, S. A.; Rosenbrock, G.; Barth, P. T.; Taylor, I. W. F.; Paupit, R. A.; Timms, D. *Biochemistry* **1997**, *36*, 9663-9673.

(96) Lewis, R. J.; Singh, O. M. P.; Smith, C. V.; Skarzyknski, T.; Maxwell, A.; Wonacott, A. J.; Wigley, D. B. *EMBO J.* **1996**, *15*, 1412-1420.

(97) Tsai, F. T. F.; Singh, O. M. P.; Skarzynski, T.; Wonacott, A. J.; Weston, S.; Tucker, A.; Pauptit, R. A.; Breeze, A. L.; Poyser, J. P.; O'Brien, R.; Ladbury, J. E.; Wigley, D. B. *Proteins* **1997**, *28*, 41-52.

(98) Gobernado, M.; Canton, E. S., M. *J. Clin. Microbiol.* **1984**, *3*, 371.

(99) Schwartz, G. N.; Teicher, B. A.; Eder, J. P., Jr.; Korbut, T.; Holden, S. A.; Ara, G.; Herman, T. S. *Cancer Chemother. Pharmacol.* **1993**, *32*, 455-462.

(100) Nordenberg, J.; Albukrek, D.; Hadar, T.; Fux, A.; Wasserman, L.; Novogrodsky, A.; Sidid, Y. *Br. J. Cancer* **1992**, *65*, 183-188.

(101) Hombrouck, C.; Capmau, M.; Moreau, N. *Cell Mol. Biol.* **1999**, *45*, 347-352.

(102) Burlison, J. A.; Avila, C.; Vielhauer, G.; Lubbers, D. J.; Holzbeierlein, J.; Blagg, B. S. J. *J. Org. Chem.* **2008**, *73*, 2130-2137.

(103) Burlison, J. A.; Blagg, B. S. J. *Org. Lett.* **2006**, *8*, 4855-4858.

(104) Huang, Y.-T.; Blagg, B. S. J. *J. Org. Chem.* **2007**, *72*, 3609-3613.

(105) Le Bras, G.; Radanyi, C.; Peyrat, J.-F.; Brio, J.-D.; Alami, M.; Marsaud, V.; Stella, B.; Renoir, J.-M. *J. Med. Chem.* **2007**, *50*, 6189-6200.

(106) Radanyi, C.; Le Bras, G.; Messaoudi, S.; Bouclier, C.; Peyrat, J.-F.; Brion, J.-D.; Marsaud, V.; Renoir, J.-M.; Alami, M. *Bioorg. Med. Chem. Lett.* **2008**, *18*, 2495-2498.

(107) Galanski, M. *Recent Patents Anticancer Drug Discov.* **2006**, *1*, 285-295.

(108) Goodisman, J.; Hagrman, D.; Tacka, K. A.; Souid, A. K. *Cancer Chemother. Pharmacol.* **2006**, *57*, 257.

(109) Brabec, V.; Kasparkova, J. *Drug Resist. Updat.* **2005**, *8*, 131.

(110) Frankenberg-Schwager, M.; Kirchermeier, D.; Greif, G.; Baer, K.; Becker, M.; Frankenberg, D. *Toxicology* **2005**, *212*, 175.

(111) Sreedhar, A. S.; Soti, C.; Csermely, P. *Biochim. Biophys. Acta* **2004**, *1697*, 233-242.

(112) Rosenhagen, M. C.; Soti, C.; Schmidt, U.; Wochnik, G. M.; Hartl, F. U.; Hosboer, F.; Young, J. C.; Rein, T. *Mol. Endocrinol.* **2003**, *17*, 1991.

(113) Itoh, H.; Ogura, M.; Komatsuda, A.; Wakui, H.; Miura, A. B.; Tashima, Y. *Biochem. J.* **1999**, *343*, 697-703.

(114) Perez, R. P. *Eur J. Cancer* **1998**, *34*, 1535-1542.

(115) Huang, R. Y.; Eddy, M.; Vujcic, M.; Kowalski, D. *Cancer Res.* **2005**, *65*, 5890-5897.

(116) Schenk, P. W.; Brok, M.; M., B. A. W.; Brandsma, J. A.; Kulk, H. D.; Brok, M.; Burger, H.; Stoter, G.; Brouwer, J.; Nooter, K. *Mol. Pharmacol.* **2003**, *64*, 259-268.

(117) Niedner, H.; Christen, R.; Lin, X.; Kondo, A.; Howell, S. B. *Mol. Pharmacol.* **2001**, *60*, 1153-1160.

(118) Liao, C.; Hu, B.; Arno, M. J.; Panaretou, B. *Mol. Pharmacol.* **2007**, *71*, 416-425.

(119) Palermo, C. M.; Westlake, C. A.; Gasiewicz, T. A. *Biochemistry* **2005**, *44*, 5041-5052.

(120) Wani, M. C.; Taylor, H. L.; Wall, M. E.; Coggon, P.; McPhail, A. T. *J. Am. Chem. Soc.* **1971**, *93*, 2325-2327.

(121) Ding, A. H.; Porteu, F.; Sanchez, E.; Nathan, C. F. *Science* **1990**, *248*, 370-372.

(122) Byrd, C. A.; Bornmann, W.; Erdjument-Bromage, H.; Tempst, P.; Pavletich, N.; Rosen, N.; Nathan, C. F.; Ding, A. *Proc. Natl. Acad. Sci. USA* **1999**, *96*, 5645-5650.

(123) Solit, D. B.; Basso, A. D.; Olshen, A. B. S., H. I.; Rosen, N. *Cancer Res.* **2003**, *63*, 2139-2144.

(124) Adams, J.; Elliot, P. J. *Oncogene* **2000**, *19*, 6687-6692.

(125) Yufu, Y.; Nishimura, J.; Nawata, H. *Leuk. Res.* **1992**, *16*, 597-605.

(126) Franzen, B.; Linder, S.; Alaiya, A. A.; Eriksson, E.; Fujioka, K.; Bergman, A. C. *Electrophoresis* **1997**, *18*, 582-587.

(127) Luparello, C.; Noel, A.; Pucci-Minafra, I. *DNA Cell Biol.* **1997**, *16*, 1231-1236.

(128) Banerji, U. *Proc. Am. Assoc. Cancer Ther.* **2003**, *44*, 677.

(129) Sausville, E. A. *Curr. Cancer Drug Targets* **2003**, *3*, 337-383.

(130) Hurst, D. R.; Mehta, A.; Moore, B. P.; Phadke, P. A.; Meehan, W. J.; Accavitti, M. A.; Shevde, L. A.; Hopper, J. E.; Xie, Y.; Welch, D. R.; Samant, R. S. *Biochem. Biophys. Res. Commun.* **2006**, *348*, 1429-1435.

(131) Neckers, L. *J. Biosci.* **2007**, *32*, 517-530.

(132) Eustace, B. K.; Sakurai, T.; Stewart, J. K.; Yimlamai, D.; Unger, C. Z., C.; Lain, B.; Torella, C.; Henning, S. W.; Beste, G.; Scroggins, B. T.; Neckers, L.; Ilag, L. L.; Jay, D. G. *Nature Cell. Biol.* **2004**, *6*, 507-510.

(133) Whitesell, L.; Lindquist, S. L. *Nat. Rev. Cancer* **2005**, *5*, 761-772.

(134) Aubert, G.; Lansdorp, P. M. *Physiol. Rev.* **2008**, *88*, 557-579.

(135) Monneret, C. *Anticancer Drugs* **2007**, *4*, 363-370.

(136) Hamamoto, R.; Furukawa, Y.; Morita, M.; Iimura, Y.; Piettella Silva, F.; Li, M.; Ragyu, R.; Nakamura, Y. *Nature Cell Biology* **2004**, *6*, 731-740.

(137) Brown, M. A.; Sims, R. J.; Gottlieb, P. D.; Tucker, P. W. *Mol. Cancer* **2006**, *5*, 26.

(138) Zhang, R.; Luo, D.; Miao, R.; Vai, L.; Ge, Q.; Sessa, W. C.; Min, W. *Oncogene* **2005**, *24*, 3954-3963.

(139) Cross, D. A.; Alessi, D. R.; Cohen, P.; Andjelkovich, M.; Hemmings, B. A. *Nature* **1995**, *378*, 785-789.

(140) Datta, S. R.; Dudek, H.; Tao, X.; Masters, S.; Fu, H.; Gotoh, Y.; Greenberg, M. E. *Cell* **1997**, *91*, 231-241.

(141) Cardone, M. H.; Roy, N.; Stennicke, H. R.; Salvesen, G. S.; Franke, T. F.; Stanbridge, E.; Frisch, S.; Reed, J. C. *Science* **1998**, *282*, 1318-1321.

(142) Kops, G. J.; de Ruiter, N. D.; De Vries-Smits, A. M.; Powell, D. R.; Bos, J. L.; Burgering, B. M. *Nature* **1999**, *398*, 630-634.

(143) Shiojima, I.; Walsh, K. *Circ. Res.* **2002**, *90*, 1243-1250.

(144) Tsuruo, T.; Naito, M.; Tomida, A.; Fujita, N.; Mashima, T.; Sakamoto, H.; Haga, N. *Cancer Science* **2003**, *94*, 15-21.

(145) Sattler, M.; Salgia, R. *Curr. Oncol. Rep.* **2007**, *9*, 102-108.

(146) Neckers, L. *Trends. Mol. Med.* **2002**, *8*, S55-61.

(147) Webb, C. P.; Hose, C. D.; Koochekpour, S.; Jeffers, M.; Oskarsson, M.; Sausville, E.; Monks, A.; Vande Woude, G. F. *Cancer Res.* **2000**, *60*, 342-349.

(148) Xie, Q.; Gao, C.-F.; Shinomiya, N.; Sausville, E.; Hay, R.; Gustafson, M.; Shen, Y.; Wenkert, D.; Vande Woude, G. F. *Oncogene* **2005**, *24*, 3697-3707.

(149) Peruzzi, B.; Bottaro, D. P. *Clin. Cancer Res.* **2006**, *12*, 3657-3660.

(150) Sturgill, T. W.; Wu, J. *Biochim. Biophys. Acta.* **1991**, *1092*, 350-357.

(151) Ahn, N. G.; Seger, R.; Krebs, E. G. *Curr. Opin. Cell. Biol.* **1992**, *4*.

(152) Nishida, E.; Gotoh, Y. *Trends Biochem. Sci.* **1993**, *18*, 128-131.

(153) Davis, R. J. *Trends Biochem. Sci.* **1994**, *19*, 470-473.

(154) Marshall, C. J. *Curr. Opin. Genet. Dev.* **1994**, *4*, 82-89.

(155) Cobb, M. H.; Goldsmith, E. J. *J. Biol. Chem.* **1995**, *270*, 14843-14846.

(156) Kyriakis, J. M.; Avruch, J. *BioEssays* **1996**, *18*, 567-577.

(157) Lavoie, J. N.; Rivard, N.; L'Allemain, G.; Poyssegur, J. *Prog. Cell Cycle Res.* **1996**, *2*, 49-58.

(158) Miyata, Y.; Ikawa, Y.; Shibuya, M.; Nishida, E. *J. Biol. Chem.* **2001**, *276*, 21841-21848.

(159) Kim, H. R.; Kang, H. S.; Kim, H. D. *IUBMB Life* **1999**, *48*, 429-433.

(160) Alonso, A. d. C.; Zaidi, T.; Novak, M.; Grundke-Iqbal, I.; Iqbal, K. *Proc. Natl. Acad. Sci. USA* **2001**, *98*, 6923-6928.

(161) Delacourte, A. *Folia Neuropathol.* **2005**, *43*, 244-257.

(162) Sahara, N.; Maeda, S.; Yoshiike, Y.; Mizoroki, T.; Yamashita, S.; Murayama, M.; Park, J. M.; Saito, Y.; Murayama, S.; Takashima, A. *J. Neurosci. Res.* **2007**, *85*, 3098-3108.

(163) Lau, L. F.; Schachter, J. B.; Seymour, P. A.; Sanner, M. A. *Curr Top Med Chem.* **2002**, *4*, 395-415.

(164) Lee, V. M.; Goedert, M.; Trojanowski, J. Q. *Annu. Rev. Neurosci.* **2001**, *24*, 1121–1159.

(165) Goedert, M.; Jakes, R. *Biochim. Biophys. Acta* **2005**, *1739*, 240-250.

(166) Zheng, Y. L.; Kesavapany, S.; Gravell, M.; Hamilton, R. S.; Schubert, M.; Amin, N.; Albers, W.; Grant, P.; Pant, H. C. *EMBO J.* **2005**, *24*, 209-220.

(167) Luo, W.; Dou, F.; Rodina, A.; Chip, S.; Kim, J.; Zhao, Q.; Moulick, K.; Aquirre, J.; Wu, N.; Greengard, P.; Chiosis, G. *Proc. Natl. Acad. Sci. USA* **2007**, *104*, 9511-9516.

(168) Kim, H. Y.; Heise, H.; Fernandez, C. O.; Baldus, M.; Zweckstetter, M. *ChemBioChem* **2007**, *8*, 1671-1674.

(169) Culvenor, J. G.; McLean, C. A.; Cutt, S.; Campbell, B. C. V.; Maher, F.; Jakala, P.; Hartmann, T.; Beyreuther, K.; Masters, C. L.; Li, Q.-X. *Am. J. Pathol.* **1999**, *255*, 1173-1181.

(170) Donnelly, A. C.; Mays, J. R.; Burlison, J. A.; Nelson, J. T.; Vielhauer, G.; Holzbeierlein, J.; Blagg, B. S. J. *J. Org. Chem.* **2008**, *73*, 8901-8920.

(171) Shen, G.; Yu, X. M.; Blagg, B. S. J. *Bioorg. Med. Chem. Lett.* **2004**, *14*, 5903 – 5906.

(172) Klaholz, B. P.; Moras, D. *Structure* **2002**, *10*, 1197-1204.

(173) Nabaei-Bidhendi, G.; Bannerjee, N. R. *J. Indian Chem. Soc.* **1990**, *67*, 43-45.

(174) Horvath, R. F.; Chan, T. H. *J. Org. Chem.* **1986**, *52*, 4489-4494.

(175) Miyake, M.; Hanaoka, Y.; Fujimoto, Y.; Sato, Y.; Taketomo, N.; Yokota, I.; Yoshiyama, Y. *Heterocycles* **1996**, *43*, 665-674.

(176) Carreno, M. C.; Garcia Ruano, J. L.; Toledo, M. A.; Urbano, A. *Tetrahedron Asymmetry* **1997**, *8*, 913-921.

(177) Wang, Y.; Tan, W.; Li, W. Z.; Li, Y. *J. Nat. Prod.* **2001**, *64*, 196-199.

(178) Ruenitz, P. C.; Bagley, J. R.; Nanavati, N. T. *J. Med. Chem.* **1988**, *31*, 1471-1475.

(179) Milne, J. E.; Buchwald, S. L. *J. Am. Chem. Soc.* **2004**, *126*, 13028-13032.

(180) Elliger, C. A. *Synth Commun* **1985**, *15*, 1315-1324.

(181) Robinson, A. J.; Lim, C. Y.; He, L.; Ma, P.; Li, H.-Y. *J. Org. Chem.* **2001**, *66*, 4141-4147.

(182) Toplak, R.; Svete, J.; Stanovnik, B.; Grdadolnik, S. G. *J. Hetero. Chem.* **1999**, *36*, 225-235.

(183) Lu, Y.; Ansar, S.; Michaelis, M. L.; Blagg, B. S. *Bioorg. Med. Chem.* **2009**, *17*, 1709-1715.

(184) Tao, Y.; Hart, J.; Lichtenstein, L.; Joseph, L. J.; Ciancio, M. J.; Hu, S.; Chang, E. B.; Bissonnette, M. *Carcinogenesis* **2009**, *30*, 175-182.

(185) Urban, M. J.; Li, C.; Yu, C.; Lu, Y.; Krise, J. M.; McIntosh, M. P.; Rajewski, R. A.; Blagg, B. S.; Dobrowsky, R. T. *ASN Neuro.* **2010**, *2*, 189-199.

(186) Selvam, J. J. P.; Suresh, V.; Rajesh, K.; Reddy, S. R.; Venkateswarlu, Y. *Tetrahedron Lett.* **2006**, *47*, 2507-2509.

(187) Singh, V.; Kanojiya, S.; Batra, S. *Tetrahedron* **2006**, *62*, 10100-10110.

(188) Corey, E. J.; Suggs, W. *J. Org. Chem.* **1973**, *38*, 3223-3224.

(189) Wilkinson, H. S.; Tanoury, G. J.; Wald, S. A.; Senanayake, C. H. *Tetrahedron Lett.* **2001**, *42*, 167-170.

(190) VanVliet, D. S. *Tetrahedron Lett.* **2005**, *46*, 6741-6743.

(191) Varala, R.; Enugala, R.; Adapa, S. R. *J. Iran. Chem. Soc.* **2007**, *4*, 370-374.

(192) Matts, R. L.; Dixit, A.; Peterson, L. B.; Sun, L.; Voruganti, S.; Kalyanaraman, P.; Hartson, S. D.; Blagg, B. S. J. *ACS Chem. Biol.* **2011**, *Submitted*.

(193) Zhao, H.; Donnelly, A. C.; Reddy, K. B.; Brandt, G. E. L.; Brown, D.; Rajewski, R. A.; Vielhauer, G.; Holzbeierlein, J.; Cohen, M. S.; Blagg, B. S. J. *J. Med. Chem.* **2011**, *accepted*.

(194) Donnelly, A.; Zhao, H.; Kusuma, B. R.; Blagg, B. S. J. *MedChemComm* **2010**, *1*, 165-170.

(195) Zhao, H.; Kusuma, B. R.; Blagg, B. S. J. *ACS Med. Chem. Lett.* **2010**, *1*, 311-315.

(196) Ramadas, S.; Krupadanam, G. L. D. *Tetrahedron Asymmetry* **2000**, *11*, 3375-3393.

(197) Boger, D. L.; Wysocki, R. J. *J. Org. Chem.* **1989**, *54*, 1238-1240.

(198) Tabart, M. *Bioorg. Med. Chem. Lett.* **2003**, *13*, 1329-1331.

(199) Sajiki, H.; Hirota, K. *Tetrahedron* **1998**, *54*, 13981-13996.

(200) Hajipour, A. R.; Ruoho, A. E. *Tetrahedron Lett.* **2005**, *46*, 8307-8310.

(201) Elokdah, H. M.; McFarlane, G. R.; Mayer, S. C.; Crandall, D. L.; Int, P., Ed. US, 2003; Vol. WO/2003/000671.

(202) Fang, Y.-G.; Lautens, M. *J. Org. Chem.* **2007**, *73*, 538-549.

(203) Lankalapalli, R. S.; Ouro, A.; Arana, L.; Gomez-Munoz, A.; Bittman, R. *J. Org. Chem.* **2009**, *74*, 8844-8847.

(204) Cresp, T. M.; Giles, R. G. F.; Sargent, M. V. *J. Chem. Soc.* **1974**, *1974*, 2435-2447.

(205) Ito, T.; Ito, M.; Arimoto, H.; Takamura, H.; Uemura, D. *Tetrahedron Lett.* **2007**, *48*, 5465-5469.

(206) Takamura, H.; Yamagami, Y.; Ito, T.; Ito, M.; Arimoto, H.; Kadota, I.; Uemura, D. *Heterocycles* **2009**, *77*, 351-364.

(207) Xie, L.; Xie, J.-X.; Kashiwada, Y.; Cosentino, M.; Liu, S.-H.; Pai, R. B.; Cheng, Y.-C.; Lee, K.-H. *J. Med. Chem.* **1995**, *38*, 3003-3008.

(208) O'Brien, C. J.; Kantchev, E. A. B.; Valente, C.; Hadei, N.; Chass, G. A.; Lough, A.; Hopkinson, A. C.; Organ, M. G. *Chem. Eur. J.* **2006**, *12*, 4743-4748.

(209) Sidduri, A.; Rozema, M. J.; Knochel, P. *J. Org. Chem.* **1993**, *58*, 2694-2713.

(210) Monguchi, Y.; Maejima, T.; Mori, S.; Maegawa, T.; Sajiki, H. *Chem. Eur. J.* **2010**, *16*, 7372-7375.

(211) Lebel, H.; Leogane, O. *Org. Lett.* **2006**, *8*, 5717-5720.

(212) Doyle, M. P.; Bryker, W. J. *J. Org. Chem.* **1978**, *44*, 1572-1574.

(213) Kikukawa, K.; Kono, K.; Wada, F.; Matsuda, T. *J. Org. Chem.* **1983**, *48*, 1333-1336.

(214) Cornforth, J.; Sierakowski, A. F.; Wallace, T. W. *J. Chem. Soc.* **1982**, *1982*, 2299-2315.

(215) Rassias, G.; Stevenson, N. G.; Curtis, N. R.; Northall, J. M.; Gray, M.; Prodger, J. C.; Walker, A. J. *Org. Process Res. Dev.* **2010**, *14*, 92-98.

(216) Doherty, E. M.; Fotsch, C.; Bannon, A. W.; Bo, Y.; Chen, N.; Dominguez, C.; Falsey, J.; Gavva, N. R.; Katon, J.; Nixey, T.; Ognyanov, V. I.; Pettus, L.; Rzasa, R. M.; Stec, M.; Surapaneni, S.; Tamir, R.; Zhu, J.; Treanor, J. J. S.; Norman, M. H. *J. Med. Chem.* **2007**, *50*, 3515-3527.

(217) Henderson, E. A.; Bavetsias, V.; Theti, D. S.; Wilson, S. C.; Clauss, R.; Jackman, A. L. *Bioorg. Med. Chem.* **2006**, *14*, 5020-5042.

(218) Webber, S. E.; Bleckman, T. M.; Attard, J.; Deal, J. G.; Kathardekar, V.; Welsh, K. M.; Webber, S.; Janson, C. A.; Matthews, D. A.; Smith, W. W.; Freer, S. T.; Jordan, S. R.; Bacquet, R. J.; Howland, E. F.; Booth, C. L. J.; Ward, R. W.; Hermann, S. M.; White, J.; Morse, C. A.; Hilliard, J. A.; Bartlett, C. A. *J. Med. Chem.* **1993**, *36*, 733-746.

(219) Malmgren, H.; Backstrom, B.; Solver, E.; Wennerberg, J. *Org. Process Res. Dev.* **2008**, *12*, 1195-1200.

(220) Wu, Z.-Q.; Jiang, X.-K.; Zhu, S.-Z.; Li, Z.-T. *Org. Lett.* **2004**, *6*, 229-232.

(221) Gao, L.-J.; Herdewijn, P. A.; De Jonghe, S. C.; Watkins, W. J.; Chong, L. S.; Int, P., Ed. US, 2008; Vol. WO/2008/009077.

(222) Davidson, A. H.; Davies, S. J.; Moffat, D. F. C.; Int, P., Ed. GB, 2006; Vol. WO/2006/117552.

(223) Baumgarten, H. E.; DeBrunner, M. R. *J. Am. Chem. Soc.* **1954**, *76*, 3489-3493.

(224) Cheng, Y.; Albrecht, B. K.; Brown, J.; Buchanan, J. L.; Buckner, W. H.; DiMauro, E. F.; Emkey, R.; Fremeau, R. T.; Harmange, J.-C.; Hoffman, B. J.; Huang, L.; Huang, M.; Lee, J. H.; L, F.-F.; Martin, M. W.; Nguyen, H. Q.; Patel, V. F.; Tomlinson, S. A.; White, R. D.; Xia, X.; Hitchcock, S. A. *J. Med. Chem.* **2008**, *51*, 5019-5034.

(225) Saari, W. S.; Wai, J. S.; Fisher, T. E.; Thomas, C. M.; Hoffman, J. M.; Rooney, C. S.; Smith, A. B.; Jones, J. H.; Bamberger, D. L.; Golman, M. E.; O'Brien, J. A.; Nunberg, J. H.; Quintero, J. C.; Schleif, W. A.; Emini, E. A.; Anderson, P. S. *J. Med. Chem.* **1992**, *35*, 3792-3802.

(226) Bachman, G. B.; Welton, D. E.; Jenkins, G. L.; Christian, J. E. *J. Am. Chem. Soc.* **1947**, *69*, 365-371.

(227) Krishnan, R.; Lang, S. A.; Siegel, M. M. *J. Heterocyclic Chem.* **1986**, *23*, 1801-1804.

(228) Jogireddy, R.; Maier, M. *J. Org. Chem.* **2006**, *71*, 6999-7006.

(229) Akritopoulou-Zanze, I.; Patel, J. R.; Hartandi, K.; Brenneman, J.; Winn, M.; Pratt, J. K.; Grynfarb, M.; Goos-Nisson, A.; von Geldern, T. W.; Kym, P. R. *Bioorg. Med. Chem. Lett.* **2004**, *14*, 2079-2082.

(230) Klarmann, E. *J. Am. Chem. Soc.* **1926**, *48*, 791-794.

(231) Greig, L. M.; Slawin, A. M. Z.; Smith, M. H.; Philp, D. *Tetrahedron* **2007**, *63*, 2391-2403.

(232) Green, K. *J. Org. Chem.* **1991**, *56*, 4325-4326.

(233) Kruse, I.; Lawrence, I. *Heterocycles* **1981**, *16*, 1119-1124.

(234) Saenz, J.; Mitchell, M.; Bahmanyar, S.; Stankovic, N.; Perry, M.; Craig-Woods, B.; Kline, B.; Yu, S.; Albizati, K. *Org. Process Res. Dev.* **2007**, *11*, 30-38.

(235) Noguchi, T.; tanaka, N.; Nishimata, T.; Goto, R.; Hayakawa, M.; Sugidachi, A.; Ogawa, T.; Asai, F.; Mastsui, Y.; Fujimoto, K. *Chem. Pharm. Bull.* **2006**, *54*, 163-174.

(236) Boyd, D. R.; Berchtold, G. A. *J. Am. Chem. Soc.* **1979**, *101*, 2470-2474.

(237) Yu, X. M.; Shen, G.; Blagg, B. S. J. *J. Org. Chem.* **2004**, *69*, 7375.

(238) Garg, H.; Francella, N.; Tony, K. A.; Augustine, L. A.; Barchi, J. J.; Fantini, J.; Puri, A.; Mootoo, D. R.; Blumenthal, R. *Antiviral Res.* **2008**, *80*, 54-61.

(239) Anizon, F.; Moreau, P.; Sancelme, M.; Laine, W.; Bailly, C.; Prudhomme, M. *Bioorg. Med. Chem.* **2003**, *11*, 3709-3722.

(240) Yu, Y. M.; Han, H.; Blagg, B. S. J. *J. Org. Chem.* **2005**, *70*, 5599.

(241) Matts, R. L.; Brandt, G. E. L.; Lu, Y.; Dixit, A.; Mollapour, M.; Wang, S.; Donnelly, A. C.; Neckers, L.; Verkhivker, G.; Blagg, B. S. J. *Bioorg. Med. Chem.* **2011**, *19*, 684-692.

(242) Chen, L.; Georges, G.; Mertens, A.; Wu, X.; Int, P., Ed. 2007; Vol. WO/2007/071348.

(243) Baganz, H.; Teichert, P. *Arch. Pharm. Ber. Dtsch. Pharm. Ges.* **1961**, *294*, 725-739.

(244) Weymouth-Wilson, A. C. *Nat. Prod. Rep.* **1997**, *14*, 99-110.

(245) Thorson, J. S.; Hosted, T. J.; Jiang, J.; Biggins, J. B.; Ahlert, J. *Curr. Org. Chem.* **2001**, *5*, 139–167.

(246) Nicolaou, K. C.; Mitchell, H. J. *Angew. Chem. Int. Ed. Engl.* **2001**, *40*, 1576-1624.

(247) In *Carbohydrates in Chemistry and Biology*; Ernst, B., Hart, G. W., Sinay, P., Ed.; Wiley-VCH: Weinheim, 2000.

(248) Wang, P. G., Bertozzi, C. R., Ed.; Marcel Dekker, Inc.: New York, 2001.

(249) Vogel, P. In *Glycoscience*; Fraser-Reid, B. O., Tatsuta, K., Thiem, J., Ed.; Springer: Berlin, 2001; Vol. 2.

(250) Capon, R. J.; Peng, C.; Dooms, C. *Org. Biomol. Chem.* **2008**, *6*, 2765-2771.

(251) Kolocouris, N.; Zoidis, G.; Foscolos, G. B.; Fytas, G.; Prathalingham, S. R.; Kelly, J. M.; Naesens, L.; De Clercq, E. *Bioorg. Med. Chem. Lett.* **2007**, *17*, 4358-4362.

(252) Ke, S. Y.; Qian, X. H.; Liu, F. Y.; Wang, N.; Yang, Q.; Li, Z. *Eur. J. Med. Chem.* **2009**, *44*, 2113-2121.

(253) Andrew, J. R.; Olga, V. S.; Andrei, V. N. *Carbohydrate Research* **2006**, *341*, 1954.

(254) Huber-Ruano, I.; Pastor-Anglada, M. *Curr. Drug Metab.* **2009**, *10*, 347-358.

(255) Bernardi, A.; Cheshev, P. *Chemistry* **2008**, *14*, 7434-7441.

(256) Hosmane, R. S.; Hong, M. *Biochim. Biophys. Res. Commun.* **1997**, *236*, 88-93.

(257) Eis, C.; Nidetzky, B. *Biochem. J.* **2002**, *363*, 335-340.

(258) Werz, D. B.; Seeberger, P. H. *Chemistry* **2005**, *11*, 3194-3206.

(259) Shelton, S. N.; Shawgo, M. E.; Comer, S. B.; Lu, Y.; Donnelly, A. C.; Szabla, K.; Tanol, M.; Vielhauer, G. A.; Rajewski, R. A.; Matts, R. L.; Blagg, B. S.; Robertson, J. D. *Mol. Pharmacol.* **2009**, *76*, 1314-1322.

(260) Cunningham, C. W.; Mukhopadyay, A.; Lushington, G. H.; Blagg, B. S.; Prisinzano, T. E.; Krise, J. P. *Mol. Pham.* **2010**, *7*, 1301-1310.

(261) Zych, A. J.; Iverson, B. L. *J. Am. Chem. Soc.* **2000**, *122*, 8898-8909.

(262) Yan, Y.; Qin, B.; Shu, Y.; Chen, X.; Yip, Y. K.; Zhang, D.; Su, H.; Zeng, H. *Org. Lett.* **2009**, *11*, 1201-1204.

(263) Priet, S.; Zlatev, I.; Barvik, I.; Geerts, K.; Leyssen, P.; Neyts, J.; Dutartre, H.; Canard, B.; Vasseur, J.-J.; Morvan, F.; Alvarez, K. *J. Med. Chem.* **2010**, *53*, 6608-6617.

(264) Bartoli, G.; Bosco, M.; Locatelli, M.; Marcantoni, E. *Org. Lett.* **2005**, *7*, 427-430.

(265) Lunazzi, L.; Mancinelli, M.; Mazzanti, A. *J. Org. Chem.* **2008**, *73*, 2198-2205.

(266) Shibahara, F.; Kinoshita, S.; Nozaki, K. *Org. Lett.* **2004**, *6*, 2437-2439.

(267) Grosse Brinkhaus, K. H.; Steckhan, E.; Degner, D. *Tetrahedron* **1986**, *42*, 553-560.

(268) Peddibhotla, S.; Shi, R.; Khan, P.; Smith, L. H.; Mangravita-Novo, A.; Vicchiarelli, M.; Su, Y.; Okolotowicz, K. J.; Cashman, J. R.; Reed, J. C.; Roth, G. P. *J. Med. Chem.* **2010**, *53*, 4793-4797.

(269) Schmidt, M.; Barbayianni, E.; Fotakopoulou, I.; Hoehne, M.; Constantinou-Kokotou, V.; Bornscheuer, U. T.; Kokotos, G. *J. Org. Chem.* **2005**, *70*, 3737-3740.

(270) Hou, Y.; Meyers, C. *J. Org. Chem.* **2004**, *69*, 1186-1195.

(271) Boyer, A.; Isono, N.; Lackner, S.; Lautens, M. *Tetrahedron* **2010**, *66*, 6468-6482.

(272) Piper, P. W.; Panaretou, B.; Millson, S. H.; Truman, A.; Mollapour, M.; Pearl, L. H.; Prodromou, C. *Gene* **2003**, *302*, 165-70.

(273) Millson, S. H.; Truman, A. W.; Racz, A.; Hu, B.; Panaretou, B.; Nuttall, J.; Mollapour, M.; Soti, C.; Piper, P. W. *FEBS J* **2007**, *274*, 4453-63.

(274) Zou, J.; Guo, Y.; Guettouche, T.; Smith, D. F.; Voellmy, R. *Cell* **1998**, *94*, 471-80.

(275) Nathan, D. F.; Lindquist, S. *Mol Cell Biol* **1995**, *15*, 3917-25.

(276) Mollapour, M.; Tsutsumi, S.; Donnelly, A. C.; Beebe, K.; Tokita, M. J.; Lee, M.-J.; Lee, S.; Morra, G.; Bourboulia, D.; Scroggins, B. T.; Colombo, G.; Blagg, B. S.; Panaretou, B.; Stetler-Stevenson, W. G.; Trepel, J. B.; Piper, P. W.; Prodromou, C.; Pearl, L. H.; Neckers, L. *Mol. Cell* **2010**, *37*, 333-343.

(277) Palmer, B. D.; Thompson, A. M.; Booth, R. J.; Dobrusin, E. M.; Kraker, A. J.; Lee, H. H.; Lunney, E. A.; Mitchell, L. H.; Ortwine, D. F.; Smaill, J. B.; Swan, L. M.; Denny, W. A. *J. Med. Chem.* **2006**, *49*, 4896-4911.

(278) Tsotinis, A.; Afroudaki, P. A.; Davidson, K.; Prashar, A.; Sugden, D. *J. Med. Chem.* **2007**, *50*, 6436-6440.

(279) Yusubov, M. S.; Tveryakova, E. N.; Krasnokutskaya, E. A.; Perederyna, I. A.; Zhdankin, V. V. *Synth. Commun.* **2007**, *37*, 1259-1265.

(280) Adams, A.; Gottschling, D. E.; Kaiser, C. A.; Stearns, T. *Methods in Yeast Genetics.*; Cold Spring Harbor Laboratory Press: Cold Spring Harbor, New York, 1997.

(281) Xu, Y.; Singer, M. A.; Lindquist, S. *Proc Natl Acad Sci U S A* **1999**, *96*, 109-14.

(282) Nathan, D. F.; Vos, M. H.; Lindquist, S. *Proc Natl Acad Sci U S A* **1997**, *94*, 12949-56.

(283) Panaretou, B.; Siligardi, G.; Meyer, P.; Maloney, A.; Sullivan, J. K.; Singh, S.; Millson, S. H.; Clarke, P. A.; Naaby-Hansen, S.; Stein, R.; Cramer, R.; Mollapour, M.; Workman, P.; Piper, P. W.; Pearl, L. H.; Prodromou, C. *Mol Cell* **2002**, *10*, 1307-18.

(284) Hjorth-Sorensen, B.; Hoffmann, E. R.; Lissin, N. M.; Sewell, A. K.; Jakobsen, B. K. *Mol Microbiol* **2001**, *39*, 914-23.

(285) Panaretou, B.; Piper, P. *Methods Mol Biol* **1996**, *53*, 117-21.